

# Mechanisms of the Intriguing Rearrangements of Activated Organic Species

A Thesis Submitted for the Degree  
of  
**Doctor of Philosophy**  
of  
The Australian National University

by

David Grant Harman



Department of Chemistry  
Faculty of Science  
Canberra

April 2003



## **Declaration**

This thesis is an original work. None of the work has been previously submitted by me for the purpose of obtaining a degree or diploma in any university or other tertiary education institution. To the best of my knowledge, this thesis does not contain material previously published by another person, except where due reference is made in the text.

*To those who tell me the truth in love,  
particularly when I do not want to hear it.*

## Acknowledgements

Many people, too numerous to mention individually, assisted in the production of this thesis. Corporately I wish to thank them and to express my deep and sincere gratitude. I would briefly like to mention those to whom I am particularly indebted and I apologise to anyone whom I have inadvertently omitted.

Professor Athel Beckwith was my supervisor while I was working in the laboratories of the Research School of Chemistry. Athel and his wife Kaye made me feel welcome in Canberra. I'm grateful to have worked on such challenging projects and to have had such expert guidance. Athel's love for chemistry, his vast knowledge, his view of the bigger picture and the humility to admit when he didn't know something have been the source of much inspiration.

My RSC advisers were Professor Lew Mander, Professor Rod Rickards and Dr John MacLeod. I would like to thank them and other academic, technical and administrative staff for valuable advice and assistance. Mr Robert Longmore deserves a particular mention for his laboratory prowess, his willingness to share his expertise and his friendship. So does Mrs Joan Smith—RSC Librarian Extraordinaire—for her helpfulness, patience, encouragement and continual grace when loans were overdue.

Dr Steven Brumby helped me record the esr spectra. My brother, Mr Ian Harman, helped me with the computer program used to determine the rotational barriers in  $\beta$ -substituted ethyl radicals. Ms Peta Simmonds, Mrs Tin Culnane and Mr Chris Blake of the ANU NMR Centre helped me with two-dimensional and  $^{17}\text{O}$  nmr. Drs Graham Heath, Richard Webster and Brett Yeomans assisted me with the recording and interpretation of cyclic voltammograms.

I thank the Australian Government for a Commonwealth Postgraduate Research Award, known later as the Australian Postgraduate Research Award. I'm grateful to have received an Australian National University PhD Scholarship for six months upon the expiration of my APRA.

I'm one of the lucky few who have worked in both the Research School of Chemistry and the Department of Chemistry. Professor Jack Elix has been my

supervisor during my time in the Department. I'd like to thank him for taking on a student from a field quite different to his own, for his efforts in correcting thesis drafts and for his gentle advice. Drs Christina Chai and Geoff Salem, my current advisers, I thank for their assistance. My passage into the Department was facilitated by past Heads Professor Jack Elix and Dr Gad Fischer. Thanks also to the current Head, Dr Geoff Salem, for his support. Mr Warren Griffiths provided tireless assistance with computer problems.

And last, but by no means the least, I'd like to acknowledge the unending support my parents Kay and Grant have given me in realms moral, spiritual and financial and for some proof reading.

## Abstract

The  $\beta$ -acyloxyalkyl radical rearrangement has been known since 1967 but its mechanism is still not fully understood, despite considerable investigation. Since the migration of a  $\beta$ -trifluoroacetoxy group generally proceeds more rapidly and with more varied regiochemistry than its less electronegative counterparts, this reaction was studied in the hope of understanding more about the subtleties of the mechanism of the  $\beta$ -acyloxyalkyl radical rearrangement. The mechanism of the catalysed rearrangement of *N*-alkoxy-2(1*H*)-pyridinethiones was also explored because preliminary studies indicated that the transition state (TS) for this process was isoelectronic with TSs postulated for the  $\beta$ -acyloxyalkyl radical and other novel rearrangements.

A kinetic study of the rearrangement of the 2-methyl-2-trifluoroacetoxy-1-heptyl radical in solvents of different polarity was undertaken using a radical clock method. Arrhenius equations for the rearrangement in each solvent were: hexane,  $\log_{10}[k_r \text{ (s}^{-1})] = 11.8 \pm 0.3 - (48.9 \pm 0.7)/\theta$ ; benzene,  $\log_{10}[k_r \text{ (s}^{-1})] = 12.0 \pm 0.2 - (43.7 \pm 0.8)/\theta$ ; and propionitrile,  $\log_{10}[k_r \text{ (s}^{-1})] = 11.9 \pm 0.2 - (42.0 \pm 0.3)/\theta$ . Rate constants at 75°C were: hexane,  $k_r = 2.9 \times 10^4$ ; benzene,  $k_r = 2.8 \times 10^5$ ; and propionitrile,  $k_r = 4.0 \times 10^5 \text{ s}^{-1}$ . The equilibrium constant for the reversible rearrangement at 80°C in benzene was  $15.1 < K < 52.9$ .

A regiochemical study with oxygen-labelled radicals revealed that trifluoroacetoxy group migration occurs with 66-83% label transposition (3,2 shift). The proportion of 3,2 shift is decreased by polar solvent, high temperature and low concentration of the reducing agent. Results of labelling experiments were consistent with cooperative 1,2 and 3,2 shifts, the former having  $E_a$  9.5 kJmol<sup>-1</sup> higher than the latter in benzene solution.

An esr study of nine  $\beta$ -oxygenated radicals revealed that the temperature-dependent equilibrium conformation is controlled by a balance between steric and stereoelectronic effects. The influence of the latter is increased by electron-attracting  $\beta$ -substituents. Barriers to  $C_\alpha$ - $C_\beta$  rotation in  $\beta$ -oxyethyl radicals are approximately the same as for the propyl radical. Consequently, there is no significant through-space

interaction between the  $\beta$ -substituent and the unpaired electron.

Experimental results were consistent with a mechanism involving a combination of polarized 1,2 and 3,2 concerted shifts. The results may also be rationalised by the intermediacy of a contact ion pair, as well as combinations of the three options.

The rearrangement of *N*-alkoxy-2(1*H*)-pyridinethiones is catalysed by oxidants, Lewis acids and protic acids. Pseudo first order kinetics are observed and there are moderate solvent effects. The migration of a 1,1-dideuteroallyl group occurs almost exclusively in a 1,4 sense. Migration of an enantiomerically enriched 1-phenylethyl group proceeds with predominant retention of configuration in chloroform, but with virtual racemisation in acetonitrile. Migrating groups do not become diffusively free during the rearrangement. Substituents which stabilise positive charge at C1 migrate more rapidly. The bulk of evidence indicates that a catalyst activates the pyridinethione for rearrangement by promoting aromatisation. Mass-spectrometric analysis of an isolated intermediate and kinetic results are consistent with an intermolecular mechanism.



## Abbreviations and symbols

A	adenine
A	Arrhenius frequency factor
abs.	absolute
Ac	acetyl
ACS	American Chemical Society
AIBN	azobis(isobutyronitrile)
AM1	Austin Model 1
AM1-SM2	Solvation Model 2 based on the Austin Model 1
amu	atomic mass units
ANU	Australian National University
Ar	aryl
ASTM	American Society for Testing and Materials
B3LYP	Becke three parameter hybrid function, using the Lee-Yang-Parr correction
bp	boiling point
BP1	GC stationary phase consisting of dimethylpolysiloxane
BP5	GC stationary phase consisting of 5% phenyl / 95% dimethylpolysiloxane
BP10	GC stationary phase consisting of 14% cyanopropylphenyl / 86% dimethyl polysiloxane
BP20	GC stationary phase consisting of polyethylene glycol
BSTFA	bis(trimethylsilyl)trifluoroacetamide
Bu	<i>n</i> -butyl
cal	calorie
calc.	calculated
CIDNP	chemically induced dynamic nuclear polarisation
CIMS	chemical ionisation mass spectrometry
CIP	contact ion pair
conc.	concentrated <i>or</i> concentration
COSY	correlated nmr spectroscopy
CT	charge transfer
$\Delta$	heat applied
DMAP	dimethylaminopyridine
DME	1,2-dimethoxyethane
DMF	dimethylformamide
DMPO	5,5-dimethyl-1-pyrroline <i>N</i> -oxide

DMSO	dimethylsulfoxide
DNA	deoxyribonucleic acid
$\epsilon$	dielectric constant
$E_a$	Arrhenius activation energy
e.e	enantiomer(ic) excess
EI	electron impact
EIMS	electron impact mass spectrum/spectrometry
eq.	equivalent(s) <i>or</i> equation
esr	electron spin resonance spectroscopy
Et	ethyl
$E_T$	Dimroth-Reichardt parameter for the ionising power of a solvent
Fc	ferrocenium
$F_r$	fraction of retention of configuration upon rearrangement
FTIR <i>or</i> ftir	fourier transform infrared spectroscopy
G3(MP2)	Gaussian 3 theoretical calculations applied to a geometry determined by second order Moller-Plesset perturbation theory
GC	gas chromatography
GCMS	gas chromatography / mass spectrometry
HETCOR	heteronuclear correlated nmr spectroscopy
hfs	hyperfine splitting
HP1	GC stationary phase consisting of dimethylpolysiloxane
HPLC	high performance liquid chromatography
HRMS	high resolution mass spectrometry
I.D.	inner diameter
INDO	molecular orbital theory incorporating the intermediate neglect of differential overlap
ir	infrared spectroscopy
IUPAC	International Union of Pure and Applied Chemistry
$J$	symbol for nmr coupling constant
$K$	equilibrium constant
$k$	rate constant
KIE	kinetic isotope effect
lit.	literature value
LR HETCOR	long-range (2 and 3 bond) $^{13}\text{C}$ - $^1\text{H}$ shift-correlated heteronuclear nmr
<i>m</i> -CPBA	<i>m</i> -chloroperbenzoic acid
$m/z$	mass to charge ratio
Me	methyl
min(s)	minute(s)

MO	molecular orbital
mp	melting point
MS	mass spectrometry
Ms	methanesulfonyl
<i>MW</i>	molecular weight
n.d.	not detected
<i>n</i> -Pr	<i>n</i> -propyl
n.r.	not resolved
Nu	nucleophile
NBA	<i>N</i> -bromoacetamide
NBS	<i>N</i> -bromosuccinimide
NMA	<i>N</i> -methylacetamide
nmr	nuclear magnetic resonance spectroscopy
PFK	perfluorokerosene
PFMC	perfluoromethylcyclohexane
Ph	phenyl
PM3	third parametrisation of the Modified Neglect of Diatomic Differential Overlap
ppm	parts per million
Pr	<i>n</i> -propyl
PT	pyridinethione
$\rho$	Hammett parameter measuring the susceptibility of the reaction to electronic effects
<i>R</i>	gas constant
R	alkyl radical <i>or</i> substituted alkyl radical
RBF	round-bottomed flask
$R_E$	proportion of original concentration of label remaining in the oxygen of the same hybridisation in the product ester
Rf	chromatographic retardation factor
$\sigma$	standard deviation
$\sigma_p^+$	Hammett parameter describing the degree to which a <i>para</i> electron-donating group interacts with a developing positive charge in the transition state
SAR	sarcophagine
SGE	Scientific Glass Engineering (company)
SOMO	singly occupied molecular orbital
SSIP	solvent-separated ion pair

STO-3G	basis set consisting of Slater-type orbitals approximated by three primitive Gaussian functions
SVF	standard volumetric flask
<i>T</i>	temperature
<i>t</i>	time
<i>t</i> -Bu	<i>tert</i> -butyl
TBAF	tetrabutylammonium fluoride
TBDMS	<i>t</i> -butyldimethylsilyl
TBTH	tributyltin hydride
TCD	thermal conductivity detector
TFAA	trifluoroacetic anhydride
<i>tfc</i>	3-(trifluoromethylhydroxymethylene)camphorato
TFE	trifluoroethanol
THF	tetrahydrofuran
TLC	thin layer chromatography
TMS	trimethylsilyl <i>or</i> tetramethylsilane
Tol	<i>p</i> -tolyl
Tos	<i>p</i> -toluenesulfonyl
triflic	trifluoromethanesulfonic
TS	transition state/structure
TTMSS	tris(trimethylsilyl)silane
U	uracil
UV	ultraviolet
Val	valine
vis	visible
VLC	vacuum liquid chromatography
w.r.t.	with respect to
WCOT	wall-coated open-tubular
[X]	concentration of substance X

## Word Count

Chapter	Words
1	5263
2	15546
3	17761
4	15263
5	26896
6	6091
7	3272
Total	90092

## Contents

<b>Declaration</b>	iii
<b>Dedication</b>	iv
<b>Acknowledgements</b>	v
<b>Abstract</b>	vii
<b>Abbreviations and symbols</b>	ix
<b>Word Count</b>	xiii
<b>Chapter 1: Introduction</b>	<b>1</b>
1.1 Aims of this thesis	2
1.2 A review of the mechanism of the $\beta$ -acyloxyalkyl radical rearrangement	2
1.3 The $\beta$ -trifluoroacetoxyalkyl radical rearrangement	14
1.4 Other isomerisations which may share the same mechanism: The rearrangement of <i>N</i> -alkoxy-2(1 <i>H</i> )-pyridinethiones	16
1.5 References	19
<b>Chapter 2: Kinetics of the <math>\beta</math>-trifluoroacetoxyalkyl radical rearrangement</b>	<b>23</b>
2.1 Introduction	24
2.2 A review of $\beta$ -acyloxyalkyl radical rearrangement kinetics	24
2.3 The search for a suitable system for study	31
2.3.1 2-Trifluoroacetoxy-1-hexyl radical	31
2.3.2 Reaction of $\beta$ -bromoester <b>2.50</b> with Bu <sub>3</sub> SnH	32
2.3.3 A faster rearrangement	34
2.3.4 Reaction of $\beta$ -bromoester <b>2.59</b> with Bu <sub>3</sub> SnH	34
2.4 Determination of the equilibrium constant	34
2.4.1 Theory	35

2.4.2	Preparation of $\beta$ -bromoester <b>2.66</b>	36
2.4.3	Reaction of $\beta$ -bromoester <b>2.66</b> with $\text{Bu}_3\text{SnH}$	37
2.5	Kinetics experiments	38
2.5.1	The kinetic scheme and analytical method	38
2.5.2	Conducting the kinetic experiments and product analysis	41
2.5.3	Management of analytical complexities	43
2.5.4	Kinetics results	46
2.6	Discussion of results	53
2.7	Conclusions	57
2.8	Experimental	58
2.9	References	72

**Chapter 3: A labelled-oxygen study of the  
regiochemistry of the  $\beta$ -trifluoroacetoxyalkyl  
radical rearrangement** 74

3.1	Introduction	75
3.2	Literature review	75
3.3	Choice of a suitable system for study	79
3.4	An attempt to observe the 1,2 shift of a hydroxy group in a $\beta$ -hydroxyalkyl radical	80
3.5	A study of the regiochemistry of the rearrangement of <b>3.32</b> → <b>3.33</b> using $^{18}\text{O}$ -labelling techniques	81
3.5.1	Preparation of an $^{18}\text{O}$ -labelled radical precursor	81
3.5.2	Determination of $^{18}\text{O}$ enrichment in bromohydrin <b>3.30a</b>	83
3.5.3	Determination of $^{18}\text{O}$ enrichment of labelled $\beta$ -bromoester <b>3.31a</b>	84
3.5.4	Determination of the distribution of $^{18}\text{O}$ label in the ether and carbonyl oxygens of the product esters <b>3.34</b> and <b>3.35</b>	85

3.5.5 Results	90
3.5.6 Validation of the analytical method	91
3.5.7 Experiments with a 92 % $^{18}\text{O}$ -enriched $\beta$ -bromoester	93
3.6 Study of the regiochemistry of the rearrangement of <b>3.32</b> → <b>3.33</b> using $^{17}\text{O}$ nmr	95
3.6.1 Preparation and characterisation of $^{17}\text{O}$ -labelled bromohydrin <b>3.30c</b> and $\beta$ -bromoester <b>3.31c</b>	95
3.6.2 Results	97
3.6.3 Validation of the results	99
3.7 A crossover experiment	100
3.8 An attempt to trap an ion pair intermediate	105
3.9 Discussion of results with regard to mechanism	108
3.10 Conclusions	116
3.11 Experimental	118
3.12 References	131
<b>Chapter 4: An esr study of <math>\beta</math>-oxygenated alkyl radicals</b>	<b>133</b>
4.1 Introduction	134
4.2 Estimation of the time-averaged dihedral angles	135
4.3 Recording of the esr spectra and extraction of $g$ -values and hyperfine splitting constants	138
4.4 Results	140
4.4.1 Spectra of 2-(oxysubstituted)-1-hexyl radicals <b>4.1a-c</b>	140
4.4.2 Spectra of 3-(oxysubstituted)-2-butyl radicals <b>4.2a-c</b>	142
4.4.3 Spectra of 2-(oxysubstituted)ethyl radicals <b>4.3a-c</b>	144
4.5 Calculations, analysis and discussion	146
4.5.1 General	146



4.5.2	2-(Oxysubstituted)hexyl radicals <b>4.1a-c</b>	152
4.5.3	3-(Oxysubstituted)-2-butyl radicals <b>4.2a-c</b>	157
4.5.4	2-(Oxysubstituted)ethyl radicals <b>4.3a-c</b>	160
4.6	Estimation of the energy barrier to internal rotation about the $C_{\alpha}-C_{\beta}$ bond in the $\beta$ -oxygenated ethyl radicals <b>4.3a-c</b>	170
4.7	Final discussion	176
4.8	Conclusions	180
4.9	Experimental	181
4.10	References	187
<b>Chapter 5: The mechanism of the catalysed rearrangement of <i>N</i>-alkoxy-2(1<i>H</i>)-pyridinethiones</b>		<b>192</b>
5.1	Introduction	193
5.2	Review of the chemistry of <i>N</i> -alkoxy-2(1 <i>H</i> )-pyridinethiones and related compounds	193
5.2.1	Prevalence of <i>N</i> -alkoxy-2(1 <i>H</i> )-pyridinethione research	193
5.2.2	Barton esters and related classes of compounds	194
5.2.3	Radical chemistry of <i>N</i> -alkoxy-2(1 <i>H</i> )-pyridinethiones	195
5.2.4	Related rearrangements	199
5.2.5	Catalysed <i>N</i> -alkoxy-2(1 <i>H</i> )-pyridinethione rearrangement	202
5.2.6	The chemistry of 4 and 6 electron 1,4 sigmatropic shifts and 5-electron, 6-centre electrocyclic processes	204
5.3	The mechanism of the rearrangement of <i>N</i> -alkoxy-2(1 <i>H</i> )-pyridinethiones	206
5.3.1	The mode of catalysis	206
5.3.1.1	Can the rearrangement of 2-alkoxypyridine <i>N</i> -oxides be catalysed in the same manner?	211
5.3.2	Kinetics	212
5.3.3	A study of rearrangement regiochemistry	219
5.3.4	A study of rearrangement stereochemistry	224

5.3.4.1	Preparation of optically active reactants and products	225
5.3.4.2	Results	230
5.3.4.3	Determination of the extent of solution-phase racemisation of both the pyridinethione <b>5.1d</b> and the <i>N</i> -oxide <b>5.2d</b>	232
5.3.4.4	Discussion of results	233
5.3.5	Electronic structure of the migrating group at C1 during rearrangement	234
5.3.6	Substituent effects	237
5.3.7	Attempted detection and isolation of intermediates	239
5.3.7.1	Addition of a radical scavenger	239
5.3.7.2	Esr spectroscopy	240
5.3.7.3	Cyclic voltammetry	241
5.3.7.4	Isolation and attempted identification of intermediates	244
5.4	Conclusions	247
5.5	Future work	249
5.6	Experimental	250
5.7	References	277
	<b>Chapter 6: General discussion and conclusions</b>	<b>284</b>
6.1	Introduction	285
6.2	The $\beta$ -trifluoroacetoxyalkyl radical rearrangement	285
6.2.1	What is known about the rearrangement of the 2-methyl-2-trifluoroacetoxy-1-heptyl radical?	285
6.2.2	Migrating group electronic effects	287
6.2.3	Relationship between rearrangement regiochemistry and kinetics	288
6.2.4	Is the regiochemistry controlled by the conformation of the ester group?	289
6.2.5	Predicted dynamics for a radical ion pair intermediate	291

6.2.6 The mechanism of the rearrangement of $\beta$ -trifluoroacetoxyalkyl radicals	295
6.3 Related radical-mediated rearrangements and $\beta$ -eliminations	297
6.4 The mechanism of the rearrangement of <i>N</i> -alkoxy-2(1 <i>H</i> )-pyridinethiones	301
6.5 Final remarks	301
6.6 References	303
<b>Chapter 7: General experimental</b>	<b>306</b>
7.1 Melting points	307
7.2 Elemental analyses	307
7.3 Infrared spectroscopy	307
7.4 Optical rotations	307
7.5 Molecular ultraviolet and visible spectra	307
7.6 Bulb to bulb distillations	307
7.7 Liquid chromatography	307
7.7.1 Flash chromatography	307
7.7.2 Vacuum-liquid chromatography	307
7.7.3 Analytical thin layer chromatography	308
7.7.4 Preparative scale thin layer chromatography	308
7.7.5 Radial chromatography	308
7.8 Gas chromatography	308
7.8.1 Analytical gas chromatography	308
7.8.2 Chiral analytical gas chromatography	309
7.8.3 Preparative scale gas chromatography	309
7.9 Mass spectrometry	309
7.9.1 EIMS	309
7.9.2 HRMS	309

7.9.3	CIMS	310
7.9.4	GCMS	310
7.9.5	FAB	310
7.9.6	Electrospray	310
7.10	Electron spin resonance spectroscopy	310
7.11	Nuclear magnetic resonance spectroscopy	310
7.11.1	$^1\text{H}$ nmr	310
7.11.2	$^2\text{H}$ nmr	311
7.11.3	$^{13}\text{C}$ nmr	311
7.11.4	$^{17}\text{O}$ nmr	311
7.11.5	$^{19}\text{F}$ nmr	312
7.11.6	2-Dimensional nmr	312
7.12	Cyclic voltammetry	312
7.13	Purification of solvents for radical reactions	312
7.13.1	Hexane	313
7.13.2	Benzene	313
7.13.3	Toluene	313
7.13.4	<i>tert</i> -Butylbenzene	313
7.13.5	Acetonitrile	313
7.13.6	Propionitrile	313
7.13.7	<i>N</i> -methylacetamide	314
7.13.8	Perfluoromethylcyclohexane	314
7.14	Purification of solvents for other purposes	314
7.14.1	Chloroform for pyridinethione rearrangements	314
7.14.2	Acetonitrile for electrochemistry	314
7.15	Reagents for synthesis	314
7.16	Evaporation of solvents	314
7.17	Drying of extract solutions	315
7.18	Nomenclature	315
7.19	References	316

<b>Appendix A:</b>	
<b>A description of the analytical method used to obtain rearrangement rate constants and a derivation of the integrated rate expression</b>	<b>317</b>
A.1 Analytical method	317
A.2 Derivation of the integrated rate expression	318
A.3 References	320

<b>Appendix B:</b>	
<b><math>^{17}\text{O}</math> nmr spectroscopy: Optimisation of acquisition parameters for accurate quantification of the ratio of <math>^{17}\text{O}</math> label in carbonyl and alkoxy oxygens of esters</b>	<b>322</b>
B.1 Introduction	322
B.2 Overcoming transmitter breakthrough	324
B.3 Spectrometer parameters and method of acquisition	325
B.3.1 Spectrometer parameters	325
B.3.2 Method for obtaining spectra	326
B.4 $^{17}\text{O}$ nmr spectra	328
B.5 References	331

<b>Appendix C:</b>	
<b>The assignment of the <math>^{13}\text{C}</math> and <math>^1\text{H}</math> nmr chemical shifts of the heterocyclic ring systems of <i>N</i>-alkoxy-2(1<i>H</i>)-pyridinethiones and 2-(alkylsulfanyl)pyridine <i>N</i>-oxides</b>	<b>333</b>
C.1 Introduction	333
C.2 Assignment of the chemical shifts of <i>N</i> -cyclohexylmethoxy-2(1 <i>H</i> )-pyridinethione	334

C.3 Assignment of the chemical shifts of 2-(cyclohexylmethylsulfanyl)pyridine <i>N</i> -oxide	340
C.4 References	343

**Appendix D:  
The preparation, purification, purity  
determination and storage of  
tributyltin hydride**

	344
D.1 Introduction	344
D.2 Preparation	345
D.3 Purification	346
D.4 Purity determination	347
D.5 Storage	348
D.6 References	349

I had learned that all the greatest and most important problems of life are fundamentally insoluble. They must be so, for they express the necessary polarity in every self-regulating system. They can never be solved, but only outgrown....What a fool I was! How I tried to force everything to go the way I thought it ought to!

C. G. Jung

Commentary on 'The Secret of the Golden Flower', *Collected Works* 13 (1938).

## Chapter 1

### Introduction

1.1	Aims of this thesis	2
1.2	A review of the mechanism of the $\beta$ -acyloxyalkyl radical rearrangement	2
1.3	The $\beta$ -trifluoroacetoxyalkyl radical rearrangement	14
1.4	Other isomerizations which may share the same mechanism: The rearrangement of <i>N</i> -alkoxy-2(1 <i>H</i> )-pyridinethiones	16
1.5	References	19



## 1.1 Aims of this research

The primary objective of this research was to elucidate the mechanism of the  $\beta$ -acyloxyalkyl radical rearrangement. Generally, a  $\beta$ -trifluoroacetoxyalkyl radical is known to rearrange more quickly and display more interesting regiochemistry than a  $\beta$ -acetoxyalkyl radical. Chapter 2 contains a study of the solvent effects upon the kinetics of the rearrangement of a  $\beta$ -trifluoroacetoxyalkyl radical. An investigation into the solvent effects upon the regiochemistry of the same rearrangement is the topic of chapter 3. In an attempt to probe stereoelectronic effects, chapter 4 describes an electron spin resonance study of the temperature dependence of radical conformations and the barriers to internal rotation of alkyl radicals bearing three different, oxygenated  $\beta$ -substituents.

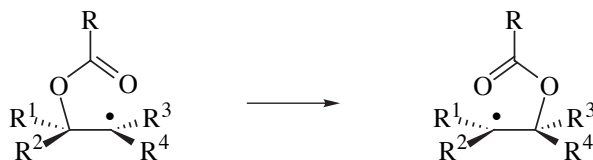
Chapter 5 comprises an enquiry into the mechanism of the catalysed rearrangement of *N*-alkoxy-2(1*H*)-pyridinethiones. Preliminary investigations indicated that this type of rearrangement may proceed *via* a pericyclic transition structure, isoelectronic with that postulated for the  $\beta$ -acyloxyalkyl radical rearrangement.

A discussion of the experimental results, an analysis of the conformation of the  $\beta$ -ester group, an investigation into the plausibility of a short-lived intermediate and a summary of the chemistry of related rearrangements and  $\beta$ -eliminations are presented in chapter 6. Implications for the mechanism of the  $\beta$ -trifluoroacetoxyalkyl radical rearrangement, and more broadly for the  $\beta$ -acyloxyalkyl radical and related rearrangements in general, are discussed.

## 1.2 A review of the mechanism of the $\beta$ -acyloxyalkyl radical rearrangement

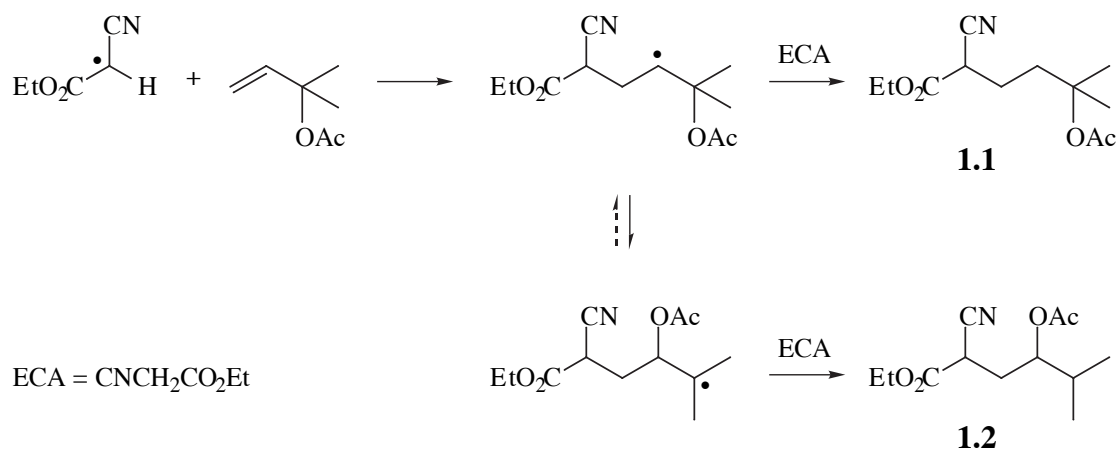
Like many other intriguing chemical reactions, the  $\beta$ -acyloxyalkyl radical rearrangement (scheme 1.1) was discovered by accident.<sup>1</sup> Its mechanism has been of particular interest to investigators because it appeared to have no intermolecular analogue, unlike ordinary radical rearrangements. Forty-seven research papers dealing directly with the chemistry the  $\beta$ -acyloxyalkyl radical rearrangement have been published.<sup>1-47</sup> These articles include a 1997 review of the  $\beta$ -acyloxyalkyl radical isomerization and related rearrangements and fragmentations,<sup>35</sup> *ab initio* computational studies,<sup>14,32,34,45,47</sup> a

mechanistic commentary<sup>25</sup> and an *Organic Syntheses* procedure for the stereospecific preparation of a 2-deoxy sugar.<sup>20</sup>

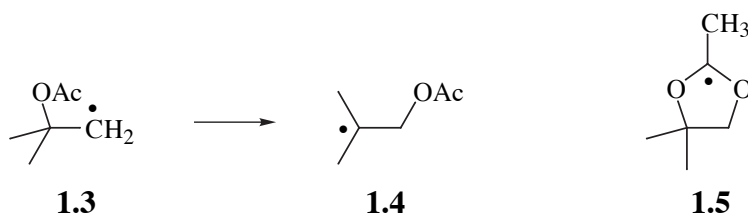


**Scheme 1.1.** The general form of the  $\beta$ -acyloxyalkyl radical rearrangement

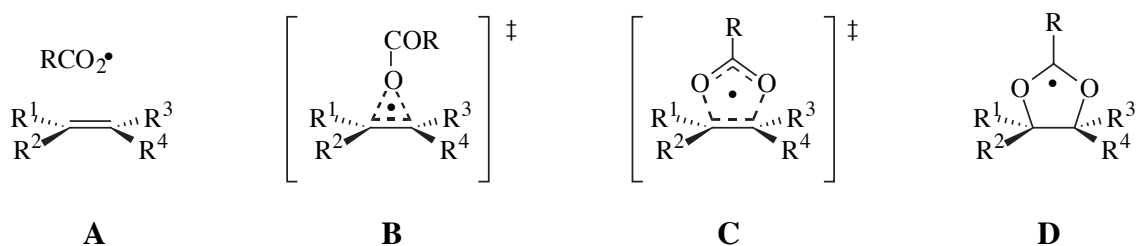
In 1967 Surzur and Tiessier<sup>1</sup> reported an unexpected migration of an acetoxy group whilst studying the dibenzoyl peroxide initiated addition of ethyl cyanoacetate to 1,1-dimethylallyl acetate. In addition to the expected product **1.1** (70%), there was 30% of product in which a 1,2 acetoxy shift had occurred (**1.2**). When the reaction was repeated with cyclohexane in the place of ethyl cyanoacetate, the yield of the corresponding rearrangement product was 95%. This result indicated that the acetoxy shift was in competition with a hydrogen abstraction reaction. The C–H bonds in cyclohexane are stronger than that for the abstractable hydrogen in ethyl cyanoacetate.



Tanner and Law, unaware of Surzur's and Tiessier's results, reported the rearrangement of the 2-acetoxy-2-methyl-1-propyl radical (**1.3**) to the 1-acetoxy-2-methyl-1-propyl radical (**1.4**) two years later.<sup>2</sup> They suggested that a bridged dioxolanyl radical (**1.5**) was an intermediate.



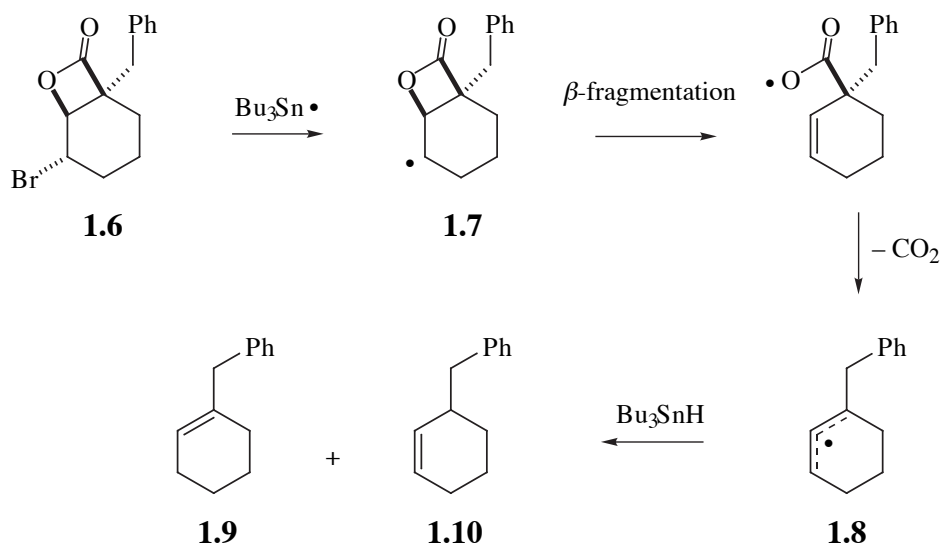
In 1973 Beckwith and Thomas presented four possible mechanistic pathways for the rearrangement.<sup>7</sup> Mechanism **A** consisted of the  $\beta$ -elimination and subsequent  $\alpha$ -readdition of an acyloxy radical. Mechanisms **B** and **C** were concerted 1,2 and 3,2 shifts respectively. The transition structures shown and were analogous to those observed in carbocation chemistry. Structure **D** is a 1,3-dioxolan-2-yl radical intermediate formed by attack of the unpaired electron upon the carbonyl oxygen. **D** may then fragment to give the rearranged radical.



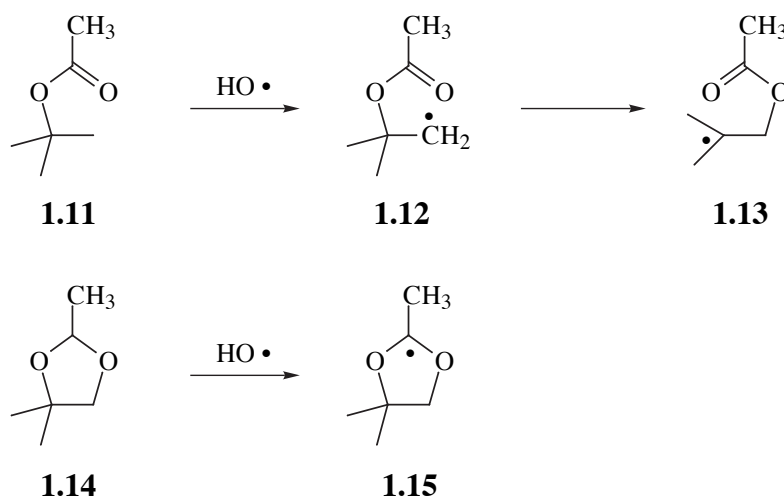
Option **A** was considered by Tanner and Law, but was dismissed after the rearrangement of **1.3** conducted in the presence of isobutylene, resulted in the complete recovery of the alkene. Tanner and Law knew that acyloxy radicals decarboxylate extremely rapidly (now known that  $k \approx 10^9 \text{s}^{-1}$  at room temperature<sup>48</sup>), certainly much faster than the migration of the acetoxy group occurred. The failure to trap acetoxy or methyl radicals with isobutylene meant that such species were not dissociatively free. It was known at the time that acetoxy radicals may be trapped by addition to alkenes.<sup>49-51</sup>

Instances of the elimination of an acyloxy radical from a  $\beta$ -acyloxyalkyl radical, resulting in the formation of an alkene, are also known but are very rare.<sup>35</sup> A recent example comes from a study of the chemistry of 2-oxetanon-4-ylcarbinyl radicals.<sup>36</sup> When the  $\beta$ -bromolactone **1.6** was irradiated in the presence of  $\text{Bu}_3\text{SnH/AIBN}$  the isomeric cyclohexenes **1.9** and **1.10** were formed, in the ratio 7.3:1. The results

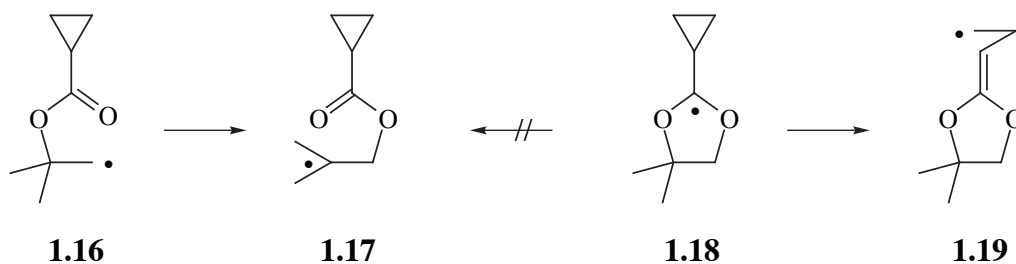
indicated that ring expansion of the highly-strained radical **1.7** by the  $\beta$ -acyloxyalkyl radical rearrangement was an unfavourable process in this case, presumably because of stereoelectronic and ring strain effects.



Evidence against the intermediacy of **D** was obtained by esr spectroscopy.<sup>4</sup> When *t*-butyl acetate (**1.11**) was exposed to hydroxyl radicals in the cavity of an esr spectrometer, spectra corresponding to both **1.12** and **1.13** were detected, but no spectrum of the dioxolanyl radical **1.15** was present. However, when the dioxolanyl radical **1.15** was generated by the reaction of the hydroxyl radical with **1.14**, the spectrum of **1.13** could not be detected. Therefore the workers concluded that radical **1.15** could not be an intermediate in the reaction of **1.12**.

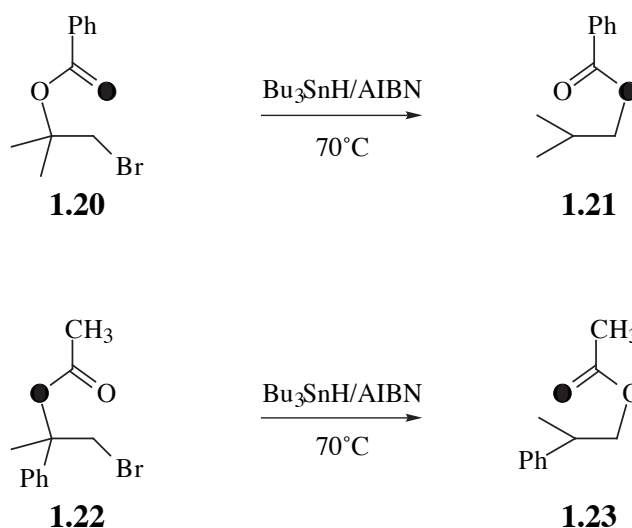


A rate constant of  $7 \times 10^2 \text{ s}^{-1}$  for the  $\beta$ -scission of **1.15** to **1.13** at  $72^\circ\text{C}$  was later determined by Perkins and Roberts by esr.<sup>8</sup> This created a problem. Beckwith and Thomas had measured a rate constant for the **1.12**→**1.13** rearrangement at  $75^\circ\text{C}$  of  $k = 6.2 \times 10^3 \text{ s}^{-1}$  using a product-ratio/competition-clock method.<sup>7</sup> Experimental uncertainties associated with each of the measurements meant that the two values might be of a similar magnitude. Rigorous exclusion of **D** finally came with the aid an elegant esr experiment.<sup>12</sup> The radical **1.16** rearranged exclusively to the radical **1.17** in the esr cavity with  $k = 1.2 \times 10^2 \text{ s}^{-1}$  at  $75^\circ\text{C}$ . The 2-dioxolanyl radical **1.18** did not undergo C–O scission to radical **1.17**, but instead underwent a rapid opening of the cyclopropyl ring to form **1.19** with  $k = 8.7 \times 10^5 \text{ s}^{-1}$  at the same temperature. Thus, radical **1.18** could not possibly be an intermediate for the **1.16**→**1.17** rearrangement. Jung and Xu have recently used the same mechanistic probe to rule out the intermediacy of the dioxolanyl radical in the migration of acyloxy groups in pentose sugar radicals.<sup>43</sup> The intermediacy of 1,3-dioxolanyl radicals in  $\beta$ -acyloxyalkyl radical rearrangements has also been excluded by *ab initio* MO calculations.<sup>14,34,47</sup>

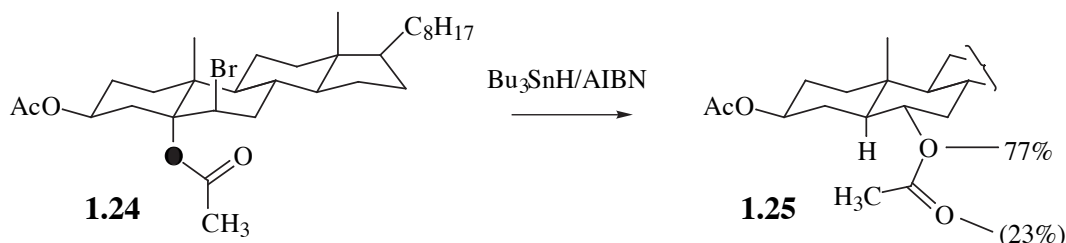


In an effort to discriminate between the remaining options **B** and **C**, Beckwith and Thomas studied the  $\beta$ -acyloxyalkyl rearrangement of radicals which were specifically labelled with  $^{18}\text{O}$  at one of the two ester oxygens.<sup>7</sup> A benzene solution of the  $^{18}\text{O}$ -carbonyl labelled  $\beta$ -bromobenzoate **1.20** was heated with tributyltin hydride and AIBN to give isobutyl benzoate (**1.21**) with virtually all the label in the ether oxygen. This translocation of ester oxygens was also observed when the  $\beta$ -bromoacetate **1.22** (labelled specifically in the ether oxygen) was heated with  $\text{Bu}_3\text{SnH/AIBN}$ . Only

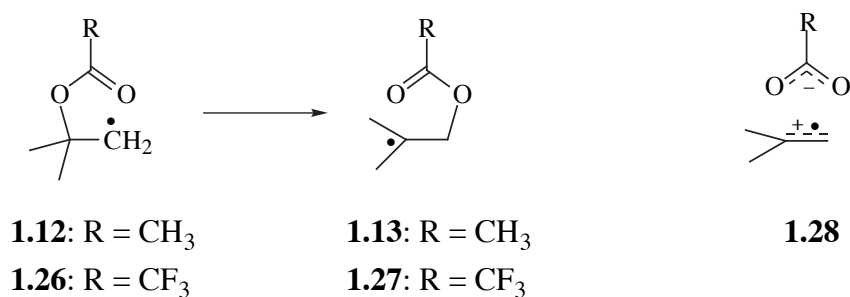
mechanism **C** was consistent with these results. The question of mechanism appeared to be answered.



However, in 1986 Kocovsky and coworkers stumbled upon a stereospecific migration of an acetoxy group while attempting to replace the bromine in a  $\beta$ -bromoacetoxy steroid with a hydrogen atom using tributyltin hydride.<sup>15</sup> Intrigued by this unexpected reaction, they studied the rearrangement of an acetoxy group labelled with  $^{18}\text{O}$  at the ether oxygen. When compound **1.24** was heated in benzene with tributyltin hydride, the rearrangement product (**1.25**) was isolated and found to contain 77% of the label in the ether oxygen of the acetoxy group using mass spectrometric methods. This result meant that **C** could not be the only mechanism of the  $\beta$ -acyloxyalkyl radical rearrangement. Beckwith and Duggan immediately checked Kocovsky's result by studying the migration in the same steroid of a butanoyloxy group specifically labelled with  $^{18}\text{O}$  in the carbonyl oxygen.<sup>19,21</sup> Their results equated with 76% of the label remaining in the carbonyl oxygen of the rearranged product, confirming that there must be an alternative mechanism to **C**. A rate constant for the migration of the butanoyloxy group was obtained ( $k = 1.9 \times 10^6 \text{ s}^{-1}$  at  $75^\circ\text{C}$ ), which indicated that the rearrangement was several orders of magnitude faster than other  $\beta$ -acyloxyalkyl radical rearrangements whose rate constants were known ( $k = 10^2\text{-}10^4 \text{ s}^{-1}$ ).



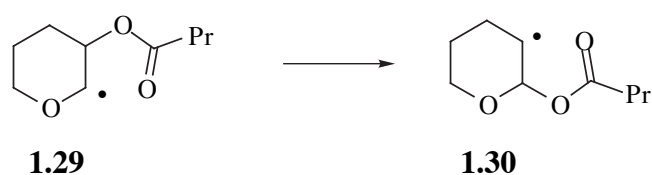
Ingold and coworkers had discovered that the  $\beta$ -acyloxyalkyl radical rearrangement was facilitated by the use of a polar solvent and by electronegative substituents on the migrating group during their kinetic esr spectroscopy experiments.<sup>13</sup> At 75°C, the rate constant for the rearrangement of **1.12**→**1.13** in *t*-butylbenzene was  $4.5 \times 10^2 \text{ s}^{-1}$ , but in water  $k$  rose sharply to  $2.1 \times 10^4 \text{ s}^{-1}$ . At the same temperature, the migration of the trifluoroacetoxy group in the rearrangement of **1.26** to **1.27** proceeded with  $k = 7.0 \times 10^4 \text{ s}^{-1}$  in the non-polar,<sup>52</sup> halogenated solvent Freon 113.<sup>13</sup> Since none of the mechanisms **A-D** was consistent with the observed solvent and electronic effects, it was proposed that charge-separation in canonical structures such as **1.28** played an important role in the transition states of these rearrangements.<sup>12,13</sup>



The canonical structure represented by **1.28** later came to be interpreted by Beckwith and Duggan as an intimate radical ion pair.<sup>21</sup> This structure was used in conjunction with mechanism **C** to explain Kocovsky's <sup>18</sup>O-labelling results in the rearrangement of the steroidal radical **1.24**.<sup>21</sup> They realised that the results were also explicable by mechanism **B** operating in conjunction with **C**, but three-membered transition structures such as **B** had no literature precedent. Kocovsky and coworkers did search for a 1,2 OH shift by treatment of a steroidal bromohydrin (from which **1.24** was

prepared by acetylation) with tributyltin hydride/AIBN, but only observed the replacement of the bromine atom with hydrogen.<sup>15</sup> However 1,2 OH shifts were reported to be observed in biological systems subject to the action of enzymes.<sup>53</sup> In addition, early *ab initio* MO calculations predicted that the 1,2 shift of a hydroxyl group in a  $\beta$ -hydroxyalkyl radical is energetically feasible provided that the oxygen is protonated.<sup>54</sup> Gilbert and coworkers have observed the acid-catalysed interconversion of  $\beta$ -hydroxyalkyl radicals in aqueous solution, but concluded that the mechanism involved formation and subsequent solvent-hydration of an alkene radical cation.<sup>55</sup>

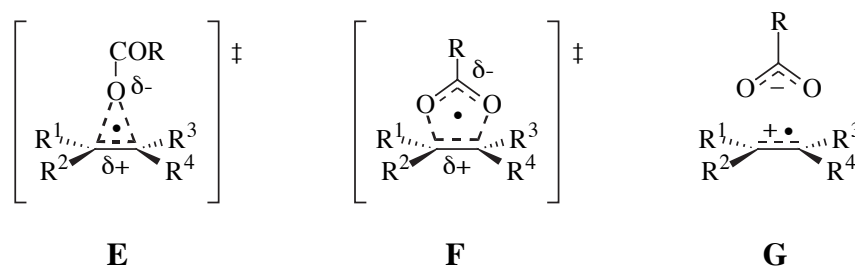
Beckwith and Duggan studied the rearrangement of the 3-butanoyloxytetrahydropyran-2-yl radical (**1.29**),<sup>22</sup> as a model for the a 1,2 acetoxy group shifts Giese and coworkers had discovered in peracetylated hexose radicals.<sup>17,18,20</sup> Experiments with <sup>17</sup>O- and <sup>18</sup>O-labelled substrates indicated that the rearrangement of **1.29**→**1.30** proceeded with 67% formal 1,2 shift.<sup>22</sup> Since such a large degree of formal 1,2 shift was no longer confined to the rearrangement of **1.24**, it was concluded that the three-membered transition structure **B** may possibly play a role in the mechanism of other  $\beta$ -acyloxyalkyl radical rearrangements.<sup>22</sup> However, the high value of  $\log_{10}A/s^{-1}$  (12.7) obtained from analysis of the kinetics of the **1.29**→**1.30** rearrangement indicated that there was a considerable degree of bond breakage at the rate limiting step, thereby favouring a dissociative mechanism.<sup>22</sup>



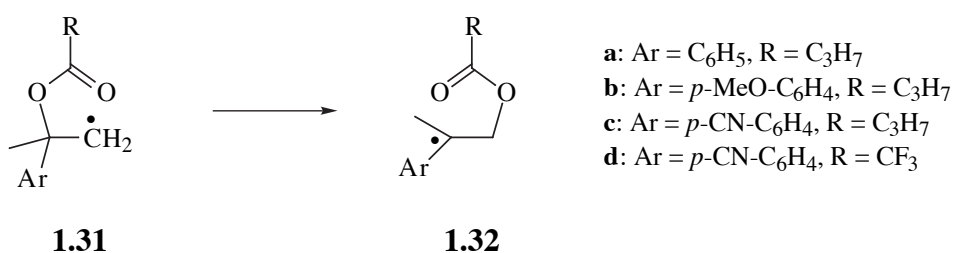
Eventually, the course of mechanistic evolution resulted in the rejection of transition structures **B** and **C** because they could not account for the observed solvent and substituent effects. To rectify this problem, these structures were replaced with the polarized versions **E** and **F** respectively by Crich and Filzen in 1995.<sup>26</sup> Previously, *ab initio* MO calculations had indicated that structures like **C** possessed considerable dipolar character.<sup>14</sup> In 1994 Sprecher had argued in a *Chemtracts* commentary that the kinetic



and oxygen-labelling results for all the  $\beta$ -acyloxyalkyl radical rearrangements known at that time could be rationalised by a mechanism involving an intimate ion pair composed of an alkene radical cation and a carboxylate anion (**G**).<sup>25</sup> He claimed that the diversity in rate constant and degree of formal 1,2 shift could be explained by a varying degree of intimacy of the ion pair and the mutual orientation of the fragments, which in turn would depend critically on the respective charge distributions.<sup>25</sup>



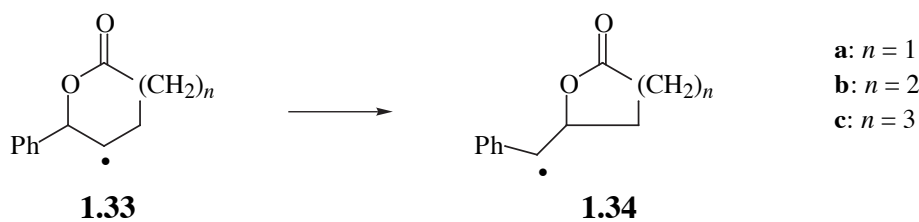
Beckwith and Duggan managed to establish a relationship between the electronic environment, rearrangement rate constant and the degree of oxygen scrambling in a single system from a study of the rearrangement of 2-acyloxy-2-arylpropyl radicals.<sup>33</sup> They discovered that the rate constant for the rearrangement of **1.31a**→**1.32a** showed a weak, yet significant, dependence upon solvent polarity. A Hammett plot yielded a  $\rho$  value of  $-0.71$ , which is small in comparison to that for ionic processes, yet clearly demonstrates that aryl substituents which stabilise positive charge at the benzylic position accelerate the rearrangement. In benzene at  $75^\circ\text{C}$ , the rate constant for the rearrangement of **1.31d** was 156 times that for **1.31c**, demonstrating the facilitation of acyloxy migration where electron-attracting substituents are present. Oxygen-labelling experiments revealed that in benzene, **1.31a** migrated with essentially 0% 1,2 shift, but in methanol the faster rearrangement proceeded with 25% 1,2 shift.



In a thoughtful conclusion to their 1997 review, the authors stated that the  $\beta$ -acyloxyalkyl radical rearrangement has a spectrum of mechanisms.<sup>35</sup> The type of mechanism(s) manifested depends primarily upon radical structure and the solvent. Slow rearrangements generally proceed *via* the relatively non-polarized, 5-membered transition structure, **F**. Fast rearrangements generally proceed *via* the polarized, 3-membered transition structure, **E**. In rare cases, it is possible that  $\beta$ -acyloxyalkyl radical rearrangements proceed at least in part by caged, contact radical ions, **G**. Most fragmentations of  $\beta$ -acyloxyalkyl radicals occur *via* the permanent separation of the carboxylate and alkene-radical-cation moieties of **G**. Of course, rearrangements proceeding at an intermediate rate were believed to proceed by a mixture of transition structures **E** and **F**, possibly with a minor involvement of **G**. It is a difficult undertaking to devise ways of enabling experimental differentiation between these mechanistic alternatives, yet since the mid-1990s this has been the major goal of workers in the field.

There have been a number of important recent developments. Crich, Newcomb and coworkers have measured rate constants for  $\beta$ -acyloxyalkyl radical rearrangements directly by a laser flash photolysis technique, confirming that migrations are accelerated by electron-donating groups on the alkyl framework, electron-withdrawing substituents on the migrating group and more polar solvents.<sup>40</sup> Rate constants were obtained directly from time-resolved UV-vis spectra of the product radicals,<sup>40</sup> thus addressing Sprecher's<sup>25</sup> reservations that kinetic parameters determined from competition methods depend on some arguable assumptions.

Beckwith, Crich and coworkers have also studied the  $\beta$ -acyloxyalkyl-radical-mediated ring contraction of lactones.<sup>31,41</sup> Six-, seven- and eight-membered lactones each contract entirely by a 1,2 shift, as indicated by <sup>17</sup>O-labelling experiments.<sup>41</sup> Radicals **1.33a,b** and **c** each rearrange with  $k \approx 10^6 \text{ s}^{-1}$  at 80°C, making these processes among the fastest of the  $\beta$ -acyloxyalkyl radical rearrangements.<sup>41</sup> The regiochemical results are attributed to high energy barriers to transition structures of the type **F**.<sup>41</sup>



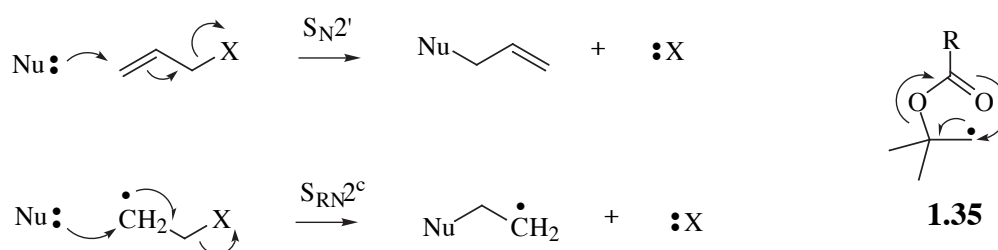
Renaud and coworkers have reported that  $\beta$ -acyloxyalkyl radicals which undergo rearrangement in the presence of a Lewis acid can experience rate acceleration of up to three orders of magnitude.<sup>38,44</sup> The effect was attributed to the stabilisation of negative charge in the migrating substituent upon complexation of the Lewis acid with the ester group.

The stereospecific shifts of a pivaloxy group from C1' to C2' in radicals generated from modified uridines and adenosines have been studied.<sup>28,29,37</sup> Chatgialloglu and coworkers have measured rate constants of  $5\text{-}10 \times 10^4 \text{ s}^{-1}$  for these processes at  $80^\circ\text{C}$ .<sup>37</sup> These rearrangements produce C1' anomeric nucleoside radicals, illustrating their importance in biochemistry.

A 1998 review of the free radical reactions of anomeric monosaccharide and C-nucleoside radicals includes a section on the use of the  $\beta$ -acyloxyalkyl radical rearrangement as a synthetic tool for the preparation of 2-deoxy sugars from readily available precursors, illustrating the growing importance of this intriguing reaction.<sup>39</sup>

*Ab initio* molecular orbital calculations<sup>14,32,34,45,47</sup> on the  $\beta$ -acyloxyalkyl radical rearrangement have provided meaningful mechanistic information where laboratory-based experiments reach the limit of their capacity to discriminate mechanisms **E-G**. The way forward will undoubtedly be a close collaboration of theory and experiment. In a comparison of the 3,3 acyloxy shift in allyl formate with the 3,2 acyloxy shift in the 2-formyloxyethyl radical, Zipse found that the open-shell reaction had a barrier of 92 to 113  $\text{kJmol}^{-1}$  lower than the closed-shell process, showing that the transition state **F** is energetically viable.<sup>32</sup> Both reactions could be viewed as intramolecular, nucleophilic substitutions.<sup>32</sup> The idea of these rearrangements being seen as intramolecular displacements was expanded into a general "methyleneology principal", which states that

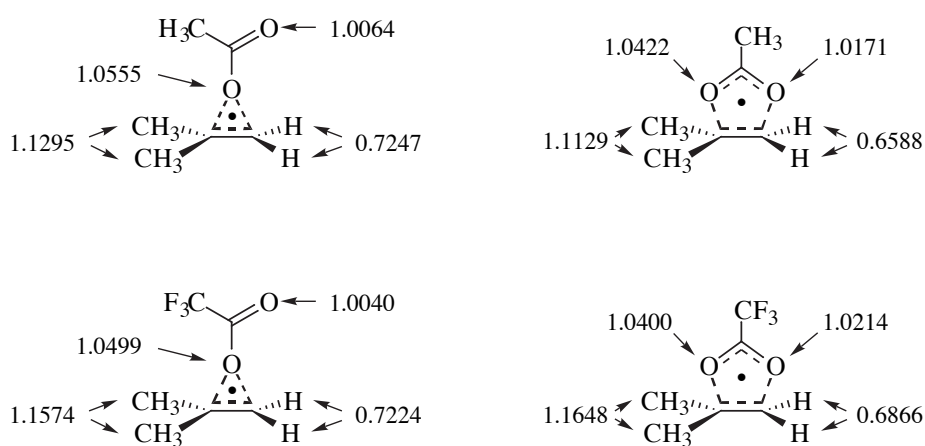
$\beta$ -elimination initiated by nucleophilic attack upon a radical centre is an open-shell analogy to the  $S_N2'$  reaction.<sup>45</sup> The source of the low barriers to these polar reactions in open-shell systems is the mixing in behaviour of homolytic and heterolytic bond cleavage processes.<sup>45</sup> The similarity in the  $S_{RN}2^c$  ('c' represents cine regiochemistry) and  $S_N2'$  reactions is shown below, together with a diagram of valence electron delocalisation in the  $\beta$ -acyloxyalkyl radical rearrangement, viewed as an  $S_{RN}2^i$  (intramolecular) reaction (1.35).



In a computational exploration of the rearrangement of 2-acyloxyethyl radicals, Zipse found that a 3,2 shift was always favoured over a 1,2 shift, that trifluoroacetoxy migration possessed a lower barrier than acetoxy migration and that a 3,2 acyloxy shift will proceed more quickly in water than in the gas phase, in conformity with most experimental evidence.<sup>34</sup> In addition, protonation of a formyloxy group was found to lower the rearrangement barrier by more than 40 kJmol<sup>-1</sup> compared with the unprotonated species.<sup>34</sup> However, the solvent effects predicted were much smaller than those observed experimentally.<sup>34</sup>

The results most pertinent to the work of this thesis come from Zipse and Bootz, who investigated the rearrangements of 2-acyloxy-2-methyl-1-propyl radicals (**1.12**→**1.13** and **1.26**→**1.27**) with a variety of theoretical methods.<sup>47</sup> They found no evidence of an ion pair intermediate (**G**) for either acetoxy or trifluoroacetoxy migration. The three-membered transition structure (**E**) was always slightly less favourable (by *ca.* 4 kJmol<sup>-1</sup>) than the five-membered transition structure (**F**), but became more competitive as absolute reaction barriers were lowered by electron-withdrawing migrating groups and polar solvents. In effect, the amount of formal 1,2 shift is predicted to increase in polar

solvents and the effect will be greater for a trifluoroacetoxy group than for acetoxy.<sup>65</sup> Solvent effects were predicted to be minor for both **E** and **F** and the barrier difference between acetoxy and trifluoroacetoxy migration was less than half the size of that measured experimentally. The large rate constant increase for acetoxy migration observed experimentally in water was rationalised by protonation of the ester group. Carboxylate group charge in both acetoxy and trifluoroacetoxy groups varied little between transition states **E** and **F**, contrasting with the assumption that **E** must be significantly more polarized than **F**.<sup>26,30,33,35</sup> Kinetic isotope effects calculated for structures **E** and **F** were generally small except for the strong inverse KIEs (0.66-0.72) found upon dideuteration of the radical centre (dideuteration at C1 accelerates the rearrangement). It is claimed that the ratio of the <sup>18</sup>O KIEs of the ester oxygen atoms may be used to distinguish **E** from **F**, but in practice the magnitude of such effects may be small compared with experimental uncertainties. Pertinent KIEs are provided in scheme 1.2. Unfortunately, KIEs could not be calculated for intermediate **G** since no transition structure for it could be found.



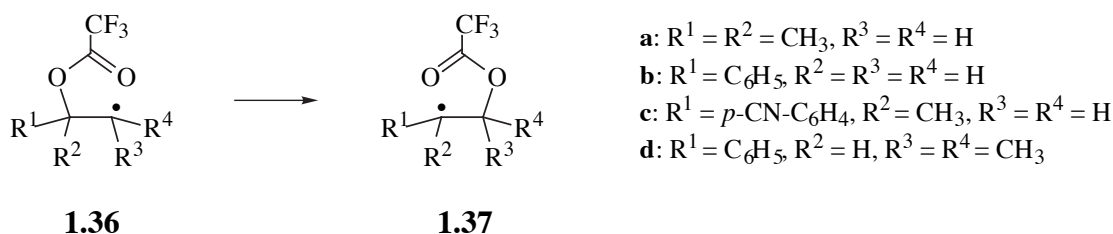
**Scheme 1.2.** Kinetic effects calculated for <sup>16</sup>O/<sup>18</sup>O and <sup>2</sup>H/<sup>1</sup>H isotopic substitutions upon the transition states **E** and **F** for rearrangements of the 2-acetoxy-2-methyl-1-propyl and 2-trifluoroacetoxy-2-methyl-1-propyl radicals.

### 1.3 The $\beta$ -trifluoroacetoxyalkyl radical rearrangement

It is known that groups with electron-withdrawing substituents facilitate the  $\beta$ -trifluoroacetoxyalkyl radical rearrangement and that faster rearrangements usually proceed

with a higher proportion of formal 1,2 shift. Given that an acetoxy group migrates over an aliphatic framework with approximately 0% 1,2 shift, the question of the degree of 1,2 shift which accompanies the faster trifluoroacetoxy group migration is an interesting one. Despite the considerable theoretical interest in the  $\beta$ -trifluoroacetoxyalkyl radical rearrangement,<sup>34,47</sup> there is comparatively little experimental data available.

Kinetic data for the rearrangement of radicals **1.36a-d** have previously been obtained. The Arrhenius parameters and/or rate constant,  $k$ , at 75°C are supplied in table 1.1 and are extracted from table 2.1 (of chapter 2). The isomerization of radical **1.36d** is the fastest  $\beta$ -acyloxyalkyl radical rearrangement yet reported. Values of  $\log_{10}A$  are approximately the same, indicating a similar degree of order in the transition state(s) of the rate limiting step. Faster rearrangements have lower activation energy, consonant with more facile cleavage of the C–O alkoxy ester bond.



**Table 1.1.** Kinetic data for the  $\beta$ -trifluoroacetoxyalkyl radical rearrangement

Rearrangement	Solvent	$\log_{10}(A/s^{-1})$	$E_a$ (kJmol <sup>-1</sup> )	$k$ at 75°C (s <sup>-1</sup> )	Ref.
<b>1.36a</b> → <b>1.37a</b>	CF <sub>2</sub> ClCFCl <sub>2</sub>	11.0	41.0	$7.0 \times 10^4$	13
<b>1.36c</b> → <b>1.37c</b>	benzene			$2.5 \times 10^6$	33
<b>1.36d</b> → <b>1.37d</b>	THF	10.7	25.9	$6.5 \times 10^6$	40
<b>1.36d</b> → <b>1.37d</b>	CH <sub>3</sub> CN	11.2	24.7	$3.1 \times 10^7$	40

Only one example of a labelled-oxygen study of trifluoroacetoxy migration has been published.<sup>26</sup> In benzene at 80°C, the rearrangement **1.36c**→**1.37c** proceeds with 19% 1,2 shift, demonstrating that a formal 3,2 shift is predominant but not exclusive.

We saw the need to study the relationship between the degree of oxygen scrambling and rearrangement rate as a function of solvent polarity in a single, simple system. Chapter 2 is concerned with the determination of the kinetics of a simply-constituted, aliphatic  $\beta$ -trifluoroacetoxyalkyl radical in the solvents hexane, benzene and propionitrile. Chapter 3 is concerned with an investigation of solvent-dependent oxygen scrambling behaviour in the same rearrangement studied in chapter 2.


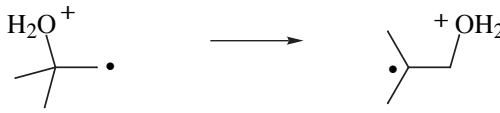

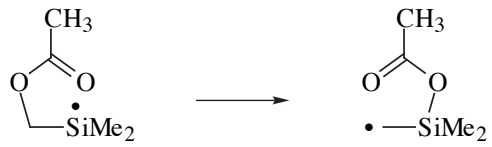
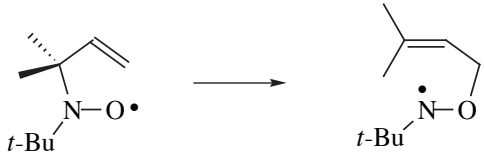
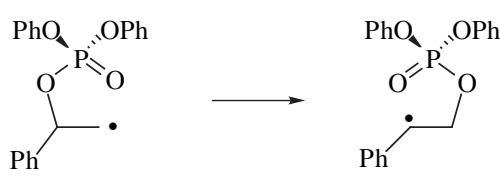
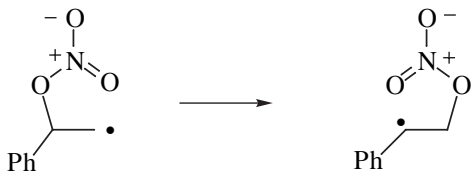
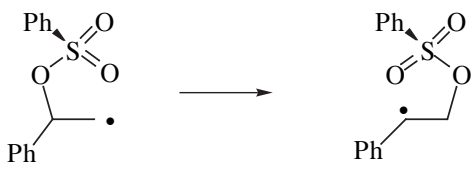
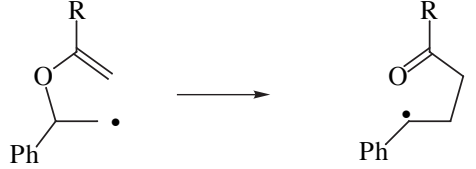
Zipse's MO calculations have indicated that the  $\beta$ -acyloxyalkyl radical rearrangement can be viewed as an intramolecular nucleophilic substitution reaction.<sup>32</sup> Chapter 4 comprises an electron spin resonance study of the temperature-dependent average conformation of a series of  $\beta$ -oxygenated alkyl radicals. This work was undertaken to evaluate whether there exists a significant electronic interaction between the unpaired spin and the ester carbonyl oxygen, as suggested by theoretical calculations.

#### ***1.4 Other isomerizations which may share the same mechanism: The rearrangement of N-alkoxy-2(1H)-pyridinethiones***

Since the discovery of the  $\beta$ -acyloxyalkyl radical rearrangement, there has been a steadily growing number of rearrangements discovered which appear to have the same type of mechanism. Rearrangements which display a radical mediated 1,2 or 3,2 shift are illustrated in table 1.2.

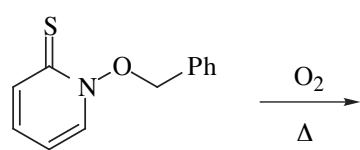
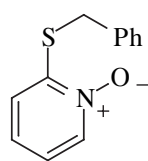
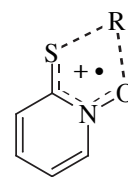
In 1989 the unexpected, oxygen-catalysed rearrangement of *N*-benzyloxy-2(1*H*)-pyridinethione (**1.38**) was reported, in which a formal 1,4 benzyloxy group migration had occurred.<sup>62</sup> Since then reports of the facile rearrangement of other *N*-alkoxy-2(1*H*)-pyridinethiones have appeared in the literature.<sup>63,64</sup> With a growing awareness that various rearrangements could plausibly proceed through a pericyclic transition state in which five electrons were delocalised over five atoms, it was envisaged that the catalysed rearrangement of *N*-alkoxy-2(1*H*)-pyridinethiones may proceed *via* a 5-electron, 5-centre transition structure (**1.40**) resulting in 1,4 migration. Chapter 5 describes attempts to determine the mechanism of this interesting isomerization.

**Table 1.2.** Some types of radical-mediated 1,2 and 3,2 rearrangements

Name of rearrangement	Reaction type	Ref.
$\beta$ -chloroalkyl		56
$\beta$ -hydroalkyl <sup>a</sup>		55
$\beta$ -allyperoxidyl		57
$\beta$ -acyloxysilyl		58
$\beta$ -allylnitroxyl		59
$\beta$ -phosphatoxyalkyl		60
$\beta$ -nitroxyalkyl		60
$\beta$ -sulfonatoxyalkyl		60
$\beta$ -allyloxyalkyl		61

a: Mechanism may not be intramolecular



**1.38****1.39****1.40**

## 1.5 References

1. Surzur, J.-M. and Teissier, P. *C. R. Seances Acad. Sci.* **1967**, 264C, 1981.
2. Tanner, D. D. and Law, F. C. P. *J. Am. Chem. Soc.* **1969**, 91, 7535.
3. Surzur, J.-M. and Teissier, P. *Bull. Soc. Chim. Fr.* **1970**, 3060.
4. Beckwith, A. L. J. and Tindal, P. K. *Aust. J. Chem.* **1971**, 24, 2099.
5. Julia, S. and Lorne, R. *C. R. Seances Acad. Sci. Series C* **1971**, 273, 174.
6. Lewis, S. N.; Miller, J. J. and Winstein, S. *J. Org. Chem.* **1972**, 37, 1478.
7. Beckwith, A. L. J. and Thomas, C. B. *J. Chem. Soc., Perkin Trans. 2* **1973**, 861.
8. Perkins, M. J. and Roberts, B. P. *J. Chem. Soc., Perkin Trans. 2* **1975**, 77.
9. Evanochko, W. T. and Shevlin, P. B. *J. Org. Chem.* **1979**, 44, 4426.
10. Beckwith, A. L. J. and Ingold, K. U. in *Rearrangements in Ground and Excited States*, De Mayo, P. (Ed.), Academic Press, New York, **1980**, Vol 1.
11. Shahidi, F. and Tidwell, T. T. *Can. J. Chem.* **1982**, 60, 1092.
12. Barclay, L. R. C.; Griller, D. and Ingold, K. U. *J. Am. Chem. Soc.* **1982**, 104, 4399.
13. Barclay, L. R. C.; Luszyk, J. and Ingold, K. U. *J. Am. Chem. Soc.* **1984**, 106, 1793.
14. Saebo, S.; Beckwith, A. L. J. and Radom, L. *J. Am. Chem. Soc.* **1984**, 106, 5119.
15. Kocovsky, P.; Stary, I. and Turecek, F. *Tetrahedron Lett.* **1986**, 27, 1513.
16. Julia, S. A. and Lorne, R. *Tetrahedron* **1986**, 42, 5011.
17. Giese, B.; Groninger, K. S.; Witzel, T.; Korth, H.-G. and Sustmann, R. *Angew. Chem. Int. Ed. Engl.* **1987**, 26, 233.
18. Korth, H.-G.; Sustmann, R.; Groninger, K. S.; Liesung, M. and Giese, B. *J. Org. Chem.* **1988**, 53, 4364.
19. Beckwith, A. L. J. and Duggan, P. J. *J. Chem. Soc. Chem. Commun.* **1988**, 1000.
20. Giese, B. and Groninger, K. S. *Org. Synth.* **1990**, 69, 66.
21. Beckwith, A. L. J. and Duggan, P. J. *J. Chem. Soc. Perkin Trans. 2* **1992**, 1777.
22. Beckwith, A. L. J. and Duggan, P. J. *J. Chem. Soc. Perkin Trans. 2* **1993**, 1673.
23. Katora, M.; Hájek, M.; Kvícala, J.; Ameduri, B. and Boutevin, B. *J. Fluorine*

*Chem.* **1993**, 64, 259.

24. Crich, D. and Yao, Q. *J. Am. Chem. Soc.* **1994**, 116, 2631.

25. Sprecher, M. *Chemtracts Org. Chem.* **1994**, 7, 120.

26. Crich, D. and Filzen, G. F. *J. Org. Chem.* **1995**, 60, 4834.

27. Furber, M.; Kraft-Klaunzer, P.; Mander, L. N.; Pour, M.; Yamauchi, T.; Murofushi, N.; Yamane, H.; Schraudolf, H. *Aust. J. Chem.* **1995**, 48, 427-44.

28. Itoh, Y.; Haraguchi, K.; Tanaka, H.; Matsumoto, K.; Nakamura, K. T. and Miyasaka, T. *Tetrahedron Lett.* **1995**, 36, 3867.

29. Gimisis, T.; Ialongo, G.; Zamboni, M. and Chatgililoglu, C. *Tetrahedron Lett.* **1995**, 36, 6781.

30. Crich, D.; Yao, Q. and Filzen, G. F. *J. Am. Chem. Soc.* **1995**, 117, 11455.

31. Crich, D.; Beckwith, A. L. J.; Filzen, G. F. and Longmore, R. W. *J. Am. Chem. Soc.* **1996**, 118, 7422.

32. Zipse, H. *J. Chem. Soc. Perkin Trans. 2* **1996**, 1797.

33. Beckwith, A. L. J. and Duggan, P. J. *J. Am. Chem. Soc.* **1996**, 118, 12838.

34. Zipse, H. *J. Am. Chem. Soc.* **1997**, 119, 1087.

35. Beckwith, A. L. J.; Crich, D.; Duggan, P. J. and Yao, Q. *Chem. Rev.* **1997**, 97, 3273.

36. Crich, D. and Mo, X. -S. *J. Am. Chem. Soc.* **1998**, 120, 8298.

37. Gimisis, T.; Ialongo, G. and Chatgililoglu, C. *Tetrahedron* **1998**, 54, 573.

38. Lacôte, E. and Renaud, P. *Angew. Chem. Int. Ed. Engl.* **1998**, 37, 2259.

39. Togo, H.; He, W.; Waki, Y. and Yokoyama, M. *Synlett* **1998**, 700.

40. Choi, S.-Y.; Crich, D.; Horner, J. H.; Huang, X.; Newcomb, M. and Whitted, P. *O. Tetrahedron* **1999**, 55, 3317.

41. Crich, D.; Huang, X. and Beckwith, A. L. J. *J. Org. Chem.* **1999**, 64, 1762.

42. Crich, D.; Hao, X. L. and Lucas, M. *Tetrahedron* **1999**, 55, 14261.

43. Jung, M. E. and Xu, Y. *Org. Lett.* **1999**, 1, 1517.

44. Renaud, P.; Andrau, L.; Gerster, M. and Lacôte, E. In *Current Trends in Organic Synthesis*; Scolastico, C. and Nicotra, F., Eds.; Plenum: New York, 1999; pp 117-122.

45. Zipse, H. *Acc. Chem. Res.* **1999**, 32, 571.
46. Clive, D. L. J. and Subedi, R. *Chem. Commun.* **2000**, 237.
47. Zipse, H. and Bootz, M. *J. Chem. Soc. Perkin Trans. 2* **2001**, 1566.
48. Howard, J. A. and Scaiano, J. C. In *Landolt-Bornstein : Numerical data and functional relationships in science and technology : Group 2: Radical Reaction Rates in Liquids*; Fischer, H., Ed.; Springer-Verlag: Berlin, 1984; Vol. 13, Subvolume d, pp 128-129.
49. Shine, H. J. and Slagle, J. R. *J. Am. Chem. Soc.* **1959**, 81, 6309.
50. Martin, J. C. and Drew, E. H. *J. Am. Chem. Soc.* **1961**, 83, 1232.
51. Martin, J. C.; Taylor, J. W. and Drew, E. H. *J. Am. Chem. Soc.* **1967**, 89, 129.
52. a) Reichardt, C. *Chem. Rev.* **1994**, 94, 2319. b) Reichardt, C. and Schäfer, G. *Liebigs Ann.* **1995**, 1579. c) Eberhardt, R.; Löbbecke, S.; Neidhart, B. and Reichardt, C. *Liebigs Ann. /Recueil* **1997**, 1195.
53. a) Wollowitz, S. and Halpern, J. *J. Am. Chem. Soc.* **1988**, 110, 3112; and b) Halpern, J. *Science* **1985**, 227, 869.
54. Golding, B. T. and Radom, L. *J. Am. Chem. Soc.* **1976**, 98, 6331.
55. Gilbert, B. C.; Norman, R. O. C. and Williams, P. S. *J. Chem. Soc. Perkin Trans. 2* **1981**, 1401.
56. This type of reaction has been reviewed. See for example reference 10.
57. See for example a) Porter, N. A.; Mills, K. A.; Caldwell, S. E. and Dubay, G. R. *J. Am. Chem. Soc.* **1994**, 116, 6697 and b) Schenck, G. O. *Angew. Chem.* **1957**, 69, 579.
58. Wilt, J. W. and Keller, S. M. *J. Am. Chem. Soc.* **1983**, 105, 1395.
59. Craig, R. L. and Roberts, J. S. *J. Chem. Soc., Chem. Commun.* **1972**, 1142.
60. For a review see reference 35.
61. Crich, D. and Yao, Q. *J. Chem. Soc., Chem. Commun.* **1993**, 1265.
62. Hay, B. P. and Beckwith, A. L. J. *J. Org. Chem.* **1989**, 54, 4330.
63. Hartung, J.; Hiller, M. and Schmidt, P. *Chem. Eur. J.* **1996**, 2, 1014.
64. Hartung, J.; Hiller, M. and Schmidt, P. *Liebigs Ann.* **1996**, 1425.

65. Zipse, H. personal communication, April 2003.

## Chapter 2

### Kinetics of the $\beta$ -trifluoroacetoxyalkyl radical rearrangement

2.1	Introduction	24
2.2	A review of $\beta$ -acyloxyalkyl radical rearrangement kinetics	24
2.3	The search for a suitable system for study	31
2.4	Determination of the equilibrium constant	34
2.5	Kinetics experiments	38
2.6	Discussion of results	53
2.7	Conclusions	57
2.8	Experimental	58
2.9	References	72

## 2.1 Introduction

This chapter is concerned with the kinetics of the  $\beta$ -trifluoroacetoxyalkyl radical rearrangement. To put the subject into perspective, this chapter begins with a review of the kinetics of  $\beta$ -acyloxyalkyl radical rearrangements in general. A description of the search for an appropriately-structured radical for the study follows. An equilibrium constant is determined for the reversible rearrangement of the chosen radical in benzene solution. The kinetic scheme, experimental method and solutions to attendant analytical complexities are described. Arrhenius parameters,  $\log_{10}A$  and  $E_a$ , are obtained for the rearrangement of the 2-methyl-2-trifluoroacetoxy-1-heptyl radical in each of three solvents of varying polarity. The kinetics results and their implications for the rearrangement mechanism are discussed.

## 2.2 A review of $\beta$ -acyloxyalkyl radical rearrangement kinetics

A substantial contribution to the elucidation of the mechanism of the  $\beta$ -acyloxyalkyl radical rearrangement has come from the determination of the kinetics of the ester migration step.<sup>1-10,40</sup> In particular, the relationship of radical structure and solvent polarity to the rearrangement rate constant have yielded vital information about the nature of transition states or intermediates. For several rearrangements, the Arrhenius frequency factor ( $A$ ) and the activation energy ( $E_a$ ) have been determined. A high  $\log_{10}A$  value ( $>13$ ) can indicate that a radical frequently achieves a geometry similar to that of the rearrangement transition state, whereas a characteristic such as a strong alkoxy C–O bond between the carbon framework and the ester group will contribute to a high  $E_a$ .

A comprehensive review,<sup>11</sup> incorporating the kinetics of the  $\beta$ -acyloxyalkyl radical rearrangement, covers the literature up to mid 1997. The amount of work in the field is extensive but not exhaustive. Accordingly, these kinetic results are reproduced here (table 2.1), including work published to date.

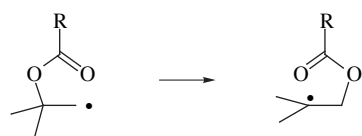
The earliest kinetic results (entries 3,6,8 and 13) were obtained by Beckwith and Thomas in 1973<sup>2</sup> who used a product ratios technique. Ingold and coworkers<sup>1,3</sup> who

used kinetic esr spectroscopy (entries 1,2,4,5,7 and 9), discovered that comparable rearrangement rate constants were an order of magnitude smaller than those of the initial work. However, when a fully integrated rate expression which allows for a changing  $\text{Bu}_3\text{SnH}$  concentration is applied to the earlier data, the rate constants decrease and thus correspond better to those obtained by the esr technique.<sup>1</sup>

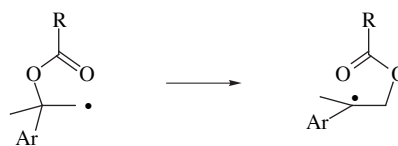
Considerable evidence on the rearrangement mechanism is provided by the results in table 2.1. It is clear that the rearrangement is thermodynamically favoured when the product radical is more stabilised than the reactant radical. Furthermore, a greater degree of product stabilisation generally results in faster rearrangement. This is exemplified by the difference in rate constants for the rearrangement of the 2-acetoxy-2-methyl-1-propyl radical (**2.1**→**2.6**, entry 4) and the 2-acetoxy-2-phenyl-1-propyl radical (**2.11**→**2.16**, entry 13). The latter rearrangement results in a highly stabilised benzylic radical.

A comparison of entries 5 (**2.1**→**2.6**) and 9 (**2.5**→**2.10**) reveals that a trifluoroacetoxy group migrates more than two orders of magnitude as fast as an acetoxy group in an otherwise identically-structured radical. This observation is corroborated by a comparison of entries 21 and 22, as well as 31 and 32. For an appropriate comparison of the latter, at 20°C in  $\text{CH}_3\text{CN}$ , radical **2.22** rearranges with  $k_r = 6.2 \times 10^6 \text{ s}^{-1}$ . This effect can be attributed to the stabilisation of negative charge that  $-\text{CF}_3$  brings to the ester group. Renaud and coworkers report that Lewis acids can accelerate certain  $\beta$ -acyloxyalkyl radical rearrangements by three orders of magnitude.<sup>12,13</sup> For instance, treatment of the lactate bromide **2.45** with tributyltin-hydride/AIBN in the absence of Lewis acid affords only the directly-reduced product. However, the same reaction in the presence of one equivalent of scandium (III) triflate/2,6-lutidine affords the rearrangement product **2.46** in 60% yield at the extraordinarily low temperature of  $-20^\circ\text{C}$ . This rate acceleration effect is consistent with the intermediacy of a complex of the type shown (**2.47**), expected to stabilise developing negative charge in the migrating group. Zipse's theoretical calculations<sup>14</sup> predict a large decrease in energy of the three-membered transition state (**i**) for a  $\beta$ -acyloxyalkyl radical 1,2 shift upon protonation of the carbonyl oxygen.

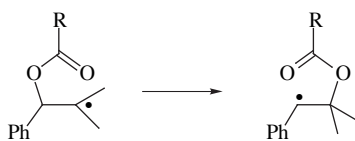




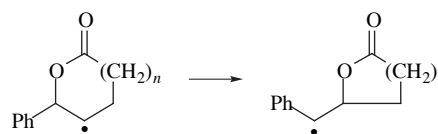
- 2.1:** R = Me **2.6**  
**2.2:** R = *n*-hex **2.7**  
**2.3:** R = Ph **2.8**  
**2.4:** R = *cyclo*-C<sub>3</sub>H<sub>5</sub> **2.9**  
**2.5:** R = CF<sub>3</sub> **2.10**



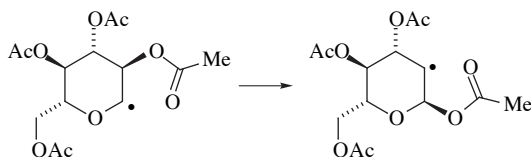
- 2.11:** R = Me, Ar = Ph **2.16**  
**2.12:** R = *n*-Pr, Ar = Ph **2.17**  
**2.13:** R = *n*-Pr, Ar = *p*-MeO-C<sub>6</sub>H<sub>4</sub> **2.18**  
**2.14:** R = *n*-Pr, Ar = *p*-CN-C<sub>6</sub>H<sub>4</sub> **2.19**  
**2.15:** R = CF<sub>3</sub>, Ar = *p*-CN-C<sub>6</sub>H<sub>4</sub> **2.20**



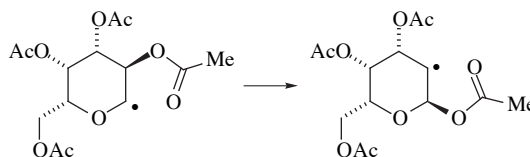
- 2.21:** R = Me **2.23**  
**2.22:** R = CF<sub>3</sub> **2.24**



- 2.25** **2.28**  
**2.26** **2.29**  
**2.27** **2.30**



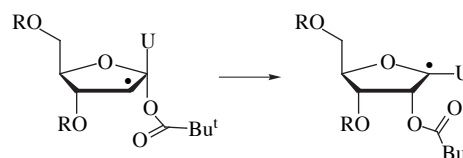
- 2.31** **2.32**



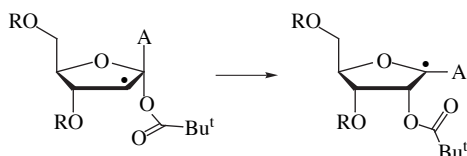
- 2.33** **2.34**



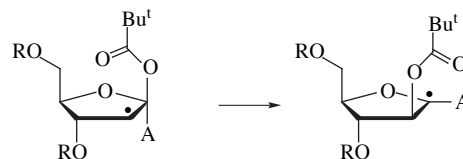
- 2.35** **2.36**



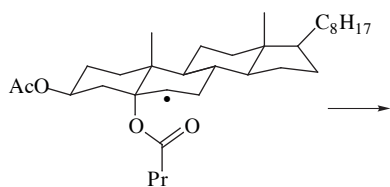
- 2.37:** R = TBDMS **2.38**



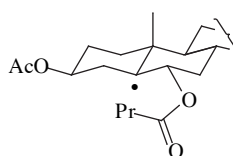
- 2.39:** R = TBDMS **2.40**



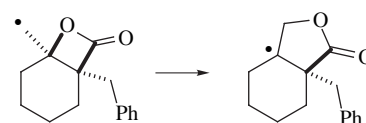
- 2.41:** R = TBDMS **2.42**



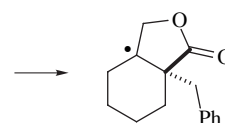
- 2.43**



- 2.44**



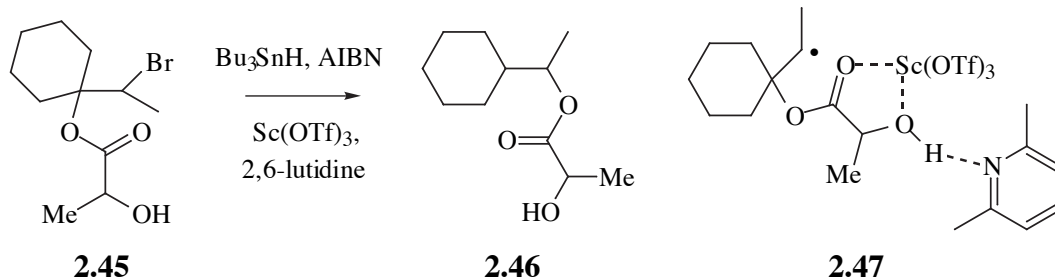
- 2.68**



- 2.69**

**Table 2.1.** Kinetic data for the rearrangement of  $\beta$ -acyloxyalkyl radicals of varying structure and in solvents of differing polarity

Entry	Rearrangement	Solvent	$T$ ( $^{\circ}\text{C}$ )	$k_r$ ( $\text{s}^{-1}$ )	$\log_{10}A$	$E_a$ ( $\text{kJmol}^{-1}$ )	Ref.
1	2.4 $\rightarrow$ 2.9	hydrocarbon	75	$1.2 \times 10^2$	13.2	74.5	1
2	2.3 $\rightarrow$ 2.8	hydrocarbon	75	$2.5 \times 10^2$	13.2	72.4	1
3	2.3 $\rightarrow$ 2.8	benzene	70	$3.9 \times 10^3$			2
4	2.1 $\rightarrow$ 2.6	<i>t</i> -butylbenzene	75	$4.5 \times 10^2$	13.9	74.9	3
5	2.1 $\rightarrow$ 2.6	hydrocarbon	75	$5.1 \times 10^2$	13.2	70.3	1
6	2.1 $\rightarrow$ 2.6	benzene	75	$6.2 \times 10^3$			2
7	2.1 $\rightarrow$ 2.6	H <sub>2</sub> O	75	$2.1 \times 10^4$	12.3	53.1	3
8	2.2 $\rightarrow$ 2.7	benzene	75	$3.6 \times 10^3$			2
9	2.5 $\rightarrow$ 2.10	CF <sub>2</sub> ClCFCl <sub>2</sub>	75	$7.0 \times 10^4$	11.0	41.0	3
10	2.31 $\rightarrow$ 2.32	benzene	75	$4.0 \times 10^2$	8.1	36.4	4
11	2.33 $\rightarrow$ 2.34	benzene	75	$5.4 \times 10^3$	11.8	53.6	4
12	2.35 $\rightarrow$ 2.36	benzene	75	$1.0 \times 10^4$	12.7	58.0	5
13	2.11 $\rightarrow$ 2.16	benzene	70	$4.1 \times 10^4$			2
14	2.12 $\rightarrow$ 2.17	cyclohexane	75	$3.7 \times 10^4$			6
15	2.12 $\rightarrow$ 2.17	DME	75	$5.8 \times 10^4$			6
16	2.12 $\rightarrow$ 2.17	benzene	75	$6.3 \times 10^4$	11.7	46.0	6
17	2.12 $\rightarrow$ 2.17	DMF	75	$8.4 \times 10^4$			6
18	2.12 $\rightarrow$ 2.17	EtOH	75	$1.3 \times 10^5$			6
19	2.12 $\rightarrow$ 2.17	MeOH	75	$1.6 \times 10^5$			6
20	2.13 $\rightarrow$ 2.18	benzene	75	$1.7 \times 10^5$			6
21	2.14 $\rightarrow$ 2.19	benzene	75	$1.6 \times 10^4$			6
22	2.15 $\rightarrow$ 2.20	benzene	75	$2.5 \times 10^6$			6
23	2.37 $\rightarrow$ 2.38	C <sub>6</sub> D <sub>6</sub>	80	$6.6 \times 10^4$			7
24	2.39 $\rightarrow$ 2.40	C <sub>6</sub> D <sub>6</sub>	80	$5.5 \times 10^4$			7
25	2.41 $\rightarrow$ 2.42	C <sub>6</sub> D <sub>6</sub>	80	$1.3 \times 10^5$			7
26	2.43 $\rightarrow$ 2.44	benzene	75	$1.9 \times 10^6$	14.8	56.9	8
27	2.25 $\rightarrow$ 2.28	benzene	80	$9.9 \times 10^5$			9
28	2.26 $\rightarrow$ 2.29	benzene	80	$1.7 \times 10^6$	11.8	37.7	9
29	2.27 $\rightarrow$ 2.30	benzene	80	$1.1 \times 10^6$			9
30	2.68 $\rightarrow$ 2.69	benzene	75	$3.2 \times 10^6$	8.2	11.3	40
31	2.21 $\rightarrow$ 2.23	CH <sub>3</sub> CN	20	$< 1 \times 10^4$			10
32	2.22 $\rightarrow$ 2.24	THF	75	$6.5 \times 10^6$	10.7	25.9	10
33	2.22 $\rightarrow$ 2.24	CH <sub>3</sub> CN	75	$3.1 \times 10^7$	11.2	24.7	10

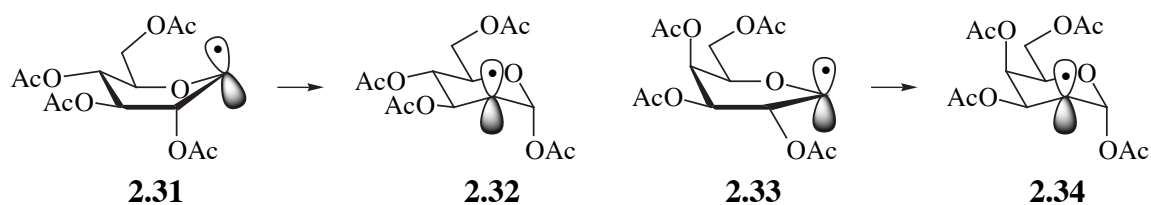


Larger rate constants will also result if the alkoxy carbon framework can stabilise a developing positive charge. A Hammett plot of  $\log_{10}(k_X/k_H)$  against substituent parameter  $\sigma_p^+$  for the *p*-substituted radicals **2.12-2.14** yielded a slope of  $\rho = -0.71$ , quite significant for a radical reaction.<sup>6</sup> However, this value is small considering that  $\rho$  is typically  $-4.5$  for  $S_N1$  solvolysis of *tert*-cumyl chlorides.<sup>15</sup> Nevertheless, the slightly negative slope indicates that stabilisation of positive charge at the benzylic position accelerates rearrangement.

As might now be expected, acceleration of the rearrangement is also promoted by polar solvents. Rearrangement **2.1**→**2.6** (entry 5) in hydrocarbon solvent at 75°C proceeds with  $k_r = 5.1 \times 10^2 \text{ s}^{-1}$ .<sup>1</sup> With water as solvent (entry 7),  $k_r$  increases to  $2.1 \times 10^4 \text{ s}^{-1}$ .<sup>3</sup> In a study of rearrangement of 2-butanoyloxy-2-phenyl-1-propyl radical (**2.12**→**2.17**), the logarithm of rate constant shows a weak linear dependence upon the solvent polarity parameter  $E_T$ ,<sup>22</sup> as given by an equation of the form  $\log_{10}k_r = 0.024E_T + 3.882$  ( $r = 0.978$ ).<sup>6</sup> A coefficient of 0.024 is substantial for a radical reaction. Again, a comparison of entries 32 and 33 illustrates how radical **2.22** rearranges more quickly in acetonitrile than in the less polar solvent THF.

Stereoelectronic requirements are also important kinetically, as exemplified by the difference in  $k_r$  between the rearrangements of the tetra-*O*-acetylgalactosyl radical (**2.33**) and the tetra-*O*-acetylglucosyl radical (**2.31**). Giese and coworkers have studied the kinetics of the rearrangements of **2.31** and **2.33** and have used esr spectroscopy to determine the conformation of the radicals.<sup>4</sup> Esr coupling constants reveal that both the product radicals, **2.34** and **2.32** respectively, exist in a standard  ${}^4C_1$  chair formation. Above  $-30^\circ\text{C}$ , radical **2.31** resides in a boat conformation, in which there is periplanarity

of the SOMO and the C2 acetoxy group. Radical **2.33** rearranges faster, and has a much larger  $\log_{10}A$  value than that for **2.31**. A larger  $A$  suggests that **2.33** favours a conformation which is preoriented towards rearrangement. Above  $-15^{\circ}\text{C}$  radical **2.33** occupies a half-chair conformation in which the radical orbital and the C2 acetoxy group are no longer periplanar, but there is planarity of O-C1-C2-C3. Such a conformation might be expected to facilitate scission of the C2–O bond by the formation of an alkene radical cation, or alternatively provide an optimal geometry for passage into transition states **i** and/or **ii**.

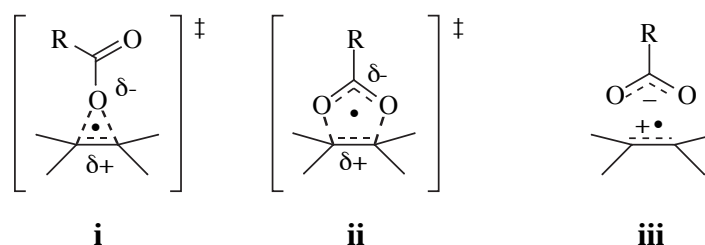


A similar stereoelectronic effect may exist in the very fast rearrangement of steroidal radical **2.43** (entry 26). The extremely high  $\log_{10}A$  value of 14.8 implies that the geometry of the radical is strongly preoriented towards rearrangement. Models demonstrate that carbons 4,5,6 and 7 lie in approximately the same plane, thus providing a favourable alignment for the formation of a cholesteryl acetate alkene radical cation, or alternatively for passage into transition structures **i** or **ii**. Additionally, at  $80^{\circ}\text{C}$ , nucleoside radical **2.39** rearranges with a rate constant of  $5.5 \times 10^4 \text{ s}^{-1}$ . The epimeric radical **2.41**, rearranges approximately twice as fast, with  $k_r = 1.3 \times 10^5 \text{ s}^{-1}$ . The exact cause of this reactivity difference is unknown, but it is possible that in **2.39** steric hindrance between the bulky C-1' pivaloyloxy group and the *cis* C-3' TBDMSO group makes it more difficult for the C-1' adenosine substituent to achieve a favourable position (closer to the pentose ring plane) than for **2.41**.

The low  $\log_{10}A$  value (8.2) for the rearrangement of **2.68** (entry 30) indicates that the radical does not achieve a favourable geometry for rearrangement as frequently as most of the other radicals. However, the activation energy ( $E_a = 11.3 \text{ kJmol}^{-1}$ ) is the lowest yet measured and is attributable to the high degree of ring strain relief upon

rearrangement. The low activation energy term (weak C–O ether bond) more than compensates for the poor stereoelectronic situation, making this rearrangement one of the fastest yet measured ( $k_r(75^\circ\text{C}) = 3.2 \times 10^6$ ).

Although rate constants for  $\beta$ -acyloxyalkyl radical rearrangements show significant electronic and solvent effects for radical reactions, such influences are small in comparison to those associated with ionic reactions. The cooperation of polarized 1,2 (i) and 2,3 (ii) shifts is a mechanism which is consistent with kinetic data. Alternatively, a mechanism involving solely an alkene radical cation/carboxylate ion pair intermediate (iii) also fits the data, as do various combinations of the three possibilities.

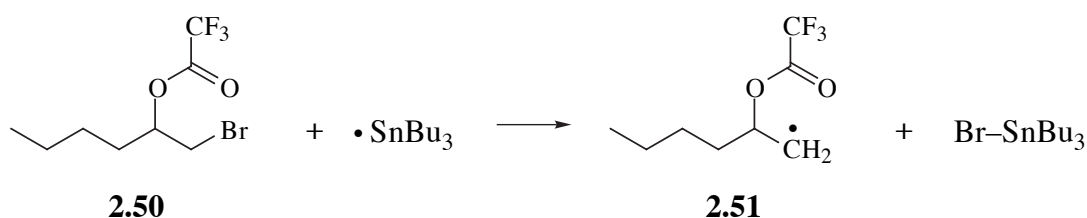


In this current work the kinetics of the  $\beta$ -trifluoroacetoxyalkyl radical rearrangement in simple, aliphatic systems is investigated. The Arrhenius parameters,  $\log_{10}A$  and  $E_a$ , have been determined in the solvents hexane, benzene and propionitrile. A limited amount of kinetic data for a 1,2 trifluoroacetoxy group shifts have previously been collected (entries 9,22,33 and 33). In fact, the rearrangement of **2.22**→**2.24** is the fastest  $\beta$ -acyoxyalkyl radical rearrangement yet recorded. However, much of the data (entries 22,32 and 33) were obtained from systems containing aromatic  $\alpha$ -substituents in which the complicating neophyl rearrangement can occur coincidentally with the target rearrangement.<sup>6,10</sup> In a purely aliphatic system (entry 9), the data was obtained by the integration of complex esr signals. Occasionally this technique suffers from experimental difficulties which give rise to errors. We wanted to obtain rate data by a product-studies/competitive-clock method to validate that obtained by esr. And finally, there has not yet been a systematic study of a  $\beta$ -trifluoroacetoxyalkyl radical rearrangement where both kinetic and labelling data have been obtained as a function of solvent polarity. Thus, a reaction system was chosen where both sets of data could also be obtained.

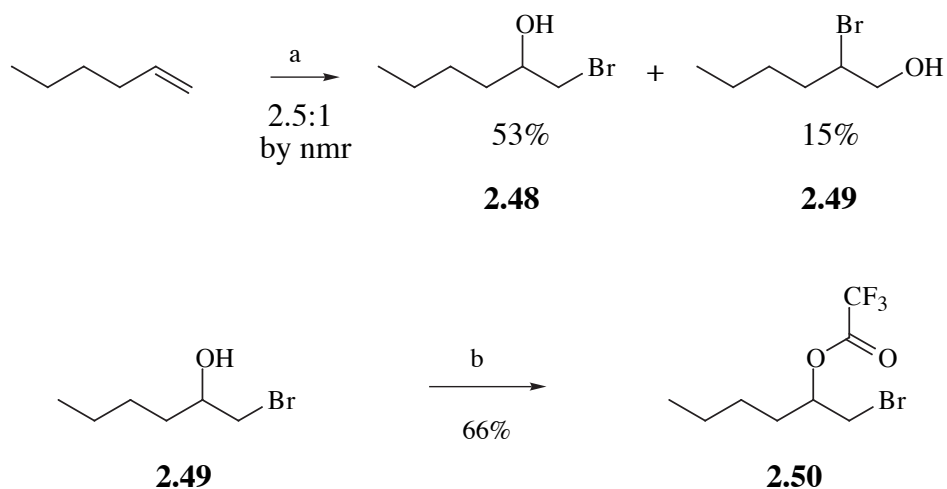
## 2.3 The search for a suitable system for study

### 2.3.1 2-Trifluoroacetoxy-1-hexyl radical

We sought a radical precursor which could be easily prepared, would react readily with tributyltin radicals, would provide scope for the introduction of an oxygen isotopic label and would yield products that are sufficiently involatile so as to permit straightforward laboratory manipulation. The tributyltin radical is known to react readily with an alkyl bromide to produce an alkyl radical and tributyltin bromide.<sup>16-18</sup> Accordingly, 1-bromo-2-trifluoroacetoxyhexane (**2.50**) was prepared in order to provide access to 2-trifluoroacetoxy-1-hexyl radicals (**2.51**).



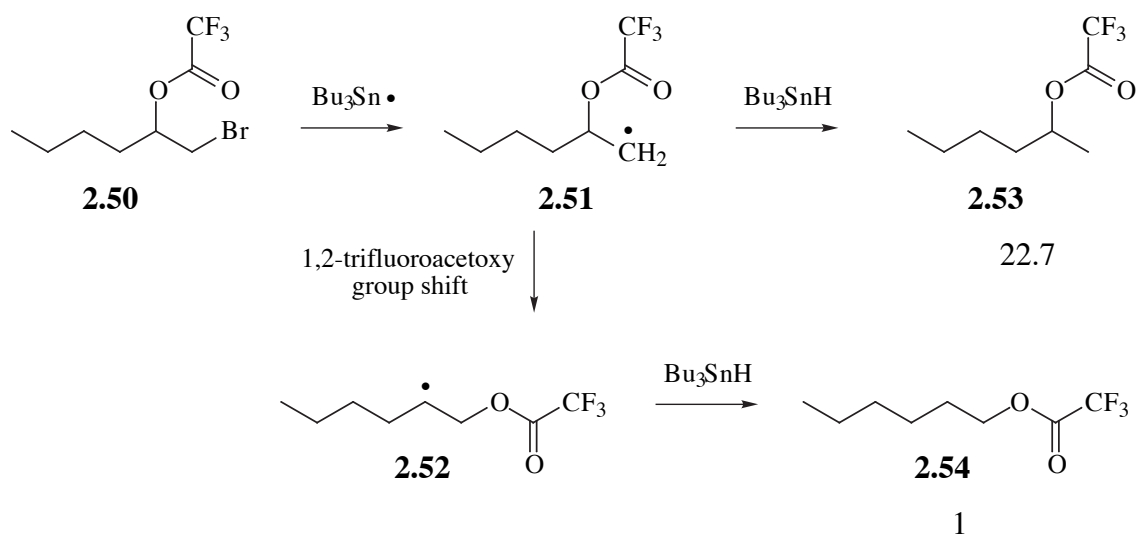
A moist DMSO solution of 1-hexene was treated with *N*-bromosuccinimide, according to an established procedure,<sup>19</sup> to give a mixture of the regioisomeric bromohydrins **2.48** and **2.49** in the ratio 2.5:1 by nmr. Upon separation by flash chromatography, the isolated yields were 53% and 15% respectively. The bromohydrin with the tertiary hydroxyl group (**2.48**) was esterified with trifluoroacetic anhydride and sodium trifluoroacetate, yielding the desired  $\beta$ -bromoester, **2.50**.



a: NBS, H<sub>2</sub>O in DMSO; b: (CF<sub>3</sub>CO)<sub>2</sub>O, NaOCOCF<sub>3</sub>

### 2.3.2 Reaction of $\beta$ -bromoester **2.50** with $\text{Bu}_3\text{SnH}$

To a 4.3 mM deoxygenated solution of **2.50** in benzene at reflux was added a benzene solution containing one equivalent of  $\text{Bu}_3\text{SnH}$  (13.8 mM) and catalytic AIBN over 106 minutes. After a total time of 3 hr, GC revealed that all the tributyltin hydride had been consumed and only a trace of **2.50** remained. The products included 2-trifluoroacetoxyhexane (**2.53**), resulting from direct reduction of **2.50** and 1-trifluoroacetoxyhexane (**2.54**), resulting from a 1,2 trifluoroacetoxy group shift. Unfortunately the ratio of **2.54**:**2.53** was only 1:22.7, demonstrating that the rearrangement is slow. When a 0.5 M solution of **2.50** in *tert*-butylbenzene was heated at the higher temperature of 130°C and treated with one equivalent of tributyltin hydride over 30 min, the ratio of **2.54**:**2.53** increased only modestly to 1:18.8. Thus, the rearrangement is too slow to give yields of **2.54** high enough for labelling and kinetic purposes. A faster rearrangement was therefore sought.



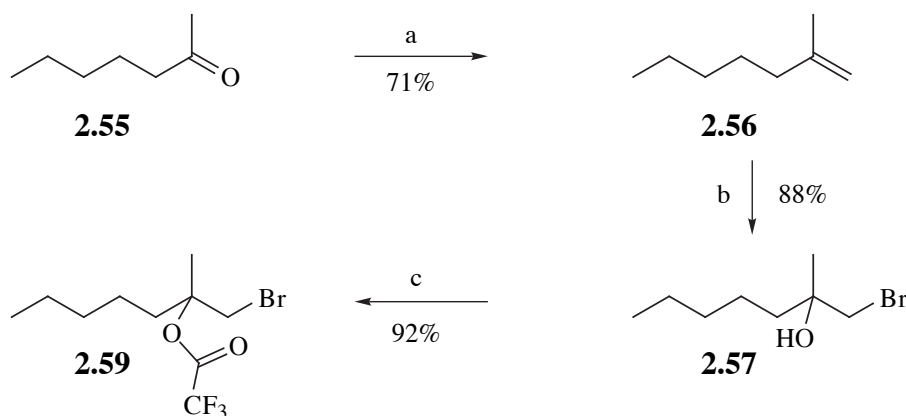
**Scheme 2.1.** Generation and reactions of  $\beta$ -trifluoroacetoxyalkyl radical **2.51**

### 2.3.3 A faster rearrangement

Since tertiary alkyl radicals are more stabilised by hyperconjugation than secondary radicals, the 1,2 migration of an ester group from a tertiary to a primary carbon is generally faster than that from a secondary to a primary terminus. Accordingly, the

tertiary ester 1-bromo-2-methyl-2-trifluoroacetoxyheptane (**2.59**) was prepared.

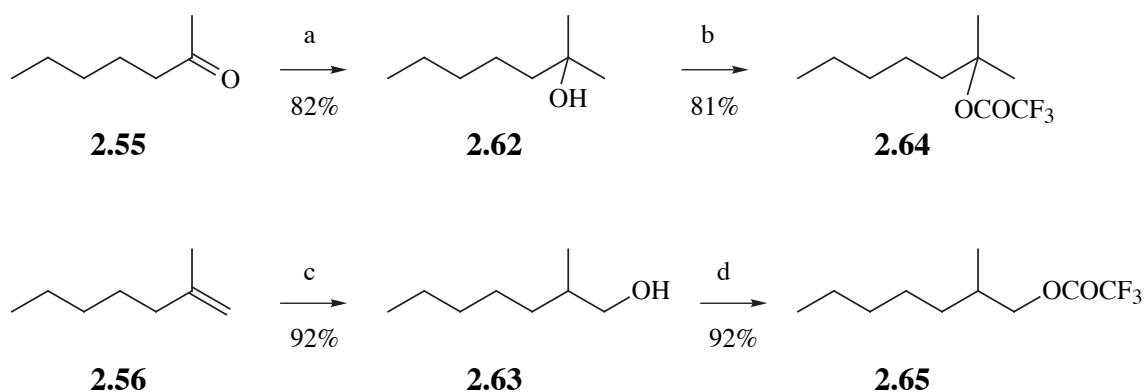
A Wittig reaction of  $\text{Ph}_3\text{P}=\text{CH}_2$  and 2-heptanone (**2.55**) gave 2-methyl-1-heptene (**2.56**) in reasonable yield. Conversion to the bromohydrin **2.57** was effected by treatment of a wet DMSO solution of **2.56** with NBS.<sup>19</sup> As expected, the regioisomer 2-bromo-2-methylheptan-1-ol (**2.58**) was also formed, although nmr indicated that the ratio of **2.57**:**2.58** was  $\geq 20:1$ . Purification of the desired isomer by flash chromatography was straightforward since **2.57** had the higher  $R_f$ , eluting before **2.58**. The  $\beta$ -bromoester **2.59** was obtained in high yield by esterification of **2.57**.



a:  $\text{Ph}_3\text{P}=\text{CH}_2$ , diglyme; b: NBS,  $\text{H}_2\text{O}$  in DMSO; c:  $(\text{CF}_3\text{CO})_2\text{O}$ , pyridine,  $\text{CH}_2\text{Cl}_2$ .

Authentic samples of the esters **2.64** and **2.65**—both products expected from the reaction of the  $\beta$ -bromoester **2.59** with  $\text{Bu}_3\text{SnH}$ —were prepared. Treatment of 2-heptanone (**2.55**) with methylmagnesium bromide in diethyl ether afforded the tertiary alcohol, **2.62**. Hydroboration of 2-methyl-1-heptene (**2.56**) in THF, followed by treatment with basic hydrogen peroxide gave the primary alcohol **2.63**. Alcohols **2.62** and **2.63** were converted to their respective esters **2.64** and **2.65** in high yield by standard trifluoroacetylation.

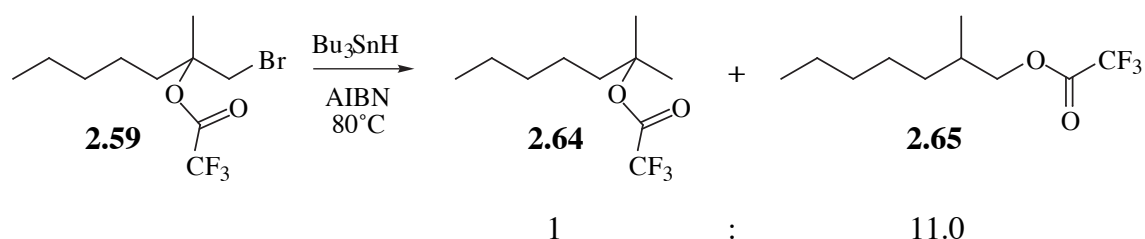




a:  $\text{CH}_3\text{MgBr}$  in  $\text{Et}_2\text{O}$ ; b:  $(\text{CF}_3\text{CO})_2\text{O}$ , pyridine in hexane; c:  $\text{BH}_3\cdot\text{THF}$  in THF, then  $\text{H}_2\text{O}_2$ ,  $\text{NaOH}$ ;  
d:  $(\text{CF}_3\text{CO})_2\text{O}$ ,  $\text{NaOCOFCF}_3$ .

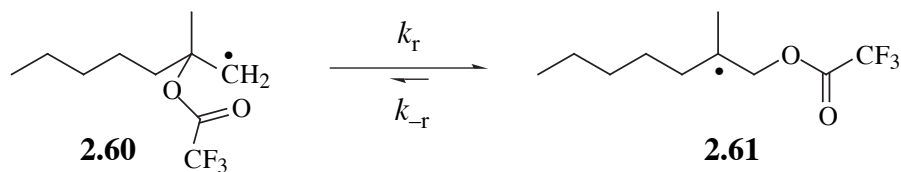
### 2.3.4 Reaction of $\beta$ -bromoester 2.59 with $\text{Bu}_3\text{SnH}$

A 4.2 mM, deoxygenated solution of **2.59** in benzene was heated to reflux and one equivalent of  $\text{Bu}_3\text{SnH}$  and catalytic AIBN were added over 30 min. After a total of 100 min, GC analysis showed the reaction to be virtually complete. The ratio of **2.65** to **2.64** was 11.0:1, indicating that the rearrangement step was much faster than that for the 2-trifluoroacetoxy-1-hexyl radical (**2.51**). This system was deemed highly suitable for both kinetic and labelling studies since it gave high, but not exclusive, yields of rearranged product **2.65**.



### 2.4 Determination of the equilibrium constant

Aware that the rearrangement of **2.60**  $\rightarrow$  **2.61** may be reversible and might therefore affect kinetic results at low concentrations of tributyltin hydride, an experiment was designed to determine the equilibrium constant,  $K$ , in benzene solution at  $80^\circ\text{C}$ .



**Scheme 2.2.** The equilibrium between radicals **2.60** and **2.61**.

### 2.4.1 Theory

For equilibria in which the forward and reverse reactions are both first order,  $K$  is equal to the forward rate constant ( $k_r$ ) divided by the reverse rate constant ( $k_{-r}$ ), as given by equation 2.1.

$$K = \frac{k_r}{k_{-r}} \quad (2.1)$$

A rate law for the equilibrium reaction **2.60**  $\leftrightarrow$  **2.61** may be written:

$$\frac{d[\mathbf{2.60}]}{dt} = [\mathbf{2.60}]k_r - [\mathbf{2.61}]k_{-r} \quad (2.2)$$

Under conditions of infinite  $\text{Bu}_3\text{SnH}$  dilution, where the reaction is at equilibrium, the rate of change of concentration of reactants is zero, so that equation 2.2 becomes:

$$0 = [\mathbf{2.60}]k_r - [\mathbf{2.61}]k_{-r} \quad (2.3)$$

$$\therefore [\mathbf{2.60}]k_r = [\mathbf{2.61}]k_{-r}$$

and so

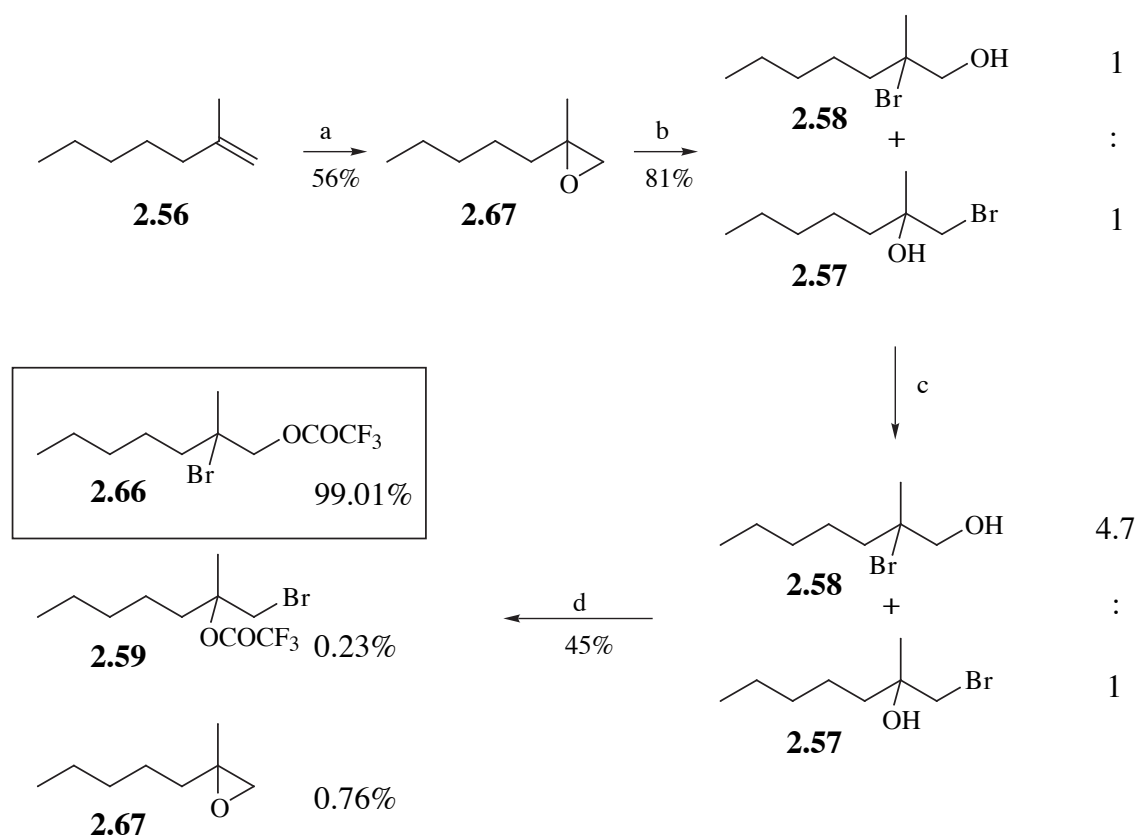
$$\frac{k_r}{k_{-r}} = \frac{[\mathbf{2.61}]}{[\mathbf{2.60}]} \quad (2.4)$$

Since the reaction of carbon-centred radicals with tributyltin hydride is irreversible, the concentrations of radicals **2.60** and **2.61** are directly proportional to the

product esters **2.64** and **2.65** respectively. Thus,  $K$  is equal to the ratio of products, according to equation 2.5.

$$K = \frac{k_r}{k_{-r}} = \frac{[\mathbf{2.65}]}{[\mathbf{2.64}]} \quad (2.5)$$

### 2.4.2 Preparation of $\beta$ -bromoester **2.66**



a: *m*-CPBA,  $\text{CH}_2\text{Cl}_2$ ; b: conc. HBr (aq); c: flash chromatography;  
d: 0.5 eq.  $(\text{CF}_3\text{CO})_2\text{O}$ , 0.5 eq. pyridine,  $\text{CH}_2\text{Cl}_2$ ,  $-78^\circ\text{C} \rightarrow \text{RT}$ , flash chromatography.

The  $\beta$ -bromoester, 2-bromo-2-methyl-1-trifluoroacetoxyheptane (**2.66**), was prepared in three reaction steps from 2-methyl-1-heptene (**2.56**). Oxidation of alkene **2.56** with *m*-CPBA in dichloromethane gave the epoxide **2.67**. Treatment of the epoxide with concentrated HBr yielded the expected mixture of regioisomeric bromohydrins, **2.57** and **2.58**, in approximately equal proportions. Flash chromatography enabled significant enrichment (82.5 mol%) in the desired, more polar

isomer, 2-bromo-2-methylheptan-1-ol (**2.58**). Selective esterification of the major isomer was achieved by treatment of a cold, dichloromethane solution of the bromohydrins with trifluoroacetic anhydride (0.5 eq.) and pyridine. Flash chromatography enabled the desired  $\beta$ -bromoester **2.66** to be separated from the unreacted bromohydrins.

Analysis of the purified product by GC showed it to consist of 2-bromo-2-methyl-1-trifluoroacetoxyheptane (**2.66**, 99.01%), 1-bromo-2-methyl-2-trifluoroacetoxyheptane (**2.59**, 0.23%) and 1,2-epoxy-2-methylheptane (**2.67**, 0.76%).

### 2.4.3 Reaction of $\beta$ -bromoester **2.66** with $\text{Bu}_3\text{SnH}$

A stirred 2.8 mM solution of 2-bromo-2-methyl-1-trifluoroacetoxyheptane (**2.66**) in dry benzene was deoxygenated with a stream of nitrogen, heated to 80°C and injected quickly with one equivalent of tributyltin hydride followed by catalytic AIBN. After two hours the reaction was concentrated and analysed by GC. All of the  $\beta$ -bromoester **2.66** had been consumed.

Unfortunately, retention times for the epoxide impurity **2.67** and the product tertiary trifluoroacetate **2.64** were identical on a dimethylpolysiloxane (BP1) capillary column, making the indicated proportion of **2.64** higher than its true value. Under these conditions, the lower limit for the equilibrium constant was calculated to be 15.1. However, these compounds did separate well on a polyethyleneglycol (BP20) stationary phase, yielding a ratio of the product esters of 52.9:1, in favour of the primary trifluoroacetate **2.65**. There were small amounts of 2-methyl-1-heptene (**2.56**) and 2-methyl-2-heptene (**2.56a**) present in the mixture, from the eliminative decomposition of **2.64**. Therefore,  $K < 52.9$ .

It was assumed that the low concentration of  $\text{Bu}_3\text{SnH}$  used in this experiment allowed radicals **2.60** and **2.61** to reach equilibrium prior to their hydrogen atom transfer reaction with tributyltin hydride. The small amount of 1-bromo-2-methyl-2-trifluoroacetoxyheptane (**2.59**) present initially in the sample of **2.66** is therefore deemed insignificant.

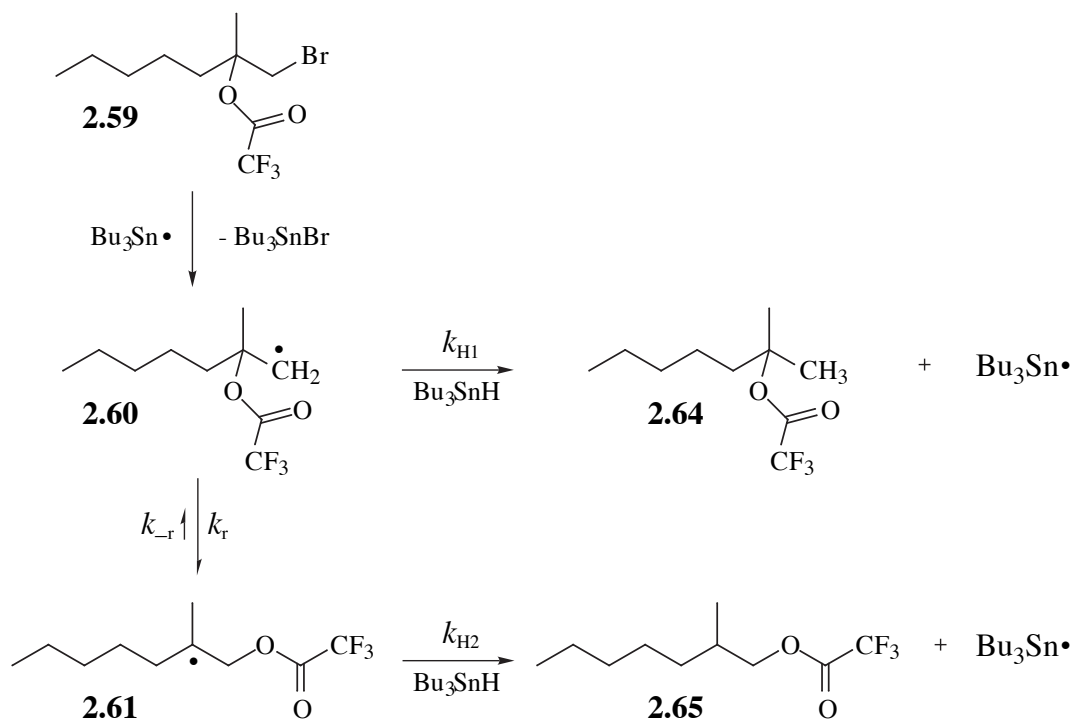
In conclusion, the equilibrium constant at 80°C in benzene is  $15.1 < K < 52.9$ , in favour of the tertiary 2-methyl-1-trifluoroacetoxyheptan-2-yl radical (**2.61**). It was deemed desirable to check this result using a different analytical method (e.g. HPLC) and to determine  $K$  at a number of temperatures in solvents of widely differing polarity.

## 2.5 Kinetics experiments

### 2.5.1 The kinetic scheme and analytical method

Scheme 2.3 illustrates the kinetically important reaction steps from which a numerical method of analysis may be derived. Removal of the bromine atom from bromoester **2.59** by a tributyltin radical forms the incipient radical **2.60** in a kinetically unimportant step. Disregarding the very small proportion of radical-radical termination events which occur, radical **2.60** may react in two possible ways. The first of these involves the abstraction of a hydrogen atom from tributyltin hydride, with second order rate constant  $k_{H1}$ , irreversibly forming the unrearranged product ester, **2.64**. The second path involves rearrangement to tertiary radical **2.61** with first order rate constant  $k_r$ . Radical **2.61** reacts irreversibly with tributyltin hydride with second order rate constant  $k_{H2}$  to form the rearranged ester **2.65**.

If the rearrangement step is irreversible, the size of  $k_{H2}$  is not important since reduction of **2.61** occurs as a matter of course. However, the rearrangement is reversible, with the radical **2.61** re-forming radical **2.60** with rate constant  $k_{-r}$ . If  $K = 53$  at 80°C in benzene, then  $k_{-r}$  is only about 2% the magnitude of  $k_r$  under these conditions. Owing to the relative slowness of the reverse reaction, the rearrangement was treated as being irreversible for the purposes of the analytic method. Noticeable deviations in the observed results for those expected from an irreversible rearrangement should only be encountered at very low concentrations of  $\text{Bu}_3\text{SnH}$  and at the highest temperatures.



**Scheme 2.3.** Generation and reactions of  $\beta$ -trifluoroacetoxyalkyl radical **2.60**

An analytic method for this type of reaction scheme has been developed by Beckwith and Moad.<sup>20</sup> The essence of the analysis lies in the competition between the rearrangement of radical **2.60** measured (clocked) against its direct reduction by  $\text{Bu}_3\text{SnH}$ . It can be shown (see appendix A) that:

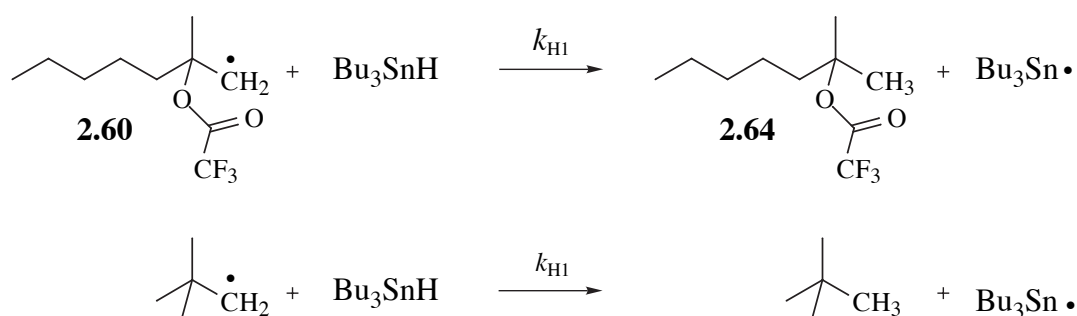
$$[\mathbf{2.65}]_f = \frac{k_r}{k_{\text{H1}}} \left\{ \ln\left([\text{Bu}_3\text{SnH}]_i + \frac{k_r}{k_{\text{H1}}}\right) - \ln\left([\text{Bu}_3\text{SnH}]_f + \frac{k_r}{k_{\text{H1}}}\right) \right\} \quad (2.6)$$

where  $[\mathbf{2.65}]_f$  is the final concentration of the rearranged product ester,  $k_r/k_{\text{H1}}$  is the ratio of rate constants for the competing processes and  $[\text{Bu}_3\text{SnH}]_i$  and  $[\text{Bu}_3\text{SnH}]_f$  are the initial and final concentrations of tributyltin hydride respectively.

A computer program is used to iteratively solve for values of  $k_r/k_{\text{H1}}$ , given values for  $[\mathbf{2.65}]_f$ ,  $[\text{Bu}_3\text{SnH}]_i$  and  $[\text{Bu}_3\text{SnH}]_f$ . Matters were simplified somewhat by ensuring  $[\text{Bu}_3\text{SnH}]_f = 0$ , achieved by making  $\text{Bu}_3\text{SnH}$  the limiting reagent. Ratios for  $k_r/k_{\text{H1}}$  were determined in this way at four different concentrations, as a test for reversibility and precision, and at four different temperatures: 40, 60, 80 and 100°C. Plots of  $\ln(k_r/k_{\text{H1}})$

versus reciprocal absolute temperature would be expected to show a linear relationship if the rearrangement step is truly first-order.

A value for  $k_r$  is obtained by multiplication of the corresponding  $k_r/k_{H1}$  value by  $k_{H1}$ , determined for that reaction temperature from literature data. Laser flash photolysis has been used to determine Arrhenius kinetic parameters for the second order reaction of simple alkyl, vinyl and aryl radicals with tributyltin hydride.<sup>21</sup> Of the radicals for which rate data are available, the radical judged to have greatest structural similarity to the 2-methyl-2-trifluoroacetoxyheptan-1-yl radical (**2.60**) is the 2,2-dimethyl-propyl (neopentyl) radical. Arrhenius parameters for the reaction of this radical with tributyltin hydride appear in table 2.2.



**Table 2.2.** Arrhenius parameters for the reaction of 2,2-dimethylpropan-1-yl radical with tributyltin hydride in isooctane solvent, as determined by laser flash photolysis<sup>21</sup>

$\log_{10} (A/M^{-1}s^{-1})$	$E_a$ (kJmol <sup>-1</sup> )
8.5±0.2	11.3±0.8

Uncertainties are at  $2\sigma$  limit (95% confidence)

The rate constant  $k_{H1}$  is not totally solvent-independent. Beckwith and Duggan have shown that  $k_{H1}$  for the reaction of 2-butanoyloxy-2-phenyl-1-propyl radical (**2.12**) with tributyltin hydride at 75°C exhibits only a weak solvent dependence, of the form  $\log[k_{H1}/M^{-1}s^{-1}] = 0.004E_T + 6.667$ .<sup>6</sup> The size of the likely solvent effect upon  $k_{H1}$  was

therefore judged to be too weak to be significant in this current work.

Values of  $k_{H1}$  at each reaction temperature were calculated by substitution of the  $\log_{10} A$  and  $Ea$  values into the Arrhenius expression:

$$k_{H1} = A e^{-\left(\frac{Ea}{RT}\right)} \quad (2.7)$$

Multiplication of these  $k_{H1}$  values by the corresponding, experimentally-determined values for  $k_r/k_{H1}$  yielded the desired  $k_r$  values. Normal Arrhenius plots were constructed to obtain  $\log_{10} A$  and  $Ea$  values for the rearrangement step.

## 2.5.2 Conducting the kinetic experiments and product analysis

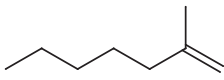
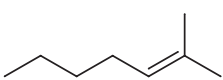
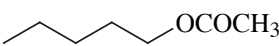
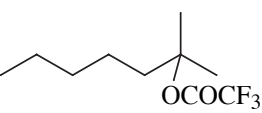
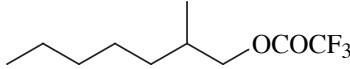
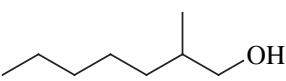
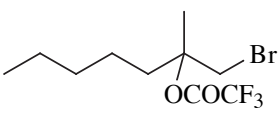
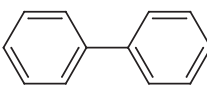
A detailed account of the procedure can be found in the experimental section (2.8) at the end of this chapter. Stirred, deoxygenated solutions containing a known concentration of  $\beta$ -bromoester **2.59** and the internal standard biphenyl (*n*-pentyl acetate for reactions in benzene solvent) in the desired solvent were heated at the nominated temperatures ( $\pm 0.3^\circ\text{C}$ ) of 40, 60, 80 and  $100^\circ\text{C}$  in Reactivials. The vials were equipped with Mininert valves which permitted addition to and removal of liquid from the hot solutions, even at temperatures exceeding the boiling point of the solvent. After 15 minutes,  $\text{Bu}_3\text{SnH}$  (0.9 molar equivalents with respect to **2.59**) and 1 mol% of radical initiator were injected. Reactions were monitored periodically by withdrawing small aliquots for GC analysis. Once the peak corresponding to  $\text{Bu}_3\text{SnH}$  had disappeared from the chromatogram a reaction was judged to be complete.

Molar yields were determined by GC for each of the pertinent reaction products and the sums were all found to be in excess of 95% that of the limiting reagent,  $\text{Bu}_3\text{SnH}$ . Values for  $[\mathbf{2.65}]_f$  (corrected),  $[\text{Bu}_3\text{SnH}]_i$  and  $[\text{Bu}_3\text{SnH}]_f (= 0)$  were used to determine a  $k_r/k_{H1}$  value for each reaction, with the iterative computer program which calculates solutions to equation 2.6. Plots of  $\ln(k_r/k_{H1})$  vs.  $1/T$  were constructed, all of which indicated a linear relationship. Uncertainties in the kinetic parameters obtained from these plots represent one standard deviation from the average of the parameters obtained from



plots of each concentration set. A list of the compounds quantified and their respective GC retention times appears in table 2.3.

**Table 2.3.** Gas chromatographic retention times<sup>a</sup>, on the stationary phase dimethylpolysiloxane (BP1), for relevant compounds<sup>b</sup> detected in the kinetic analysis.

Compound	Typical retention time (min)	Comments
 <b>2.56</b>	3.07	formed by thermal elimination from unrearranged product trifluoroacetate <b>2.64</b>
 <b>2.56a</b>	3.20	formed by thermal elimination from unrearranged product trifluoroacetate <b>2.64</b>
 <b>2.64</b>	4.62	GC detector analytical standard used for reactions in the solvent benzene
 <b>2.64</b>	5.40	unrearranged product ester
 <b>2.65</b>	6.31	rearranged product ester
 <b>2.63</b>	6.67	formed from (hydrolysis of?) rearranged product ester <b>2.65</b>
 <b>2.59</b>	9.65	$\beta$ -bromoester, the radical precursor
	12.52	GC detector internal analytical standard for reactions in the solvents hexane and propionitrile
<b>Bu<sub>3</sub>SnH</b>	13.06	limiting reagent; concentration not quantitatively determined
<b>Bu<sub>3</sub>SnBr</b>	16.96	concentration not quantitatively determined

a: Column temperature program: 100°C (0 min); ramp at 10°C/min; final temp 250°C (5 min); b: The compounds isobutyronitrile and *tert*-butanol, products formed from the initiators AIBN and di-*tert*-butyl hyponitrite (40°C reactions) respectively, do not appear in the table, but were detected by GC.

Values of  $k_{\text{HI}}$  at each temperature were determined from the literature data, then  $k_{\text{r}}$  values were calculated. Uncertainties in both the  $k_{\text{HI}}$  and  $k_{\text{r}}$  values represent two standard deviations (95% confidence) and are derived entirely from the uncertainties in the  $k_{\text{HI}}$  Arrhenius parameters.

Plots of  $\ln k_{\text{r}}$  vs.  $1/T$  were constructed and show a linear relationship, as expected. Arrhenius parameters for the radical rearrangement step were obtained. Uncertainties in these values are a sum of those inherent in the calculation of  $k_{\text{r}}$  values, and from the average of the Arrhenius parameters from plots of each concentration set. These uncertainties are at one standard deviation limits.

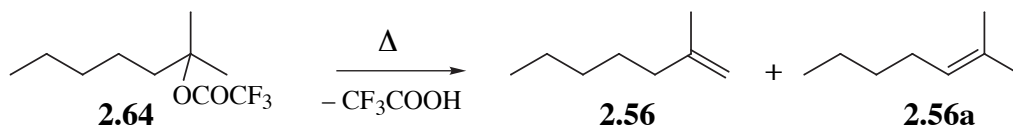
Both *experimental* and *recommended* values of the kinetic parameters are given. *Experimental* values are averages of the values obtained from the series of reactions at each concentration, using all the experimental data. *Recommended* values are those obtained by omitting lower quality data, usually from reactions for which the molar yields were lowest and/or where there was a large proportion of alkenes formed by elimination of trifluoroacetic acid from the product trifluoroacetate esters. This increased the uncertainty in the yield of the product ester.

### 2.5.3 Management of analytical complexities

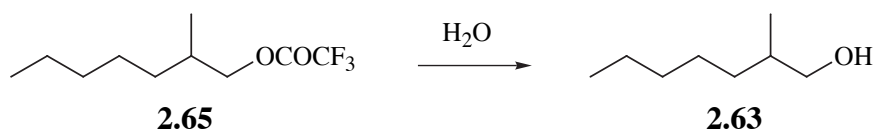
Owing to the relative lability of the trifluoroacetate products **2.64** and **2.65**, the analysis of the product concentrations was more complex than initially envisaged. As table 2.3 illustrates, there are three by-products formed, namely 2-methyl-1-heptene (**2.56**), 2-methyl-2-heptene (**2.56a**), and 2-methylheptan-1-ol (**2.63**). Some adjustments were therefore made to the procedure used to determine the final concentration of ester **2.65**.

Injection of a benzene solution of 2-methyl-2-trifluoroacetoxyheptane (**2.64**) into the GC (injector temperature of 250°C) caused the formation of a small amount of the two alkenes, **2.56** and **2.56a**. They were produced in approximately equal proportions as the only detectable products in a combined yield of about 5%, presumably by thermal elimination of trifluoroacetic acid from **2.64**. The identity and relative retention times of

the isomeric alkenes were established by GCMS.



The primary alcohol 2-methylheptan-1-ol (**2.63**) is presumably formed from the rearranged ester **2.65** ( $\leq 5\%$  the concentration of **2.65** in dilute propionitrile solution) in the reaction solution. However, the exact manner of its formation is unknown. Although dry solvents, reagents and apparatus were used, hydrolysis of the parent ester with adventitious water does still seem the most likely cause of the formation of **2.63**.



Injection of a benzene solution of 2-methyl-1-(trifluoroacetoxy)heptane (**2.65**) into the GC did not result in the formation of either of the alkenes, nor the alcohol **2.63**. Therefore, both alkenes are formed solely from the unrearranged ester **2.64**. Primary alcohol **2.63** is presumed to arise solely from the rearranged ester **2.65**. Consequently, the value of the final concentration of the rearranged ester,  $[\mathbf{2.65}]_f$ , was taken to be the sum of the concentrations of the ester itself and the alcohol subsequently formed from it (equation 2.8).

$$[\mathbf{2.65}]_f = [\mathbf{2.65}] + [\mathbf{2.63}] \quad (2.8)$$

Likewise, the value of the final concentration of the unrearranged ester,  $[\mathbf{2.64}]_f$ , was taken to be the sum of the concentrations of **2.64** and the isomeric alkenes formed by thermal elimination of  $\text{CF}_3\text{COOH}$  from it (equation 2.9).

$$[\mathbf{2.64}]_f = [\mathbf{2.64}] + [\mathbf{2.56}] + [\mathbf{2.56a}] \quad (2.9)$$

The computer program which calculated the  $k_r/k_{HI}$  values employed a ratio of the rearranged and unrearranged products to iteratively solve equation 2.6, with the assumption that these were the only two products. To avoid calculational errors, the values of  $[2.65]_f$  were corrected to equal the fraction of the total concentrations of product esters, multiplied by the initial concentration of the limiting reagent,  $Bu_3SnH$  (equation 2.10).

$$[2.65]_f^{corr.} = \frac{[2.65]_f}{[2.65]_f + [2.64]_f} \times [Bu_3SnH]_i \quad (2.10)$$

The value of  $[Bu_3SnH]_i$  for each reaction was calculated, in turn, by measuring the number of moles of unreacted  $\beta$ -bromoester **2.59** remaining at the end of the reaction by GC, subtracting this value from the number of moles present initially, then dividing by the reaction solution volume (equation 2.11).

$$[Bu_3SnH]_i = \frac{n(2.65)_i - n(2.65)_f}{\text{reaction solution volume (L)}} \quad (2.11)$$

This final correction was employed because trifluoroacetic acid—formed during the reaction by elimination from the unrearranged product ester **2.64**—reacts with  $Bu_3SnH$ , to form hydrogen and tributyltin trifluoroacetate. Tributyltin trifluoroacetate,  $Bu_3SnOCOCF_3$ , can be detected in small proportions in the reaction mixtures by GC, having a retention time approximately midway between that for  $Bu_3SnH$  and  $Bu_3SnBr$ . The iterative computer program does not account for this manner of consumption of  $Bu_3SnH$ , hence necessitating a corrective response. Tables 2.4 to 2.6 reveal slight variations in the  $[Bu_3SnH]_i$  values between reactions in each concentration set. The lowest  $[Bu_3SnH]_i$  values are usually found in the highest temperature (373 K/100°C) reactions, where the largest amount of trifluoroacetic acid is produced by elimination from the product ester **2.64**.

## 2.5.4 Kinetics results

Table 2.4. Kinetic data for reactions with **hexane** as the solvent

Nominal [Bu <sub>3</sub> SnH] <sub>i</sub>	<i>T</i> (K)	[ <b>2.65</b> ] <sub>f</sub> <i>corr.</i> (M)	[Bu <sub>3</sub> SnH] <sub>i</sub> (M)	[Bu <sub>3</sub> SnH] <sub>f</sub> (M)	$\frac{k_r}{k_{H1}}$ (M)	$10^{-6} \times k_{H1}$ <i>calc.</i> (M <sup>-1</sup> s <sup>-1</sup> )	$10^{-3} \times k_r$ (s <sup>-1</sup> )
0.015 M	313.9	0.00287	0.0144	0	0.00107	4.17±1.7	4.48±1.8
	332.5	0.00479	0.0149	0	0.00244	5.31±2.1	13.0±3.4
	353.6	0.00704	0.0149	0	0.00524	6.78±2.7	35.5±15
	373.2	0.00911	0.0146	0	0.0103	8.29±3.2	85.4±35
0.050 M	313.9	0.00500	0.0503	0	0.00138	4.17±1.7	5.75±2.4
	332.5	0.00845	0.0499	0	0.00292	5.31±2.1	15.5±6.4
	353.6	0.00140	0.0497	0	0.00651	6.78±2.7	44.1±18
	373.2	0.0211	0.0491	0	0.0140	8.30±3.2	116±48
0.10 M	313.9	0.00682	0.0996	0	0.00166	4.17±1.7	6.91±2.8
	332.5	0.0112	0.0990	0	0.00326	5.31±2.1	17.3±7.1
	353.6	0.0190	0.0975	0	0.00705	6.78±2.7	47.8±20
	373.2	0.0318	0.0977	0	0.0164	8.30±3.2	136±56
0.15 M	313.9	0.00837	0.147	0	0.00193	4.17±1.7	8.03±3.3
	332.5	0.0136	0.146	0	0.00367	5.31±2.1	19.5±8.0
	353.6	0.0239	0.145	0	0.00813	6.78±2.7	55.1±23
	373.2	0.0414	0.144	0	0.0194	8.30±3.2	161±66

**Table 2.5.** Kinetic data for reactions with **benzene** as the solvent

Nominal [Bu <sub>3</sub> SnH] <sub>i</sub>	T (K)	[ <b>2.65</b> ] <sub>f</sub> <i>corr.</i> (M)	[Bu <sub>3</sub> SnH] <sub>i</sub> (M)	[Bu <sub>3</sub> SnH] <sub>f</sub> (M)	$\frac{k_r}{k_{H1}}$ (M)	$10^{-6} \times k_{H1}$ <i>calc.</i> (M <sup>-1</sup> s <sup>-1</sup> )	$10^{-4} \times k_r$ (s <sup>-1</sup> )
0.010 M	313.6	0.00613	0.00904	0	0.00838	4.15±1.7	3.48±1.4
	331.0	0.00717	0.00906	0	0.0159	5.21±2.1	8.27±3.4
	353.3	0.00806	0.00922	0	0.0307	6.75±2.7	20.7±8.5
	372.5	0.00823	0.00908	0	0.0426	8.24±3.2	35.1±14
0.070 M	313.6	0.0210	0.0661	0	0.0106	4.15±1.7	4.39±1.8
	331.0	0.0299	0.0664	0	0.0209	5.21±2.1	10.9±4.5
	353.3	0.0395	0.0641	0	0.0437	6.75±2.7	29.5±12
	372.5	0.0458	0.0626	0	0.0766	8.24±3.2	63.1±26
0.130 M	313.6	0.0300	0.133	0	0.0121	4.15±1.7	5.01±2.1
	331.0	0.0434	0.132	0	0.0226	5.21±2.1	11.8±4.8
	353.3	0.0635	0.132	0	0.0481	6.75±2.7	32.5±13
	372.5	0.0794	0.130	0	0.0874	8.24±3.2	72.0±30
0.175 M	313.6	0.0320	0.174	0	0.0115	4.15±1.7	4.78±2.0
	331.0	0.0479	0.173	0	0.0219	5.21±2.1	11.4±4.7
	353.3	0.0733	0.168	0	0.0496	6.75±2.7	33.5±14
	372.5	0.0804	0.140	0	0.0783	8.24±3.2	64.5±26

**Table 2.6.** Kinetic data for reactions with **propionitrile** as the solvent

Nominal [Bu <sub>3</sub> SnH] <sub>i</sub>	T (K)	[ <b>2.65</b> ] <sub>f</sub> corr. (M)	[Bu <sub>3</sub> SnH] <sub>i</sub> (M)	[Bu <sub>3</sub> SnH] <sub>f</sub> (M)	$\frac{k_r}{k_{H1}}$ (M)	$10^{-6} \times k_{H1}$ calc. (M <sup>-1</sup> s <sup>-1</sup> )	$10^{-4} \times k_r$ (s <sup>-1</sup> )
0.036 M	314.4	0.0186	0.0360	0	0.0156	4.20±1.7	6.54±2.7
	332.4	0.0244	0.0366	0	0.0319	5.30±2.1	16.9±6.9
	352.2	0.0285	0.0361	0	0.0623	6.67±2.7	41.6±17
	373.2	0.0304	0.0352	0	0.115	8.29±3.2	95.0±39
0.075 M	314.4	0.0308	0.0742	0	0.0198	4.20±1.7	8.30±3.4
	332.4	0.0402	0.0727	0	0.0370	5.30±2.1	19.6±8
	352.2	0.0496	0.0722	0	0.0700	6.67±2.7	46.7±19
	373.2	0.0567	0.0706	0	0.134	8.29±3.2	111±46
0.15 M	314.4	0.0384	0.128	0	0.0186	4.20±1.7	7.80±3.2
	332.4	0.0575	0.136	0	0.0374	5.30±2.1	19.8±8
	352.2	0.0699	0.124	0	0.0661	6.67±2.7	44.1±18
	373.2	0.0828	0.117	0	0.126	8.29±3.2	105±43
0.30 M	314.4	0.0605	0.284	0	0.0235	4.20±1.7	9.87±4.0
	332.4	0.0874	0.280	0	0.0436	5.30±2.1	23.1±9.5
	352.2	0.122	0.280	0	0.0826	6.67±2.7	55.1±23
	373.2	0.143	0.278	0	0.118	8.29±3.2	97.9±40

The Arrhenius equation for the first order rearrangement of radical **2.60** can be written:

$$\ln k_r = \ln A_r - \frac{E_{a_r}}{RT} \quad (2.12)$$

Likewise, the Arrhenius equation for the second order reaction of radical **2.60** with tributyltin hydride can be written:

$$\ln k_{H1} = \ln A_{H1} - \frac{E_{a_{H1}}}{RT} \quad (2.13)$$

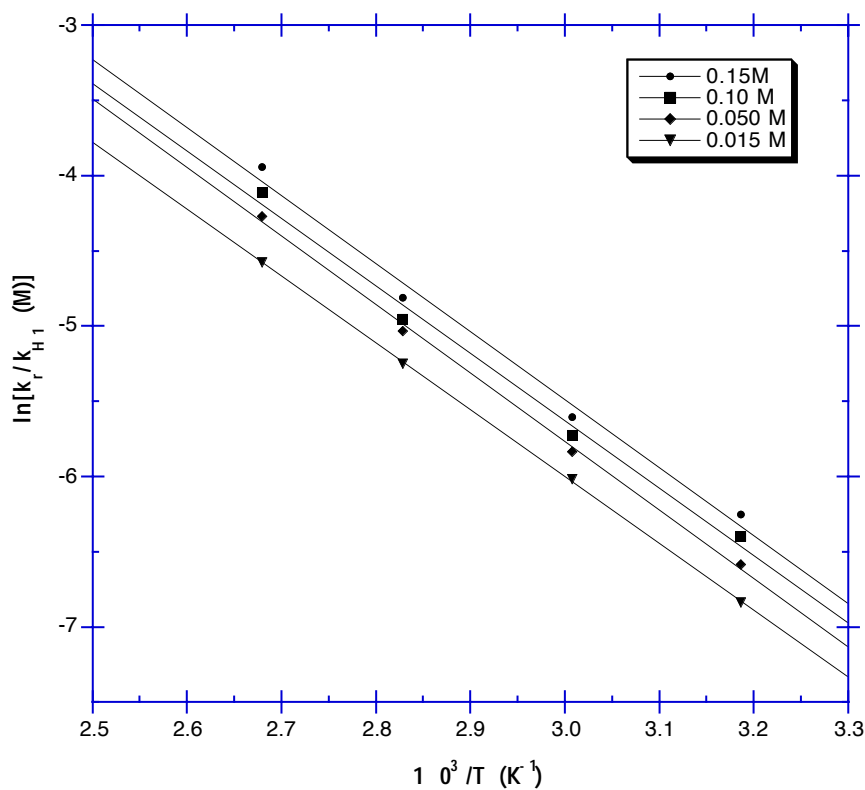
Subtraction of equation 2.13 from equation 2.12 gives:

$$\ln\left(\frac{k_r}{k_{H1}}\right) = \ln\left(\frac{A_r}{A_{H1}}\right) - \frac{(E_{a_r} - E_{a_{H1}})}{RT} \quad (2.14)$$

or, alternatively:

$$\ln\left(\frac{k_r}{k_{H1}}\right) = 2.3026 \log_{10}\left(\frac{A_r}{A_{H1}}\right) - \frac{(E_{a_r} - E_{a_{H1}})}{RT} \quad (2.15)$$

As expected, plots of  $\ln(k_r/k_{H1})$  against  $1/T$  (figures 2.1-2.3), displayed a linear relationship. The gradient was  $-(E_{a_r} - E_{a_{H1}})/R$  and the vertical intercept  $2.3026 \log_{10}(A_r/A_{H1})$ . Kinetic parameters extracted from each of the graphs appear in table 2.7.



**Figure 2.1.** Plot of  $\ln(k_r/k_{H1})$  against reciprocal temperature for the reactions of radical **2.60** in the solvent **hexane**



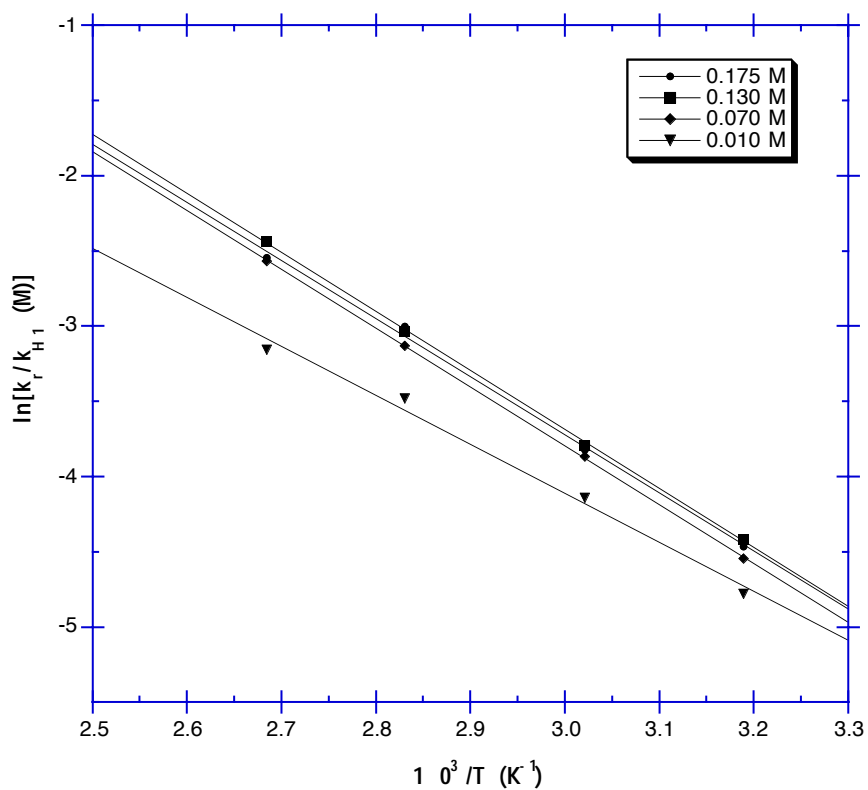


Figure 2.2. Plot of  $\ln(k_r/k_{H1})$  against  $1/T$  for the reactions of radical **2.60** in **benzene**

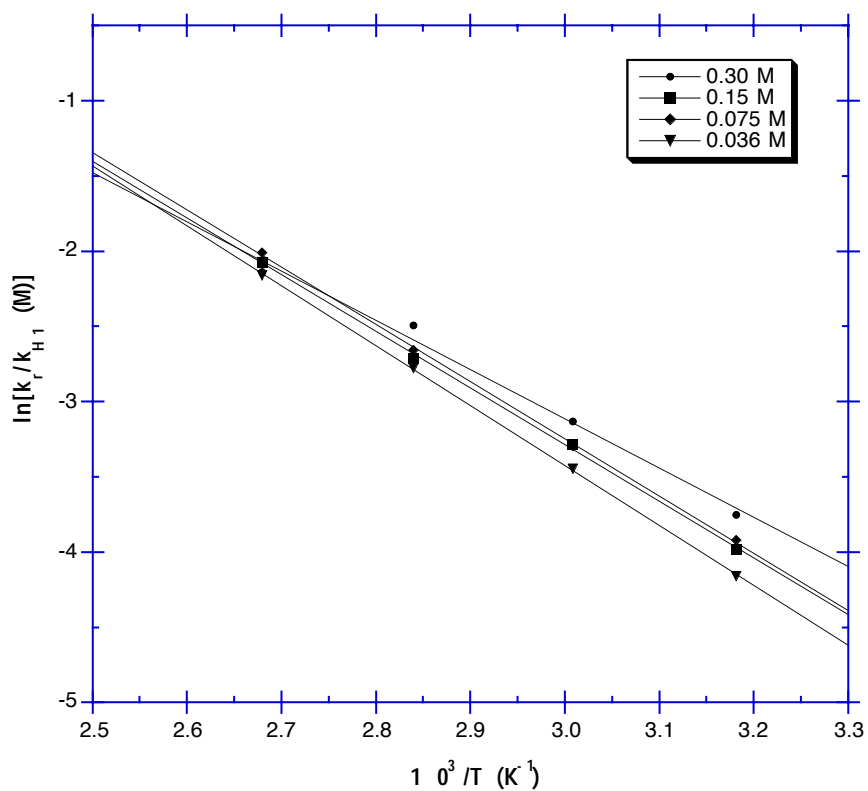


Figure 2.3. Plot of  $\ln(k_r/k_{H1})$  against  $1/T$  for the reactions of radical **2.60** in **propionitrile**

Both *experimental* and *recommended* values of the kinetic parameters are supplied in tables 2.7 and 2.8. *Experimental* values are averages of the values obtained from the series of reactions at each concentration, using all the experimental data. *Recommended* values are those obtained by omitting lower quality data. Since the rearrangement reaction was reversible, data obtained at the lowest initial concentrations of tributyltin hydride was considered to have the larger possible error. Reactions with lower mole balances (*ca.* 95%) were also considered to provide less reliable data.

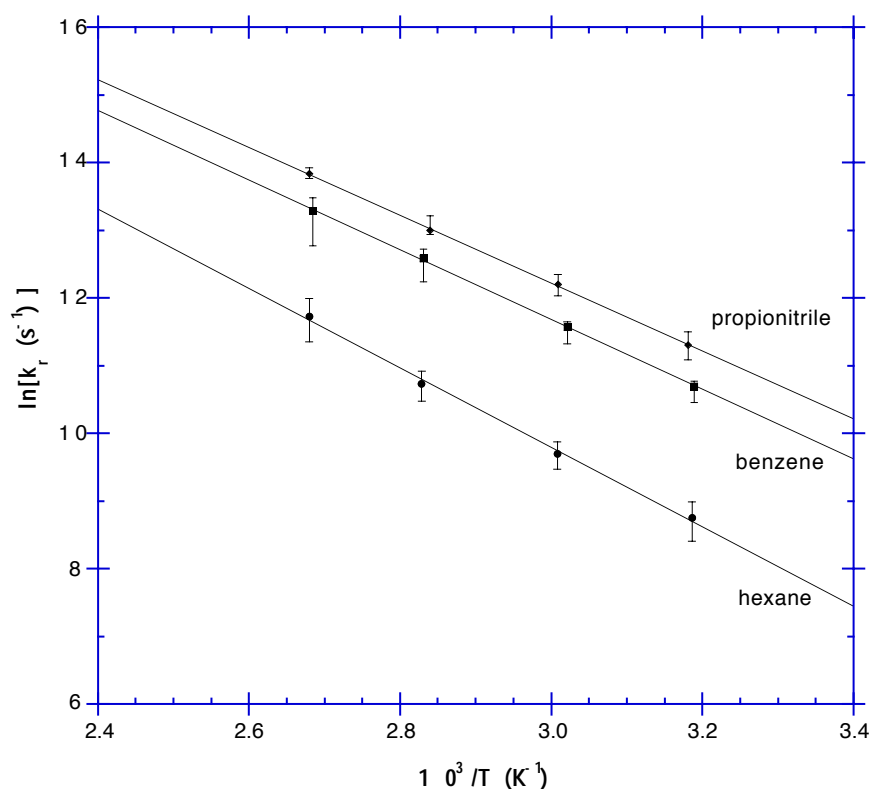
**Table 2.7.** Kinetic parameters extracted from the data plots of  $\ln(k_r/k_{H1})$  vs.  $1/T$

Solvent	Entry type	$\log_{10}\left(\frac{A_r}{A_{H1}}(\text{M})\right)$	$E_{a_r} - E_{a_{H1}}$ (kJmol <sup>-1</sup> )
hexane	experimental values	3.38±0.14	37.4±0.4
	recommended values	3.45±0.06	37.6±0.3
benzene	experimental values	3.21±0.50	31.1±1.8
	recommended values	3.46±0.04	32.4±0.3
propionitrile	experimental values	3.55±0.11	31.7±1.1
	recommended values	3.42±0.03	30.7±0.1

Uncertainties represent one standard deviation from the mean (68% confidence)

Figure 2.4 shows a plot of  $\ln k_r$  versus  $1/T$ . Arrhenius parameters have been extracted and appear in table 2.8. To allow the kinetic parameters to be expressed in familiar units, the Arrhenius equation can be written in the form:

$$\ln k_r = 2.3026 \log_{10} A_r - \frac{E_{a_r}}{RT} \quad (2.16)$$



**Figure 2.4.** Comparative Arrhenius plots of  $\ln k_r$  against reciprocal absolute temperature for the rearrangement of radical **2.60** in the solvents hexane, benzene and propionitrile. Data points represent  $k_r$  mean values from each of the four concentrations and error bars represent the spread of  $k_r$  values.

**Table 2.8.** Arrhenius parameters for the rearrangement of 2-methyl-2-trifluoroacetoxy-1-heptanyl radical (**2.60**) in the solvents hexane, benzene and propionitrile

Solvent	Entry type	$\log_{10}[A \text{ (s}^{-1}\text{)}]$	$E_{a_r} \text{ (kJmol}^{-1}\text{)}$
hexane	experimental values	$11.9 \pm 0.3$	$48.7 \pm 0.9$
	recommended values	$11.8 \pm 0.3$	$48.9 \pm 0.7$
benzene	experimental values	$11.7 \pm 0.6$	$42.4 \pm 3.2$
	recommended values	$12.0 \pm 0.2$	$43.7 \pm 0.8$
propionitrile	experimental values	$11.9 \pm 0.5$	$42.2 \pm 2.9$
	recommended values	$11.9 \pm 0.2$	$42.0 \pm 0.3$

Uncertainties represent one standard deviation from the mean (68% confidence limit).

## 2.6 Discussion of results

It was found that the rearrangement of radical **2.60** to **2.61** was reversible, having an equilibrium constant,  $K$ , of between 15 and 53, depending upon the method of determination. This reversibility was reflected in the plots of  $\ln(k_r/k_{H1})$  against reciprocal temperature (figures 2.1-2.3), where it was observed that the lowest data points at each temperature were those belonging to the reactions performed at the lowest concentrations of tributyltin hydride.

The accuracy of the  $k_r$  values are dependent on the respective  $k_{H1}$  values and therefore on how well the model system mirrored the actual hydrogen atom transfer reaction between **2.60** and  $\text{Bu}_3\text{SnH}$ . It is believed that the model system selected to mimic actual  $k_{H1}$  values was a good choice. If anything,  $k_{H1}$  for the reaction of 2-methyl-2-trifluoroacetoxyheptan-1-yl radical (**2.60**) with  $\text{Bu}_3\text{SnH}$  would be a little smaller than for its model, neopentyl radical, owing to the increased steric bulk of a trifluoroacetate group over a methyl substituent. Therefore, the true corresponding  $k_r$  values are probably slightly smaller than indicated, although certainly not as much as an order of magnitude, since  $k_{H1}$  for the reaction of methyl radical with  $\text{Bu}_3\text{SnH}$  at  $75^\circ\text{C}$  is only 7.5 times that for the reaction with the much more highly hindered *tert*-butyl radical.<sup>21</sup> It has been established previously that  $k_{H1}$  does show a solvent dependence, but the effect is very weak.<sup>6</sup>

Table 2.9 contains rate constants,  $k_r$ , for the radical rearrangement of radical **2.60** at  $75^\circ\text{C}$ , calculated using the *recommended* Arrhenius parameters. Also included are the values of the empirical solvent polarity parameter  $E_T$  (30).<sup>22</sup> It is clear that  $k_r$  increases as the solvent changes from hexane to benzene to propionitrile, supporting others' findings that polar solvents accelerate the  $\beta$ -acyloxyalkyl radical rearrangement.<sup>3,6,10</sup> The  $A$  frequency factors are identical within experimental uncertainty, therefore the rate constant differences lie with the activation energy term,  $E_{a_r}$ . The decrease observed in  $E_{a_r}$  is consistent with a weakening of the C2–O alkoxy ester bond with increasing solvent polarity.

**Table 2.9.** Arrhenius parameters and rate constants for the rearrangement of radical **2.60** in various solvents

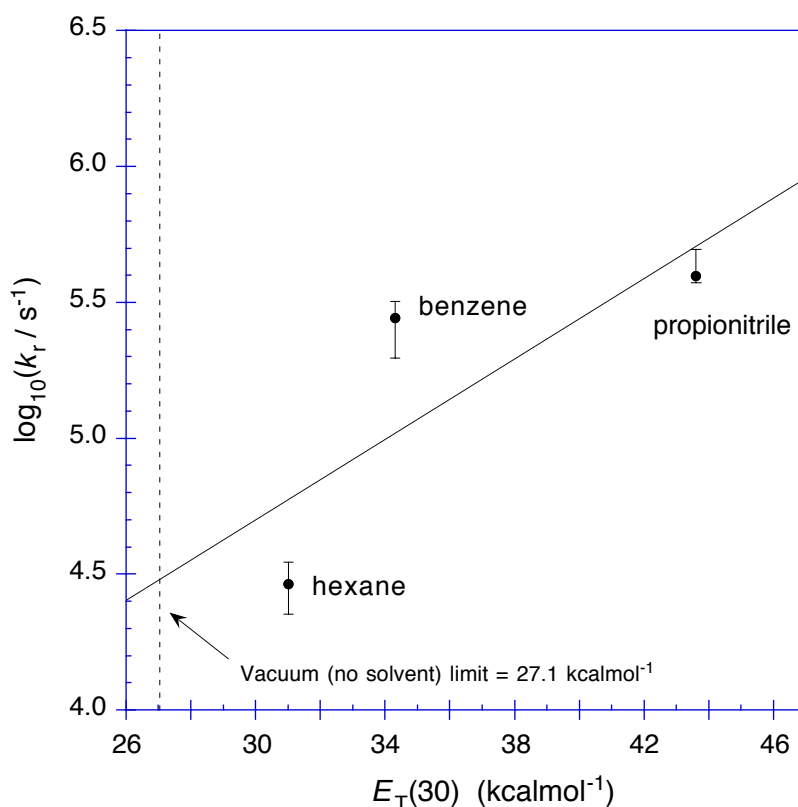
Solvent	$E_T(30)$ (kcalmol <sup>-1</sup> )	$\log_{10}[A \text{ (s}^{-1}\text{)}]$	$E_{a_r}$ (kJmol <sup>-1</sup> )	$k_r$ at 75°C (s <sup>-1</sup> )
hexane	31.0	11.8±0.3	48.9±0.7	$2.91 \times 10^4$
benzene	34.3	12.0±0.2	43.7±0.8	$2.78 \times 10^5$
propionitrile	43.6	11.9±0.2	42.0±0.3	$3.97 \times 10^5$

The current kinetics results are comparable with those obtained for other  $\beta$ -trifluoroacetoxyalkyl radical shifts,<sup>3,6,10</sup> particularly those for the rearrangement of the 2-methyl-2-trifluoroacetoxypropyl radical (**2.5**) in CF<sub>2</sub>ClCFCl<sub>2</sub>.<sup>3</sup> The rearrangement of radical **2.5** possesses Arrhenius parameters of  $\log_{10}[A \text{ (s}^{-1}\text{)}] = 11.0 \pm 1.0$  and  $E_{a_r} = 41.0 \pm 5.0 \text{ kJmol}^{-1}$ , with  $k_r(75^\circ\text{C}) = 7.0 \times 10^4 \text{ s}^{-1}$ .<sup>3</sup> Therefore, results from this current study agree reasonably well with those obtained from a similarly-structured radical by the independent method of kinetic esr spectroscopy.<sup>3</sup> Rate constants at 75°C for the  $\beta$ -acyloxyalkyl radical rearrangement (table 2.1) vary from  $>1.2 \times 10^2$  to  $3.1 \times 10^7 \text{ s}^{-1}$ . On this scale the isomerization of radical **2.60** can be described as moderately fast.

Beckwith and Duggan observed a linear relationship between the  $\log_{10}(k_r/\text{s}^{-1})$  and the solvent polarity parameter  $E_T(30)$  for the rearrangement at 75°C of the 2-butanoyloxy-2-phenyl-1-propyl radical (**2.12**).<sup>6</sup> When data for the rearrangement of radical **2.60** was plotted in this way (figure 2.5), no linear relationship was observed. The rate constant for the rearrangement in hexane is significantly smaller than  $k_r$  in benzene solution. This result is not yet well understood, but it would appear to indicate a change in mechanism as the solvent is changed from benzene to hexane.

One explanation for this unusual behaviour arises from an examination of the properties of the two hydrocarbon solvents. The dielectric constant for benzene (2.3) is only slightly larger than for hexane (1.9). Both solvents have permanent dipole moments of zero and similar polarisabilities (ease of inducing a temporary dipole).<sup>23</sup> However, the quadrupole moment for benzene of  $-29.7 \times 10^{-40} \text{ Cm}^2$  is much greater than for simple alkanes such as ethane ( $-3.34 \times 10^{-40} \text{ Cm}^2$ ), meaning that the change of charge density is

much greater across the benzene molecule than for aliphatic, straight chain alkanes.<sup>24</sup> The  $\pi$  electrons in the benzene aromatic ring are responsible for this effect, and might be cause of an increase in  $k_r$  through a stabilising interaction with the electrophilic carbon of the ester carbonyl group. It has been suggested that this type of interaction is responsible for the large difference in the rate of solvolysis of 1-acetoxy-2-bromopropane in octane and in benzene.<sup>25</sup> Since the compound used in the determination of the  $E_T(30)$  values<sup>22</sup> has no carbonyl group, this parameter does not allow for such an electronic interaction. Alternatively, there might be an interaction between the benzene ring and the radical centre at C1, promoting trifluoroacetate scission by an  $S_{RN}2^c$  reaction.<sup>26</sup> Another possible cause for the apparent size of  $k_r$  in benzene is that  $k_{H1}$  is decreased through an interaction between the solvent and  $Bu_3SnH$ , or because of an interaction between incipient radical **2.60** and benzene which hinders reaction with  $Bu_3SnH$ . However, no precedent could be found for a significant decrease in  $k_{H1}$  upon a change in solvent from *n*-alkane to benzene.



**Figure 2.5.** Plot of  $\log_{10}(k_r/s^{-1})$  vs.  $E_T(30)$  for rearrangement of radical **2.60** at 75°C. The equation of the line of best fit is  $\log_{10}[k_r/s^{-1}] = 0.0741E_T + 2.479$  ( $r = 0.787$ ).

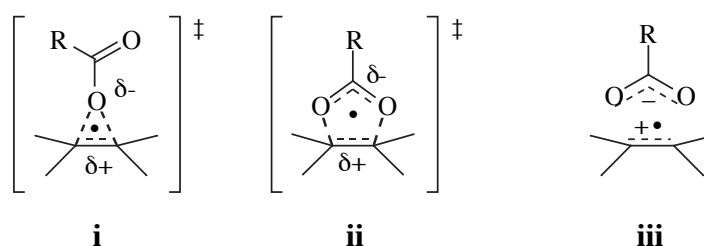
The solvent effects observed in the rearrangement of  $\beta$ -trifluoroacetoxyalkyl radical **2.60** are significant for a radical reaction but are very small in comparison to those observed in ionic chemistry. Rate constants for the first order elimination of HCl from *tert*-butyl chloride at 120°C in various solvents<sup>27</sup> are displayed in table 2.10. A huge relative rate acceleration is observed as the solvent polarity is increased. However, for the rearrangement of **2.60**, the acceleration effect is at best only a few percent as large as that for the elimination reaction.



**Table 2.10.** Absolute and relative rate constants for the decomposition of *t*-butyl chloride

Solvent	Rate constant, $k$ ( $s^{-1}$ )	Relative rate constant
heptane	$1.0 \times 10^{-9}$	1
benzene	$2.45 \times 10^{-7}$	245
acetonitrile	$6.92 \times 10^{-5}$	69200

The kinetic data obtained in the present study are consistent with a rearrangement mechanism for radical **2.60** which involves the coincidence of polarized 1,2 (**i**) and 3,2 (**ii**) concerted shifts, although it is not possible (at this stage) to exclude the possibility that the rearrangement mechanism involves the intermediacy of an ion pair (**iii**). However, the insensitivity of  $k_r$  to solvent polarity relative to ionic processes initially suggests that there is not complete scission of the trifluoroacetoxy group from the carbon framework prior to the formation of the new bond.



## 2.7 Conclusions

The rearrangement of 2-methyl-2-trifluoroacetoxy-1-heptyl (**2.60**) to the 2-methyl-1-trifluoroacetoxy-2-heptyl radical (**2.61**) is a reversible process. At 80°C in benzene, an equilibrium mixture consists of between 93.8% and 98.1% of **2.61**.

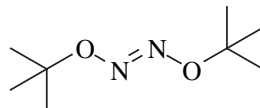
The kinetics of the rearrangement of **2.60**→**2.61** have been determined by a product-studies/competition-clock method in three different solvents. There was good agreement with results obtained by kinetic esr spectroscopy for the rearrangement of the structurally-similar 2-methyl-2-trifluoroacetoxy-1-propyl radical (**2.5**) in CF<sub>2</sub>ClCFCl<sub>2</sub>. Arrhenius equations for the rearrangement of **2.60** in each solvent were: hexane,  $\log_{10}[k_r (\text{s}^{-1})] = 11.8 \pm 0.3 - (48.9 \pm 0.7)/\theta$ ; benzene,  $\log_{10}[k_r (\text{s}^{-1})] = 12.0 \pm 0.2 - (43.7 \pm 0.8)/\theta$ ; and propionitrile,  $\log_{10}[k_r (\text{s}^{-1})] = 11.9 \pm 0.2 - (42.0 \pm 0.3)/\theta$ . Rate constants at 75°C in each solvent were: hexane,  $k_r = 2.9 \times 10^4$ ; benzene,  $k_r = 2.8 \times 10^5$ ; and propionitrile,  $k_r = 4.0 \times 10^5 \text{ s}^{-1}$ . It is the activation energy term which is primarily responsible for the dependence of the rate constant upon solvent polarity, indicating that the C–O ether bond of **2.60** is weakened by polar solvent. It was unusual that  $k_r$  in benzene was 9.5 times as large as that in hexane, yet  $k_r$  in propionitrile was only 13.6 times as large as that in hexane. This effect is not well understood.

These solvent effects, although large for a radical reaction, were only a few percent as large as those observed for a comparable solvolysis reaction. Overall, the results most closely fit a mechanism which involves a combination of concerted and polarized 1,2 and 3,2 pericyclic shifts, although the intermediacy of an alkene-radical-cation/trifluoroacetate-anion pair cannot yet be excluded.



## 2.8 Experimental

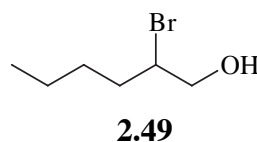
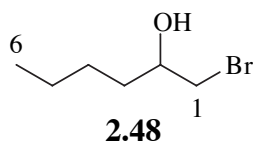
### *E*-Di-*tert*-butyl Hyponitrite [82554-97-0]



The preparation of this low-temperature, free-radical initiator was based on the method of Mendenhall.<sup>28</sup> Anhydrous  $\text{FeCl}_3$  (4.67 g, 28.8 mmol) was stirred with 35 mL of diethyl ether and cooled to  $0^\circ\text{C}$  before adding *tert*-butyl chloride (30 mL, 276 mmol), followed by sodium hyponitrite,  $\text{Na}_2\text{N}_2\text{O}_2$  (3.33 g of  $88\pm 5\%$  purity, 27.6 mmol). The mixture was allowed to warm to room temperature and stirring was continued for a further 30 min. The suspension was filtered through a small column of celite, eluting with diethyl ether until no further orange/yellow colour was present in the filtrate. The filtrate was washed with  $5 \times 50$  mL of water, by which time the washings were colourless. After drying ( $\text{MgSO}_4$ ), the solvent was evaporated to yield a yellow solid of mass 4.06 g (23.3 mmol, 84% crude, lit.<sup>28</sup> 82%).

The crude product was purified by flash chromatography on silica, eluting with 1.5% diethyl ether in 40/60 pet. spirit. A total mass of 3.31 g (19.0 mmol, 69%) was retrieved from the column, 2.32 g of which was present as white crystals and the remainder as an off-white solid. The off-white product was purified further by recrystallisation from  $\text{MeOH}/\text{H}_2\text{O}$  (10:1, *v/v*) at  $-50^\circ\text{C}$ , yielding material which gave one spot by TLC. The purified compound was stored in an airtight, dark glass bottle at  $-18^\circ\text{C}$ .

### (±) 1-Bromohexan-2-ol [26818-04-2] and (±) 2-Bromohexan-1-ol [112586-72-8]



A mixture of the isomeric bromohydrins **2.48** and **2.49** was prepared by the method of Langman and Dalton.<sup>19</sup> These compounds have been prepared and partially characterised previously, but without separation.<sup>29</sup>

A stirred solution of 1-hexene (5.00 g, 59.4 mmol) and water (3.0 mL, 167 mmol) in 180 mL of DMSO was treated with portions of *N*-bromosuccinimide (NBS) (21.15 g, 119 mmol) over 10 minutes. The solution warmed and became yellow,

gradually darkening to an orange colour. After the final addition of NBS, the mixture was stirred for a further 15 minutes then poured into 500 mL of ice-water and extracted four times with 100 mL portions of diethyl ether. The combined extracts were washed consecutively with 125 mL of water, 125 mL of saturated aqueous NaCl, then dried. Evaporation of solvent yielded an orange oil of mass 10.37 g which was dissolved in 200 mL of hexane and washed with 50 mL of 5% aqueous sodium metabisulfite then 50 mL of water and redried. Removal of solvent afforded a pale yellow oil (9.19 g). A portion of this oil (1.00 g) was purified by flash chromatography using 5% ethyl acetate in hexane as the eluent. Three compounds were isolated and identified. In order of elution they were:

i) 1,2-dibromohexane (0.02 g, 1%), Rf = 0.46

ii) 1-bromohexan-2-ol (**2.48**, 0.62 g, 53%), Rf = 0.19

$^1\text{H}$  nmr: 0.92 (t, 3H,  $\text{CH}_3$ ), 1.25-1.45 (m, 4H,  $\text{CH}_3\text{-CH}_2\text{CH}_2$ ), 1.55 (m, 2H, 3- $\text{CH}_2$ ), 2.20 (s, 1H, OH), 3.39 (dd, 1H,  $^2J = 10$  Hz,  $^3J = 7$  Hz, BrCH), 3.56 (dd, 1H,  $^2J = 10$  Hz,  $^3J = 3$  Hz, BrCH), 3.78 (m, 1H, CHO).

$^{13}\text{C}$  nmr: 13.9 (6), 22.5 (5), 27.7 (4), 34.8 (3), 40.6 (1), 71.0 (2).

EIMS: 181 (0.04) & 179 (0.03)  $\text{M}^+$ , 165 (0.5), 163 (0.7), 87 (56), 83 (21), 69 (100), 57 (24), 55 (27);

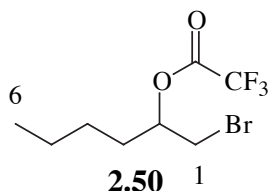
iii) 2-bromohexan-1-ol (**2.49**, 0.17 g, 15%), Rf = 0.13

$^1\text{H}$  nmr: 0.95 (t, 3H,  $\text{CH}_3$ ), 1.25-1.60 (m, 4H,  $\text{CH}_3\text{-CH}_2\text{CH}_2$ ), 1.85 (m, 2H,  $\text{CH}_3(\text{CH}_2)_2\text{CH}_2$ ), 2.20 (s, 1H, OH), 3.78 (m, 2H,  $\text{CH}_2\text{-O}$ ), 4.14 (m, 1H, BrCH).

$^{13}\text{C}$  nmr: 13.8 (6), 22.1 (5), 29.5 (4), 34.6 (3), 60.0 (2), 67.2 (1).

The nmr spectra of **2.48**<sup>30</sup> and **2.49**<sup>29</sup> have been published previously and conform with the current spectra.

### (±) 1-Bromomethylpentyl Trifluoroacetate



A stirred mixture of 1-bromohexan-2-ol (**2.48**, 0.3087 g, 1.71 mmol) and dry sodium trifluoroacetate (0.1118 g, 0.822 mmol) was treated with trifluoroacetic anhydride (1.17 mL, 8.28 mmol). After 20 min the resulting suspension was treated with 20 mL of pentane and filtered, washing the precipitate with 13 mL more pentane. After washing with water (33 mL) and back-extracting the aqueous washings with 2 × 10 mL of pentane, the combined organic phase was dried. Careful removal of solvent under vacuum left a colourless oil which was distilled by kugelrohr (90°C/10 mmHg), to

give the desired  $\beta$ -bromoester (**2.50**, 0.3106 g, 1.12 mmol, 66%) which was 99.7% pure by GC.

$^1\text{H}$  nmr: 0.92 (t, 3H,  $\text{CH}_3$ ), 1.35 (m, 4H,  $\text{CH}_3(\underline{\text{C}}\text{H}_2)_2$ ), 1.80 (m, 2H,  $\text{CH}_3(\text{CH}_2)_2\underline{\text{C}}\text{H}_2$ ), 3.46-3.59 (m, 2H,  $\text{BrCH}_2$ ), 5.21 (m, 1H,  $\text{CH-O}$ ).

$^{13}\text{C}$  nmr: 13.7 (6), 22.2 (5), 26.8 (4), 32.0 (1\*), 32.1 (3\*), 77.5 (2), 114.5 (q,  $^1J^{19}\text{F}-^{13}\text{C} = 286$  Hz,  $\text{CF}_3$ ), 156.9 (q,  $^2J^{19}\text{F}-^{13}\text{C} = 43$  Hz,  $\text{C=O}$ ).

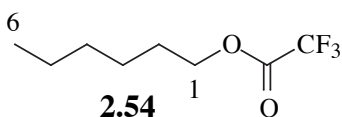
ir (neat): 2963 s, 2937 s, 2869 s, 1786 vs, 1224 vs, 1160 vs, br, asym, 667 m, asym.

EIMS: 183 (3), 164 (6), 162 (6), 83 (82), 69 (100), 55 (71).

CIMS: 296 (9) & 294 (11)  $\text{MNH}_4^+$ , 201 (49), 184 (39), 165 (98), 163 (100).

Found: C, 34.62; H, 4.63; N, 0.00%.  $\text{C}_8\text{H}_{12}\text{BrF}_3\text{O}_2$  requires: C, 34.68; H, 4.37; N, 0.00%.

### 1-Hexyl Trifluoroacetate [400-61-3]



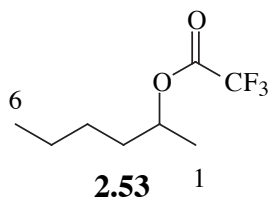
A stirred mixture of 1-hexanol (1.00 g, 9.78 mmol) and dry sodium trifluoroacetate (0.922 g, 4.97 mmol) was treated with trifluoroacetic anhydride (6.9 mL, 49 mmol). The exothermic reaction caused the mixture to boil, then form a thick, white suspension. Stirring was continued for another 20 minutes before the mixture was filtered under vacuum, washing the precipitate several times with a total of 50 mL of pentane. The filtrate was washed with 200 mL of water and the aqueous phase was back-extracted twice with 50 mL portions of pentane. The combined organic phase was dried and evaporated carefully (volatile product) under reduced pressure to give a yellow oil which was distilled by kugelrohr (70°C/49 mmHg, lit.<sup>31</sup> 68.9°C/49 mmHg) to yield **2.54** as a colourless oil (1.91 g, 9.64 mmol, 99%).

$^1\text{H}$  nmr: 0.90 (t, 3H,  $\text{CH}_3$ ), 1.25-1.45 (m, 6H,  $\text{CH}_3(\underline{\text{C}}\text{H}_2)_3$ ), 1.75 (m, 2H, 2- $\text{CH}_2$ ), 4.35 (t, 2H, 1- $\text{CH}_2$ ).

$^{13}\text{C}$  nmr: 13.9 (6), 22.4 (5), 25.2 (3\*), 28.1 (2\*), 31.2 (4), 68.3 (1), 114.6 (q,  $^1J^{19}\text{F}-^{13}\text{C} = 286$  Hz,  $\text{CF}_3$ ), ca.157.6 (q,  $\text{C=O}$ ).

ir (neat): 2962 s, 2937 s, 2877 m, 2867 m, 1787 vs, 1470 m, asym, 1406 m, 1350 s, 1225 vs, 1162 vs, 779 m, 733 m.

EIMS: 99 (12), 97 (14), 85 (40), 84 (16), 83 (29), 71 (53), 69 (91), 57 (100), 56 (69), 55 (80).

**(±) 1-Methylpentyl Trifluoroacetate [763-50-8]**

A stirred mixture of 2-hexanol (1.00 g, 9.78 mmol) and dry sodium trifluoroacetate (0.928 g, 6.78 mmol) was treated with 6.9 mL (49 mmol) of trifluoroacetic anhydride. A vigorous reaction resulted, which caused much of the anhydride to boil off. The reaction mixture was cooled to 0°C and more trifluoroacetic anhydride (4.0 mL, 28 mmol) was added and stirring continued for 20 minutes at room temperature to complete the reaction. The mixture was filtered under vacuum, washing the precipitate with 50 mL of pentane. The filtrate was washed with 200 mL of water and the aqueous washings were back-extracted with 50 mL more pentane, then dried. The solvent was evaporated carefully (volatile product) and the residue was distilled by kugelrohr (80°C/67 mmHg) to yield **2.53** as a colourless oil (1.11 g, 5.61 mmol, 57%), 99.5% pure by GC.

<sup>1</sup>H nmr: 0.91 (t, 3H, CH<sub>2</sub>CH<sub>3</sub>), 1.25-1.40 (m, 4H, CH<sub>3</sub>(CH<sub>2</sub>)<sub>2</sub>), 1.35 (d, 3H, <sup>3</sup>J = 6.2 Hz, 1-CH<sub>3</sub>), 1.55-1.80 (m, 2H, CH<sub>3</sub>(CH<sub>2</sub>)CH<sub>2</sub>), 5.10 (m, 1H, <sup>3</sup>J = 6.2 Hz, 2-CH).

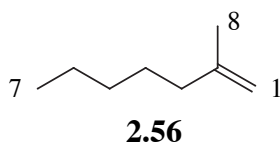
<sup>13</sup>C nmr: 13.8 (6), 19.5 (1), 22.3 (5), 27.2 (4\*), 35.1 (3\*), 76.6 (2), 114.6 (q, <sup>1</sup>J<sup>19</sup>F-<sup>13</sup>C = 286 Hz, CF<sub>3</sub>), 157.2 (q, <sup>2</sup>J<sup>19</sup>F-<sup>13</sup>C = 42 Hz, C=O).

ir (neat): 2962 s, 2939 s, 2879 s, 2870 s, 1783 vs, 1471 m, asym, 1385 m, 1340 m, 1222 vs, 1116 s, 866 m, 779 m, 732 m.

EIMS: 141 (8), 122 (19), 91 (19), 85 (30), 83 (37), 81 (48), 71 (55), 69 (47), 59 (45), 57 (100), 56 (46), 55 (87).

CIMS: 213 (30), 199 (5) MH<sup>+</sup>, 196 (28), 189 (22), 149 (48), 141 (51), 135 (85), 122 (83), 109 (100).

Found: C, 48.65; H, 6.60; N, 0.00; F, 28.88%. C<sub>8</sub>H<sub>13</sub>F<sub>3</sub>O<sub>2</sub> requires: C, 48.48; H, 6.61; N, 0.00; F, 28.76%.

**2-Methyl-1-heptene [15870-10-7]**

Methyltriphenylphosphonium bromide was purified by recrystallisation from EtOH/Et<sub>2</sub>O (mp 233.5-234°C). A mixture of methyltriphenylphosphonium bromide

(35.72 g, 100 mmol) and a 60% suspension of NaH in mineral oil (4.15 g, 104 mmol) in 150 mL of dry diglyme was magnetically-stirred *slowly* at 65°C, venting the hydrogen evolved. Formation of the phosphorane was deemed complete when the mixture was an egg-yolk colour and no dense, white solid could be seen on the bottom of the flask (*ca.* 10 hr).

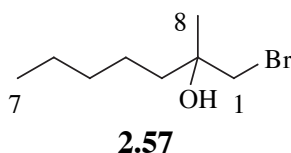
The mixture was cooled with an ice-water bath while 2-heptanone (**2.55**, 14.00 mL, 98.3 mmol, dried by passage through a column of anhydrous CaSO<sub>4</sub>) was added dropwise, which caused the solution colour to fade from yellow to cream. A distillation head was fitted to the flask and the product alkene was distilled from the mixture, under reduced pressure (96 mmHg) until a constant boiling point (~90°C) was reached. The distillate was washed first with saturated aqueous NaCl (four times), then with water, until the volume of the organic phase seemed to no longer decrease, then dried over MgSO<sub>4</sub>.

The crude alkene was redistilled, collecting the fraction boiling in the range 120-124°C (lit.<sup>32</sup> 119°C). This colourless oil (8.26 g) was analysed by <sup>1</sup>H nmr and consisted of 95% the desired alkene (**2.56**), 4% 2-heptanone (**2.55**) and a trace of benzene, making the reaction yield 7.85 g (70 mmol 71%).

<sup>1</sup>H nmr: 0.90 (t, 3H, 7-CH<sub>3</sub>), 1.22-1.38 (m, 4H, 6+5-CH<sub>2</sub>), 1.43 (m, 2H, 4-CH<sub>2</sub>), 1.71 (s, 3H, 8-CH<sub>3</sub>), 2.00 (t, 2H, 3-CH<sub>2</sub>), 4.68 (d, 2H, =CH<sub>2</sub>).

The <sup>1</sup>H nmr resonances matched those of an authentic sample.<sup>33</sup>

### (±) 1-Bromo-2-methylheptan-2-ol



The method of Langman and Dalton<sup>19</sup> was adapted to prepare this compound. 2-Methyl-1-heptene (**2.56**, 5.35 g, 47.8 mmol) and water (2.5 mL, 140 mmol) were added to 150 mL of DMSO. The stirred solution was cooled with an ice bath so that the temperature of the solution remained below 20°C, while *N*-bromosuccinimide (10.2 g, 57.3 mmol) was added in portions until the solution remained permanently yellow. After pouring the mixture into 500 g of ice-water, the product was extracted with 4 × 100 mL of diethyl ether (100 mL), and with ethyl acetate (50 mL). The combined extracts were washed consecutively with 125 mL portions of water and saturated aqueous NaCl, then dried and evaporated to yield an orange oil (10.58 g). Initial purification was achieved by flash chromatography over 100 g of silica, eluting first with 7% ethyl acetate in hexane, then 15% ethyl acetate once the sweet odour of the bromohydrin was detected. Evaporation of the solvents afforded **2.57** (8.79 g, 42.0 mmol, 88%) as a colourless oil

which was distilled by kugelrohr (85°C/0.8 mmHg) to give analytically pure material.

$^1\text{H}$  nmr: 0.90 (t, 3H, 7-CH<sub>3</sub>), 1.20-1.40 (m, 6H, CH<sub>3</sub>(CH<sub>2</sub>)<sub>3</sub>), 1.31 (s, 3H, 8-CH<sub>3</sub>), 1.55-1.65 (m, 2H, 3-CH<sub>2</sub>), 1.91 (s, 1H, OH), 3.45 (d, 1H,  $^2J = 10.2$  Hz, CHBr), 3.49 (d, 1H,  $^2J = 10.2$  Hz, CHBr).

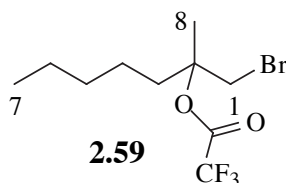
$^{13}\text{C}$  nmr: 13.9 (7), 22.5 (6), 23.6 (4), 24.9 (8), 32.1 (5), 39.9 (3), 45.3 (1), 71.3 (2).

ir (neat): 3425 s, br, asym, 2959 s, 2935 s, 2873 m, 2862 m, 1462 m, 1378 m, 1232 m, asym, 1042 s, 773 m, 670 s.

EIMS: 195 (8), 193 (12), 139 (15), 137 (16), 115 (14), 95 (32), 93 (32), 71 (97), 69 (96), 58 (89), 57 (100), 55 (68).

Found: C, 45.72; H, 8.53; N, 0.00; Br, 38.56%. C<sub>8</sub>H<sub>17</sub>BrO requires: C, 45.94; H, 8.19; N, 0.00; Br, 38.21%.

### (±) 1-Bromomethyl-1-methylhexyl Trifluoroacetate



A stirred solution of 1-bromo-2-methylheptan-2-ol (**2.57**, 8.79 g, 42.0 mmol) in dry CH<sub>2</sub>Cl<sub>2</sub> (150 mL) was cooled to 0°C. Dry pyridine (3.40 mL, 42.0 mmol) was added, followed by the dropwise addition of trifluoroacetic anhydride (5.95 mL, 42.1 mmol) over 2 minutes. The mixture was allowed to warm to room temperature then stirred for 20 minutes more. Pentane (100 mL) was added and the mixture was washed with 100 mL of water. The aqueous phase was back-extracted with 20 mL of pentane, the combined organic phases were dried, and the solvents were evaporated under reduced pressure. TLC (7% ethyl acetate in 40-60°C pet. spirit) revealed that some hydrolysis of the ester had occurred during work-up. The product was purified by flash chromatography (eluent: pentane), giving a colourless oil (12.15 g). Distillation by kugelrohr (86°C/2 mmHg) afforded analytically pure **2.59** (11.80 g, 38.7 mmol, 92%). Analysis by GC (BP1) revealed that the product contained 98.78% of the desired isomer **2.59** and 0.79% 2-bromo-1-methylhexyl trifluoroacetate (**2.66**).

$^1\text{H}$  nmr: 0.90 (t, 3H, 7-CH<sub>3</sub>), 1.25-1.40 (m, 6H, CH<sub>3</sub>(CH<sub>2</sub>)<sub>3</sub>), 1.64 (s, 3H, CH<sub>3</sub>-CO), 1.87 (m, 1H, 3-CH), 2.07 (m, 1H, 3-CH), 3.75 (d, 1H,  $^2J = 11.2$  Hz, CHBr), 3.82 (d, 1H,  $^2J = 11.2$  Hz, CHBr).

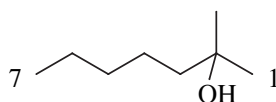
$^{13}\text{C}$  nmr: 13.9 (7), 22.3 (8), 22.4 (4\*), 22.9 (6\*), 31.6 (5), 36.63 (1<sup>†</sup>), 36.69 (3<sup>†</sup>), 87.9 (2), 114.2 (q,  $^1J^{19}\text{F}-^{13}\text{C} = 287$  Hz, CF<sub>3</sub>), 155.9 (q,  $^2J^{19}\text{F}-^{13}\text{C} = 42$  Hz, C=O).

ir (neat): 2960 s, 2935 s, 2870 m, 1780 vs, 1464 m, 1370 s, asym, 1221 vs, 1160 s, br, asym, 1040 m, 852 m, 777 s, 729 m, asym, 677 m, asym.

GCMS: 263 (0.2), 261 (0.2), 235 (5), 233 (5), 211 (16), 192 (6), 190 (6), 111 (32), 97 (70), 69 (73), 55 (100).

Found: C, 39.19; H, 5.43; N, 0.00%.  $C_{10}H_{16}BrF_3O_2$  requires: C, 39.36; H, 5.29; N, 0.00%.

**(±) 2-Methylheptan-2-ol [625-25-2]**



**2.62**

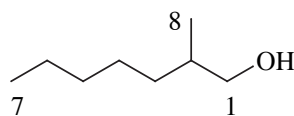
A stirred solution of methylmagnesium bromide in diethyl ether (29.0 mL of Aldrich 3.0 M solution, 87 mmol) was cooled in an ice-salt bath, while a solution of 2-heptanone (**2.55**, 8.59 g, 75.2 mmol) in 20 mL of dry diethyl ether was added dropwise, over 20 min. The mixture was heated at reflux for 30 min. The cooled mixture was poured onto 100 g of cracked ice, followed by 50 mL of 1.5 M aqueous sulfuric acid, with stirring. The aqueous phase was extracted twice with 50 mL portions of diethyl ether and the combined extracts were washed consecutively with 50 mL each of sat. aqueous  $NaHCO_3$ ,  $NaCl$  and then dried. Removal of solvent under vacuum yielded a slightly yellow oil which was distilled by kugelrohr (78°C/15 mmHg, lit.<sup>34</sup> 66-68°C/15 mmHg), providing **2.62** (8.07 g, 62.0 mmol, 82%) as a colourless oil with a pleasant smell.

$^1H$  nmr: 0.90 (t, 3H, 7- $CH_3$ ), 1.21 (s, 6H, 2 × 1- $CH_3$ ), 1.25-1.40 (m, 6H,  $CH_3(CH_2)_3$ ), 1.41-1.57 (m, 3H, 3- $CH_2$  and OH).

$^{13}C$  nmr: 14.0 (7), 22.6 (6\*), 24.0 (4\*), 29.1 (C1 x 2), 32.3 (5), 43.9 (3), 71.0 (2).

GCMS: 115 (13), 112 (2), 97 (3), 69 (8), 59 (100).

**(±) 2-Methylheptan-1-ol [60435-70-3]**



**2.63**

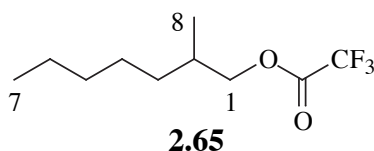
A procedure to prepare 1-hexanol by the hydroboration of 1-hexene<sup>35</sup> was adapted to prepare **2.63**. Dry conditions were used throughout the hydroboration step. A stirred solution of 2-methyl-1-heptene (**2.56**, 1.0816 g, 9.64 mmol) in dry THF (4.5 mL) was cooled to 0°C before a solution of  $BH_3:THF$  complex in THF (3.21 mL of a 1.01 M solution, standardised by hydrogen evolution from its reaction with water, 3.25 mmol) was added by syringe pump over 20 minutes. After stirring for an hour at room temperature 3.00 M aqueous  $NaOH$  solution (1.07 mL, 3.21 mmol) was added, followed

by the dropwise addition of a 29% solution of aqueous hydrogen peroxide (1.37 mL, 11.7 mmol) over 5 minutes, while cooling the reaction vessel sufficiently to keep the temperature below 35°C. Stirring at room temperature was continued for an additional 100 minutes, by which time a thick, white precipitate was present.

Water (10 mL) and diethyl ether (15 mL) were added, the mixture was filtered to remove the precipitate and the layers were separated. The aqueous layer was extracted twice more with 10 mL portions of diethyl ether and the combined organic extracts were washed thrice with 5 mL portions of saturated aqueous NaCl, then dried (MgSO<sub>4</sub>). Removal of solvents under reduced pressure yielded a colourless oil (1.28 g). This was distilled by kugelrohr (105-115°C/28 mmHg, lit.<sup>36</sup> *R* enantiomer 94-96°C/30 mmHg) to give **2.63** as a sweet smelling, colourless oil (1.16 g, 8.91 mmol, 92%) which was 98.7% pure by GC (BP1).

<sup>1</sup>H nmr: 0.89 (t, 3H, 7-CH<sub>3</sub>), 0.91 (d, 3H, 8-CH<sub>3</sub>), 1.10 (m, 1H, 3-CH), 1.20-1.45 (m, 7H, CH<sub>3</sub>(CH<sub>2</sub>)<sub>3</sub> & 3-CH), 1.60 (m, 1H, 2-CH), 1.71 (s, 1H, OH), 3.41 (dd, 1H, <sup>2</sup>*J* = 10.5 Hz, <sup>3</sup>*J* = 6.5 Hz, HOCH), 3.51 (dd, 1H, <sup>2</sup>*J* = 10.5 Hz, <sup>3</sup>*J* = 5.8 Hz, HOCH).  
<sup>13</sup>C nmr: 14.1 (7), 16.5 (8), 22.6 (6), 26.6 (4), 32.1 (5\*), 33.1 (3\*), 35.7 (2), 68.4 (1).  
 GCMS: 112 (3), 98 (4), 97 (4), 84 (11), 83 (17), 70 (31), 69 (21), 57 (100), 43 (40), 41 (53).

**(±) 2-Methyl-1-heptyl Trifluoroacetate [53800-03-6]**



A stirred mixture of 2-methylheptan-1-ol (**2.63**, 0.5058 g, 3.88 mmol) and dry sodium trifluoroacetate (0.2574 g, 1.89 mmol) was cooled to 0°C with an ice bath. Trifluoroacetic anhydride (2.71 mL, 19.2 mmol) was added dropwise over 2 min. Stirring was continued at room temperature for a further 20 minutes to complete the reaction. Pentane (25 mL) was added and the mixture was washed with 5 mL of water, then dried and evaporated carefully (volatile product) under reduced pressure. The crude product (0.83 g) was distilled by kugelrohr (85°C/60 mmHg) to give **2.65** as a colourless oil (0.81 g, 3.6 mmol, 92%) which was 98.9% pure by GC.

<sup>1</sup>H nmr: 0.89 (t, 3H, 7-CH<sub>3</sub>), 0.97 (d, 3H, 8-CH<sub>3</sub>), 1.15-1.43 (m, 8H, CH<sub>3</sub>(CH<sub>2</sub>)<sub>4</sub>), 1.90 (m, 1H, 2-CH), 4.14 (dd, 1H, <sup>2</sup>*J* = 10.6 Hz, <sup>3</sup>*J* = 6.9 Hz, 1-CH), 4.24 (dd, 1H, <sup>2</sup>*J* = 10.6 Hz, <sup>3</sup>*J* = 5.8 Hz, 1-CH).

<sup>13</sup>C nmr: 14.0 (7), 16.4 (8), 22.5 (6), 26.3 (4), 31.9 (5\*), 32.3 (2) 32.9 (3), 72.8 (1), 114.6 (q, <sup>1</sup>*J*<sup>19</sup>F-<sup>13</sup>C = 286 Hz, CF<sub>3</sub>), 157.6 (q, <sup>2</sup>*J*<sup>19</sup>F-<sup>13</sup>C = 42 Hz, C=O).

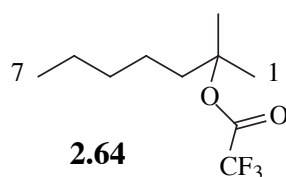


ir (neat): 2965 s, 2939 s, 2882 m, 2868 m, 1790 vs, 1474 m, asym, 1408 m, 1386 m, 1350 m, asym, 1227 vs, 1168 vs, br, 953 w, 782 m, 737 m.

EIMS: 226 (2)  $M^+$ , 155 (8), 127 (2), 126 (2), 113 (3), 112 (2), 99 (9), 98 (13), 85 (17), 71 (30), 57 (100).

Found: C, 52.83; H, 7.78; N, 0.00; F, 24.39%.  $C_{10}H_{17}F_3O_2$  requires: C, 53.09; H, 7.57; N, 0.00; F, 25.19%.

**(±) 1,1-Dimethylhexyl Trifluoroacetate [77949-48-5]**



A stirred solution of 2-methylheptan-2-ol (**2.62**, 1.50 g, 11.5 mmol) in distilled hexane (40 mL) was treated with pyridine (0.935 mL, 11.6 mmol). Trifluoroacetic anhydride (1.65 mL, 11.7 mmol) was added slowly, while cooling the reaction flask with a water bath. A thick, white precipitate was formed which stopped the mixture from being stirred. The addition of more hexane (10 mL) overcame this problem. Stirring was continued until the solid mass was broken up, then the mixture was filtered and washed with hexane (20 mL). The filtrate was washed with 20 mL of water, dried ( $MgSO_4$ ), then the solvent was carefully evaporated (volatile product) under reduced pressure and the residue was distilled by kugelrohr (100°C at 50 mmHg), to give **2.64** (2.10 g, 9.28 mmol, 81%) as a colourless oil, having a GC purity (BP1) of 99.8%.

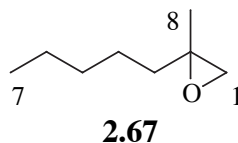
$^1H$  nmr: 0.89 (t, 3H, 7- $CH_3$ ), 1.25-1.40 (m, 6H,  $CH_3(CH_2)_3$ ), 1.54 (s, 6H, 2 × 1- $CH_3$ ), 1.80-1.85 (m, 2H, 3- $CH_2$ ).

$^{13}C$  nmr: 13.9 (7), 22.4 (6), 23.3 (4), 25.5 ( $C1 \times 2$ ), 31.8 (5), 40.3 (3), 89.3 (2), 114.5 (q,  $^1J^{19}F-^{13}C = 287$  Hz,  $CF_3$ ), 156.2 (q,  $^2J^{19}F-^{13}C = 41$  Hz,  $C=O$ ).

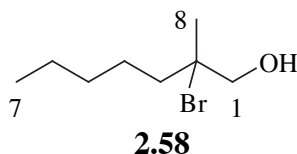
ir (neat): 2964 s, 2940 s, 2880 m, 2870 m, 1782 vs, 1474 m, asym, 1397 m, 1375 s, 1222 vs, 1160 vs, br, 876 m, 783 m, 767 m.

GCMS: 155 (100), 113 (12), 112 (12), 97 (13), 71 (12), 69 (64).

Found: C, 52.81; H, 7.79; N, 0.00%.  $C_{10}H_{17}F_3O_2$  requires: C, 53.09; H, 7.57; N, 0.00%.

**(±) 2-Methyl-2-pentyloxirane [53907-75-8]**

The sample of 2-methyl-1-heptene used in this preparation was 80% pure by GC, the remainder being benzene. A solution of 2-methyl-1-heptene (**2.56**, 1.20 g = 0.96 g alkene, 8.6 mmol) in 15 mL of CH<sub>2</sub>Cl<sub>2</sub> was stirred and cooled to 0°C. To this was added a solution of *m*-CPBA (2.4 g of stated purity 85%, 12 mmol) in 30 mL of CH<sub>2</sub>Cl<sub>2</sub>. The solution of the oxidant was dried with MgSO<sub>4</sub> before addition to remove droplets of water evident upon dissolution of the *m*-CPBA. After 30 minutes, the mixture was filtered and the solvent evaporated to yield a white, crystalline solid suspended in a colourless oil. Pentane was added and the resulting suspension was filtered to remove solid, acidic components. Evaporation of the filtrate yielded an oil which was purified by flash chromatography using 5% diethyl ether in hexane as the eluent. The epoxide **2.67** (0.62 g, 4.8 mmol, 56%) was obtained as a colourless oil. <sup>1</sup>H nmr: 0.90 (t, 3H, 7-CH<sub>3</sub>), 1.25-1.35 (m, 6H, CH<sub>3</sub>(CH<sub>2</sub>)<sub>3</sub>), 1.32 (s, 3H, CH<sub>3</sub>CO), 1.35-1.70 (m, 2H, 3-CH<sub>2</sub>), 2.65-2.72 (2 × d, 2H, CH<sub>2</sub>O). <sup>13</sup>C nmr: 14.0 (7), 20.8 (8), 22.6 (6), 24.9 (4), 31.8 (5), 36.7 (3), 53.9 (1), 57.0 (2). The partial <sup>1</sup>H nmr spectrum of **2.22** has been published<sup>37</sup> and conforms with that recorded here.

**(±) 2-Bromo-2-methylheptan-1-ol**

A method based on that of Thayer, Marvel and Hiers<sup>38</sup> was used to prepare **2.58**. Hydrobromic acid (0.8501 g of a 48% aqueous solution, 5.1 mmol), was cooled to 0°C and stirred while 2-methyl-1,2-epoxyheptane (**2.67**, 500 μL, 3.01 mmol) was added by syringe over 1 min. The mixture was allowed to warm to room temperature over 90 min, then diluted with water (15 mL) and extracted twice with 10 mL portions of CH<sub>2</sub>Cl<sub>2</sub>. The combined organic phase was washed with 5 mL of water, then dried (MgSO<sub>4</sub>) and evaporated to yield a colourless oil (0.51 g).

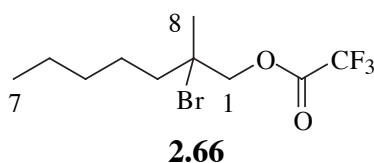
Analysis of the oil by TLC (15% diethyl ether in hexane) showed two main components of R<sub>f</sub> 0.23 and 0.25, the latter being the most abundant. By repeated flash

chromatography (eluent: ethyl acetate/hexane mixtures) of this mixture, 21.1 mg (0.101 mmol, 3.4%) of an oil was isolated, significantly enriched in the later eluting compound. The major component was identified as **2.58** since it had an identical  $^1\text{H}$  nmr spectrum to that of an isomeric by-product identified in the preparation of 1-bromo-2-methylheptan-2-ol (**2.57**). By nmr, the ratio of **2.58:2.57** was 4.7:1. Analysis by GC revealed that **2.58** largely decomposes to the epoxide **2.67** in the injector port.

$^1\text{H}$  nmr: 0.91 (t, 3H, 7- $\text{CH}_3$ ), 1.25-1.40 (m, 4H,  $\text{CH}_3(\underline{\text{CH}_2})_2$ ), 1.42-1.53 (m, 2H, 4- $\text{CH}_2$ ), 1.71 (s, 3H,  $\text{CH}_3\text{-CBr}$ ), 1.76 (m, 1H, 3- $\text{CH}$ ), 1.89 (m, 1H, 3- $\text{CH}$ ), 1.95 (s, br, 1H, OH), 3.60 (d, 1H,  $^2J = 12.2$  Hz,  $\text{CH-O}$ ), 3.66 (d, 1H,  $^2J = 12.2$  Hz,  $\text{CH-O}$ ).

$^{13}\text{C}$  nmr: 14.0 (7), 22.5 (6), 25.1 (4), 27.5 (8), 31.8 (5), 41.7 (3), 72.0 (1), 75.7 (2).

### (±) 2-Bromo-2-methylheptyl Trifluoroacetate



Compound **2.66** was prepared from a mixture of the regioisomeric bromohydrins, **2.58** and **2.57**, using the principle that esterification of a primary hydroxy group would be faster than for a tertiary hydroxyl. A stirred solution of a 4.7:1 mixture of **2.58:2.57** (9.5 mg, 0.026 mmol of 2-bromo-2-methylheptan-1-ol and 0.0055 mmol of 1-bromo-2-methylheptan-2-ol) in  $\text{CH}_2\text{Cl}_2$  (300  $\mu\text{L}$ ) was cooled to  $-78^\circ\text{C}$  with a dry ice/acetone bath. Pyridine (2.0  $\mu\text{L}$ , 0.025 mmol) was added, followed by trifluoroacetic anhydride (3.4  $\mu\text{L}$ , 0.024 mmol). The mixture was stirred overnight, the bath temperature being  $10^\circ\text{C}$  the following morning.

The mixture was treated with 1 mL of pentane, washed with 1 mL of water, dried over  $\text{MgSO}_4$  and concentrated. The residue was purified by flash chromatography (hexane as eluent) to give a colourless oil of mass (3.3 mg, 0.011 mmol, 45% w.r.t. TFAA). It was composed of 99.01% 2-bromo-2-methylheptyl trifluoroacetate (**2.66**), 0.23% 1-bromomethyl-1-methylhexyl trifluoroacetate (**2.59**) and 0.76% of the epoxide (**2.67**) by gas chromatography (BP1).

$^1\text{H}$  nmr: 0.90 (t, 3H, 7- $\text{CH}_3$ ), 1.25-1.40 (m, 4H,  $\text{CH}_3(\underline{\text{CH}_2})_2$ ), 1.45-1.55 (m, 2H, 4- $\text{CH}_2$ ), 1.76 (s, 3H, 8- $\text{CH}_3$ ), 1.80-1.90 (m, 2H, 3- $\text{CH}_2$ ), 4.44-4.53 (2  $\times$  d, 2H,  $\text{CH}_2\text{O}$ ).

### The general procedure for radical-mediated reactions of $\beta$ -bromoesters with tributyltin hydride (non-kinetic experiments)

Reactions of this type had the following elements in common. The  $\beta$ -bromoester was weighed accurately into a round-bottomed flask, fitted with a stirrer bar. The flask was fitted with a reflux condenser and placed under a nitrogen atmosphere. The desired volume of the dry and pure solvent (see Chapter 7, General Experimental), usually benzene, was added by syringe and the resulting solution was freed of oxygen by passing a gentle stream of dry nitrogen through a long needle, into the stirred solution for approximately five min.

The apparatus was lowered into a thermostatted oil bath at the desired temperature and the solution was stirred for several minutes to permit equilibration. Tributyltin hydride (or tris(trimethylsilyl)silane) was then injected. A solution of the initiator AIBN ( $T \geq 60^\circ\text{C}^{39}$ ) or di-*tert*-butyl hyponitrite ( $20^\circ\text{C} < T < 60^\circ\text{C}$ ) in the reaction solvent was then introduced in one portion (normally 1-5 mol% relative to  $\text{Bu}_3\text{SnH}$ ). If a slow addition was required, a solution of the reducing agent in the reaction solvent, together with half of the total amount of initiator, was deoxygenated and added at the desired rate by syringe pump, by routing a long needle down the reflux condenser. The other half of the initiator was placed in the reaction solution with the  $\beta$ -bromoester, prior to deoxygenation.

The progress of a reaction was monitored by GC, withdrawing samples directly from solution. To confirm that the reaction was complete, an aliquot of *ca.* 100  $\mu\text{L}$  was withdrawn, dissolved in 500  $\mu\text{L}$  of  $\text{CCl}_4$ , then injected into the gas chromatograph. Tetrachloromethane quickly consumes any remaining  $\text{Bu}_3\text{SnH}$ , so if the limiting reagent is the  $\beta$ -bromoester, the GC-detection of the  $\beta$ -bromoester indicates that the reaction was incomplete. In the case where tributyltin hydride (or tris(trimethylsilyl)silane) is the limiting reagent, there will be no change in the ratio of rearranged and non-rearranged products and no tributyltin chloride detected when the reaction is complete.

### Determination of the equilibrium constant, $K$ , for the reversible reaction 2.60 $\rightarrow$ 2.61, at $80^\circ\text{C}$ in benzene

The sample of 2-bromo-2-methylheptyl trifluoroacetate (**2.66**, 99.01% by GC) contained 0.23% of the regioisomer 1-bromomethyl-1-methylhexyl trifluoroacetate (**2.59**) and 0.76% of the epoxide 2-methyl-2-pentyloxirane (**2.67**).

The  $\beta$ -bromoester (**2.66**, 3.3 mg,  $1.1 \times 10^{-5}$  mol) was placed into a 5 mL Reactivial with a stirrer vane and purified benzene (4 mL) was added. A Mininert valve was screwed on the top of the vial and the solution was deoxygenated with a gentle stream of dry nitrogen. The vial was placed in an  $80 \pm 1^\circ\text{C}$  bath and the solution was stirred for 5 min before tributyltin hydride (3.1  $\mu\text{L}$ ,  $1.1 \times 10^{-5}$  mol) and a 0.11 M

solution of AIBN in benzene (1.0  $\mu\text{L}$ ,  $1.1 \times 10^{-7}$  mol) were quickly injected. After a total time of 2 hours the solution was cooled, concentrated by rotary evaporation and analysed by GC using a dimethylpolysiloxane (BP1) capillary.

A GC temperature program, beginning at 100°C and ramping immediately at 10°C/min to 250°C, was used. The injector temperature was 250°C. In addition to tin-containing compounds, the chromatogram displayed peaks at 5.16 (0.59%), 5.87 (35.61%) and 6.24 min (2.16%), corresponding to the compounds 1,1-dimethylhexyl trifluoroacetate (**2.64**), 2-methyl-1-heptyl trifluoroacetate (**2.65**) and 2-methylheptan-1-ol (**2.63**), respectively. However, 2-methyl-2-pentyloxirane (**2.67**) had an identical retention time with 1,1-dimethylhexyl trifluoroacetate (**2.64**) on the dimethylpolysiloxane stationary phase. In addition, there were peaks at 3.06 (0.96%) and 3.31 min (1.06%), corresponding to 2-methyl-1-heptene (**2.56**) and 2-methyl-2-heptene (**2.56a**) respectively. It is known that the tertiary ester, 1,1-dimethylhexyl trifluoroacetate (**2.64**), undergoes thermal elimination of trifluoroacetic acid in the injector port of the chromatograph, forming these alkenes and presumably does so to some extent in hot solutions as well. The corrected ratio of **2.65:2.64**, calculated with the aid of detector response factors, is  $\geq 15.1$  assuming that both the alkenes were formed from **2.64**.

**Table 2.11.** GC yields of various products on the stationary phase dimethylpolysiloxane

Compound	GC retention time (min)	Peak area (counts)
<b>2.56</b>	3.06	15248
<b>2.56a</b>	3.11	16806
<b>2.64</b> and/or <b>2.67</b>	5.16	9342
<b>2.65</b>	5.87	563670
<b>2.63</b>	6.24	34195

Separation of **2.64**, **2.65** and **2.67** was achieved using a polyethylene glycol (BP20) capillary. With a column temperature program of 50°C (5 min), 10°C/min ramp, 240°C (5 min), the respective retention times and peak integrals were **2.64** (2.81 min, 0.4652%), **2.65** (4.60 min, 24.5992%) and **2.67** (5.78 min, 0.0781%). According to these data, the ratio of **2.65:2.64** is 52.9:1. Unfortunately, it was not possible to determine the yields of the alkenes **2.56** and **2.56a** using this system.

It is concluded that the equilibrium constant,  $K$ , is greater than 15.1, but less than 52.9.

### The procedure used to conduct the kinetics experiments

Approximately 20 mL of the selected, purified solvent (hexane, benzene or propionitrile) was placed in a 50 mL pear-shaped flask sealed with a septum, then degassed by three freeze/pump/thaw cycles and stored under a dry nitrogen atmosphere. In a 10 mL SVF was weighed the desired quantity of 1-bromomethyl-1-methylhexyl trifluoroacetate (**2.59**) and biphenyl (internal standard). The exception to this is where benzene was used as the solvent pentyl acetate was the analytical standard, a known quantity of which was added to each reaction mixture immediately prior to analysis. Approximately 3 mL of the chosen reaction solvent was added to the SVF and the resulting solution was degassed in the same manner as the solvent in the pear-shaped flask. When equilibrated to 20°C, the flask was filled to the line with the pure, degassed solvent. This solution will be referred to as the stock solution.

Four Reactivials, each fitted with a stirrer vane and capped with a Mininert valve, were flushed for 5 min with dry nitrogen, then sealed to exclude oxygen. Into each vial was placed (nominally) 2.00 mL of the stock solution via a calibrated gastight syringe. Each Mininert valve was sealed and the septa—removed previously to allow larger bore needles to pass through the valves—were refitted. One vial was placed to heat and stir in each of four thermostatted ( $\pm 0.3^\circ\text{C}$ ) oil baths, set nominally to 40, 60, 80 and 100°C. After 15 min—a time at which a test experiment revealed temperature equilibration to be complete—an identical quantity of tributyltin hydride (0.9 molar eq. w.r.t. **2.59**) was injected quickly into each vial, through the Mininert valve. An injection of a solution supplying approximately 1.0 mol% (w.r.t.  $\text{Bu}_3\text{SnH}$ ) of a free-radical initiator—di-*tert*-butyl hyponitrite for the 40°C reaction and AIBN for the remainder—followed as soon as the solution was visibly homogeneous. The Mininert valve was closed and the reactions were monitored for completeness by GC, using a dimethylpolysiloxane capillary. The GC temperature program began at 100°C and ramped immediately at 10°C/min to 250°C. The injector temperature was 250°C.

It became evident that reactions may appear to be complete by GC, but some reaction was taking place in the injector port of the gas chromatograph. Therefore, in several instances, small volumes of reaction solution were "quenched" with  $\text{CCl}_4$ , which reacted with any remaining  $\text{Bu}_3\text{SnH}$ . The resulting solutions were analysed by GC and the ratios of the peaks corresponding to relevant compounds were compared to those of the non-quenched reactions (which appeared to be complete). If the ratios were identical, it was concluded that unreacted  $\text{Bu}_3\text{SnH}$  was not present in the reaction solution and hence the reaction was complete.

The quantities of the products of interest were determined by GC (at least three analyses for each solution), using calibrated detector response factors for each compound. Molar balances were found always to be  $\geq 95\%$  that of the limiting reagent,  $\text{Bu}_3\text{SnH}$ .

## 2.9 References

1. Barclay, L. R. C.; Griller, D. and Ingold, K. U. *J. Am. Chem. Soc.* **1982**, *104*, 4399.
2. Beckwith, A. L. J. and Thomas, C. B. *J. Chem. Soc., Perkin Trans. 2* **1973**, 861.
3. Barclay, L. R. C.; Luszytk, J. and Ingold, K. U. *J. Am. Chem. Soc.* **1984**, *106*, 1793.
4. Korth, H.-G.; Sustmann, R.; Groninger, K. S.; Liesung, M. and Giese, B. *J. Org. Chem.* **1988**, *53*, 4364.
5. Beckwith, A. L. J. and Duggan, P. J. *J. Chem. Soc., Perkin Trans. 2* **1993**, 1673.
6. Beckwith, A. L. J. and Duggan, P. J. *J. Am. Chem. Soc.* **1996**, *118*, 12838.
7. Gimisis, T.; Ialongo, G. and Chatgililoglu, C. *Tetrahedron* **1998**, *54*, 573.
8. Beckwith, A. L. J. and Duggan, P. J. *J. Chem. Soc. Perkin Trans. 2* **1992**, 1777.
9. Crich, D.; Huang, X. and Beckwith, A. L. J. *J. Org. Chem.* **1999**, *64*, 1762.
10. Choi, S.-Y.; Crich, D.; Horner, J. H.; Huang, X.; Newcomb, M. and Whitted, P. O. *Tetrahedron* **1999**, *55*, 3317.
11. Beckwith, A. L. J.; Crich, D.; Duggan, P. J. and Yao, Q. *Chem. Rev.* **1997**, *97*, 3273.
12. Lacôte, E. and Renaud, P. *Angew. Chem. Int. Ed. Engl.* **1998**, *37*, 2259.
13. Renaud, P.; Andrau, L.; Gerster, M. and Lacôte, E. In *Current Trends in Organic Synthesis*; Scolastico, C. and Nicotra, F., Eds.; Plenum: New York, 1999; pp 117-122.
14. Zipse, H. *J. Am. Chem. Soc.* **1997**, *119*, 1087.
15. Okamoto, Y.; Inukai, T. and Brown, H. C. *J. Am. Chem. Soc.* **1958**, *80*, 4972.
16. Menapace, L. W. and Kuivila, H. G. *J. Am. Chem. Soc.* **1964**, *86*, 3047.
17. Kuivila, H. G. *Synthesis* **1970**, 499.
18. Neumann, W. P. *Synthesis* **1987**, 665.
19. Langman, A. W. and Dalton, D. R. *Org. Synth.* **1980**, *59*, 16.
20. Beckwith, A. L. J. and Moad, G. *J. Chem. Soc. Chem. Commun.*, **1974**, 472.
21. Johnston, L. J.; Luszytk, J.; Wayner, D. D. M.; Abeywickreyma, A. N.; Beckwith, A. L. J.; Scaiano, J. C. and Ingold, K. U. *J. Am. Chem. Soc.* **1985**, *107*, 4594.

22. a) Reichardt, C. *Chem. Rev.* **1994**, *94*, 2319; b) Reichardt, C., Schäfer G. , *Liebigs Ann.* **1995**, 1579; c) Eberhardt, R., Löbbecke S., Neidhardt, B. and Reichardt C. *Liebigs Ann. /Recueil* **1997**, 1195; d) Website: [www.chemie.uni-marburg.de/~ak39/et\\_home.html](http://www.chemie.uni-marburg.de/~ak39/et_home.html)
23. Bottcher, C. J. F. *Theory of Electric Polarization*; Elsevier Scientific Pub. Co.: New York, 1973, 2nd Ed., vol. 1, p. 88.
24. Rigby, M.; Smith, E. B.; Wakeham, W. A. and Maitland, G. C. *The Forces Between Molecules*; Clarendon Press: Oxford, 1986, p. 188.
25. Smolina, T. A.; Brusova, G. P.; Shchekut'eva, L. F.; Gopius, E. D.; Permin, A. B. and Reutov, O. A. *Izv. Akad. Nauk SSSR, Ser. Khim.* **1980**, *9*, 2079.
26. Zipse, H. *Acc. Chem. Res.* **1999**, *32*, 571.
27. Abraham, M. H. and Abraham, R. J. *J. Chem. Soc. Perkin Trans. 2* **1974**, 47.
28. Mendenhall, G. D. *Tetrahedron Lett.* **1983**, *24*, 451.
29. Cerichelli, G.; Grande, C.; Luchetti, L. and Mancini, G. *J. Org. Chem.* **1991**, *56*, 3025.
30. Kraus, G. and Gottschalk, P. *J. Org. Chem.* **1983**, *48*, 2111.
31. Macey, W. A. T. *J. Phys. Chem.* **1960**, *64*, 254.
32. *Dictionary of Organic Compounds*; 5th ed.; Buckinham, J., Ed.; Chapman and Hall: New York, 1982, M-01935.
33. Aldrich *FT-NMR* **1**(1), 33A.
34. *Dictionary of Organic Compounds*; 5th ed.; Buckinham, J., Ed.; Chapman and Hall: New York, 1982, M-01918.
35. Kono, H. and Hooz, J. *Org. Synth.* **1973**, *53*, 77.
36. Sonnet, P. E. and Gazzillo, J. *Org. Prep. Proceed. Int.* **1990**, *22*, 203.
37. Quenard, M.; Bonmarin, V. and Gelbard, G. *New. J. Chem.* **1989**, *13*, 183.
38. Thayer, F. K.; Marvel, C. S. and Hiers, G. S. *Org. Synth.* **1941**, *Coll. Vol. 1*, 117.
39. Walling, C. *Free Radicals in Solution*; John Wiley, New York, 1957; pp. 467-537.
40. Crich, D. and Mo, X.-S. *J. Am Chem. Soc.* **1998**, *120*, 8298.



## Chapter 3

### A labelled-oxygen study of the regiochemistry of the $\beta$ -trifluoroacetoxyalkyl radical rearrangement

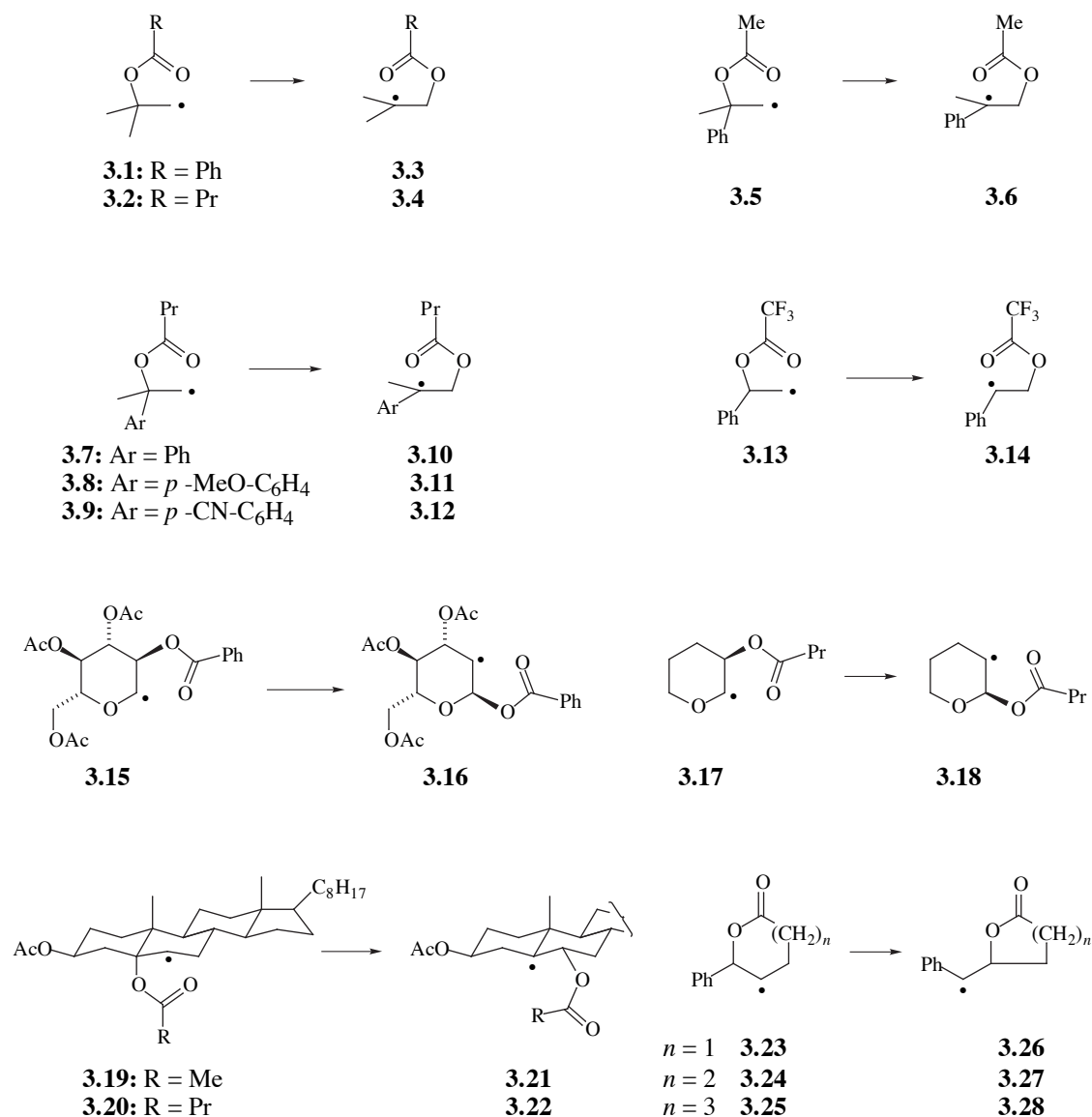
3.1	Introduction	75
3.2	Literature review	75
3.3	Choice of a suitable system for study	79
3.4	An attempt to observe the 1,2 shift of a hydroxy group in a $\beta$ -hydroxyalkyl radical	80
3.5	A study of the regiochemistry of the rearrangement <b>3.32</b> → <b>3.33</b> using $^{18}\text{O}$ -labelling techniques	81
3.6	Study of the regiochemistry of the rearrangement of <b>3.32</b> → <b>3.33</b> using $^{17}\text{O}$ nmr	95
3.7	A crossover experiment	100
3.8	An attempt to trap an ion pair intermediate	105
3.9	Discussion of results with regard to mechanism	108
3.10	Conclusions	116
3.11	Experimental	118
3.12	References	131

### 3.1 Introduction

This chapter is concerned with a study of the regiochemistry of the  $\beta$ -trifluoroacetoxyalkyl radical rearrangement. Such a study employs heavy isotopes of oxygen in order to specifically label one of the two oxygen atoms of the ester group. To place the current work in context, the chapter begins with a review of the regiochemistry of  $\beta$ -acyloxyalkyl radical rearrangements in general. The preparation of  $^{18}\text{O}$ -labelled compounds from which  $\beta$ -trifluoroacetoxyalkyl radicals may be generated, the determination of their label enrichment and the design of a mass-spectrometric method for determining the regiochemical outcome of 1,2 trifluoroacetoxy group shifts are then described. Regiochemical results are obtained for rearrangement reactions conducted in solvents of differing polarity, at different temperatures and with different concentrations of the radical-reducing agent. To verify the results from the  $^{18}\text{O}$ -labelling studies and obtain further data under different conditions, the rearrangements of  $^{17}\text{O}$ -labelled  $\beta$ -trifluoroacetoxyalkyl radicals are studied by a  $^{17}\text{O}$  nmr technique. A crossover experiment is performed to determine whether ester groups are transferred intermolecularly. An attempt is made to trap an alkene radical cation intermediate. The results and their implications for the rearrangement mechanism are discussed.

### 3.2 Literature review

Previous experiments with oxygen-labelled radicals of varying structure have provided valuable information on the regiochemistry of the  $\beta$ -acyloxyalkyl radical rearrangement. A comprehensive literature review<sup>1</sup> covers all but the most recent of the work. Data from the review have been reproduced here and updated with results published to present (table 3.1). Computational errors in the original papers have been corrected when discovered. The regiochemical results are expressed in terms of the fraction of formal 1,2 shift (**i**) observed in the rearranged product. The 1,2 shift quotient is numerically equal to the proportion of label retained by the oxygen atom of the same hybridisation in the product. A rate constant is also provided, where possible, for a temperature at or close to that under which the rearrangement reaction was conducted.



At a glance, the degree of 1,2 shift covers the complete spectrum from 0-100%. Generally, the faster the rearrangement proceeds, the higher the proportion of 1,2 shift. Polar solvents also increase the proportion of 1,2 shift, as indicated by a comparison of entries 6 and 8.

The mass-spectrometric data for the rearrangements of entries 3 and 4 indicated that the isomerizations proceeded with a high, but not total, degree of label transposition.<sup>4</sup> The authors reported complete transposition owing to the size of the uncertainties associated with the mass spectrometric enrichment results.<sup>4</sup> Results calculated using the original mass spectrometric data are displayed in table 3.1. The rearrangement of

**3.2**→**3.4** (entry 2) was studied by a  $^{13}\text{C}$  nmr technique,<sup>3</sup> as a check on the result of entry 3, further substantiating the trend that these types of simple  $\beta$ -acyloxyalkyl radical rearrangements proceed with essentially complete transposition of ester oxygens.

**Table 3.1.** A summary of the published results for oxygen-labelling experiments with various  $\beta$ -acyloxyalkyl radical rearrangements.

Entry	Rearrangement	Solvent	Temp. (°C)	% 1,2 shift	Rate constant $k_r$ ( $\text{s}^{-1}$ ) at reaction (or other specified) temperature	Ref.
1	<b>3.15</b> → <b>3.16</b>	benzene	80	~ 0	$5.2 \times 10^2$ (for acetoxy shift)	2
2	<b>3.2</b> → <b>3.4</b>	methylcyclohexane	101	~ 0	$3.6 \times 10^3$ at 75°C ( $R = \text{hex}$ )	3, 4
3	<b>3.1</b> → <b>3.3</b>	benzene	70	≤ 4	$3.9 \times 10^3$	4
4	<b>3.5</b> → <b>3.6</b>	benzene	70	≤ 6	$4.1 \times 10^4$	4
5	<b>3.9</b> → <b>3.12</b>	benzene	80	~ 0	$1.6 \times 10^4$ at 75°C	5
6	<b>3.7</b> → <b>3.10</b>	benzene	80	~ 0	$6.4 \times 10^4$ at 75°C	5
7	<b>3.13</b> → <b>3.14</b>	benzene	80	19	not measured ( $10^5$ ?)	6
8	<b>3.7</b> → <b>3.10</b>	methanol	65	25	$1.6 \times 10^5$ at 75°C	5
9	<b>3.8</b> → <b>3.11</b>	benzene	80	39	$1.7 \times 10^5$ at 75°C	5
10	<b>3.17</b> → <b>3.18</b>	benzene	80	67-75	$1.2 \times 10^4$	7
11	<b>3.20</b> → <b>3.22</b>	benzene	80	76	$2.5 \times 10^6$	3
12	<b>3.19</b> → <b>3.21</b>	benzene	80	77	not measured	8
13	<b>3.23</b> → <b>3.26</b>	benzene	80	~ 100	$9.9 \times 10^5$	9
14	<b>3.24</b> → <b>3.27</b>	benzene	80	~ 100	$1.7 \times 10^6$	9
15	<b>3.25</b> → <b>3.28</b>	benzene	80	~ 100	$1.1 \times 10^6$	9

It is clear that an increase in the amount of 1,2 shift is generally accompanied by an increase in the rearrangement rate constant,  $k_r$ . There is no direct correlation between these quantities however, since the situation is complicated by such factors as differences in the electronic properties of migrating groups, alkoxy framework structure, stereoelectronic requirements and solvent properties. But generally the fastest rearrangements favour a 1,2 shift. For example, **3.15** rearranges comparatively slowly

to radical **3.16** (entry 1) with essentially complete transposition of the ester oxygens.<sup>2</sup> In contrast, the rearrangement **3.20**→**3.22** (entry 11) proceeds 4800 times as fast and with 76% 1,2 shift.<sup>3</sup>

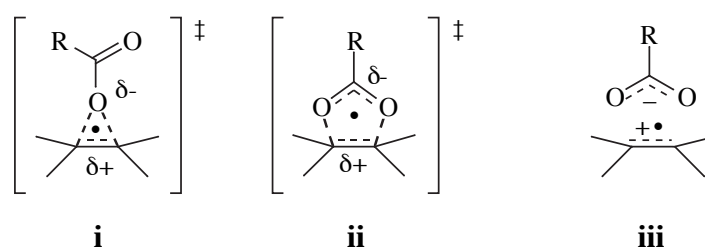
The lactone radicals **3.23-3.25** each undergo a 1-carbon ring contraction rearrangement with a rate constant of approximately  $10^6 \text{ s}^{-1}$  and with 100% 1,2 shift.<sup>9</sup> Radicals **3.23** and **3.24** are obviously constrained to the *E* conformation, but the authors point out that the eight-membered ring of **3.25** should permit a significant proportion of the lower energy *Z* conformation to be present.<sup>9</sup> Computer calculations suggest, however, that for **3.25** the 2,3 shift has a significantly higher barrier than the 1,2 shift, making the *Z* conformer relatively unreactive towards rearrangement.<sup>9</sup>

Although obtained at different temperatures, data for the rearrangement of the 2-butanoyloxy-2-phenyl-1-propyl radical (**3.7**) in benzene (0% 1,2) and methanol (25% 1,2) indicate that a more polar solvent simultaneously increases the rearrangement rate and the proportion of 1,2 shift. A study of solvent polarity upon the rearrangement rate of **3.7** obtained a correlation with the parameter  $E_T$ , of the form  $\log_{10} k_r (\text{s}^{-1}) = 0.024 E_T + 3.882$ .<sup>5</sup> This indicates a weak, yet significant, dependence of  $k_r$  upon solvent polarity. A Hammett plot for the rearrangement of radicals **3.7-3.9** resulted in a linear relationship of the form  $\log_{10}(k_{rX}/k_{rH}) = -0.71 \sigma_p^+$ , indicating that stabilisation of positive charge at the benzylic carbon has a small but significant effect upon the rate constant.<sup>5</sup> Unfortunately, an extensive study of the effect of solvent upon the rearrangement regiochemistry has not been reported for this or any other system.

Unrearranged ester products, resulting from the direct reduction of radicals **3.2**,<sup>3</sup> **3.7**,<sup>5</sup> **3.20**<sup>3</sup> and **3.23-3.25**<sup>9</sup> are reported to have experienced no scrambling of the oxygen label. However, <sup>17</sup>O-carbonyl-3-(butanoyloxy)tetrahydropyran, the unrearranged product resulting from the reaction of **3.17** with Bu<sub>3</sub>SnH, bore 6% of the label in the ether oxygen. Such scrambling of the label has important mechanistic consequences. Since the label distribution in the unrearranged product is often not reported, other systems might also experience this type of label scrambling.

A migration of the trifluoroacetoxy group in **3.13**→**3.14** resulted in 19% 1,2

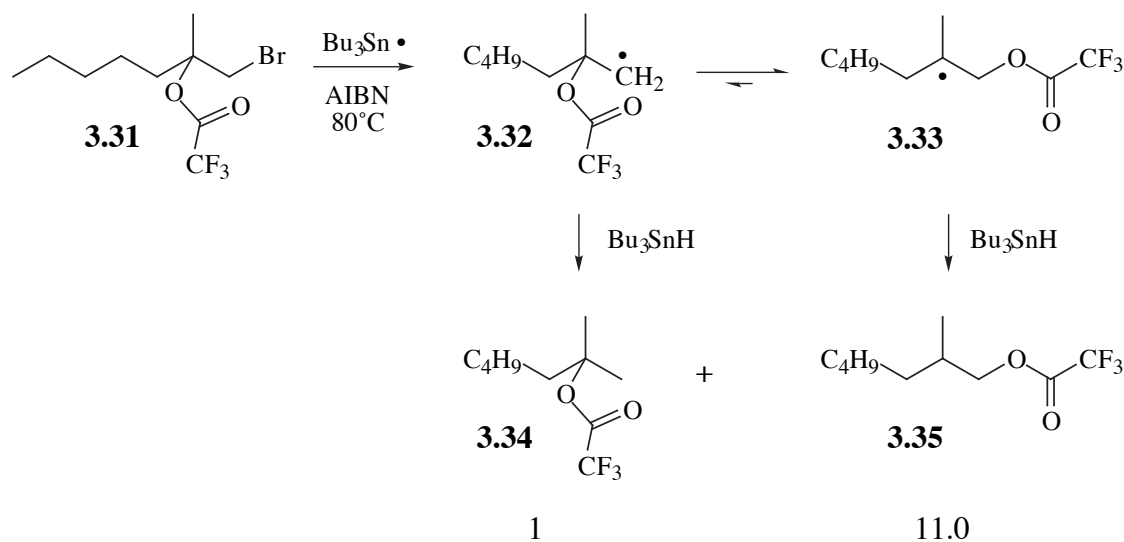
shift, whereas a ~0% 1,2 shift result might be expected for the migration of an acetoxy group in an analogous situation, if entries 2-6 are any guide. This increase in 1,2 shift suggests that there is a cooperation of 1,2 (**i**) and 3,2 (**ii**) shifts for electron-attracting migrating groups, or an involvement of an alkene radical cation/carboxylate ion intermediate (**iii**). This situation prompted an investigation into the factors affecting the regiochemistry of the  $\beta$ -trifluoroacetoxyalkyl rearrangement.



The purpose of this current work was to investigate the effect of solvent, temperature and radical-reducing agent concentration upon the regiochemistry of the rearrangement of a  $\beta$ -trifluoroacetoxyalkyl radical of invariant structure. A radical with a simple, aliphatic alkoxy framework was studied, to avoid the complications associated with the propensity for 2-aryl substituents to migrate *via* the neophyl rearrangement.<sup>5</sup> To allow for the possibility of establishing a correlation with the rearrangement rate constant, a radical identical in structure to that used for the kinetic study was used. The distribution of the oxygen label in the unrearranged product ester was also studied.

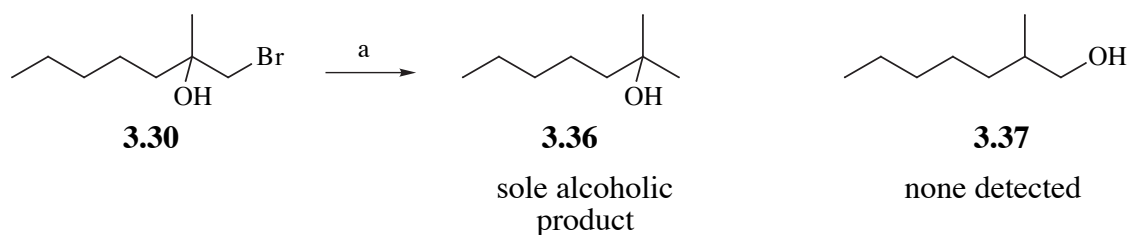
### 3.3 Choice of a suitable system for study

In chapter 2, the 2-methyl-2-trifluoroacetoxy-1-heptyl radical (**3.32**) was utilised for the kinetics study owing to the ease with which its precursors could be prepared, the rate of its rearrangement and because the products from its reactions could be manipulated easily in the laboratory. The same radical was deemed highly suitable for labelling studies, making the regiospecific oxygen-labelling of the  $\beta$ -bromoester 1-bromo-2-methyl-2-trifluoroacetoxyheptane (**3.31**) the paramount synthetic task.



### 3.4 An attempt to observe the 1,2 shift of a hydroxy group in a $\beta$ -hydroxyalkyl radical

According to the data in table 3.1, rearrangements of  $\beta$ -acyloxyalkyl radicals proceed with a proportion of 1,2 shift somewhere between 0 and 100%. The question arose as to whether it was possible to observe the analogous 1,2 shift of an OH group experimentally. To answer this question, 1-bromo-2-methylheptan-2-ol (**3.30**) was treated with  $\text{Bu}_3\text{SnH/AIBN}$  in benzene at  $80^\circ\text{C}$ . At an average tin hydride concentration of 0.013 M—a concentration at which a significant proportion ( $\geq 80\%$ ) of the  $\beta$ -trifluoroacetoxyalkyl rearrangement product (**3.35**) should form—the only alcohol detected by GC was that resulting from direct reduction, 2-methylheptan-2-ol (**3.36**). The detection limit of **3.37** was estimated at 0.15% that of the major product (**3.36**). Therefore, the rate constant for the rearrangement of 2-hydroxy-2-methyl-1-heptyl radical is less than 0.2% that of 2-methyl-2-trifluoroacetoxy-1-heptyl radical (**3.32**), i.e.  $\leq 5 \times 10^2 \text{ s}^{-1}$ .



a:  $\text{Bu}_3\text{SnH/AIBN}$ , benzene,  $80^\circ\text{C}$

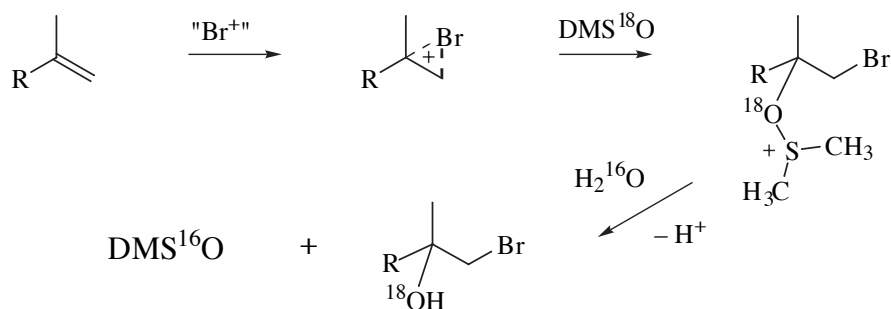
After accidentally discovering a 1,2 acetoxy group shift in a steroidal  $\beta$ -acetoxyalkyl radical, Kocovsky and coworkers went in search of the analogous 1,2 OH shift.<sup>8</sup> They were also unsuccessful in observing such a rearrangement. However, other workers at first appeared to have met with more success. Gilbert and coworkers observed the rearrangement of  $\bullet\text{CH}_2\text{CMe}_2\text{OH}$  to  $\bullet\text{CMe}_2\text{CH}_2\text{OH}$  by esr spectroscopy, under acidic aqueous conditions, although they doubted that this was a true, concerted 1,2 OH shift.<sup>10</sup> Further experiments using pulsed radiolysis and esr have established that protonation of the hydroxyl group of  $\bullet\text{CMe}_2\text{CMe}_2\text{OH}$  results in C–O bond scission, forming the tetramethylethylene radical cation by the elimination of water.<sup>11</sup> Consequently, there is good evidence that the apparent 1,2 OH shift in question occurs *via* the eliminative formation and subsequent hydration of the 2-methylpropene radical cation.

### **3.5 A study of the regiochemistry of the rearrangement 3.32→3.33 using $^{18}\text{O}$ -labelling techniques**

#### **3.5.1 Preparation of an $^{18}\text{O}$ -labelled radical precursor**

We preferred to oxygen-label the  $\beta$ -bromoester **3.31** at the *ether* position since this site is considerably less prone to exchange processes than the carbonyl oxygen. The logical precursor to the labelled  $\beta$ -bromoester **3.31a** was the bromohydrin **3.30a**. However, the standard synthetic method<sup>12</sup> of hypobromous acid addition to an alkene is uneconomical with respect to water, the intended source of labelled oxygen. Langman and Dalton<sup>13</sup> have prepared bromohydrins by the treatment of an alkene in DMSO with *N*-bromosuccinimide (NBS) and a comparatively small amount of water. Unfortunately, labelling experiments reveal that the bromohydrin oxygen comes not from water, but from dimethylsulfoxide.<sup>14</sup> Dalton and coworkers proposed that DMSO reacts with the initial bromonium ion to form a sulfoxonium intermediate which is later hydrolysed (scheme 3.1).<sup>14</sup>



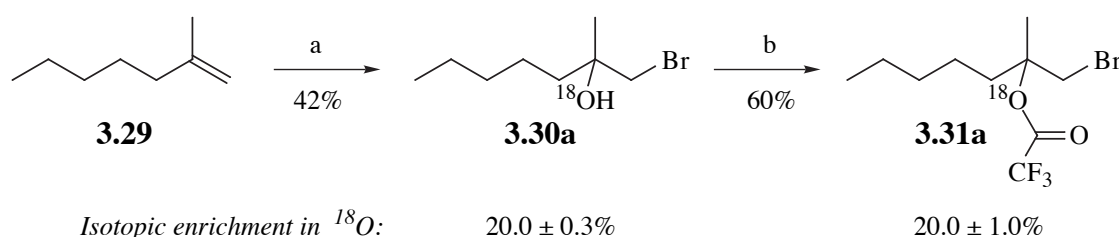


**Scheme 3.1:** Proposed mechanism<sup>14</sup> for bromohydrin formation in <sup>18</sup>O-DMSO

A new method of bromohydrin formation was therefore sought, one economical with water and avoiding solvent exchange processes which decrease the level of label enrichment. Such a procedure was developed, providing the bromohydrin in reasonable yield, with an oxygen label enrichment essentially the same as that for the labelled water.

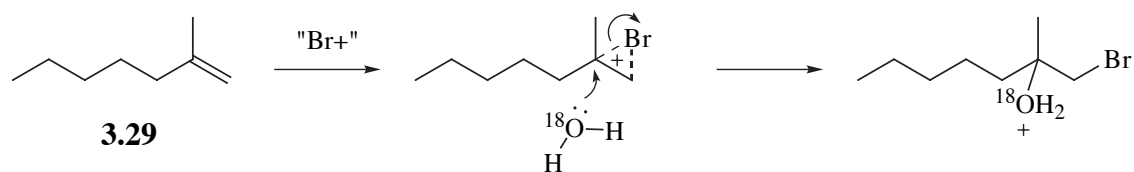
### 1-Bromo-2-methyl-2-trifluoro-oxy-<sup>18</sup>O-acetoxyheptane (20 atom%)

A solution of 2-methyl-1-heptene (**3.29**) in dry THF was treated with five molar equivalents of H<sub>2</sub><sup>18</sup>O (20.1 atom% <sup>18</sup>O, 19.9% enriched) and two equivalents of *N*-bromoacetamide (NBA) and catalytic trifluoromethanesulfonic (triflic) acid to give the labelled bromohydrin **3.30a** in 42% yield. Esterification of **3.30a** with trifluoroacetic anhydride and sodium trifluoroacetate gave the desired β-bromoester **3.31a** in reasonable yield.



a: 5 eq. H<sub>2</sub><sup>18</sup>O (20.1 atom%), 2 eq. NBA, cat. CF<sub>3</sub>SO<sub>3</sub>H, THF; b: (CF<sub>3</sub>CO)<sub>2</sub>O, NaOCOCF<sub>3</sub>

The mechanism of the labelling reaction is thought to be straightforward, the first step being electrophilic attack of positive bromine upon the double bond. Subsequent nucleophilic attack of the resulting bromonium ion with labelled water forms the protonated alcohol, which deprotonates readily. It was later discovered that triflic acid is not required to catalyse the formation of positive bromine from the *N*-bromoacetamide and so may be omitted.

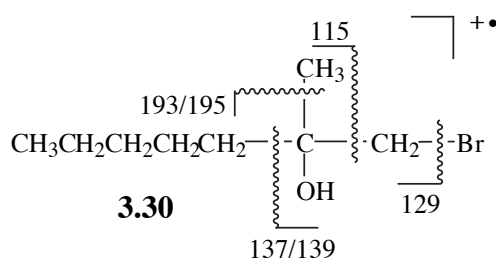


### 3.5.2 Determination of $^{18}\text{O}$ enrichment in bromohydrin **3.30a**

The presence of the  $^{18}\text{O}$  label in **3.30a** was verified by a  $^{13}\text{C}$  nmr spectrum, which contained peaks at  $\delta$  71.29 ( $^{18}\text{O}-\text{C}$ , 20.1%) and  $\delta$  71.32 ( $^{16}\text{O}-\text{C}$ , 79.9%), corresponding to the quaternary carbon resonances of the isotopomers. Percentages represent relative heights of peaks which were resolved using the Varian RESOLV nmr resolution enhancement program.

The  $\text{H}_2^{18}\text{O}$  used to label **3.30a** was hydrogen-normalised, i.e. the hydrogen isotopes were in naturally abundant proportions. Furthermore, a  $\text{D}_2\text{O}$  exchange experiment resulted in an immediate and complete disappearance of the hydroxyl resonance in the  $^1\text{H}$  nmr spectrum of **3.30a**, indicating that rapid hydroxyl proton exchange had taken place during the aqueous work-up of the bromohydrin-forming reaction. Hence, there cannot be inaccuracy in the mass spectroscopic determination of the  $^{18}\text{O}$  enrichment determination owing to an enrichment of heavy *hydrogen* isotopes at the hydroxyl proton.

The isotopic composition of **3.30a** was determined accurately using gas chromatography/mass spectrometry (GCMS). A molecular ion ( $MW$  209) was not detected. The base peak at  $m/z$  115 was ascribed to  $\text{C}_7\text{H}_{15}\text{O}^+$ , formed by loss of  $\text{BrCH}_2\cdot$  from the molecular ion as illustrated in figure 3.1. The peak group corresponding to this oxygen-containing ion was used for the isotopic analysis.



**Figure 3.1.** Some plausible fragmentation pathways for the molecular ion of unlabelled 1-bromo-2-methylheptan-2-ol ( $MW$  209), yielding ions containing oxygen

An averaged mass spectrum (5 trials) of the peak group at  $m/z$  115-119 was obtained for the unlabelled bromohydrin **3.30**. Natural abundance levels of other stable oxygen isotopes are 0.200% for  $^{18}\text{O}$  and 0.038% for  $^{17}\text{O}$ . Using the respective natural abundances, predicted mass spectra were calculated for isotopomers of **3.30** having the oxygen composed entirely of  $^{18}\text{O}$  and entirely  $^{17}\text{O}$ . The averaged mass spectrum for the labelled bromohydrin **3.30a** was treated as being a linear combination of the mass spectra of the natural abundance (**3.30**),  $^{17}\text{O}$  and  $^{18}\text{O}$  isotopomers (equation 3.1), where  $A$ ,  $B$  and  $C$  represent the respective proportions. This type of procedure was used for all analyses of oxygen isotope enrichments. Using this method, the bromohydrin **3.30a** was determined to have an  $^{18}\text{O}$  enrichment of  $20.0\pm 0.3\%$  ( $20.2\pm 0.3$  atom%  $^{18}\text{O}$ ) and a  $^{17}\text{O}$  enrichment of  $0.66\pm 0.08\%$ , where uncertainties represent one standard deviation. It is clear that the label introduction method does not significantly decrease the  $^{18}\text{O}$  enrichment in **3.30a** relative to that of the  $\text{H}_2^{18}\text{O}$  (20.1 atom%).

$$\text{Mass spectrum (3.30a)} = A (\text{3.30}) + B (\text{3.30 } ^{17}\text{O}) + C (\text{3.30 } ^{18}\text{O}) \quad (3.1)$$

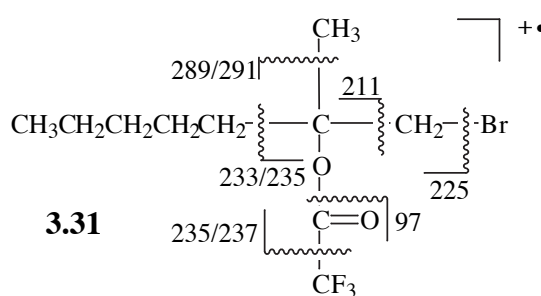
Concentrations of  $^{18}\text{O}$  label are expressed in terms of *enrichment* rather than *content*. This convention requires no further compensation for natural abundance  $^{18}\text{O}$  and thus simplifies later calculations of label distribution in the esters **3.34** and **3.35**, resulting from the radical-mediated reduction of  $\beta$ -bromoester **3.31a**. The simple relationship between  $^{18}\text{O}$  content and enrichment is given by equation 3.2.

$$\begin{aligned} \text{atom\% } ^{18}\text{O} &= \%^{18}\text{O enrichment} + 0.200\%(100\% - \%^{18}\text{O enrichment}) \\ &= 99.796(\%^{18}\text{O enrichment}) + 0.200\% \end{aligned} \quad (3.2)$$

### 3.5.3 Determination of $^{18}\text{O}$ enrichment of labelled $\beta$ -bromoester **3.31a**

A  $^{13}\text{C}$  nmr spectrum of **3.31a** contained resonances at  $\delta$  87.834 ( $^{18}\text{O-C}$ , 19.6%) and  $\delta$  87.883 ( $^{16}\text{O-C}$ , 80.4%), corresponding to the quaternary carbons at the 2-heptyl

position of the isotopomers. Isotopic enrichment was again determined by GCMS. Figure 3.2 illustrates some plausible fragmentation paths for the unlabelled bromoester. No molecular ion ( $MW$  305) was detected and neither was a peak corresponding to  $M^+ - Br\cdot$  ( $m/z$  225). The group used for the analysis was one with the lowest peak at  $m/z$  211 (16%), ascribed to  $C_9H_{14}F_3O_2^+$ , formed by the loss of  $\cdot CH_2Br$  from the molecular ion. An  $^{18}O$  enrichment of  $20.0 \pm 1.0\%$  was determined ( $0.90 \pm 0.66\%$   $^{17}O$ ), identical in magnitude to that for the labelled bromohydrin **3.30a**.



**Figure 3.2.** Some plausible fragmentation pathways for the molecular ion of natural abundance 1-bromo-2-methyl-2-trifluoroacetoxyheptane **3.31** ( $MW$  305), yielding ions containing oxygen

As a check of the integrity of the label, bromoester **3.31a** was hydrolysed back to bromohydrin **3.30a** with dilute  $K_2CO_3$  in aqueous THF at room temperature. GCMS analysis of the **3.30a** so formed indicated an  $^{18}O$  enrichment of  $20.0 \pm 0.6\%$ , demonstrating that none of the label had been displaced by base-catalysed hydrolysis. Unhydrolysed bromoester **3.31a** recovered from the reaction had a  $20.4 \pm 2.1\%$   $^{18}O$  enrichment.

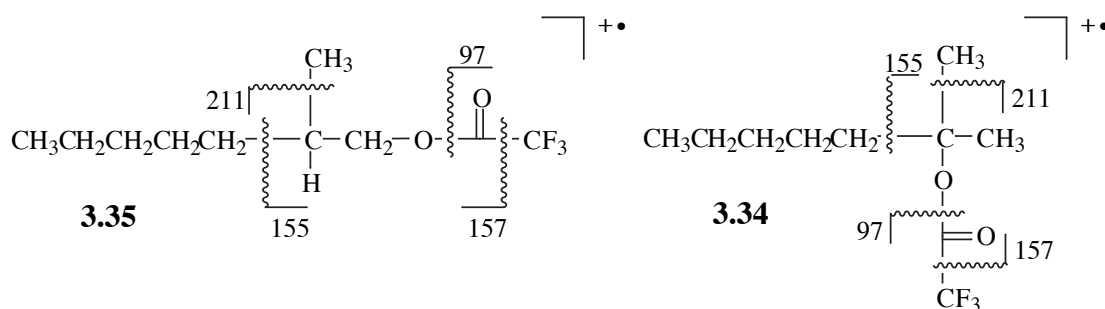
#### 3.5.4 Determination of the distribution of $^{18}O$ label in the ether and carbonyl oxygens of the product esters **3.34** and **3.35**

Unfortunately, it was not possible to establish the distribution of the  $^{18}O$  label in the product esters **3.34** and **3.35** directly by mass spectrometry alone. The GCMS spectral data ( $m/z$  (%)) for each of the unlabelled esters is provided below and relevant fragmentation pathways are illustrated in figure 3.3.

**3.35:** 169 (0.2), 157 (3), 155 (0.3), 112 (4), 99 (5), 97 (7), 83 (19), 69 (62), 57 (100).

**3.34:** 157 (0.5), 155 (100), 113 (12), 112 (12), 97 (13), 71 (12), 69 (64), 57 (27), 56 (41), 55 (40).

For an accurate determination of the enrichment of  $^{18}\text{O}$  in the entire ester group, an ion of relatively high abundance containing both oxygens is required. From figure 3.3, suitable ions have  $m/z$  of 211, 157 or 155. Unfortunately the relative abundance of each of these peaks was relatively low or zero in the GCMS of **3.35**. Such a situation makes  $^{18}\text{O}$  enrichment level determinations unreliable or impossible. The GCMS of ester **3.34** lacks a peak at  $m/z$  211, but the base peak at  $m/z$  155 provides scope for an enrichment determination. However, the peak at  $m/z$  157 corresponds not only to the  $^{18}\text{O}$  isotopomer of the  $m/z$  155 ion, but also to a structurally different ion. Such a situation is unsuitable for an accurate  $^{18}\text{O}$  enrichment determination in either **3.34** or **3.35**.

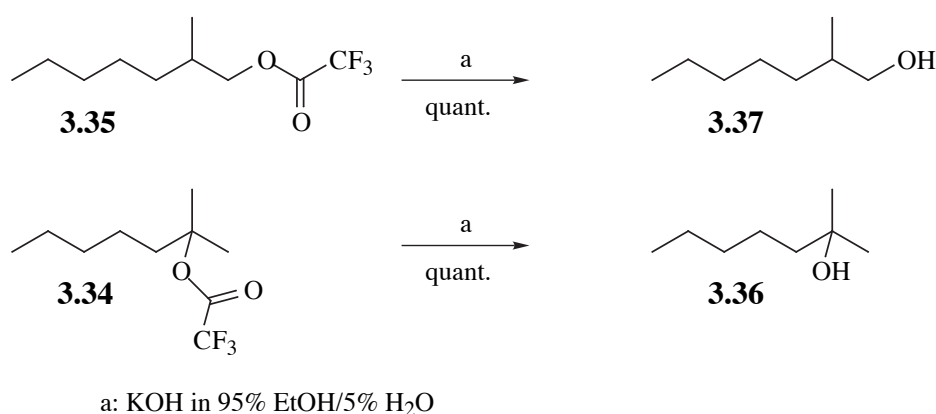


**Figure 3.3.** Some plausible fragmentation pathways for the molecular ions of unlabelled 2-methyl-1-trifluoroacetoxyheptane **3.35** and 2-methyl-2-trifluoroacetoxyheptane **3.34**, yielding ions containing one or both oxygen atoms

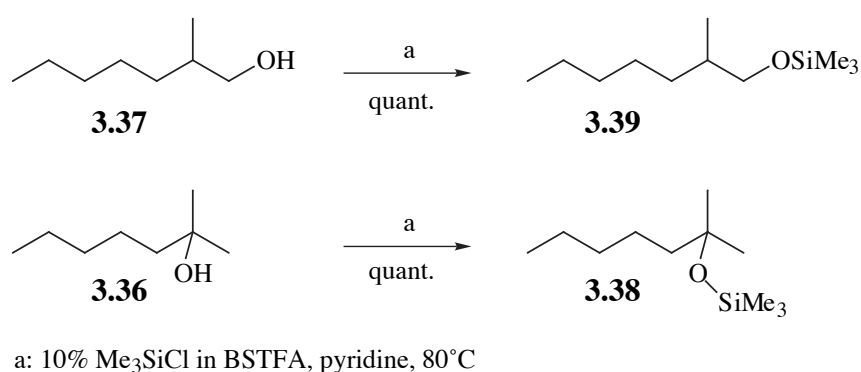
The ions corresponding to the peaks at  $m/z$  97 contained only the carbonyl oxygen of each ester group. Unfortunately, not only are such peaks low in relative abundance in the GCMS of both **3.34** and **3.35**, but in the case of **3.35** the peak at  $m/z$  99—which corresponds to a fragment ion of different structure—prohibits an accurate  $^{18}\text{O}$  determination. An indirect method of analysing the proportions of  $^{18}\text{O}$  in the ester and carbonyl oxygens of each ester was therefore developed.

With a view to determining the  $^{18}\text{O}$  enrichment of the ether oxygen alone, each

ester was hydrolysed with ethanolic hydroxide to its corresponding alcohol, as indicated below. The GCMS of 2-methylheptan-2-ol (**3.36**, *MW* 130) had a base peak at  $m/z$  59, assigned to  $C_3H_7O^+$  which was formed by loss of  $\bullet C_5H_{11}$  from the molecular ion. This oxygen-containing fragment could be used to determine the  $^{18}O$  enrichment of alcohol **3.36**. Unfortunately, the GCMS of the alcohol of greatest interest, 2-methylheptan-1-ol (**3.37**), contained no relatively intense peaks corresponding to oxygen-containing ions.



The analytical problem was finally solved by the conversion of each alcohol to its corresponding trimethylsilyl ether. To effect the derivatisation, each alcohol was treated with a large excess of both pyridine and 10%  $Me_3SiCl$  in bis(trimethylsilyl)trifluoroacetamide (BSTFA) and heated at 80°C for 20 minutes.

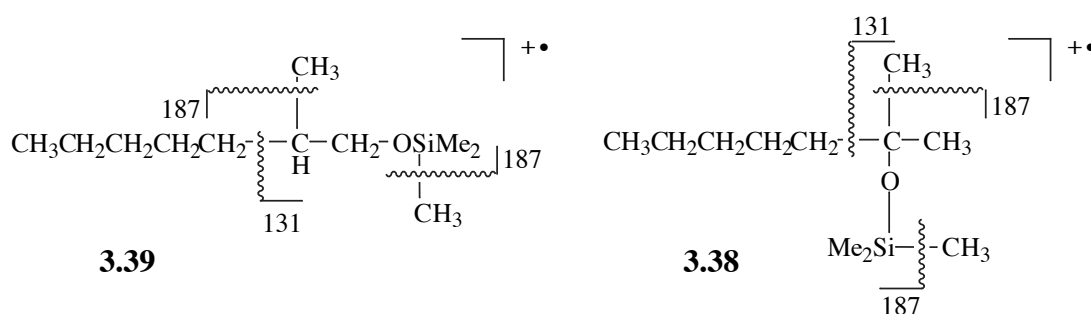


GCMS data for each TMS ether (*MW* 202) are provided below and fragmentation paths for each of the compounds **3.39** and **3.38** are displayed in figure 3.4.

**3.39**: 187 (100), 129 (5), 103 (67), 75 (96), 73 (63), 69 (13).

**3.38**: 187 (19), 131 (100), 115 (4), 75 (40), 73 (45), 61 (4).

Neither mass spectrum contained a molecular ion. However, the GCMS of the primary TMS ether **3.39** had the base peak at  $m/z$  187. This was ascribed to  $C_{10}H_{23}OSi^+$ , formed by the loss of methyl radical from  $M^+$ . The base peak for the tertiary TMS ether **3.38** appeared at  $m/z$  131. This was ascribed to  $C_6H_{15}OSi^+$ , formed from  $M^+ - \cdot C_5H_{11}$ .



**Figure 3.4.** Some of the plausible fragmentation paths for the molecular ions of the trimethylsilyl ethers **3.39** and **3.38**, yielding ions containing oxygen

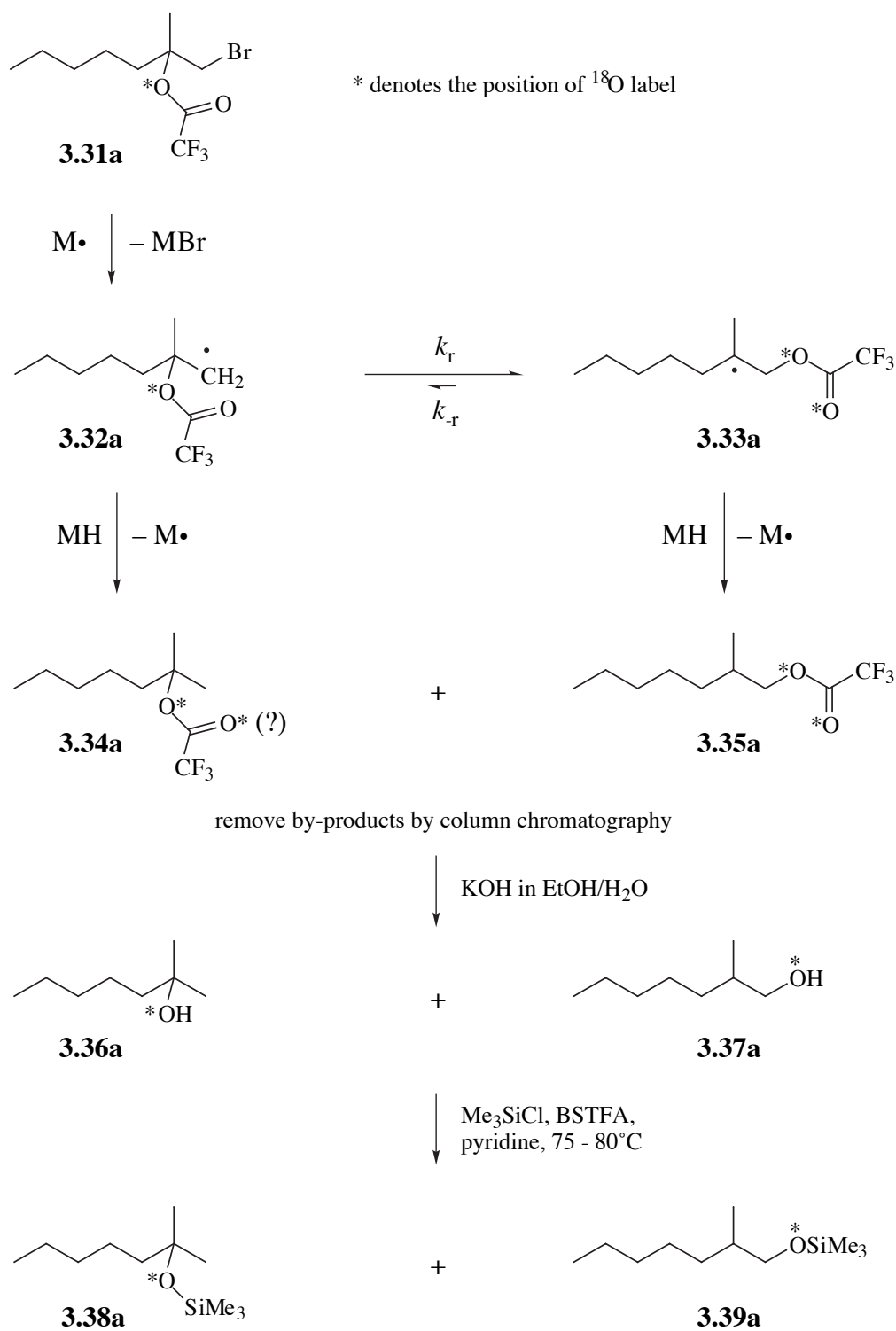
Thus, the enrichment of  $^{18}O$  in the ether oxygen of trifluoroacetate esters **3.35** and **3.34** was determined by a GCMS analysis of the respective trimethylsilyl ether derivatives **3.39** and **3.38**. Scheme 3.2 illustrates a flow diagram from the reaction of **3.31a**, through product isolation, to the derivatisation process.

Removal of the bromine atom by  $M\cdot$  (either  $Bu_3Sn\cdot$  or  $(Me_3Si)_3Si\cdot$ ) from the labelled  $\beta$ -bromoester **3.31a** produces the incipient radical **3.32a**. This primary radical can rearrange with rate constant  $k_r$  to form the tertiary product radical **3.33a**. Alternatively, it may react with the hydrogen atom source,  $MH$ , to form the non-rearranged tertiary trifluoroacetate ester **3.34a**. The rearrangement step is slightly reversible, having a reverse step rate constant of  $k_{-r}$ .

The proportion of label retained in the ether position of either ester ( $R_E$ ) is simply the  $^{18}O$  enrichment of the trimethylsilyl ether divided by the  $^{18}O$  enrichment of the labelled  $\beta$ -bromoester **3.31a** (equations 3.3, 3.4).

$$R_E(\mathbf{3.35a}) = \frac{^{18}O \text{ enrichment } \mathbf{3.39a}}{^{18}O \text{ enrichment } \mathbf{3.31a}} \quad (3.3)$$

$$R_E(\mathbf{3.34a}) = \frac{^{18}O \text{ enrichment } \mathbf{3.38a}}{^{18}O \text{ enrichment } \mathbf{3.31a}} \quad (3.4)$$



**Scheme 3.2.** Generation and subsequent reactions of  $\beta$ -trifluoroacetoxyalkyl radical **3.32a**, as well as the procedure for preparing product esters **3.34a** and **3.35a** for a determination of the  $^{18}\text{O}$  enrichment in the ether oxygen



### 3.5.5 Results

In these experiments, tris(trimethylsilyl)silane (TTMSS,  $(\text{Me}_3\text{Si})_3\text{SiH}$ ) was used instead of tributyltin hydride (TBTH,  $\text{Bu}_3\text{SnH}$ ) as the hydrogen atom source, MH. Traces of organotin compounds remaining on the GCMS injector port septum and capillary column have reportedly contaminated very dilute samples of natural products, injected frequently by other users of the same instrument. Neither TTMSS nor the products from its reaction with alkyl bromides cause this type of contamination.

TTMSS is an efficient chain transfer agent and silicon-centred radicals readily abstract bromine atoms from alkyl bromides.<sup>15</sup> It has advantages over tributyltin hydride in other regards.<sup>15-18</sup> The Si–H bond strength ( $330 \text{ kJmol}^{-1}$ ) is greater than that for Sn–H ( $309 \text{ kJmol}^{-1}$ ),<sup>16</sup> making TTMSS a less reactive H atom donor. Since  $(\text{Me}_3\text{Si})_3\text{SiH}$  reacts more slowly than  $\text{Bu}_3\text{SnH}$  with incipient radical **3.32a**, this direct reduction step competes less strongly with the rearrangement step, leading to a higher proportion of the rearranged product **3.35a** for identical initial MH concentrations.

All labelling experiments were performed in the absence of air in Reactivials fitted with Mininert<sup>19</sup> syringe valve caps (see experimental section 3.11). This apparatus permitted addition or removal of fluids during the reaction at temperatures greater than the boiling point of the solvent. A deoxygenated solution of the labelled  $\beta$ -bromoester **3.31a** in the desired solvent was heated at  $80 \pm 1^\circ\text{C}$  (or another nominated temperature) for at least two minutes, then injected with an excess of TTMSS and catalytic AIBN. When the reaction was complete by GC, the reaction was cooled and the solvent was evaporated. In the case of the water-miscible solvents acetonitrile and *N*-methylacetamide, the reaction mixture was taken up in diethyl ether, washed with water, dried and evaporated. The trifluoroacetate ester products **3.34a** and **3.35a** were separated from other components by flash chromatography, hydrolysed by aqueous base to the corresponding alcohols **3.36a** and **3.37a**, converted to the respective trimethylsilyl ethers **3.38a** and **3.39a**, then analysed by GCMS. Equations 3.3 and 3.4 were used to calculate the proportion of  $^{18}\text{O}$  label residing in the ether position of esters **3.35a** and **3.34a** respectively. The  $^{18}\text{O}$  enrichment of **3.31a** was taken to be identical

to that for the bromohydrin **3.30a**, namely  $20.0\pm 0.3\%$ . Results are displayed in table 3.2.

**Table 3.2.** Results from the AIBN-initiated reaction of  $(\text{Me}_3\text{Si})_3\text{SiH}$  with the  $^{18}\text{O}$ -labelled  $\beta$ -bromoester **3.31a** at  $80\pm 1^\circ\text{C}$ , in four different solvents.  $R_E$  represents the proportion of  $^{18}\text{O}$  label residing in the ether oxygen of the product esters **3.35a** and **3.34a**.

Entry	Solvent	Solvent dielectric constant $\epsilon$ , at $25^\circ\text{C}$	Average [TTMSS] (M)	Mole ratio <b>3.35a</b> : <b>3.34a</b>	$^{18}\text{O}$ enrichment in silylether <b>3.39a</b> (%)	$^{18}\text{O}$ enrichment in silylether <b>3.38a</b> (%)	$R_E$ for <b>3.35a</b> (%)	$R_E$ for <b>3.34a</b> (%)
1	hexane	1.88	0.029	2.00	$3.7\pm 0.4$	$20.2\pm 0.5$	<b><math>18.5\pm 2</math></b>	<b><math>101\pm 4</math></b>
2	benzene	2.27	0.029	10.1	$6.4\pm 0.4$	$19.1\pm 0.6$	<b><math>32.0\pm 2</math></b>	<b><math>95.3\pm 4</math></b>
3	benzene	2.27	0.0083	11.8	$6.7\pm 0.6$	a	<b><math>33.5\pm 4</math></b>	<b>a</b>
4	$\text{CH}_3\text{CN}$	35.94	0.029	70.3	$7.8\pm 0.4$	a	<b><math>38.8\pm 2</math></b>	<b>a</b>
5	$\text{CH}_3\text{CN}$	35.94	0.158	9.00	$6.7\pm 0.4$	$19.4\pm 1.0$	<b><math>33.7\pm 2</math></b>	<b><math>97.1\pm 6</math></b>
6	NMA <sup>b</sup>	$191.3^c$	0.083	57.2	$7.8\pm 0.4$	a	<b><math>39.2\pm 3</math></b>	<b>a</b>

a: not measured owing to insufficient amount of compound; b: *N*-methylacetamide; c: at  $32^\circ\text{C}$ . Uncertainties represent one standard deviation from the mean (68% confidence).

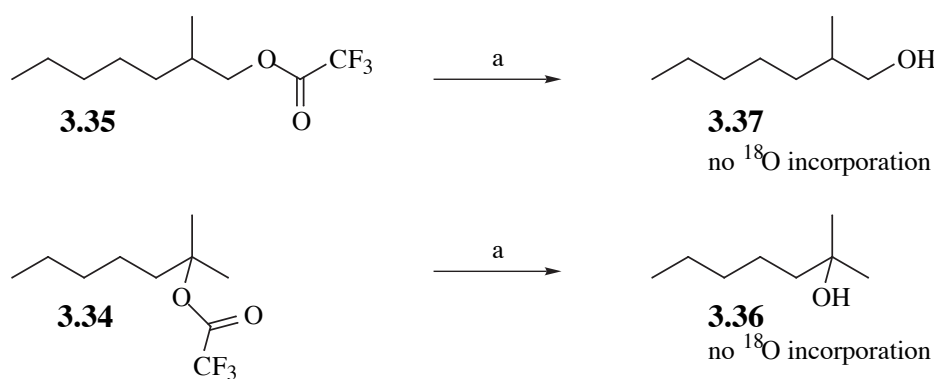
### 3.5.6 Validation of the analytical method

The values of  $R_E$  will suffer inaccuracy if there exist processes which scramble or exchange the oxygen label before the reaction of  $\beta$ -bromoester **3.31a** with  $(\text{Me}_3\text{Si})_3\text{Si}\cdot$ , or in solution after the formation of the product esters **3.34a** and **3.35a**, or during the isolation/derivatisation process to TMS ethers **3.39a** and **3.38a**. Experiments were designed to test for scrambling of the oxygen label in  $\beta$ -bromoester **3.31a** prior to rearrangement and the displacement of labelled trifluoroacetate by unlabelled hydroxide during the basic hydrolysis of esters **3.34a** and **3.35a**.

A reaction between TTMSS and **3.31a** was stopped at half-completion to establish whether scrambling of the label—by  $\text{S}_{\text{N}}1$  heterolysis then (internal) ion-pair return—had taken place. A 0.032 M solution of **3.31a** in benzene solution at  $80^\circ\text{C}$ , was treated with 0.5 equivalents of  $(\text{Me}_3\text{Si})_3\text{SiH}$  and catalytic AIBN. When the reaction was

complete, the remaining bromoester **3.31a** was separated from silicon-containing by-products by flash chromatography, then hydrolysed with aqueous 1M  $\text{K}_2\text{CO}_3$  in THF at room temperature. The resulting, purified bromohydrin had a  $20.4 \pm 1.1\%$   $^{18}\text{O}$  enrichment. At the limits of uncertainty, the oxygen label in **3.31a** is scrambled  $\leq 1.8\%$  (9 relative%), but probably not at all. When the experiment was repeated in  $\text{CH}_3\text{CN}$  solution, the resulting bromohydrin had a  $20.1 \pm 0.9\%$   $^{18}\text{O}$  enrichment, also indicating negligible oxygen scrambling.

To assess whether the basic hydrolysis of esters **3.34a** and **3.35a** decreases the  $^{18}\text{O}$  enrichment by exchange with unlabelled hydroxide/water, the unlabelled esters **3.34** and **3.35** were hydrolysed in the presence of  $^{18}\text{O}$ -labelled water.



a: 1.5 eq.  $\text{KOH}$ ,  $\frac{1}{2}$   $\text{H}_2\text{O}$ , 3.8 eq.  $\text{H}_2^{18}\text{O}$  (20.1 atom%) in dry EtOH

Esters **3.34** and **3.35** were hydrolysed separately with  $\text{KOH}$ ,  $\frac{1}{2}$   $\text{H}_2\text{O}$  and  $\text{H}_2^{18}\text{O}$  (20.1 atom%) in dry ethanol. Proportions were such that the isotopic composition of exchangeable "-OH equivalent" was calculated to be 12.5 atom%  $^{18}\text{O}$ . The alcohols **3.36** and **3.37** were isolated, converted to the corresponding TMS ethers **3.38** and **3.39** and analysed isotopically by GCMS. Compound **3.39** had an  $^{18}\text{O}$  enrichment of  $0.00 \pm 0.28\%$  and **3.38** had  $-0.03 \pm 0.27\%$ , indicating an incorporation of oxygen from the hydrolysis reagents in each case to be  $\leq 2.2$  relative%.

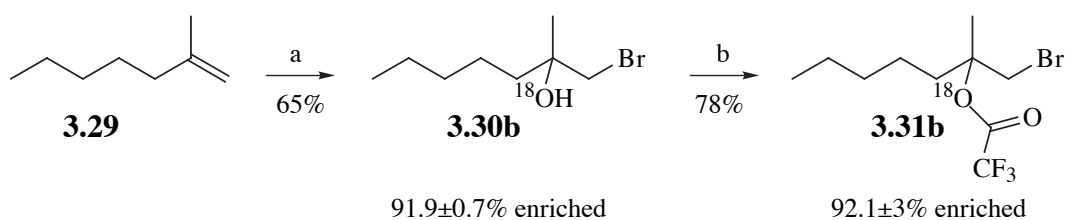
In summary, the values of  $R_E$  in table 3.2 cannot be much in error owing to label exchange or scrambling processes external to the rearrangement step. The values of  $R_E$  for **3.34a** indicate that a small amount of scrambling of the oxygen label is observed in

the non-rearranged product ester. Unfortunately, the relatively large uncertainties in  $R_E$  (**3.34a**) undermine the reliability of these results. Since a genuine scrambling of the label in **3.34a** has important mechanistic implications, it was necessary to obtain more accurate values for  $R_E$ . In an effort to achieve this, the  $\beta$ -bromoester **3.31** was prepared, possessing a much higher level of label enrichment.

### 3.5.7 Experiments with a 92 % $^{18}\text{O}$ -enriched $\beta$ -bromoester

#### 1-Bromo-2-methyl-2-trifluoro-*oxy*- $^{18}\text{O}$ -acetoxyheptane (92 atom%)

The  $^{18}\text{O}$ -labelled bromohydrin **3.30b** was prepared in reasonable yield by the treatment of 2-methyl-1-heptene (**3.29**) in dry diethyl ether with  $\text{H}_2^{18}\text{O}$  (reported 97-98 atom%) and *N*-bromoacetamide. GCMS analysis gave a  $91.9\pm 0.7\%$   $^{18}\text{O}$  enrichment for **3.30b**. Since a high integrity in the introduction of the label into bromohydrin **3.30a** (20 atom%) was realised, it is assumed that the small decrease in the  $^{18}\text{O}$  enrichment of the bromohydrin **3.30b** relative to that of the  $\text{H}_2^{18}\text{O}$  was caused by a decrease in enrichment of the labelled water by exposure (upon storage) to atmospheric moisture, or by the 2-methyl-1-heptene (**3.29**) or solvent being slightly wet.



a: 1.5 eq. NBA, 2.5 eq.  $\text{H}_2^{18}\text{O}$  (97-98%  $^{18}\text{O}$ ),  $\text{Et}_2\text{O}$ ,  $-7^\circ\text{C} \rightarrow \text{RT}$ ; b:  $(\text{CF}_3\text{CO})_2\text{O}$ , pyridine,  $\text{CH}_2\text{Cl}_2$

Esterification of **3.30b** with trifluoroacetic anhydride and pyridine in dichloromethane afforded the labelled ester **3.31b** in good yield. GCMS analysis gave an  $^{18}\text{O}$  enrichment of  $92.1\pm 3\%$ , but for a more accurate calculation of  $R_E$  values the enrichment is taken as being identical to that for the bromohydrin, **3.30b**. Reactions of **3.31b** with TTMSS and the isotopic analyses were conducted in a manner identical with that for **3.31a**. The suffix **b** denotes compounds derived from 91.9%  $^{18}\text{O}$  enriched

bromoester **3.31b**. Results appear in table 3.3.

The relatively small uncertainties confirm that  $R_E$  (**3.34b**) values are truly less than 100%. Thus, scrambling of the oxygen label in the non-rearranged product ester **3.34b** is real and significant. It is clear from the results in tables 3.2 and 3.3 that there is a substantial amount of scrambling of the  $^{18}\text{O}$  label upon migration of the ester group in  $\beta$ -trifluoroacetoxyalkyl radicals **3.32a** and **3.32b**, as indicated by  $R_E$  for the compounds **3.35a** and **3.35b**. A convincing amount of label scrambling is also evident in the unrearranged esters **3.34a** and **3.34b**. The latter results are important since they indicate that the rearrangement, or alternatively the ion-pair-forming, process is reversible.

**Table 3.3.** Results from the AIBN-initiated reaction of  $(\text{Me}_3\text{Si})_3\text{SiH}$  with the labelled  $\beta$ -bromoester **3.31b** ( $91.9\pm 0.7\%$   $^{18}\text{O}$  enriched) in benzene at different temperatures and various concentrations of  $(\text{Me}_3\text{Si})_3\text{SiH}$ .

Entry	Temperature ( $\pm 1^\circ\text{C}$ )	Average [TTMSS] (M)	Mole ratio <b>3.35b</b> : <b>3.34b</b>	$^{18}\text{O}$	$^{18}\text{O}$	$R_E$ for <b>3.35b</b> (%)	$R_E$ for <b>3.34b</b> (%)
				enrichment in silylether <b>3.39b</b> (%)	enrichment in silylether <b>3.38b</b> (%)		
1	40	0.028	4.00	$19.75\pm 0.81$	$90.53\pm 0.58$	<b><math>21.5\pm 1</math></b>	<b><math>98.5\pm 1</math></b>
2 <sup>a</sup>	80	0.029	10.1			<b><math>32.0\pm 2</math></b>	<b><math>95.3\pm 4</math></b>
3	100	0.028	12.6	$29.96\pm 1.0$	$82.11\pm 0.91$	<b><math>32.6\pm 1</math></b>	<b><math>89.4\pm 2</math></b>
4	80	0.0029	7.70	$38.06\pm 0.92$	$59.03\pm 0.60$	<b><math>41.4\pm 1</math></b>	<b><math>64.2\pm 1</math></b>

Uncertainties represent one standard deviation (68% confidence). a: From data in table 3.2

Experiments using the  $^{18}\text{O}$ -labelling GCMS technique have yielded very informative results, but suffer from several deficiencies. Despite the investigation into possible sources of error, the extent to which product esters **3.34a/b** and **3.35a/b** must be manipulated in preparation for GCMS analysis allows for the possibility of systematic errors in the results. In addition, the exclusion of  $\text{Bu}_3\text{SnH}$  as the hydrogen atom source/chain transfer agent places limitations upon the validity of comparisons between labelling and kinetic (chapter 2) experiments. Finally, the  $R_E$  values determined by the

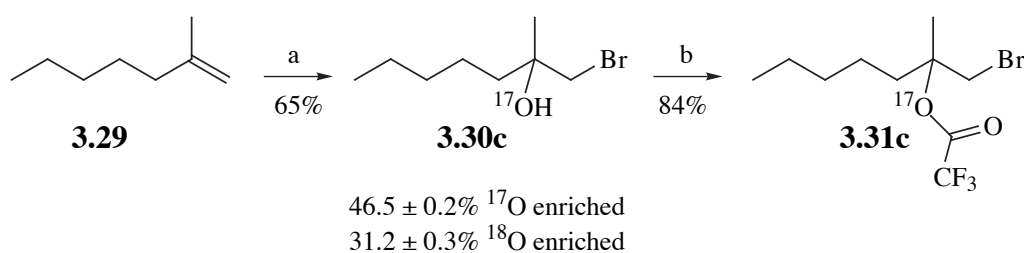
$^{18}\text{O}$ -GCMS method bear unacceptably high random uncertainties in certain instances. An analytical technique was desired which was direct, more accurate and which permitted the use of  $\text{Bu}_3\text{SnH}$ .

### 3.6 Study of the regiochemistry of the rearrangement 3.32→3.33 using $^{17}\text{O}$ nmr

The technique of  $^{17}\text{O}$  nmr spectroscopy has been used previously to successfully determine the proportions of  $^{17}\text{O}$  label in different oxygen atoms of esters.<sup>5,20-23</sup> The technique requires only the measurement of the ratio of peak integrals for ether and carbonyl  $^{17}\text{O}$  resonances.

#### 3.6.1 Preparation and characterisation of $^{17}\text{O}$ -labelled bromohydrin 3.30c and $\beta$ -bromoester 3.31c

The treatment of 2-methyl-1-heptene (**3.29**) in dry diethyl ether with 1.5 equivalents of *N*-bromoacetamide and 2.5 equivalents of  $\text{H}_2^{17}\text{O}$  (48.6 atom%  $^{17}\text{O}$ ) gave the labelled bromohydrin **3.30c** in reasonable yield. Compound **3.30c** was then trifluoroacetylated successfully to yield the desired  $\beta$ -bromoester **3.31c**. The suffix **c** denotes the presence of a  $^{17}\text{O}$  label.



a: 1.5 eq. NBA, 2.5 eq.  $\text{H}_2^{17}\text{O}$  (48.6 atom%  $^{17}\text{O}$ ),  $\text{Et}_2\text{O}$ ,  $-7^\circ\text{C} \rightarrow \text{RT}$ ; b:  $(\text{CF}_3\text{CO})_2\text{O}$ , pyridine,  $\text{CH}_2\text{Cl}_2$

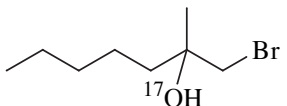
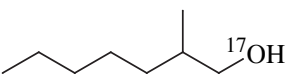
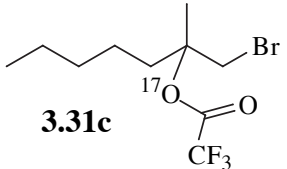
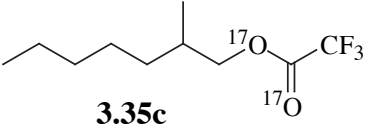
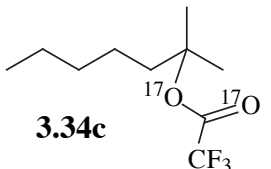
Prior to isotopic analysis by GCMS, a  $\text{CDCl}_3$  solution of the bromohydrin **3.30c** was subject to  $\text{D}_2\text{O}$  exchange nmr experiment. The hydroxyl resonance at 1.71 ppm disappeared immediately and completely. Hence, the aqueous work-up of the reaction which formed **3.30c** ensures that the hydroxyl hydrogen is normalised (at natural-

abundance isotopic composition). Using GCMS, in conjunction with an adapted version of equation 3.1, the bromohydrin **3.30c** analysed for  $46.5 \pm 0.2\%$   $^{17}\text{O}$  enrichment and  $31.2 \pm 0.3\%$   $^{18}\text{O}$  enrichment.

The presence of an  $^{18}\text{O}$  label in **3.30c** was corroborated by a  $^{13}\text{C}$  nmr spectrum containing quaternary resonances at 71.279 (58%) and 71.309 (42%) ppm, assigned to the tertiary carbons of the  $^{18}\text{O}$  and  $^{16}\text{O}$  isotopomers respectively. No resonance was detected for the  $^{17}\text{O}$  isotopomer, owing presumably to the combination of the effects of the signal multiplicity resulting from  $^{13}\text{C} - ^{17}\text{O}$  coupling (sextet) and the broadening of the  $^{13}\text{C}$  signal owing to rapid relaxation brought about by the quadrupole moment ( $I = \frac{5}{2}$ ) of the  $^{17}\text{O}$  nucleus.<sup>24</sup>

An  $^{17}\text{O}$  nmr spectrum of a pentane solution of labelled bromohydrin **3.30c** contained a single resonance, 50.6 ppm downfield of external  $\text{H}_2^{17}\text{O}$  (0 ppm), within the expected shift range of  $-40$  to  $+70$  ppm for aliphatic alcohols.<sup>25</sup> A pentane solution of the labelled  $\beta$ -bromoester **3.31c** gave a spectrum with a single peak at 176.7 ppm, assigned to the alkoxy oxygen. A normal range for alkoxy resonances is 125-210 ppm, whereas carbonyl oxygens resonate in the range 352-392 ppm.<sup>26</sup> For instance, methyl trifluoroacetate in acetonitrile at  $75^\circ\text{C}$  gives a carbonyl peak at 352.8 and an alkoxy peak at 133.0 ppm.<sup>26</sup> The chemical shifts of the various  $^{17}\text{O}$ -labelled compounds isolated during this work are displayed in table 3.4. To view some of the  $^{17}\text{O}$  nmr spectra, see appendix B.

**Table 3.4.**  $^{17}\text{O}$  nmr chemical shifts of selected compounds in pentane solution, relative to  $\text{H}_2^{17}\text{O} = 0$  ppm.

Compound	$^{17}\text{O}$ chemical shift of ether or hydroxyl oxygen (ppm)	$^{17}\text{O}$ chemical shift of carbonyl oxygen (ppm)
 <b>3.30c</b>	50.6	-
 <b>3.37c</b>	-6.3	-
 <b>3.31c</b>	176.7	not measured—carbonyl position unlabelled
 <b>3.35c</b>	148.5	356.7
 <b>3.34c</b>	186.0	363.3

### 3.6.2 Results

Reactions were performed using 50 mg (170  $\mu\text{mol}$ ) of the labelled  $\beta$ -bromoester **3.31c**. A deoxygenated solution of **3.31c** in the solvent of choice was stirred in a Reactivial or pressure bottle, fitted with a Mininert valve, at  $80\pm 1^\circ\text{C}$  for 15 min before adding 1.35 eq of  $(\text{Me}_3\text{Si})_3\text{SiH}$  (or 1.20 eq of  $\text{Bu}_3\text{SnH}$ ), followed by a solution of AIBN (5-6 mol%). The progress of the reaction was monitored by GC. When complete, a reaction involving  $(\text{Me}_3\text{Si})_3\text{SiH}$  was analysed by GCMS to determine the approximate isotopic compositions of the ester products **3.34c** and **3.35c**. With this hydrogen atom source, no ester was ever found to have a measurably lower label enrichment than the parent bromoester, hence ruling out the possibility of unlabelled oxygen exchange



processes occurring during the reaction.

The reaction mixture was carefully concentrated under reduced pressure to  $\leq 10\%$  of its initial volume and the residue (where miscible) was dissolved in pentane. An  $^{17}\text{O}$  nmr spectrum was then obtained. Where a residue was not miscible with pentane, a spectrum was run after diluting with the reaction solvent. The product trifluoroacetates **3.34c** and **3.35c** were isolated by preparative GC, using a column oven temperature of  $60^\circ\text{C}$ . A separation by flash chromatography on silica gel was attempted, but 22% (relative) of the  $^{17}\text{O}$  label was lost from the carbonyl group of rearranged ester **3.35c**, making this method of purification inappropriate. Once purified, the esters **3.34c** and **3.35c** were dissolved separately in pentane, checked for purity by GC, then analysed by  $^{17}\text{O}$  nmr. The acquisition parameters for the nmr spectrometer were optimised to ensure accurate quantification (see appendix B) and the results are displayed in table 3.5.

**Table 3.5.** Results from the AIBN-initiated reaction of the  $^{17}\text{O}$ -labelled  $\beta$ -bromoester **3.31c** with  $(\text{Me}_3\text{Si})_3\text{SiH}$  or  $\text{Bu}_3\text{SnH}$  at  $80\pm 1^\circ\text{C}$  in various solvents. Uncertainties in  $R_E$  are estimated at  $\pm 0.2$ - $0.3$  abs.%.

Solvent	Solvent dielectric constant $\epsilon_s$ , at $25^\circ\text{C}$	Reducing agent type and average concentration (mM)	Molar product ratio <b>3.35c</b> : <b>3.34c</b>	$R_E$ for <b>3.35c</b> (%)	$R_E$ for <b>3.34c</b> (%)
hexane	1.88	TTMSS, <sup>a</sup> 28.9	1.98	<b>17.7</b>	<b>98.8</b>
benzene	2.27	TTMSS, 30.2	9.15	<b>30.6</b>	<b>91.2</b>
$\text{CH}_3\text{CN}$	35.94	TTMSS, 28.9	27.0	<b>39.1</b>	not measured <sup>e</sup>
$\text{CH}_3\text{CN}$	35.94	TTMSS, 150	6.78	<b>33.3</b>	<b>95.4</b>
hexane	1.88	TBTH, <sup>b</sup> 5.95	0.752	<b>18.5</b>	<b>99.3</b>
benzene	2.27	TBTH, 6.40	4.66	<b>26.4</b>	<b>97.9</b>
$\text{CH}_3\text{CH}_2\text{CN}^c$	28.86 <sup>f</sup>	TBTH, 5.93	8.46	<b>36.0</b>	<b>96.7</b>
PFMC <sup>d</sup>	1.85 <sup>f</sup>	TBTH, 8.75	0.127	<b>44.8</b>	<b>&gt; 99.6</b>

a: Tris(trimethylsilyl)silane,  $(\text{Me}_3\text{Si})_3\text{SiH}$ ; b: Tributyltin hydride,  $\text{Bu}_3\text{SnH}$ ; c:  $\text{Bu}_3\text{SnH}$  soluble in EtCN but not  $\text{CH}_3\text{CN}$ ; d: Perfluoromethylcyclohexane,  $\text{C}_6\text{F}_{11}\text{CF}_3$ ; e: insufficient quantity; f: at  $20^\circ\text{C}$

### 3.6.3 Validation of the results

As for the  $^{18}\text{O}$  labelling work, it was necessary to establish that unanticipated label-scrambling or exchange processes which may perturb the value of  $R_E$  were not operative during reactions of **3.31c** with the reducing agent  $\text{Bu}_3\text{SnH}$  or  $(\text{Me}_3\text{Si})_3\text{SiH}$ .

A deoxygenated 0.029 M solution of the  $\beta$ -bromoester **3.31c** in dry  $\text{CH}_3\text{CN}$  was heated at  $80^\circ\text{C}$  for three hours in the presence of 5.6 mol% AIBN. A  $^{17}\text{O}$  nmr spectrum of the concentrated solution displayed a single peak at 181 ppm, with no trace of a resonance in the range 350-360 ppm (where carbonyl oxygens of these types of esters resonate<sup>26</sup>). The detection limit for the carbonyl resonance is estimated at  $\leq 0.5\%$  that of the alkoxy peak. It can be concluded that no detectable scrambling of the  $^{17}\text{O}$  label in **3.31c** takes place, even in the most polar solvent,  $\text{CH}_3\text{CN}$ .

To determine whether any scrambling of the  $^{17}\text{O}$  label in the product trifluoroacetate esters takes place after the rearrangement, solutions of **3.34c** and **3.35c** were heated under reaction conditions then analysed by  $^{17}\text{O}$  nmr. To mimic more closely actual conditions, 1-bromopentane was reduced to pentane with  $(\text{Me}_3\text{Si})_3\text{SiH/AIBN}$  in the presence of each ester. A deoxygenated benzene solution, 5.7 mM in **3.34c** and 8.9 mM in bromopentane was heated to  $80^\circ\text{C}$  and treated with  $(\text{Me}_3\text{Si})_3\text{SiH}$  (1.45 eq) and AIBN (0.043 eq). A deoxygenated benzene solution, 44.2 mM in **3.35c** and 35.4 mM in bromopentane was subject to identical temperature, and reagent proportions. Both reactions were stopped after 4.0 hours, concentrated under reduced pressure and analysed by  $^{17}\text{O}$  nmr. The results (table 3.6) indicate that no scrambling of label took place in either **3.34c** or **3.35c**, within the experimental uncertainty of  $\pm 0.2$ - $0.3\%$ .

**Table 3.6.**  $R_E$ , as determined by  $^{17}\text{O}$  nmr, for product esters **3.34c** and **3.35c** before and after being subject to radical rearrangement conditions.

Compound	$R_E$ before experiment (%)	$R_E$ after experiment (%)	Change in $R_E$ (relative%)
Rearranged <b>3.35c</b>	26.5	26.7	+0.8
Unrearranged <b>3.34c</b>	97.3	97.0	-0.3

There existed the possibility that some of the  $^{17}\text{O}$  label, in the carbonyl oxygen in particular, of **3.34c** or **3.35c** may be lost by exchange on the preparative GC packed column during purification. The benzene solution resulting from a reaction between the labelled  $\beta$ -bromoester **3.31c** and TTMSS at  $80^\circ\text{C}$  was analysed by GCMS to determine the level of  $^{17}\text{O}$  enrichment in the product trifluoroacetate esters **3.34c** and **3.35c**. Each ester was then isolated by preparative GC and the  $^{17}\text{O}$  enrichments were redetermined. It was clear from the results (table 3.7) that within experimental uncertainty there is no loss of the label during preparative GC. In summary, it may be concluded that the values of  $R_E$  in table 3.5 are free from the effects of label scrambling and/or exchange processes.

**Table 3.7.** Results of experiments designed to test for loss of  $^{17}\text{O}$  label from trifluoroacetate esters **3.35c** and **3.34c**, during separation by preparative GC.

Compound	$^{17}\text{O}$ enrichment <b>before</b> preparative GC (%)	$^{17}\text{O}$ enrichment <b>after</b> preparative GC (%)
Rearranged product <b>3.35c</b>	48.1 $\pm$ 0.7	48.9 $\pm$ 0.2
Unrearranged product <b>3.34c</b>	47.8 $\pm$ 0.2	47.9 $\pm$ 0.3

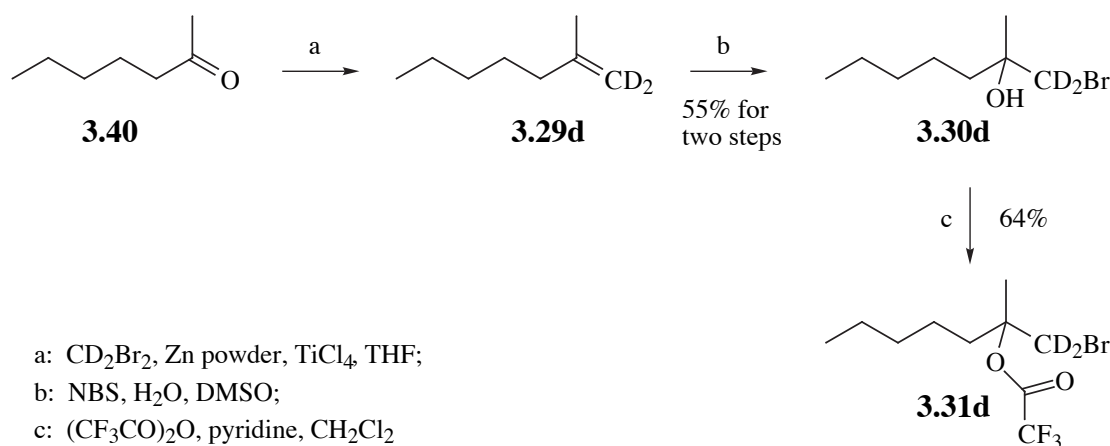
Uncertainties represent one standard deviation (68% confidence)

### 3.7 A crossover experiment

If the rearrangement of radical **3.32** to **3.33** proceeds in part by intermolecular processes, the  $R_E$  values for **3.35** and particularly **3.34**, cannot accurately represent the intramolecular regiochemistry. A crossover experiment was therefore performed to measure the limits of intermolecularity in the rearrangement step. The experiment consisted of the reaction of  $(\text{Me}_3\text{Si})_3\text{SiH}$  with an equimolar mixture of two  $\beta$ -bromoesters, one of which (**3.31b**) bears an  $^{18}\text{O}$  label in the trifluoroacetoxy group and the other (**3.31d**) possesses a  $\text{CD}_2$  label in the 2-methylheptyl moiety. Mass spectrometry was used to determine the extent of crossover.

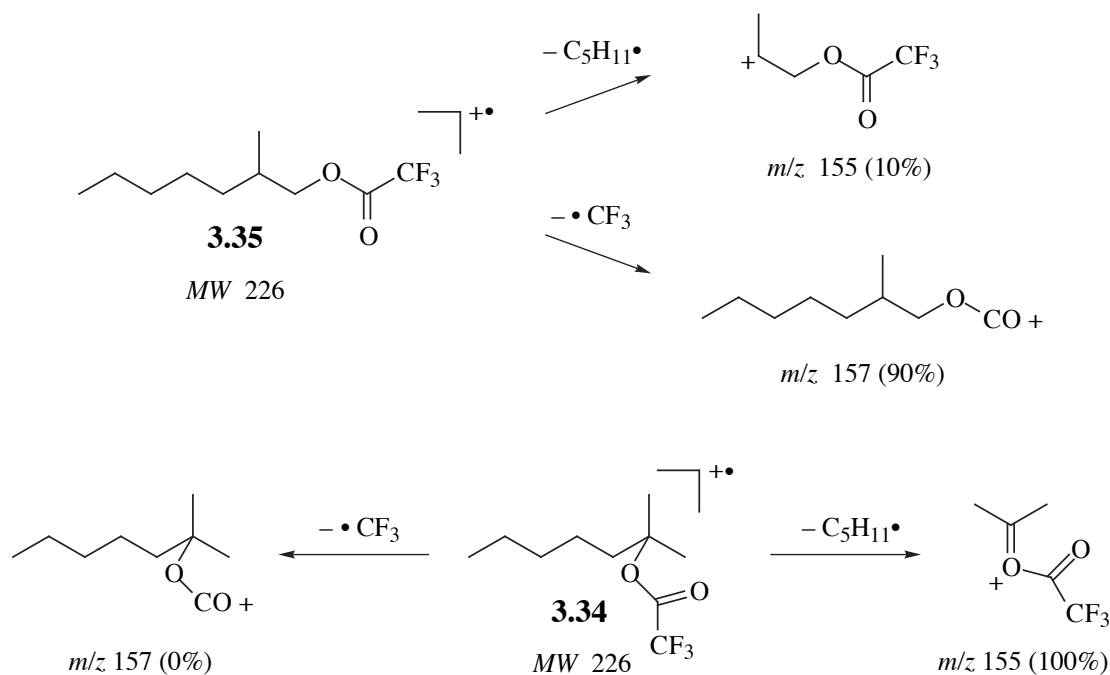
The dideuterated bromoester **3.31d** was prepared in three steps from 2-heptanone (**3.40**). A Lombardo olefination<sup>27</sup> of **3.40**—using a procedure adapted for dideuteration by Mander<sup>28</sup>—gave the deuterium-labelled alkene **3.29d**, which was not

isolated owing to its volatility. A diethyl ether solution of **3.29d** was treated with NBS in moist DMSO to form the dideuterated bromohydrin **3.30d** in reasonable yield. By GCMS it was determined that  $99.2\pm 0.5\%$  of the 1-methylene group of **3.30d** existed as  $\text{CD}_2$ . The trifluoroacetylation of **3.30d** in the usual manner afforded the labelled  $\beta$ -bromoester **3.31d**.



In an effort to locate suitable fragment ions for isotopic analysis, unlabelled product esters **3.35** and **3.34** were subject to GCMS. For the tertiary ester **3.34**, the fragment ion  $\text{C}_5\text{H}_6\text{F}_3\text{O}_2^+$  ( $m/z$  155), which was formed by loss of  $\cdot\text{C}_5\text{H}_{11}$  from  $\text{M}^{+\bullet}$ , was chosen for the analysis. For the primary ester **3.35**, the loss of  $\cdot\text{C}_5\text{H}_{11}$  from the molecular ion theoretically gives a fragment ion with  $m/z$  155, but in practice this is a disfavoured pathway. The major fragmentation route was by the loss of  $\cdot\text{CF}_3$  from the molecular ion, giving  $\text{C}_9\text{H}_{17}\text{O}_2^+$  of  $m/z$  157. This latter pathway predominated over the former by a factor of approximately 9:1 (scheme 3.3).

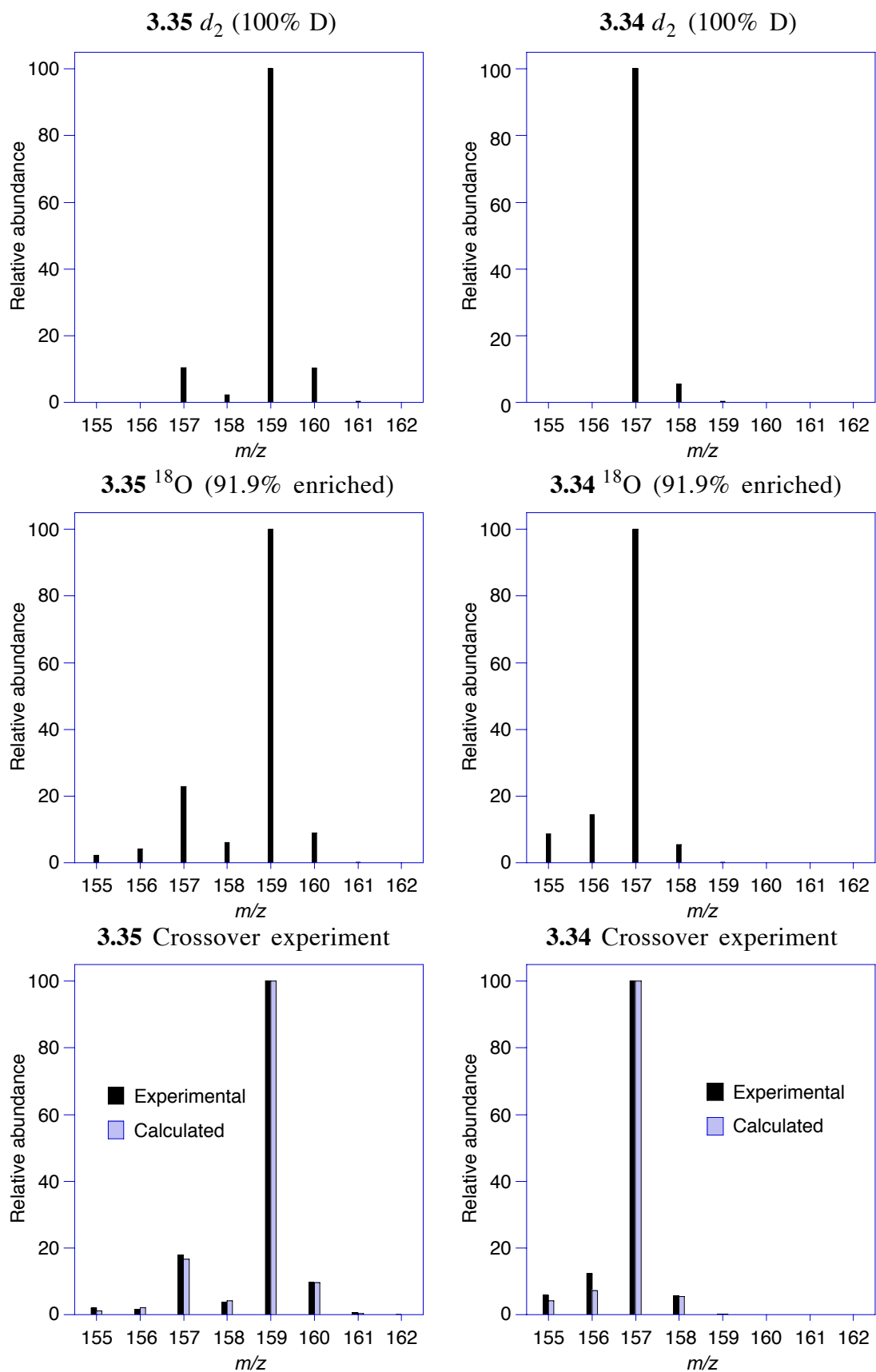
A benzene solution, 0.0192 M in the  $91.9\pm 0.7\%$   $^{18}\text{O}$  enriched bromoester **3.31b** and 0.0193 M in the  $99.2\pm 0.5$  atom%  $d_2$  bromoester **3.31d** was deoxygenated with a stream of dry nitrogen and heated to  $80^\circ\text{C}$ . Statistically,  $95.6\pm 0.6\%$  of the  $\beta$ -bromoester molecules bore either a  $\text{CD}_2$  or an  $^{18}\text{O}$  label. The solution was treated with 1.35 equivalents of TTMSS and catalytic AIBN and heated until GC indicated the absence of the  $\beta$ -bromoester peak. The molar ratio of **3.35:3.34** was 9.47:1.



**Scheme 3.3.** Competing fragmentation paths for the molecular ions of each of the product esters **3.34** and **3.35**

Three partial mass spectra (figure 3.5) are shown for each ester. The uppermost charts are calculated spectra for the completely dideuterated esters, obtained simply by adding two  $m/z$  units to the natural abundance spectrum. These spectra are expected to differ negligibly from the authentic spectra of the 99.2%  $d_2$  esters, for which experimental mass spectra were not available. The spectra in the middle are of the 91.9%  $^{18}\text{O}$  enriched esters. At the bottom a comparison is made between the product ester spectra from the crossover experiment and those calculated for zero crossover (a linear combination of the spectra of the  $\text{CD}_2$ - and  $^{18}\text{O}$ -labelled ions).

It can be seen that the calculated and the experimental crossover spectra for a particular ester are very similar, particularly at the higher  $m/z$  values. This similarity indicates that there is an insignificant amount of crossover in each case. To calculate the maximum amount of crossover it was necessary to measure the relative abundance of the peak at  $m/z$  161 in the case of **3.35** and  $m/z$  159 for **3.34**. Ions which bear both a  $d_2$  and an  $^{18}\text{O}$  label have these respective  $m/z$  values.



**Figure 3.5.** Partial mass spectra of the rearranged (**3.35**) and unrearranged (**3.34**) product esters which are  $d_2$  labelled (top),  $^{18}\text{O}$ -labelled (middle) and the result of the crossover experiment (bottom)

**Table 3.8.** Relative abundance data from partial mass spectra, for quantification of the extent of crossover. Uncertainties are at  $1\sigma$  limits (68% confidence).

$m/z$	<b>3.35</b> Crossover experimental (%)	<b>3.35</b> Crossover calculated (%)	<b>3.34</b> Crossover experimental (%)	<b>3.34</b> Crossover calculated (%)
157			100	100
159	100	100	0.21±0.09	0.25±0.09
161	0.45±0.31	0.33±0.08		

The experimental mass spectrum for **3.35** is very similar to the calculated mass spectrum. This indicates that the rearrangement of the deuterated radical **3.32d** proceeds at approximately the same rate as the  $^{18}\text{O}$ -labelled radical **3.32b**. This result is in contrast to the significant inverse kinetic isotope effects predicted by *ab initio* calculations for the 1,2 and 3,2 concerted rearrangements of 2-acyloxy-2-methyl-1-propyl radicals which are dideuterated at the radical centre.<sup>32</sup> According to these predictions, radical **3.32d** should rearrange noticeably faster than **3.32b**.

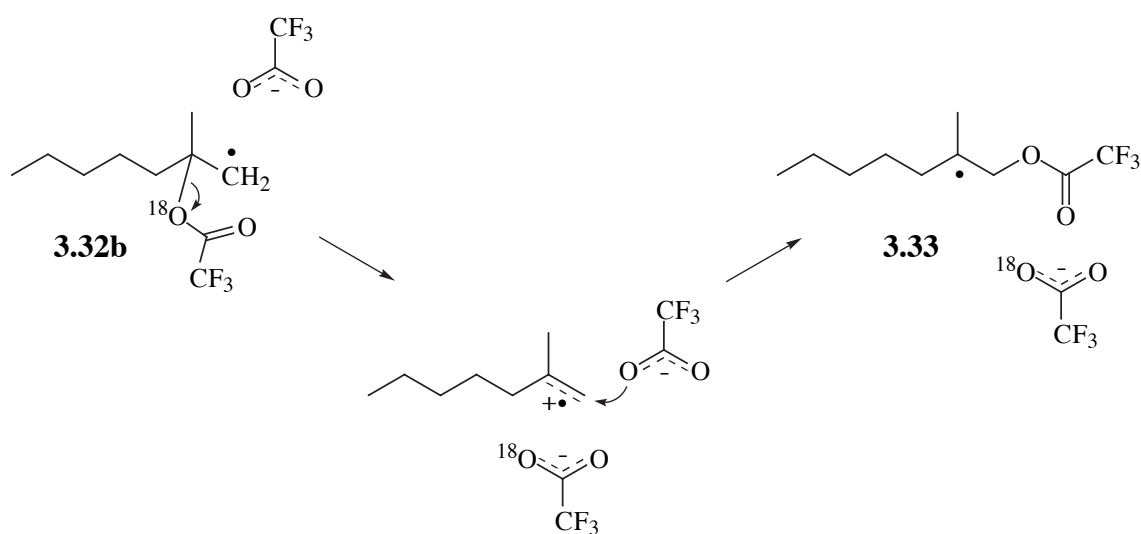
Statistically, in the absence of isotope effects, complete randomisation of all labels by crossover reactions will result in 27.2% of the molecules of a particular product ester having no label, 50.0% bearing either a  $\text{CD}_2$  or  $^{18}\text{O}$  label and 22.8% possessing both a  $\text{CD}_2$  and a  $^{18}\text{O}$  label. Theoretical partial mass spectra can now be calculated simply for the completely label-randomised products, since the relative abundances will be directly proportional to the prevalence of the corresponding isotopomers. For **3.35**, the spectrum will be  $m/z$  159 (100%) and 161 (45.6%) and for **3.34**,  $m/z$  157 (100) and 159 (45.6%). For each ester, the experimental crossover spectrum was treated as a linear combination of the randomised spectrum and the calculated spectrum for zero crossover. The maximum amount of label randomisation was calculated according to the limits of uncertainty ( $1\sigma$ ).

For the rearranged ester **3.35**, the extent of label randomisation is  $\leq 1.14\%$  and for the unrearranged ester **3.34** the amount is  $\leq 0.31\%$ . It is clear from table 3.8 that the experimental and calculated partial mass spectra are the same for a particular ester, within experimental uncertainty. It is therefore likely that there is no crossover whatsoever. It is

concluded that crossover reactions do not contribute to any significant extent towards the labelling results in tables 3.2, 3.3 and 3.5.

### 3.8 An attempt to trap an ion pair intermediate

One possible mechanism for the  $\beta$ -acyloxyalkyl radical rearrangement involves the formation and subsequent collapse of a carboxylate-anion/alkene-radical-cation pair. In the rearrangement of the  $^{18}\text{O}$ -labelled radical **3.32b**, an attempt was made to trap the 2-methyl-1-heptene radical cation with a nucleophile, unlabelled trifluoroacetate anion. A successful trapping encounter would produce the rearranged radical **3.33** by the substitution of unlabelled for labelled trifluoroacetate (scheme 3.4). It may also produce some of the unlabelled incipient radical **3.32**. Unlabelled tetraethylammonium trifluoroacetate was prepared from the reaction of aqueous tetraethylammonium hydroxide and trifluoroacetic acid and the product was dried carefully. The salt  $\text{Et}_4\text{NOCOCF}_3$  is soluble in  $\text{CH}_3\text{CN}$ , providing a convenient source of unlabelled trifluoroacetate ion. The ion pair dissociation constant,  $K$ , for  $\text{Et}_4\text{NOCOCF}_3$  is  $7 \times 10^{-3}$  M in acetonitrile at electrolyte concentrations up to  $3 \times 10^{-4}$  M.<sup>29</sup> Above this concentration, conductivity data indicates that triple ion formation occurs.<sup>29</sup>



**Scheme 3.4.** An envisaged mechanism by which the 2-methyl-1-heptene radical cation fragment would be trapped by unlabelled trifluoroacetate ion



The degree of ionisation,  $\alpha$ , of a weak electrolyte is given by equation 3.5, where  $c$  represents the concentration.<sup>30</sup> At a typical tetraethylammonium trifluoroacetate concentration of 0.78 M, the electrolyte is calculated to be  $\leq 9.0\%$  dissociated.

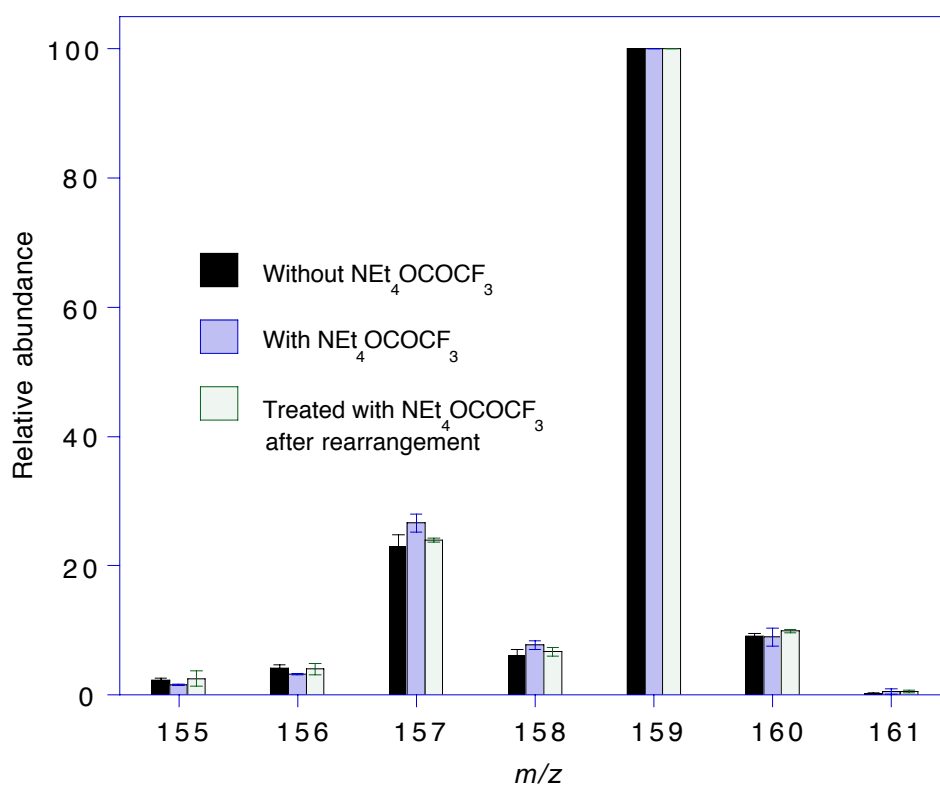
$$\alpha = \frac{K}{2c} \left( \sqrt{1 + \frac{4c}{K}} - 1 \right) \quad (3.5)$$

An initial experiment was performed to ensure that trifluoroacetate exchange does not occur by nucleophilic substitution in the  $\beta$ -bromoester **3.31b**, the (91.9 $\pm$ 0.7%) <sup>18</sup>O-enriched radical precursor. A solution of **3.31b** (0.032 M) and tetraethylammonium trifluoroacetate (0.78 M) in dry acetonitrile was heated at 80°C for 90 min. GCMS analysis yielded an <sup>18</sup>O enrichment of 91.7 $\pm$ 0.2% in the recovered **3.31b**, establishing that trifluoroacetate exchange does not occur in the radical precursor.

A 0.037 M solution of **3.31b** in dry acetonitrile containing tetraethylammonium trifluoroacetate (0.78 M) was deoxygenated, heated to 80°C and treated with 2.6 equivalents of (Me<sub>3</sub>Si)<sub>3</sub>SiH and catalytic AIBN. When the GC peak corresponding to the  $\beta$ -bromoester **3.31b** could no longer be detected, heating was ceased and the reaction mixture was analysed by GCMS. The <sup>18</sup>O enrichment in the unrearranged product ester **3.34b** was 72.7 $\pm$ 0.4%. For comparison, the same product from a control reaction (without Et<sub>4</sub>NOCOCF<sub>3</sub>) yielded an <sup>18</sup>O enrichment of 92.1 $\pm$ 0.3%. This indicates that about one fifth of the label is lost due to substitution reactions involving the unlabelled trifluoroacetate ion.

A test was devised to check whether the loss of label might have occurred simply by reaction of **3.34b** with the trifluoroacetate ion. The reaction solution from the previous control experiment (in which Et<sub>4</sub>NOCOCF<sub>3</sub> was omitted) was treated with an equal volume of a 0.78 M solution of tetraethylammonium trifluoroacetate in acetonitrile and heated at 80°C for 90 min. The ester now displayed an <sup>18</sup>O enrichment of 79.4 $\pm$ 0.8%, indicating that the loss of label in **3.34b** may well occur entirely after its formation and not from a reaction between radical **3.32b** and unlabelled trifluoroacetate.

Difficulty was encountered in measuring the  $^{18}\text{O}$  enrichment in the rearranged ester **3.35b** since two fragment ions contribute (in varying amounts) to the ester-containing peak group in the  $m/z$  155-161 range. Although reliable label enrichments could not be determined, a semi-quantitative analysis was performed by a comparison of the partial mass spectrum for **3.35b** with that for the control reaction (lacking  $\text{Et}_4\text{NOCOCF}_3$ ) and for the control reaction which was subsequently heated with  $\text{Et}_4\text{NOCOCF}_3$  (figure 3.6). It is obvious that the spectra are quite similar, so the amount of substitution of unlabelled for labelled trifluoroacetate can only be of the order of a few percent, if such a process occurs at all. As indicated by the error bars, treatment of **3.35b** with trifluoroacetate ion causes negligible incorporation of unlabelled trifluoroacetate.



**Figure 3.6.** Partial mass spectra of the rearranged ester **3.35b**, subjected to various conditions. Uncertainty bars represent one standard deviation (68% confidence).

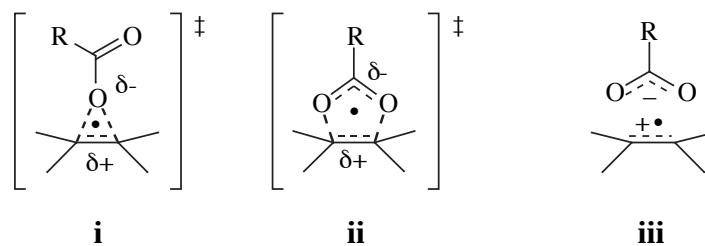
Minimum possible  $^{18}\text{O}$  enrichments of **3.35b** were calculated from the ratio of the relative abundances at  $m/z$  157 and 159. These were 80.2% for the control reaction,

80.5% for the control reaction subsequently heated with  $\text{Et}_4\text{NOCOCF}_3$  and 78.1% for the rearrangement reaction performed in the presence of  $\text{Et}_4\text{NOCOCF}_3$ . According to this data, 97.4% of the amount of label present in **3.35b** from the control experiment remained in **3.35b** when it was formed in the presence of unlabelled trifluoroacetate ion. Thus, there appeared to be very little exchange of trifluoroacetate, if any at all, during the rearrangement step. It can be concluded that if a radical ion pair is an actual intermediate it must exist as a contact ion pair (CIP) and not as a solvent-separated (SSIP), a solvent-shared ion pair, or a dissociated ion pair.

It is envisaged that more accurate results might be obtained if the experiment was repeated by conducting the TTMSS/AIBN reduction of the unlabelled  $\beta$ -bromoester **3.31** in the presence of  $\text{Et}_4\text{NOCO}^{14}\text{CF}_3$ . The product esters could be separated by preparative GC, then analysed for radioactivity by beta particle detection. Radioactivity in the product esters would indicate exchange.

### **3.9 Discussion of results with regard to mechanism**

It is clear that the rearrangement of the 2-methyl-2-trifluoroacetoxy-1-heptyl radical (**3.32**) to the 2-methyl-1-trifluoroacetoxy-2-heptyl radical (**3.33**) proceeds with neither complete positional retention nor complete transposition of the ester oxygens, but rather with considerable scrambling of the oxygen label. A formal 3,2 shift predominated over a formal 1,2 shift under all the experimental conditions of this study. An increase in the proportion of 1,2 shift in polar solvents is in agreement with theoretical predictions for a mechanism consisting of concerted 3- and 5-membered transition structures<sup>32</sup> and with labelling results from the rearrangement of the 2-butanoyloxy-2-phenyl-1-propyl radical.<sup>5</sup> In addition, the unrearranged product ester (**3.34**) displays a usually small but significant amount of scrambling of the label. Therefore, the rearrangement of **3.32** cannot occur by a single, concerted mechanism. The results dictate that the mechanism consists of the cooperation of reversible, polarized 1,2 (**i**) and 2,3 (**ii**) shifts; or involves the intermediacy of an alkene radical cation/trifluoroacetate anion pair (**iii**); or is a combination of these options.

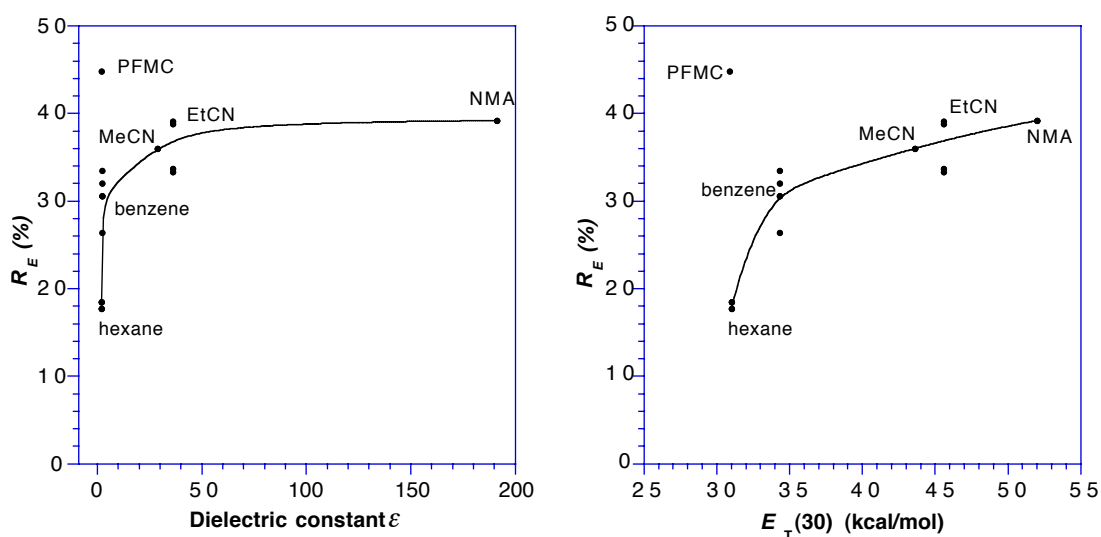


According to the various verification experiments, the results in tables 3.2, 3.3 and 3.5 are an accurate representation of the regiochemistry of the rearrangement reactions. There is good agreement between comparable  $^{17}\text{O}$  and  $^{18}\text{O}$  experiments. The crossover experiment established that there is a negligible transfer of trifluoroacetoxy groups intermolecularly. The attempt to trap the alkene radical cation of the postulated intermediate (**iii**) resulted in product esters which essentially retained their initial  $^{18}\text{O}$  enrichment levels. This last result indicates that if the intermediate **iii** is indeed operative, it cannot exist predominantly as a dissociated or solvent-separated ion pair (SSIP), but must exist as a contact ion pair (CIP), dwelling within the solvent cage.

Several trends are conspicuous from the results of the labelling experiments. For reactions performed in the same solvent, the  $R_E$  values depend little on whether the reducing/chain-transfer agent is  $\text{Bu}_3\text{SnH}$  or  $(\text{Me}_3\text{Si})_3\text{SiH}$ , indicating that the reducing agent is not implicitly involved in the actual trifluoroacetoxy group migration step. For the rearranged product ester **3.35**, the factors which result in an increase in  $R_E$  (more 1,2 shift) are increased solvent polarity, higher temperature and low reducing agent concentration. The latter variable is particularly significant, as exemplified by comparing entries 2 and 4 in table 3.3. At  $80^\circ\text{C}$ , for an average TTMSS concentration of 0.029 M,  $R_E = 32.0\%$ . However,  $R_E$  rises significantly to 41.4% at the lower average [TTMSS] of 0.0029 M.

Values of  $R_E$  for **3.35** vary from 17.7–41.4% in non-fluorinated solvents. In perfluoromethylcyclohexane (PFMC) with TBTH as the reducing agent,  $R_E$  reaches its maximum value of 44.8%. This anomalous behaviour is possibly caused by an attractive interaction between the  $\text{CF}_3$  of the trifluoroacetoxy group and the solvent, which affects the conformation of the migrating substituent.

Figure 3.7 contains plots of  $R_E$  for the rearrangement **3.32**→**3.33** against the solvent polarity parameters of dielectric constant  $\epsilon$  and  $E_T(30)$ .<sup>33</sup> The line of fit in each graph illustrates the trend that  $R_E$  decreases sharply in non-polar solvents. It is clear from both plots that the behaviour in the perfluorinated solvent PFMC is anomalous. The value of  $E_T(30)$  for PFMC has been estimated to be about the same as hexane, since the experimental value could not be found. It is clear that the solvent has a large effect on the regiochemistry of the rearrangement. It is therefore important that theoretical MO calculations take solvent effects into account.



**Figure 3.7.** Plots of  $R_E$  against dielectric constant and against  $E_T(30)$  for the rearrangement of radical **3.32** at 80°C in various solvents

It was surprising to observe the sharp decrease in  $R_E$  as the solvent changes from benzene ( $\epsilon = 2.27$ ,  $R_E = 26-34\%$ ) to hexane ( $\epsilon = 1.88$ ,  $R_E = 18-19\%$ ), whereas the vast increase in dielectric constant of acetonitrile ( $\epsilon = 35.9$ ,  $R_E = 33-39\%$ ) might be expected to produce a larger increase in  $R_E$ . According to Coulomb's equation (eq. 3.6), the dielectric constant,  $\epsilon$ , is a measure of the capacity of a medium to reduce the force,  $F$ , between two charges,  $q_1$  and  $q_2$ , separated by distance  $r$ . If the mechanism involves ion

$$F = \frac{1}{\epsilon} \frac{q_1 q_2}{4\pi\epsilon_0 r^2} \quad (3.6)$$

pairs, benzene probably promotes an increase in distance  $r$  between the oppositely-charged fragments relative to hexane since the difference in dielectric constants is considered too small by itself to cause such a large change in  $R_E$ . Alternatively, the  $\pi$ -electron cloud of the benzene ring may have enough nucleophilic character to interact with the electron-deficient carbonyl carbon of the trifluoroacetoxy group, affecting not only the regiochemistry but the rate constant of the rearrangement. Such interactions have been used previously to explain the large difference in the rate of solvolysis of 1-acetoxy-2-bromopropane in octane and in benzene.<sup>31</sup>

If the mechanism for the rearrangement of radical **3.32** involves the cooperation of concerted 1,2 (**i**) and 3,2 (**ii**) shifts, then the increase in  $R_E$  in polar solvent implies that the 3-membered transition structure **i** is more polarized than the 5-membered structure **ii**. Theoretical calculations of carboxylate group charge for the ground state (**3.32**-like) and for structures **i** and **ii** ( $R = CF_3$ ) indicate that the charge separation in structures **i** and **ii** is essentially the same,<sup>32</sup> conflicting with the mechanistic hypotheses of some experimental chemists.<sup>1,5</sup>

The regiochemistry of the rearrangement of the 2-methyl-2-trifluoroacetoxy-1-heptyl radical (**3.32**) resembles that of the 2-phenyl-2-trifluoroacetoxyethyl radical (**3.13**,  $R_E = 19\%$ ), and also that of the 2-aryl-2-butanoyloxypropyl radicals **3.7** (25% in methanol) and **3.8** (39%). Like **3.7**, radical **3.32** experiences greater label scrambling as solvent polarity increases.

From the data in table 3.3 it can be seen that  $R_E$  increases at higher temperatures. This indicates that a greater randomisation of the label is taking place in the radical cation/carboxylate anion pair intermediate (**iii**) at higher temperatures, or alternatively that the activation energy for a concerted 1,2 shift (**i**) is greater than that for a 3,2 shift (**ii**). In latter alternative, it is possible to estimate the difference in activation energy,  $\Delta E_a$ , and Arrhenius frequency factor,  $A$ , between the two transition states. The ratio of rate constants from the 3,2 and 1,2 rearrangements can be calculated simply from the regiochemical results (table 3.9). The Arrhenius expressions (equations 3.7 and 3.8) for the two competing rate constants,  $k_{3,2}$  and  $k_{1,2}$  are:

$$k_{3,2} = A_{3,2} e^{-\left(\frac{Ea_{3,2}}{RT}\right)} \quad (3.7)$$

$$k_{1,2} = A_{1,2} e^{-\left(\frac{Ea_{1,2}}{RT}\right)} \quad (3.8)$$

Division of equation 3.7 by 3.8 gives:

$$\frac{k_{3,2}}{k_{1,2}} = \frac{(100 - R_E)\%}{R_E\%} = \frac{A_{3,2}}{A_{1,2}} e^{-\left(\frac{Ea_{3,2} - Ea_{1,2}}{RT}\right)} \quad (3.9)$$

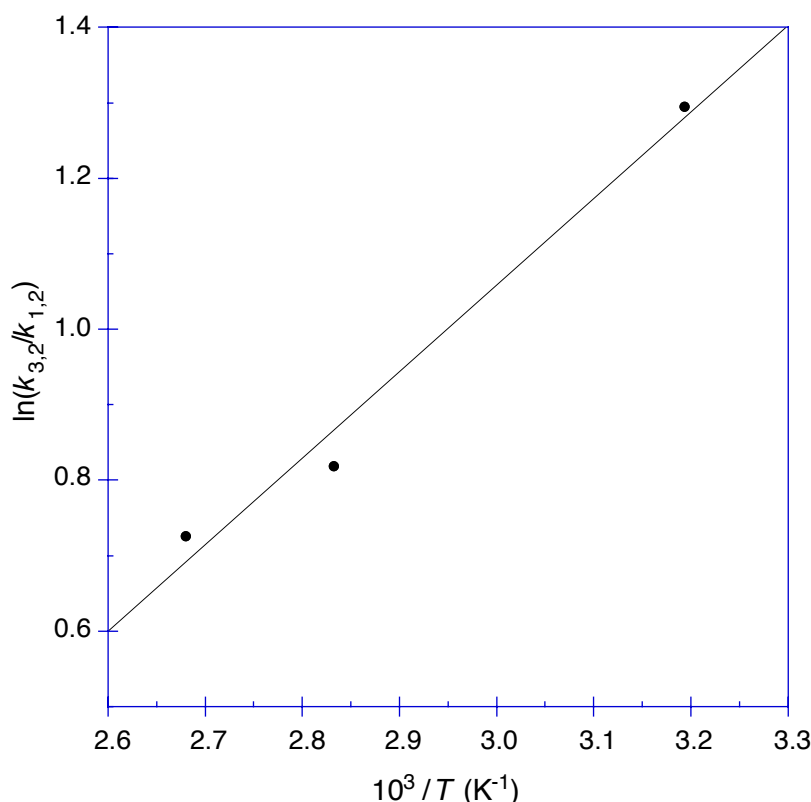
$$\text{and so } \ln\left(\frac{k_{3,2}}{k_{1,2}}\right) = \ln\left(\frac{(100 - R_E)\%}{R_E\%}\right) = \frac{-(Ea_{3,2} - Ea_{1,2})}{RT} + \ln\left(\frac{A_{3,2}}{A_{1,2}}\right) \quad (3.10)$$

**Table 3.9.**  $R_E$  data<sup>a</sup> at several temperatures,<sup>b</sup> from which the difference in Arrhenius parameters between hypothetical 3,2 and 1,2 mechanisms may be approximated

Temperature (°C)	$R_E$ (%)	$\left(\frac{(100 - R_E)\%}{R_E\%}\right)$	$\ln\left(\frac{(100 - R_E)\%}{R_E\%}\right)$
40	21.5	3.65	1.30
80	30.6 <sup>c</sup>	2.27	0.819
100	32.6	2.07	0.726

a: From table 3.3; b: benzene solution; c: From table 3.5

Figure 3.8 is a plot of  $\ln(k_{3,2}/k_{1,2})$  against  $1/T$ . A good data fit was achieved with a line of equation  $\ln(k_{3,2}/k_{1,2}) = -2.377 + 1145/T$  ( $R^2 = 0.9807$ ). The gradient of 1145 K corresponds to  $(Ea_{1,2} - Ea_{3,2}) = 9.5 \text{ kJmol}^{-1}$  and the intercept of  $-2.38$  corresponds to  $\log_{10}(A_{3,2}/A_{1,2}) = -1.03$ . By this analysis, the 3-centred pericyclic process has a higher activation energy and a larger  $A$  factor than that for the 5-centred process, consistent with a transition structure requiring the constraint of one less degree of rotational freedom, but possessing more ring strain.



**Figure 3.8.** Plot of  $\ln(k_{3,2}/k_{1,2})$  against  $1/T$  for the rearrangement of radical **3.32b**.

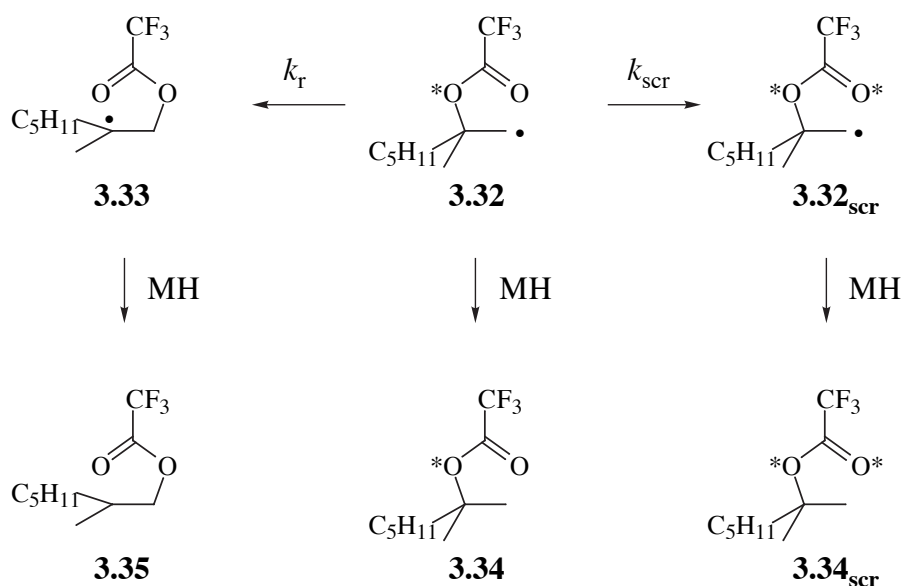
A theoretical value for  $(E_{a_{1,2}} - E_{a_{3,2}})$  of  $4 \pm 1$   $\text{kJmol}^{-1}$  for the rearrangement of the 2-methyl-2-trifluoroacetoxypropyl radical has been obtained by *ab initio* calculations.<sup>32</sup> Energies were calculated at the B3LYP level with several basis sets, although at the G3(MP2) level (composite, high degree of theory)  $\Delta E_a$  for the B3LYP-optimised geometry rose steeply to  $12$   $\text{kJmol}^{-1}$ ,<sup>32</sup> comparing favourably with the current experimental value.

An interesting result was obtained at a very low reducing agent concentration. For  $[\text{TTMSS}] = 2.9$  mM (entry 4, table 3.3) the  $R_E$  values are 41.4% for the rearranged product **3.35b** and 64.2% for **3.34b**. Such a large degree of label scrambling in both products indicates the involvement of one or more dynamic, reversible processes which result in considerable label randomisation in each direction. Interestingly, the ratio **3.35b:3.34b** is only 7.70 at this concentration, yet when  $[\text{TTMSS}] = 29$  mM (entry 2, table 3.2) the ratio increases to 12.6. This depletion in **3.35b** at low reducing agent concentration may be caused by the elimination of trifluoroacetate ion from the incipient



radical **3.32b** during rearrangement. Unfortunately, it was not possible to establish the yield of an expected elimination product, 2-methyl-1-heptene (**3.29**), since the low concentration of the reaction mixture caused the benzene solvent GC peak tail to largely obscure the peak expected for **3.29**. It may be profitable to further explore this area.

It was possible to obtain approximate rate constants and Arrhenius parameters for the process which results in scrambling of the label in the unrearranged product ester **3.34**. The scrambling process which converts radical **3.32** to label-randomised radical **3.32<sub>scr</sub>** was treated as having first order kinetics, with rate constant  $k_{scr}$ . In direct competition with this was the first order rearrangement of **3.32** to **3.33**, with rate constant  $k_r$ . Thus, the situation was treated as a simple competition between two first-order processes.



Owing to the irreversibility of the reaction of each radical with the reducing agent MH, the ratio of two first order rate constants is equal to the ratio of the concentrations of the products formed by each respective process (equation 3.11). Since the rate constants for the rearrangement step,  $k_r$ , have been determined in chapter 2,  $k_{scr}$  can be obtained for each temperature (equation 3.12). The quantity  $[3.34_{scr}]$  refers to the concentration of a form of **3.34** in which the label has been completely randomised ( $R_E = 50\%$ ). For

example, an  $R_E$  value for **3.34** of 95.4% means that  $[3.34_{\text{scr}}] = (100-95.4) \times 2 = 9.2\%$  the concentration of **3.34**.

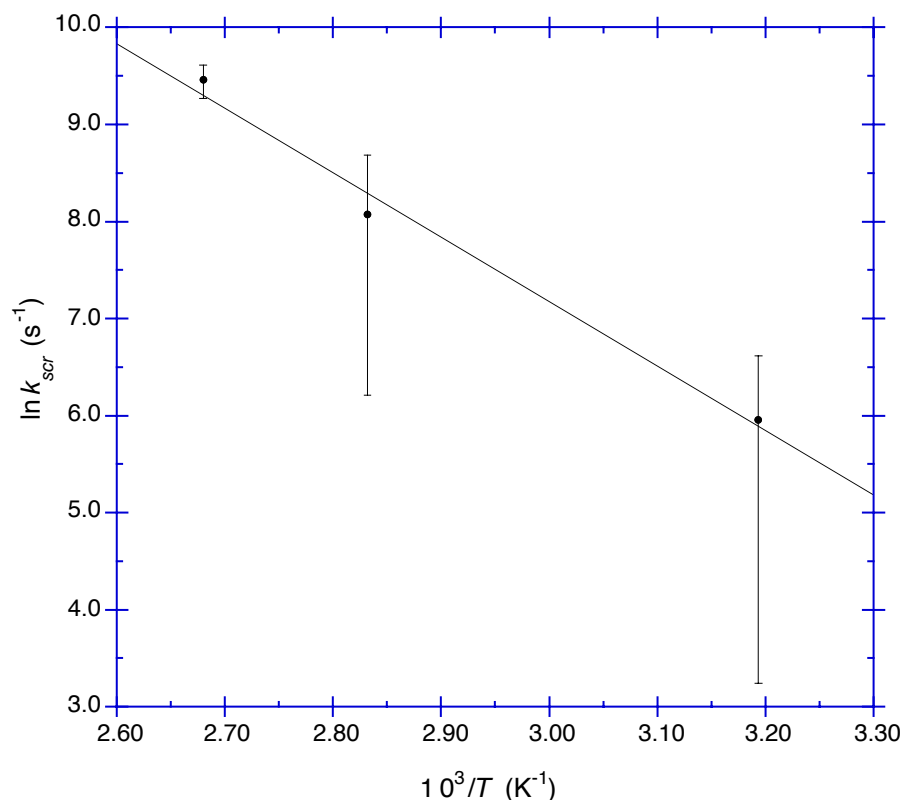
$$\frac{k_{\text{scr}}}{k_{\text{r}}} = \frac{[3.34_{\text{scr}}]}{[3.35]} \quad (3.11)$$

$$k_{\text{scr}} = \frac{k_{\text{r}} [3.34_{\text{scr}}]}{[3.35]} \quad (3.12)$$

It is interesting to note (table 3.10) that at normal temperatures,  $k_{\text{scr}}$  is only 1-2% as large as  $k_{\text{r}}$ , demonstrating that the process that scrambles the label in **3.34** is much slower than the migration of the ester group. From an Arrhenius plot of this data (figure 3.9), the kinetic parameters extracted were  $\log_{10}A = 11.8 \text{ s}^{-1}$  and  $E_a = 55.3 \text{ kJmol}^{-1}$ , although the uncertainties in these values are large. In benzene, the Arrhenius parameters for trifluoroacetoxy migration are  $\log_{10}A = 12.0 \pm 0.2 \text{ s}^{-1}$  and  $E_a = 43.7 \pm 0.8 \text{ kJmol}^{-1}$ . Initial results therefore indicate that it is the activation energy term which is primarily responsible for the difference in rate between the two processes. At this time it is not clear what mechanistic conclusion to draw from these parameters.

**Table 3.10.** Concentration ratio and rate data required for the calculation of  $k_{\text{scr}}$  at three temperatures

$T$ ( $^{\circ}\text{C}$ )	$[3.34_{\text{scr}}] \div [3.35]$	$k_{\text{r}}$ ( $\text{s}^{-1}$ )	$k_{\text{scr}}$ ( $\text{s}^{-1}$ )
40	$0.0075 \pm 0.0070$	$5.14 \times 10^4$	$3.9 \pm 3.6 \times 10^2$
80	$0.0093 \pm 0.0079$	$3.44 \times 10^5$	$3.2 \pm 2.7 \times 10^3$
100	$0.0168 \pm 0.0029$	$7.64 \times 10^5$	$1.28 \pm 0.22 \times 10^4$



**Figure 3.9.** Plot of  $\ln k_{scr}$  against reciprocal temperature. The error bars represent the uncertainty in  $R_E$  for **3.34b**, from table 3.3. The line of best fit is described by the equation  $27.13 - 6652/T$ .

### 3.10 Conclusions

In summary, the rearrangement of the 2-trifluoroacetoxy-2-methyl-1-heptyl radical (3.32) proceeds with between 17-44% formal 1,2 shift, demonstrating that the translocation of ester oxygens is favoured under the conditions of this study. The proportion of 1,2 shift in the rearrangement **3.32**→**3.33** is increased by polar solvents, high temperatures and low concentrations of the hydrogen atom source. These same factors also increase the degree of label scrambling in the unrearranged product **3.34**. The rearrangement is truly intramolecular and reversible. One mechanism consistent with these facts involves the cooperation of reversible 1,2 and 3,2 shifts possessing polarized transition structures. The labelling results agree qualitatively, but not quantitatively, with theoretical calculations which predict that the 3,2 shift becomes less favoured in polar solvents. The 1,2 shift was estimated to have an  $E_a$  9.5  $\text{kJmol}^{-1}$  higher and  $\log_{10}(A/s^{-1})$

1.01 units larger for the 3,2 shift. This is consistent with the 3-membered TS possessing greater ring strain but more degrees of freedom than its 5-membered counterpart. The difference in energy between the two transition structures is consonant with one high-level theoretical calculation.

A second mechanism which is compatible with the results is a reversible process involving an alkene-radical-cation/trifluoroacetate-anion contact pair. This ion pair collapses to form either the rearranged radical **3.33**—in which the label is preferentially distributed into the carbonyl oxygen—or radical **3.32**, in which the label has been partly scrambled. Such an ion pair must exist primarily inside the solvent cage and not as a solvent-separated, solvent-shared or dissociated pair. At this stage it is not possible to confidently exclude either of these possible mechanisms using the available evidence.

### 3.11 Experimental

#### Tetraethylammonium Trifluoroacetate $\text{Et}_4\text{NOCOCF}_3$ [30093-29-9]

A 20% aqueous solution of tetraethylammonium hydroxide (50.0 g, 67.9 mmol) was cooled to 0°C and stirred while 5.5 mL (71.4 mmol) of trifluoroacetic acid was added over 30 seconds. Rotary evaporation was used to concentrate the mixture. The resulting colourless liquid was transferred to a Quickfit test tube and dried on the kugelrohr at 110°C/0.1 mmHg for several hours. A bulb containing  $\text{P}_2\text{O}_5$  was positioned in the vapour path to absorb moisture. The product was obtained as a very hygroscopic white solid upon cooling and was stored under dry nitrogen.

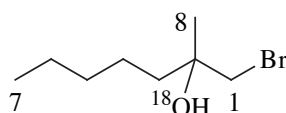
$^1\text{H}$  nmr: 1.32 (t, 3H, 4 ×  $\text{CH}_3$ ), 3.36 (q, 2H, 4 ×  $\text{CH}_2$ ).

#### Attempt to observe a 1,2 OH shift in the 2-hydroxy-2-methyl-1-heptyl radical

The preparations of the compounds 1-bromo-2-methylheptan-2-ol (**3.30**), 2-methylheptan-2-ol (**3.36**) and 2-methylheptan-1-ol (**3.37**) are described in the experimental section of chapter 2. The compounds are there numbered **2.57**, **2.62** and **2.63** respectively.

In a sturdy, brown reagent bottle (10 mL) was placed 10.7 mg (0.0512 mmol) of 1-bromo-2-methylheptan-2-ol (**3.30**) and 5.0 mL of pure, dry benzene. The bottle was capped with a Mininert valve and the solution was purged of oxygen with a gentle nitrogen bubble stream. After heating the stirred solution at 80°C for 15 minutes,  $\text{Bu}_3\text{SnH}$  (25  $\mu\text{L}$ , 0.093 mmol, 1.8 eq.) and AIBN (0.0036 mmol, 0.071 eq.) were added, each by one quick injection. After 2 hours, analysis of the reaction solution by GC revealed that all of **3.30** had been consumed. Among the compounds present were 2-methylheptan-2-ol (**3.36**, 43.8%),  $\text{Bu}_3\text{SnH}$  (14.3%) and  $\text{Bu}_3\text{SnBr}$  (39.9%) with the relative peak integrals indicated. A peak corresponding to the product expected from a 1,2 OH shift—2-methylheptan-1-ol (**3.37**)—could not be detected. The estimated limit of detection of the **3.37** peak was 0.15% the area of the **3.36** peak.

#### (±)-1-Bromo-2-methylheptan-2-ol- $^{18}\text{O}$ (20 atom%).



**3.30a**

All glassware involved in this reaction was dried in a 120°C oven before use and a dry nitrogen atmosphere was used. Dry triflic acid (1 drop) was added to a stirred

solution of 2-methyl-1-heptene (**3.29**, 158  $\mu\text{L}$ , 1.00 mmol) and 90  $\mu\text{L}$  of 20.1 atom%  $\text{H}_2^{18}\text{O}$  in  $\text{H}_2^{16}\text{O}$  ( $\rho = 1.029 \text{ g mL}^{-1}$ , 5.15 mmol) in 5.0 mL of dry THF under nitrogen. *N*-bromoacetamide (0.2757 g, 1.998 mmol) was added in one portion, under a blanket of dry nitrogen. The mixture was stirred for a further 20 min, diluted with 10 mL of diethyl ether and washed with 30 mL of water. The aqueous phase was extracted twice with 10 mL portions of ether and the combined organic extract was washed consecutively with 5 mL of 0.5 M aqueous  $\text{NaHCO}_3$ , 10 mL of 0.3 M aqueous  $\text{Na}_2\text{S}_2\text{O}_3$ , then 5 mL of water. Pentane was added until the solution became cloudy, to aid drying ( $\text{MgSO}_4$ ). Concentration yielded an orange oil (272.3 mg).

Purification was achieved by flash chromatography on 37 mL of silica, eluting with 3% ethyl acetate in hexane (8 mL fractions) until the sweet smell of the bromohydrin was detected, then 6% ethyl acetate in hexane was used as eluent. Fractions that also contained a second spot of slightly higher  $R_f$  were not discarded since this impurity could be removed after the next (esterification) step. Compound **3.30a** was obtained as a colourless oil (88.1 mg, 0.418 mmol, 42%).

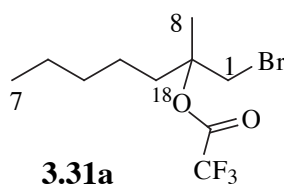
$^1\text{H}$  nmr: 0.90 (t, 3H, 7- $\text{CH}_3$ ), 1.20-1.40 (m, 6H,  $\text{CH}_3(\underline{\text{CH}_2})_3-$ ), 1.31 (s, 3H,  $\underline{\text{CH}_3}\text{C}-\text{OH}$ ), 1.55-1.65 (m, 2H, 3- $\text{CH}_2$ ), 1.91 (s, 1H, OH), 3.45 (d, 1H,  $^2J = 10.2 \text{ Hz}$ ,  $\text{CHBr}$ ), 3.49 (d, 1H,  $^2J = 10.2 \text{ Hz}$ ,  $\text{CHBr}$ ).

$^{13}\text{C}$  nmr: 14.0 (7), 22.5 (6), 23.7 (4), 24.9 (8), 32.1 (5), 39.9 (3), 45.5 (1), 71.292 (2- $^{18}\text{O}$ , 20.1%), 71.324 (2- $^{16}\text{O}$ , 79.9%).

The percentages refer to the relative peak heights for the quaternary carbon resonances.

GCMS:  $20.0 \pm 0.3\%$   $^{18}\text{O}$  enriched.

**(±)-1-Bromomethyl-1-methylhexyl Trifluoro-*oxy*- $^{18}\text{O}$ -acetate (20 atom%)**



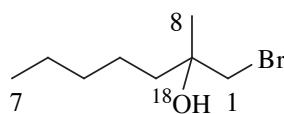
A stirred mixture of sodium trifluoroacetate (34.7 mg, 0.255 mmol) and labelled bromohydrin **3.30a** (88.1 mg, 0.422 mmol) was cooled to  $0^\circ\text{C}$  and trifluoroacetic anhydride (300  $\mu\text{L}$ , 2.12 mmol) was added. After 20 min, TLC (6% ethyl acetate in hexane) indicated the reaction was incomplete. A further 33.5 mg (0.246 mmol) of sodium trifluoroacetate was added, followed by portionwise additions of trifluoroacetic anhydride (*ca.* 400  $\mu\text{L}$ ), continued until the reaction appeared complete by TLC. Pentane (10 mL) was added and the mixture was washed with 10 mL of water. The aqueous phase was extracted with 10 mL of pentane and the combined organic phase was dried and evaporated to yield an oil (102.4 mg). Flash chromatography on silica (4.0 g), using hexane as the eluent, afforded pure **3.31a** as an oil (77.5 mg, 0.254 mmol, 60%).

$^1\text{H}$  nmr: 0.90 (t, 3H, 7- $\text{CH}_3$ ), 1.25-1.40 (m, 6H,  $\text{CH}_3(\underline{\text{CH}_2})_3-$ ), 1.64 (s, 3H,  $\text{CH}_3\text{CO}$ ), 1.87 (m, 1H, 3-CH), 2.07 (m, 1H, 3-CH), 3.75 (d, 1H,  $^2J = 11.2$  Hz,  $\text{CHBr}$ ), 3.82 (d, 1H,  $^2J = 11.2$  Hz,  $\text{CHBr}$ ).

$^{13}\text{C}$  nmr: 13.9 (7), 22.3 (8), 22.4 (4\*), 22.9 (6\*), 31.6 (5), 36.63 (1 $^\dagger$ ), 36.69 (3 $^\dagger$ ), 87.837 (2-  $^{18}\text{O}$ , 19.6%), 87.882 (2-  $^{16}\text{O}$ , 80.4%), 114.2 (q,  $^1J^{19}\text{F}-^{13}\text{C} = 287$  Hz,  $\text{CF}_3$ ), 156.0 (q,  $^2J^{19}\text{F}-^{13}\text{C} = 42$  Hz,  $\text{C=O}$ ).

GCMS:  $20.0 \pm 1.0\%$   $^{18}\text{O}$  enrichment.

**( $\pm$ )-1-Bromo-2-methylheptan-2-ol- $^{18}\text{O}$  (92 atom%).**



**3.30b**

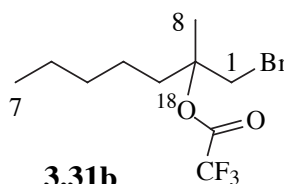
This compound was prepared using the same method as that for the synthesis of 1-bromo-2-methylheptan-2-ol- $^{17}\text{O}$  (48 atom%, **3.30c**). The reaction of 2-methyl-1-heptene (325  $\mu\text{L}$ , 2.06 mmol),  $\text{H}_2^{18}\text{O}$  (reported 97-98 atom%, Cambridge Isotopes, 90  $\mu\text{L}$ , 5.00 mmol) and *N*-bromoacetamide (0.4147 g, 3.01 mmol) in 10 mL of dry diethyl ether at an initial temperature of  $-7^\circ\text{C}$  gave an orange oil (0.5463 g) upon work-up. Flash chromatography using 30 g of silica yielded **3.30b** as a pale orange oil (0.2811 g, 64.6%).

$^1\text{H}$  nmr: 0.90 (t, 3H, 7- $\text{CH}_3$ ), 1.25-1.42 (m, 6H,  $\text{CH}_3(\text{CH}_2)_3-$ ), 1.30 (s, 3H,  $\underline{\text{CH}_3}\text{COH}$ ), 1.55-1.65 (m, 2H, 3- $\text{CH}_2$ ), 2.16 (s, 1H, OH), 3.44 (d, 1H,  $^2J = 10.2$  Hz,  $\text{CHBr}$ ), 3.48 (d, 1H,  $^2J = 10.2$  Hz,  $\text{CHBr}$ ).

$^{13}\text{C}$  nmr: 13.9 (7), 22.5 (6), 23.6 (4), 24.9 (8), 32.1 (5), 39.8 (3), 45.3 (1), 71.248 (2-  $^{18}\text{O}$ , 91.8%), 71.278 (2-  $^{16}\text{O}$ , 8.2%). The percentages refer to relative peak heights for the resolved quaternary (2) carbons.

GCMS:  $91.9 \pm 0.7\%$   $^{18}\text{O}$  enrichment.

**( $\pm$ )-1-Bromomethyl-1-methylhexyl Trifluoro-oxy- $^{18}\text{O}$ -acetate (92 atom%  $^{18}\text{O}$ )**



**3.31b**

Trifluoroacetic anhydride (146  $\mu\text{L}$ , 1.03 mmol) was added to a stirred solution of 202.8 mg (0.961 mmol) of the labelled bromohydrin **3.30b** (92 atom%  $^{18}\text{O}$ ), and

pyridine (84  $\mu\text{L}$ , 1.04 mmol) in 5.0 mL of  $\text{CH}_2\text{Cl}_2$  at  $0^\circ\text{C}$ . TLC revealed that the reaction was complete within 20 min. Pentane (5 mL) was added and the mixture was washed with 5 mL of water. The aqueous phase was extracted with  $2 \times 10$  mL of pentane and the combined organic phase was dried and evaporated to give an orange oil (0.23 g). Purification was achieved by flash chromatography on 3 g of silica, eluting with pentane. The labelled  $\beta$ -bromoester **3.31b** was obtained as a colourless oil (0.2294 g, 77.7%).

$^1\text{H}$  nmr: 0.90 (t, 3H, 7- $\text{CH}_3$ ), 1.25-1.40 (m, 6H,  $\text{CH}_3(\underline{\text{CH}}_2)_3-$ ), 1.64 (s, 3H,  $\text{CH}_3\text{CO}$ ), 1.87 (m, 1H, 3-CH), 2.07 (m, 1H, 3-CH), 3.75 (d, 1H,  $^2J = 11.1$  Hz, CHBr), 3.82 (d, 1H,  $^2J = 11.1$  Hz, CHBr).

$^{13}\text{C}$  nmr: 13.8 (7), 22.2 ( $\underline{\text{C}}\text{H}_3\text{CO}$  or 8), 22.3 (4\*), 22.9 (6\*), 31.6 (5), 36.63 (1 $^\dagger$ ), 36.66 (3 $^\dagger$ ), 87.830 (2- $^{18}\text{O}$ , 92.5%), 87.884 (2- $^{16}\text{O}$ , 7.5%), 114.3 (q,  $^1J^{19}\text{F}-^{13}\text{C} = 287$  Hz,  $\text{CF}_3$ ), 155.9 (q,  $^2J^{19}\text{F}-^{13}\text{C} = 42$  Hz, C=O). The percentages refer to relative resolved peak heights.

GCMS:  $92.1 \pm 3\%$   $^{18}\text{O}$  enrichment.

### Procedure for regiochemical studies with $^{18}\text{O}$ -labelled $\beta$ -bromoesters **3.31a** and **3.31b**

In a dried 1 mL Reactivial, fitted with a stirrer vane and capped with a Mininert valve,<sup>19</sup> was placed the labelled  $\beta$ -bromoester (5-6 mg, 0.015-0.020 mmol). The appropriate type and quantity of dry solvent (usually 250-1000  $\mu\text{L}$ , depending upon concentration required) was added by syringe and the resulting solution was freed of oxygen by bubbling a slow stream of dry nitrogen through it for approximately 1 min. The Mininert valve was closed, sealing the vessel and the flask was lowered into an  $80 \pm 1^\circ\text{C}$  (or other nominated temperature) thermostatted oil bath and stirred for at least 2 minutes to allow temperature equilibration.

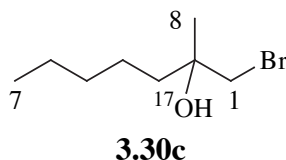
The desired quantity of tris(trimethylsilyl)silane was injected (nominally 1.35 eq.), in one shot, followed by a volume of AIBN solution (usually 5-10  $\mu\text{L}$ , about 5 mol% relative to the silane) in the reaction solvent. For reactions performed in hexane solution, benzene was the solvent for the initiator solution owing to the very low solubility of AIBN in hexane. The progress of the reaction was monitored by GC (dimethylpolysiloxane capillary) and more initiator was injected if the reaction appeared to have stalled. When the reaction was judged to be complete, the reaction vessel was cooled to room temperature and the bulk of the solvent was removed carefully on the rotary evaporator, under reduced pressure. The water-miscible solvents acetonitrile and *N*-methylacetamide were not removed in this way. Acetonitrile and NMA solutions were taken up in 5 mL of diethyl ether, washed with 1 mL of water, treated with 5 mL of pentane, dried over  $\text{MgSO}_4$  and concentrated under reduced pressure.



Flash chromatography over silica, with hexane or pentane eluent, was used to isolate the desired esters **3.34a/b** and **3.35a/b** ( $R_f \approx 0.3$ ) from silicon-containing reactants and by-products ( $R_f \approx 0.9$ ). Solvents were removed carefully under vacuum and the esters were hydrolysed to their respective alcohols by treatment with 20  $\mu\text{L}$  of a solution of 1.5 M KOH in 95% aqueous ethanol (95% ethanol, 5%  $\text{H}_2\text{O}$  v/v), and heating in a capped vial for 20 min at 75°C. After cooling, 5 mL of diethyl ether was added and the resulting solution was washed with 1 mL of water and treated with 5 mL of pentane to aid drying ( $\text{MgSO}_4$ ). Removal of the solvents under vacuum yielded a mixture of the desired alcohols, **3.36a/b** and **3.37a/b**.

Quantitative conversion of the alcohols to the corresponding trimethylsilyl ethers **3.38a/b** and **3.39a/b** was effected by treatment with 5  $\mu\text{L}$  (0.062 mmol) of pyridine and 15  $\mu\text{L}$  of Regisil (10%  $\text{Me}_3\text{SiCl}$  in BSTFA, capable of silylating 0.06 mmol of hydroxyl groups) and heating in a capped vial for 20 min at 75°C. After cooling, the mixture was diluted with  $\text{CH}_2\text{Cl}_2$  to a concentration (usually 0.1 mg/mL for the most abundant TMS ether) appropriate for GCMS analysis. Results appear in tables 3.2 and 3.3 in the text.

**(±)-1-Bromo-2-methylheptan-2-ol- $^{17}\text{O}$  (48 atom%)**



In preparation for this experiment, all syringes, spatulas and solids transfer containers were dried under vacuum overnight in a desiccator, over silica gel. Glassware was dried at 130°C overnight. Diethyl ether was distilled from sodium, in the presence of benzophenone (15  $\text{mgL}^{-1}$ ), once the blue ketyl was persistent. *N*-Bromoacetamide was recrystallized (mp 106.5-107.5°C) from 1,2-dichloroethane/hexane and dried over  $\text{P}_2\text{O}_5$ , under high vacuum for three days. Exposure to light was minimised after addition of the NBA until the completion of the reaction.

A solution composed of 800  $\mu\text{L}$  (0.5697 g, 5.08 mmol) of 2-methyl-1-heptene (**3.29**), 225  $\mu\text{L}$  of  $\text{H}_2^{17}\text{O}$  (48.6 atom%  $^{17}\text{O}$ , Cambridge Isotopes, 12.5 mmol) and 25 mL of dry diethyl ether was stirred whilst cooling to  $-7^\circ\text{C}$  in an ice/salt/acetone bath. *N*-Bromoacetamide (1.0299 g, 7.465 mmol) was added in one portion, under a blanket of dry nitrogen and the temperature of the cooling bath was allowed to rise slowly. After 195 min, the bath temperature was 3°C and the solution was pale yellow/orange (bromine), indicating consumption of the alkene. Diethyl ether (30 mL) was added and the mixture was washed with 150 mL of water. The aqueous washing was back-

extracted with 2 × 50 mL of ether and the combined organic phases were dried (MgSO<sub>4</sub>) and evaporated to yield an orange oil. Purification was achieved by flash chromatography (53 g of silica), eluting with 5% ethyl acetate in 40-60°C pet. spirit (10 mL fractions) until the sweet smell of the bromohydrin was detected, then elution continued using 15% ethyl acetate. Any mixed fractions containing a contaminant of immediately higher R<sub>f</sub> were not discarded since the contaminant was unreactive in the next (esterification) step and was removed at that stage. The bromohydrin **3.30c** was obtained as a pale orange oil (0.6864 g, 3.27 mmol, 64.5%).

It was not known whether the labelled water was normalised with respect to hydrogen. A D<sub>2</sub>O exchange experiment caused the hydroxyl signal in the <sup>1</sup>H nmr spectrum of **3.30c** to disappear immediately.

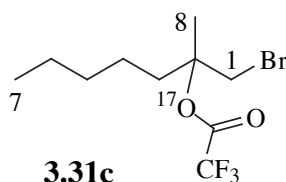
<sup>1</sup>H nmr: 0.90 (t, 3H, 7-CH<sub>3</sub>), 1.25-1.40 (m, 6H, CH<sub>3</sub>(CH<sub>2</sub>)<sub>3</sub>-), 1.30 (s, 3H, CH<sub>2</sub>COH), 1.55-1.65 (m, 2H, 3-CH<sub>2</sub>), 2.02 (s, br, 1H, D<sub>2</sub>O exch., OH), 3.44 (d, 1H, <sup>2</sup>J = 10.2 Hz, CHBr), 3.48 (d, 1H, <sup>2</sup>J = 10.2 Hz, CHBr).

<sup>13</sup>C nmr: 14.0 (7), 22.5 (6), 23.6 (4), 24.9 (8), 32.1 (5), 39.9 (3), 45.4 (1), 71.279 (2-<sup>18</sup>O, 58.1%), 71.309 (2-<sup>16</sup>O, 41.9%). The percentages refer to the relative peak heights of the quaternary carbon 2.

<sup>17</sup>O nmr (40.7 MHz, pentane): 50.6 (s, OH).

GCMS: 46.5±0.2% <sup>17</sup>O enriched, 31.2±0.3% <sup>18</sup>O enriched.

### (±)-1-Bromomethyl-1-methylhexyl Trifluoro-oxy-<sup>17</sup>O-acetate



Dry pyridine (0.213 mL, 2.63 mmol) was added to **3.30c** (0.5120 g, 2.44 mmol) in 10 mL of dry CH<sub>2</sub>Cl<sub>2</sub>. After cooling to 0°C, the stirred solution was treated dropwise with trifluoroacetic anhydride (0.371 mL, 2.63 mmol) over 1 min, then allowed to warm to room temperature. TLC (7% ethyl acetate in 40-60°C pet. spirit) showed a faint spot remaining with the same R<sub>f</sub> (0.20) as **3.30c**. Another 20 μL (total of 2.77 mmol) of trifluoroacetic anhydride did not result in the disappearance of this spot. The spot in question displayed fluorescence under UV light but the bromohydrin did not. Thus, it was concluded that all of **3.30c** had been converted to **3.31c** and the spot was an impurity. After dilution with 10 mL of pentane, the solution was washed with 10 mL of water. The aqueous phase was back-extracted with 2 × 10 mL portions of pentane and the combined organic phases were dried (MgSO<sub>4</sub>) and concentrated to yield an oil (0.77 g). Flash chromatography (pentane) over 10 g of silica afforded **3.31c** as a colourless

oil (0.6289 g, 2.06 mmol, 84%) which was 99.0% pure by GC (BP1).

$^{17}\text{O}$  nmr (40.7 MHz, pentane): 176.7 (s, alkoxy oxygen).

### Procedure for regiochemical studies with $^{17}\text{O}$ -labelled $\beta$ -bromoester **3.31c**

Two separate series of experiments were conducted: the first using tris(trimethylsilyl)silane as the hydrogen atom source; and the second using tributyltin hydride. For each series of reactions, approximately 52 mg (0.17 mmol) of  $\beta$ -bromoester **3.31c** was used, to provide sufficient quantities of products for nmr analysis. For the tris(trimethylsilyl)silane reactions the quantity of the reducing agent was usually about 71  $\mu\text{L}$  (0.23 mmol), corresponding to an intended 1.35 molar equivalents and the amount of AIBN was approximately 3.5 mol% relative to the silane. The volume of each solvent (hexane, benzene, acetonitrile) was 5.0 mL. For reactions performed with tributyltin hydride the quantity of reducing agent used was approximately 55  $\mu\text{L}$  (0.20 mmol), corresponding to an intended 1.2 molar equivalents and approximately 4.5 mol% AIBN relative to the hydride. The volume of each solvent (hexane, benzene, propionitrile, perfluoromethylcyclohexane) was 20 mL (16 mL for PFMC).

An appropriately-sized (10 or 50 mL), sturdy, brown glass bottle was equipped with a stirrer bar and charged with the labelled  $\beta$ -bromoester **3.31c**. The vessel was capped with a Mininert valve<sup>19</sup> and the dry, purified solvent of choice was introduced by syringe. A slow stream of dry nitrogen bubbles was passed through the stirred solution—*via* a needle inserted through the Mininert valve—for three minutes, to remove oxygen. The valve was then closed and the bottle was placed in an  $80\pm 1^\circ\text{C}$  thermostatted oil bath, and surrounded with a metal gauze protective shield. The solution was stirred at this temperature for 15 min prior to a rapid injection of the reducing agent, followed by a solution of the initiator. The progress of reactions was monitored by GC (polydimethylsiloxane stationary phase) and the reaction vessel was withdrawn from the bath and cooled after consumption of  $\beta$ -bromoester **3.31c**. Reactions involving tris(trimethylsilyl)silane were analysed by GCMS to determine the isotopic composition of each of the ester products (table 3.11). Reactions involving tributyltin hydride were not analysed directly because of GCMS contamination issues and were only analysed after tin-containing residues had been removed by preparative GC.

Solvents were removed by distillation under reduced-pressure through a column comprising a B10 still head packed with glass rings. The heating bath temperature was kept below  $55^\circ\text{C}$ . The residue was transferred to an nmr tube, sometimes with the aid of a little pentane to lower the solution viscosity, and a  $^{17}\text{O}$  nmr spectrum of the mixture was obtained (see  $^{17}\text{O}$  nmr appendix).

Preparative GC (see general experimental section, column temperature  $60^\circ\text{C}$ ) was then used to separate the non-rearranged (**3.34c**) and rearranged (**3.35c**) esters from

one another and from other by-products. For each ester,  $^{17}\text{O}$  nmr spectra were obtained in pentane solution. These spectra were all consistent with the spectra of the reaction mixtures obtained previously.

Isotopic compositions of each ester were again determined after nmr to check whether any of the label had been lost from the molecule during preparative GC or nmr (tables 3.11 and 3.12).

**Table 3.11.**  $^{17}\text{O}$  enrichments of esters **3.34c** and **3.35c**—obtained from the reaction of  $46.5\pm 0.2\%$   $^{17}\text{O}$ -enriched  $\beta$ -bromoester **3.31c** with tris(trimethylsilyl)silane—before and after preparative GC.

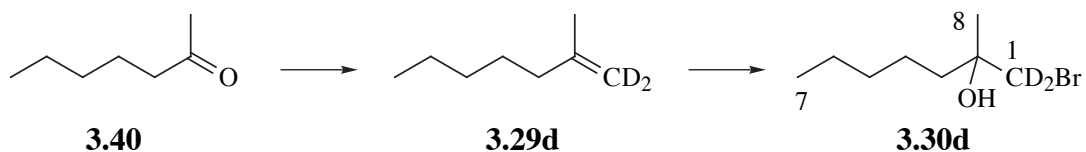
Solvent	Average [TTMSS] (M)	$^{17}\text{O}$ enrichment in non-rearranged ester <b>3.34c</b> before prep. GC (%)	$^{17}\text{O}$ enrichment in rearranged ester <b>3.35c</b> before prep. GC (%)	$^{17}\text{O}$ enrichment in non-rearranged ester <b>3.34c</b> after prep. GC (%)	$^{17}\text{O}$ enrichment in rearranged ester <b>3.35c</b> after prep. GC (%)
hexane	0.0302	47.8	47.4	47.8	48.7
benzene	0.0289	47.8	48.1	47.9	47.9
acetonitrile	0.0289	44.3*	48.3	---	---
acetonitrile	0.150	47.3	48.6	47.6	47.9

\* High uncertainty due to a low concentration of **3.34c**

**Table 3.12.**  $^{17}\text{O}$  enrichments, after preparative GC, for reactions involving tributyltin hydride.

Solvent	Average [TBTH] (M)	$^{17}\text{O}$ enrichment in non-rearranged ester <b>3.34c</b> (%)	$^{17}\text{O}$ enrichment in rearranged ester <b>3.35c</b> (%)
hexane	0.00595	47.6	38.0*
benzene	0.00640	47.6	44.7*
propionitrile	0.00593	47.4	35.3*
PFMC	0.00875	---	---

\* These values are considered to be highly uncertain for several reasons. The first is that the isotope ratio analysis for the rearranged isomer is complicated because two fragment ions contribute to the peak group in the mass spectrum. The second is that a relatively high proportion of 2-methylheptan-1-ol (**3.37**), which has a GC retention time only slightly larger than its trifluoroacetate, was present and may interfere with the GCMS analysis. Finally, the ratio between  $^{17}\text{O}$  and  $^{18}\text{O}$  varies for these analyses, which would not be so if the label was merely undergoing dilution by exchange. Since there is negligible exchange for the non-rearranged isomer in all cases, it is assumed that negligible exchange occurs in the rearranged ester **3.35c**.

**(±)-1-Bromo-2-methylheptan-2-ol-1,1-*d*<sub>2</sub> (99 atom% D)**

This labelled bromohydrin was prepared from 2-methyl-1-heptene-1,1-*d*<sub>2</sub> (**3.29d**), in turn synthesised by the Lombardo olefination<sup>27</sup> of 2-heptanone (**3.40**), utilising CD<sub>2</sub>Br<sub>2</sub> as the source of the label. Unfortunately, the expected yield of alkene was low owing to an error in stoichiometry initiated by a typographical error in the reference. In the synthesis of compound **25** (p. 4868), 0.230 g of compound **24** represents 0.593 mmol, not 5.93 mmol, as reported.<sup>28</sup> The alkene was then converted, without isolation, to the bromohydrin **3.30d**.

**2-Methyl-1-heptene-1,1-*d*<sub>2</sub> (3.29d)**

A vigorously stirred suspension of zinc powder (0.415 g, 6.35 mmol) in 3.5 mL of dry THF, under an atmosphere of dry nitrogen, was treated with 140 μL (2.00 mmol) of CD<sub>2</sub>Br<sub>2</sub> (99 atom% D, Icon Chemicals). The mixture was cooled to -55°C before 165 μL (1.50 mmol) of freshly distilled TiCl<sub>4</sub> was added dropwise. A thick, grey suspension resulted, which was stirred at 4°C for 17 hr. After warming the solution to room temperature 840 μL (6.00 mmol) of 2-heptanone (**3.40**, dried by passage through powdered CaSO<sub>4</sub>) was added and stirring was continued for one hr, resulting in a dark brown/grey suspension. Saturated aqueous NaHCO<sub>3</sub> solution (15 mL) was added cautiously, causing a vigorous effervescence. A further 1.0 g of solid NaHCO<sub>3</sub> was then added and the product was extracted with 4 × 10 mL of diethyl ether, decanting the organic phase each time. The combined extracts were dried and the solvent was reduced to a volume of approximately 3 mL by careful distillation through a short column packed with glass rings, down to a volume of approximately 3 mL.

**(±)-1-Bromo-2-methylheptan-2-ol-1,1-*d*<sub>2</sub> (3.30d)**

The residue from the preceding experiment was treated with 15 mL of DMSO and 500 μL (27.8 mmol) of water, then cooled to 0°C with stirring. *N*-Bromosuccinimide (2.05 g, 11.5 mmol) was added in portions, resulting in an orange solution. This was poured into 70 mL of ice/water and then extracted with 4 × 15 mL of diethyl ether. The combined organic layer was washed with 15 mL of saturated aqueous NaCl, then dried (MgSO<sub>4</sub>) and evaporated, yielding an orange oil (0.64 g). Purification of the crude product was achieved by flash chromatography over 25 g of silica, eluting with 6% ethyl acetate in 40-60°C pet. spirit until the sweet odour of the product was detected, then elution continued with 10% ethyl acetate. The labelled bromohydrin **3.30d** was obtained

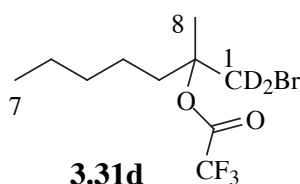
as a colourless oil (69.4 mg, 0.329 mmol, 55%).

$^1\text{H}$  nmr: 0.90 (t, 3H, 7- $\text{CH}_3$ ), 1.20-1.40 (m, 6H,  $\text{CH}_3(\underline{\text{C}}\text{H}_2)_3$ ), 1.30 (s, 3H,  $\underline{\text{C}}\text{H}_3\text{COH}$ ), 1.55-1.64 (m, 2H, 3- $\text{CH}_2$ ), 2.33 (s, br, OH). Small multiplets were present, centred at 3.45 and 3.49 ppm, corresponding to non- or partially-deuterated isotopomers. From the relative integrals of these, **3.30d** was  $\geq 98.5$  atom% D.

$^{13}\text{C}$  nmr: 13.9 (7), 22.5 (6), 23.6 (4), 24.8 (8), 32.1 (5), 39.8. The expected quintet (*ca.* 45 ppm), corresponding to carbon-1 was too weak in intensity to be observed.

GCMS:  $99.2 \pm 0.5$  atom% D (as  $\text{CD}_2$ ), using the peak group at  $m/z$  135-143 ( $\text{C}_3\text{H}_6\text{BrO}^+$  in unlabelled bromohydrin **3.30**).

### (±)-1-Bromomethyl-1-methylhexyl Trifluoroacetate-1,1- $d_2$ (99 atom% D)



A stirred solution of the labelled bromohydrin **3.30d** (66.9 mg, 0.317 mmol) in 2.0 mL of dry  $\text{CH}_2\text{Cl}_2$  was cooled to  $0^\circ\text{C}$ . Pyridine (27.7  $\mu\text{L}$ , 0.342 mmol) was added, followed by trifluoroacetic anhydride (48.2  $\mu\text{L}$ , 0.341 mmol) and the solution was allowed to warm to room temperature. After 10 min, 5 mL of pentane was added and the mixture was washed with 10 mL of water. The aqueous phase was extracted with  $2 \times 10$  mL of pentane, and the combined organic phase was dried ( $\text{MgSO}_4$ ) and evaporated, to yield an oil (0.10 g). Flash chromatography (pentane) over 3 g of silica provided pure **3.31d** as a colourless oil (61.8 mg, 0.201 mmol, 64%).

### Crossover experiment

A mixture of 5.88 mg ( $1.91 \times 10^{-5}$  mol) of  $^{18}\text{O}$ -labelled (91.9% enriched)  $\beta$ -bromoester **3.31b** and 5.93 mg ( $1.93 \times 10^{-5}$  mol) of  $d_2$ -labelled (99.2 atom% D)  $\beta$ -bromoester **3.31d** was placed in a 3 mL Reactivial, fitted with a stirrer vane and capped with a Mininert valve. To this mixture was added 1.00 mL of dry, purified benzene and the resulting solution was stirred while a stream of dry nitrogen was bubbled through for 3 min to remove oxygen. The Mininert valve was closed and the vial was placed in an  $80 \pm 1^\circ\text{C}$  bath for 15 min before tris(trimethylsilyl)silane (16.0  $\mu\text{L}$ ,  $5.19 \times 10^{-5}$  mol) was rapidly injected, followed by 10.0  $\mu\text{L}$  of an 0.118 M AIBN solution in benzene ( $1.18 \times 10^{-6}$  mol, 3.1 mol% relative to silane). The progress of the reaction was monitored by GC, the reaction requiring two more 10.0  $\mu\text{L}$  injections of the initiator solution to ensure that it went to completion. The molar ratio of the rearranged to non-rearranged ester was

determined from the GC peak integration to be 9.47:1.

After cooling to room temperature, 50  $\mu\text{L}$  of the solution was dissolved in 2 mL of pentane, to provide a solution of appropriate concentration for GCMS analysis. Relevant mass-spectral data for the rearranged (table 3.13) and unrearranged (table 3.14) esters are provided.

**Table 3.13.** Partial mass-spectral data for the rearranged product ester **3.35** from the crossover experiment

<i>m/z</i>	<b>3.35</b> (pure $d_2$ ) (%)	<b>3.35b</b> ( $^{18}\text{O}$ ) (%)	<b>3.35</b> From crossover experiment (%)	<b>3.35</b> Calculated for zero crossover (%)
155	0	2.32 $\pm$ 0.29	1.96 $\pm$ 0.34	1.16 $\pm$ 0.15
156	0	4.13 $\pm$ 0.53	1.61 $\pm$ 0.33	2.06 $\pm$ 0.27
157	10.43 $\pm$ 0.47	22.90 $\pm$ 1.85	17.88 $\pm$ 1.43	16.64 $\pm$ 1.16
158	2.25 $\pm$ 0.50	6.15 $\pm$ 0.89	3.78 $\pm$ 0.37	4.19 $\pm$ 0.70
159	100	100	100	100
160	10.23 $\pm$ 0.32	9.05 $\pm$ 0.49	9.75 $\pm$ 0.85	9.64 $\pm$ 0.41
161	0.40 $\pm$ 0.09	0.26 $\pm$ 0.07	0.45 $\pm$ 0.31	0.33 $\pm$ 0.08
162			0.03 $\pm$ 0.07	

**Table 3.14.** Partial mass-spectral data for the unrearranged product ester **3.34** from the crossover experiment

<i>m/z</i>	<b>3.34</b> (pure $d_2$ ) (%)	<b>3.34b</b> ( $^{18}\text{O}$ ) (%)	<b>3.34</b> From crossover experiment (%)	<b>3.34</b> Calculated for zero crossover (%)
155	0	8.59 $\pm$ 0.27	5.85 $\pm$ 0.44	4.27 $\pm$ 0.14
156	0	14.41 $\pm$ 0.44	12.33 $\pm$ 0.31	7.18 $\pm$ 0.22
157	100	100	100	100
158	5.51 $\pm$ 0.33	5.51 $\pm$ 0.14	5.56 $\pm$ 0.26	5.51 $\pm$ 0.24
159	0.38 $\pm$ 0.14	0.12 $\pm$ 0.04	0.21 $\pm$ 0.09	0.25 $\pm$ 0.09

### Attempt to trap the 2-methyl-1-heptene radical cation

A reaction of the  $^{18}\text{O}$ -oxy-labelled  $\beta$ -bromoester **3.31b** ( $91.9\pm 0.7\%$  enriched) with tris(trimethylsilyl)silane in acetonitrile solution, in the presence of unlabelled trifluoroacetate ion was conducted to test whether any exchange of unlabelled for labelled trifluoroacetate occurs during the rearrangement of the incipient radical **3.32b**. Successful trapping of the radical-cation fragment of the postulated intermediate may be detected by a decrease in the  $^{18}\text{O}$  enrichment of the ester products **3.34b** and **3.35b** relative to the bromoester. Difficulties encountered in the GCMS analysis necessitated a control experiment as a basis for comparison.

#### 1) Rearrangement of radical **3.32b** in the presence of unlabelled trifluoroacetate ion.

The labelled bromoester **3.31b** (5.71 mg,  $1.86 \times 10^{-5}$  mol) was dissolved in a solution of anhydrous tetraethylammonium trifluoroacetate (500  $\mu\text{L}$  of a 0.78 M solution,  $3.9 \times 10^{-4}$  mol, 21 eq.) in dry acetonitrile in a 1 mL Reactivial fitted with a Mininert valve. After deoxygenating with nitrogen, the solution was heated to  $80\pm 1^\circ\text{C}$  and stirred at this temperature for 15 min before rapidly injecting 15.0  $\mu\text{L}$  ( $4.86 \times 10^{-5}$  mol) of tris(trimethylsilyl)silane and 5  $\mu\text{L}$  of an 0.24 M solution of AIBN ( $1.2 \times 10^{-6}$  mol) in acetonitrile. The reaction was monitored by GC and stopped when no **3.31b** remained (several hours). The GC integration ratio for **3.35b**:**3.34b** was 8.5:1. Unrearranged ester **3.34b** gave an  $^{18}\text{O}$  enrichment of  $72.7\pm 0.4\%$  and rearranged ester **3.35b** gave  $\geq 78.1\%$ . See table 3.15 for the relevant mass-spectral data for **3.35b**.

#### 2) Control experiment

This was performed in an identical manner to the prior experiment, with the exception that the solvent contained no tetraethylammonium trifluoroacetate. The following quantities were used: 5.81 mg ( $1.89 \times 10^{-5}$  mol) of bromoester **3.31b**, 500  $\mu\text{L}$  of dry acetonitrile, 15.0  $\mu\text{L}$  ( $4.86 \times 10^{-5}$  mol) of tris(trimethylsilyl)silane and 5  $\mu\text{L}$  ( $1.2 \times 10^{-6}$  mol) of AIBN solution. Two further 5  $\mu\text{L}$  injections of AIBN were required to ensure the reaction went to completion. The GC integration ratio for **3.35b**:**3.34b** was 12.3:1. Unrearranged ester **3.34b** gave an  $^{18}\text{O}$  enrichment of  $92.1\pm 0.3\%$  and rearranged ester **3.35b** gave  $\geq 80.2\%$ . See table 3.15 for the relevant mass-spectral data for **3.35b**.

#### 3) Test for exchange in **3.31b** prior to rearrangement

To test for exchange prior to rearrangement, 5.0 mg ( $1.6 \times 10^{-5}$  mol, 0.032 M) of the labelled  $\beta$ -bromoester **3.31b** in 500  $\mu\text{L}$  of a 0.78 M solution of tetraethylammonium trifluoroacetate in dry acetonitrile was heated at  $80^\circ\text{C}$  for 1.5 hours. The  $^{18}\text{O}$  isotopic enrichment of the recovered **3.31b** was determined by GCMS to be  $91.7\pm 0.2\%$ , comparing favourably with the initial enrichment of  $91.9\pm 0.7\%$ .



4) Test for exchange in ester products **3.34b** and **3.35b** after rearrangement

To test for exchange after rearrangement, the reaction solution from the undoped reaction was treated with 500  $\mu\text{L}$  of an 0.78 M solution of anhydrous tetraethylammonium trifluoroacetate in dry acetonitrile, making the overall concentration of the dissolved salt 0.39 M, and heated at 80°C for a further 1.5 hours. The  $^{18}\text{O}$  enrichment of the non-rearranged isomer **3.34b** was determined to be  $79.4\pm 0.8\%$  and that of the rearranged isomer **3.35b** was  $\geq 80.5\%$ . See table 3.15 for the relevant mass-spectral data for **3.35b**.

**Table 3.15.** Partial mass spectral data for the rearranged ester **3.35b**, from experiments 1,2 and 4 (plotted in figure 3.6)

$m/z$	(1) Test for trapped trifluoroacetate (%)	(2) Control (%)	(4) Control then heated with tetraethylammonium trifluoroacetate (%)
155	1.55 $\pm$ 0.07	2.32 $\pm$ 0.29	2.51 $\pm$ 1.17
156	3.20 $\pm$ 0.050	4.13 $\pm$ 0.53	3.98 $\pm$ 0.84
157	26.61 $\pm$ 1.36	22.90 $\pm$ 1.85	23.96 $\pm$ 0.32
158	7.72 $\pm$ 0.66	6.15 $\pm$ 0.89	6.67 $\pm$ 0.66
159	100	100	100
160	8.95 $\pm$ 1.39	9.05 $\pm$ 0.49	9.88 $\pm$ 0.24
161	0.57 $\pm$ 0.41	0.26 $\pm$ 0.07	0.54 $\pm$ 0.20

Uncertainties are at one standard deviation.

### 3.12 References

1. Beckwith, A. L. J.; Crich, D.; Duggan, P. J. and Yao, Q. *Chem. Rev.* **1997**, *97*, 3273.
2. Korth, H.-G.; Sustmann, R.; Groninger, K. S.; Liesung, M. and Giese, B. *J. Org. Chem.* **1988**, *53*, 4364.
3. Beckwith, A. L. J. and Duggan, P. J. *J. Chem. Soc., Perkin Trans. 2* **1992**, 1777.
4. Beckwith, A. L. J. and Thomas, C. B. *J. Chem. Soc., Perkin Trans. 2* **1973**, 861.
5. Beckwith, A. L. J. and Duggan, P. J. *J. Am. Chem. Soc.* **1996**, *118*, 12838.
6. Crich, D. and Filzen, G. F. *J. Org. Chem.* **1995**, *60*, 4834.
7. Beckwith, A. L. J. and Duggan, P. J. *J. Chem. Soc., Perkin Trans. 2* **1993**, 1673.
8. Kocovsky, P.; Stary, I. and Turecek, F. *Tetrahedron Lett.* **1986**, *27*, 1513.
9. Crich, D.; Huang, X. and Beckwith, A. L. J. *J. Org. Chem.* **1999**, *64*, 1762.
10. Gilbert, B. C.; Norman, R. O. C. and Williams, P. S. *J. Chem. Soc. Perkin Trans. 2* **1981**, 1401.
11. Asmus, K.-D.; Williams, P. S.; Gilbert, B. C. and Winter, J. N. *J. Chem. Soc. Chem. Commun.* **1987**, 208.
12. Guss, C. O. and Rosenthal, R. *J. Am. Chem. Soc.* **1955**, *77*, 2549.
13. Langman, A. W. and Dalton, D. R. *Org. Synth.* **1980**, *59*, 16.
14. Dalton, D. R.; Dutta, V. P. and Jones, D. C. *J. Am. Chem. Soc.* **1968**, *90*, 5498.
15. Chatgililoglu, C.; Griller, D. and Lesage, M. *J. Org. Chem.* **1988**, *53*, 3641.
16. Giese, B.; Kopping, B. and Chatgililoglu, C. *Tetrahedron Lett.* **1989**, *30*, 681.
17. Dickhaut, J. and Giese, B. *Org Synth.* **1992**, *70*, 164.
18. Chatgililoglu, C.; Ferreri, C. and Gimisis, T. In *Chemistry of Organic Silicon Compounds*; Rappoport, Z. and Apeloig, Y., Eds.; Wiley: Chichester, 1998; Vol. 2(pt. 2), pp 1539-1579.
19. Aldrich *Fine Chemicals and Laboratory Equipment Catalogue*, Australia and New Zealand Edition, **2000-2001**, T778.
20. Nakanishi, W.; Jo, T.; Miura, K.; Ikeda, Y.; Sugawara, T.; Kawada, Y. and Iwamura, H. *Chem. Lett.* **1981**, 387.

21. Creary, X. and Inocenio, P. A. *J. Am. Chem. Soc.* **1986**, *108*, 5979.
22. See reference 7.
23. Crich, D.; Huang, X. and Beckwith, A. L. J. *J. Org. Chem.* **1999**, *64*, 1762.
24. See appendix B
25. McFarlane, W. and McFarlane, H. C. E. in *Multinuclear NMR*; Mason, J., Ed.; Plenum Press: New York, 1987.
26. Boykin, D. W. and Baumstark, A. L. in *<sup>17</sup>O NMR Spectroscopy in Organic Chemistry*; Boykin, D. W., Ed.; CRC Press: Boston, 1991, p. 205.
27. Lombardo, L. *Org. Synth.* **1993**, *Coll. Vol. 8*, 386.
28. Furber, M.; Mander, L. N. and Patrick, G. L. *J. Org. Chem.* **1990**, *55*, 4860.
29. Forcier, G. A. and Olver, J. W. *Electrochim. Acta* **1970**, *15*, 1609.
30. Atkins, P. W. *Physical Chemistry*; 3rd ed.; Oxford University Press Oxford, 1986; p. 667.
31. Smolina, T. A.; Brusova, G. P.; Shchekut'eva, L. F.; Gopius, E. D.; Permin, A. B. and Reutov, O. A. *Izv. Akad. Nauk SSSR, Ser. Khim.* **1980**, *9*, 2079.
32. Zipse, H. and Bootz, M. *J. Chem. Soc. Perkin Trans. 2* **2001**, 1566.
33. a) Reichardt, C. *Chem. Rev.* **1994**, *94*, 2319; b) Reichardt, C., Schäfer G., *Liebigs Ann.* **1995**, 1579; c) Eberhardt, R., Löbbecke S., Neidhardt, B. and Reichardt C. *Liebigs Ann. /Recueil* **1997**, 1195; d) Website: [www.chemie.uni-marburg.de/~ak39/et\\_home.html](http://www.chemie.uni-marburg.de/~ak39/et_home.html)

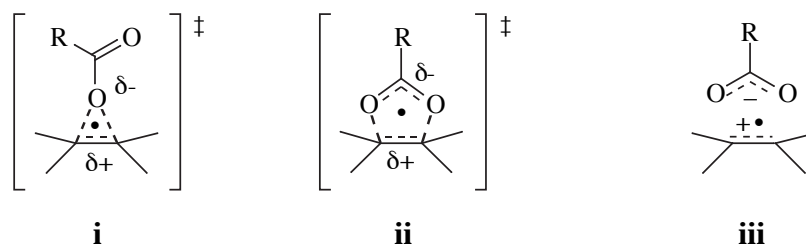
## Chapter 4

### An esr study of $\beta$ -oxygenated alkyl radicals

4.1	Introduction	134
4.2	Estimation of time-averaged dihedral angles	135
4.3	Recording of the esr spectra and extraction of $g$ -values and hyperfine splitting constants	138
4.4	Results	140
4.5	Calculations, analysis and discussion	146
4.6	Estimation of the energy barrier to internal rotation about the $C_{\alpha}-C_{\beta}$ bond in the $\beta$ -oxygenated ethyl radicals <b>4.3a-c</b>	170
4.7	Final discussion	176
4.8	Conclusions	180
4.9	Experimental	181
4.10	References	187

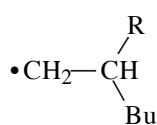
## 4.1 Introduction

This chapter describes an electron spin resonance study of alkyl radicals which possess an oxygenated  $\beta$ -substituent. Such work was undertaken for two main reasons. Firstly, labelling experiments<sup>1-3</sup> reveal that most simple, acyclic  $\beta$ -acetoxyalkyl radicals undergo a net 1,2 acetoxy shift with almost complete transposition of ester oxygens. However, the migration of the electronegative trifluoroacetoxy group proceeds more quickly with approximately 65%<sup>4</sup> to 81%<sup>5</sup> oxygen label translocation. In a recent *ab initio* MO investigation into the  $\beta$ -acyloxyalkyl radical rearrangement, workers could not locate a stationary point on the energy surface corresponding to a contact ion pair (**iii**) for reactions involving the shift of either an acetoxy or trifluoroacetoxy group.<sup>6</sup> Rather, the results indicated that the mechanism involved a combination of primarily 5-membered (**ii**) and to a lesser extent 3-membered (**i**) polarized transition structures, with **i** being higher in energy by approximately 4.7 kJmol<sup>-1</sup> for acetoxy and 4.3 kJmol<sup>-1</sup> for trifluoroacetoxy migration. The question then arose as to whether there is a stereoelectronic interaction between the ester carbonyl oxygen and the radical orbital which is detectable by esr and might account for the preponderance of a 3,2 (5-membered TS **ii**) shift over a 1,2 (3-membered TS **i**) shift. Barriers to internal rotation about the  $C_{\alpha}$ - $C_{\beta}$  bond were determined for radicals **4.3a-c** in order to estimate the magnitude of any stereoelectronic interaction between the  $\beta$ -substituent and the radical orbital.

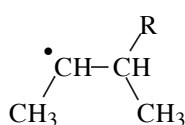


Secondly, although vicinal shifts of  $\beta$ -acetoxy and  $\beta$ -trifluoroacetoxy groups in alkyl radicals are well documented, attempts to observe a 1,2 hydroxy shift in  $\beta$ -hydroxyalkyl radicals under similar conditions have failed.<sup>7,8</sup> Although 1,2 hydroxy rearrangements do occur in the presence of enzymes<sup>9</sup> and protonated hydroxy groups are

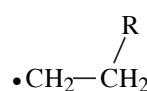
known to migrate,<sup>10</sup> such shifts are considered special cases with significant differences in chemistry. In light of the difference in reactivity between  $\beta$ -hydroxy, acetoxy and trifluoroacetoxy alkyl radicals, an obvious question which arises is whether the propensity for migration of a  $\beta$ -substituent correlates with a particular radical conformation. In an attempt to answer this question, the stable conformation was determined for each of three series of radicals (4.1-4.3) bearing  $\beta$ -substituents (a) OH, (b) OCOCH<sub>3</sub> and (c) OCOCF<sub>3</sub>.



4.1



4.2



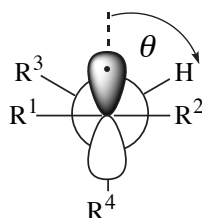
4.3

a: R = OH

b: R = OCOCH<sub>3</sub>c: R = OCOCF<sub>3</sub>

## 4.2 Estimation of the time-averaged dihedral angles

The esr  $\beta$ -hydrogen hyperfine coupling constant is dependent upon the configuration about the  $C_\alpha$ - $C_\beta$  bond. One such relationship<sup>11</sup> is given by equation 4.1, where  $\alpha_\beta$  is the  $\beta$ -coupling constant;  $Q_{\text{CCH}}^{\text{H}}$  is a proportionality constant, characteristic of the  $\bullet\text{C}-\text{CH}$  system representing the coupling constant at maximum spin density ( $\leq 58.6 \text{ G}^{12}$ );  $\rho_{\text{C}}$  is the spin density in the carbon  $2p_z$  orbital and  $\theta$  is the dihedral angle between the  $\beta$ -C-H bond and the axis of the singly occupied molecular orbital.



$$\alpha_\beta = Q_{\text{CCH}}^{\text{H}} \rho_{\text{C}} \cos^2 \theta \quad (4.1)$$

For systems in which there can be complete rotation or other rapid conformational interconversion about the  $C_\alpha$ - $C_\beta$  bond, equation 4.1 still holds, but  $\alpha_\beta$  and  $\theta$  represent time-averaged, or equilibrium, values. A temperature dependence of the  $\beta$ -coupling

constant can be observed in many systems. A classical explanation of this phenomenon states that with a decrease in temperature, the proportion of time spent by the radical in a more stable conformations increases, as governed by the Boltzmann distribution. A change in the equilibrium conformation naturally results in a corresponding change in the time-averaged  $\beta$ -coupling constant. At very low temperatures, conformational freezing may occur if the radical does not have sufficient energy to surmount the potential well of the most stable conformation(s). A quantum mechanical treatment specifies that depopulation of discrete, higher energy rotational states occurs with a decrease of temperature.

For unrestricted rotation about the  $C_\alpha$ - $C_\beta$  bond, the average value of  $\theta$  is  $\cos^{-1}\sqrt{0.5} = 45^\circ$ , as derived from equation 4.2. Consequently, values of  $\theta_{\text{average}}$  calculated from  $\beta$ -hydrogen coupling constants using equation 4.1 represent deviations from the free-spin value of  $45^\circ$  because of the increasing contribution to the equilibrium conformation by potential minima at lower temperature.

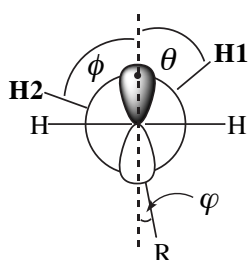
$$\frac{1}{2\pi} \int_0^{2\pi} \cos^2\theta \, d\theta = \frac{1}{2} \quad (4.2)$$

For primary radicals **4.1a-c** and **4.3a-c**, a value of  $Q_{\text{CCH}}^{\text{H}}\rho_{\text{C}} = 53.8 \text{ G}$  was used in equation 4.1 for the calculation of  $\theta$  values. This value is derived from equation 4.1, using the temperature-invariant  $\beta$ -coupling constant for ethyl radical ( $\alpha_\beta$ - $\text{CH}_3 = 26.9 \text{ G}$ ),<sup>13</sup> assuming free rotation ( $\theta_{\text{average}} = 45^\circ$ ). It is broadly accepted that the barrier for rotation about the  $C_\alpha$ - $C_\beta$  bond in the ethyl radical is very small since the methyl hydrogens are still magnetically equivalent at 4K,<sup>14</sup> although quantum mechanical tunnelling through the barrier may well occur. For the secondary radicals **4.2a-c**, an internally consistent value of  $Q_{\text{CCH}}^{\text{H}}\rho_{\text{C}}$  was calculated for each radical in the same way as for the ethyl radical, using the respective, averaged  $\beta$ - $\text{CH}_3$  coupling constants. Values appear in table 4.1.

**Table 4.1.** Internally consistent values of  $Q_{\text{CCH}}^{\text{H}}\rho_{\text{C}}$ , for radicals **4.2a-c**

Radical species		$Q_{\text{CCH}}^{\text{H}}\rho_{\text{C}}$ (G)
$\text{CH}_3\dot{\text{C}}\text{HCH}(\text{CH}_3)\text{OH}$	<b>4.2a</b>	50.43
$\text{CH}_3\dot{\text{C}}\text{HCH}(\text{CH}_3)\text{OCOCH}_3$	<b>4.2b</b>	50.98
$\text{CH}_3\dot{\text{C}}\text{HCH}(\text{CH}_3)\text{OCOCF}_3$	<b>4.2c</b>	51.47

A modified version of equation 4.1 was required for conformational analysis of radicals **4.3a-c** since there are two  $\beta$ -hydrogens as opposed to the usual one. Equation 4.3 is an expression for a hypothetical sum of  $\beta$ -coupling constants, where  $\alpha_{\beta 1}$  and  $\alpha_{\beta 2}$  represent the splittings from H1 and H2 respectively and  $\theta$  and  $\phi$  are the respective dihedral angles.<sup>12</sup>



$$\Sigma\alpha_{\beta} = \alpha_{\beta 1} + \alpha_{\beta 2} = Q_{\text{CCH}}^{\text{H}}\rho_{\text{C}} (\cos^2\theta + \cos^2\phi) \quad (4.3)$$

In situations of high frequency ( $> 10^8 \text{ s}^{-1}$ ) conformational interconversion, the  $\beta$ -hydrogens become spectroscopically equivalent, so

$$\Sigma\alpha_{\beta} = \alpha_{\beta 1} + \alpha_{\beta 2} = 2\langle\alpha_{\beta}\rangle = Q_{\text{CCH}}^{\text{H}}\rho_{\text{C}} (\cos^2\theta + \cos^2\phi)$$

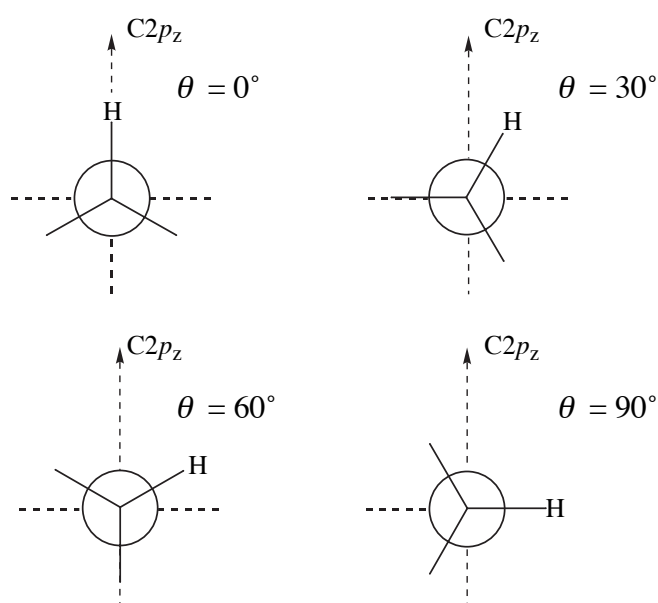
$$\text{and hence } \langle\alpha_{\beta}\rangle = Q_{\text{CCH}}^{\text{H}}\rho_{\text{C}} \left( \frac{\cos^2\theta + \cos^2\phi}{2} \right)$$

where  $\langle\alpha_{\beta}\rangle$  is the time-averaged value of the coupling constant. This is more conveniently expressed by equation 4.4 in terms of  $\varphi$ , the dihedral angle to the oxygenated  $\beta$ -substituent.



$$\langle \alpha_{\beta} \rangle = Q_{\text{CCH}}^{\text{H}} \rho_{\text{C}} (0.5 \sin^2 \varphi + 0.25) \quad (4.4)$$

There are four conformations commonly encountered at the potential minima of simple alkyl radicals,<sup>13</sup> as displayed in figure 4.1. The  $\text{H}_{\beta}\text{-C}_{\beta}$  bond may adopt torsion angles to the  $\text{C}2p_z$  semi-occupied orbital axis of 0, 30, 60 and 90°. To aid conformational analysis,  $\theta_{\text{average}}$  values were calculated and plotted against absolute temperature. An estimation of the geometry of the most stable conformation of each radical was made from  $\alpha_{\beta\text{H}}$  and its temperature dependence, by considering selective line broadening phenomena in the esr spectra and evaluating relative steric effects.

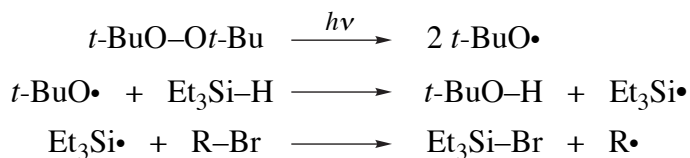


**Figure 4.1.** The four basic geometries of alkyl radicals, which correspond to potential minima upon rotation about the  $\text{C}_{\alpha}\text{-C}_{\beta}$  bond

### 4.3 Recording of the esr spectra and extraction of g-values and hyperfine splitting constants

The desired radicals were generated in the cavity of an esr spectrometer by high-pressure Hg/Xe irradiation of a mixture of the appropriate  $\beta$ -bromoester or alcohol (1 volume), triethyl silane (2 volumes) and di-*tert*-butylperoxide (4 volumes) in cyclopropane (mp 145 K) solution, according to an established procedure.<sup>15,16</sup> The

sequence of reactions responsible for generation of the carbon centred radicals is shown below.



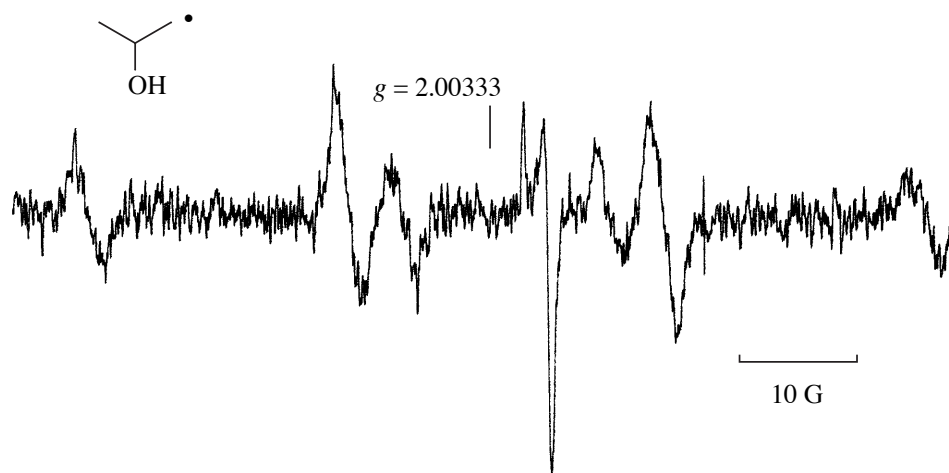
Occasionally, ethylene oxide (mp 162 K) was used instead of, or in conjunction with, cyclopropane when the solubility of the components was poor at lower temperatures. The solutions were cooled to  $-78^\circ\text{C}$  and deoxygenated with dry nitrogen for five minutes prior to their insertion into the spectrometer. The temperature controlling device was calibrated using a thermocouple and temperatures are estimated to be accurate to better than  $\pm 5$  K.

The spectra of the  $\beta$ -hydroxyalkyl radicals were the most difficult to obtain due to the line broadening, presumably caused by hydrogen bonding. The hydroxylated precursors were less soluble and crystallized at higher temperatures than their ester counterparts. Well resolved spectra for the 2-hydroxy-1-hexyl radical (**4.1a**) were particularly difficult to obtain at certain temperatures since the comparatively large size of the alkyl chain reduces the frequency of molecular tumbling in solution, resulting in larger linewidths. Consequently, data for the 2-hydroxy-1-propyl radical were used in these instances owing to the relative ease of recording this spectrum and the high degree of similarity expected for the coupling constants.

Isotropic  $g$  factors were determined relative to a calibrated spectrometer field marker at  $g = 2.00333$  and are uncorrected with respect to second and higher order effects. The  $g$  values and coupling constants, together with the multiplicities (in brackets) of the resonances are tabulated for each species over a typical temperature range of 150-250 K. If splittings were not resolved, this is indicated by the abbreviation n.r..

## 4.4 Results

### 4.4.1 Spectra of 2-(oxysubstituted)-1-hexyl radicals 4.1a-c

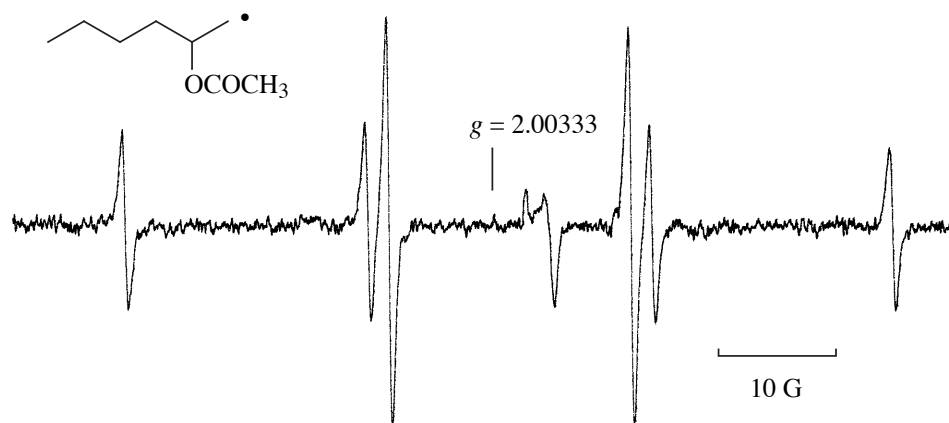


**Figure 4.2.** ESR spectrum of 2-hydroxy-1-propyl radical (in place of the very poorly resolved 2-hydroxy-1-hexyl species **4.1a**), at 172 K, spectral width 80 G

**Table 4.2.** ESR spectral data for the 2-hydroxy-1-hexyl radical (**4.1a**)

$T$ (K)	$g$	$\alpha_\alpha$ (G)	$\alpha_\beta$ (G)	$\alpha_\gamma$ (G)
153*	~2.0024	~21.9 (t)	~27.3 (d)	n.r.
172*	2.00240	21.93	26.61	n.r.
190	2.00247	21.97	25.60	n.r.
211	2.00248	21.99	25.34	n.r.

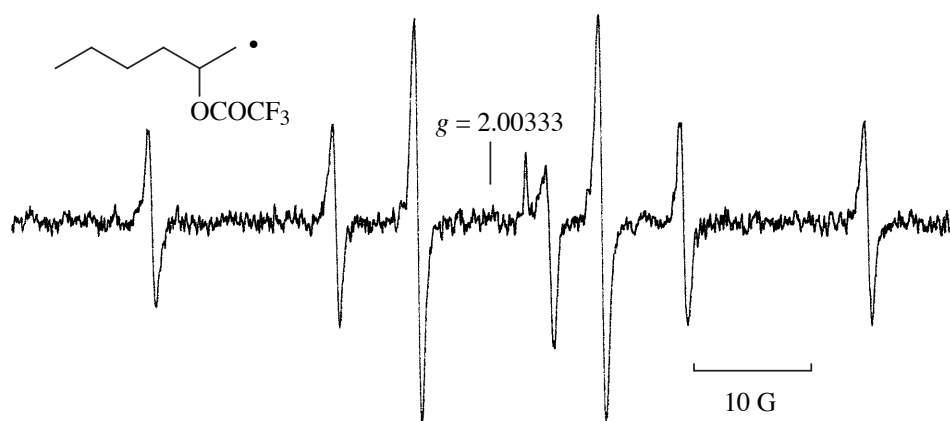
\* data for 2-hydroxy-1-propyl radical



**Figure 4.3.** ESR spectrum of 2-acetoxy-1-hexyl radical (**4.1b**) at 172 K, spectral width 80 G

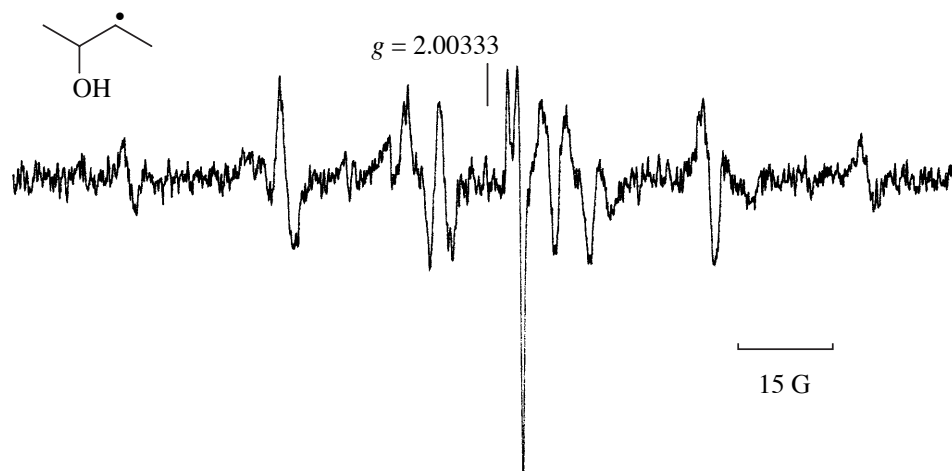
**Table 4.3.** ESR spectral data for the 2-acetoxy-1-hexyl radical (**4.1b**)

$T$ (K)	$g$	$\alpha_\alpha$ (G)	$\alpha_\beta$ (G)	$\alpha_\gamma$ (G)
135	~2.0024	~22.3(t)	~20.7 (d)	n.r.
153	2.00245	22.37	20.62	n.r.
172	2.00241	22.30	20.53	n.r.
190	2.00244	22.31	20.97	n.r.
211	2.00246	22.28	21.56	n.r.
231	2.00247	22.28	21.78	n.r.

**Figure 4.4.** ESR spectrum of 2-trifluoroacetoxy-1-hexyl radical (**4.1c**) at 172 K, spectral width 80 G**Table 4.4.** ESR spectral data for the 2-trifluoroacetoxy-1-hexyl radical (**4.1c**)

$T$ (K)	$g$	$\alpha_\alpha$ (G)	$\alpha_\beta$ (G)	$\alpha_\gamma$ (G)
135	2.00241	22.54 (t)	14.69 (d)	n.r.
153	2.00243	22.55	15.09	n.r.
172	2.00243	22.52	15.59	n.r.
191	2.00245	22.52	16.29	n.r.
211	2.00248	22.48	17.51	n.r.
231	2.00247	22.44	18.18	n.r.
251	2.00244	22.37	18.46	n.r.
271	2.00241	22.38	18.66	n.r.

## 4.4.2 Spectra of 3-(oxysubstituted)-2-butyl radicals 4.2a-c

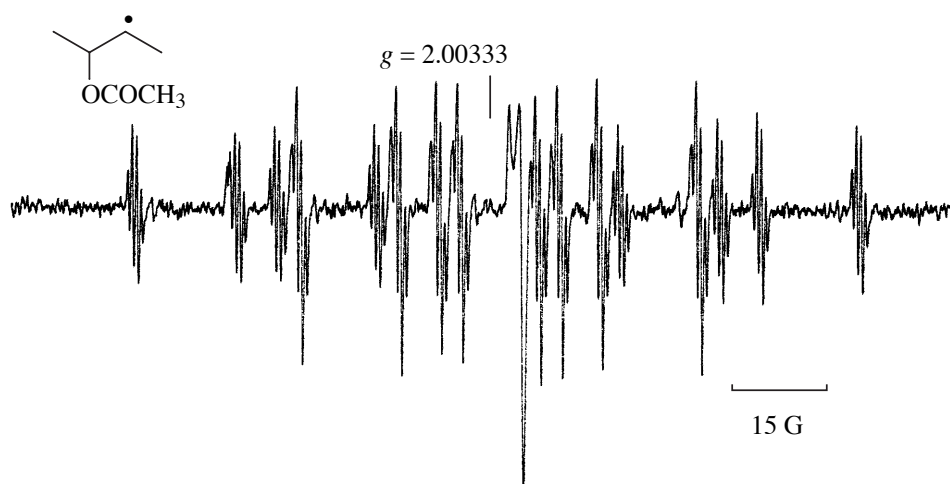


**Figure 4.5.** ESR spectrum of 3-hydroxy-2-butyl radical (**4.2a**) at 231 K, spectral width 150 G

**Table 4.5.** ESR spectral data for the 3-hydroxy-2-butyl radical (**4.2a**)

$T$ (K)	$g$	$\alpha_\alpha$ (G)	$\alpha_\beta$ -CH (G)	$\alpha_\beta$ -CH <sub>3</sub> (G)	$\alpha_\gamma$ (G)
172	2.00251	21.95 (d)	19.82 (d)	25.21 (q)	0.5* (q)
190	2.00249	22.02	19.35	25.35	0.5*
211	2.00252	21.82	18.84	25.08	0.5*

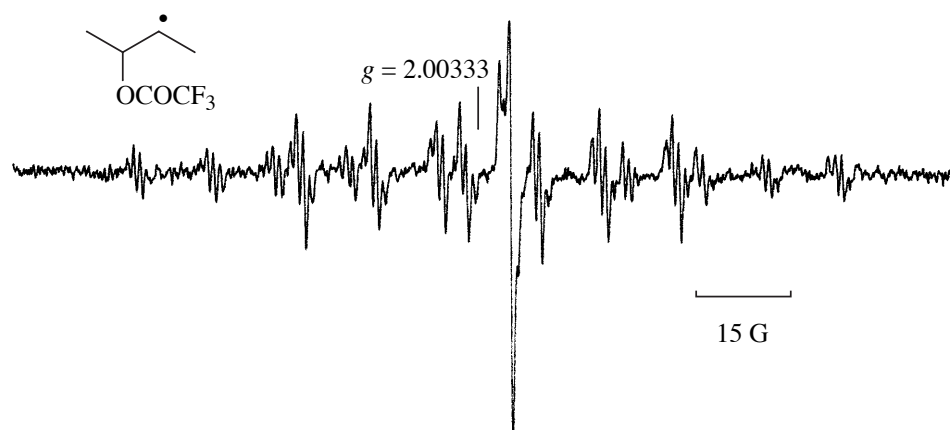
\* poorly resolved



**Figure 4.6.** ESR spectrum of 3-acetoxy-2-butyl radical (**4.2b**) at 172 K, spectral width 150 G

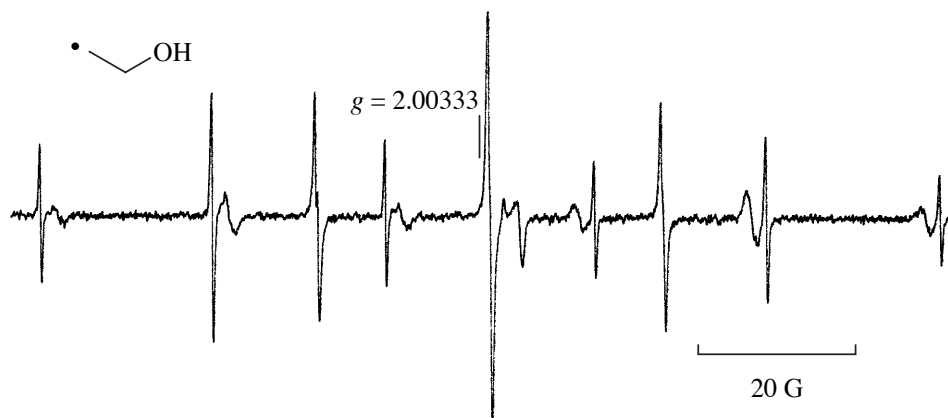
**Table 4.6.** ESR spectral data for the 3-acetoxy-2-butyl radical (**4.2b**)

$T$ (K)	$g$	$\alpha_\alpha$ (G)	$\alpha_\beta$ -CH (G)	$\alpha_\beta$ -CH <sub>3</sub> (G)	$\alpha_\gamma$ (G)
135	~2.0025	~21.8 (d)	15.85 (d)	25.6 (q)	n.r. (q)
153	2.00252	22.21	15.82	25.58	0.72
172	2.00251	22.09	15.83	25.48	0.72
190	2.00249	22.09	15.91	25.44	0.73
211	2.00248	22.06	16.07	25.48	0.75
231	2.00248	22.01	16.16	25.46	0.76

**Figure 4.7.** ESR spectrum of 3-trifluoroacetoxy-2-butyl radical (**4.2c**) at 172 K, spectral width 150 G**Table 4.7.** ESR spectral data for the 3-trifluoroacetoxy-2-butyl radical (**4.2c**)

$T$ (K)	$g$	$\alpha_\alpha$ (G)	$\alpha_\beta$ -CH (G)	$\alpha_\beta$ -CH <sub>3</sub> (G)	$\alpha_\gamma$ (G)
153	2.00248	22.19 (d)	11.18 (d)	25.88 (q)	1.00 (q)
172	2.00251	22.07	11.53	25.77	1.02
191	2.00248	22.03	12.02	25.77	0.97
211	2.00252	21.96	12.46	25.70	0.99
261	2.00245	21.89	13.24	25.56	0.99

## 4.4.3 Spectra of 2-(oxysubstituted)ethyl radicals 4.3a-c

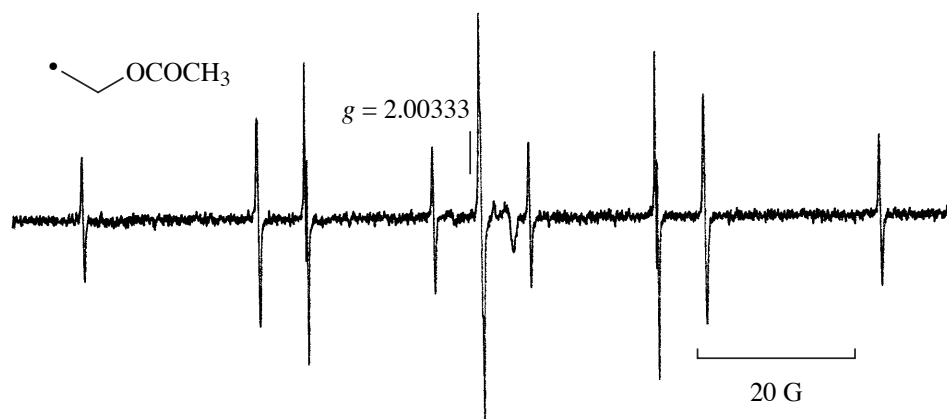


**Figure 4.8.** ESR spectrum of 2-hydroxyethyl radical (**4.3a**) at 153 K, spectral width 120 G. Note the second spectrum also present, in which the  $M_I = \pm 1$  lines due to the  $\beta$ -hydrogen splitting are greatly broadened.

**Table 4.8.** ESR spectral data for the 2-hydroxyethyl radical (**4.3a**)

$T$ (K)	$g$	$\alpha_\alpha$ (G)	$\alpha_\beta$ (G)
135	2.00273	22.16 (t), 22.19 (t)	35.94 (t), 33.99 (t)
153	2.00267	22.06, 22.10	35.31, 33.31
172	2.00268	22.09, 22.19	34.76, 33.16
191	2.00267	22.04, 22.19	34.18, 32.58
201	2.00263	22.09, 22.19	33.77, 32.45
231	2.00261	22.06, 22.17	32.66, 30.69

Numbers in italics represent splitting constants for a second species present, with great broadening of the  $M_I = \pm 1$  lines of the  $\beta$ -hydrogen coupling.

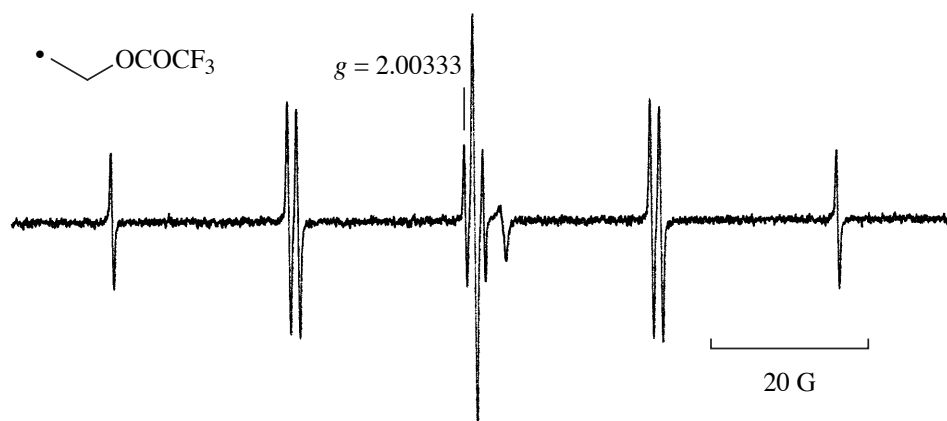


**Figure 4.9.** ESR spectrum of 2-acetoxyethyl radical (**4.3b**) at 172 K, spectral width 120 G

**Table 4.9.** ESR spectral data for the 2-acetoxyethyl radical (**4.3b**)

$T$ (K)	$g$	$\alpha_\alpha$ (G)	$\alpha_\beta$ (G)
135	~2.0027	22.32 (t)	29.97 (t)
153	2.00259	22.29	29.27
172	2.00258	22.38	28.51
191	2.00259	22.33	27.82
211	2.00257	22.35	27.29
231*	2.00258	22.27	26.77
251*	2.00253	22.24	26.42
271*	2.00257	22.23	26.11

\* Propane and ethylene oxide were omitted in the preparation of these sample solutions.

**Figure 4.10.** ESR spectrum of 2-trifluoroacetoxyethyl radical (**4.3c**) at 172 K, spectral width 120 G**Table 4.10.** ESR spectral data for the 2-trifluoroacetoxyethyl radical (**4.3c**)

$T$ (K)	$g$	$\alpha_\alpha$ (G)	$\alpha_\beta$ (G)
135	2.00256	22.54 (t)	24.25 (t)
153	2.00258	22.54	23.91
171	2.00260	22.53	23.70
191	2.00258	22.51	23.49
211	2.00256	22.54	23.33
231	2.00256	22.48	23.22
251	2.00257	22.48	23.15



## 4.5 Calculations, analysis and discussion

### 4.5.1 General

A compilation of the  $g$  values and pertinent hyperfine coupling constants for each of the nine species studied is provided in table 4.11, along with those for comparable hydrocarbon radicals. The  $g$  values for most of the radicals are slightly lower than the range 2.0026-2.0028 normally expected for alkyl radicals, although they are still greater than that for a free spin (2.00232). Such values are consistent with a  $\pi$ -type radical which possesses an electronegative  $\beta$ -heteroatom substituent. For example, 2-trifluoromethoxyethyl radical,  $\text{CF}_3\text{OCH}_2\dot{\text{C}}\text{H}_2$ , has a  $g$  factor of 2.00257.<sup>17</sup>

**Table 4.11.** Summary of esr spectral parameters and comparison with those of analogous hydrocarbon radicals.

Species		$g$ (average)	$\alpha_{\alpha H}$ (average, G)	$\alpha_{\beta H}$ at <i>ca.</i> 170 K (G)
$\dot{\text{C}}\text{H}_2\text{CH}(\text{Bu})\text{OH}$	<b>4.1a</b>	2.00245	21.96	26.7
$\dot{\text{C}}\text{H}_2\text{CH}(\text{Bu})\text{OCOCH}_3$	<b>4.1b</b>	2.00245	22.31	20.6
$\dot{\text{C}}\text{H}_2\text{CH}(\text{Bu})\text{OCOCF}_3$	<b>4.1c</b>	2.00244	22.48	15.5
$\dot{\text{C}}\text{H}_2\text{CH}(\text{CH}_3)_2$		2.0026 <sup>b</sup>	21.93 <sup>a</sup>	32.3 <sup>c</sup>
$\text{CH}_3\dot{\text{C}}\text{HCH}(\text{CH}_3)\text{OH}$	<b>4.2a</b>	2.00251	21.93	19.9
$\text{CH}_3\dot{\text{C}}\text{HCH}(\text{CH}_3)\text{OCOCH}_3$	<b>4.2b</b>	2.00250	22.09	15.8
$\text{CH}_3\dot{\text{C}}\text{HCH}(\text{CH}_3)\text{OCOCF}_3$	<b>4.2c</b>	2.00249	22.03	11.5
$\text{CH}_3\dot{\text{C}}\text{HCH}(\text{CH}_3)\text{CH}_2\text{CH}_3$		unreported	22.0 <sup>d</sup>	22.0 (at 77 K) <sup>d</sup>
$\dot{\text{C}}\text{H}(\text{CH}_3)_2$		2.00268 <sup>e</sup>	21.87 <sup>e</sup>	24.7 <sup>f</sup>
$\dot{\text{C}}\text{H}_2\text{CH}_2\text{OH}$	<b>4.3a</b>	2.00267	22.08	34.8
$\dot{\text{C}}\text{H}_2\text{CH}_2\text{OCOCH}_3$	<b>4.3b</b>	2.00257	22.30	28.6
$\dot{\text{C}}\text{H}_2\text{CH}_2\text{OCOCF}_3$	<b>4.3c</b>	2.00257	22.52	23.7
$\dot{\text{C}}\text{H}_2\text{CH}_2\text{CH}_3^g$		2.00265	22.10	30.2 <sup>c</sup>

For convenience all coupling constants are represented as having positive sign.

a: Reference 24; b:  $g$  value for aqueous solution: reference 25; c: Reference 45; d: Reference 49; e: Reference 26; f: in diethyl ether solution: reference 20; g: Reference 18

These lower  $g$  values are consistent with delocalisation of the odd electron on to the  $\beta$ -substituent, as postulated for  $\beta$ -chloroethyl radicals,<sup>18-21</sup> although this may not be the case with  $\beta$ -oxyalkyl radicals. The low  $g$  value of 2.00199 for  $\beta$ -chloroethyl radical is attributed to a delocalisation of the odd electron into the p orbitals of the chlorine atom.<sup>20</sup> However, Kochi and coworkers doubt that such homoconjugation with  $\beta$ -oxygen substituents is detectable in  $g$  since the spin orbit coupling constant of oxygen ( $\xi_p = 151 \text{ cm}^{-1}$ ) is only a fraction of that for Cl ( $\xi_p = 586 \text{ cm}^{-1}$ ).<sup>17</sup> More recent theoretical calculations discount the significance of such homoconjugation altogether.<sup>22,23</sup> Furthermore, since many workers do not indicate whether the  $g$  factors have been corrected for second-order field effects, care should be taken before drawing conclusions about radical structure from small deviations in this parameter.

Values for the  $\alpha$  coupling constants are often slightly larger than, yet consonant with, those of comparable alkyl radicals. Values of  $\alpha_{\alpha H}$  are relatively invariant between species, deviating not more than 1.5% from the mean. This indicates that spin density at  $C_\alpha$  varies little with changes in radical structure according to equation 4.5,<sup>27</sup> where  $Q_{CH}^H$  is a proportionality constant estimated to be between  $-22$ <sup>28</sup> and  $-28$  gauss<sup>27</sup> and  $\rho_C$  is the spin density at  $C_\alpha$ .

$$\alpha_\alpha = Q_{CH}^H \rho_C \quad (4.5)$$

However, in the series **4.1a-c** and **4.3a-c**, it is clear that  $\alpha_{\alpha H}$  increases steadily in the order  $R = OH < OCOCH_3 < OCOCF_3$ . It is to be expected that  $\alpha_{\alpha H}$  will increase only slightly with a correspondingly large decrease in  $\alpha_{\beta H}$  since the hyperfine splitting at the  $\beta$ -hydrogens does not exceed 10% that of the 507 G splitting of an isolated hydrogen atom.<sup>29</sup>

Also affecting  $\alpha_{\alpha H}$  is the degree of geometric distortion at the radical site. It is known that  $\alpha$ -coupling constants are usually negative in sign and become more positive with increasing pyramidalisation at the radical centre.<sup>28</sup> The ethyl radical is known to be slightly pyramidal at  $C_\alpha$  due to its low resistance to pyramidalisation and for steric and hyperconjugative reasons.<sup>30</sup> So the correlation between the  $\beta$ -substituent  $R$  and  $\alpha_{\alpha H}$  is

consistent with a flattening at  $C_\alpha$  as R becomes more electronegative.

Accompanying the increase in  $\alpha_{\alpha H}$ , in the series **4.1a-c** and **4.3a-c**, is a corresponding and large decrease in  $\alpha_{\beta H}$ . This phenomenon has been observed previously with radicals possessing electronegative  $\beta$ -substituents, a good example being a series of  $\beta$ -oxyethyl radicals,<sup>17</sup> the esr parameters of which are displayed in table 4.12. It can be seen that  $\alpha_{\alpha H}$  increases with both the increasing electronegativity of the substituent and increasing alkyl substitution at  $C_\alpha$ . This is consistent with the participation of a  $\beta$ -oxyanion/alkene radical cation structure (see further on) in stabilising the radical. Such radical cations are stabilised by increasing alkyl substitution, as indicated by the corresponding oxidation potentials<sup>31</sup> of the parent alkenes.

As mentioned previously, it is in the  $\beta$ -hfs that we observe the most obvious differences between  $\beta$ -oxygenated and ordinary alkyl radicals. Hyperfine splittings for acyclic hydrocarbons radicals are normally in the range 23-35 G.<sup>32,33</sup> Not only are the  $\beta$ -couplings for  $\beta$ -oxygenated species often significantly smaller than this, but in all cases

**Table 4.12.** Spectral parameters for a series of  $\beta$ -oxyethyl radicals, from reference 17

Radical	Temp. K	$g$	$\alpha_\alpha$ (G)	$\alpha_\beta$ (G)	$\alpha_\beta$ -CH <sub>3</sub> (G)
$\dot{C}H_2CH_2OH^a$	135	2.00273 <sup>b</sup>	22.16	35.94	-
$\dot{C}H_2CH_2OCH_3$	137	2.00257	22.17	34.61	-
$\dot{C}H_2CH_2OCF_3$	137	2.00257	22.59	31.21	-
$CH_3\dot{C}HCH_2OCF_3$	173	2.00255	22.69	16.56	25.56
$(CH_3)_2\dot{C}CH_2OCF_3$	172	2.00256	-	10.02	23.45

a: this current work; b: not corrected for second order effects

within a series of the same carbon framework, the splitting magnitude decreases as a function of the substituent, in the order OH > OCOCH<sub>3</sub> > OCOF<sub>3</sub> and as the degree of alkyl substitution at  $C_\alpha$  and  $C_\beta$  increases. Such trends are illustrated clearly by examining the free-spin  $\alpha_{\beta H}$  values in table 4.13 and their deviation from that for the benchmark

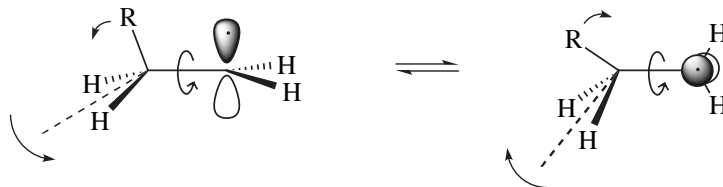
ethyl radical. It is clear that the nature of the  $\beta$ -substituent and radical alkyl structure affect the  $\beta$ -coupling constant markedly.

**Table 4.13.** Approximate extrapolated free-spin values for  $\alpha_{\beta H}$  and the deviation from that for ethyl radical ( $\approx 27$  G)

Radical		$\alpha_{\beta H}$ at free-spin (G)	$27 - (\alpha_{\beta H}$ at free-spin) (G)
$\dot{\text{C}}\text{H}_2\text{CH}(\text{Bu})\text{OH}$	<b>4.1a</b>	24	3
$\dot{\text{C}}\text{H}_2\text{CH}(\text{Bu})\text{OCOCH}_3$	<b>4.1b</b>	23	4
$\dot{\text{C}}\text{H}_2\text{CH}(\text{Bu})\text{OCOCF}_3$	<b>4.1c</b>	20	7
$\text{CH}_3\dot{\text{C}}\text{HCH}(\text{CH}_3)\text{OH}$	<b>4.2a</b>	17	10
$\text{CH}_3\dot{\text{C}}\text{HCH}(\text{CH}_3)\text{OCOCH}_3$	<b>4.2b</b>	16.5	10.5
$\text{CH}_3\dot{\text{C}}\text{HCH}(\text{CH}_3)\text{OCOCF}_3$	<b>4.2c</b>	14	13
$\dot{\text{C}}\text{H}_2\text{CH}_2\text{OH}$	<b>4.3a</b>	27	0
$\dot{\text{C}}\text{H}_2\text{CH}_2\text{OCOCH}_3$	<b>4.3b</b>	24	3
$\dot{\text{C}}\text{H}_2\text{CH}_2\text{OCOCF}_3$	<b>4.3c</b>	22	5

Three main theories have been put forward to explain this phenomenon. Kochi and coworkers,<sup>20,34</sup> building on an earlier idea,<sup>13</sup> argued that the reduction in  $\alpha_{\beta H}$  as a function of the  $\beta$ -substituent was caused by a geometric distortion at  $C_\beta$  which tilts the  $\beta$ -hydrogen(s) towards the nodal plane, lessening interaction with the unpaired spin. In  $\beta$ -oxygenated alkyl radicals, such tilting is attributed<sup>17</sup> to asymmetric oxygen bridging caused by a homoconjugative interaction between the  $\beta$ -oxygenated substituent and the radical centre. Such a theory requires that the degree of distortion at  $C_\beta$  is dependent upon the  $\text{R}-\text{C}_\beta-\text{C}_\alpha$ -SOMO dihedral angle, being largest at 0 and 180°. The angle of tilt affects the magnetic field experienced at the  $\beta$ -hydrogens such that an in-phase modulation of  $\alpha_{\beta H}$  between two limiting values is expected, the width of a particular line being proportional to  $(M_H)^2$ .<sup>16</sup> This leads to selective broadening of only the outer pair of lines of a triplet, with spin quantum number  $\pm 1$ . Huge linewidths are not observed in the  $M_\beta = \pm 1$  lines of the esr spectra. So, for this theory to be correct a time-averaged tilt

angle must exist, resulting from interconversion between rotational states at a rate significantly exceeding the esr timescale ( $\sim 10^8 \text{ s}^{-1}$ ).



Lloyd and Wood<sup>35</sup> offered a second explanation, after an esr study of  $\beta$ -halo-*tert*-butyl radicals. The coupling constants indicated pyramidalisation of  $C_\alpha$  which reduces the interaction of the unpaired electron with the  $\beta$ -hydrogens since the SOMO is tilted away from a position perpendicular to the  $C_\alpha$ - $C_\beta$  bond. The equilibrium conformation of chloro-*tert*-butyl radical is shown from two different angles, illustrating the pyramidalisation at  $C_\alpha$ . A good measure of the degree of pyramidalisation is the  $^{13}\text{C}$



coupling constant at  $C_\alpha$ .<sup>36</sup> Unfortunately this parameter was not measured in the present study. The lowering of both  $\alpha_{\alpha H}$  and  $\alpha_{\beta H}(\text{CH}_3)$  by pyramidalisation at  $C_\alpha$  is illustrated by the difference between ethyl and 1-fluoroethyl radicals<sup>37</sup> in table 4.14.

**Table 4.14.** ESR parameters<sup>37</sup> and values of  $P$  for ethyl and 1-fluoroethyl radical

Radical	$T$ (K)	$g$	$\alpha_{\alpha H}$ (G)	$\alpha_{\beta H} - \text{CH}_3$ (G)	$P$
$\text{CH}_3\dot{\text{C}}\text{H}_2$	160	2.00260	22.37	26.99	1.207
$\text{CH}_3\dot{\text{C}}\text{HF}$	167	2.00366	17.31	24.48	1.414

Beckwith, Ruchardt and coworkers<sup>38</sup> have developed an earlier idea<sup>39</sup> to provide a means for estimating of the degree of pyramidalisation at  $C_\alpha$  in radicals of structure  $\dot{C}HMeX$ . The pyramidalisation quotient,  $P$ , is defined as the ratio of  $\alpha_{\beta H}$  ( $CH_3$ ) to  $\alpha_{\alpha H}$ , the former being less sensitive to a change in geometry.<sup>40</sup> If  $P > 1.25$ , the radical is considered to be significantly pyramidal at  $C_\alpha$ .

$$P = \frac{\alpha_{\beta H} - CH_3}{\alpha_{\alpha H}}$$

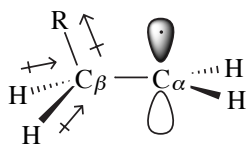
**Table 4.15.** ESR parameters and values of  $P$  for **4.2a-c** at 172 K

Radical		$\alpha_{\alpha H}$ (G)	$\alpha_{\beta H} - CH_3$ (G)	$P$
$CH_3\dot{C}HCH(CH_3)OH$	<b>4.2a</b>	21.95	25.21	1.149
$CH_3\dot{C}HCH(CH_3)OCOCH_3$	<b>4.2b</b>	22.09	25.48	1.153
$CH_3\dot{C}HCH(CH_3)OCOCF_3$	<b>4.2c</b>	22.07	25.77	1.168

According to the  $P$  index, radicals **4.2a-c** are *less* pyramidal at  $C_\alpha$  than the propyl radical, but do become slightly more pyramidal with increasing  $\beta$ -substituent electronegativity. From the values of  $P$  in table 4.15 it is concluded that pyramidalisation at  $C_\alpha$  cannot be responsible for the large reduction in the  $\alpha_{\beta H}$  free-spin values.

A third theory was formulated when *ab initio* calculations<sup>23,41</sup> revealed no significant geometric distortions in the optimised structures of  $\beta$ -substituted ethyl radicals. A correlation was however found between calculated spin densities at  $H_\beta$  and the electronegativity of the  $\beta$ -substituent.<sup>41,42</sup> Guerra<sup>42</sup> reports that an electronegative  $\beta$ -substituent reduces the "electron releasing power" of the  $C_\beta-H_\beta$  bond towards the unpaired spin and he has even formulated a modified Heller-McConnell<sup>43</sup> expression for  $\alpha_{\beta H}$  in  $\beta$ -substituted ethyl radicals.  $A$  and  $B$  are constants which are relatively invariant for second-row substituents ( $CH_3$ ,  $NH_2$ ,  $OH$ ,  $F$ ). The variable  $C$  is related to substituent electronegativity and is responsible for the majority of the difference in  $\beta$ -coupling constant between species.  $\theta$  and  $\varphi$  refer to the dihedral angles between the

SOMO axis and  $C_{\beta}$ - $H_{\beta}$  and  $C_{\beta}$ - $R$  bonds respectively. This equation accurately predicts  $\alpha_{\beta H}$  values obtained from *ab initio* calculations,<sup>42</sup> yet shows significant deviations when used to predict experimental free-spin values in the present work.



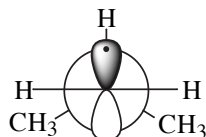
$$\langle \alpha_{\beta, \varphi} \rangle = A + B \cos^2 \theta + C \cos \theta \cos \varphi$$

In summary,  $\alpha_{\alpha H}$  values for  $\beta$ -oxysubstituted alkyl radicals are slightly larger than those for alkyl radicals owing to the combined effects of an increase in the spin density at  $C_{\alpha}$ —caused by a corresponding decrease at  $H_{\beta}$ —and to increased planarity at the radical centre. Free-spin values for  $\alpha_{\beta H}$  are considerably lower than those observed in alkyl radicals owing to either a spectroscopically time-averaged tilt of the  $\beta$ -hydrogens towards the nodal plane and/or a spin density decrease at  $H_{\beta}$  caused by the electronegativity of the  $\beta$ -substituent, rather than pyramidalisation at  $C_{\alpha}$ .

#### 4.5.2 2-(Oxysubstituted)hexyl radicals 4.1a-c

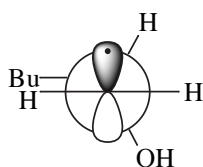
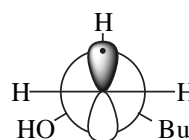
As expected, the esr spectra for each of the species (**4.1a-c**) yielded six major lines, consisting of a doublet of triplets. Longer range  $\gamma$  coupling to the C3 methylene group was not resolved. The temperature dependences of  $\alpha_{\beta H}$  for radicals **4.1a-c** each contain points of inflexion (figure 4.11). This indicates that steric and electronic effects are of similar strength, sometimes acting antagonistically upon the equilibrium conformation of these species and that the degree of their participation changes with temperature.

The isobutyl radical, the simplest hydrocarbon analogue of radicals **4.1a-c**, is widely believed to have a lowest energy conformation in which the  $\beta$ -hydrogen eclipses the radical orbital,<sup>34</sup> as shown by the negative temperature dependence ( $\alpha_{\beta H}$  magnitude decreases with increasing temperature) of the  $\beta$ -hydrogen splitting (see figure 4.11).

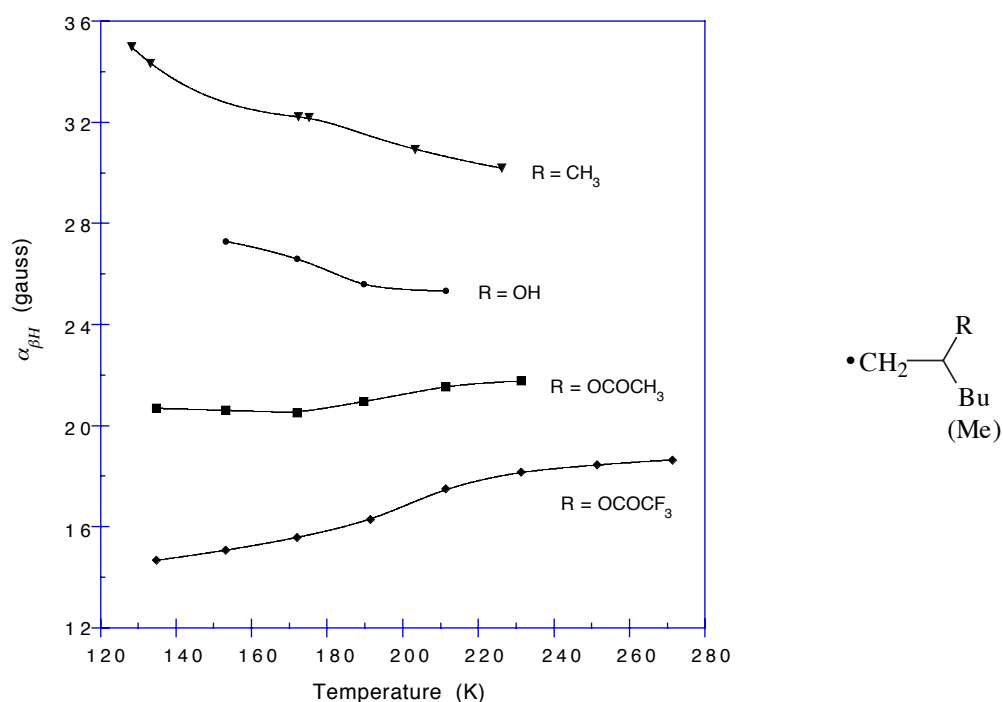


The 2-hydroxyhexyl radical (**4.1a**) has the same sense of  $\alpha_{\beta H}$  temperature dependence. The maximum value of  $\alpha_{\gamma H}$  in alkyl radicals is approximately 8 G, which is achieved in a frozen *W*-plan conformation.<sup>44</sup> The experimental hfs of *trans*  $\gamma$ -hydrogens have been shown to fit a relationship of the form  $\alpha_{\gamma H} = 0.1 + 7.9 \cos^2 \Phi$ , where  $\Phi$  is the dihedral angle between the SOMO and the plane through  $C_{\alpha}-C_{\beta}-C_{\gamma}$ .<sup>44</sup> It follows that the maximum  $\alpha_{\gamma H}$  value for a *freely rotating*  $\gamma$ -hydrogen is about 4 G and so a relationship of the form  $\alpha_{\gamma H} = 4 \cos^2 \Phi$  has been used to approximate the position of alkyl groups. Long-range hfs are resolvable for the 2-methylpentyl radical for  $T > 140\text{K}$ .<sup>44</sup> Therefore, it is reasonable to assume that the  $\gamma$ -hydrogens are time-averaged by free  $C_{\beta}-C_{\gamma}$  rotation in radicals **4.1a-c**, for  $T > 140\text{ K}$ .

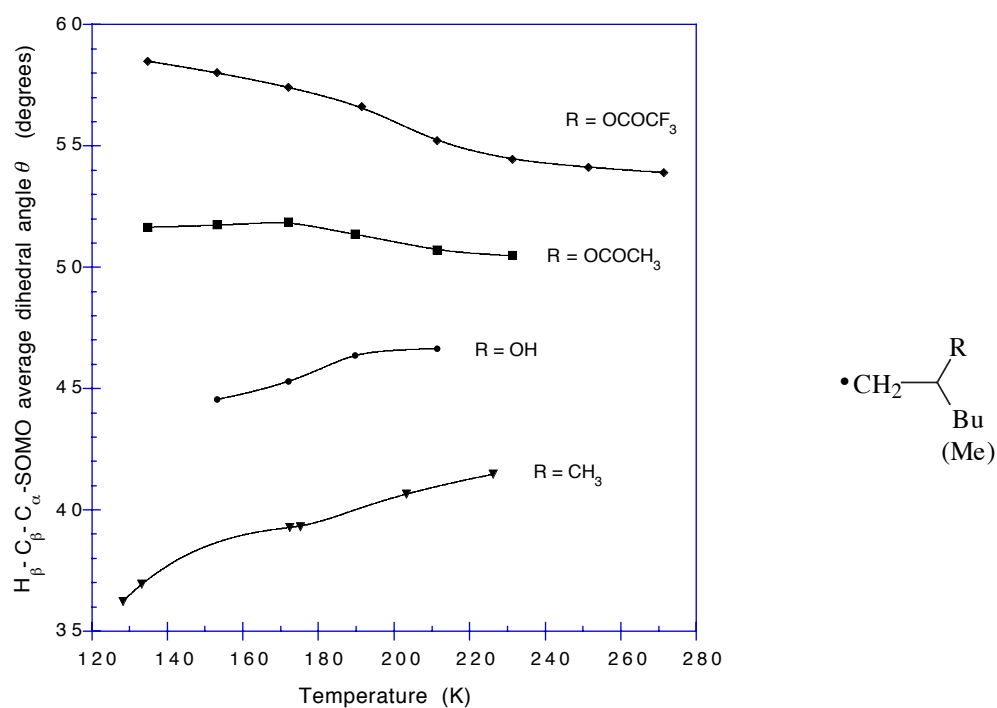
Since  $\gamma$ -coupling was not resolved in the spectra of **4.1a-c**, it was not possible to calculate the exact equilibrium position of the butyl (or methyl) group. But base-to-base esr linewidths for **4.1a** are approximately 4 G, so  $\alpha_{\gamma H}$  for the C3-methylene is  $< 2\text{ G}$ . This places the alkyl substituent at  $> 45^\circ$  away from the radical orbital axis. Therefore, the most likely low temperature conformation is closer to that depicted in **4.4**, because the  $\alpha_{\beta H}$  values are significantly lower than those for isobutyl radical and have a less significant temperature dependence at low temperature. However, **4.5**, a less probable contender, cannot be excluded owing to the unavailability of hfs data at lower temperatures.

**4.4****4.5**





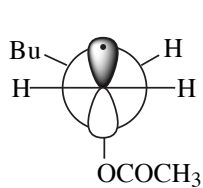
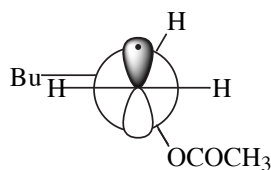
**Figure 4.11.** Plot of the  $\beta$  coupling constant versus temperature for 2-(oxysubstituted)hexyl radicals (4.1a-c). Data for the isobutyl radical in alkane solvent, is included for comparison.<sup>45</sup>



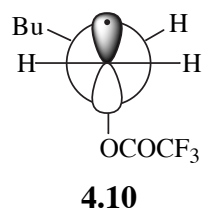
**Figure 4.12.** Plot of the dependence of the time-averaged  $\beta$ -H-SOMO dihedral angle upon temperature for 2-(oxysubstituted)hexyl radicals (4.1a-c). Angles calculated for the isobutyl radical<sup>45</sup> are shown for comparison.

Radical **4.1c** (and to some extent **4.1b**) shows a *positive* temperature dependence of the  $\beta$ -coupling constant, in contrast to the negative temperature dependence of the isobutyl radical. The 2-acetoxy-1-hexyl radical (**4.1b**) shows an invariance in  $\alpha_{\beta H}$  at lower temperatures. This radical is not conformationally frozen, however, since the esr spectra indicate that the  $\alpha$ -hydrogens are magnetically equivalent at all temperatures. Therefore exchange between magnetically equivalent conformations is still occurring at rates significantly above the esr time scale of about  $10^8 \text{ s}^{-1}$ . Such a temperature dependence for **4.1b** has a gradient intermediate between those of **4.1a** and **4.1c** and is consistent with the lower temperature invariance being caused by a balance of weak steric and electronic effects rather than by strong conformational locking due to a stereoelectronic effect. However, it should be noted that the linewidths are large in the spectra of **4.1a-c**. Such broadening might be due in part to rate processes which exchange conformations in which  $\alpha$ -hydrogens are inequivalent.

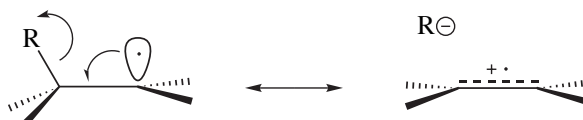
At 231 K, the base-to-base width of each major line in the spectrum of **4.1b** is approximately 2.2 G and the line shape is consistent with a poorly resolved triplet. In the considerably more highly strained 2,2-di(*trideuteromethyl*)-1-butyl radical, the spectroscopic coalescence temperature for rotation about the C2-C3 bond is 225K.<sup>44</sup> Hence it may be confidently concluded that the  $\gamma$ -hydrogens in **4.1b** are magnetically equivalent by fast exchange at 231K. If the  $\gamma$ -hydrogens resonate as a poorly resolved triplet, the coupling constant cannot exceed 1.1 G. Hence the butyl group can be calculated to be twisted away from the axis of the radical orbital by *ca.*  $58^\circ$ . Therefore, **4.6** appears to be the more stable conformation, although the less probable conformation **4.7** cannot yet be excluded since hfs data below 135 K have not been obtained.

**4.6****4.7**

The widths of the major lines in the spectrum of **4.1c** are also *ca.* 2 G, so the position of the butyl group must be at  $> 45^\circ$  to the SOMO. This information, in conjunction with the positive temperature dependence of the  $\beta$ -coupling constant, is consistent with **4.10** being the most stable conformation.



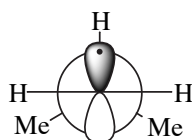
A comparison of the low temperature conformations of **4.1a-c** indicates that as the electronegativity of the  $\beta$ -oxy substituent increases, the group is more prone to eclipse the SOMO. Consequently, the butyl group tends to lie closer to the nodal plane than to the SOMO. These geometries are consistent with a significant contribution from an anion/radical cation hyperconjugative mechanism towards the equilibrium conformations.



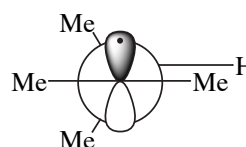
### 4.5.3 3-(Oxysubstituted)-2-butyl radicals 4.2a-c

Radicals **4.2a-c** each displayed an esr spectrum consisting of 16 major lines, composed of a quartet of double doublets. Within each major line, a quartet due to  $\gamma$ -splitting (0.5-1 G) was evident, although the resolution was poor in the case of **4.2a**.

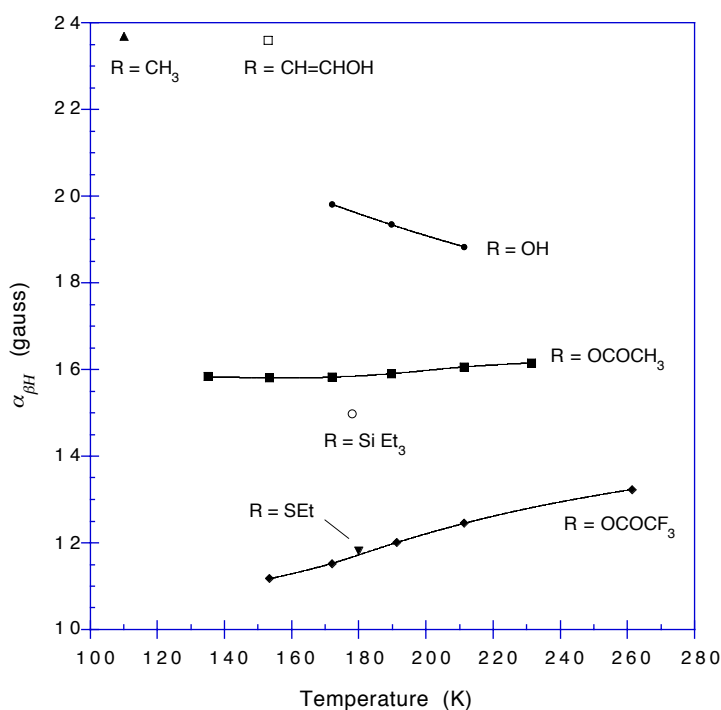
The most stable conformation of the 3-methyl-2-butyl radical,  $\text{CH}_3\dot{\text{C}}\text{HCH}(\text{CH}_3)_2$ , has not yet been reported. At low temperature, the isobutyl radical (**4.13**) adopts an equilibrium conformation with the  $\beta$ -hydrogen eclipsing the half filled orbital,<sup>13,34,45</sup> whereas in the 2,3-dimethyl-2-butyl radical (**4.14**) the  $\beta$ -H eclipses an  $\alpha$ -methyl group.<sup>34</sup>



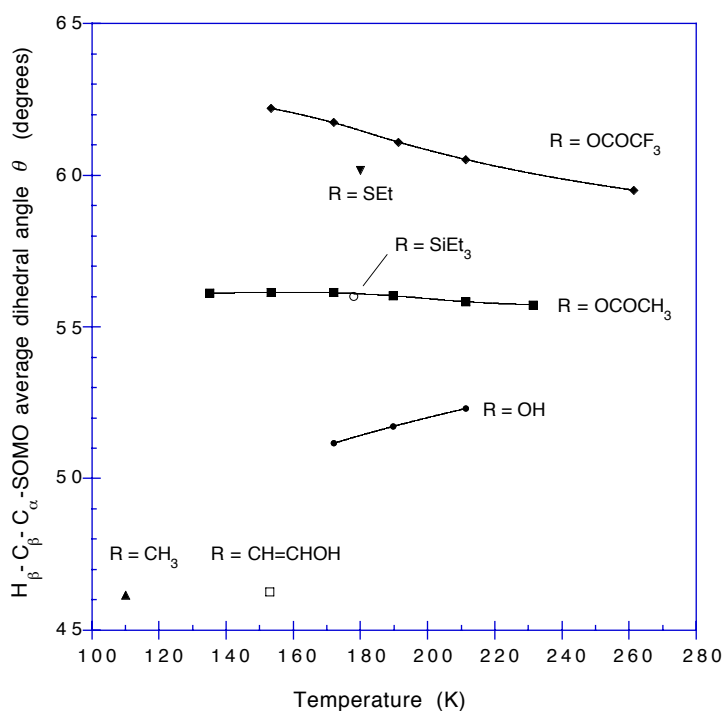
**4.13**



**4.14**

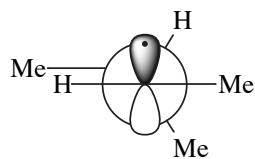


**Figure 4.13.** Plot of the  $\beta$ -coupling constant versus temperature for 3-oxysubstituted-2-butyl radicals (**4.2a-c**). Data points are included for  $\text{R} = \text{CH}_3$ ,<sup>46</sup>  $\text{CH}=\text{CHOH}$ ,<sup>47</sup>  $\text{SiEt}_3$ <sup>48</sup> and  $\text{SEt}$ <sup>48</sup>.

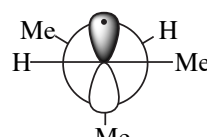


**Figure 4.14.** Plot of the time-averaged  $\beta$ -H-SOMO dihedral angle versus temperature for 3-oxy-substituted-2-butyl radicals (**4.2a-c**). Angles for additional radicals are included. If no  $\alpha_{\beta H}(\text{CH}_3)$  coupling constants were available, that for isopropyl radical ( $24.7 \text{ G}$ )<sup>26</sup> was used.

On steric grounds, one would expect the lowest energy conformation of the 3-methyl-2-butyl radical,  $\text{CH}_3\dot{\text{C}}\text{HCH}(\text{CH}_3)_2$ , to lie somewhere between **4.13** and **4.14**, with  $\theta_0 = 30$  or  $60^\circ$ . The options are therefore **4.15** and **4.16** and models suggest that the  $\beta$ -methyl will lie in closer proximity to the  $\alpha$ -hydrogen than the  $\alpha$ -methyl for steric reasons. Since the  $\beta$ -splitting at 110 K ( $23.7 \text{ G}$ )<sup>46</sup> is slightly *less* ( $\theta_0 > 45^\circ$ ) than the expected free spin value ( $\alpha_\beta(\text{CH}_3) = 24.68 \text{ G}$  for isopropyl radical<sup>33</sup>), the favoured conformation is most likely **4.16**. This conclusion is supported by the still smaller  $\beta$ -splitting for 3-methyl-2-pentyl radical,  $\text{CH}_3\dot{\text{C}}\text{HCH}(\text{CH}_3)\text{CH}_2\text{CH}_3$  ( $22.0 \text{ G}$ ) at the lower temperature of 77 K.<sup>49</sup> This low temperature conformation will be used as a benchmark for the  $\beta$ -oxygenated radicals **4.2a-c**.



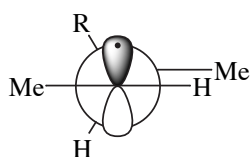
4.15



4.16

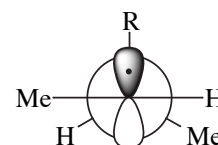
The calculated angles for **4.2a-c** (figure 4.14) must be erroneously large, due to an overestimation of  $Q_{\text{CCH}}^{\text{H}}\rho_{\text{C}}$  values. The temperature dependences of  $\alpha_{\beta\text{H}}$  for **4.2a-c** (figure 4.13) reveal that the extrapolated free-spin (high temperature)  $\alpha_{\beta\text{H}}$  values are considerably less than those expected from the  $\alpha_{\beta\text{H}}(\text{CH}_3)$  values of 25.22, 25.49 and 25.74 G respectively (from table 4.1). However, from the negative temperature dependence for **4.2a**, it can be concluded that **4.17a** is the more stable conformation. Likewise, the positive temperature dependence observed for **4.2c** means that conformation **4.18c** is favoured. Since low temperature data was not available for **4.2b**, the low energy conformation cannot be determined with certainty, but must be either **4.17b** or **4.18b**. If the extrapolated free-spin value of  $\alpha_{\beta\text{H}}$  for **4.2b** is taken to be 16.5 G, then  $\alpha_{\beta\text{H}}$  of 15.85 G at 153 K corresponds to  $\theta = 46.1^\circ$ , slightly favouring **4.18b** over **4.17b**. Since the relatively invariant temperature dependence of **4.2b** is intermediate in gradient between **4.2a** and **4.2c**, it can be concluded that a dynamic balance of weak steric and electronic effects is responsible, rather than a strong conformational locking.

From the  $\gamma_{\beta\text{H}}$  values, the approximate (relative) position of the  $\beta$ -methyl group may be established. For **4.2a**, the  $\text{CH}_3\text{-C}_\beta\text{-C}_\alpha\text{-C}2p_z$  equilibrium dihedral angle is *ca.*  $70^\circ$ ; for **4.2b**,  $65^\circ$ ; and for **4.2c**,  $60^\circ$ . Such values correspond reasonably well with the dihedral angles for the  $\beta$ -hydrogens, in support of the conformational assignments.



4.17

- a: R = OH  
b: R = OCOCH<sub>3</sub>  
c: R = OCOF<sub>3</sub>



4.18

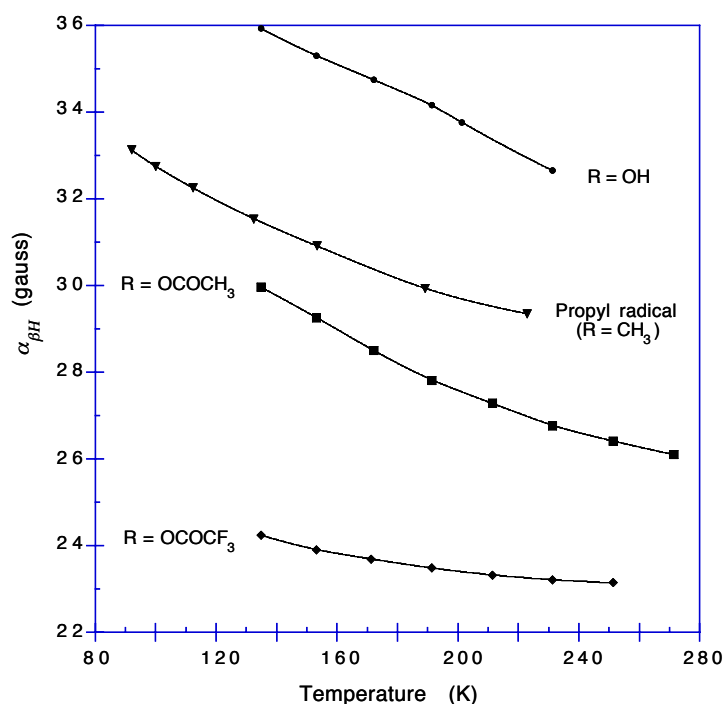
Such pronounced lowering of the  $\alpha_{\beta H}$  values is consistent with an increased participation of heterolytic hyperconjugation, promoted by the increased alkene radical cation stabilisation which accompanies greater methyl substitution.

#### 4.5.4 2-(Oxysubstituted)ethyl radicals 4.3a-c

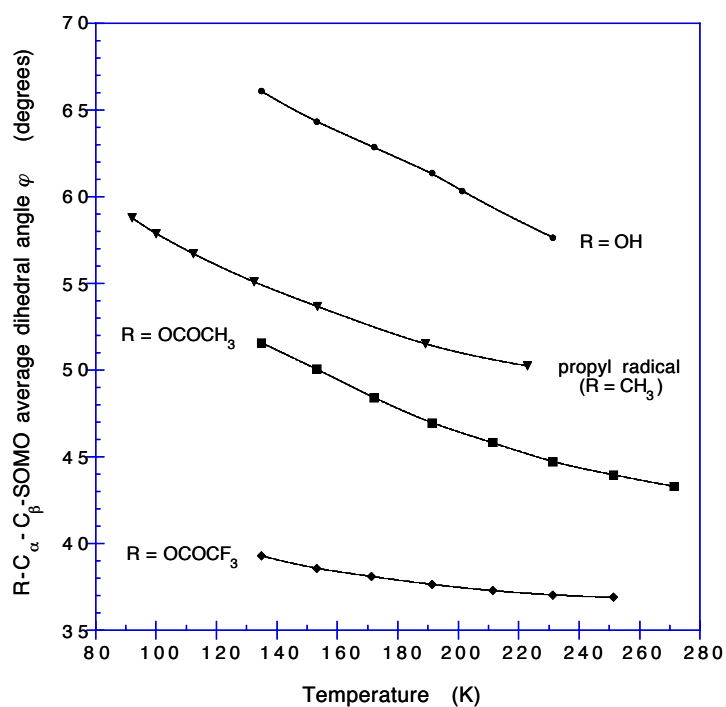
As expected, the esr spectra of the radicals **4.3a-c** consisted of 9 lines (triplet of triplets). With the 2-hydroxyethyl radical (**4.3a**), a second species was observed (figure 4.8), in which the  $M_I = \pm 1$  lines of the  $\beta$ -splitting are considerably broadened and the  $\beta$ -couplings are slightly smaller than for the species with sharper lines. The esr spectra of 2-hydroxyethyl (e.g. reference 50) and 2-acetoxyethyl<sup>16, 51</sup> radicals have been recorded previously and are essentially identical with those recorded here.

A small splitting is observed in the  $M_\beta = 0, M_\alpha = \pm 1$  lines (lines 3 and 7) in the spectra of the 2-hydroxyethyl (0.4 G) and 2-acetoxyethyl (0.15 G) radicals. This is due to a second-order effect<sup>50</sup> since the  $\beta$ -couplings are relatively large with respect to the applied magnetic field (3360 G). Such a splitting is too small to be resolved in the case of **4.3c**.

Like the propyl radical,<sup>34</sup> the low temperature equilibrium conformation of both **4.3a**<sup>32</sup> and **4.3b**<sup>16, 51</sup> has generally been accepted to be **4.19**, in which the oxygenated substituent R eclipses an  $\alpha$ -hydrogen and  $\varphi = 90^\circ$ . Arguments used to support this conclusion include: these species all display a negative temperature dependence of  $\alpha_{\beta H}$ ; the propyl<sup>13</sup> and 2-hydroxyethyl<sup>32</sup> radicals both exhibit broadening of  $M_\alpha = 0$  lines, rationalised by an out-of-phase modulation of the  $\alpha$ -hydrogens, which should be most pronounced at  $\varphi = 90^\circ$  (figure 4.17); and the 2-acetoxyethyl radical shows broadening of the  $M_\beta = \pm 1$  lines,<sup>16</sup> rationalised by an in-phase modulation of the  $\beta$ -hydrogens caused

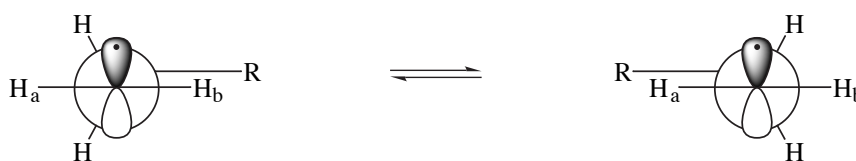


**Figure 4.15.** Plot of the  $\beta$ -coupling constant versus temperature for 2-(oxysubstituted)ethyl radicals (4.3a-c). Data for the propyl radical in hydrocarbon solvent is included for comparison.<sup>45</sup>



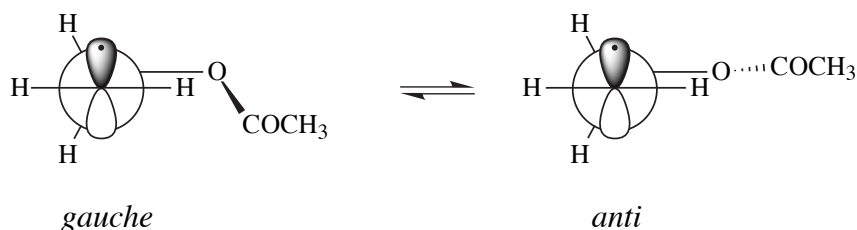
**Figure 4.16.** Plot of the time-averaged dihedral angle between the R-O bond and the SOMO axis versus temperature for 2-(oxysubstituted)ethyl radicals (4.3a-c). Calculated angles for the propyl radical<sup>45</sup> are included for reference.





**Figure 4.17.** Medium-rate conformational exchange in a rotationally hindered radical can account for time-inequivalence of the  $\alpha$ -hydrogens, broadening the  $M_\alpha = 0$  spectral lines.

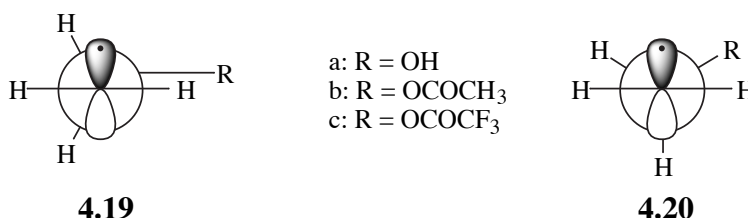
by oscillation of the acetoxy group about the hindered  $C_\beta$ -O bond between two positions in which the  $\beta$ -hydrogens are magnetically equivalent. In figure 4.18 it is apparent that the *anti* conformer has  $C_S$ -like symmetry in which the  $\beta$ -hydrogens are equivalent, but the *gauche* conformer has  $C_1$ -like symmetry in which the  $\beta$ -hydrogens must be inequivalent. Hence this mechanism cannot result in in-phase modulation of solely the  $M_\beta = \pm 1$  lines, but must cause some degree of broadening of the  $M_\alpha = 0$  lines owing to the time-averaged inequivalence of the  $\beta$ -hydrogens. It is highly likely, however, that such phenomena would also be observed if the most stable conformation was not **4.19**, but **4.20**, in which  $\varphi = 60^\circ$ .



**Figure 4.18.** An earlier rationalisation for the modulation of the  $M_\beta = \pm 1$  spectral lines observed with 2-acetoxyethyl radical

*Ab initio* calculations predict that in the minimum energy conformation of the propyl<sup>23</sup> and 2-hydroxyethyl<sup>23,52,53</sup> radicals,  $\varphi$  is approximately  $60^\circ$ . In addition, the isotropic  $\beta$ -coupling of the propyl radical in an argon matrix at 4.2 K is 35.1 G.<sup>54</sup> Such a radical appears not to be conformationally frozen, but tunnels through the rotational barrier with an estimated reorientation correlation time of  $6 \times 10^{-10}$  s.<sup>54</sup> Using  $Q_{CCH}^H \rho_C = 53.8$  G in equation 4.4, the methyl group is calculated to occupy an equilibrium position

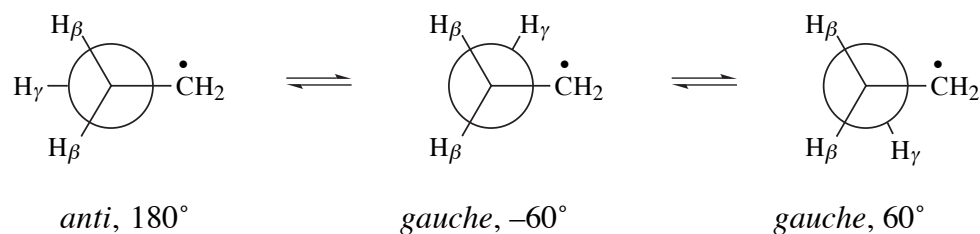
with  $\varphi = 63^\circ$  away from the SOMO. However, Brumby<sup>50</sup> claims that a purely classical analysis under these conditions may be in error. It is therefore concluded that the propyl radical has a low temperature conformation of either **4.19** or **4.20**, the weight of evidence indicating that the latter is the more probable.



Using a value of  $Q_{\text{CCH}}^{\text{H}}\rho_{\text{C}} = 54 \text{ G}$  for **4.3a**, at 135 K, the OH substituent is calculated to lie at  $\varphi = 66^\circ$ . The slope of the temperature dependence suggests that  $\alpha_{\beta\text{H}}$  will continue to increase somewhat at lower temperatures, so the esr evidence indicates that **4.19** is the more stable conformation of the 2-hydroxyethyl radical. This radical shows no preference for stereoelectronic interaction with the half filled orbital. In our hands, the broadening of  $M_{\alpha} = 0$  lines reported by Kochi and Krusic,<sup>32</sup> was difficult to detect until the solvent was changed from cyclopropane to ethylene oxide. At temperatures at or below 211 K obvious broadening of the lines with  $M_{\alpha} = 0$  did occur and is consistent with out-of-phase modulation of time-inequivalent  $\alpha$ -hydrogens. Kochi and Krusic<sup>32</sup> generated the 2-hydroxyethyl radical by photolysis of a solution of hydrogen peroxide in ethanol. Initial indications are that an increased solvent polarity may slow conformational interconversion, making the time-inequivalence of the  $\alpha$ -hydrogens more prominent.

As mentioned previously, a second species was observed in the spectrum of **4.3a** (figure 4.8) in which the  $M_1 = \pm 1$  lines of the  $\beta$ -hydrogen splittings are greatly broadened due partly to in-phase modulation, with the  $\beta$  coupling constants being slightly smaller than for the species displaying sharper resonances. This second spectrum becomes less intense as the temperature is decreased, being almost undetectable at 135 K. However, in the more polar solvent ethylene oxide, the species having the smaller  $\alpha_{\beta\text{H}}$  values was predominant. In fact, another species was not observed until the temperature was

reduced to 191 K. In ethylene oxide, the major spectrum displayed an  $\alpha_\gamma$  OH coupling of about 0.35 G in all major lines. It is believed that this coupling is present—but unresolved, resulting in further line broadening—for the same species in cyclopropane solvent. It is proposed that the two species are the *gauche* and *anti* conformers, resolved by restricted rotation about the C–O bond. The *anti* conformer is the only one in which the OH coupling is large enough to be resolved. The OH coupling for the *gauche* conformers is  $0.35 \text{ G} \times \cos^2(60^\circ) = 0.088 \text{ G}$ , which is too small to be resolved. Presumably H-bonding between the OH and ethylene oxide stabilises the *anti* conformer. Pople and coworkers<sup>52</sup> report that gas phase *ab initio* calculations show that the *gauche* conformer is more stable than the *anti* by up to  $5.4 \text{ kJmol}^{-1}$  at a potential minimum ( $\varphi \approx 60^\circ$ ). Earlier work supports this finding.<sup>41,53</sup> However, when the OH is locked in the *anti* conformation, calculations predict the most stable radical geometry to have  $\varphi = 80^\circ$ .<sup>41</sup>

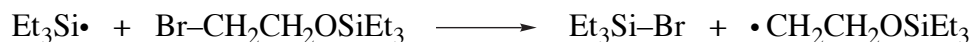
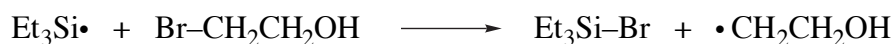
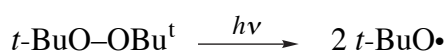


**Figure 4.19.** Stable conformations about the  $\text{C}_\beta\text{-O}$  bond in 2-hydroxyethyl radical **4.3a**

Internal rotational barriers about the C–O bond have been determined for ethanol from vibrational spectra.<sup>55</sup> The *anti/gauche* barrier is  $4.82 \text{ kJmol}^{-1}$  and the *gauche/gauche* barrier  $4.77 \text{ kJmol}^{-1}$ , with *anti*  $0.50 \text{ kJmol}^{-1}$  more stable than the *gauche* conformer. It is expected that the C–O barrier for **4.3a** should be about this size, but this barrier seems too small to spectroscopically resolve the *anti* and *gauche* conformers, even at the low temperatures used.

Another possible explanation for the appearance of the two spectra is that the species with the narrower lines in the esr spectrum of **4.3a** is actually  $\dot{\text{C}}\text{H}_2\text{CH}_2\text{OSiEt}_3$ , formed by the following sequence of reactions. The esr spectrum of  $\dot{\text{C}}\text{H}_2\text{CH}_2\text{OSiMe}_3$

has been recorded,<sup>56</sup> yielding  $g = 2.00259$ ,  $\alpha_{\alpha H} = 22.10$  G and  $\alpha_{\beta H} = 34.36$  G at 160 K. Such parameters are very similar to those for **4.3a**, but the authors report that the spectrum undergoes no detectable linewidth alternation with changes in temperature, contrary to the behaviour observed with **4.3a**. In addition, a preponderance of  $\dot{\text{C}}\text{H}_2\text{CH}_2\text{OSiEt}_3$  in the spectrum would necessitate that the triethylsilyl radicals react much faster with the tiny proportion of  $\text{Et}_3\text{SiOCH}_2\text{CH}_2\text{Br}$  formed than with 2-bromoethanol, a scenario which is highly unlikely.

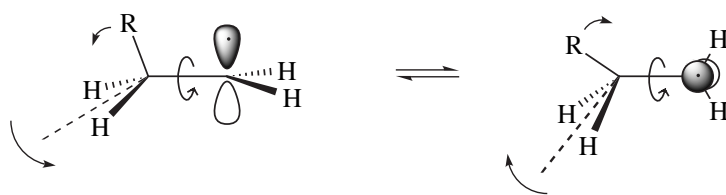


Smaller  $\beta$ -splittings were observed for **4.3a** in the more polar solvent. At 172 K, the *anti* conformer gave  $\alpha_{\beta H} = 33.16$  G in cyclopropane, and 32.60 G in ethylene oxide, with values of 34.77 and 34.69 G respectively for the *gauche* conformers. The dielectric constant for liquid cyclopropane remains unreported, but the refractive index at 230.65 K is known to be 1.3799.<sup>57</sup> Since Maxwell's equation states that the refractive index is equal to approximately the square root of the dielectric constant,  $\epsilon$  is approximately equal to  $(1.3799)^2 = 1.90$ . Ethylene oxide, having  $\epsilon = 12.42$  at 293 K<sup>58</sup> is significantly more polar than cyclopropane. Such a lowering in  $\alpha_{\beta H}$  values is consistent with an increasing contribution of the  $\varphi = 0^\circ$  rotamer to the time-averaged conformation by stabilisation of the charged, hyperconjugative canonical structure. Thus, in ethylene oxide the  $\beta$ -oxygen lone pairs appear to exhibit more steric repulsion from the  $\alpha$ -H's or alternatively, greater interaction with the SOMO, in support of some theoretical results.<sup>52</sup>

The most stable conformation of the 2-acetoxyethyl radical appears to be **4.19b** as judged from the slope of the temperature dependence, although steric and electronic

effects would be expected to destabilise this conformation relative to **4.19a**. Since the ester conformations of  $\beta$ -formyloxy radicals agree with those of the parent formates,<sup>59</sup> it is reasonable to assume that the *Z* conformation of  $\beta$ -acyloxyalkyl radicals is favoured, as observed in the corresponding acetates and trifluoroacetates.<sup>60</sup> In-phase modulation of the  $M_I = \pm 1$  lines of the  $\beta$ -hydrogen splittings is also detected in spectra of **4.3b**, although it is less pronounced than for **4.3a**. Kochi<sup>16</sup> points out that such in-phase modulation occurs because the magnetic environment of the  $\beta$ -hydrogens fluctuates periodically and in such a way that each hydrogen is spectroscopically equivalent at all times, with field fluctuation driven by oscillations of the  $\beta$ -substituent. Such processes must occur at a rate not so slow that two discrete resonances are resolved (slow exchange limit) and not so fast that a spectroscopically averaged field results (fast exchange limit). However such an effect must also broaden the  $M_\alpha = 0$  spectral lines (2,5 and 8) of radicals **4.3a-c**, since rotamers about the  $C_\beta$ -O can occupy one *anti* or two *gauche* positions. When in the *gauche* conformation, the  $\beta$ -hydrogens are inequivalent. In figures 4.8 and 4.9 it can be seen that line 2 is less than twice the height of line 1, an outcome which supports the in-phase modulation explanation.

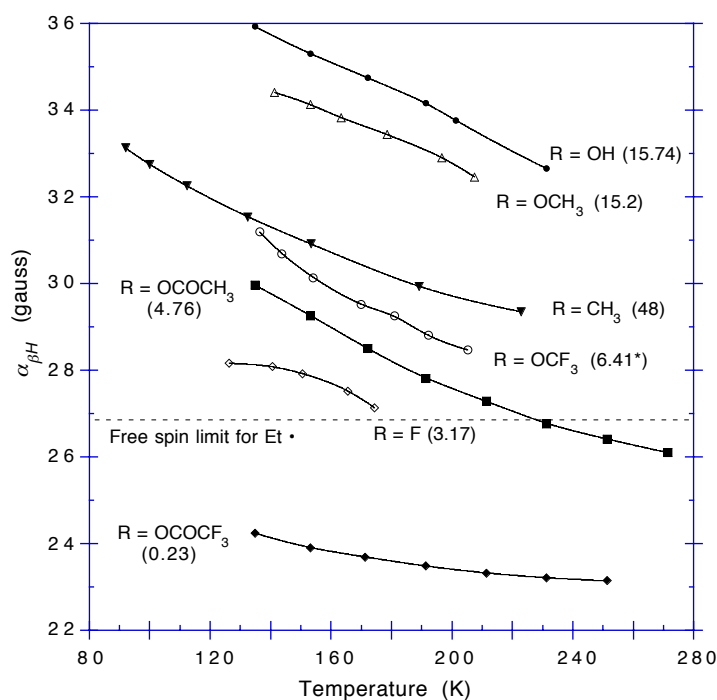
The selective broadening of the  $M_\beta = \pm 1$  lines can also be rationalised by the  $\beta$ -CH<sub>2</sub> group rocking in phase with  $C_\alpha$ - $C_\beta$  bond rotation processes. As the  $\beta$ -methylene group plane tilts toward the nodal plane, the  $\beta$ -hyperfine splitting decreases in size. It is noteworthy that the in-phase modulation is most noticeable when the rotational barrier is largest (see section 4.6); that is, the energy difference between the mutually perpendicular conformations illustrated is large and conformational interconversion is slower. At high interconversion rates, a time-averaged tilt angle results. As the temperature is decreased and lower interconversion frequencies result, the averaged  $\beta$ -hyperfine splitting moves away from the fast exchange limit and a broader range of magnetic field strength is detected at the  $\beta$ -hydrogens. A time-averaged rock of amplitude 1° either side of an equilibrium position may correspond to line broadening of up to 0.75 G, for a 30 G  $\beta$ -coupling, assuming a  $\cos^2$  relationship with the tilt angle.



In-phase modulation of the  $\beta$ -hyperfine splittings is not observed in the esr spectrum of 2-trifluoroacetoxy radical (**4.3c**) until the temperature is decreased to approximately 135 K, when rotational state interconversion becomes slow enough for the  $\beta$ -methylene group rocking to be detected. Using a value of 44 G for  $Q_{\text{CCH}}^{\text{H}}\rho_{\text{C}}$ , at 135 K, **4.3c** adopts an equilibrium conformation in which  $\varphi = 51^\circ$ . This information, combined with the slight temperature dependence of  $\alpha_{\beta\text{H}}$ , indicates that at low temperature the favoured conformation is **4.20c**, where  $\varphi = 60^\circ$ . It is expected that the *Z* conformer of the ester group is highly favoured, as observed for alkyl trifluoroacetates.<sup>60</sup>

Like radicals **4.1a-c** and **4.2a-c**, it is obvious that the  $\alpha_{\beta\text{H}}$  values for **4.3b** and **4.3c**, as well as the other  $\beta$ -acyloxyalkyl radicals studied, are often considerably less than the ethyl radical free-spin ( $45^\circ$ ) value of 26.87 G.<sup>33</sup> This is because the values of  $Q_{\text{CCH}}^{\text{H}}\rho_{\text{C}}$  used to calculate the angle  $\varphi$  with equation 4.4 are too large. Since the  $\alpha_{\alpha\text{H}}$  values indicate that  $\rho_{\text{C}}$  (the spin density at  $\text{C}_\alpha$ ) is relatively invariant across radicals **4.3a-c**, the problem must be that  $Q_{\text{CCH}}^{\text{H}}$  is smaller than for ordinary alkyl radicals. The changes in  $\alpha_{\beta\text{H}}$  between species cannot be accounted for by different equilibrium conformations alone. This problem prompted further investigation.

Figure 4.20 shows a plot of  $\alpha_{\beta\text{H}}$  vs.  $T$ , gleaned from current research and literature data for ethyl radicals with a variety of second row substituents. Values of the  $\text{p}K_{\text{a}}$  of the parent acid RH are in brackets, adjacent to the temperature dependence curves. Apart from propyl radical, there is a steady decrease in the size of  $\beta$ -coupling constant as the substituent becomes a weaker conjugate base.

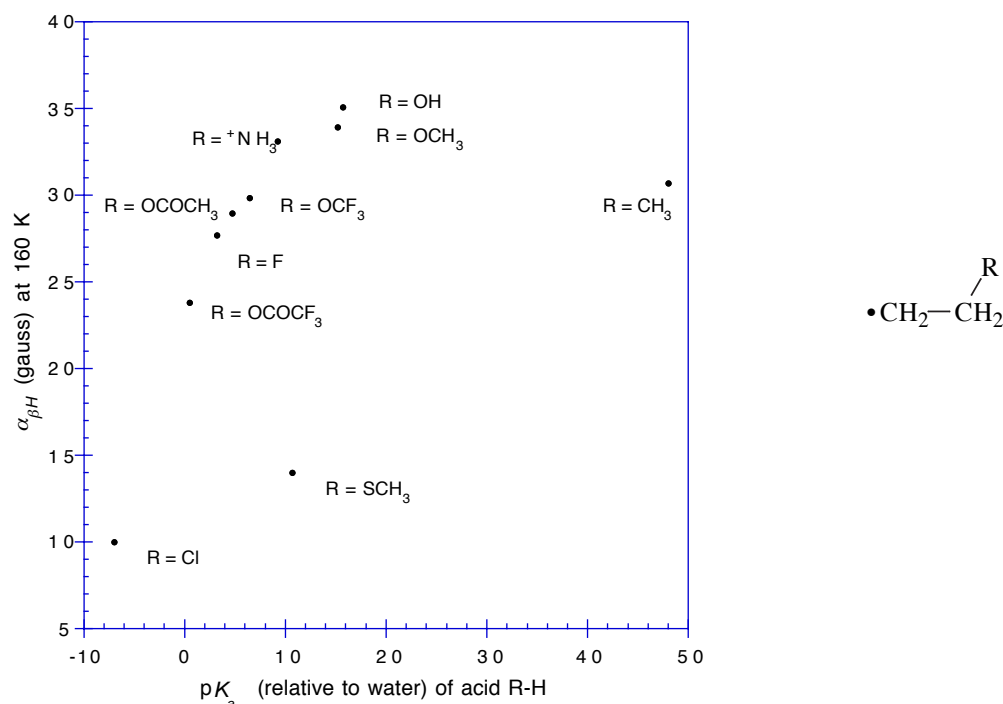


**Figure 4.20.** Comparative plot of  $\beta$ -coupling constant against temperature for ethyl radicals with varying  $\beta$ -substituents having the joining atom from the first row of the periodic table. R = F data is from reference 19, R = OCF<sub>3</sub> and OCH<sub>3</sub> from reference 17. Numbers in brackets represent the  $pK_a$  value for the acid RH.

**Table 4.16.** Values of  $pK_a$  for several acids

Acid	$pK_a$
H-CH <sub>3</sub>	48
H-H	35
H-OH	15.74
H-OCH <sub>3</sub>	15.2
H-SCH <sub>3</sub>	10.7
H-OCF <sub>3</sub>	6.41 <sup>a</sup>
H-OCOCH <sub>3</sub>	4.76
H-F	3.17
H-OCOCF <sub>3</sub>	0.52 <sup>b</sup>
H-Cl	-7

Values come mostly from reference 61. a: Unstable above 0°C—see reference 62; b: from reference 63



**Figure 4.21.** Plot of  $\alpha_{\beta H}$  for  $\beta$ -substituted ethyl radicals at 160 K, versus the  $pK_a$  of the parent acid R-H. R = SCH<sub>3</sub> data is from reference 32 and R = Cl from reference 18. The  $\beta$ -coupling constant for R = <sup>+</sup>NH<sub>3</sub> was calculated, assuming a linear  $\alpha_{\beta H}$ -temperature dependence, from two known data points, at 300 K (26.6 G)<sup>64</sup> and 77 K (37 G).<sup>65</sup>

Figure 4.21 is a plot of  $\alpha_{\beta H}$  at 160K for ethyl radicals with  $\beta$ -substituent R against the  $pK_a$  of the acid R-H. There is a reasonable correlation for the substituents with a leading second-row atom, apart from the methyl substituent. It is believed that the propyl radical (R = CH<sub>3</sub>) is anomalous because steric factors are more influential than electronic factors in determining the conformation. Third-row substituents such as Cl and SCH<sub>3</sub> are significantly different because of their greater size and probable homoconjugation with the unpaired electron.<sup>18-21,32</sup> The correlation observed in figure 4.21 indicates that the base strength of a second row  $\beta$ -substituent plays an important role in determining the size of  $\alpha_{\beta H}$ .



## 4.6 Estimation of the energy barrier to internal rotation about the $C_{\alpha}-C_{\beta}$ bond in the $\beta$ -oxygenated ethyl radicals 4.3a-c

The temperature dependence of  $\alpha_{\beta H}$  results from hindered rotation about the  $C_{\alpha}-C_{\beta}$  bond. Recent  $^{13}\text{C}$  nmr studies<sup>66</sup> indicate that internal rotational barriers in *n*-alkanes vary from 14 to 20  $\text{kJmol}^{-1}$ . The rotational barriers for alkyl radicals<sup>34, 67</sup> (which usually range between 1.25 and 4.9  $\text{kJmol}^{-1}$ ) are considerably smaller, due largely to the decrease in steric hindrance associated with the change in hybridisation at  $C_{\alpha}$  from  $sp^3$  to  $sp^2$ .

Internal rotational barriers have been determined for the series of  $\beta$ -substituted ethyl radicals (**4.3a-c**) in an attempt to discover whether a significant stereoelectronic interaction exists between the unpaired electron and the vicinal substituent. The propyl radical, which lacks any significant stereoelectronic effect, was used as a benchmark. A repulsive electrostatic interaction would be expected to result in an increased barrier due to an increase in the energy of the least stable conformation ( $\varphi = 0, 180^\circ$ ). Similarly, a weakly-attracting interaction should lower the barrier. A significantly stabilising interaction ( $> 15 \text{ kJmol}^{-1}$ ) would be expected to lock a radical into a particular conformation, creating a large rotational barrier, as in the  $\beta$ -haloethyl radicals.<sup>18-21</sup> However, this latter effect was not observed. Radicals **4.3a-c** were chosen specifically for reasons of structural simplicity and degree of symmetry, so enabling a greater confidence in the suitability of the theoretical model and a simplification of the calculations.

Rotational energy barriers have previously been determined experimentally from temperature dependent esr  $\beta$ -coupling constants by quantum mechanical,<sup>32,45,68</sup> classical limit approximation<sup>32,67,68</sup> and lineshape analysis<sup>13,37,44,69-71</sup> methods. Numerous attempts have also been made to estimate rotational barriers by theoretical methods.<sup>22,23,41,52,67,72-76</sup> An adapted classical limit approximation method was chosen in this study.

An expression for the averaged, temperature-dependent value of the  $\beta$ -coupling constant at the classical limit of a quantum mechanical analysis is given by equation 4.6,<sup>13</sup>

$$\langle \alpha_\beta \rangle = \frac{\int_{-\pi}^{\pi} \alpha_\beta(\omega) e^{-V(\omega)/RT} d\omega}{\int_{-\pi}^{\pi} e^{-V(\omega)/RT} d\omega} \quad (4.6)$$

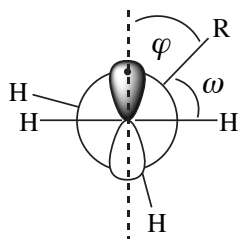
where  $V(\omega)$  represents the twofold sinusoidal potential for rotation about the  $C_\alpha-C_\beta$  bond and  $\alpha_\beta(\omega)$  is the angular dependent  $\beta$ -coupling constant expression. For cases of one  $\beta$ -hydrogen, the angular dependence of  $\alpha_\beta$  is approximated by the Heller-McConnell<sup>43</sup> equation (eq. 4.7), where  $\theta$  is the usual  $H_\beta$  dihedral angle and  $A$  (0-4 G) and  $B$  (40-50 G) are constants.

$$\alpha_\beta(\theta) = A + B \cos^2 \theta \quad (4.7)$$

In species with two  $\beta$ -hydrogens, the angular dependence is approximated by equation 4.8, where  $\varphi$  is the dihedral angle between the  $C_\beta-R$  bond and the axis of

$$\alpha_\beta(\varphi) = A + 0.25 B + 0.5 B \sin^2 \varphi \quad (4.8)$$

the  $C_\alpha 2p_z$  orbital. The lowest energy conformation of radicals **4.3a-c** is taken to be that where R eclipses an  $\alpha$ -hydrogen ( $\varphi = 90^\circ$ ). If  $\omega$  is defined as the dihedral angle of torsion away from the most stable conformation ( $\omega_0 = 0^\circ$ ), then equation 4.8 can now be expressed in terms of  $\omega$ , by equation 4.9.



$$\alpha_\beta(\omega) = A + 0.25 B + 0.5 B \sin^2 (90 - \omega) \quad (4.9)$$

In a system where internal rotation has  $C_2$  symmetry, the expression<sup>13</sup> for  $V(\omega)$  is

given by equation 4.10, where  $V_0$  is the barrier to internal rotation.

$$V(\omega) = \frac{V_0}{2} (1 - \cos 2\omega) \quad (4.10)$$

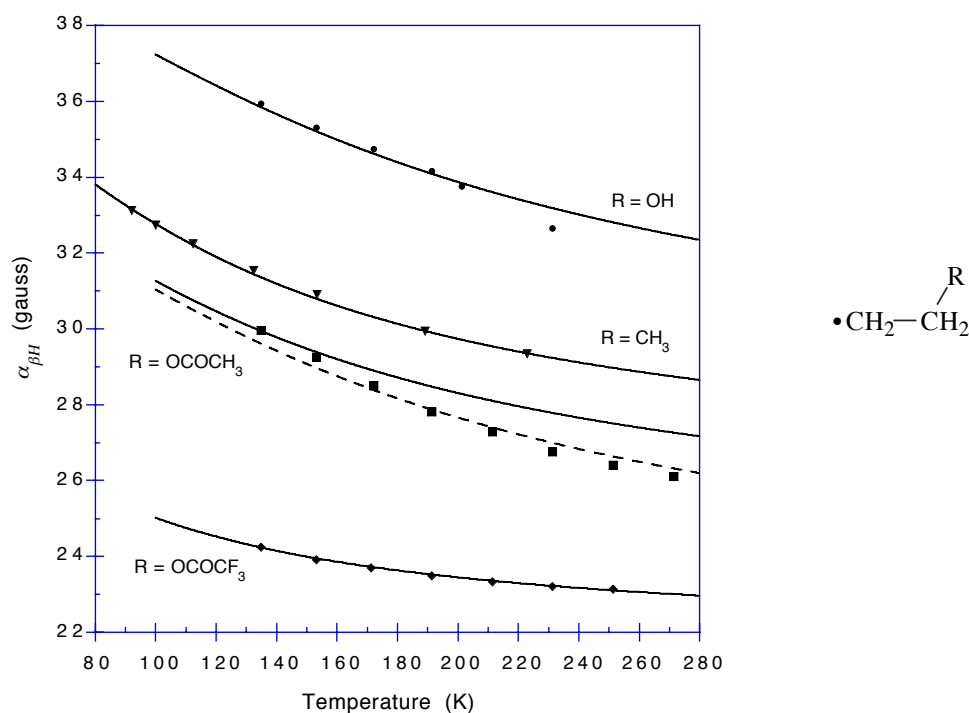
Substitution of equations 4.9 and 4.10 into equation 4.6 results in the desired expression, equation 4.11.

$$\langle \alpha_\beta \rangle = \frac{\int_{-\pi}^{\pi} \left( A + 0.25B + 0.5B \sin^2(90 - \omega) \right) e^{-\left( \frac{V_0(1-\cos 2\omega)}{2RT} \right)} d\omega}{\int_{-\pi}^{\pi} e^{-\left( \frac{V_0(1-\cos 2\omega)}{2RT} \right)} d\omega} \quad (4.11)$$

With the aid of an established numerical integration method<sup>77</sup> a simple computer routine was written, in the C++ language, which outputted  $\langle \alpha_\beta \rangle$  when given values for  $A$ ,  $B$ ,  $T$  and  $V_0$ . Calculations were performed in 1 K increments and parameters  $A$ ,  $B$  and  $V_0$  were varied manually until a fit with experimental data points was achieved, as shown in figure 4.22. Values for the optimised parameters are displayed in table 4.17.

**Table 4.17.** Values of  $A$ ,  $B$  and  $V_0$  giving the curves of best fit in figure 4.22

Radical		$A$ (G)	$B$ (G)	$V_0$ (kJmol <sup>-1</sup> )
$\dot{\text{C}}\text{H}_2\text{CH}_2\text{CH}_3$	<b>propyl</b>	0	51.4	2.20
$\dot{\text{C}}\text{H}_2\text{CH}_2\text{OH}$	<b>4.3a</b>	0.6	54.0	3.50
$\dot{\text{C}}\text{H}_2\text{CH}_2\text{OCOCH}_3$	<b>4.3b</b>	0	47.9	2.60
$\dot{\text{C}}\text{H}_2\text{CH}_2\text{OCOCF}_3$	<b>4.3c</b>	0	43.5	1.05



**Figure 4.22.** Plot of the fit of calculated coupling constant values from equation 4.11 to temperature dependent values for species **4.3a-c**, determined experimentally. The dashed curve represents the calculated fit to the experimental values for **4.3b**, using  $A = -5.1$  G,  $B = 53.74$  G (from ethyl radical free spin value)<sup>33</sup> and  $V_0 = 3.25$  kJmol<sup>-1</sup>.

Although inaccuracy will be present in the value of  $V_0$  to the degree to which the method fails to model actual behaviour, it is clear from the shape of the temperature dependence curves that the barriers to  $C_\alpha-C_\beta$  rotation are small in all cases. If  $\varphi = 90^\circ$  and  $270^\circ$  are not the lowest energy conformations, then a twofold potential (eq. 4.10) cannot accurately model real behaviour. However, such a situation is unlikely to result in huge inaccuracies in  $V_0$  since experimental  $\alpha_{\beta H}$  values are consistent with  $\varphi = 0^\circ$  and  $180^\circ$  remaining the potential maxima. Although the  $\alpha_{\beta H}$  values are markedly affected by variation in spin density (or alternatively tilt angle at the  $\beta$ -hydrogens), such behaviour is accounted for in the differing values of  $A$  and  $B$  between species.

Our value for  $V_0$  in the propyl radical is 2.20 kJmol<sup>-1</sup>. Earliest values are 1.76 kJmol<sup>-1</sup> by the classical limit method<sup>32</sup> and between 1.72 and 2.26 kJmol<sup>-1</sup> by quantum mechanical means.<sup>45</sup> Meakin and coworkers<sup>13</sup> estimated a value of 13 kJmol<sup>-1</sup> from esr

linewidth analysis. Despite admitting that assumptions involved in the technique might lead to significant errors, they concluded that the presence of a linewidth effect demands that the barrier must be considerably larger than  $1.7 \text{ kJmol}^{-1}$ . A likely source of overly small rotational barriers in earlier studies is the omission of a modified expression of the angular dependence of  $\alpha_{\beta H}$  (eq. 4.8) in situations where there are two  $\beta$ -hydrogens. Such an omission has been the cause of a poor match between calculated curves and experimental data. Brumby,<sup>50</sup> however, using an unmodified Heller-McConnell expression in combination with a square wave potential, achieved a good match with experimental data using an internal rotational barrier of  $2.193 \text{ kJmol}^{-1}$ . Remarkably, this value agrees almost perfectly with that in the present work. It is concluded that  $2.20 \text{ kJmol}^{-1}$  is a reasonable value of  $V_0$  for propyl radical.

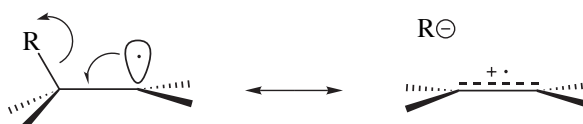
Values for  $V_0$  in **4.3a** have not been determined previously by experimental means, but early INDO calculations gave large barriers of  $17.3^{74}$  and  $11.8^{75} \text{ kJmol}^{-1}$ , while *ab initio* methods<sup>22,23,41,52,73,76</sup> have yielded  $V_0$  values between  $0.4^{73}$  and  $8.4^{52} \text{ kJmol}^{-1}$ . The classical limit approach value of  $3.50 \text{ kJmol}^{-1}$  is substantially smaller than the INDO values, but moderate by *ab initio* standards. Temperature dependence data used in the calculations was taken from what was ascribed to the *gauche* isomer of **4.3a**. Increased steric hindrance resulting from this situation may be the reason for a larger barrier than for propyl radical. Microwave spectroscopy yields a C–C rotational barrier of  $14.2 \text{ kJmol}^{-1}$  for the *anti* conformer of ethanol in the gas phase,<sup>80</sup> so it is clear that  $\beta$ -hydroxylated alkyl radicals have much lower internal rotational barriers than analogous alcohols.

A value of  $V_0 = 2.60 \text{ kJmol}^{-1}$  was obtained for 2-acetoxy ethyl radical, **4.3b**. No previous determination of this  $C_\alpha$ – $C_\beta$  internal rotational barrier, either experimental or theoretical, could be found. The slightly larger barrier than that for propyl radical indicates no significant repulsive or attractive interaction between the SOMO and the acetoxy group. The ester group conformation in **4.3b** is not known, yet experimental esr evidence<sup>59</sup> for 2-formyloxyethyl radical,  $\dot{\text{C}}\text{H}_2\text{CH}_2\text{OCHO}$ , indicates the *Z* isomer is more stable and in conformity with the favoured conformation of ethyl formate.<sup>60</sup> It is

therefore likely that the *Z* conformer of **4.3b** is favoured. The fact that the experimental temperature dependence is steeper than the best calculated curve is perhaps indicative of a higher rotational barrier than the one calculated. A better fit was obtained with the values  $A = -5.1$  G,  $B = 53.74$  G and  $V_0 = 3.25$  kJmol<sup>-1</sup>, so demonstrating the dependence of the barrier upon the quality of the data fit. The  $B$  value is derived from the free spin value of  $\alpha_{\beta H}$  for the ethyl radical.<sup>33</sup> Other workers have used negative  $A$  values in the conformational analysis of hydroxy hydrogens.<sup>40</sup>

A smaller rotational barrier of 1.05 kJmol<sup>-1</sup> was determined for 2-trifluoroacetoxyethyl radical, **4.3c**. A low temperature conformation of  $\varphi_0 = 60^\circ$  is consistent with a smaller  $V_0$ . As mentioned previously, since the expression for the twofold potential will no longer be accurate, inaccuracy in  $V_0$  is expected. Nevertheless, the current value is considered to be a good approximation to the real one, since *ab initio* calculations<sup>23</sup> on the benchmark propyl radical predict the difference in energy between  $\varphi_0 = 60^\circ$  and  $90^\circ$  conformations to be only 0.59 kJmol<sup>-1</sup>. Acetoxy and trifluoroacetoxy groups are of similar size, although **4.3c** is expected to favour the *Z* ester conformation more than **4.3b**. However, it is the increased contribution of heterolytic hyperconjugation which is expected to be the major contributor to the change in stable conformation between **4.3b** and **4.3c**.

Esr evidence<sup>78</sup> indicates that the ethylene radical cation in solution is not planar, but has an equilibrium twist angle of  $45 \pm 5^\circ$  between the methylene planes at 77 K. In contrast, the radical cation of propylene is planar.<sup>79</sup> So are the *cis* and *trans* 2-butene radical cations which give the same esr hyperfine splittings, indicating a small barrier for conformational interconversion about the C2–C3 bond.<sup>79</sup> However, stereoelectronic requirements for this type of hyperconjugative interaction in  $\beta$ -oxygenated radicals necessitate that the radical geometry must be conducive to the formation of an alkene radical cation.



In summary, the  $C_{\alpha}$ - $C_{\beta}$  rotational barriers in radicals **4.3a-c** are all small and within the range of those for acyclic alkyl radicals. In particular, due to the small barrier difference between propyl radical and **4.3b**, any attractive stereoelectronic effect between the acetoxy group and the singly occupied orbital must be very small, i.e.  $\leq 1 \text{ kJmol}^{-1}$ . Such an effect is negligible in comparison with the activation energy for 1,2- acetoxy ( $36\text{--}70 \text{ kJmol}^{-1}$ )<sup>81</sup> and even trifluoroacetoxy ( $26^{82}\text{--}49^4 \text{ kJmol}^{-1}$ ) group shifts. In light of this esr study, it is unlikely that a through-space stereoelectronic interaction is responsible for the regioselectivity observed in oxygen labelling experiments with 1,2- acetoxy group shift in alkyl radicals. However, a 1,2 acetoxy shift is likely to be very slow in **4.3b** and differently structured  $\beta$ -acetoxy alkyl radicals may well have significantly stronger SOMO-acetoxy interactions. In addition, such interactions may not become significant until  $C_{\beta}$ -O bond fission begins, and this will not occur at low temperature.

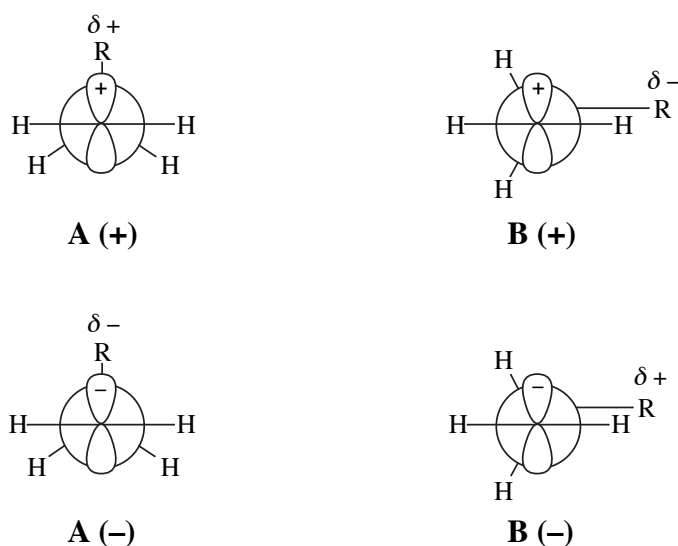
#### 4.7 Final Discussion

Variations in  $\alpha_{\beta H}$  between  $\beta$ -substituted ethyl radicals arise from  $\beta$ -hydrogen tilting and/or spin density reduction as well as from differences in the equilibrium conformation (as illustrated by the data in table 4.18). Except for propyl radical, as the conjugate base strength of the anion of R decreases, so too does the angle  $\varphi$ .

**Table 4.18.** Calculation of substituent equilibrium angle,  $\varphi$  (equation 4.4) for 2-substituted ethyl radicals, using the values of  $B$  obtained from the calculation of the internal rotational barriers (table 4.17)

Radical		$\alpha_{\beta H}$ at 135 K (G)	$B$ (G)	$\varphi$ (degrees)
$\dot{\text{C}}\text{H}_2\text{CH}_2\text{CH}_3$	<b>propyl</b>	31.46	51.4	58.4
$\dot{\text{C}}\text{H}_2\text{CH}_2\text{OH}$	<b>4.3a</b>	35.94	54.0	65.7
$\dot{\text{C}}\text{H}_2\text{CH}_2\text{OCOCH}_3$	<b>4.3b</b>	29.97	47.9	60.1
$\dot{\text{C}}\text{H}_2\text{CH}_2\text{OCOCF}_3$	<b>4.3c</b>	24.25	43.5	51.7

Roald Hoffmann and coworkers<sup>72</sup> have rationalised conformational preference differences in  $\beta$ -substituted ethyl cations and anions in terms of positive and negative hyperconjugation (depicted in figure 4.23). If R is more electronegative than H, the cation prefers conformation B(+), while the anion favours A(-). If R is less electronegative than H, the cation favours A(+), the anion B(-). More recent work<sup>76</sup> showed that this explanation was somewhat simplistic since anions can undergo a direct 1,3 interaction between the anionic  $2p$  orbital and the vacant  $2p$  substituent orbital. Similarly, 1,3 hypervalent interactions can dominate control over the conformation of cations. Yet, the theorem provides a basic understanding of the relationship between conformation and electronic effects.

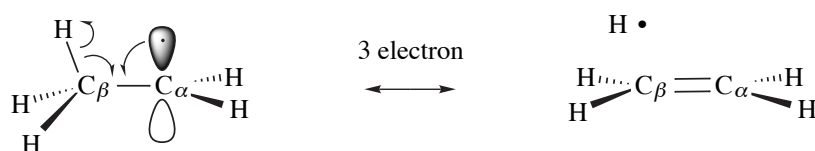


**Figure 4.23.** Favoured conformations for cations and anions with electronegative and electropositive substituent R

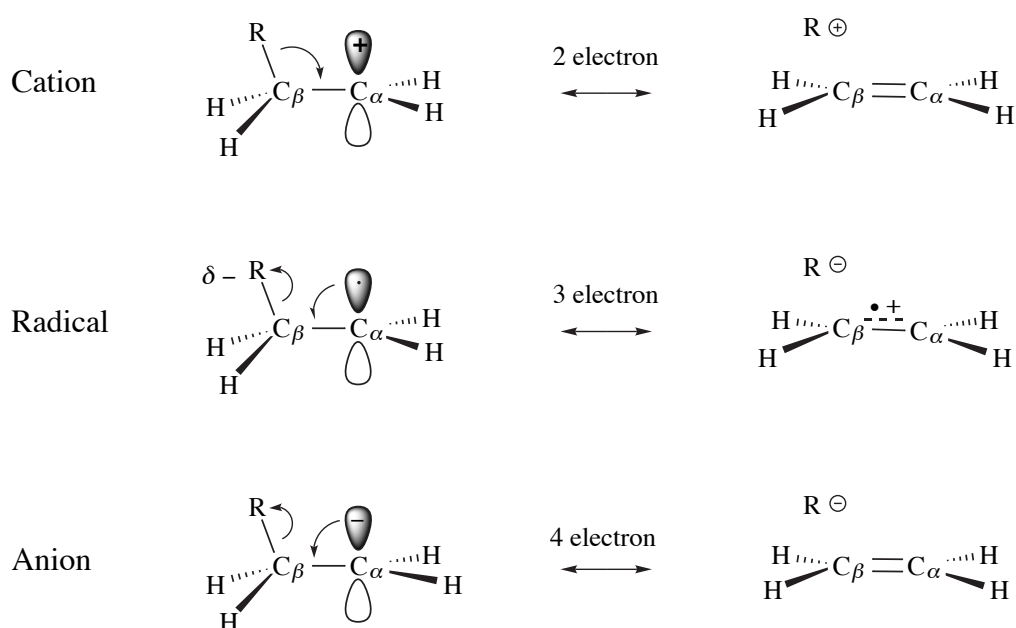
Radicals are expected intuitively to display conformational preferences between those observed for cations and anions and to possess lower rotational barriers. *Ab initio* calculations<sup>76</sup> support this prediction and indicate that in radicals such an effect arises from participation of both positive and negative hyperconjugation—donation of charge into (cation-like) and acceptance of charge from (anion-like) the SOMO, respectively. Since such electronic effects in radicals largely cancel one another, steric factors are more important than in ions. Hyperconjugative stabilisation of a radical occurs by overlap of a



$\beta$ -CH bond with the half filled  $C2p_z$  orbital. This process may be viewed as a three electron interaction, as illustrated with the ethyl radical.



It is proposed that as a  $\beta$ -substituent becomes a weaker conjugate base, it develops a greater tendency to involve an electron pair from the  $C_\beta$ -R bond rather than a single electron. Such behaviour makes radicals of this type more anion-like, as illustrated in figure 4.24. The weaker the conjugate base, the stronger the hyperconjugative stabilisation and hence the more the  $\varphi = 0^\circ$  conformation is favoured. Theoretical work<sup>23</sup> on  $\beta$ -substituted ethyl radicals indicates that the  $C_\beta$ -R bond is longer in the conformation where R eclipses the SOMO than when it eclipses an  $\alpha$ -hydrogen, consistent with such a hyperconjugative mechanism.



**Figure 4.24.** Hyperconjugative mechanisms for the stabilisation of the  $\varphi = 0^\circ$  conformation of cations, anions and of radicals with electronegative  $\beta$ -substituents

As well as  $\beta$ -substituent base strength, the degree of alkyl substitution of the carbon skeleton influences the radical conformation. Alkyl substitution stabilises alkene radical cations. At 191 K, the esr spectrum of 2-methyl-2-trifluoroacetoxy-1-heptyl radical,  $C_5H_{11}(CH_3)C(OCOCF_3)\dot{C}H_2$ , has resolved  $\gamma$  splitting, where  $\alpha_{\gamma H}$  averages to about 1.0 G<sup>83</sup>. This is consistent with a conformation in which the trifluoroacetoxy group eclipses the half-filled orbital. This radical is known to rearrange in a facile manner.<sup>4</sup>

Kochi argues that it is not necessary to have a direct correlation between a radical's stable conformation and propensity for rearrangement,<sup>16</sup> yet many radicals known to rearrange possess a favourable stereoelectronic preorientation. For instance,  $\beta$ -chloroalkyl radicals, many of which are known to rearrange extremely rapidly, are known to exist in an asymmetrically-bridged conformation in which the chlorine is eclipsed by the SOMO.<sup>84</sup> Similar conformational preferences are observed in carbohydrate radicals with a  $\beta$ -C–O bond<sup>85</sup> where such radicals undergo facile 1,2 acyloxy rearrangement.<sup>86</sup> The neophyl radical,  $PhC(CH_3)_2\dot{C}H_2$ , which rearranges readily to  $(CH_3)_2\dot{C}CH_2Ph$ , displays a  $\gamma$  splitting to the methyl groups of 1.05 G at 177 K.<sup>16</sup> Such a splitting places each methyl group at 60° to the SOMO so that the phenyl group eclipses the radical orbital, the perfect preorientation for rearrangement. However 2-phenylethyl radical,  $PhCH_2\dot{C}H_2$ , which does not rearrange readily, gives  $\alpha_{\beta H} = 30.94$  G at 173 K.<sup>16</sup> This result is consistent with the favoured conformation where the phenyl group lies instead in the equatorial plane ( $\varphi = 90^\circ$ ).

In summary, the equilibrium conformation of alkyl radicals bearing second row  $\beta$ -substituents is controlled by a combination of steric and electronic effects. The conformation where the  $\beta$ -substituent eclipses the radical orbital becomes increasingly favoured as the conjugate base strength of the  $\beta$ -substituent decreases and as the degree of alkyl substitution at  $C_\alpha$  and  $C_\beta$  increases. This effect is attributed to an increasing contribution from three electron, heterolytic hyperconjugation. In several cases a correlation exists between this eclipsed conformation and the propensity for 1,2 rearrangement.

## 4.8 Conclusions

The esr spectra of  $\beta$ -oxysubstituted alkyl radicals are similar to those of unsubstituted hydrocarbon radicals. There is no evidence for symmetric bridging or tight conformational locking. The  $g$  factors are slightly lower than for alkyl radicals. Values of  $\alpha_{\alpha H}$  are slightly larger owing to an increase in spin density and decreased pyramidalisation at  $C_{\alpha}$ . Most conspicuous, however, is the large decrease in  $\alpha_{\beta H}$  for radicals with  $\beta$ -substituents R in the order  $R = OH > OCOCH_3 > OCOCF_3$ . This is caused not by pyramidalisation at  $C_{\alpha}$ , but by either geometric distortion at  $C_{\beta}$ , or by spin density decrease at  $H_{\beta}$  due to the electronegativity of R, or both.

Low temperature studies indicate that the conformation where R eclipses the SOMO is favoured in radicals where R• has low conjugate basicity and where there is alkyl substitution at  $C_{\alpha}$  and  $C_{\beta}$ . An eclipsed conformation is optimal for  $\beta$ -acyloxyalkyl radical rearrangement and is also stereoelectronically favourable for the formation of a radical cation by the elimination of R•. For  $\beta$ -substituents where the linking atom is from the second row of the periodic table, there is a correlation between  $\alpha_{\alpha H}$  and  $pK_a$  of the acid RH at 160 K.

Barriers to internal rotation are very low, within the range of normal alkyl radicals and decrease in the order  $R = OH > OCOCH_3 > OCOCF_3$ . This situation is consistent with increasing stabilisation by R of the conformation where the oxygenated substituent and the half filled orbital are eclipsed. Any stereoelectronic interaction between the acetoxy group and the SOMO is negligible, estimated to be  $< 1 \text{ kJmol}^{-1}$ .

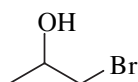
The conformation of the radicals is governed by a balance of steric and stereoelectronic effects. The principle stereoelectronic effect in this study was 3 electron heterolytic hyperconjugation.

## 4.9 Experimental

### Esr spectroscopy

For a description of the equipment and method used to obtain the esr spectra see section 7.10 of chapter 7 (General Experimental).

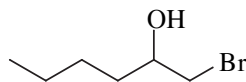
#### (±)-1-Bromopropan-2-ol [19686-73-8]



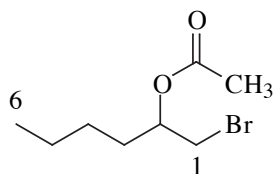
A sample of (Aldrich) 70% 1-bromo-2-propanol (the remainder 2-bromo-1-propanol) was subject to TLC analysis in a view to separating the regioisomers by chromatography. Unfortunately, both compounds had the same  $R_f$ . Therefore, the two compounds were separated by their different reactivity. A stirred 0.1 M solution of the isomeric bromohydrins in  $\text{CHCl}_3$  was cooled to  $-10^\circ\text{C}$  and treated dropwise with 0.5 equivalents of acetic anhydride/pyridine, which resulted in preferential acetylation of 2-bromo-1-propanol over the desired isomer. When complete by TLC, the mixture was washed with 0.1 M aqueous HCl, then water and dried over  $\text{MgSO}_4$ . Removal of solvent yielded an oil which was purified by flash chromatography (eluent  $\text{CH}_2\text{Cl}_2$ ). The desired bromohydrin was successfully separated from the  $\beta$ -bromoacetate isomers, which had a much larger  $R_f$ . By  $^1\text{H}$  nmr, the purified material was  $\geq 96\%$  1-bromo-2-propanol and was used without further purification.

$^1\text{H}$  nmr: 1.30 (d, 3H,  $\text{CH}_3\text{-CO}$ ), 2.16 (s, 1H, OH), 3.36 (dd, 1H, CHBr), 3.51 (dd, 1H, CHBr), 4.00 (m, 1H, CH-O).

#### (±)-1-Bromohexan-2-ol [26818-04-2]



The preparation of this compound is described in chapter 2, compound **2.48**.

**(±)-1-Bromomethylpentyl Acetate [28078-71-9]**

This compound has been prepared previously<sup>87</sup> but not fully characterised. A stirred solution of 1-bromo-2-hexanol (204.8 mg, 1.13 mmol), in 5 mL of dry CH<sub>2</sub>Cl<sub>2</sub> was treated with pyridine (101 µL, 1.25 mmol) and acetic anhydride (118 µL, 1.25 mmol), then 4-dimethylaminopyridine (DMAP, 13 mg, 0.11 mmol) was added to catalyse the reaction. By TLC (30% ether in hexane) it was estimated that the reaction was approximately 80% complete after 1 hour. Further additions of acetic anhydride (total of 100 µL more, 1.06 mmol) and of DMAP (total of 15 mg more, 0.12 mmol) did not appear to effect complete conversion to the product. Stirring was ceased and the mixture was diluted with 5 mL of CH<sub>2</sub>Cl<sub>2</sub> and washed consecutively with 3 mL each of dilute aqueous HCl, dilute aqueous NaHCO<sub>3</sub>, water, then dried. Evaporation of the solvent yielded a yellow oil (210.4 mg) which was purified by flash chromatography, using 4% ether in hexane as the eluent. The purified product (207.9 mg, 0.932 mmol, 82%) was obtained as a colourless oil. It was necessary to distil the sample (kugelrohr, 96°C/19 mmHg) to obtain an analytically pure sample.

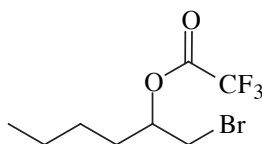
<sup>1</sup>H nmr: 0.91 (t, 3H, CH<sub>2</sub>-CH<sub>3</sub>), 1.33 (m, 4H, CH<sub>3</sub>(CH<sub>2</sub>)<sub>2</sub>), 1.68 (m, 2H, CH<sub>3</sub>(CH<sub>2</sub>)<sub>2</sub>CH<sub>2</sub>), 2.10 (s, 3H, CH<sub>3</sub>-CO), 3.40-3.54 (2 × dd, 2H, BrCH<sub>2</sub>), 5.00 (m, 1H, O-CH).

<sup>13</sup>C nmr: 13.9 (6), 21.0 (COCH<sub>3</sub>), 22.4 (5), 27.2 (4), 32.2 (1\*), 34.2 (3\*), 72.4 (2), 170.5 (C=O).

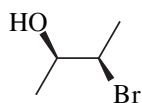
ir (neat): 2959 s, 2935 s, 2873 s, 2864 s, 1740 vs, 1375 s, asym, 1235 vs, br, 1026 s, asym, 669 m.

EIMS: 223 (0.05), 221(0.04), 167 (4), 165 (5), 164 (4), 162 (4), 129 (100), 101 (23), 83 (80), 69 (22), 61 (29).

Found: C, 43.03; H, 6.76; N, 0.00%. C<sub>8</sub>H<sub>15</sub>BrO<sub>2</sub> requires: C, 43.07; H, 6.78; N, 0.00%.

**(±)-1-Bromomethylpentyl Trifluoroacetate**

The preparation of this compound (numbered **2.50**) is described in chapter 2.

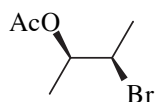
***Threo*-3-Bromobutan-2-ol [116051-24-2](*R,R*) and [19773-41-2](*S,S*)**(and *2S*, *3S* enantiomer)

The *threo* diastereomers have been prepared previously,<sup>88</sup> according to the method of Guss and Rosenthal.<sup>89</sup> A mixture of *N*-bromosuccinimide (23.7 g of 98% pure, 130 mmol) and water (50 mL, 2.78 mol) was stirred in a two-necked 100 mL RBF fitted with a dry ice-ethanol condenser. To this was added *cis*-2-butene (Fluka Chemicals, bp 4°C) by condensing the gas into a cooled, sealed measuring cylinder then heating the cylinder to transfer the gas *via* cannula to the reaction solution. Addition of the alkene ( $\approx$  19 mL, 12 g, 0.22 mol) was continued until all of the solid NBS visibly disappeared. The reaction mixture was extracted thrice with 20 mL portions of diethyl ether and the combined extract was washed with 20 mL of water and treated with 20 mL of pentane to aid drying (MgSO<sub>4</sub>). Evaporation of the solvents yielded an oil (19.89 g, largest component = 95.3% by GC). The crude bromohydrin was distilled twice: 71–77°C/43 mmHg; and 72.5–74°C/43 mmHg (lit.<sup>90</sup> 66–68°C/30 mmHg), affording the bromohydrin as a colourless oil (14.83 g, 96.9 mmol 75% w.r.t. NBS). The NBS was recovered in 56% yield by treatment of the aqueous solution of succinimide from the separation of the bromohydrin with NaOH (5.00 g, 125 mmol), cooling to 0°C then adding bromine (6.8 mL, 130 mmol) as described previously.<sup>89</sup>

<sup>1</sup>H nmr: 1.27 (d, 3H, CH<sub>3</sub>-CO), 1.73 (d, 3H, CH<sub>3</sub>-CBr), 2.21 (s, 1H, OH), 3.70 (dq, 1H, CHBr), 4.10 (dq, 1H, CH-O).

<sup>13</sup>C nmr: 20.5 (1\*), 22.4 (4\*), 59.3 (3), 71.7 (2).

The <sup>1</sup>H nmr spectrum was almost identical with that reported in CCl<sub>4</sub> solution.<sup>88</sup>

***Threo*-2-Bromo-1-methylpropyl Acetate [19773-39-8](*R,R*)**(and *2S*, *3S* enantiomer)

Acetic anhydride (1.01 mL, 10.7 mmol) and pyridine (0.87 mL, 10.7 mmol) were added to a stirred solution of *threo*-3-bromobutan-2-ol (1.50 g, 9.80 mmol) in 10 mL of dry CH<sub>2</sub>Cl<sub>2</sub>. The reaction was monitored by TLC (20% ether in hexane). The reaction was still incomplete after stirring overnight. Treatment with 4-dimethylaminopyridine (5 mg, 0.04 mmol) and more acetic anhydride (500  $\mu$ L, 5.30 mmol) and pyridine (430  $\mu$ L, 5.32 mmol) forced the reaction to completion within a further 4 hours. Pentane (30 mL) was added and the mixture was washed consecutively with 20 mL portions of water, 0.1 M aqueous HCl, 0.5 M aqueous NaHCO<sub>3</sub>, water, and then dried. Evaporation of the

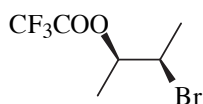
solvents yielded a pale yellow oil (1.9 g), which was distilled by kugelrohr (95°C/30 mmHg, lit.<sup>90</sup> 64°C/8 mmHg). The desired product was obtained as a colourless oil (1.67 g, 8.56 mmol, 87%).

<sup>1</sup>H nmr: 1.32 (d, 3H, <sup>3</sup>J = 6.5 Hz, CH<sub>3</sub>-CH-O), 1.67 (d, 3H, <sup>3</sup>J = 7.0 Hz, CH<sub>3</sub>-CBr), 2.09 (s, 3H, CH<sub>3</sub>C=O), 4.14 (dq, 1H, <sup>3</sup>J = 7.0, 4.6 Hz, CHBr), 5.01 (dq, <sup>3</sup>J = 6.5, 4.6 Hz, 2-CH). The <sup>1</sup>H nmr spectrum in CDCl<sub>3</sub> corresponded reasonably well with that reported in CCl<sub>4</sub> solution.<sup>91</sup>

<sup>13</sup>C nmr: 17.1 (1), 21.0 (CH<sub>3</sub>C=O\*), 21.4 (4\*), 50.8 (3), 72.8 (2), 170.1 (C=O).

ir (neat): 2985 s, 2936 s, 2875 m, 1742 vs, 1446 s, 1375 s, 1235 vs, br, 1199 s, 1072 s, 1025 s, 971 m, 952 m, 939 m, 605 s.

### ***Threo*-2-Bromo-1-methylpropyl Trifluoroacetate**



(and 2*S*, 3*S* enantiomer)

Pyridine (872 μL, 10.7 mmol) was added to a stirred solution of *threo*-3-bromobutan-2-ol (1.50 g, 9.80 mmol) in 35 mL of dry CH<sub>2</sub>Cl<sub>2</sub>. Trifluoroacetic anhydride (1.52 mL, 10.7 mmol) was then added over 1 min by syringe. After 5 min, the solution was diluted with 35 mL of pentane then washed successively with 30 mL of water then 20 mL portions of 0.1 M aqueous HCl, 0.5 M aqueous NaHCO<sub>3</sub> and water. The solution was dried and the solvent was evaporated carefully (volatile product) to yield a colourless oil (2.45 g). Distillation by kugelrohr (83°C/40 mmHg) afforded the desired product as a colourless oil (1.60 g, 6.43 mmol, 66%).

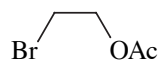
<sup>1</sup>H nmr: 1.46 (d, 3H, <sup>3</sup>J = 6.5 Hz, 1-CH<sub>3</sub>), 1.71 (d, 3H, <sup>3</sup>J = 7.0 Hz, 4-CH<sub>3</sub>), 4.16 (dq, 1H, <sup>3</sup>J = 5.1, 7.0 Hz, CHBr), 5.19 (dq, 1H, <sup>3</sup>J = 5.1, 6.5 Hz, CHCO).

<sup>13</sup>C nmr: 16.5 (1), 21.1 (4), 48.3 (3) 77.6 (2), 114.4 (q, <sup>1</sup>J<sup>19</sup>F-<sup>13</sup>C = 286 Hz, CF<sub>3</sub>), 156.6 (q, <sup>2</sup>J<sup>19</sup>F-<sup>13</sup>C = 43 Hz, C=O).

ir (neat): 2995 s, 2940 m, 2880 w, 1788 vs, 1448 s, asym, 1380 s, 1330 s, 1222 vs, 1162 vs, br, 1065 m, 1008 s, 962 m, 865 s, 775 s, 730 s, 642 m.

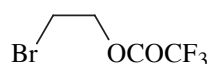
EIMS: 169 (7), 141 (22), 137 (6), 136 (12), 135 (6), 134 (12), 113 (9), 69 (100).

Found: C, 28.98; H, 3.35; N, 0.00%. C<sub>6</sub>H<sub>8</sub>BrF<sub>3</sub>O<sub>2</sub> requires: C, 28.94; H, 3.24; N, 0.00%.

**2-Bromoethyl Acetate [927-68-4]**

A stirred solution of 2-bromoethanol (2.76 g, 22.1 mmol) in 15 mL of dry  $\text{CH}_2\text{Cl}_2$  was treated with acetic anhydride (3.45 mL, 36.6 mmol), pyridine (2.96 mL, 36.6 mmol) and 4-dimethylaminopyridine (10 mg, 0.08 mmol). After 6 hours the mixture was poured into 50 mL of water, shaken and the layers were separated. The aqueous phase was extracted twice with 10 mL portions of  $\text{CH}_2\text{Cl}_2$ , the organic phases were combined and washed with 20 mL portions of 0.1 M aqueous HCl until the washings were acidic. The organic extract was then washed with 20 mL of 0.5 M aqueous  $\text{NaHCO}_3$  and 20 mL of water then dried. Careful removal of solvent under reduced pressure (volatile product) and distillation by kugelrohr (96°C/60 mmHg, lit.<sup>93</sup> 159°C), afforded 2-bromoethyl acetate as a colourless oil (2.17 g, 13.0 mmol, 59%). Accidental spillage was primarily responsible for the lowered yield.

$^1\text{H}$  nmr: 2.11 (s, 3H,  $\text{CH}_3$ ), 3.52 (t, 2H,  $\text{CH}_2\text{Br}$ ), 4.39 (t, 2H,  $\text{CH}_2\text{O}$ ). The nmr spectrum was identical with that of authentic material (Aldrich).

**2-Bromoethyl Trifluoroacetate [76045-93-7]**

Pyridine (1.60 mL, 19.8 mmol) was added to a stirred solution of 2-bromoethanol (2.24 g, 17.9 mmol) in 50 mL of  $\text{CH}_2\text{Cl}_2$  at 0°C. Trifluoroacetic anhydride (2.79 mL, 19.8 mmol) was added slowly over 1 min. The mixture was stirred at room temperature overnight (10 min is enough) then washed with 100 mL of water and the aqueous washings were back-extracted twice with 50 mL portions of pentane. The organic extracts were combined and washed successively with 30 mL each of 0.1 M aqueous HCl, 0.5 M aqueous  $\text{NaHCO}_3$ , water and then dried. Careful evaporation (volatile product) of the solvent yielded a mobile oil which was distilled by kegelrohr (80°C/60 mmHg) to give 2-bromoethyl trifluoroacetate as a colourless oil (2.76 g, 12.5 mmol, 70%). The  $^1\text{H}$  nmr spectrum was similar to that previously published in trifluoroacetic acid solution.<sup>92</sup>

$^1\text{H}$  nmr: 3.59 (t, 2H,  $^3J = 6.2$  Hz,  $\text{CH}_2\text{Br}$ ), 4.66 (t, 2H,  $^3J = 6.2$  Hz,  $\text{CH}_2\text{O}$ ).

$^{13}\text{C}$  nmr: 26.5 (2), 66.7 (1), 114.4 (q,  $^1J^{19}\text{F}-^{13}\text{C} = 286$  Hz,  $\text{CF}_3$ ), 157.0 (q,  $^2J^{19}\text{F}-^{13}\text{C} = 43$  Hz,  $\text{C=O}$ ).



ir (neat): 2975 w, asym, 1791 vs, 1398 m, 1350 s, 1283 m, asym, 1222 vs, 1160 vs, br, 989 w, 949 w, 775 m, sharp, 734 m, sharp, 672 w.

EIMS: 141 (13), 109 (18), 108 (8), 107 (18), 106 (8), 79 (92), 69 (53), 57 (29), 52 (100).

Found: C, 21.87; H, 2.02; N, 0.00%.  $C_4H_4BrF_3O_2$  requires: C, 21.74; H, 1.82; N, 0.00%.

#### 4.10 References

1. Beckwith, A. L. J. and Thomas, C. B. *J. Chem. Soc., Perkin Trans. 2* **1973**, 861.
2. Beckwith, A. L. J. and Duggan, P. J. *J. Chem. Soc., Chem. Commun.* **1988**, 1000.
3. Beckwith, A. L. J. and Duggan, P. J. *J. Chem. Soc., Perkin Trans. 2* **1992**, 1777.
4. Harman, D. G. *This thesis*, Chapter 3.
5. Crich, D. and Filzen, G. F. *J. Org. Chem.* **1995**, *60*, 4834. Note that there is a calculational error, giving the amount of translocation as 93%.
6. Zipse, H. and Bootz, M. *J. Chem. Soc., Perkin Trans. 2* **2001**, 1566.
7. Kocovsky, P.; Stary, I. and Turecek, F. *Tetrahedron Lett.* **1986**, *27*, 1513.
8. Harman, D. G. *This thesis*, Chapter 3; Section 3.4
9. Halpern, J. *Science* **1985**, *227*, 869.
10. Gilbert, B. C., Norman, R. O. C. and Williams, P. S. *J. Chem. Soc., Perkin Trans. 2* **1981**, 1401.
11. Ayscough, P. B. *Electron Spin Resonance in Chemistry*; Methuen and Co. Ltd: London, 1967; p 76.
12. Radtsig, V. A. *J. Struct. Chem.* **1970**, *11*, 221.
13. Krusic, P. J.; Meakin, P. and Jesson, J. P. *J. Phys. Chem.* **1971**, *75*, 3438.
14. Cochran, E. L.; Adrian, F. J. and Bowers, V. A. *J. Chem. Phys.* **1961**, *34*, 1161.
15. Hudson, A. and Jackson, R. A. *Chem. Commun.* **1969**, 1323.
16. Edge, D. J. and Kochi, J. K. *J. Am. Chem. Soc.* **1972**, *94*, 7695.
17. Chen, K. S. and Kochi, J. K. *J. Am. Chem. Soc.* **1974**, *96*, 1383.
18. Kawamura, T.; Edge, D. J. and Kochi, J. K. *J. Am. Chem. Soc.* **1972**, *94*, 1752.
19. Edge, D. J. and Kochi, J. K. *J. Am. Chem. Soc.* **1972**, *94*, 6485.
20. Chen, K. S.; Elson, I. H. and Kochi, J. K. *J. Am. Chem. Soc.* **1973**, *95*, 5341.
21. Elson, I. H.; Chen, K. S. and Kochi, J. K. *Chem. Phys. Lett.* **1973**, *21*, 72.
22. Bernardi, F.; Bottoni, A.; Fossey, J. and Sorba, J. *Tetrahedron* **1986**, *42*, 5567.
23. Guerra, M. *J. Am. Chem. Soc.* **1992**, *114*, 2077.
24. Kochi, J. K. and Krusic, P. J. *J. Am. Chem. Soc.* **1969**, *91*, 3940.
25. Davies, M. J.; Gilbert, B. C.; Thomas, C. B. and Young, J. *J. Chem. Soc., Perkin*

*Trans.* 2 **1985**, 1199.

26. Elson, I. H. and Kochi, J. K. *J. Org. Chem.* **1974**, 39, 2091.

27. Ayscough, P. B. *Electron Spin Resonance in Chemistry*; Methuen and Co. Ltd: London, 1967; p 73.

28. Fischer, H. In *Free Radicals*; Kochi, J. K., Ed.; John Wiley and Sons: New York, 1973; Vol. 2, p 445.

29. *Ibid.* p 442.

30. Fossey, J.; Lefort, D. and Sorba, J. *Free Radicals in Organic Chemistry*; John Wiley and Sons/Masson Paris, 1995, p 23.

31. Ebersson, L.; Utley, J. H. P. and Hammerich, O. In *Organic Electrochemistry*; 3rd ed.; Lund, H. and Baizer, M. M., Eds.; Marcel Dekker: New York, 1991; p 516.

32. Krusic, P. J. and Kochi, J. K. *J. Am. Chem. Soc.* **1971**, 93, 846.

33. Fessenden, R. W. and Schuler, R. H. *J. Chem. Phys.* **1963**, 39, 2147.

34. Kochi, J. K. *Adv. Free-Radical Chem.* **1975**, 5, 189.

35. Lloyd, R. V. and Wood, D. E. *J. Am. Chem. Soc.* **1975**, 97, 5986.

36. Fischer, H. In *Free Radicals*; Kochi, J. K., Ed.; John Wiley and Sons: New York, 1973; Vol. 2, p 448.

37. Chen, K. S.; Krusic, P. J.; Meakin, P. and Kochi, J. K. *J. Phys. Chem.* **1974**, 78, 2014.

38. Brocks, J. J.; Beckhaus, H.-D.; Beckwith, A. L. J. and Ruchardt, C. *J. Org. Chem.* **1998**, 63, 1935.

39. Dobbs, A. J.; Gilbert, B. C. and Norman, R. O. C. *J. Chem. Soc. (A)* **1971**, 124.

40. See reference 36

41. Bernardi, F. and Fossey, J. *J. Mol. Struct.* **1988**, 180, 79.

42. Guerra, M. *Chem. Phys. Lett.* **1987**, 139, 463.

43. Heller, C. and McConnell, H. M. *J. Chem. Phys.* **1960**, 32, 1535.

44. Ingold, K. U.; Nonhebel, D. C. and Walton, J. C. *J. Phys. Chem.* **1986**, 90, 2859.

45. Fessenden, R. W. *J. Chim. Phys. Phys.-Chim. Biol.* **1964**, 61, 1570.

46. Nunome, K.; Toriyama, K. and Iwasaki, M. *Chem. Phys. Lett.* **1984**, 105, 414.

47. Mariano, P. S. and Bay, E. *J. Org. Chem.* **1980**, *45*, 1763.
48. Leardini, R.; Tundo, A.; Zanardi, G. and Pedulli, G. F. *Tetrahedron* **1983**, *39*, 2715.
49. Lin, D. P. *J. Chin. Chem. Soc.* **1974**, *21*, 201.
50. Brumby, S. *J. Phys. Chem.* **1983**, *87*, 1917.
51. Smith, P. and Karukstis, K. K. *J. Mag. Reson.* **1982**, *46*, 200.
52. Curtiss, L. A.; Lucas, D. J. and Pople, J. A. *J. Chem. Phys.* **1995**, *102*, 3292.
53. Sosa, C. and Schlegel, H. B. *J. Am. Chem. Soc.* **1987**, *109*, 4193.
54. McDowell, C. A. and Shimokoshi, K. *J. Chem. Phys.* **1974**, *60*, 1619.
55. Durig, J. R. and Larsen, R. A. *J. Mol. Struct.* **1989**, *238*, 195.
56. Edge, D. J. and Kochi, J. K. *J. Chem. Soc. Perkin Trans. 2* **1973**, 182.
57. Grosse, A. V. *J. Am. Chem. Soc.* **1937**, *59*, 2739.
58. *CRC Handbook of Physics and Chemistry*, 82nd ed. (2001-2002); Lide, D. R., Ed.; CRC Press: Boca Raton, 2001; p 6-154.
59. Smith, P. and Karukstis, K. K. *J. Mag. Reson.* **1981**, *43*, 122.
60. Deslongchamps, P. *Stereoelectronic Effects in Organic Chemistry*; Pergamon: Oxford, 1983; p 54.
61. March, J. *Advanced Organic Chemistry*; 3rd ed.; John Wiley: New York, 1985; pp 220-222, 230.
62. Kloter, G. and Seppelt, K. *J. Am. Chem. Soc.* **1979**, *101*, 347. Value of  $pK_a$  predicted by SciFinder Scholar database (CAS, 2002).
63. *CRC Handbook of Physics and Chemistry*, 82nd ed. (2001-2002); Lide, D. R., Ed.; CRC Press: Boca Raton, 2001; p 8-46.
64. Taniguchi, H.; Fukui, K.; Ohnishi, S.-i.; Hatano, H.; Hasegawa, H. and Maruyama, T. *J. Phys. Chem.* **1968**, *72*, 1926.
65. Kotov, A. G.; Pukhal'skaya, G. V. and Pshezhetskii, S. Y. *Khim. Vys. Energ.* **1970**, *4*, 93.
66. Min, B. and Lee, J. W. *J. Mol. Liq.* **1999**, *80*, 33.
67. Kemball, M. L.; Walton, J. C. and Ingold, K. U. *J. Chem. Soc., Perkin Trans. 2*

1982, 1017.

68. Stone, E. W. and Maki, A. H. *J. Chem. Phys.* **1962**, *37*, 1326.

69. Hudson, A. and Luckhurst, G. R. *Chem. Rev.* **1969**, *69*, 191.

70. Kawamura, T.; Meakin, P. and Kochi, J. K. *J. Am. Chem. Soc.* **1972**, *94*, 8065.

71. Ingold, K. U.; Nonhebel, D. C. and Walton, J. C. *J. Phys. Chem.* **1985**, *89*, 4424.

72. Hoffmann, R.; Radom, L.; Pople, J. A.; Schleyer, P. v. R.; Hehre, W. J. and Salem, L. *J. Am. Chem. Soc.* **1972**, *94*, 6221.

73. Radom, L.; Paviot, J. and Pople, J. A. *Chem. Commun.* **1974**, 58.

74. Gilbert, B. C.; Trenwith, M. and Dobbs, A. J. *J. Chem. Soc. Perkin Trans. 2* **1974**, 1772.

75. Wunsche, P. and Grossohme, T. *Z. Phys. Chem. (Leipzig)* **1977**, *258*, 426.

76. Pross, A. and Radom, L. *Tetrahedron* **1980**, *36*, 1999.

77. Press, W. H.; Flannery, B. P.; Teukolsky, A. S. and Vetterling, W. T. *Numerical Recipes*; Cambridge University Press: Cambridge, 1986; pp 110-114.

78. Shiotani, M.; Nagata, Y. and Sohma, J. *J. Am. Chem. Soc.* **1984**, *106*, 4640.

79. Shiotani, M.; Nagata, Y. and Sohma, J. *J. Phys. Chem.* **1984**, *88*, 4078.

80. Sasada, Y. *J. Mol. Struct.* **1988**, *190*, 93.

81. Beckwith, A. L. J. and Duggan, P. J. *J. Chem. Soc., Perkin Trans. 2* **1993**, 1673.

82. Choi, S.-Y.; Crich, D.; Horner, J. H.; Huang, X.; Newcomb, M. and Whitted, P. O. *Tetrahedron* **1999**, *55*, 3317.

83. Beckwith, A. L. J. and Harman D. G. Unpublished results.

84. Beckwith, A. L. J. and Ingold, K. U. In *Rearrangements in Ground and Excited States*; Mayo, P. d., Ed.; Academic Press: New York, 1980; pp 162-310.

85. Korth, H. G.; Sustmann, R.; Dupuis, J.; Groninger, K. S.; Witzel, T. and Giese, B. In *Substituent Effects in Radical Chemistry*; Viehe, H. G., Janousek, Z. and Merenyi, R., Eds.; D. Reidel: Dordrecht, 1986; Vol. NATO ASI Series. Series C: Vol 89, p 297.

86. Beckwith, A. L. J.; Crich, D.; Duggan, P. J. and Yao, Q. *Chem. Rev.* **1997**, *97*, 3273.

87. Heasley, V. L.; Frye, C. L.; Heasley, G. E.; Martin, K. A.; Redfield, D. A. and

Wilday, P. S. *Tetrahedron Lett.* **1970**, 1573.

88. Maurette, M.-T.; Gaset, A.; Mathis, R. and Lattes, A. *Bull. Soc. Chim. Fr.* **1975**, 398.

89. Guss, G. O. and Rosenthal, R. *J. Am. Chem. Soc.* **1955**, 77, 2549.

90. *Dictionary of Organic Compounds*; 5th ed.; Buckinham, J., Ed.: Chapman and Hall: New York, 1982; Vol. 1, p 765, listing B-02025.

91. Gelas, J. and Michaud, S. *Bull. Soc. Chim. Fr.* **1972**, 2445.

92. Smolina, T. A.; Brusova, G. P.; Shchekut'eva, L. F.; Gopius, E. D.; Permin, A. B. and Reutov, O. A. *Izv. Akad. Nauk SSSR, Ser. Khim.* **1980**, 2079.

93. Aldrich *Fine Chemicals and Laboratory Equipment Catalogue*, Australia and New Zealand Edition, **2000-2001**.

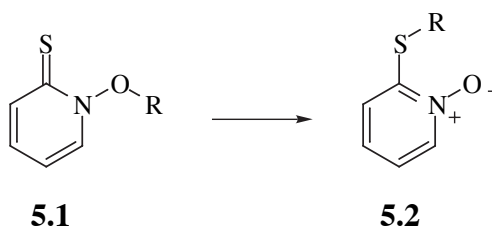
## Chapter 5

### The mechanism of the catalysed rearrangement of *N*-alkoxy-2(1*H*)-pyridinethiones

5.1	Introduction	193
5.2	Review of the chemistry of <i>N</i> -alkoxy-2(1 <i>H</i> )-pyridinethiones and related compounds	193
5.3	The mechanism of the rearrangement of <i>N</i> -alkoxy-2(1 <i>H</i> )-pyridinethiones	206
5.3.1	The mode of catalysis	206
5.3.2	Kinetics	212
5.3.3	A study of rearrangement regiochemistry	219
5.3.4	A study of rearrangement stereochemistry	224
5.3.5	Electronic structure of the migrating group at C1 during rearrangement	234
5.3.6	Substituent effects	237
5.3.7	Attempted detection and isolation of intermediates	239
5.4	Conclusions	247
5.5	Future work	249
5.6	Experimental	250
5.7	References	277

## 5.1 Introduction

This chapter is concerned with the mechanism of the catalysed rearrangement of *N*-alkoxy-2(1*H*)-pyridinethiones (**5.1**) to 2-(alkylsufanyl)pyridine *N*-oxides (**5.2**). *N*-alkoxy-2(1*H*)-pyridinethiones (**5.1**),<sup>1-19, 125-127</sup> exist as yellow oils or crystalline solids with low melting points, whereas 2-(alkylsufanyl)pyridine *N*-oxides (**5.2**) are colourless, crystalline solids which are considerably more polar than **5.1**.



The rearrangement was first reported by Hay and Beckwith<sup>7</sup> in 1989, where the apparent 1,4 migration of a benzyl group was unexpectedly observed upon heating a solution of *N*-benzyloxy-2(1*H*)-pyridinethione. It was assumed that the isomerization was catalysed by molecular oxygen. In 1996, Hartung and coworkers<sup>11,12</sup> reported that the 1,4 migration of various substituted benzyl groups was so facile that complete rearrangement would occur in a matter of days upon storage in the dark of the neat pyridinethiones, at 5°C to 20°C. Although no formal study of the mechanism of this isomerization was made, Hartung<sup>11</sup> concluded that the reaction was exothermic and that the increased product stability resulted from the formation of the heteroaromatic pyridine *N*-oxide ring from a cross-conjugated cyclic olefin.

## 5.2 Review of the chemistry of *N*-alkoxy-2(1*H*)-pyridinethiones and related compounds

### 5.2.1 Prevalence of *N*-alkoxy-2(1*H*)-pyridinethione research

Although *N*-alkoxypyridine-2-thiones (**5.1**) first appeared in the literature in 1963,<sup>1</sup> only about 20 research papers on their chemistry have been published to date,<sup>1-19, 125-127</sup> almost one third of them in the past five years. A recent microreview has been

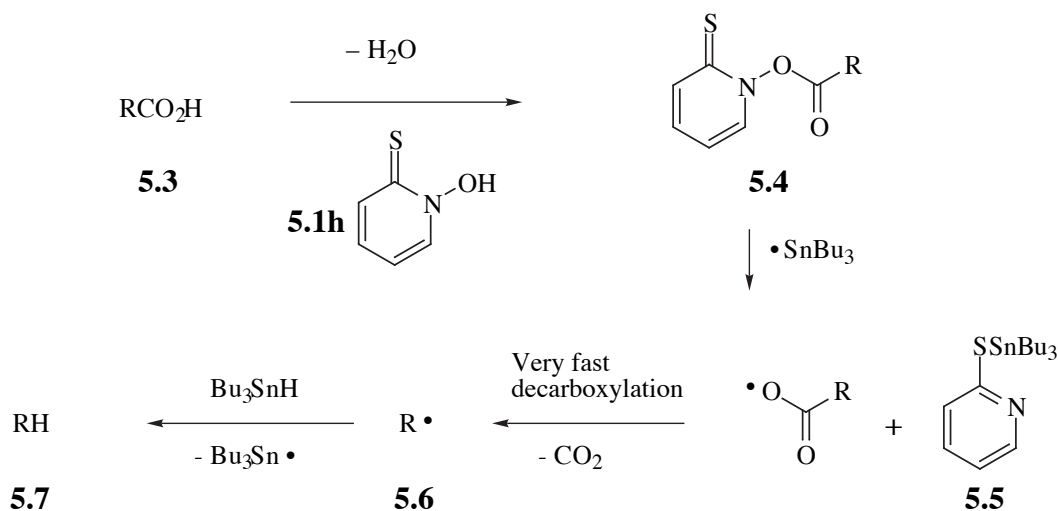


published on the use of *N*-alkoxy-pyridine-2-thiones in the synthesis of tetrahydrofurans and tetrahydropyrans by alkoxy radical cyclization<sup>125</sup> and a full review (2002) on the formation of C–O bonds using alkoxy radical chemistry describes the utility of **5.1** in such processes.<sup>129</sup> The closely related *N*-acyloxy-2(1*H*)-pyridinethiones (**5.4**)—colloquially named Barton esters (actually mixed anhydrides of thiohydroxamic and carboxylic acids)—were first reported in 1957.<sup>20</sup> Their chemistry is much better documented, judging by the number of reviews<sup>21-23</sup> published and the fact that more than 400 different Barton esters bear CAS registry numbers. Since Barton esters provide a convenient means for the decarboxylation of carboxylic acids *via* carbon-centred radicals<sup>24</sup>, much has been published on their radical chemistry.

### 5.2.2 Barton esters and related classes of compounds

Barton esters (**5.4**) can be prepared in high yield by condensation of a carboxylic acid (**5.3**) and *N*-hydroxypyridine-2-thione (**5.1h**). A common method for generating carbon-centred radicals consists of the treatment of **5.4** with Bu<sub>3</sub>SnH and a radical initiator such as AIBN. A tributyltin radical attacks the sulfur of the pyridinethione ring, forming 2-(tributyltinsulfanyl)pyridine (**5.5**) and liberating an acyloxy radical. Rapid decarboxylation of this radical forms a carbon-centred radical (**5.6**), which in turn can abstract a hydrogen atom from tributyltin hydride, producing an alkane (**5.7**)—see scheme 5.1. Of course, the carbon-centred radical may undergo further reactions—intramolecular cyclization or intermolecular addition to multiple bonds for instance—prior to reaction with tributyltin hydride, making Barton esters valuable precursors in synthetic radical chemistry.<sup>21</sup>

The utility of *N*-oxy-pyridine-2-thiones has been extended to the generation of alkoxy,<sup>5-12,16,17,19</sup> hydroxy,<sup>16,17,25-29</sup> alkoxy-carbonyloxy,<sup>30,31</sup> alkylsilyloxy,<sup>25</sup> alkylaminyl,<sup>32,33</sup> alkylamidyl<sup>34,35</sup> and carbon-centred radicals *via* radical dephosphorylation,<sup>36</sup> usually by photolysis of pyridinethione solutions with visible light.

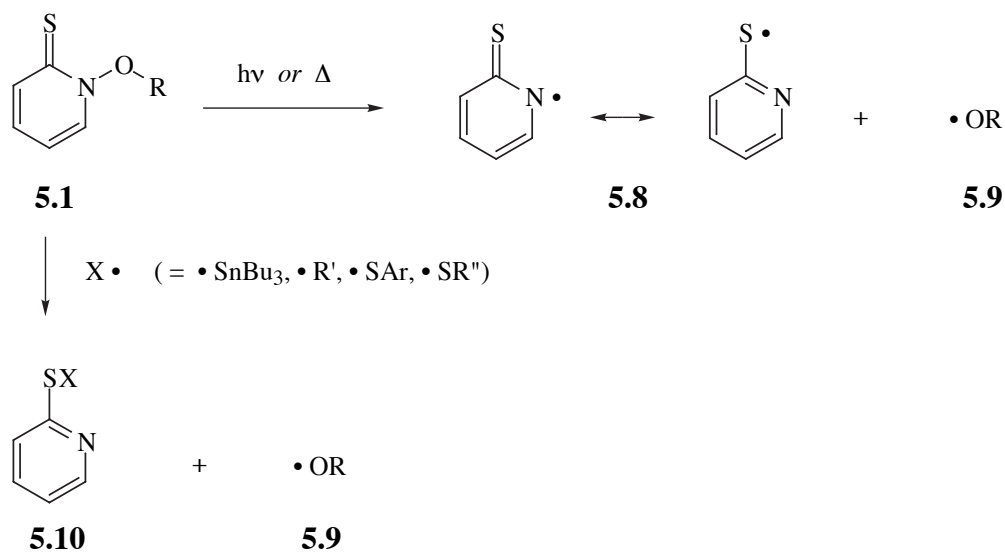


**Scheme 5.1.** Synthesis of Barton esters and mechanism of reaction with  $\text{Bu}_3\text{SnH}$

### 5.2.3 Radical chemistry of *N*-alkoxy-2(1*H*)-pyridinethiones

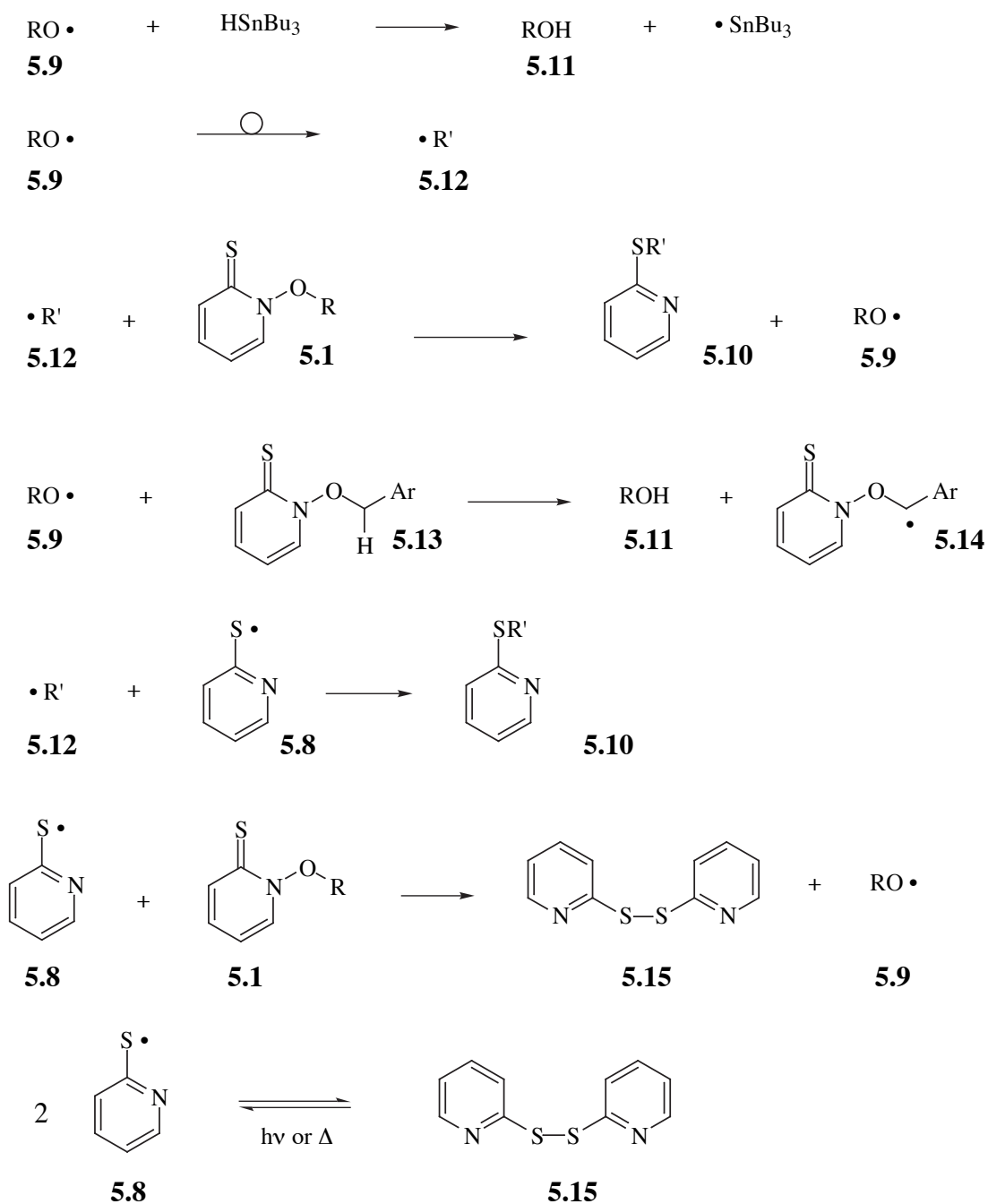
The radical chemistry of *N*-alkoxy-2-pyridinethiones (**5.1**) is comparable to that of the Barton esters (**5.4**), although differs significantly in that an alkoxy radical is incapable of decarboxylation. Photolysis of *N*-hydroxypyridine-2-thione,<sup>16,17,25-29</sup> generates hydroxy radicals but the photochemistry is more complex than a cursory glance reveals.<sup>28</sup> However, alkoxy radicals can be generated cleanly from *N*-alkoxy-2-pyridinethiones.<sup>5-12,16,17,19</sup> Other methods of generating alkoxy radicals include the homolysis of peroxides,<sup>37</sup> alkyl hypohalites,<sup>38-40</sup> and alkyl nitrites;<sup>41,42</sup> the treatment of alcohols with lead tetraacetate;<sup>43</sup> and treatment *O*-alkyl benzenesulfenates with tributyltin hydride.<sup>44,45</sup>

Scission of the N–O bond of **5.1** generates an alkoxy radical (**5.9**) and is achieved by photolysis with visible light,<sup>9,11,12,16,17,19,125</sup> thermolysis,<sup>7,125</sup> reaction with the tributylstannyl radical,<sup>5,6,8,9,12,125</sup> and reaction with arylthiyl radicals,<sup>12</sup> alkylthiyl radicals<sup>24</sup> or carbon-centred radicals.<sup>24,46</sup> A 2-substituted sulfanylpiperidine (**5.10**) is a by-product of these reactions (scheme 5.2).



**Scheme 5.2.** Methods of N–O bond scission in *N*-alkoxy-2(1*H*)-pyridinethiones

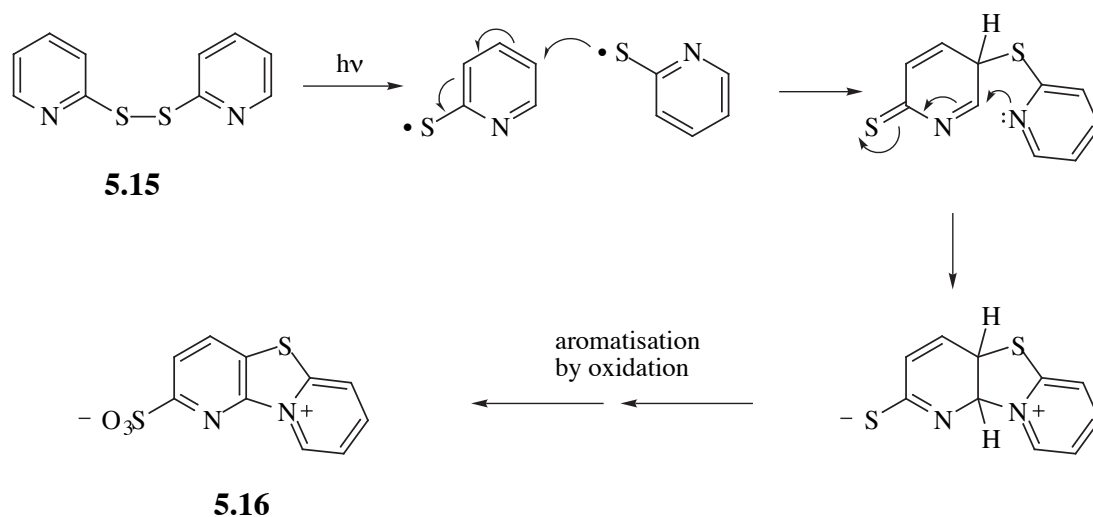
Such an alkoxy radical (**5.9**) may undergo a variety of further reactions<sup>125</sup> (not explicitly shown) including  $\beta$ -scission,<sup>5,6,8</sup> intra-<sup>10</sup> and intermolecular<sup>5-8</sup> hydrogen abstraction, and intra-<sup>6,9-12,19</sup> and intermolecular<sup>16</sup> addition to double bonds. The resulting carbon-centred radical (**5.12**) may then attack the sulfur atom of another pyridinethione molecule, generating an alkoxy radical and 2-(alkylsulfanyl)pyridine (**5.10**). Radical **5.12** may also react with 2-pyridylthiyl radical (**5.8**) in a termination step, forming the same product. Other reactions, including radical-radical termination, disproportionation and atom abstraction may also occur, to a lesser extent (scheme 5.3).



**Scheme 5.3.** Overview of the radical chemistry of *N*-alkoxy-2(1*H*)-pyridinethiones

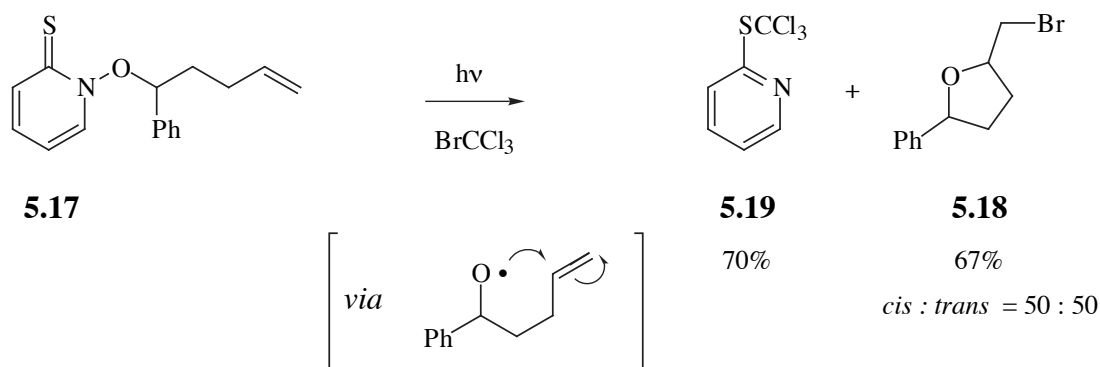
The 2-pyridylthiyl radical (**5.8**) is known to react with Barton esters (**5.4**) at an almost diffusion controlled rate.<sup>46</sup> Radical **5.8** is expected also to react rapidly with **5.1** to liberate another alkoxy radical (**5.9**) and 2,2'-dipyridyl disulfide (**5.15**). The disulfide **5.15** may also be formed by combination of two 2-pyridylthiyl radicals (**5.8**). Photolysis of **5.15** at 350 nm results in homolysis of the disulfide bond and the formation of two 2-pyridylthiyl radicals (**5.8**) which may then react further.<sup>17</sup> The novel

tricyclic betaine **5.16** is formed in aqueous solution and a mechanism<sup>17</sup> suggested for its formation is shown below (scheme 5.4). It is more likely that the first addition product results not from the reaction of two pyridine-2-thiyl (**5.8**) radicals, but by attack of **5.8** upon a molecule of **5.15**, with displacement of another **5.8** radical.



**Scheme 5.4.** The mechanism proposed<sup>17</sup> for the fate of photolysed 2,2'-dipyridyl disulphide

Hartung and coworkers<sup>11</sup> report that photolysis of *N*-(1-phenyl-4-penten)oxy-pyridine-2-thione (**5.17**) in benzene, in the presence of the radical trap  $\text{BrCCl}_3$ , produces 2-(trichloromethylsulfanyl)pyridine (**5.19**) and 2-bromomethyl-5-phenyltetrahydrofuran (**5.18**)—see scheme 5.5. This procedure illustrates the synthetic usefulness of *N*-alkoxy-pyridinethione radical chemistry. Similar methodology has been used to synthesize other substituted tetrahydrofurans<sup>9,11,12,19,125</sup> as well as tetrahydropyrans.<sup>9,11,12,125</sup>

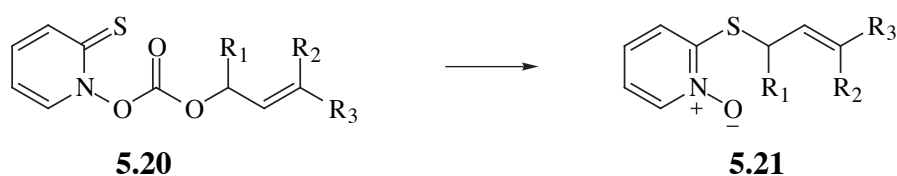


**Scheme 5.5.** Synthesis of substituted tetrahydrofurans using the radical chemistry of *N*-alkoxy-2(1*H*)-pyridinethiones

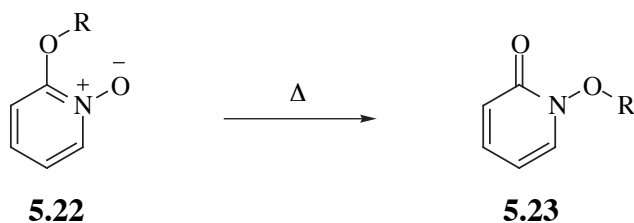
Direct evidence for the intermediacy of alkoxy radicals was obtained when solutions of *N*-alkoxy-2-thiones were irradiated in the presence of the radical trap, dimethylpyrrolone *N*-oxide (DMPO), and esr signals corresponding to DMPO adducts of alkoxy radicals were observed.<sup>16</sup> In addition, the same workers<sup>16</sup> found that supercoiled DNA suffered strand breaks and base modifications—results characteristic of the action of alkoxy and hydroxy radicals—when photolysed in the presence of *N*-alkoxy-2-thiones.

#### 5.2.4 Related rearrangements

Although Barton esters (**5.4**) do not undergo a 1,4 alkyl group shift similar to that observed with the *N*-alkoxy-2-thiones, it has been postulated that a 3,3 sigmatropic rearrangement to a thioperoxide actually initiates the radical chain reaction.<sup>47</sup> By contrast, it has been reported<sup>30,31</sup> that the closely related substituted *N*-allyloxycarbonyloxypyridine-2-thiones (**5.20**) slowly isomerize to 2-allylsulfanylpyridine *N*-oxides (**5.21**) on storage. This apparently decarboxylative rearrangement was assumed to proceed "via a concerted or dissociative intramolecular process",<sup>30</sup> but nothing further has yet been published on the mechanism.



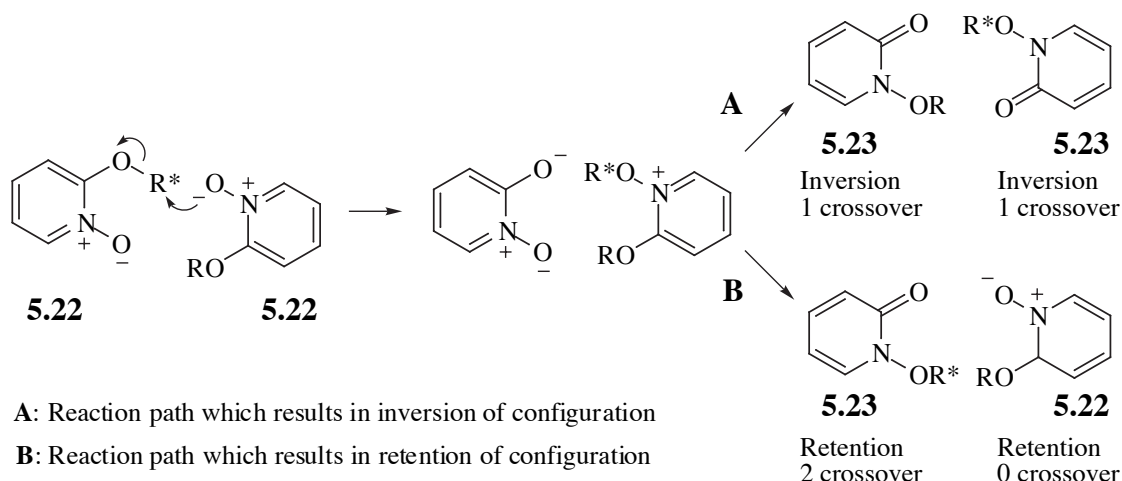
A reaction analogous to the rearrangement of *N*-alkoxy-2-thiones, albeit in the reverse direction, is the isomerization of a 2-alkoxy-1,4-dihydropyridine *N*-oxide (**5.22**) to an *N*-alkoxy-2(1*H*)-pyridone (**5.23**).<sup>48-57, 117-119</sup>



First reported in 1962,<sup>48</sup> this rearrangement has been subject to considerable mechanistic scrutiny. Due to the comparatively low temperatures required for rearrangement and the fact that radical scavengers did not retard the reaction rate, early researchers concluded that radicals were not intermediates but that the mechanism involved either intermolecular nucleophilic substitution or ion pair intermediates.<sup>50</sup> A more comprehensive study found the rearrangement to exhibit first order kinetics, show a small rate difference between migration of benzyl and alkyl groups, and have an extremely negative  $\Delta S^\ddagger$  and unusually low  $\Delta H^\ddagger$ .<sup>52,53</sup> Since the migration of benzhydryl groups displayed vastly different kinetic parameters to other groups and CIDNP was observed only in the products of benzhydryl migration, it was concluded that the mechanism involved radical pairs for groups that form stable radicals, but proceeded otherwise by a 1s,4s sigmatropic shift.<sup>53</sup> This conclusion was supported by le Noble and Daka, who determined a negative activation volume for benzyl migration (concerted) but a positive value (dissociative) for benzhydryl groups.<sup>55</sup> Ollis and coworkers concluded that the general mechanism involves a concerted 1,4 sigmatropic shift and not ion pairs.<sup>56</sup>

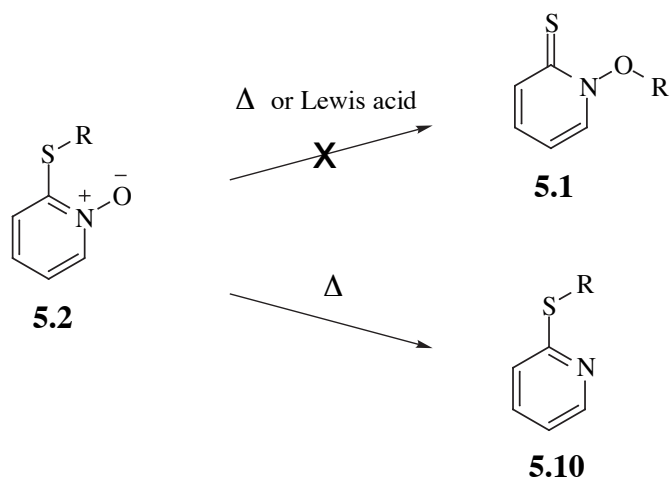
In very recent work, Wolfe and coworkers report that the rearrangement mechanism cannot involve solely an intramolecular 1s,4s sigmatropic migration of the alkyl group.<sup>118, 119</sup> A variety of experiments including crossover studies, study of solvent and secondary isotope effects and kinetic and stereochemical investigations have demonstrated that the mechanism involves an initial intermolecular transfer of the alkyl

group, with inversion of configuration, to the *N*-oxide. This is in accord with earlier crossover experiments.<sup>117</sup> It is proposed that inversion of configuration in the migrating group upon rearrangement arises from a single crossover encounter, whereas retention of configuration results from two crossover encounters, each with inversion of configuration.<sup>119</sup> This is illustrated in scheme 5.6.



**Scheme 5.6.** A proposed intermolecular mechanism which accounts for the stereochemical outcome of the rearrangement of 2-alkoxy pyridine *N*-oxides (**5.22**)

Attempts were also made to isomerize **5.2** to **5.1**, with<sup>58</sup> and without<sup>7,59</sup> Lewis acid catalysis. These attempts failed, demonstrating that the 2-alkylsulfanylpyridine *N*-oxide is the more stable isomer, presumably because of its aromaticity. Thermolysis of 2-alkylsulfanylpyridine *N*-oxides simply effected a reductive deoxygenation to 2-alkylsulfanylpyridines (**5.10**).<sup>59</sup>

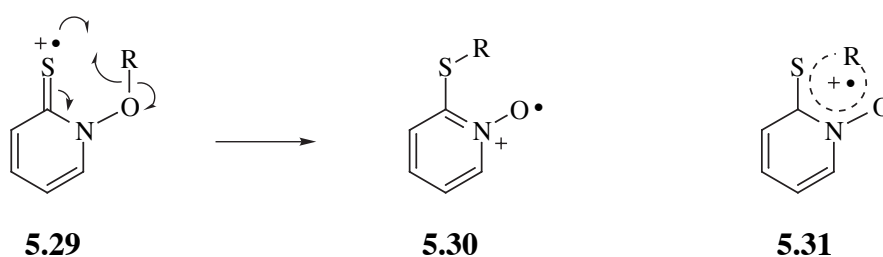


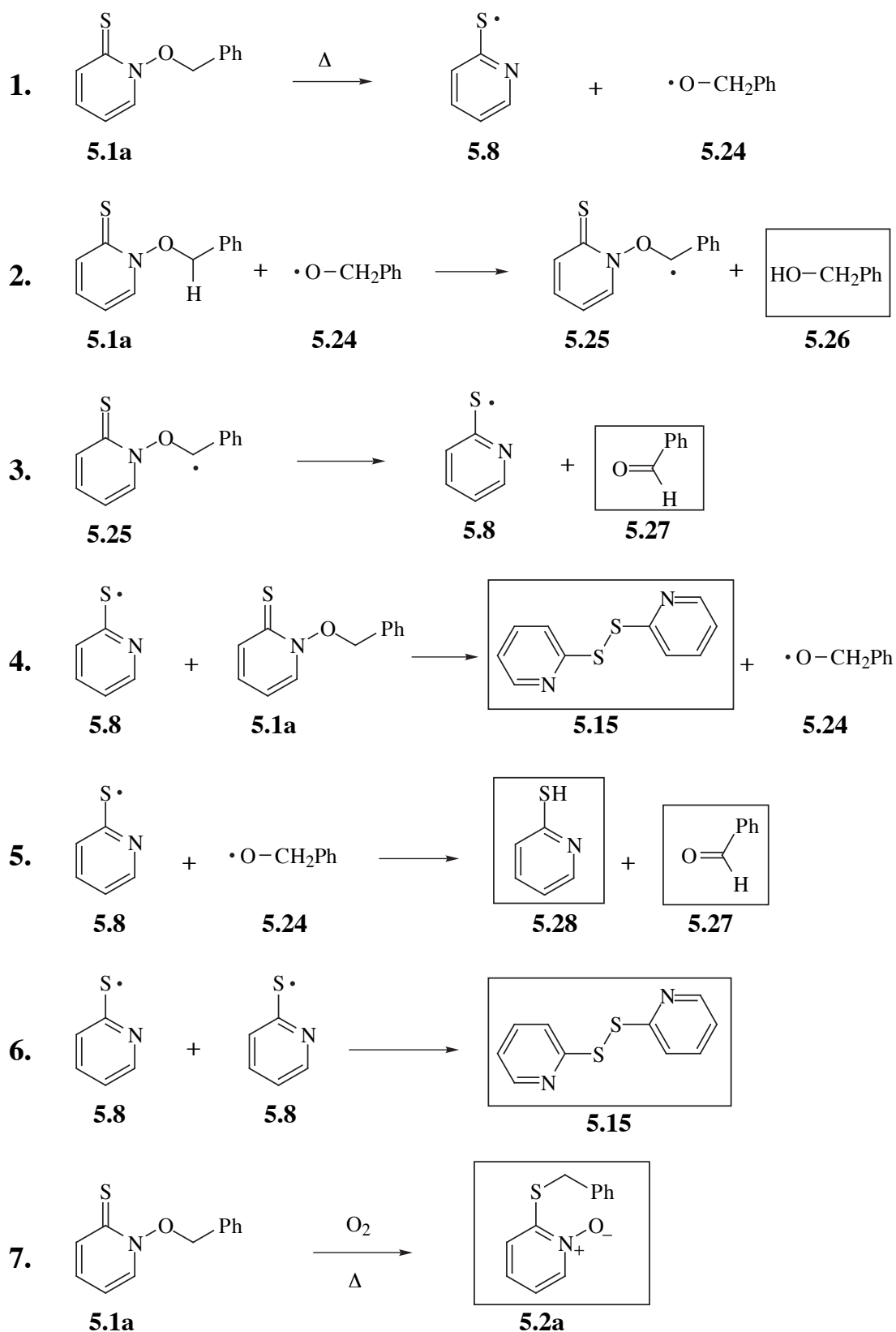


### 5.2.5 Catalysed rearrangement of *N*-alkoxy-2(1*H*)-pyridinethiones

Hay and Beckwith<sup>7</sup> found that when *N*-benzyloxy-2(1*H*)-pyridinethione (**5.1a**) in C<sub>6</sub>D<sub>6</sub> was heated in the dark at 100°C under vacuum for 36 hours, the products included benzaldehyde (**5.27**, 40%), benzyl alcohol (**5.26**, 40%) and 2-benzylsulfanylpyridine *N*-oxide (**5.2a**, 8%).<sup>7</sup> When the same experiment was conducted under an atmosphere of air, the proportions changed to **5.27**: 6%, **5.26**: 9% and **5.2a**: 71%. Whilst under an atmosphere of pure oxygen, the yield of the *N*-oxide **5.2a** increased to 78%.<sup>7</sup> The authors attributed these results to a dioxygen catalysed 1,4 benzyl migration competing with N–O bond homolysis. When these experiments were repeated in the course of this present study, it was found that 2,2'-dipyridyl disulfide (**5.15**) and pyridine-2-thiol (**5.28**) were also produced, although yields of **5.28** were low. Scheme 5.7 illustrates mechanisms which account for the formation of the products (in boxes) and are in conformity with what is already known about the chemistry of *N*-alkoxy-2(1*H*)-pyridinethiones.

Dioxygen is a known one electron oxidant,<sup>60</sup> so it is likely that the pyridinethione molecule is oxidised to a radical cation (**5.29**). **5.29** may then undergo a novel, open-shell, pericyclic reaction, forming the radical cation of the 2-alkylsulfanylpyridine *N*-oxide (**5.30**). Rearrangement of **5.29** to **5.30** involves the delocalisation of 5 electrons over 5 atoms, the transition structure of which is represented by **5.31**. Such a structure is isoelectronic with those postulated for reactions such as the isomerization of  $\beta$ -acyloxyalkyl radicals.<sup>128</sup> Such a transition structure would represent membership of a recently-postulated class of open-shell reactions which might be expected to display reactivity intermediate between that of 4 and 6 electron systems. A comprehensive mechanistic investigation was undertaken to determine whether such a transition structure exists, and if not, what the mechanism may indeed be.





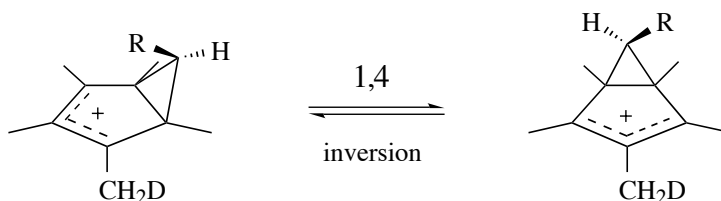
**Scheme 5.7.** A mechanistic scheme which accounts for the 5 identifiable products formed when a benzene solution of *N*-benzyloxy-2(1*H*)-pyridinethione (**5.1a**) is heated under an atmosphere of air

### 5.2.6 The chemistry of 4 and 6 electron 1,4 sigmatropic shifts and 5-electron, 6-centre electrocyclic processes

There appears to be no literature precedent for a solution phase, thermal 1,4 alkyl sigmatropic shift in radical cations. Although solution phase 1,4 H shifts have been reported,<sup>61,62</sup> evidence is scarce for such shifts being truly intramolecular. However, isomerizations which may be relevant to the rearrangement of the proposed radical cation intermediate (**5.29**) are:

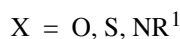
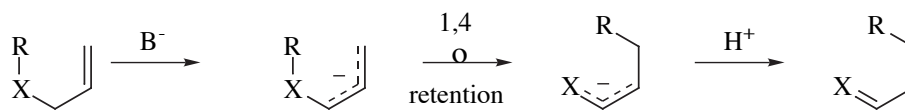
- closed-shell thermal 1,4 alkyl shifts in cations (4 electron processes);
- closed-shell thermal 1,4 alkyl shifts in anions and dipolar ylides (6 electron); and
- 6 centre, 5 electron radical cation mediated electrocyclic processes.

Cationic 1,4 sigmatropic rearrangements,<sup>63-69</sup> as exemplified by the degenerate migration of a cyclopropyl moiety in bicyclo [3.1.0] hexenyl cations,<sup>64</sup> apparently proceed in a 1a,4s mode, necessitating inversion of configuration at the terminus of the migrating group. Such a mode of migration dictates that substituent R remains endo.

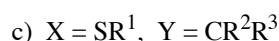
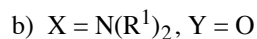
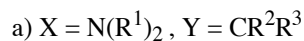
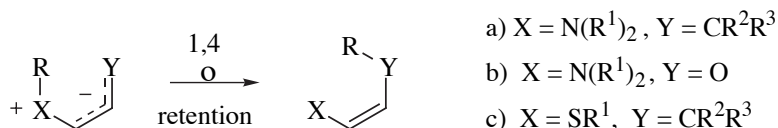


Anionic<sup>70-77</sup> and dipolar<sup>78</sup> 1,4 alkyl shifts apparently proceed in a 1s,4s fashion, the stereoconfiguration of the migrating group being predominantly retained in the product. There is evidence<sup>52-55,70,71,73,76,77</sup> for the intermediacy of tight radical/radical or radical/radical anion pairs. These rearrangements may involve the formal delocalisation of 6 electrons over 5 atoms. The general form of these, typically base catalysed shifts, are shown below.

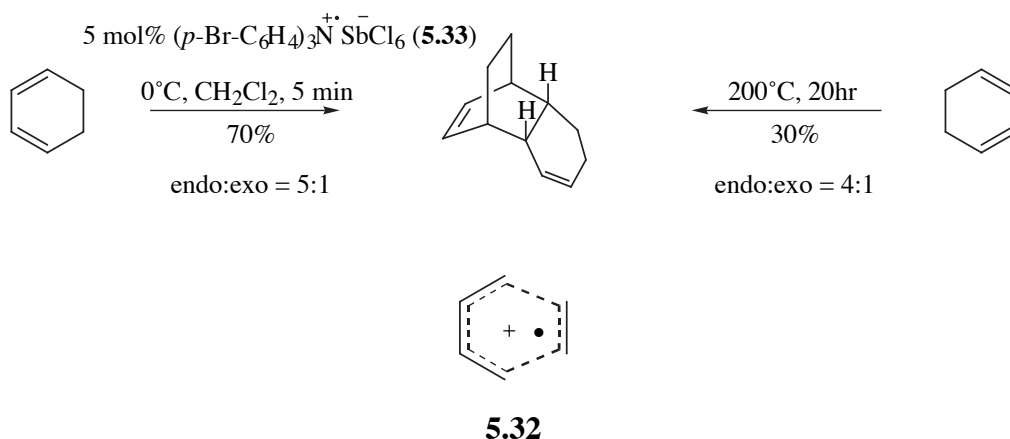
## Anionic



## Dipolar



Bauld and coworkers<sup>79-85</sup> have reported that Diels-Alder cycloaddition is effectively catalysed by the one electron oxidation of the dienophile to its radical cation. This highly electron deficient species adds to many cisoid dienes in a facile manner, retaining typical suprafacial stereospecificity and often improved stereoselectivity. Although the dimerisation of 1,3-cyclohexadiene affords only poor yields under standard reaction conditions,<sup>86</sup> treatment of this diene with a catalytic quantity of the stable radical salt tris(4-bromophenyl)aminium hexachloroantimonate (**5.33**) gives a good dimer yield at 0°C in minutes, with improved endo selectivity.<sup>82</sup>



The mechanism may be regarded as a [4+1] cycloaddition, featuring an open shell transition structure (**5.32**) with 5 electrons delocalised over 6 atoms. Aminium salt **5.33** also effectively catalyses some other electrocyclic processes,<sup>82</sup> so raising the possibility that open shell processes may participate in the mechanism of other common electrocyclic reactions.

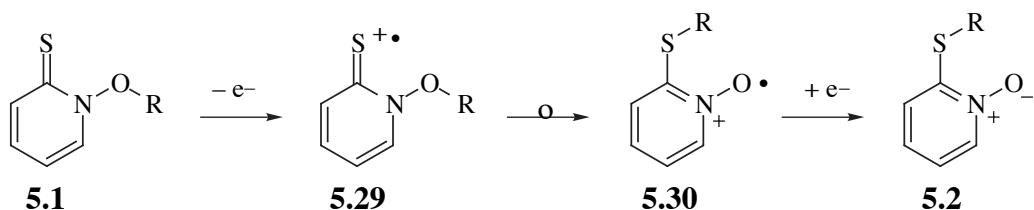
### 5.3 The mechanism of the rearrangement of *N*-alkoxy-2(1*H*)-pyridinethiones

The investigation of this rearrangement consisted of exploring the following areas:

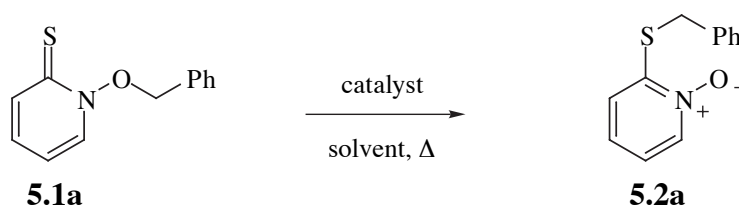
1. the mode of catalysis;
2. reaction kinetics;
3. rearrangement regiochemistry;
4. rearrangement stereochemistry;
5. the electronic structure at C1 of the migrating group during migration;
6. migrating group substituent effects; and
7. the attempted detection and isolation of intermediates.

#### 5.3.1 The mode of catalysis

Molecular oxygen catalyses the rearrangement *N*-alkoxy-2(1*H*)-pyridinethiones<sup>7</sup> which indicates that the reaction involves the formation of one or more reactive intermediates, which subsequently rearrange. An initial hypothesis of the mechanism was made, consistent with the few facts known. A molecule of the pyridinethione (**5.1**) may react with a molecule of dioxygen in a single electron redox reaction, forming a radical cation (**5.29**) of the pyridinethione and presumably the dioxygen radical anion. These oppositely charged species may or may not remain as a charge transfer complex. Subsequent reduction of rearranged radical cation **5.30**, to give *N*-oxide **5.2**, can presumably occur by the reduction of **5.30** with either the dioxygen radical anion or a molecule of the pyridinethione **5.1**, in a chain process. Since dioxygen is known to behave as a single electron oxidant<sup>60</sup> investigation of the mode of catalysis is likely to reveal valuable information about reaction intermediates.

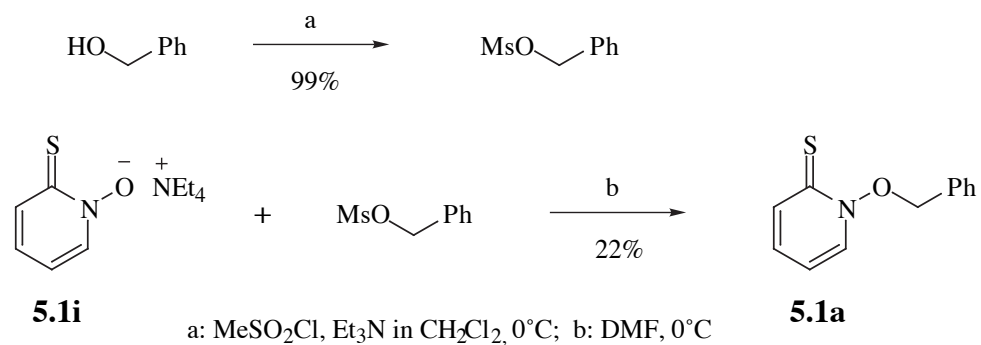


A variety of reagents were tested for catalytic activity. These included one electron oxidants, Lewis acids and Brønsted (protic) acids. Unless a selected atmosphere was used, a test reaction was conducted by heating a degassed 0.23 M solution of *N*-benzyloxy-2(1*H*)-pyridinethione (**5.1a**) in sealed glass ampoule, in the absence of light. The extent of reaction and yield of *N*-oxide **5.2a** were determined from <sup>1</sup>H nmr peak integrals corresponding to **5.1a**, **5.2a** and the other identifiable products. Results appear in table 5.1.



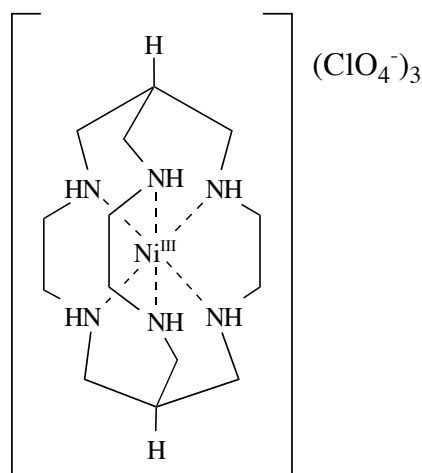
Each solvent was tested for catalytic activity by a control experiment, consisting simply of an otherwise identical reaction procedure minus catalyst. Negligible catalysis was observed in each case.

A sample of yellow, crystalline *N*-benzyloxy-2(1*H*)-pyridinethione (**5.1a**) was prepared in two steps from benzyl alcohol, by the method of Hay and Beckwith.<sup>7</sup> Mesylation<sup>99</sup> of the alcohol was facile and efficient, but the nucleophilic displacement reaction between the mesylate and tetraethylammonium 2(1*H*)-pyridinethione *N*-oxide (**5.1i**) gave consistently low yields of **5.1a**. This is due largely to the ambident nucleophilicity of the pyridinethione *N*-oxide anion, which results in the formation of a large proportion of the *N*-oxide **5.2a**. Hartung has recently reported a simpler and higher yielding route to *N*-alkoxy-2(1*H*)-pyridinethiones, consisting of the reaction between 2,2'-dithiopyridine-1,1'-dioxide and an alcohol, in the presence of a tertiary phosphine.<sup>14</sup>



**Table 5.1.** Effect of different reagents upon the rearrangement of (0.23 M) *N*-benzyloxy-2(1*H*)-pyridinethione (**5.1a**) under various conditions

Entry	Reagent	Relative conc. (mole %)	Solvent	<i>T</i> (°C)	Time (hr)	Extent of reaction of <b>5.1a</b> (%)	Yield of <i>N</i> -oxide <b>5.2a</b> (%)
1	None (vacuum)	0	C <sub>6</sub> D <sub>6</sub>	100	30.00	100	<1
2	Air	Uncert.	C <sub>6</sub> D <sub>6</sub>	100	4.00	95	71
3	Oxygen	Uncert.	C <sub>6</sub> D <sub>6</sub>	100	4.00	95	78
4	<i>m</i> -CPBA	1.08	C <sub>6</sub> D <sub>6</sub>	100	4.00	80	71
5	Iodine	4.94	C <sub>6</sub> D <sub>6</sub>	100	4.00	100	100
6	Iodine	0.51	C <sub>6</sub> D <sub>6</sub>	100	4.00	100	94
7	Iodine	0.49	CD <sub>3</sub> CN	100	4.00	100	95
8	Iodine	0.45	CDCl <sub>3</sub>	80	4.00	97	91
9	Cu(II)ethylhexanoate	0.50	CDCl <sub>3</sub>	80	4.50	5	2
10	( <i>p</i> -BrC <sub>6</sub> H <sub>4</sub> ) <sub>3</sub> N <sup>+</sup> SbCl <sub>6</sub> <sup>-</sup>	0.50	CD <sub>3</sub> CN	80	4.00	36	33
11	Fc <sup>+</sup> BF <sub>4</sub> <sup>-</sup>	~ 0.5	CD <sub>3</sub> CN	80	4.50	97	91
12	Fc <sup>+</sup> PF <sub>6</sub> <sup>-</sup>	0.50	CD <sub>3</sub> CN	80	4.00	97	96
13	Ni(III)SAR <sup>3+</sup> (ClO <sub>4</sub> <sup>-</sup> ) <sub>3</sub>	0.50	CD <sub>3</sub> CN	80	4.00	97	95
14	BF <sub>3</sub> ·Et <sub>2</sub> O	0.50	CDCl <sub>3</sub>	80	4.00	~90	~90
15	CF <sub>3</sub> SO <sub>3</sub> H	0.42	CDCl <sub>3</sub>	80	3.67	99	98
16	D <sub>2</sub> O	250	CD <sub>3</sub> CN	80	4.00	3	3
17	DCl in D <sub>2</sub> O	0.50	CD <sub>3</sub> CN	80	4.00	22	19
18	Bu <sub>4</sub> N <sup>+</sup> BF <sub>4</sub> <sup>-</sup>	5.0	CDCl <sub>3</sub>	80	4.00	3	3
19	<i>p</i> -Chloranil	0.49	CDCl <sub>3</sub>	80	4.00	2	1
20	Li <sup>+</sup> ClO <sub>4</sub> <sup>-</sup>	0.50	CD <sub>3</sub> CN	80	4.00	15	12



The structure of Ni (III) SAR perchlorate, the catalyst used in entry 13

The reagents  $\text{AgBF}_4$  and *p*-toluenesulfonic acid also displayed catalytic activity but are not included in table 5.1 since solubility problems prevented the determination of their concentration. Small amounts of benzyl alcohol and benzaldehyde were present in the reaction mixtures indicating that radical reactions resulting from thermal N–O bond homolysis occur simultaneously with the rearrangement reaction. Such radical processes usually consume only a few percent of **5.1a**, although homolytic reactions become increasingly favoured at higher temperature.

Reagents which displayed excellent catalysis included the oxidants  $\text{I}_2$ ,  $\text{O}_2$ , the Ni(III) sarcophagine complex and the ferrocenium salts; the proton donor triflic acid; and the Lewis acid  $\text{BF}_3 \cdot \text{Et}_2\text{O}$ . Hence, catalysis is not effected solely by one class of reagent.

Reagents displaying weak or negligible activity included: aqueous DCl; the oxidants copper (II) ethylhexanoate and  $(p\text{-BrC}_6\text{H}_4)_3\text{N} \cdot \text{SbCl}_6$  (**5.33**); the CT complex electron acceptor *p*-chloranil (2,3,5,6-tetrachlorobenzoquinone);<sup>88</sup> the electrolytes  $\text{Bu}_4\text{NBF}_4$  and  $\text{LiClO}_4$ ; and water. The concentration of DCl is expected to be much lower than that stated owing to its removal by the freeze/vacuum/thaw degassing procedure. This acid may actually be an effective catalyst.

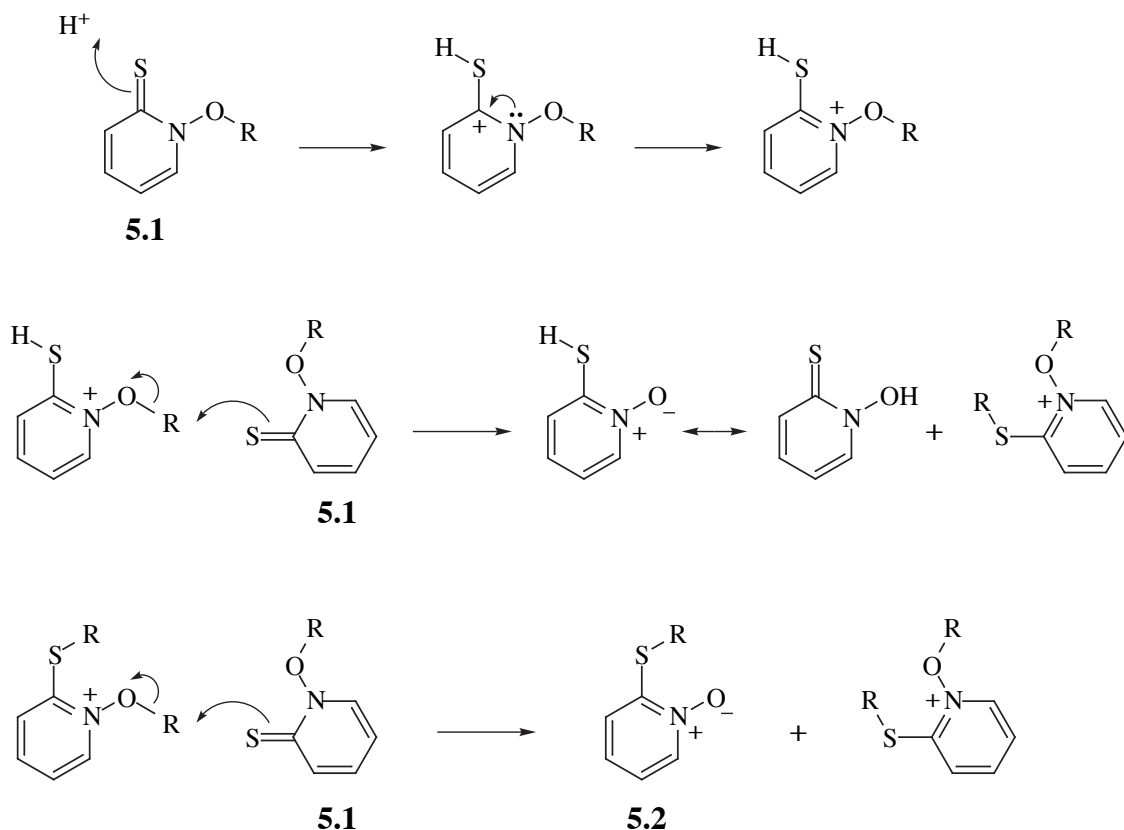
Mechanistic interpretation of these results is difficult since the chemical action of reagents can be quite ambiguous. Iodine acts as a one electron oxidant,<sup>89, 90</sup> but also as a Lewis acid when it forms the electron donor-acceptor complex  $\text{I}_3^-$  with iodide ion. Strong protic acids reportedly oxidise unsaturated hydrocarbons to radical cations,<sup>91</sup> as



too can Lewis acids,<sup>92, 93</sup> presumably by acting in tandem with atmospheric oxygen or solvents which are easily reduced. Lewis acids can produce strong protic acids by their reaction with adventitious water. Once formed, a radical cation (being acidic) can eliminate a proton.

In some cases it was possible to distinguish between alternative modes of catalysis with appropriately designed experiments. Addition of the hindered base, 2,6-di-*tert*-butyl-4-methylpyridine (0.5 eq)—used by Gassman to distinguish between oxidative and acidic catalysis of Diels-Alder cycloadditions<sup>94</sup>—did not inhibit the efficiency of iodine (1.0 mol%) catalysis of the rearrangement of **5.1a** in deuteriochloroform. Hence, iodine cannot be associated with protic acid catalysis. Furthermore, the aminium salt **5.33** was found to decompose at 80°C in CD<sub>3</sub>CN over a matter of minutes, as indicated by the irreversible loss of its deep blue colour. As the addition of the hindered base or pyridinethione **5.1a** also caused immediate decolourisation of the deep blue solution of **5.33** at room temperature, it was concluded that decomposition of **5.33** was probably the cause of its relatively poor catalytic activity.

It is possible that the rearrangement mechanism is different for oxidant and acid catalysis. A postulated chain mechanism for acid catalysis is provided below (scheme 5.8). The alkyl group R migrates not in an intramolecular sense, but is transferred intermolecularly. *N*-hydroxy-2(1*H*)-pyridinethione is a by-product according to this scheme and is essentially a weak acid resulting from a strong acid/weak base reaction. Consequently, it should be present in quantities less than or equal to the amount of catalyst and therefore hard to detect. However, the pungent odour of *N*-hydroxy-2(1*H*)-pyridinethione could sometimes be detected after evaporating to dryness reactions performed in chloroform, a solvent which often contains small amounts of HCl.



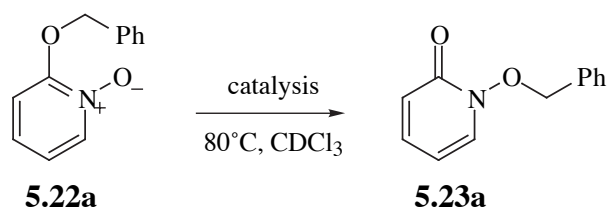
**Scheme 5.8.** A possible intermolecular chain mechanism for the acid catalysed 1,4 rearrangement of *N*-alkoxy-2(1*H*)-pyridinethiones

The catalysis experiments cannot unambiguously confirm nor exclude the formation of a radical cation intermediate by one electron oxidation of the pyridinethione. Data most supportive of a radical cation mediated mechanism are those for the reagents molecular oxygen (entry 3) and the Ni(III) SAR complex (entry 13), neither of which could be envisaged acting as Lewis or protic acids. In conclusion, catalysis by an oxidant, Lewis acid or protic acid forms the same product *N*-oxide **5.2a** from **5.1a**. It is not yet known whether catalysis occurs by significantly different paths, or by routes in which different intermediates undergo rearrangement in a similar way.

### 5.3.1.1 Can the rearrangement of 2-alkoxy-2-pyridine *N*-oxides be catalysed in the same manner?

Because of the structural similarities, we were keen to discover whether the known rearrangement<sup>48-57,117-119</sup> of 2-alkoxy-2-pyridine *N*-oxides to the corresponding *N*-alkoxy-2(1*H*)-pyridones was similarly catalysed. A sample of 2-benzyloxy-2-pyridine *N*-

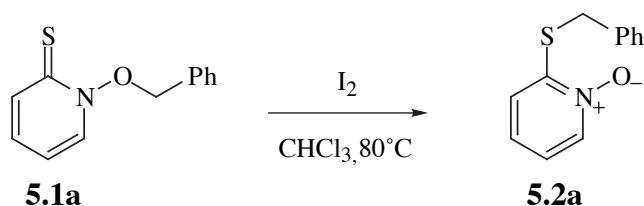
oxide<sup>53,118</sup> (**5.22a**) was prepared by the treatment of 2-chloropyridine *N*-oxide<sup>95</sup> with sodium benzyloxide in boiling THF. The attempted rearrangement of **5.22a** to *N*-benzyloxy-2(1*H*)-pyridone (**5.23a**) was studied under various conditions.



$\text{CDCl}_3$  solutions of **5.22a** (0.22 M) were heated at  $80^\circ\text{C}$  for 4 hr. All reactions proceeded cleanly, the only compounds detected by  $^1\text{H}$  nmr were the *N*-oxide **5.22a** and pyridone **5.23a**. Under vacuum-degassed conditions, a 3.7% yield of **5.23a** was obtained, while in an atmosphere of air, the yield rose slightly to 4.5%. With 1.1 mol% iodine catalysis, a 65.7% conversion to **5.23a** occurred. This rearrangement is obviously catalysed by iodine. Air (oxygen) appears to display a negligible effect. Iodine catalysis suggests a similar mechanism to that for the catalysed rearrangement of *N*-alkoxy-2(1*H*)-pyridinethiones.

### 5.3.2 Kinetics

Absolute kinetic data have been obtained for the iodine catalysed rearrangement of *N*-benzyloxy-2(1*H*)-pyridinethione (**5.1a**) to 2-benzylsulfanylpiperidine *N*-oxide (**5.2a**) in degassed chloroform, at  $80^\circ\text{C}$ . The concentration of the reactant **5.1a** (initially 0.114M) was monitored periodically by withdrawing small volumes from the reaction solution by microsyringe. After diluting an aliquot with ethanol, the absorbance at  $\lambda_{\text{max}} = 361$  nm was measured by UV-visible spectrophotometry.



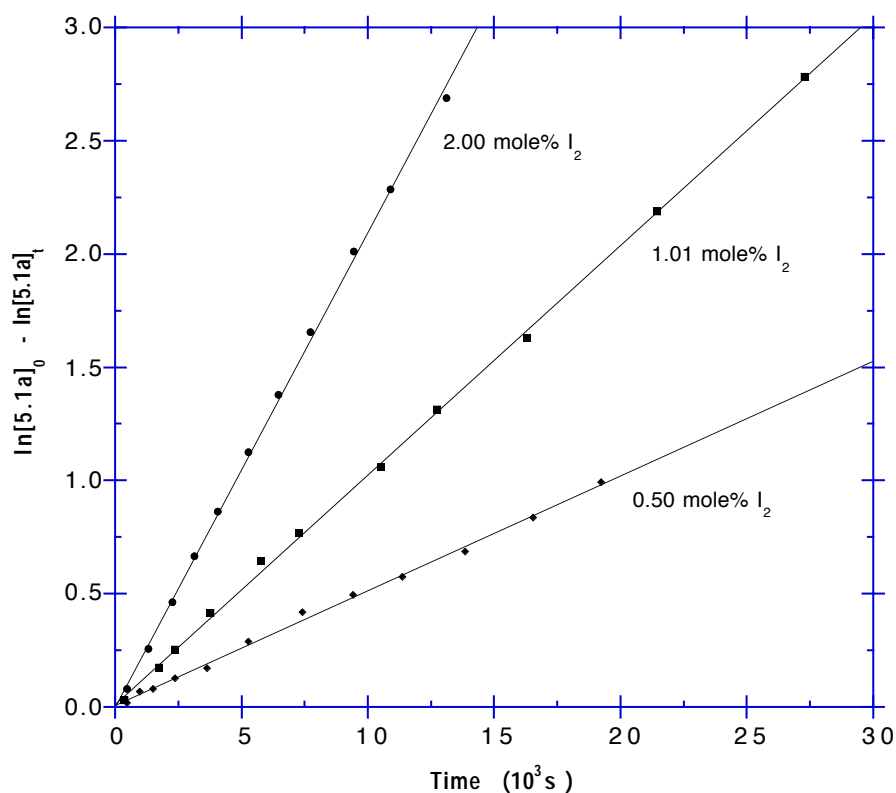
It was not possible to measure the concentration of the product **5.2a** directly by this method since the  $\lambda_{\text{max}}$  values of 244, 271 and 312 nm were all obscured to some degree by the spectrum of **5.1a** ( $\lambda_{\text{max}} = 289, 361$  nm). However, since  $^1\text{H}$  nmr spectroscopy has indicated that only a very small proportion of side reactions occur, it can be assumed that:

$$-\frac{d[\mathbf{5.1a}]}{dt} = \frac{d[\mathbf{5.2a}]}{dt} \quad (5.1)$$

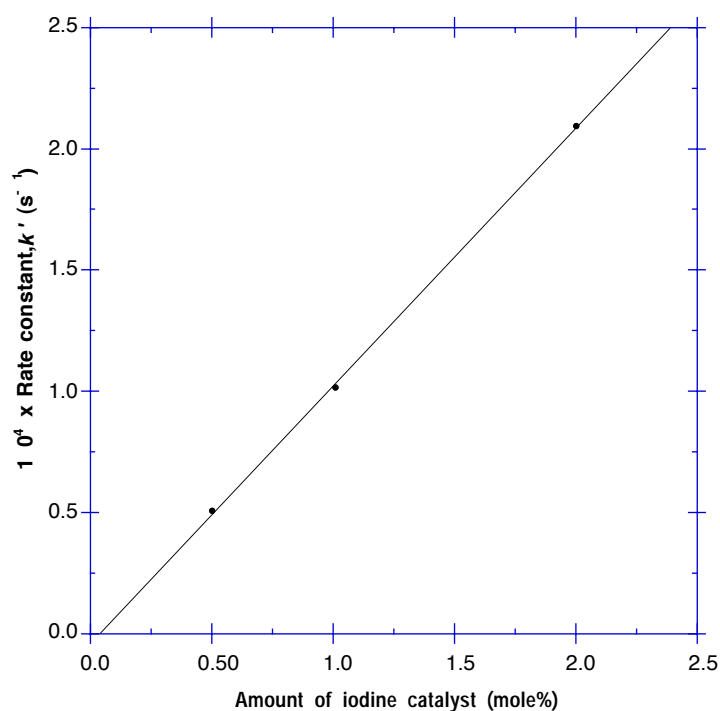
As observed in figure 5.1, plots of  $\ln\{[\mathbf{5.1a}]_0/[\mathbf{5.1a}]_t\}$  versus time are linear, indicating (pseudo) first order kinetics. The rate constant,  $k'$ , is linearly dependent upon the relative concentration of iodine, with  $k'$  effectively zero in its absence (figure 5.2). This behaviour indicates true catalysis. Therefore, the overall rate law appears to be first order in **5.1a** and catalytic in iodine. Rate constant data is displayed in table 5.2.

**Table 5.2.** Rate constants for iodine catalysed rearrangement of **5.1a** in chloroform, where  $[\mathbf{5.1a}]_0 = 0.114$  M

Initial concentration of iodine catalyst (M)	Proportion of iodine catalyst (mole%)	Pseudo first order rate constant, $k'$ (s <sup>-1</sup> )
$5.75 \times 10^{-4}$	0.50	$5.08 \times 10^{-5}$
$1.15 \times 10^{-3}$	1.01	$1.10 \times 10^{-4}$
$2.30 \times 10^{-3}$	2.00	$2.10 \times 10^{-4}$



**Figure 5.1.** Plot of  $\ln([5.1a]_t/[5.1a]_0)$  versus time for the iodine catalysed rearrangement of **5.1a** (0.114 M) in deoxygenated chloroform, at  $80^\circ\text{C}$



**Figure 5.2.** Plot of the pseudo first order rate constant,  $k'$ , versus the relative amount of catalyst present in the iodine-catalysed rearrangement of **5.1a** (0.114 M) in chloroform at  $80^\circ\text{C}$ . The gradient of the line of best fit is  $1.06 \times 10^{-4} \text{ s}^{-1}$  per mole% iodine.

The same type of rearrangement experiments were repeated, this time keeping the initial iodine concentration constant and varying the initial concentration of *N*-benzyloxy-2(1*H*)-pyridinethione **5.1a**. Table 5.3 displays the results. Doubling the initial concentration of the pyridinethione increases the rate constant by a modest 23%, demonstrating that a change in  $[\mathbf{5.1a}]_0$  has an effect of less than one quarter the magnitude of a change in  $[\text{I}_2]_0$  upon the rate constant.

**Table 5.3.** Rate constants for iodine catalysed rearrangement of **5.1a** in chloroform at 80°C<sup>†</sup>, where  $[\text{I}_2]_0$  is kept constant, but  $[\mathbf{5.1a}]_0$  is varied

$[\text{I}_2]_0$ (M)	$[\mathbf{5.1a}]_0$ (M)	Proportion of iodine catalyst (mole%)	Pseudo first order rate constant, $k'$ (s <sup>-1</sup> )
$1.15 \times 10^{-3}$	0.114	1.01	$1.10 \times 10^{-4}$
$1.16 \times 10^{-3}$	0.225	0.51	$1.35 \times 10^{-4}$

<sup>†</sup> Temperature of more concentrated reaction was 81.5±1°C

To investigate whether different catalysts produce a common intermediate, a kinetic comparison of four catalysts was performed in a solvent which would ensure complete solubility of **5.1a**, **5.2a** and all catalysts. Rate constant data is displayed in table 5.4.

**Table 5.4.** Rate constants for the rearrangement of **5.1a** ( $c = 0.115$  M) in degassed  $\text{CHCl}_3/\text{CH}_3\text{CN}$  (1:1 v/v) with 1.00mole% of each catalyst at 80±1°C

Reagent	$E^0$ in $\text{CH}_3\text{CN}$ (V)	$k'$ (s <sup>-1</sup> )
$\text{I}_2$	0.18, 0.66 <sup>a</sup>	$5.63 \times 10^{-4}$
$\text{Fc}^+\text{PF}_6^-$	0.41 <sup>b</sup>	$5.59 \times 10^{-4}$
$\text{Ni(III)SAR}(\text{ClO}_4)_3$	1.05 <sup>c</sup>	$4.57 \times 10^{-4}$
$(p\text{-BrC}_6\text{H}_4)_3\text{N}^+\text{SbCl}_6^-$ ( <b>5.33</b> )	1.05 <sup>d</sup>	$1.97 \times 10^{-5}$

a: Reference 114; b: Measured with ferrocene in acetonitrile/TBAF relative to Ag/AgCl;

c: Reference 115; d: Reference 116

Pseudo first order kinetics was obeyed in each case. The iodine and ferrocenium hexafluorophosphate catalysed reactions have approximately the same rate constant. That

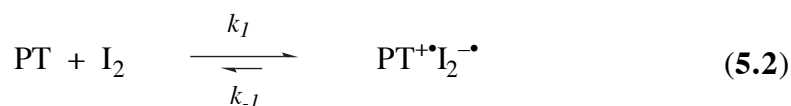
for Ni (III) SAR catalysis is about 81% of  $k'$  for iodine. The rate constant for the aminium salt (**5.33**) catalysed reaction is smaller by more than an order of magnitude, presumably owing to thermal decomposition of the catalyst, as mentioned previously. Differences may also be partially attributable due to differing solubilities of activated intermediates.

The similarity of the first three rate constants is consistent with a common intermediate, most probably a pyridinethione radical cation formed by a one electron oxidation. However, the reduction potentials for the catalysts are varied, some being below 0.5 V. Pyridinethione **5.1a** has a one electron oxidation potential of 0.9 V (section 5.3.7.3), which leaves a presently unanswered question of how it is that each catalyst is capable of oxidising **5.1a**. Mehta and Pinto<sup>116</sup> encountered the same question when they observed one electron oxidation of phenyl selenoglycosides (oxidation potential 1.35-1.50 V) by aminium salt **5.33** (reduction potential 1.05 V). They suggest that a prior complexation of the selenoglycoside and the aminium salt produces a complex of lowered oxidation potential.<sup>116</sup>

A comparison of data in tables 5.2 and 5.4, reveals a 5.5 fold increase in rate constant  $k'$  as the solvent is changed from chloroform to chloroform/acetonitrile. Such a rate acceleration with increased solvent polarity indicates a polarized rate limiting step.

The equilibrium constant for the reaction between iodine and **5.1a** in chloroform has been measured. The initial reaction between one catalyst (**5.33**) and **5.1a** is very rapid, as indicated by the immediate and complete loss of blue colour observed upon mixing a deep blue  $\text{CH}_2\text{Cl}_2$  solution of the aminium salt **5.33** with the yellow pyridinethione solution. Owing to the colours of both iodine and the pyridinethione, it was more difficult to observe such a decolourisation with this system. However, decolourisation does occur when a colourless solution of the product *N*-oxide (**5.2a**) is mixed with a  $\text{CH}_2\text{Cl}_2$  solution of either iodine, aminium salt **5.33** or ferrocenium hexafluorophosphate.<sup>96</sup> This behaviour indicates a ready oxidation of, or complexation with, the product also by the catalyst.

If the equilibrium is treated as having the stoichiometry:



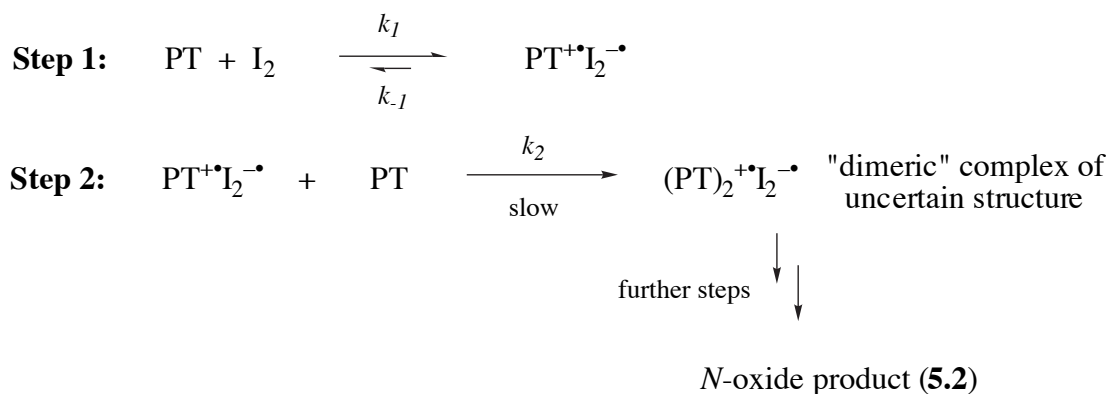
where PT stands for *N*-benzyloxy-2(1*H*)-pyridinethione **5.1a** and  $\text{PT}^+\text{I}_2^-$  represents an activated charge transfer intermediate or ion pair, then the equilibrium constant  $K$  is expressed as:

$$K = \frac{k_1}{k_{-1}} = \frac{[\text{PT}^+\text{I}_2^-]}{[\text{PT}][\text{I}_2]} \quad (5.3)$$

A solution of iodine in chloroform of concentration  $2.01 \times 10^{-4}$  M was prepared at room temperature and its UV-vis spectrum was measured, which displayed a broad absorption peak at  $\lambda_{\text{max}} = 508$  nm. A very small volume of a solution of **5.1a** in chloroform was added, so as to give an initial pyridinethione concentration of  $2.00 \times 10^{-4}$  M. Immediately another UV-vis spectrum was obtained which indicated that the absorbance at 508 nm had reduced to 79.0% of its original value. From these values,  $K$  was calculated to be  $1680 \text{ M}^{-1}$ . When the experiment was repeated at halved concentrations, where  $[\text{PT}]_0 = 9.99 \times 10^{-5}$  and  $[\text{I}_2]_0 = 9.90 \times 10^{-5}$  M, the iodine absorbance dropped to 87.5% its initial value, giving  $K = 1650 \text{ M}^{-1}$ . At room temperature, such  $K$  values correspond to approximately 99.5% consumption of iodine upon formation of the activated intermediate for typical rearrangement reaction concentrations of  $[\text{PT}]_0 = 0.10$  M and  $[\text{I}_2]_0 = 0.0010$  M. This rapid and virtually complete reaction of catalyst with pyridinethione therefore cannot be the rate limiting step.

The kinetic results are not consistent with a catalysed mechanism which involves the concerted, intramolecular rearrangement of an activated intermediate depicted by transition state **5.31**. A revised, hypothetical partial mechanism which accounts for the observed kinetics and equilibrium constant is displayed in scheme 5.9. Pseudo-first order kinetics are expected for the rate limiting second step, having rate constant  $k_2$ , since  $[\text{PT}^+\text{I}_2^-]$  will remain approximately constant owing to the large equilibrium constant for the first pre-equilibrium step. This second bimolecular process is expected to have a polarized transition structure since polar solvents increase the rate.





**Scheme 5.9.** A proposed partial mechanism for the iodine catalysed rearrangement of **5.1a**, which accounts for the kinetics being catalytic in iodine and first order in **5.1a**

For conditions under which most of the catalysed rearrangement reactions were conducted, where  $[\mathbf{5.1a}]_0 \gg [\text{I}_2]_0$ , the empirical rate law can be expressed by equation 5.4.

$$-\frac{d[\mathbf{5.1a}]}{dt} = \frac{d[\mathbf{5.2a}]}{dt} \approx k_2[\text{I}_2]_0[\mathbf{5.1a}] \quad (5.4)$$

An estimation of  $k_2$ , the true second order rate constant, at 80°C can therefore be made. Table 5.2 lists the pseudo first order rate constant,  $k'$ , for the 1.01 mole % iodine catalysed rearrangement of **5.1a** as  $1.10 \times 10^{-4} \text{ s}^{-1}$ . The initial iodine concentration of  $1.15 \times 10^{-3} \text{ M}$  will be the approximate concentration of  $\text{PT}^+\text{I}_2^-$ , assuming the equilibrium constant  $K$  is the same at 80°C as at 20°C. Division of  $k'$  by  $[\text{I}_2]_0$  gives  $k_2 = 9.57 \times 10^{-2} \text{ M}^{-1}\text{s}^{-1}$ .

Attempts were made to detect the product **5.2a** by thin layer chromatography in solutions resulting from the mixing of a relatively large proportion of a catalyst and **5.1a** at room temperature. Such attempts all failed to detect the *N*-oxide. A flocculent precipitate was formed immediately when some catalysts were mixed with **5.1a**, indicating the rapid formation of an insoluble intermediate such as a charge transfer complex. These results support the proposal that step 1 (activation) is not rate limiting.

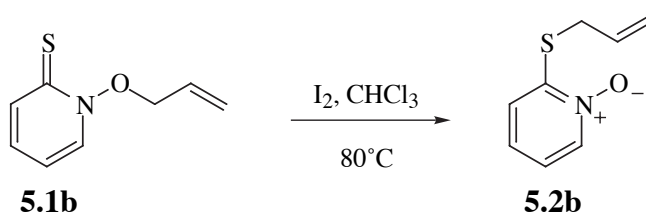
Since the kinetics are first order in the concentration of **5.1a**, the rate limiting step

must involve a reaction between **5.1a** and some type of intermediate. Consequently, the possibility exists that step 2 is not rate limiting, but some later bimolecular step is. Another mechanism accounting for the observed kinetics is one in which the rate limiting step consists of the displacement by pyridinethione **5.1a** of a molecule of the product *N*-oxide **5.2a** from a charge transfer complex intermediate in which the migrating group shift had already taken place. It is clear that much can be gained by elucidating the structures of the intermediates involved.

In summary, the kinetics indicate that the rearrangement of **5.1a** to **5.2a** is a more complex reaction than initially envisaged. This process displays pseudo first order kinetics. The initial reaction between iodine and pyridinethione **5.1a** is fast and has an equilibrium constant of approximately  $1650 \text{ M}^{-1}$  in chloroform at room temperature. The rate limiting step appears to be bimolecular, involving the reaction between an intermediate and the pyridinethione and has an estimated rate constant of  $k_2 = 9.6 \times 10^{-2} \text{ M}^{-1}\text{s}^{-1}$  in chloroform at  $80^\circ\text{C}$ . Polar solvents accelerate rearrangement, indicating a polarized transition state for the rate limiting step. Iodine exhibits true catalytic behaviour and from the similarity of rate constants, at least two other catalysts tested appear to form analogous intermediates to those formed using iodine. Little is currently known about the structure of intermediates.

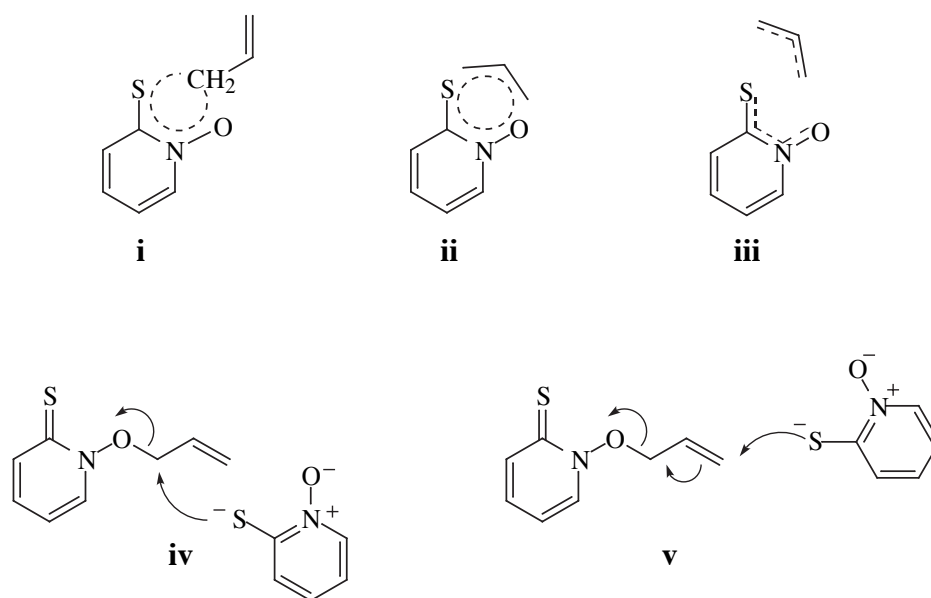
### 5.3.3 A study of rearrangement regiochemistry

It was found that *N*-allyloxy-2(1*H*)-pyridinethione (**5.1b**) rearranges exclusively to 2-allylsulfanylpyridine *N*-oxide (**5.2b**) upon catalysis with iodine.



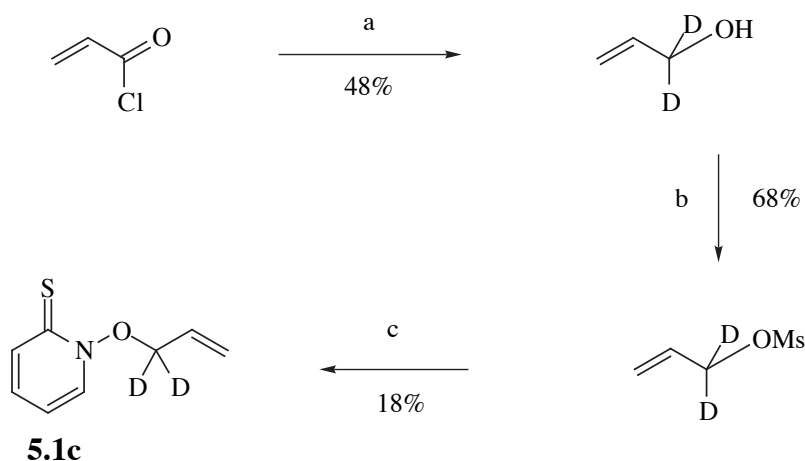
Five plausible types of mechanism which could lead to the formation of the **5.2b** came initially to mind. The first is a 1,4 sigmatropic shift involving an open or closed

shell five membered transition structure (**i**). The second is a 3,4 sigmatropic shift which proceeds *via* an open or closed shell seven membered transition structure (**ii**). Structure **iii** represents an intramolecular dissociation/recombination process which may be either heterolytic or homolytic. Mechanism **iv** exemplifies an intermolecular chain process, which may involve either ionic or radical substitution, in which attack occurs at C1 of the allyl group. Path **v** is similar to **iv**, but involves attack at C3 of the allyl group. Only options **i** and **iv** would be expected to proceed with exclusive transfer of C1 of the allyl group from oxygen to sulfur. To discriminate between the possibilities, the catalysed rearrangement of *N*-1,1-dideuteroallyloxy-2(1*H*)-pyridinethione (**5.1c**) was studied.



Compound **5.1c** was prepared in three steps. Acryloyl chloride was reduced with lithium aluminium deuteride in diethyl ether to 1,1-dideuteroallyl alcohol, according to a literature procedure.<sup>113</sup> Treatment of this alcohol with methanesulfonyl chloride in dichloromethane under basic conditions yielded the desired mesylate. The alkylating agent reacted with tetraethylammonium 2(1*H*)-pyridinethione *N*-oxide in DMF to give the desired pyridinethione **5.1c** in low yield. From the <sup>1</sup>H nmr spectrum of **5.1c** (figure 5.3) it can be concluded from the virtual absence of resonances at 5.0 ppm (O–CH<sub>2</sub>) that nucleophilic attack upon the allyl mesylate took place almost entirely at C1. A <sup>2</sup>H nmr spectrum at 30.7 MHz in CHCl<sub>3</sub> revealed that the only peak belonging to pyridinethione

**5.1c** was a broad singlet at 4.97 ppm, attributed to O-CD<sub>2</sub>. There were no peaks detected in the range 5.4-5.5 ppm, indicating no deuterium incorporation into the =CH<sub>2</sub> position. Hence, no appreciable S<sub>N</sub>2' substitution at the  $\gamma$ -carbon of the mesylate occurs during the formation of **5.1c**.

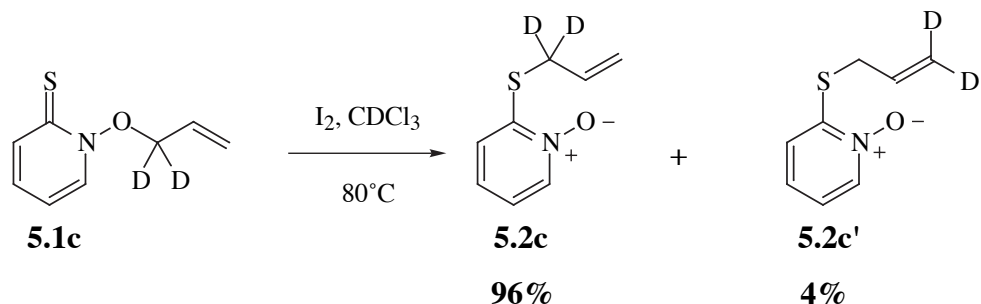


a: LiAlD<sub>4</sub> in Et<sub>2</sub>O; b: MeSO<sub>2</sub>Cl, Et<sub>3</sub>N in CH<sub>2</sub>Cl<sub>2</sub>, 0°C; c: tetraethylammonium 2(1H)-pyridinethione N-oxide (**1i**) in DMF, 0°C

The isotopic composition of pyridinethione **5.1c** could not be established accurately by mass spectrometry, although a *monodeuterated* fragment ion corresponding to a peak group at  $m/z = 111-114$  analysed for 97.6-97.9 atom% *d*. Unfortunately, this result could not be corroborated for *dideuterated* fragments owing to either low relative peak abundance or complications associated with peak groups which represent more than one species. However, from the intensity of the resonances at 5.0 ppm, <sup>1</sup>H nmr was used to establish that C1 of the allyl group was protiated to the extent of 1.2-2.4 atom% (97.6-98.8 atom% *d*), agreeing well with the mass spectrometric result for the monodeuterated fragment ion. Consequently, the isotopic composition of **5.1c** was taken to be 98 atom% *d*, identical to that stated for the LiAlD<sub>4</sub> used to incorporate the label into C1 of the allyl group. Relative yields for the isomeric rearrangement products **5.2c** and **5.2c'** have been normalised accordingly.

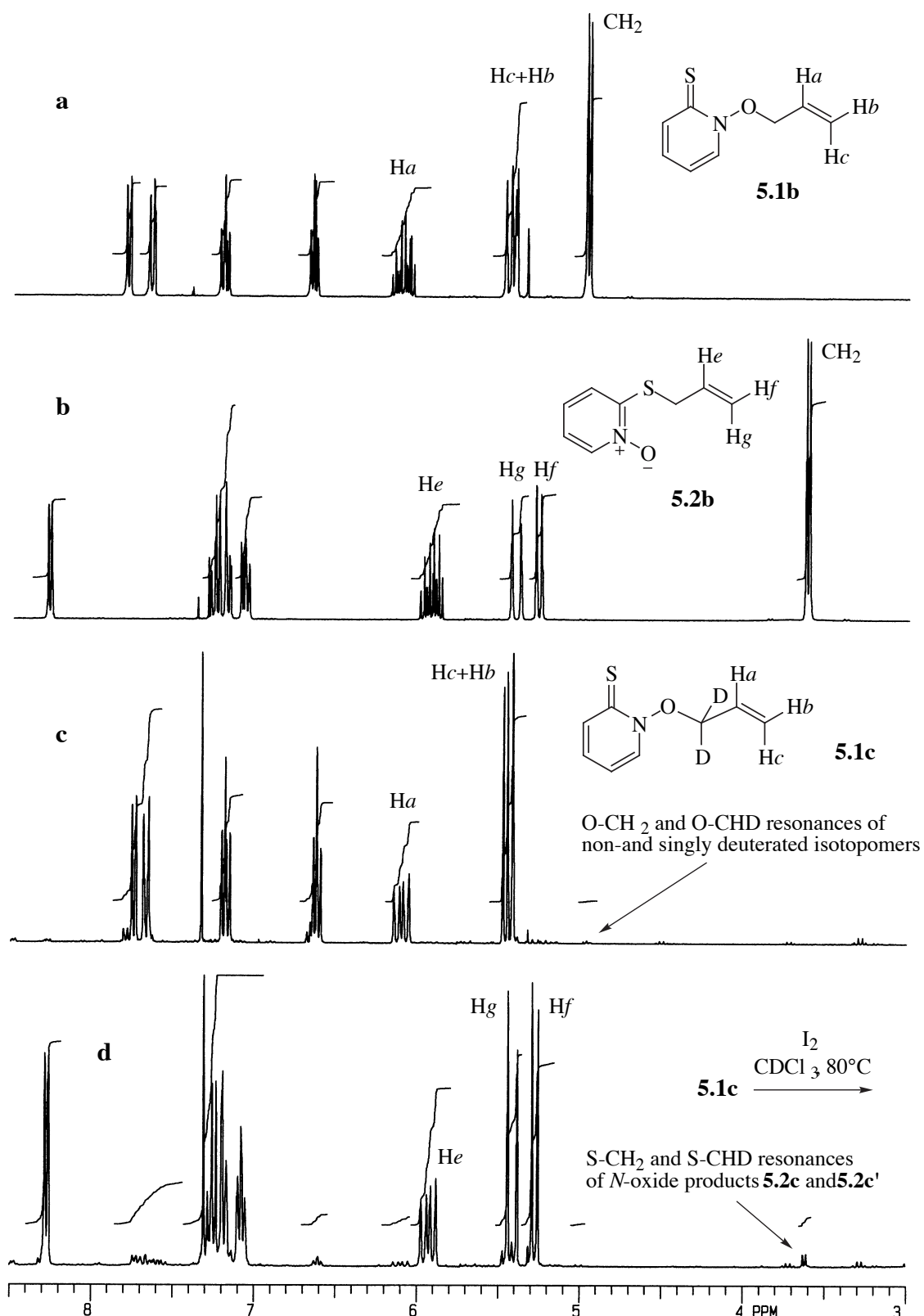
A degassed CDCl<sub>3</sub> solution of **5.1c** was heated in the dark at 80°C with 2.0 mol% iodine. After 8.5 hr, 80% of the pyridinethione had reacted, forming the products **5.2c** (96%) and **5.2c'** (4%), as determined by <sup>1</sup>H nmr. Relevant nmr spectra are

displayed in figure 5.3.



The result for iodine catalysis was checked semi-quantitatively by <sup>2</sup>H nmr. At 30.7 MHz in CHCl<sub>3</sub> solution the major product peak detected was a broad singlet at 3.62 ppm, corresponding to S-CD<sub>2</sub>. Doublet resonances of very low intensity, centred at 5.27 and 5.41 ppm were detected, corresponding to the alkene deuterons at C3 of the *N*-oxide **5.2c'**. Quantification was difficult due to the width of the lines and the low S/N ratio, but each of the alkene peaks was ≤1.8% the height of the major singlet. This indicates that ≥ (100 - (4 × 1.8)) ≈ 93% of the *d*<sub>2</sub> label is located at C1 of the allyl chain in the product **5.2c'**. Since the uncertainty is estimated at 2-3%, the <sup>2</sup>H nmr result upper limit is therefore 95-96%, close to that determined by <sup>1</sup>H nmr. It is possible that exchange of deuterons and protons (adventitious HCl in chloroform) in solution is responsible for the small amount of label scrambling, although vacuum degassing should have removed HCl.

We were eager to discover how another effective catalyst, expected to act exclusively as a protic acid, would affect the regiochemistry. The same experiment was hence repeated, replacing iodine with CF<sub>3</sub>SO<sub>3</sub>H (3.4 mol%). Relative product yields changed only slightly to **5.2c**: 98% and **5.2c'**: 2%, at *ca.* 60% consumption of **5.1c**. Allyl migration from O to S therefore occurs predominantly, though not exclusively, *via* C1 transfer for both iodine and acid catalysis. The sameness of these outcomes indicates a similar mechanism. A preponderance of mechanism **i** or **iv** is consistent with the results. Mechanism **iii** may also account for the results, but the ion or radical pair must



**Figure 5.3.** Nmr spectra of species involved in the regiochemical study. **a:** *N*-allyloxy-2(1*H*)-pyridinethione (**5.1b**); **b:** 2-allylsulfanylpyridine *N*-oxide (**5.2b**); **c:** *N*-(allyloxy-1,1-*d*<sub>2</sub>)-2(1*H*)-pyridinethione (**5.1c**); **d:** reaction mixture from iodine catalysed rearrangement of *N*-(allyloxy-1,1-*d*<sub>2</sub>)-2(1*H*)-pyridinethione (**5.1c**), consisting mostly of 2-(allylsulfanyl-1,1-*d*<sub>2</sub>)pyridine *N*-oxide

have a very short lifetime and be highly selective to produce the high level of regioselectivity observed.

In conclusion, the migration of the allyl group from O to S in the **5.1c**→**5.2c** rearrangement proceeds with high regioselectivity for C1 over C3 for both iodine and trifluoromethanesulfonic acid catalysis. The predominance of an intramolecular 1,4 shift (**i**) or an intermolecular allyl C1 substitution reaction (**iv**) is consistent with the results. A tight, short lived and highly selective ion or radical pair (**iii**) is less likely, but possible. The sameness of the results between catalysts suggests a similarity of mechanism.

### 5.3.4 A study of rearrangement stereochemistry

Results from the kinetic work of section 5.3.2 are consistent with an intermolecular rate limiting step, yet do not yet exclude the possibility that the actual alkyl group migration step is intramolecular. Mechanistic work on the rearrangement of analogous 2-alkoxy pyridine *N*-oxides<sup>117-119</sup> has shown that an intermolecular transfer of the alkyl group occurs, but such a process has not yet been tested with *N*-alkoxy-2(1*H*)-pyridinethione rearrangement. For the purposes of this current stereochemical study the initial hypothesis—that the isomerization proceeds by a catalysed 1,4 sigmatropic shift—remains intact.

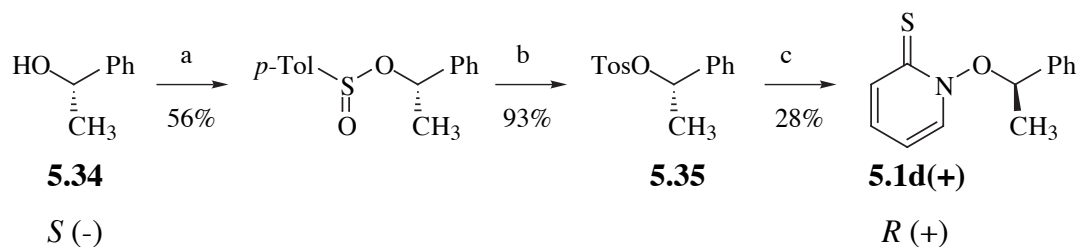
The stereochemical outcome of *closed shell*, thermal 1,4 sigmatropic rearrangements should be unambiguous. As discussed previously, those involving the redistribution of four electrons proceed in the 1a,4s mode, bringing about inversion of configuration at C1 of the migrating group, while those involving six electrons proceed with retention of configuration, *via* a 1s,4s path. Predicting the stereochemical outcome of rearrangements within *open shell* systems—having one valence orbital singly occupied—is less clear. The stereochemistry of the migration of an enantiomerically enriched 1-phenylethyl group was studied to reveal whether the rearrangement more closely resembles the characteristics of four (inversion) or of six (retention) electron systems.

### 5.3.4.1 Preparation of optically active reactants and products

The stereochemistry of the catalysed rearrangement of both the *R* (+) and *S* (–) enantiomers of *N*-(1-phenylethoxy)-2(1*H*)-pyridinethione (**5.1d**) was studied. Both the *R* and *S* enantiomers of the reactant pyridinethione (**5.1d**) and of the product *N*-oxide (**5.2d**) were prepared to ensure a high degree of confidence in the rearrangement stereochemistry results. Each enantiomer of the product and of the reactant was prepared by a different method to provide confidence in the correct assignment of absolute stereochemical configurations.

#### (i) Synthesis of *R* (+)-*N*-(1-phenylethoxy)-2(1*H*)-pyridinethione, **5.1d(+)**

A sample of *R* (+)-*N*-(1-phenylethoxy)-2(1*H*)-pyridinethione, **5.1d(+)**, was prepared in three steps from commercial, enantiomerically pure *S* (–) 1-phenethyl alcohol (**5.34**). The tosylate **5.35** was obtained indirectly<sup>97</sup> due to its thermal lability, *via* the more stable sulfinic acid. Oxidation of *S* 1-phenethyl *p*-toluenesulfinate with *m*-chloroperbenzoic acid was accomplished easily under cool conditions. Conversion of the optically active alkylating agent to the desired pyridinethione was achieved by treatment with tetraethylammonium 2(1*H*)-pyridinethione *N*-oxide in DMF at 0°C. The isolated pyridinethione **5.1d(+)** had a specific optical rotation of +771±9°, corresponding to 71.7±1.0% e.e. (see section ii). This degree of optical purity indicates that although the displacement mechanism was predominantly S<sub>N</sub>2, significant racemisation had occurred.



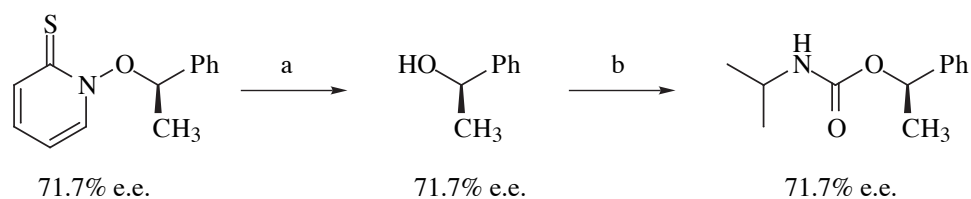
a: *p*-TolSOCl, pyridine, Et<sub>2</sub>O, 0°C; b: *m*-CPBA, CH<sub>2</sub>Cl<sub>2</sub>, 0°C;

c: tetraethylammonium 2(1*H*)-pyridinethione *N*-oxide (**1i**), DMF, 0°C

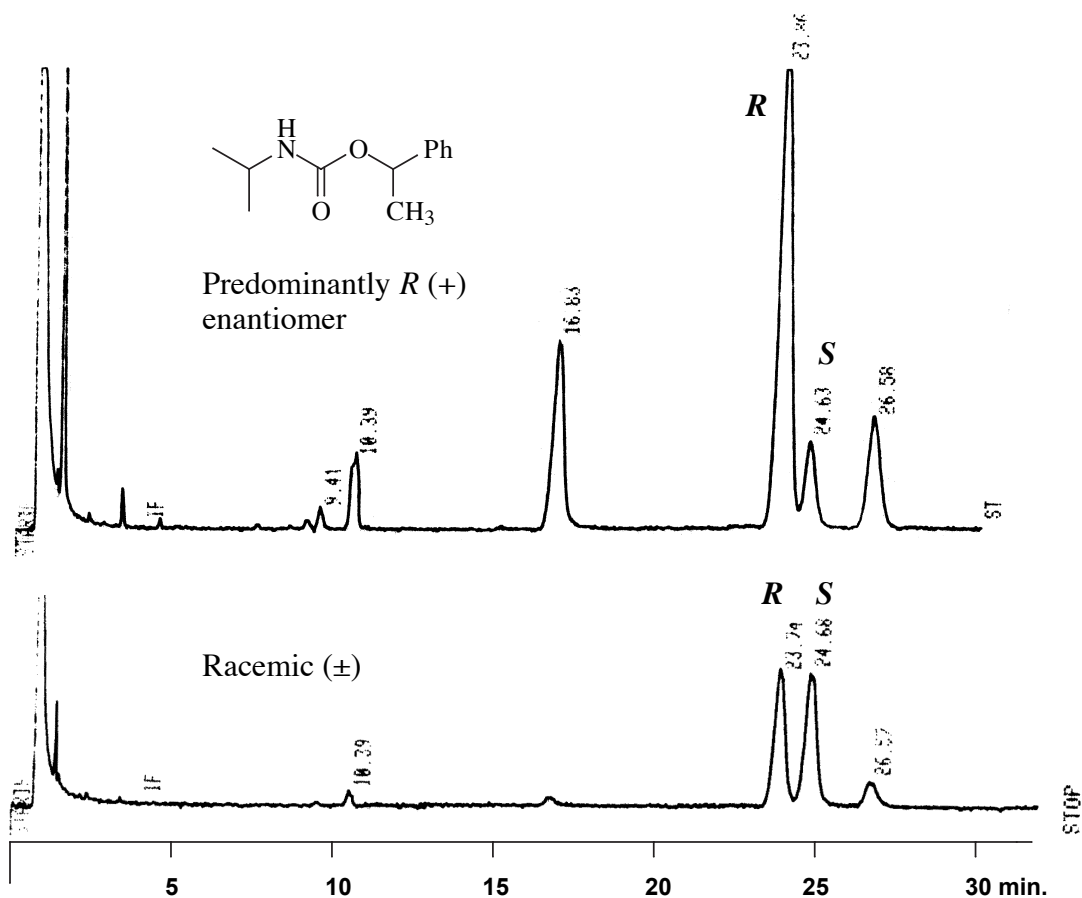
The enantiomeric composition of the pyridinethione was determined by capillary GC,<sup>87</sup> using the optically active stationary phase Chirasil-Val. Unfortunately, the mixture of pyridinethione enantiomers decomposed in the GC injector port, making a



direct analysis impossible. A method involving derivatisation of the pyridinethione was therefore developed. Photolysis of the pyridinethione in benzene yielded, among other products, acetophenone and optically active 1-phenylethanol, products expected from the intermediacy of the 1-phenylethoxy radical. The enantiomeric excess of the 1-phenylethanol is assumed to be identical to that of the pyridinethione since no plausible mechanism can be envisaged for racemisation of the alcohol during its photolytic formation. It is possible that the 1-phenylethanol-1-yl radical may be formed by the abstraction of the benzylic hydrogen atom of 1-phenylethanol by 1-phenylethoxy radical. However, the large steric compression associated with the abstraction of a benzylic hydrogen by a racemised 1-phenylethanol-1-yl radical makes this process unlikely to occur to a significant extent. Unfortunately, a good separation of the enantiomers of racemic 1-phenylethanol could not be achieved on Chirasil-Val. Success was finally encountered by derivatisation of the mixture of alcohol enantiomers to the corresponding isopropyl carbamates, achieved by adapting a literature procedure.<sup>98</sup> Only a few mg of pyridinethione were required for the entire analysis. Figure 5.4 shows the separation of enantiomers achieved by GC.



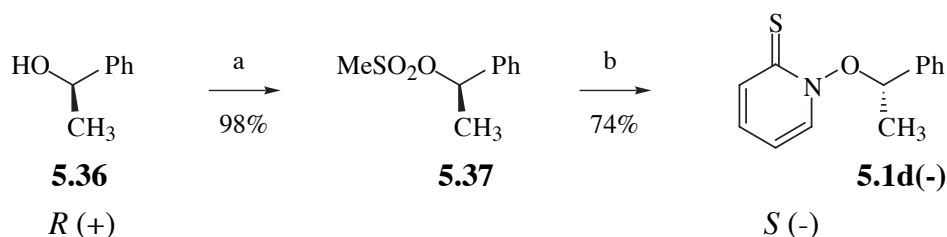
a: hv, benzene; b: isopropyl isocyanate, CH<sub>2</sub>Cl<sub>2</sub>, 100°C, 20 min



**Figure 5.4.** Determination of the enantiomeric composition of *R* (+) *N*-1-phenylethoxy-2(1*H*)-pyridinethione (**5.1d(+)**) by GC, using a ChiralSil-Val capillary column. The upper chromatogram is of the enantiomeric isopropyl urethane derivatives of the 1-phenylethanols obtained by photolytic degradation of pyridinethione **5.1d(+)** and the lower is of the same urethanes obtained from racemic ( $\pm$ ) 1-phenylethanol. The *R* enantiomer has the shorter retention time. An enantiomeric composition of  $85.8 \pm 0.5\%$  *R* (71.7% e.e.) was determined for the pyridinethione.

### (ii) Synthesis of *S* (–)-*N*-(1-Phenylethoxy)-2(1*H*)-pyridinethione, **5.1d(–)**

Preparation of *S* (–)-*N*-(1-phenylethoxy)-2(1*H*)-pyridinethione, **5.1d(–)**, was achieved in two steps from *R* (+)-1-phenylethanol (**5.36**), via the mesylate<sup>99</sup>(**5.37**). This alkylating agent was more stable than the tosylate used in the synthesis of **5.1d(+)**, although the reason is not clear. An optical rotation of  $-1047 \pm 13^\circ$  was measured for pyridinethione **5.1d(–)** and chiral GC analysis yielded an e.e. of the *S* isomer of  $95.3 \pm 0.3\%$ . The specific rotation for the pure *S* isomer is hence  $-1098 \pm 16^\circ$ .

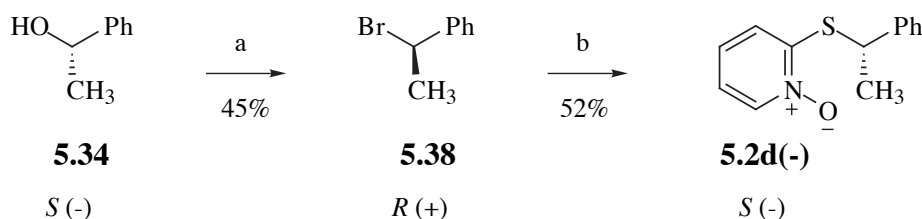


a: MeSO<sub>2</sub>Cl, Et<sub>3</sub>N, CH<sub>2</sub>Cl<sub>2</sub>, 0°C;

b: tetraethylammonium 2(1*H*)-pyridinethione *N*-oxide (**1i**), DMF, 0°C

### (iii) Synthesis of *S* (-) 2(1-Phenethylsulfanyl)pyridine *N*-oxide, **5.2d(-)**

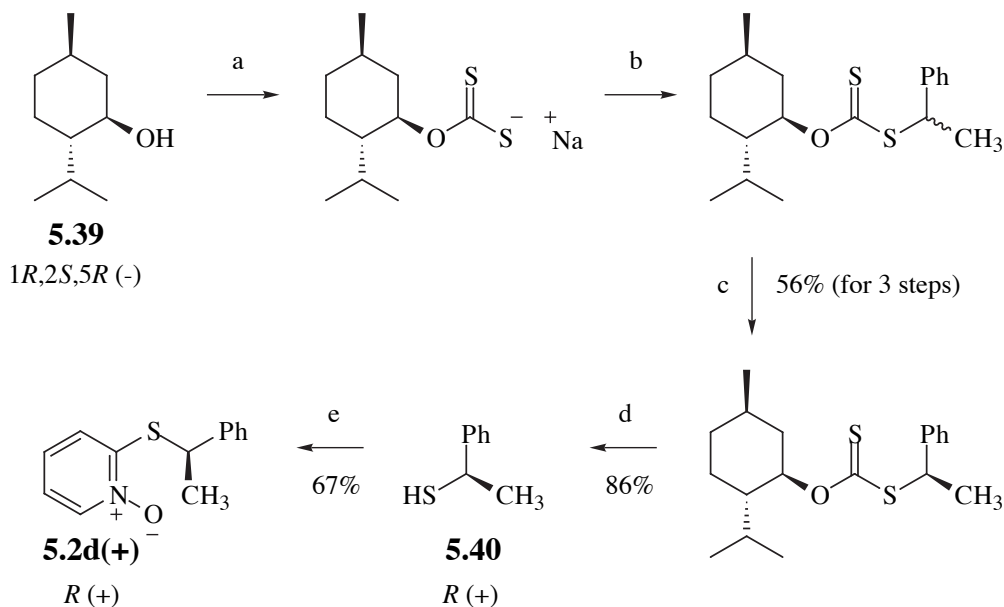
A sample of predominantly *S* (-)-2(1-phenethylsulfanyl)pyridine *N*-oxide, **5.2d(-)**, was obtained in two steps from commercial *S* (-) 1-phenylethanol (**5.34**). Unfortunately, the *R* 1-phenethyl bromide (**5.38**) obtained from **5.34** had an e.e. of only 40.4%, but this bromide is known to be prone to racemisation.<sup>100</sup> Fortunately, the racemate of the product *N*-oxide crystallized from solution in preference to the *S* enantiomer. It was possible to obtain the desired enantioenriched product from the mother liquors with an e.e. of 86.2% ( $[\alpha]_{\text{D}}^{25} = -112^\circ$ ).



a: PBr<sub>3</sub>, pyridine, Et<sub>2</sub>O; b: sodium 2(1*H*)-pyridinethione *N*-oxide, DMF, 80°C

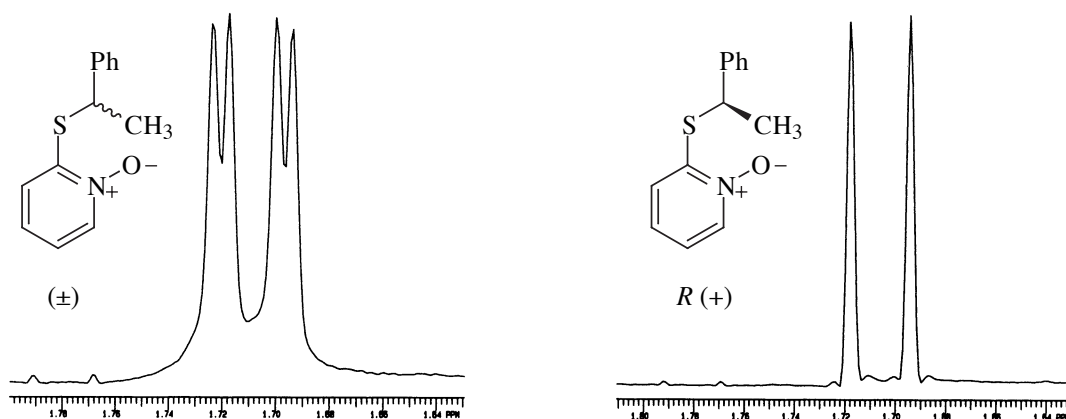
### (iv) Synthesis of *R* (+) 2(1-Phenethylsulfanyl)pyridine *N*-oxide, **5.2d(+)**

The *R* (+) isomer of 2(1-phenethylsulfanyl)pyridine *N*-oxide, **5.2d(+)**, was prepared in five steps from (-) menthol (**5.39**) in very high enantiomeric excess. This synthesis utilises a diastereomeric resolution<sup>101</sup> to provide the optically pure and intensely malodorous thiol (**5.40**), after cleavage from the chiral auxiliary. Subsequent conversion to the *N*-oxide **5.2d(+)** was achieved with chloride ion displacement from 2-chloropyridine *N*-oxide<sup>95</sup> by the thiolate anion of **5.40**. Recrystallisation of the product **5.2d(+)** from benzene/hexane was repeated to constant mp (107.0-107.5°C) and optical rotation (+130±1°).



a: Na in toluene, then CS<sub>2</sub>; b: (±) 1-phenethyl bromide; c: diastereomeric resolution by selective crystallisation from EtOH; d: morpholine, benzene, Δ; e: NaH in THF, then 2-chloropyridine *N*-oxide

The enantiomer ratio of *N*-oxide **5.2d(+)** was determined by nmr,<sup>102</sup> using the lanthanide chiral shift reagent (+) Eu(tfc)<sub>3</sub>. An optimum balance between increasing enantiomer shift difference and attendant line broadening was achieved at 10 mol% shift reagent in CDCl<sub>3</sub>. As figure 5.5 illustrates, none of the *S* isomer could be observed in the product, the estimated limit of detection being 1%. It was concluded that *N*-oxide **5.2d(+)** has an e.e. ≥ 98% and is probably enantiomerically pure.



**Figure 5.5.** Establishment of the enantiomeric purity of *R* (+) 2-(1-phenethylsulfanyl)pyridine *N*-oxide **5.2d(+)**. The partial nmr spectra show the CH<sub>3</sub> resonances for the racemic mixture (left) and *R* (+) isomer (right) respectively. Resolution enhancement of the peaks was achieved with the Varian "Resolv" function. The CH<sub>3</sub> group of the *R* isomer—the only isomer detected in the enantioenriched sample—resonates at higher field.

### 5.3.4.2 Results

The stereochemistry of the rearrangement step of the pyridinethione is expressed in terms of the degree of retention of configuration of the migrating group. Since retention of configuration demands that, for instance, the *S* enantiomer of the pyridinethione rearranges to the *S* isomer of the product *N*-oxide, this relationship is:

$$F_r = \frac{N_s + P_s - 1}{2P_s - 1} \quad (5.5)$$

where  $F_r$  is the fraction of retention of configuration in the rearrangement;  $N_s$  is the fraction of *S* enantiomer in the product *N*-oxide; and  $P_s$  is the fraction of *S* enantiomer in the reactant pyridinethione. In terms of enantiomeric excess, this equation becomes:

$$F_r = \frac{e.e.(N_s) + e.e.(P_s)}{2e.e.(P_s)} \quad (5.6)$$

where the enantiomer excesses of  $N_s$  and  $P_s$  are also expressed as fractions/percentages.

Rearrangement experiments were performed in the absence of light, under vacuum at 80°C in the chosen solvent, with a pyridinethione concentration of 0.22 M. Reaction progress was monitored by <sup>1</sup>H nmr. When complete, the optically active *N*-oxide product was isolated by flash chromatography and purified further by sublimation at 100°C/0.1 mmHg. An optical rotation measurement was then obtained and the enantiomeric composition calculated using the specific rotation for the purely *S* *N*-oxide **5.2d(-)** of  $-130 \pm 1^\circ$ . From this, the degree of retention of configuration ( $F_r$ ) was calculated using equation 5.5. Results are displayed in table 5.5.

Since Jacques, Collet and Wilen have reported<sup>103</sup> the occurrence of enantioselective sublimation of optically active compounds, a strategy was devised to avoid problems should such an effect exist in the present system. A mixture of *R* (+) *N*-oxide **5.2d(+)** (20.820 mg) and racemic *N*-oxide **5.2d(±)** (19.925 mg) was dissolved in chloroform, yielding a specific rotation of  $+64.3 \pm 0.5^\circ$ . After removal of solvent the

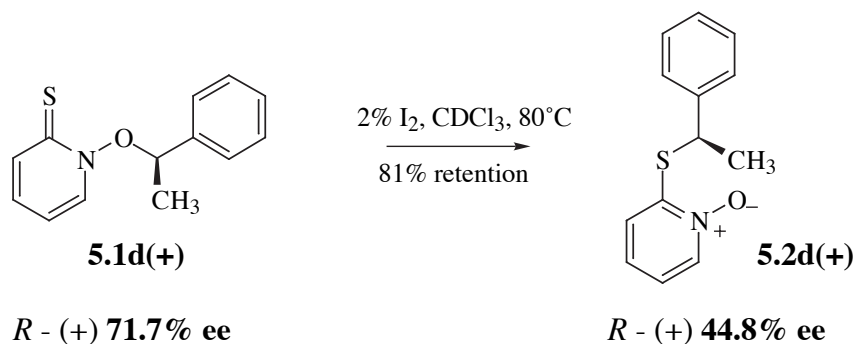
residue was sublimed completely. A homogenised sample of the sublimed *N*-oxide gave a specific rotation of  $+64.1 \pm 0.5^\circ$ . Thus, results will not be skewed by enantioselective sublimation provided the entire sample is sublimed and that the sublimate is homogenised prior to optical rotation measurement.

**Table 5.5.** Stereochemical results from catalysed rearrangements of *S* (–) pyridinethione **5.1d**(–) ( $97.65 \pm 0.16\%$  *S*,  $95.3 \pm 0.3\%$  e.e.)

Catalyst	Catalyst quantity (mole%)	Solvent	Reaction time (hr)	Fraction of <i>S</i> enantiomer in product <b>5.2d</b> (%)	Degree of retention of configuration, $F_r$ (%)
I <sub>2</sub>	5.0	CDCl <sub>3</sub>	4.0	$75.1 \pm 0.5$	$76.3 \pm 0.7$
I <sub>2</sub>	2.00	CDCl <sub>3</sub>	4.0	$79.5 \pm 0.6$	$81.0 \pm 0.7$
I <sub>2</sub>	1.92	CD <sub>3</sub> CN	4.0	$47.9 \pm 0.1$	$47.8 \pm 0.1^a$
I <sub>2</sub>	2.03	CH <sub>3</sub> CN	4.0	$48.1 \pm 0.1$	$48.0 \pm 0.1^a$
O <sub>2</sub>	145 <sup>b</sup>	CDCl <sub>3</sub>	24	$55.3 \pm 0.1$	$55.6 \pm 0.1$
O <sub>2</sub>	unknown	CH <sub>3</sub> CN	24	$31.4 \pm 0.4$	$30.5 \pm 0.5^a$
Fc <sup>+</sup> PF <sub>6</sub> <sup>–</sup>	1.00	CH <sub>3</sub> CN	4.0	$41.3 \pm 0.2$	$40.9 \pm 0.3^a$
Ni (III) SAR	1.00	CH <sub>3</sub> CN	4.0	$37.4 \pm 0.2$	$36.8 \pm 0.3^a$

a: A predominant *inversion* of configuration; b: The proportion of oxygen gas initially present above the degassed solution. Uncertainties represent one standard deviation.

To confirm the result with iodine catalysis in chloroform solution, a rearrangement of the *R* (+) isomer of the pyridinethione was performed. The iodine (2.04 mol%) catalysed rearrangement of the *R* pyridinethione **5.1d**(+) ( $71.7 \pm 1.0\%$  e.e.), at 80°C for 5 hr, produced predominantly *R* (+) 2-(1-phenethylsulfanyl)pyridine *N*-oxide **5.2d**(+) with an enantiomer excess of  $44.8 \pm 1.5\%$ . Using equation 5.6, there has been  $81.3 \pm 1.5\%$  retention of configuration in the migrating group, in excellent agreement with  $F_r = 81.0 \pm 0.7\%$  from the comparable *S* (–) pyridinethione rearrangement.



### 5.3.4.3 Determination of the extent of solution-phase racemisation of the pyridinethione and the *N*-oxide

Experiments were undertaken to establish whether the results in table 5.5 were an accurate representation of the actual stereochemistry of the rearrangement step, or whether racemisation in the reactant and/or product had introduced distortions.

A sample of *S* (–)-pyridinethione **5.1d(–)**, of 95.3%±0.3% e.e., was heated at 80°C with 5.0 mol% iodine in CHCl<sub>3</sub> for 4.0 hr and the unreacted starting material was isolated by flash chromatography. Its enantiomeric composition was established by the GC method described previously, giving 96.7±0.6% e.e., indicating that no racemisation had occurred.

A sample of *N*-oxide **5.2d(+)** of specific rotation +128.7±2°, in CHCl<sub>3</sub> solution (0.22 M) was degassed and heated at 80°C with 2 mol% iodine for 4.0 hr. The recovered *N*-oxide was purified by flash chromatography then sublimed. A specific rotation of +127.8±1° was obtained, again indicating negligible racemisation. The same result was obtained when a chloroform solution of the *N*-oxide, with or without iodine, was heated for the longer time of 16.5 hr. Furthermore, the same *N*-oxide **5.2d(+)** was heated in the more polar solvent acetonitrile for 4 hours at 80°C. A specific rotation of +127.5±1.3° indicated negligible racemisation in this solvent as well.

Pyridinethione **5.1d(–)**, of specific rotation –904±9°, was dissolved in CH<sub>3</sub>CN and heated for 4 hours at 80°C. After purification by column chromatography, the retrieved pyridinethione had a specific rotation of –787±8°, an optical purity reduction of 12.9%. Unfortunately, the e.e. could not be established accurately by chiral GC in this instance and <sup>1</sup>H nmr revealed that the pyridinethione was not chemically pure.

Recrystallisation was avoided as a purification method because it was likely to change the enantiomeric ratio. However, unreacted pyridinethione **5.1d(-)** which was retrieved from an iodine catalysed reaction in deuteriochloroform, showed a 6% reduction in optical purity by optical rotation, but no decrease in e.e. by chiral GC analysis. It is concluded that if the apparent racemisation of **5.1d(-)** in acetonitrile is real, it can only be of the order of a few percent.

In summary, there is no racemisation of either the pyridinethione or the *N*-oxide in chloroform solution. In acetonitrile, there is no racemisation of the *N*-oxide. It is possible that there is a small amount ( $\leq 6\%$ ) of racemisation of the pyridinethione in acetonitrile, but certainly not enough alone to account for the rearrangement stereochemistry results. Therefore, the results in table 5.5 are a reliable representation of the stereochemistry of the rearrangement step.

#### 5.3.4.4 Discussion of results

The most conspicuous result is that the rearrangement proceeds with predominant retention (55-81%) of configuration (cf. 6 electron) in chloroform solution and inversion (52-70%) in acetonitrile (cf. 4 electron). The solvent appears to control the sense of the stereochemical outcome of the rearrangement while the type and amount of catalyst determines the degree of stereoselectivity. Stereoselectivity is increased with smaller proportions of catalyst and also by using catalysts which give rise to smaller rearrangement rate constants. Generally, stereoselectivity is greater in chloroform than in acetonitrile solvent and there is no significant difference in results between reactions performed in deuterated and non-deuterated solvents. Data from the previous kinetic analysis indicates that the rearrangement rate constant increases in polar solvents. Initial indications are that faster rearrangement equates with lower stereoselectivity. Differences in  $F_r$  between catalysts in the same solvent suggest that the catalyst and the substrate remain associated in solution, so that the catalyst may be involved in the alkyl group migration process.

Since the rearrangement in chloroform proceeds with predominant—but not



total—retention of configuration, migration of the 1-phenethyl group in this solvent cannot occur by a single, concerted step. It is possible that, like certain 6 electron 1,4 shifts, a tight radical ion pair is involved. Alternatively, an intermolecular mechanism is possible and is consistent with kinetic results.

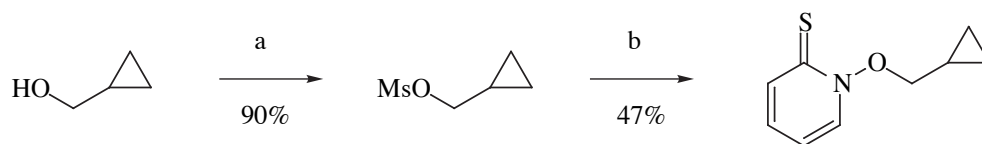
Schollkopf and Hoppe<sup>53</sup> reported  $\geq 80\%$  retention of configuration in the migrating group upon rearrangement of the optically active  $\alpha$ -deutero-2-benzyloxy pyridine *N*-oxide in chloroform at 140°C, although this result has been recently disputed.<sup>119</sup> In DMF solution, however, stereochemistry changes to 75% inversion<sup>118</sup> and in the solid state the rearrangement proceeds with essentially complete inversion of configuration.<sup>119</sup> These interesting results have been rationalised by Wolfe and coworkers,<sup>118,119</sup> who claim that the mechanism consists of a sequence of intermolecular nucleophilic displacement reactions, as evidenced by the positive results from crossover experiments (scheme 5.6). One such displacement will result in inversion of configuration in the migrating group, but two will result in overall retention. It would be desirable to study the stereochemistry of the rearrangement of *N*-alkoxyoxy-2(1*H*)-pyridinethiones in a variety of solvents and at different concentrations.

If an intermolecular mechanism is operating in the rearrangement of **5.1d(+)** and **5.1d(-)**, then a predominance of two inversive displacements must take place in chloroform solution and either one or another odd number of displacements in acetonitrile, to account for the stereochemistry results. Alternatively, an intramolecular 1s,4s sigmatropic migration is favoured in non-polar conditions, but a 1a,4s shift or intermolecular displacement reaction is favoured under polar conditions. Clearly, a crossover experiment is required to establish the molecularity of the rearrangement step.

### 5.3.5 Electronic structure of the migrating group at C1 during rearrangement

Results obtained from the stereochemical experiments indicate that the rearrangement is unlikely to involve a single, concerted step. An experiment was therefore designed to explore the nature of possible intermediates by probing the electronic configuration at C1 of the migrating group over the course of the

rearrangement. A cyclopropylmethyl group was the chosen mechanistic probe for the study, which required the preparation of *N*-cyclopropylmethoxy-2(1*H*)-pyridinethione (**5.1e**). Synthesis of **5.1e** was accomplished in two steps from cyclopropylmethanol.

**5.1e**

a: MeSO<sub>2</sub>Cl, Et<sub>3</sub>N, CH<sub>2</sub>Cl<sub>2</sub>, 0°C;

b: tetraethylammonium 2(1*H*)-pyridinethione *N*-oxide (**1i**), DMF, 0°C

A rate constant for the iodine catalysed isomerization of *N*-benzyloxy-2(1*H*) pyridinethione (**5.1a**) at 80°C in chloroform of  $k_2 = 9.6 \times 10^{-2} \text{ M}^{-1}\text{s}^{-1}$  was obtained from the kinetic study. A 1,4 shift of a cyclopropylmethyl group is known to be considerably slower than that of a benzyl group (see section 5.3.6). However, intramolecular reactions of the cyclopropylmethyl radical and ions are orders of magnitude faster than this. Therefore, if such species occur as intermediates along the reaction coordinate, their involvement should be reflected in the rearrangement products.

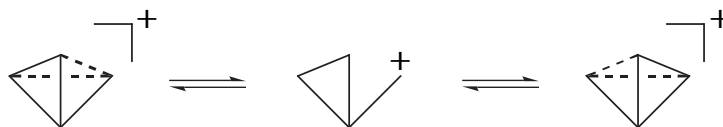
Cyclopropylmethyl radical opens to 3-buten-1-yl radical extremely rapidly, with a rate constant of  $5.2 \times 10^8 \text{ s}^{-1}$  at 80°C in cyclohexane.<sup>105</sup>



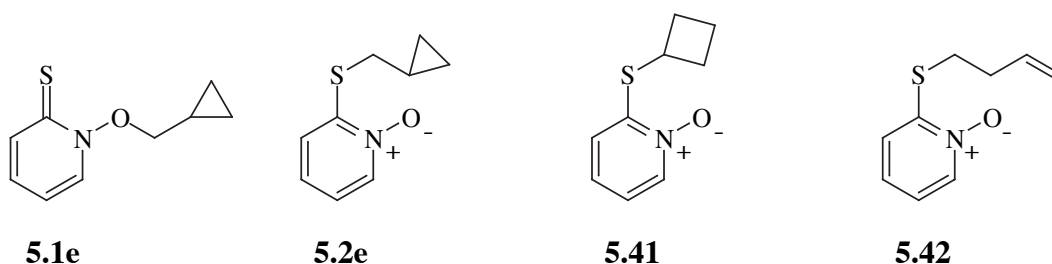
It is well established that cyclopropylmethyl radical and cyclopropyl anion both undergo ring opening to afford only the respective homoallylic radical or anion.<sup>104</sup> However, the reaction of cyclopropylmethyl cation with nucleophiles yields not only the expected cyclopropylmethyl compound, but a homoallylic product resulting from ring opening and a cyclobutyl product resulting from ring expansion.<sup>104</sup> Since oxidants and protic acids catalyse the rearrangement, it is unlikely that cyclopropylmethyl anion would be an intermediate.

Cyclopropylmethyl cation is in a very rapid dynamic equilibrium with bicyclobutonium ion. At 27°C, in the gas phase, the rate constant is in excess of  $10^{10}$

$s^{-1}$ , the equilibrium ratio being close to unity.<sup>106</sup>



Therefore, if the mechanism for the 1,4 catalysed rearrangement of **5.1e** involves the intermediacy of a cyclopropylmethyl radical, the products expected would be **5.2e** and **5.42**, but not **5.41**. If a cyclopropylmethyl cation is involved, all three *N*-oxides should be expected as products. If neither of these intermediates is involved, only product **5.2e** should result.



A 0.28 M solution of **5.1e** with 5.9 mole% iodine in chloroform was degassed, then heated in the dark at 80°C under nitrogen for 5.5 hr. The products detected by  $^1\text{H}$  nmr were 2-(cyclopropylmethylsulfanyl)pyridine *N*-oxide **5.2e** (100), unreacted *N*-cyclopropylmethyl-2(1*H*)-pyridinethione **5.1e** (20) and cyclopropylmethanol (2.7), in the relative molar amounts shown. Cyclopropylmethanol is one of the products expected from radical reactions initiated by thermal homolysis of the N–O bond. Published nmr spectra of cyclobutylthiobenzene<sup>107</sup> and 3-butenylthiobenzene<sup>108</sup> were used to predict the chemical shifts of the hydrogens of the cyclobutyl and 3-butenyl groups of **5.41** and **5.42** respectively. No resonances similar to those from either of these compounds could be detected, hence neither cyclopropyl radical nor cyclopropyl cation appear to be intermediates.

If the detection limit for both **5.41** and **5.42** is taken to be 1% that of **5.2e**, upper limits for the lifetime of cyclopropylmethyl radical and cation intermediates can be

estimated using equation 5.7:

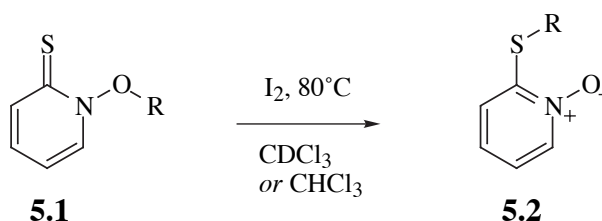
$$t = \frac{\ln\left(\frac{100}{99}\right)}{k} \quad (5.7)$$

where  $t$  is the lifetime of the intermediate in seconds and  $k$  is the rate constant for ring opening at 80°C. Accordingly, for cyclopropylmethyl radical  $t \leq 2 \times 10^{-9}$  s and for cyclopropylmethyl cation  $t \leq 2 \times 10^{-12}$  s, adjusted for the distribution of equally abundant product isomers.

Thus, in chloroform solution, if the cyclopropylmethyl cation is an intermediate, its lifetime is of the order of a molecular rotation. If the migrating group supports a radical centre at C1, the contact pair collapses at or near diffusion controlled rates. It is clear that if cyclopropylmethyl cations or radicals are indeed intermediates, they cannot be diffusively free.

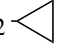
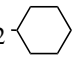
### 5.3.6 Substituent effects

A homologous series of *N*-alkoxy-2(1*H*)-pyridinethiones (**5.1a-g**) was prepared. A semi-quantitative exploration of the relationship between migrating group structure and isomerization rate was undertaken by estimating the proportion of product **5.2** present in each reaction from <sup>1</sup>H nmr peak integrals of identifiable compounds. The rate of rearrangement depends, partly, on the purity of starting pyridinethiones, catalyst and solvent. Some of the pyridinethiones were difficult to purify and/or maintain in a high state of purity. Nevertheless, a reasonable pattern of reactivity could be obtained by these experiments. Initial pyridine thione concentrations were 0.23 M and the results appear in table 5.6.



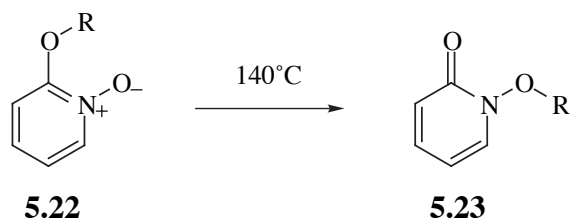
Benzylic and 1-phenylethyl substituents migrate most rapidly. A reasonably rapid reaction was observed in those compounds with a 2-alkenyl substituent (**5.1b,c**) or those where significant conjugation of ring  $\sigma$  bonds with the  $p$  orbital of the terminal carbon occurs, such as with the cyclopropylmethyl group.<sup>109</sup> Such results suggest that migration is facilitated by the capacity of the substituent to stabilise developing positive charge, or a radical, at C1. Aliphatic groups (**5.1f,g**), particularly bulky ones, migrate most slowly. Interestingly, a comparison of results of rearrangements of **5.1b** and **5.1c** indicates a deuterium isotope effect at C1.

**Table 5.6.** Reaction conditions and product yields for iodine catalysed rearrangement of a series of *N*-alkoxy-2(1*H*)-pyridinethiones **5.1a-g** in chloroform or deuteriochloroform solution at 80°C

Pyridinethione number	Substituent R	Mole fraction I <sub>2</sub> (%)	Reaction time (hr)	Yield of <i>N</i> -oxide <b>5.2a-g</b> (%)
<b>5.1a</b>	CH <sub>2</sub> Ph	0.5	4.0	91-95
<b>5.1d</b>	CH(CH <sub>3</sub> )Ph	0.5	4.7	96
<b>5.1b</b>	CH <sub>2</sub> CH=CH <sub>2</sub>	0.5	4.0	80
<b>5.1c</b>	CD <sub>2</sub> CH=CH <sub>2</sub>	1.0	4.0	50
<b>5.1e</b>	CH <sub>2</sub> 	6.3	3.5	70
<b>5.1f</b>	CH <sub>2</sub> CH <sub>2</sub> CH <sub>3</sub>	0.5	4.0	0.5
<b>5.1f</b>	CH <sub>2</sub> CH <sub>2</sub> CH <sub>3</sub>	5.0	4.0	9
<b>5.1g</b>	CH <sub>2</sub> 	5.0	4.0	2

The general trend is comparable with that reported by Ollis<sup>78</sup> (table 5.7) who observed that the degree of unsaturation in the migrating group drastically increases ease of migration in the isomerization of 2-alkoxy pyridine *N*-oxides (**5.22**) to *N*-alkoxy-2-pyridones (**5.23**). A study<sup>53</sup> of benzyl group migration in the **5.22**→**5.23**

rearrangement yielded a Hammett  $\rho$  value of  $-0.26$ , indicating that stabilisation of positive charge at the migrating group terminus significantly accelerates migration.



**Table 5.7.** Relative rate constants for a series of migrating groups in the 2-alkoxy-2(1H)-pyridinethione *N*-oxide rearrangement (**5.22**→**5.23**), from reference 78

Substituent R	Relative rate constant
CH <sub>2</sub> CH <sub>3</sub>	1
CH <sub>2</sub> CH=CH <sub>2</sub>	23.5
CH <sub>2</sub> -	2294

In summary, initial investigations suggest that substituents capable of delocalising charge, or stabilising a radical centre, at C1 of the migrating group accelerate the catalysed rearrangement of *N*-alkoxy-2(1H)-pyridinethiones. It is not yet clear how charge, or radical, stabilisation of the migrating group facilitates migration.

### 5.3.7 Attempted detection and isolation of intermediates

#### 5.3.7.1 Addition of a radical scavenger

In an attempt to test for the presence of radical intermediates, 3 mol% of the radical scavenger 1,4-benzoquinone was added to a solution of 0.23 M *N*-benzyloxy-2(1H)-pyridinethione (**5.1a**) in CDCl<sub>3</sub>, containing 0.5 mol% iodine. After heating in the dark for 2 hours, the yield of the rearrangement product **5.2a** was 72%, whereas in the same reaction without 1,4-benzoquinone the yield was 75%.



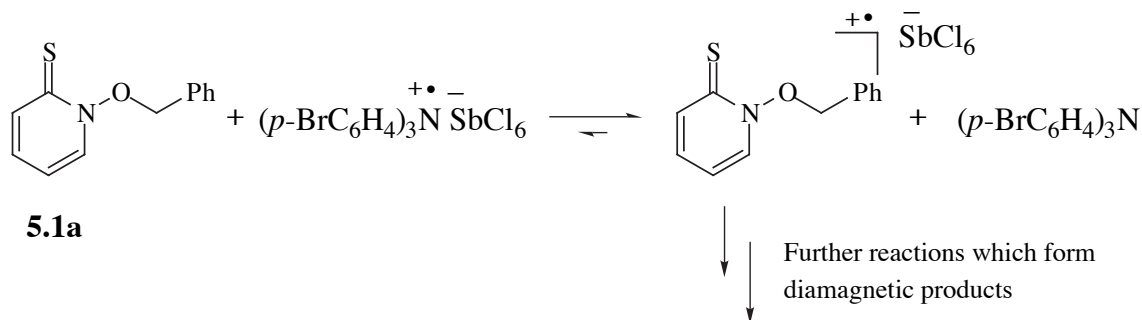
Scavenging of radicals by 1,4-benzoquinone

Since the radical scavenger caused no significant retardation of the rearrangement, it can be concluded that carbon-centred free radicals either do not appear to be intermediates in the rearrangement process or they escape detection owing to a short lifetime. It is possible that other types of radicals—thiyl radicals ( $RS\bullet$ ) for instance—may be intermediates. An S–O bond in the expected  $(RS)_2$ -benzoquinone adduct is likely to be very weak, so the trapping process would be expected to be reversible. The negative result from the scavenger addition is also consistent with a rearrangement mechanism which involves the formation of a charge transfer complex in which the catalyst and pyridinethione moieties remain in association.

### 5.3.7.2 Esr spectroscopy

Electron spin resonance spectroscopy was used in an attempt to directly observe radical intermediates. Signals due to radicals could not be detected when a dichloromethane solution of *N*-benzyloxy-2(1*H*)-pyridinethione (**5.1a**) was treated with any one of the reagents iodine, ferrocenium hexafluorophosphate, triflic acid or tris(4-bromophenyl)aminium hexachloroantimonate (**5.33**), within a temperature range 77 to 298 K, across a spectral width of 100 gauss.

A blue dichloromethane solution of the stable free radical aminium salt **5.33** gave a strong, broad signal of a poorly resolved triplet, as expected. This signal was immediately quenched upon addition of a dichloromethane solution of pyridinethione **5.1a**, simultaneous with the loss of blue colour from the solution and formation of a flocculent precipitate. No other ESR signal could be detected.



**Scheme 5.10.** Proposed initial redox reaction between free radical aminium salt **5.33** and pyridinethione **5.1a**

It is concluded that the rapid initial reaction observed is most likely a redox reaction between the aminium salt and the pyridinethione, as illustrated in scheme 5.10. Further reactions form diamagnetic products, some of which are insoluble. Diamagnetic products may result from processes such as dimerisation of the incipient pyridinethione radical cation or by its further oxidation. Attempts have been made to identify the products (see section 5.3.7.4).

### 5.3.7.3 Cyclic voltammetry

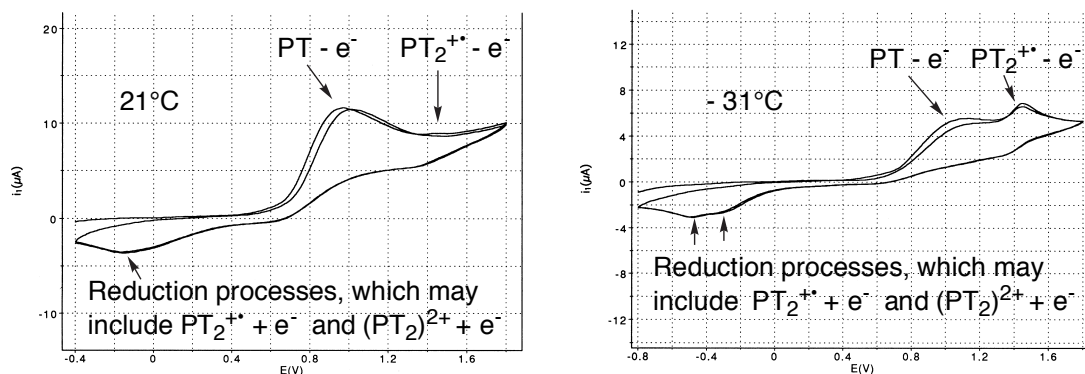
An exploration was undertaken into the electrochemistry of *N*-benzyloxy-2(1*H*)-pyridinethione (**5.1a**, denoted as PT in figure 5.6) and its rearrangement product, 2-benzylsulfanylpiperidine *N*-oxide (**5.2a**), using cyclic voltammetry. Analyte concentrations of 5.5 mM in acetonitrile were used, employing 0.1M Bu<sub>4</sub>NBF<sub>4</sub> as the electrolyte. Potentials were measured relative to the Ag/AgCl half cell. The electrochemistry of these two compounds, particularly of **5.1a**, is not simple.

At a scanning rate of 100 mVs<sup>-1</sup>, a voltammogram of *N*-oxide **5.2a** displayed a single, chemically irreversible oxidation wave at +1.7 V at room temperature, with no reduction process being detected. However, at -30°C the oxidation wave at +1.65 V gave rise to a reduction wave at -0.3 V. It is possible that the oxidation process at +1.65 V results in the formation of a new species, *via* homogeneous chemical reaction of the oxidised compound, which can be reduced at -0.3 V. Furthermore, the secondary compound that forms as a result of the electrochemical oxidation is likely to be unstable, and so can only be detected on the reverse scan at -0.3 V when the temperature is lowered to -30°C.

At room temperature, the pyridinethione **5.1a** shows an irreversible (rate of electron transfer is less than rate of diffusion away from the electrode) oxidation wave at +0.9 V and a reduction wave at -0.15 V. The reduction process at -0.15 V is only evident when the scan is extended past 1.0 V in the positive direction, hence it is likely to be associated with a product of the oxidation process. At -31°C, two oxidation waves are detected, at +0.9 and +1.4 V, both appearing irreversible, and two reduction waves at



–0.2 V and –0.45 V. At lower temperatures the species present at +1.4 V is an unstable product of the oxidation of the starting material. At higher temperatures it is not as easily detected, possibly because of its decomposition or high reactivity. Tentative assignment of the waves is given on the voltammograms displayed in figure 5.6.

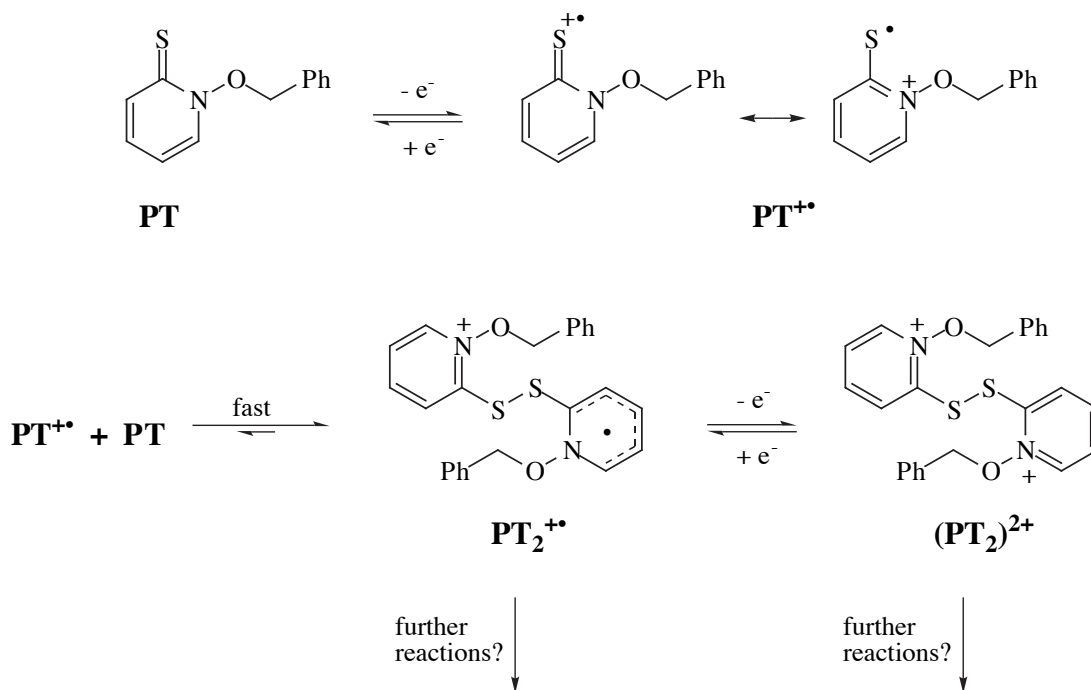


**Figure 5.6.** Cyclic voltammograms of *N*-benzyloxy-2(1*H*)-pyridinethione (PT) in acetonitrile at room temperature (left) and at –31°C (right), both recorded at a scan rate of 100 mVs<sup>-1</sup>

This type of irreversibility behaviour, in which oxidation and reduction waves are several hundred millivolts apart, is similar to the reversible dimerisation of diphenylpolyene radical cations.<sup>110</sup> Phenylthiyl radical (PhS•) is known to add rapidly to alkenes.<sup>111</sup> For instance, the rate constant<sup>112</sup> for the reaction of PhS• with butadiene at room temperature is  $3.5 \times 10^7 \text{ M}^{-1}\text{s}^{-1}$ . More specifically, it is known that 2-pyridylthiyl radical (**5.8**) adds to the S=C group of Barton esters (**5.4**) at an almost diffusion controlled rate.<sup>46</sup> Therefore, it is reasonable to assume that the addition of a pyridinethione radical cation (PT<sup>+•</sup>) to a pyridinethione molecule (PT), forming a kind of dimer (PT<sub>2</sub><sup>+•</sup>), is not only a favoured process, but would be moderately fast. Scheme 5.11 illustrates some proposed chemical reactions which can account for the observed electrochemistry.

An argument against attack of PT<sup>+•</sup> at the sulfur of another PT molecule is that this process might be expected to generate benzyloxy radicals, in a manner similar to step 4 in scheme 5.7. Redmond and coworkers have shown that 2-pyridylthiyl radical (**5.8**) can

displace  $\text{RCOO}\cdot$  radicals by its reaction with Barton esters,<sup>46</sup> although the rate of N–O bond homolysis in a structure like  $\text{PT}_2^{+\bullet}$  is difficult to estimate.



**Scheme 5.11.** Possible reactions which account for the results from cyclic voltammetry

Cyclic voltammetric results for the pyridinethione are consistent with a fast reaction that takes place between an incipient pyridinethione radical cation,  $\text{PT}^{+\bullet}$ , and another molecule of the pyridinethione,  $\text{PT}$ . The first oxidation wave corresponds to the unstable species  $\text{PT}^{+\bullet}$ , which quickly reacts with a molecule of  $\text{PT}$  to form  $\text{PT}_2^{+\bullet}$ . This rationalises the low current on the return (reduction) wave. Removal of a second electron from  $\text{PT}_2^{+\bullet}$  results in a doubly aromatised dication,  $(\text{PT}_2)^{2+}$ , a process corresponding to the second oxidation wave. Voltammetric data indicate that  $(\text{PT}_2)^{2+}$ , if this is the true structure, is unstable at room temperature and has a half life significantly less than 1 second. It may be a species of this type in which benzyl group migration takes place. There is support from mass spectrometry for dimerisation processes in solution (section 5.3.7.4). Structures  $\text{PT}_2^{+\bullet}$  and  $(\text{PT}_2)^{2+}$  have one and two aromatised heterocyclic rings respectively, in which the nitrogen atom bears a positive charge. Such aromatisation makes the 2-sulfanylpiperidine *N*-oxide moiety a better leaving group. Processes which

cause N to become positively charged may be responsible for promoting NO–R bond scission.

Cyclic voltammetry can achieve potentials exceeding those encountered in solution phase chemical reactions. Therefore, it is possible that some processes may occur during cyclic voltammetry which do not during the catalysed rearrangement of the pyridinethione.

#### 5.3.7.4 Isolation and attempted identification of intermediates

Addition of yellow *N*-benzyloxy-2(1*H*)-pyridinethione (**5.1a**) to a deep blue CH<sub>2</sub>Cl<sub>2</sub> solution of the aminium salt tris(4-bromophenyl)aminium hexachloroantimonate (**33**) results in an instantaneous loss of the blue colour with a simultaneous formation of a precipitate. An attempt was made to isolate and identify the products of this reaction.

A stirred solution of aminium salt **5.33** in dichloromethane was treated with portions of solid **5.1a** until the blue colour had just disappeared and a yellow/brown solution with a similarly coloured, flocculent precipitate resulted. This required 1.29 molar equivalents of the pyridinethione. TLC analysis at this point indicated that neither pyridinethione **5.1a** nor product *N*-oxide **5.2a** was present in solution. Centrifugation was used to settle the solid. The liquid phase was drawn off, evaporated and its constituents separated by flash chromatography. The major component from the *solution* was tris(4-bromophenyl)amine, (*p*-BrC<sub>6</sub>H<sub>4</sub>)<sub>3</sub>N (87% yield), identified by comparison of <sup>1</sup>H and <sup>13</sup>C nmr spectra with that of the authentic compound. The total mass recovery from the reaction was 96%.

Elemental analysis of the precipitate gave the results listed in table 5.8. At the limits of a conservative tolerance of 0.3% for each element, these results are consistent with the molecular formula C<sub>12</sub>H<sub>11</sub>NOSSbCl<sub>6</sub>. Such a formula indicates a molar ratio of (pyridinethione **5.1a**)<sup>+</sup>• to SbCl<sub>6</sub><sup>−</sup> of 1:1. Thus, this compound is tentatively identified as the hexachloroantimonate salt of the radical cation of *N*-benzyloxy-2(1*H*)-pyridinethione **5.1a**. Assuming that this molecular formula is correct, this compound was isolated in 92% yield.

**Table 5.8.** Elemental analysis results for the crude precipitate obtained from centrifugation of the reaction mixture

Element	Mass % calculated	Mass % found
C	26.12	27.34
H	2.01	1.70
N	2.54	2.97
Sb	22.07	22.79

This microcrystalline precipitate is sparingly soluble in methanol and acetonitrile, but insoluble in water, and most organic solvents. A  $^1\text{H}$  nmr spectrum of the sparingly soluble solid was obtained, in  $\text{CD}_3\text{CN}$  solution. The solute was very dilute, so the spectrum may represent/include by-products or impurities from the reaction. There were singlets at 4.68 (1), 5.45 (0.72), 5.70 (2) and 5.74 (1) ppm, with integral ratios shown. Multiplets ranging from 6.97 to 9.12 ppm constituted the rest of the spectrum, indicating mainly aromatic hydrogens. None of the resonances corresponded to either the pyridinethione **5.1a** or its *N*-oxide rearrangement product **5.2a** but at least two compounds appear to be present. Spectral lines are relatively sharp indicating that the material is diamagnetic in solution. There are no other peaks within the spectral range of  $-130$  to  $+130$  ppm.

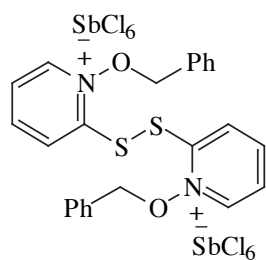
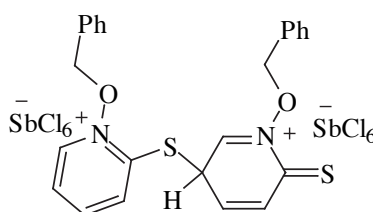
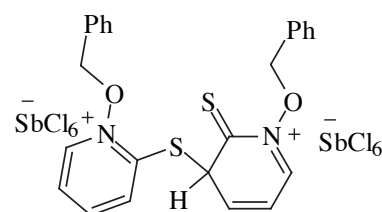
In  $\text{CD}_3\text{OD}$  solvent, a less complex nmr spectrum was obtained. It consisted of the following resonances: 4.63 (s, 2H), 5.82 (s, 2H), 7.30-7.45 (m, 4H), 7.50-7.60 (m, 7H), 7.66 (d, 2H), 8.02 (dt, 1H), 8.28 (d, 1H), 8.43 (t, 1H), 8.48 (d, 1H) and 9.49 (d, 1H). The number of hydrogens totals 22—twice the number present in the parent pyridinethione. For this reason—and the fact that there are two methylene resonances and several one hydrogen resonances—this compound cannot be a symmetric dimer. The chemical shift of the one hydrogen doublet at  $\delta$  9.49 is indicative of a proton adjacent to a positively charged nitrogen of a pyridine ring.

EIMS did not yield a useful mass spectrum and +FAB (glycerol/thioglycerol matrix) mass spectrometry exhibited a peak at  $m/z$  217.9, corresponding to the protonated

pyridinethione **5.1a**, although little else was informative. Electrospray mass spectrometry, utilising a milder ionisation method, gave a more useful spectrum. With acetonitrile as solvent, the following mass spectrum was obtained:  $m/z$  (%): 343 (100), 308 (3), 253 (43), 233 (70), 218 (6), 186 (7), 142 (8), 132 (9). None of the peaks contains the  $\text{SbCl}_6^-$  group. The base peak at 343 has the same  $m/z$  value expected for a pyridinethione dimer (434) minus a benzyl group (91). The peak group at 308 has the same  $m/z$  value expected for a pyridinethione (217) plus a benzyl cation (91). A protonated pyridinethione dimer minus two benzyl groups could account for the peak at  $m/z$  253. An asymmetric dimerisation reaction is consistent with the diamagnetism of this compound observed by nmr.

The solid isolated was tested for catalytic activity. To each of 0.23 M solutions of *N*-benzyloxy-2(1*H*)-pyridinethione (**5.1a**) in  $\text{CDCl}_3$  and in  $\text{CD}_3\text{CN}$ , was added 2.5 mol% (assumed  $MW$  1103.5  $\text{g mol}^{-1}$ ) of the solid product of unknown structure. These mixtures were degassed, sealed and heated under minimal lighting at  $80^\circ\text{C}$  for 5 hr. Ratios of *N*-oxide **5.2a** to pyridinethione **5.1a** were 0.67:1 in  $\text{CDCl}_3$  and 7.1:1 in  $\text{CD}_3\text{CN}$ , indicating that the isolated compound acts as a catalyst.

From the weight of the evidence, it is proposed that the formula of this solid is  $\text{C}_{24}\text{H}_{22}\text{Cl}_{12}\text{N}_2\text{O}_2\text{S}_2\text{Sb}_2$ ,  $MW$  1103.52  $\text{g mol}^{-1}$ . Compounds **5.44** and **5.45** are put forward as possible structures. Compound **5.43**, although expected to form easily, cannot be correct since nmr spectra indicate that the compound isolated has lower symmetry. The solid product may also be a mixture of two or more compounds. Further structural elucidation work is required.

**5.43****5.44****5.45**

## 5.4 Conclusions

The mechanism of the catalysed rearrangement of *N*-alkoxy-2(1*H*)-pyridinethiones (**5.1**) to corresponding 2-alkylsulfanylpyridine *N*-oxides (**5.2**) is more complex than initially envisaged. In particular, evidence for the participation of intermolecular reactions lessens the probability that this migration may belong to a new class of intramolecular rearrangement in which 5 electrons are delocalised over 5 atoms. However, since a crossover experiment has not been undertaken to establish the molecularity of the migration step, an intramolecular shift of the alkyl group cannot yet be excluded.

Evidence from cyclic voltammetry and catalysis experiments is consistent with an incipient pyridinethione radical cation being formed by the one electron oxidation of the pyridinethione molecule. Owing to a similarity in reactivity, the mechanisms of rearrangement with protic acid and with oxidative catalysis appear to be closely related—perhaps having several identical or analogous steps. Results from studies of stereochemistry, esr spectroscopy, radical scavenger addition and isolation of intermediates suggest that if a one electron oxidation does occur, the oxidised pyridinethione and the reduced catalyst remain associated in solution.

Kinetic studies show that the rearrangement is first order in the concentration of pyridinethione and catalytic in iodine. The similarity in rate constants between oxidant catalysts is consistent with an identical catalysis mechanism. Initial reaction between the pyridinethione and catalyst is fast and for iodine has a large equilibrium constant. Polar solvents accelerate the reaction, indicating significant charge development in the rate limiting step. Kinetic results are consistent with an intermolecular rate limiting step.

High regioselectivity was observed in the apparent 1,4 migration of the allyl group with both iodine and triflic acid catalysis, suggesting highly ordered mechanisms for the transfer of the migrating group for both types of catalyst.

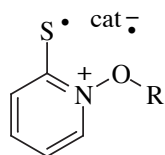
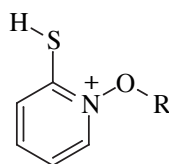
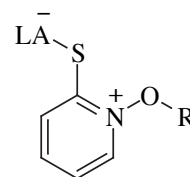
Results from the stereochemical study are difficult to interpret at this stage. The migration of an optically active 1-phenethyl group proceeds with about 80% retention of configuration in chloroform and up to 70% inversion of configuration in acetonitrile. A

sequence of intermolecular displacement reactions could account for the observed results. It is clear that the rearrangement mechanism does not involve one, concerted step.

From a study of the migration of a cyclopropylmethyl group, diffusively free radical or cationic cyclopropyl intermediates are not involved. Semi-quantitative rate data for the migration of different alkyl groups indicates that groups which can stabilise a positive charge through delocalisation migrate more quickly, consistent with a polarized transition state for the rate limiting step.

Evidence from cyclic voltammetry and from analyses of isolated intermediates indicates that the intermediate produced by reaction of the pyridinethione with the catalyst may dimerise or react through other intermolecular paths with additional pyridinethione molecules to form non-radical products. Aromatisation of the 2-sulfanylpiperidine ring—which places a positive charge on the ring N atom—appears to activate the scission of the NO–R bond.

The rearrangement of *N*-alkoxy-2(1*H*)-pyridinethiones (**5.1**) to corresponding 2-alkylsulfanylpiperidine *N*-oxides (**5.2**) is a process catalysed by oxidants, protic acids and Lewis acids, which involves a fast activation step. Initial activated intermediates probably take the form of **5.46** for oxidant, **5.47** for protic acid and **5.48** for Lewis acid (LA) catalysis. Each of these structures is one in which aromaticity exists. It is probably this aromaticity which weakens the O–R bond. A polarized rate limiting step exists, but it is not yet known whether this step is intra- or intermolecular in nature. A correlation between the rearrangement rate constant and the degree of retention of configuration upon migration of the 1-phenylethyl group suggests that the migrating group shift step is rate limiting.

**5.46****5.47****5.48**

### 5.5 Future work

First and foremost, a crossover experiment must be designed and executed to determine whether the net transfer of the migrating group takes place intramolecularly or intermolecularly. Crossover experiments should be performed with different catalysts to establish whether the molecularity of the rearrangement step is dependent on the mode of catalysis and also in solvents of different polarity to explore whether there is a correlation with results from the stereochemistry study. Secondly, more work should be put into the elucidation of the structure of isolable intermediates. Also of interest would be a Hammett study of benzyl group migration to examine the importance of charge development at C1 of the migrating group. An identification of the products from a bulk electrolysis (oxidation) of the pyridinethione would be illuminating since the results would reveal not only whether the product *N*-oxide is actually produced by this process, but how many moles of electrons must be removed per mole of pyridinethione in order for reaction to occur. A kinetic study of the triflic acid catalysis of the rearrangement of **5.1a** would provide valuable information about the similarities between acid and oxidative catalysis. A more detailed study of the effect of both solvent, catalyst and concentration upon rearrangement stereochemistry is also desirable.

In addition, testing the rearrangement of *N*-allyloxycarbonyloxy pyridine-2-thiones (**5.20**) to 2-allylsulfanylpyridine *N*-oxides (**5.21**) for crossover behaviour will establish whether rearrangement in this system is intramolecular, as early researchers assumed it was.



## 5.6 Experimental

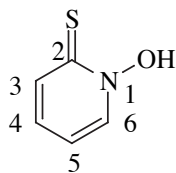
### Ferrocenium hexafluorophosphate, $\text{FcPF}_6$ [11077-24-0]

A sample of ferrocenium hexafluorophosphate was obtained by the method of Duggan and Hendrickson.<sup>96</sup> Ferrocene (1.00g, 5.38 mmol) was dissolved in 4 mL of conc.  $\text{H}_2\text{SO}_4$ , then diluted to 50 mL with water. After removing any undissolved particles by filtration, the resulting blue solution was mixed with a solution of ammonium hexafluorophosphate (0.8794 g, 5.40 mmol) in 30 mL of water. Immediately a precipitate was formed which was filtered off, washed with water and dried under high vacuum. The blue microcrystalline product (1.12 g, 3.38 mmol, 63%) had a mp > 315°C.

Found: C, 34.38; H, 2.73; N, 0.00%.  $\text{C}_{10}\text{H}_{10}\text{F}_6\text{FeP}$  requires: C, 36.29; H, 3.05; N, 0.00%.

EIMS: 186 (100)  $\text{Fc}^+$ , 129 (12), 121 (58), 107 (54), 95 (8), 88 (9), 56 (42).

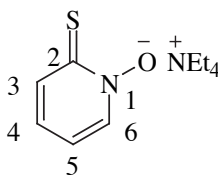
### *N*-Hydroxy-2(1*H*)-pyridinethione [1121-30-8]



**5.1h**

This compound was prepared on 0.5 mol scale, by a established method,<sup>120</sup> consisting of the treatment of a cold 40% aqueous solution of sodium 2(1*H*)-pyridinethione *N*-oxide (Harcros Chemicals) with one equivalent of concentrated HCl, then recrystallisation of the resulting precipitate from ethanol. A yield of 80% (lit.<sup>120</sup> 95%) was obtained, mp in a vacuum-sealed capillary 76-79°C (Aldrich, 69-72°C). A  $^1\text{H}$  nmr spectrum matched the published one. The product was stored at -18°C in the absence of light.

### Tetraethylammonium 2(1*H*)-pyridinethione *N*-oxide [22574-14-7]



**5.1i**

*N*-Hydroxy-2(1*H*)-pyridinethione (**5.1h**) was treated with one equivalent of 20% aqueous tetraethylammonium hydroxide and the water was evaporated under reduced

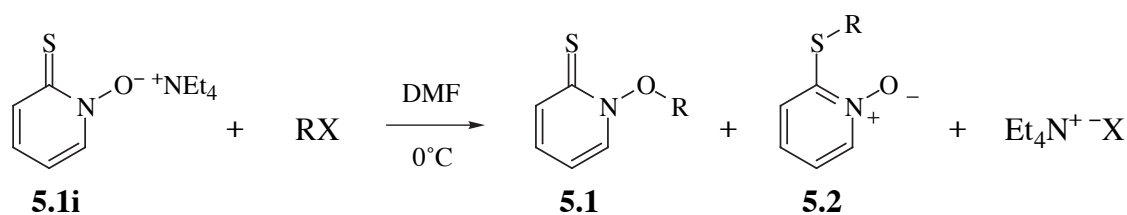
pressure as previously described.<sup>7</sup> On a scale of 230 mmol, the yield was 100%, mp in a vacuum-sealed capillary 158-163°C (lit.<sup>7</sup> 94%, 161-163°C). The product was stored at -18°C in the absence of light.

<sup>1</sup>H nmr (200 MHz): 1.24 (t, 12H, CH<sub>3</sub> × 4), 3.30 (q, 8H, CH<sub>2</sub> × 4), 6.49 (ddd, 1H, H5\*), 6.70 (ddd, 1H, H4\*) 7.53 (dd, 1H, H3), 7.99 (dd, 1H, H6).

### Synthesis of alkyl mesylates

Alkyl mesylates were prepared according to the method of Crossland and Servis<sup>99</sup> by cooling to 0°C a CH<sub>2</sub>Cl<sub>2</sub> solution of an alcohol (0.2 M) and treating with 1.5 molar equivalents of triethylamine and 1.1 equivalents of methane sulfonyl chloride. Yields of mesylates of good purity were usually above 90%. Due to their high reactivity, the mesylates were stored at -18°C and used within a short time of preparation.

### General procedure for the preparation of *N*-Alkoxy-2(1*H*)-pyridinethiones (5.1) and 2-(alkylsulfanyl)pyridine *N*-oxides (5.2)



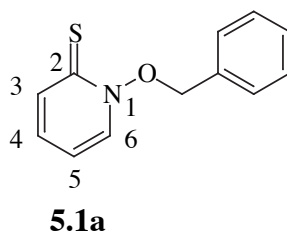
*N*-alkoxy-2(1*H*)-pyridinethiones (**5.1**) were prepared with minor alterations to an established method.<sup>7</sup> The following procedure was carried out under minimal lighting due to photolability of the products. A flame-dried, round-bottomed flask equipped with a stirrer bar was charged with tetraethylammonium 2(1*H*)-pyridinethione *N*-oxide (**5.1i**) and 25 mL of dry DMF per gram of **5.1i**. After placing the contents under a nitrogen atmosphere, the solution was cooled to 0°C and one molar equivalent of the alkylating agent was added over 15 minutes, sometimes in DMF if the alkylating agent viscosity was problematic. Occasionally the temperature was raised to *ca.* 25°C to drive the reaction to completion in reasonable time.

After approximately 1 hour, the solvent was removed under reduced pressure (0.001 mmHg, 40°C) and the residue was treated with 10 mL of 0.1 M aqueous NaOH and 15 mL of diethyl ether per gram of **5.1i** used. Any insoluble matter was removed by filtration as the two-phase mixture was transferred to a separatory funnel. The aqueous phase was repeatedly extracted until no further yellow colour was observed in the ether layer. The combined extracts were washed successively with saturated aqueous solutions of NaHCO<sub>3</sub> and NaCl. After drying (MgSO<sub>4</sub>), the ether was evaporated to give the crude product, which was purified by flash chromatography, yielding the pure product upon

drying (0.001 mmHg, 20°C, 24 hr).

Due to the ambident nucleophilicity of the 2(1*H*)-pyridinethione *N*-oxide anion,<sup>7</sup> a considerable proportion of the corresponding 2-(alkylsulfanyl)pyridine *N*-oxide (**5.2**) was formed as a by-product during the synthesis of **5.1**. The *N*-oxide was sometimes isolated and characterised, making its independent synthesis unnecessary. Following extraction with diethyl ether, the alkaline aqueous phase was extracted further with 10 mL of chloroform per gram of **5.1i**. After washing the organic phase with water and drying over MgSO<sub>4</sub>, the solvent was evaporated to yield the crude *N*-oxide (**2**) which was recrystallized from benzene/hexane.

### *N*-Benzyloxy-2(1*H*)-pyridinethione [122333-43-1]



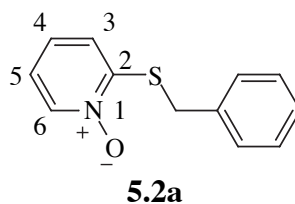
The reaction of benzyl mesylate (8.58 g, 46.1 mmol), and tetraethylammonium 2(1*H*)-pyridinethione *N*-oxide **5.1i** (11.81 g, 46.1 mmol), in 85 mL of DMF at 0°C for 1 hr afforded **5.1a** (2.20 g, 10.1 mmol, 22%), after flash chromatography (thrice) with ether as the eluent. The mp of the yellow needles, obtained by recrystallisation from EtOH/water was 89-90°C (lit.<sup>7</sup> 74-77°C).

<sup>1</sup>H nmr: 5.50 (s, 2H, CH<sub>2</sub>), 6.43 (ddd, 1H, H5), 7.12 (ddd, 1H, H4), 7.39 (m, 4H, H6 & *m+p*-Ar), 7.48 (m, 2H, *o*-Ar), 7.68 (dd, 1H, H3). Matched that reported.<sup>7</sup>

<sup>13</sup>C nmr: 77.1 (CH<sub>2</sub>), 112.5 (5), 128.6 (*m*-Ar × 2\*), 129.4 (*p*-Ar), 130.0 (*o*-Ar × 2\*), 132.8 (*i*-Ar), 132.9 (4), 137.6 (3<sup>†</sup>), 138.6 (6<sup>†</sup>), 175.3 (C=S).

ir (CCl<sub>4</sub>): 3070 w, 3037 w, 2938 w, 1610 m, 1528 s, 1447 s, 1409 s, 1278 m, 1175 m, 1130 s, 700 m.

### 2-(Benzylsulfanyl)pyridine *N*-oxide [3915-60-4]



Sodium hydride (0.185 g, 7.72 mmol) in 13 mL of dry THF under nitrogen was treated with 906 μL of benzylthiol (7.72 mmol) dropwise over 15 min. The resulting suspension was treated with 2-chloropyridine *N*-oxide<sup>95</sup> (1.00 g, 7.72 mmol) in 2.5 mL

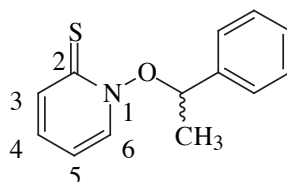
of dry THF. After heating at reflux for 10 minutes, the brown suspension was cooled, treated with 15 mL of 1M NaOH and extracted with 50 mL of chloroform. The organic phase was washed with 10 mL of water and dried over Na<sub>2</sub>SO<sub>4</sub>. Removal of solvent yielded the crude product (1.51 g, 90%). Recrystallisation from benzene afforded pure **5.2a** (0.90 g, 54%) as white needles.

<sup>1</sup>H nmr: 4.17 (s, 2H, CH<sub>2</sub>), 7.04 (ddd, 1H, H5), 7.16 (m, 2H, H3+H4), 7.35 (m, 3H, *m+p*-Ar), 7.45 (dd, 2H, *o*-Ar), 8.26 (dd, 1H, H6). Matched that reported.<sup>7</sup>

<sup>13</sup>C nmr: 35.0 (CH<sub>2</sub>), 120.7 (5), 122.0 (3), 125.9 (4), 127.9 (*p*-Ar), 128.87 (*m*-Ar\*), 128.92 (*o*-Ar\*), 134.9 (*i*-Ar), 138.8 (6), 152.2 (2).

ftir (KBr): 3066 m, 1645 w, 1590 w, 1473 s, 1455 m, 1443 m, 1426 s, 1278 m, 1249 s, 1221 s, 1152 s, 1090 s, 747 s, 716 s, 705 s, 691 s

### (±)-*N*-(1-Phenylethoxy)-2(1*H*)-pyridinethione [182194-97-4]



**5.1d**

(±)-1-Phenylethyl mesylate was prepared from (±)-1-phenethyl alcohol and mesyl chloride/Et<sub>3</sub>N in CH<sub>2</sub>Cl<sub>2</sub>, as previously reported,<sup>99</sup> in a yield of 94%. The mesylate has been described as "a highly reactive liquid which decomposes violently at room temperature".<sup>99</sup> Violent decomposition was not encountered, although the oil was used immediately due to its lability.

The reaction of **5.1i** (1.00 g, 3.90 mmol) and (±)-1-phenethyl mesylate (0.78 g, 3.9 mmol) in 25 mL of DMF at -10°C over 75 min gave **5.1d** (0.61 g, 2.6 mmol, 68%) as yellow crystals, mp 70-71.5°C (lit.<sup>11</sup> 45°C), after chromatography with 50% ether in hexane as eluent. Characterisation data is in general agreement with that published.<sup>11</sup>

<sup>1</sup>H nmr: 1.80 (d, 3H, *J* = 6.6 Hz, CH<sub>3</sub>), 6.03 (q, 1H, *J* = 6.6 Hz, CH), 6.22 (ddd, 1H, H5), 7.04 (m, 2H, H6 and H4), 7.36 (s, 5H, Ar), 7.67 (dd, 1H, H3).

<sup>13</sup>C nmr: 18.9 (CH<sub>3</sub>), 82.7 (OCH), 112.0 (5), 128.3 (*m*-Ar × 2\*), 129.0 (*o*-Ar × 2\*), 129.6 (*p*-Ar), 133.1 (4), 137.8 (3), 138.2 (*i*-Ar), 139.6 (6), 175.9 (C=S).

ir (CCl<sub>4</sub>): 3068 w, 3036 w, 2985 w, 2938 w, 1610 m, 1524 s, 1471 w, 1449 s, 1410 s, 1276 m, 1177 m, 1132 s, 1090 m, 1054 m, 700 s.

EIMS: 231 (1) M<sup>+</sup>, 220 (9), 214 (2), 182 (3), 156 (7), 127 (29), 111 (67), 105 (100), 79 (35), 78 (28), 77 (40), 67 (19), 51 (27).

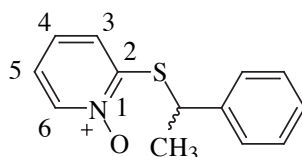
HRMS: C<sub>13</sub>H<sub>13</sub>NOS requires 231.0718. Found 231.0717

C<sub>13</sub>H<sub>12</sub>NS requires 214.0690. Found 214.0692

$C_5H_5NS$  requires 111.0143. Found 111.0144.

Found: C, 67.27; H, 5.89; N, 6.16%.  $C_{13}H_{13}NOS$  requires: C, 67.50; H, 5.66; N, 6.06%.

**(±)-2-(1-Phenylethylsufanyl)pyridine *N*-oxide [60263-93-6]**



**5.2d**

An established method<sup>7</sup> was adapted to prepare **5.2d**. The reaction of sodium 2(1*H*)-pyridinethione *N*-oxide (0.82 g, 5.5 mmol) and (±)-1-phenethyl bromide (0.75 mL, 1.02 g, 5.5 mmol) in 8 mL of DMF at 80°C for 2 hr yielded a pale yellow solid following removal of solvent. Treatment with hexane promoted crystallisation. Recrystallisation from benzene/hexane (including charcoal decolourisation) afforded a crop of fine white needles, mp 113-114°C, (0.52 g, 2.2 mmol, 41%, lit.<sup>11</sup> 118-119°C). The low yield is due partially to spillage during recrystallisation. Characterisation data is in agreement with that published.<sup>11</sup>

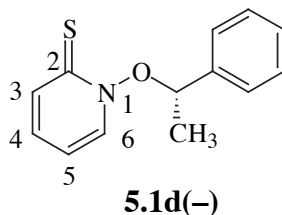
<sup>1</sup>H nmr (200 MHz): 1.73 (d, 3H, *J* = 7.1 Hz, CH<sub>3</sub>), 4.52 (q, 1H, *J* = 7.1 Hz, S-CH), 6.92-7.10 (m, 3H, H<sub>5</sub>, H<sub>4</sub>\* & *p*-Ar\*), 7.22-7.39 (m, 3H, *m*-Ar & H<sub>3</sub>\*), 7.48 (dd, 2H, *o*-Ar), 8.22 (dd, 1H, H<sub>6</sub>).

<sup>13</sup>C nmr: 23.1 (CH<sub>3</sub>), 43.8 (S-CH), 120.8 (5), 123.3 (3), 125.8 (4), 127.1 (*o*-Ar × 2), 127.8 (*p*-Ar), 129.0 (*m*-Ar × 2), 138.9 (6), 142.1 (*i*-Ar), 151.6 (2).

ir (mull): 1589 m, 1555 m, 1492 s, 1449 s, 1427 s, 1277 m, 1251 s, 1239 s, 1220 s, 1144 m, 838 s, 765 m, 741 s, 703 s.

EIMS: 231 (8) M<sup>+</sup>, 216 (5), 215 (10), 214 (35), 127 (45), 112 (20), 111 (28), 105 (100), 79 (20), 78 (18), 77 (18).

Found: C, 67.60; H, 5.80; N, 6.10%.  $C_{13}H_{13}NOS$  requires: C, 67.50; H, 5.66; N, 6.06%.

**S (-)-N-(1-Phenylethoxy)-2(1H)-pyridinethione**

*R* (+)-1-Phenylethyl mesylate was prepared from (Alfa) *R* (+)-1-phenethyl alcohol and mesyl chloride/Et<sub>3</sub>N in CH<sub>2</sub>Cl<sub>2</sub> in 98% yield. It was used immediately due to its labile nature.

The reaction between **5.1i** (1.03 g, 4.02 mmol) and *R* (+)-1-phenethyl mesylate (0.80 g, 4.0 mmol) in 25 mL of DMF at -10°C for 2 hours, afforded a viscous yellow oil after solvent removal. The residue was taken up in 25 mL of CH<sub>2</sub>Cl<sub>2</sub> and washed with 20 mL of water. The solvent was evaporated and the residue was subject to flash chromatography on silica using 50% ether in hexane as the eluent. A yellow, crystalline solid (0.6889 g, 2.98 mmol, 74%) was obtained, mp 61-66°C. A portion was recrystallized from EtOH/water to give a yellow, microcrystalline mass, mp 58-64°C,  $[\alpha]_D^{20.5} = -1047 \pm 13^\circ$  ( $c = 0.005$ , CHCl<sub>3</sub>) which corresponds to 95.30 ± 0.31% e.e.

<sup>1</sup>H nmr: 1.80 (d, 3H,  $J = 6.6$  Hz, CH<sub>3</sub>), 6.03 (q, 1H,  $J = 6.6$  Hz, CH), 6.22 (ddd, 1H, H5), 7.04 (m, 2H, H6 and H4), 7.36 (s, 5H, Ar), 7.67 (dd, 1H, H3). This was identical to the spectrum for **5.1d(±)**.

EIMS: 231 (1) M<sup>+</sup>, 220 (3), 215 (6), 214 (3), 182 (2), 156 (3), 127 (27), 111 (58), 105 (100), 79 (29), 78 (24), 77 (30), 67 (18), 51 (21).

Found: C, 66.89; H, 6.07; N, 5.90%. C<sub>13</sub>H<sub>13</sub>NOS requires: C, 67.50; H, 5.66; N, 6.06%.

**Determination of the enantiomeric composition of S (-)-N-(1-phenylethoxy)-2(1H)-pyridinethione, 5.1d(-)**

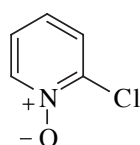
The pyridinethione (14.80 mg, 0.064 mmol, specific rotation = -1047°), was dissolved in 500 μL of benzene in an ampoule. The solution was degassed by three freeze-pump-thaw cycles, flame sealed under vacuum and irradiated at 20°C with a tungsten lamp for 30 min so as to promote the formation of *S* (-)-1-phenylethanol. The solvent was removed and the residue was transferred to a 1 mL Reactivial (Pierce), dissolved in 312 μL of CH<sub>2</sub>Cl<sub>2</sub>, and treated with isopropyl isocyanate (160 μL, 1.63 mmol). The vial was capped securely and heated at 100°C for 20 min so that the enantiomeric 1-phenylethanol (formed during the irradiation step) were converted to their respective isopropyl urethanes. All volatiles were removed under vacuum and the residue was taken up in CH<sub>2</sub>Cl<sub>2</sub> in readiness for GC analysis. The enantiomeric composition of

the mixture of urethanes was determined to be  $97.7\pm 0.16\%$  *S*, equating to an enantiomeric excess of  $95.3\pm 0.3\%$ . The specific rotation of a single enantiomer of the *S*-pyridinethione is hence calculated to be  $-1098\pm 16^\circ$  at  $21^\circ\text{C}$  in  $\text{CHCl}_3$ .

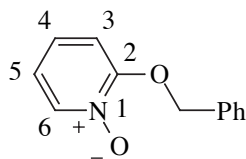
**Table 5.9.** Proportions of *R* and *S* isopropyl urethanes derived from the sample of predominantly *S* *N*-(1-phenylethoxy)-2(1*H*)-pyridinethione. Ratios were determined by GC using a capillary column with the stationary phase Chirasil-Val.

GC run number	% <i>S</i>	% <i>R</i>	% e.e.
1	97.56	2.44	95.12
2	97.66	2.34	95.32
3	97.75	2.25	95.50
4	97.63	2.37	95.26
5	97.54	2.46	95.08
6	97.42	2.58	94.84
7	97.89	2.11	95.78
8	97.56	2.44	95.12
9	97.86	2.14	95.72
average	$97.65\pm 0.16\%$	$2.35\pm 0.16\%$	$95.30\pm 0.31\%$

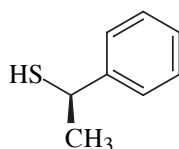
### 2-Chloropyridine *N*-oxide [2402-95-1]



This compound was prepared on a 200 mmol scale by an established procedure.<sup>95</sup> Oxidation of 2-chloropyridine was achieved with 2 equivalents of aqueous hydrogen peroxide in acetic acid at  $80^\circ\text{C}$  for 6 hours. After removal of solvent under reduced pressure and digestion with  $\text{K}_2\text{CO}_3$  at  $80^\circ\text{C}$  for 5 min, solids were filtered off and washed with chloroform. Removal of solvent from the filtrate gave the crude product which was recrystallized from ethyl acetate/hexane to yield the pure product in 55% yield (lit.<sup>95</sup> 77%).

**2-Benzylloxypyridine *N*-oxide [2683-67-6]****5.22a**

Sodium hydride (0.72 g, 30.0 mmol) in 44 mL of dry THF was treated with benzyl alcohol (3.10 mL, 30.0 mmol) then heated at reflux for 1 hour after hydrogen evolution has ceased. After cooling, 2-chloropyridine *N*-oxide (3.89 g, 30.0 mmol) in 10 mL of dry THF was added and refluxing was recommenced for 20 min. The now white suspension (NaCl) was cooled in ice and treated with 10 mL of water (which dissolved all of the white precipitate) and extracted with 100 mL of CHCl<sub>3</sub>. This organic extract was washed with 20 mL of water, 25 mL of saturated aqueous NaCl, dried over Na<sub>2</sub>SO<sub>4</sub>, then evaporated to give the crude product as an off-white solid (5.80 g). Recrystallisation of the crude product from ethyl acetate/hexane gave the pure product (3.81 g, 18.9 mmol, 63%) as a crop of white crystals, mp 106.5-107.5°C (lit.<sup>53</sup> 107°C). <sup>1</sup>H nmr: 5.46 (s, 2H, O-CH<sub>2</sub>), 6.89-6.95 (m, 2H, H<sub>3</sub>+H<sub>5</sub>), 7.19 (ddd, 1H, H<sub>4</sub>), 7.34-7.49 (m, 5H, Ar), 8.29 (dd, 1H, H<sub>6</sub>). This spectrum was in accord with that published.<sup>118</sup>

***R* (+)-1-Phenylethanethiol [33877-16-6]****5.40**

This compound was prepared by a slightly modified method of Isola and coworkers.<sup>101</sup> Sodium (4.00 g, 0.175 mol) was added gradually to a solution of (-)-menthol (25.00 g, 0.160 mol) in 25 mL of dry toluene to form the alkoxide. After heating at reflux overnight, the mixture was cooled and the remaining sodium was removed with tweezers. Dry diethyl ether (33 mL) was added, followed by the dropwise addition of carbon disulphide (18.0 mL, 0.298 mol) to give a clear yellow solution of (-)-sodium *O*-menthyl dithiocarbonate. After stirring for 15 min, (±)-1-phenethyl bromide (24.5 g, 0.132 mol) was added over 15 min to form the mixture of diastereomers of (-)-*O*-menthyl *RS*-1-phenethyl dithiocarbonate.<sup>130</sup> The mixture was stirred and heated briefly at reflux which caused a thick precipitate to form. After cooling, the mixture was washed with 40 mL of water and the aqueous phase was back-extracted with 50 mL of



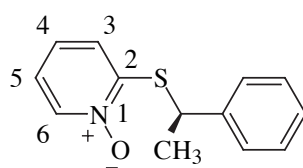
toluene. The combined organic extracts were dried over  $\text{Na}_2\text{SO}_4$  and evaporated to give a yellow/orange oil (45.02 g, 0.1338 mol, 84%).

A diastereomeric separation was effected by dissolving the oil in 100 mL of ethanol, cooling to  $0^\circ\text{C}$ , promoting crystallisation by scratching the wall of the vessel with a glass rod, then leaving the mixture at room temperature for 45 min. The white crystals which formed were filtered off and washed with a small quantity of cold ethanol and dried under vacuum to yield (–)-*O*-menthyl *S*-1-phenethyl dithiocarbonate (14.38 g, 42.7 mmol, 53%), mp  $72\text{--}73^\circ\text{C}$ . Recrystallisation was repeated from 83 mL of ethanol, leaving the solution at room temperature overnight. A yield of 12.33 g (46%) was recovered, mp  $74\text{--}75^\circ\text{C}$  (lit. 63%, mp  $76\text{--}77^\circ\text{C}$ )  $[\alpha]_{\text{D}}^{25} = +146.4 \pm 1.8^\circ$  ( $c = 0.05$ , benzene, lit.<sup>101</sup>  $+148.8^\circ$ ,  $c = 2.40$ ).

The treatment of (–)-*O*-menthyl *S*-1-phenethyl dithiocarbonate (4.00 g, 11.9 mmol) in 25 mL benzene at reflux with morpholine (7.90 g, 90.7 mmol), formed the intensely malodorous *R* (+)-1-phenylethylthiol (**5.40**). The reaction mixture was washed with  $2 \times 15$  mL water, dried over  $\text{Na}_2\text{SO}_4$  and the solvent was removed on the rotary evaporator (RT, 25 mmHg) to give a slightly yellow oil. The thiol was purified by flash chromatography (10% ether in hexane,  $R_f = 0.79$ ) to give **5.40** as a colourless oil (1.41 g, 10.2 mmol, 86%, lit.<sup>101</sup> 48%). Further purification with distillation by kugelrohr ( $95^\circ\text{C}$ , 21 mmHg) afforded the pure thiol,  $[\alpha]_{\text{D}}^{25} = +91.9 \pm 1.0^\circ$  ( $c = 0.13$ , abs. ethanol, lit.<sup>101</sup>  $[\alpha]_{\text{D}}^{25} = +91.7$ ,  $c = 6.17$ ).

$^1\text{H}$  nmr: 1.67 (d, 3H,  $J = 7.0$  Hz,  $\text{CH}_3$ ), 1.99 (d, 1H,  $J = 5.2$  Hz, SH), 4.23 (qd, 1H, CH), 7.21–7.39 (m, 5H, Ar). This was identical to a spectrum of authentic (Aldrich) (±)-1-phenethylthiol.

### ***R* (+)-2-(1-Phenylethylsulfanyl)pyridine *N*-oxide**



**5.2d(+)**

Sodium hydride, washed free of storage oil with pentane (89.6 mg, dry, 3.73 mmol), was added gradually to a stirred solution of *R* (+)-1-phenethyl thiol (0.504 mL, 0.516 g, 3.73 mmol) in 8 mL of dry THF under a nitrogen blanket. A thick, white precipitate was present once hydrogen evolution had ceased. A solution of 2-chloropyridine *N*-oxide (483.6 mg, 3.73 mmol) in 1.5 mL of dry THF was added over 1 min, which caused the precipitate to dissolve. The mixture was stirred overnight then treated cautiously with 10 mL of water and extracted with 50 mL of  $\text{CHCl}_3$ . The extract

was dried and evaporated, yielding an oil (0.86 g, 3.7 mmol, 100%) which crystallized on standing. Recrystallisation from benzene/hexane yielded **5.2d(+)** (0.58 g, 2.5 mmol, 67%) as colourless prisms, mp 107.0-107.5°C,  $[\alpha]_D^{22.4} = 130 \pm 1^\circ$  ( $c = 0.005$ ,  $\text{CHCl}_3$ ). An nmr experiment to estimate the enantiomeric composition of **5.2d(+)** (24.2 mg, 0.105 mmol) using the lanthanide shift reagent europium (III) tris(3-(trifluoromethylhydroxymethylene)camphorate) ( $\text{Eu}(\text{tfc})_3$ , 9.66 mg, 10.8  $\mu\text{mol}$ , 10.3 mol%) in 0.55 mL of  $\text{CDCl}_3$  could detect only one enantiomer, indicating an e.e. of  $\geq 98\%$ . Relevant characterisation data is in accord with that published for the racemate.<sup>11</sup>

$^1\text{H}$  nmr: 1.74 (d, 3H,  $J = 7.1$  Hz,  $\text{CH}_3$ ), 4.52 (q, 1H,  $J = 7.1$  Hz, S-CH), 6.98 (ddd, 1H, H5), 7.02-7.10 (m, 2H, H3 & H4\*), 7.22-7.30 (m, 1H,  $p$ -Ar\*), 7.34 (ddd, 2H,  $m$ -Ar), 7.49 (dd, 2H,  $o$ -Ar), 8.22 (dd, 1H, H6).

$^{13}\text{C}$  nmr: 23.0 ( $\text{CH}_3$ ), 43.6 (S-CH), 120.6 (5), 123.1 (3), 125.6 (4), 127.0 ( $o$ -Ar  $\times 2$ ), 127.7 ( $p$ -Ar), 128.9 ( $m$ -Ar  $\times 2$ ), 138.7 (6), 142.0 ( $i$ -Ar), 151.3 (2).

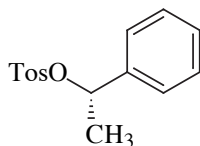
EIMS: 231 (3)  $\text{M}^+$ , 214 (14), 127 (36), 112 (21), 111(25), 105 (100), 79 (30), 78 (22), 77 (25), 67 (7), 51 (15).

Found: C, 67.47; H, 5.70; N, 6.00%.  $\text{C}_{13}\text{H}_{13}\text{NOS}$  requires: C, 67.50; H, 5.66; N, 6.06%.

### ***p*-Toluenesulfinyl Chloride, *p*-Me( $\text{C}_6\text{H}_4$ )SOCl [10439-23-3]**

The method of Kurzer<sup>121</sup> was used to prepare *p*-toluenesulfinyl chloride on a 20 mmol scale in 78% yield (lit.<sup>121</sup> 86-92%) from the reaction between sodium *p*-toluenesulfinate dihydrate and thionyl chloride (7.5 eq). Excess  $\text{SOCl}_2$  was removed under reduced pressure. The gold-coloured oil was used without further purification.

### ***S* (-)-1-Phenylethyl Toluene-4-sulfonate [188015-94-3]**



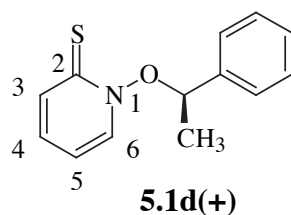
**5.35**

The method of Wilt and coworkers,<sup>122</sup> was used to prepare *S* (-)-1-phenylethyl toluene-4-sulfinate by the reaction at 0°C of (Alfa) *S* (-)-1-phenethyl alcohol (0.500 g, 4.09 mmol) with *p*-toluenesulfinyl chloride (0.72 g, 4.1 mmol) and pyridine (0.331 mL, 4.09 mmol) in 8.5 mL of dry diethyl ether. After filtering off the pyridinium hydrochloride, the filtrate was washed with 10 mL each of 2M HCl, water, 5%  $\text{NaHCO}_3$ , water and dried over  $\text{MgSO}_4$ . Removal of solvent yielded a colourless oil

(0.60 g, 2.3 mmol, 56%, lit.<sup>122</sup> 73%) which <sup>1</sup>H nmr showed to be a mixture of diastereomers due to chirality at sulfur.

Oxidation to the tosylate was achieved by the treatment of *S* (–)-1-phenylethyl toluene-4-sulfinate (0.60 g, 2.3 mmol) with *m*-CPBA (0.56 g, 3.2 mmol) in CH<sub>2</sub>Cl<sub>2</sub> at 0°C, using the procedure of Coates and Chen.<sup>97</sup> After 6 hours the mixture was washed with 10 mL each of 5% K<sub>2</sub>CO<sub>3</sub> and water, dried over MgSO<sub>4</sub>, then evaporated to yield **35** (0.59 g, 2.1 mmol, 93%) as a white solid which began to darken in colour at room temperature. Storage in a –70°C freezer halted further decomposition.

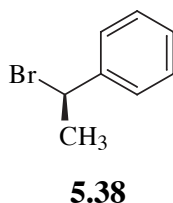
### ***R* (+)-*N*-(1-Phenylethoxy)-2(1*H*)-pyridinethione**



The reaction of *S* (–)-1-phenylethyl toluene-4-sulfonate (**5.35**, 0.59 g, 2.1 mmol) and tetraethylammonium 2(1*H*)-pyridinethione *N*-oxide (**5.1i**, 0.54 g, 2.1 mmol) in 5 mL of DMF at 0°C for 1 hr afforded a yellow oil (0.35 g) after workup. Purification by flash chromatography (50% ether in hexane) gave the desired product as a yellow oil, which crystallized when treated with hexane. The yellow crystals (140 mg, 0.605 mmol, 28%) had mp 66–68°C and  $[\alpha]_D^{21} = +771 \pm 9^\circ$  ( $c = 0.010$ , CH<sub>2</sub>Cl<sub>2</sub>), which corresponds to an e.e of 70.2±1.8%.

This compound had <sup>1</sup>H and <sup>13</sup>C nmr spectra identical with that of (±)-*N*-(1-phenylethoxy)-2(1*H*)-pyridinethione (**5.1d**).

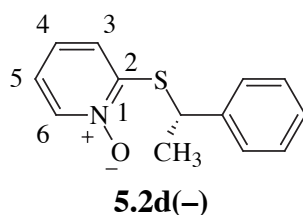
### ***R* (+)-1-(Bromoethyl)benzene [1459-14-6]**



A modified literature procedure<sup>100</sup> was used to prepare the desired bromide. The reaction at –24 to +5°C between (Alfa) *S* (–)-1-phenethyl alcohol (0.500 g, 4.09 mmol), phosphorus tribromide (0.442 mL, 4.63 mmol) and pyridine (0.757 mL, 9.34 mmol) in 6.5 mL of diethyl ether was stirred for 2 days. Excess PBr<sub>3</sub> was destroyed with ice water then the ether layer was separated and washed successively with 5 mL each of ice

water, 85% orthophosphoric acid, saturated  $\text{NaHCO}_3$ , 2 × ice water, then dried over  $\text{MgSO}_4$ . Removal of solvent under reduced pressure yielded **5.38** as a colourless oil (0.34 g, 45%, lit.<sup>100</sup> 73% distilled),  $[\alpha]_{\text{D}}^{21} = +69.2 \pm 0.7^\circ$  ( $c = 0.005$ ,  $\text{CHCl}_3$ , lit.<sup>100</sup>  $+160.8^\circ$  corresponds to 94% optical purity). The material prepared hence has an enantiomeric excess of  $40.4 \pm 0.4\%$ . This compound is reported to racemise on standing, with a half-life of 125 days at  $27^\circ\text{C}$ , catalysed by impurities.<sup>123</sup> It was stored at  $-18^\circ\text{C}$  and used within a short time.

### S (-)-2(1-Phenylethylsulfanyl)pyridine N-oxide

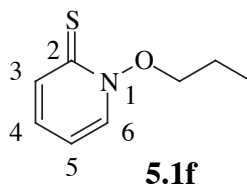


A mixture of sodium 2(1*H*)-pyridinethione *N*-oxide (0.28 g, 1.88 mmol) and *R* (+)-1-phenethyl bromide ( $40.4 \pm 0.4\%$  e.e., 0.34 g, 1.84 mmol) in 3 mL of dry DMF was stirred under nitrogen at  $80^\circ\text{C}$  for 2 hr. The mixture was cooled and the solvent was evaporated, yielding a cloudy oil which was treated twice with 7.5 mL portions of  $\text{CHCl}_3$  and filtered each time to remove  $\text{NaBr}$ . A clear yellow oil remained upon removal of solvent from the filtrate. The yellow colour was removed by treating thrice with 7.5 mL volumes of pentane, decanting the solvent each time. The remaining solid was crystallized from benzene/hexane to yield a crop of white crystals (0.22 g, 0.95 mmol, 52%), mp  $113\text{--}114^\circ\text{C}$  (**5.2d(±)** mp  $113\text{--}114^\circ\text{C}$ ).

The product was recrystallized from benzene. The precipitate had  $[\alpha]_{\text{D}}^{25} = -22.0^\circ$  ( $c = 0.006$ ,  $\text{CHCl}_3$ , 16.9% e.e.) and the evaporated filtrate  $[\alpha]_{\text{D}}^{25} = -112^\circ$  ( $c = 0.006$ ,  $\text{CHCl}_3$ , 86.2% e.e.). The optical purity of the precipitate was found to decrease on repeated recrystallisation, indicating that precipitation of the racemate was favoured over the optically pure enantiomer. The optical purity of the *N*-oxide in the filtrate was observed to correspondingly increase. Spectroscopic characterisation data is in accord with that published for the racemate.<sup>11</sup>

<sup>1</sup>H nmr: 1.74 (d, 3H,  $J = 7.1$  Hz,  $\text{CH}_3$ ), 4.52 (q, 1H,  $J = 7.1$  Hz, S-CH), 6.98 (ddd, 1H, H5), 7.02–7.10 (m, 2H, H3 & H4\*), 7.22–7.30 (m, 1H, *p*-Ar\*), 7.34 (ddd, 2H, *m*-Ar), 7.49 (dd, 2H, *o*-Ar), 8.22 (dd, 1H, H6). This spectrum matched those for both **5.2d** and **5.2d(+)**.

EIMS: 231 (3)  $\text{M}^+$ , 214 (14), 127 (36), 112 (21), 111(25), 105 (100), 79 (30), 78 (22), 77 (25), 67 (7), 51 (15).

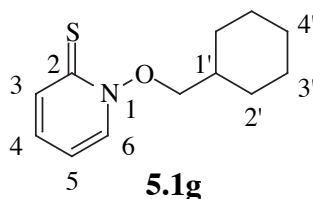
***N*-Propoxy-2(1*H*)-pyridinethione [122333-41-9]**

Propyl mesylate (2.27 g, 16.4 mmol) was prepared in 99% yield from the reaction at 0°C between propanol (1.00 g, 16.6 mmol), methanesulfonyl chloride (2.10 g, 18.3 mmol) and Et<sub>3</sub>N (3.47 mL, 24.9 mmol) in 10 mL of CH<sub>2</sub>Cl<sub>2</sub>.

The reaction of propyl mesylate (2.27 g, 16.4 mmol) and tetraethylammonium 2(1*H*)-pyridinethione *N*-oxide (**5.1i**, 4.20 g, 16.4 mmol) in 20 mL of DMF at 0°C for 1 hr afforded a yellow oil after workup. Purification by repeated flash chromatography (30% hexane in diethyl ether) gave **5.1f** as a yellow oil (0.61 g, 3.6 mmol, 22%). The <sup>1</sup>H nmr spectrum is in agreement with that published.<sup>7</sup>

<sup>1</sup>H nmr: 1.08 (t, 3H, <sup>3</sup>*J* = 7.5 Hz, CH<sub>3</sub>), 1.86 (m, 2H, CH<sub>3</sub>-CH<sub>2</sub>), 4.40 (t, 2H, <sup>3</sup>*J* = 6.7 Hz, OCH<sub>2</sub>), 6.67 (ddd, 1H, H5), 7.19 (ddd, 1H, H4), 7.67 (dd, 1H, H3), 7.82 (dd, 1H, H6).

<sup>13</sup>C nmr: 9.8 (CH<sub>3</sub>), 20.6 (CH<sub>3</sub>-CH<sub>2</sub>), 77.9 (CH<sub>2</sub>O), 113.5 (5), 133.2 (4) 137.8 (3\*), 138.2 (6\*), 175.5 (2).

***N*-Cyclohexylmethoxy-2(1*H*)-pyridinethione**

Cyclohexylmethyl mesylate was prepared in 97% yield on a 26 mmol scale, from the reaction of cyclohexylmethanol<sup>124</sup> and mesyl chloride/Et<sub>3</sub>N in CH<sub>2</sub>Cl<sub>2</sub> at 0°C.

The reaction between **5.1i** (6.52 g, 25.4 mmol) and cyclohexylmethyl mesylate (4.89 g, 25.4 mmol) in 110 mL of dry DMF at 0°C for 1 hr afforded a yellow, viscous oil upon removal of solvent. This residue was taken up in 65 mL of 0.1 M aqueous NaOH and extracted with 2 × 20 mL of diethyl ether. The ether extracts were combined and washed successively with 20 mL portions of 5% aqueous NaHCO<sub>3</sub> and saturated NaCl, which caused the precipitation of a white, crystalline solid (*N*-oxide **5.2g**) in the organic phase. After drying with MgSO<sub>4</sub> the mixture was filtered. The filter cake was added to 50 mL of CHCl<sub>3</sub> to redissolve the precipitated **5.2g**, then refiltered and evaporated to yield a white, crystalline solid which was recrystallized from benzene/hexane to give 2-(cyclohexylmethylsulfanyl)pyridine *N*-oxide (**5.2g**, 0.63 g,

2.8 mmol, 11%), mp 142-143°C. Characterisation data are provided below.

The ethereal filtrate from the first filtration was evaporated and the yellow residue was purified by flash chromatography ( $R_f = 0.39$ ) using 70% ether in hexane as the eluent. The desired product **5.1g** was obtained as a crop of yellow crystals (1.24 g, 5.55 mmol, 22%), mp 63-66.5°C. A small amount was recrystallized from EtOH/water to prepare an analytical sample. These yellow needles had mp 70-71°C.

Nmr resonances were assigned using homo- and heteronuclear 2D nmr experiments (Appendix C).

Characterisation data for *N*-cyclohexylmethoxy-2(1*H*)-pyridinethione (**5.1g**).

$^1\text{H}$  nmr: 1.13 (m, 2H, H2'a × 2), 1.20-1.40 (m, 3H, H3'a × 2 & H4'a), 1.65-1.82 (m, 3H, H3'e × 2 & H4'e), 1.81-2.00 (m, 3H, H2'e × 2 & H1'a), 4.24 (d, 2H,  $J = 6.1$  Hz,  $\text{OCH}_2$ ), 6.66 (ddd, 1H, H5), 7.17 (ddd, 1H, H4), 7.68 (dd, 1H, H3), 7.77 (dd, 1H, H6).

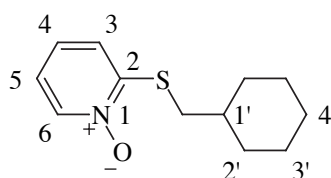
$^{13}\text{C}$  nmr: 25.2 (3' × 2), 25.9 (4'), 29.2 (2' × 2), 36.0 (1'), 81.6 ( $\text{CH}_2\text{-O}$ ), 113.6 (5), 133.1 (4), 137.8 (3\*), 138.0 (6\*), 175.6 (C=S).

ir ( $\text{CCl}_4$ ): 2932 s, asym, 2856 m, 1611 m, 1525 s, 1448 s, asym, 1412 m, 1280 m, 1134 s, 1017 w, 979 m, 715 w.

EIMS: 223 (3)  $\text{M}^{+\bullet}$ , 127 (29), 111 (24), 96 (19), 83 (34), 81 (26), 67 (49), 55 (100).

Found: C, 64.79; H, 7.82; N, 5.97%.  $\text{C}_{12}\text{H}_{17}\text{NOS}$  requires: C, 64.54; H, 7.67; N, 6.27%.

## 2-(Cyclohexylmethylsulfanyl)pyridine *N*-oxide



**5.2g**

This compound was a by-product from the preparation of **5.1g**. Nmr resonances are assigned on the basis of 2D homo- and heteronuclear nmr experiments (Appendix C).

$^1\text{H}$  nmr: 1.10 (m, 2H, H2'a × 2), 1.18-1.35 (m, 3H, H3'a × 2 & H4'a), 1.60-1.82 (m, 4H, H1'a, H4'e & H3'e × 2), 1.97 (dm, 2H, H2'e × 2), 2.78 (d, 2H,  $J = 6.8$  Hz,  $\text{S-CH}_2$ ), 7.05 (ddd, 1H, H5), 7.13 (dd, 1H, H3), 7.27 (ddd, 1H, H4), 8.28 (dd, 1H, H6).

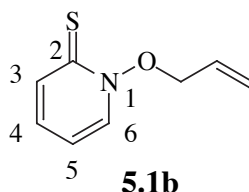
$^{13}\text{C}$  nmr: 25.6 (3' × 2), 25.8 (4'), 32.8 (2' × 2), 36.5 (1'), 37.5 ( $\text{S-CH}_2$ ), 120.0 (5), 121.3 (3), 125.9 (4), 138.9 (6), 153.3 (2).

ir (mull): 3100 w, 3073 w, 3030 w, 1589 m, 1545 m, asym, 1284 m, 1263 m, 1252 s, 1221 m, 1147 s, 1094 m, 1049 m, 840 s, 745 s, 702 m.

EIMS: 223 (2)  $M^+$ , 207 (8), 206 (6), 190 (6), 174 (10), 160 (9), 127 (87), 125 (47), 112 (83), 111 (81), 79 (50) 78 (80), 67 (78), 55 (94), 41 (100).

Found: C, 64.64; H, 7.86; N, 6.12%.  $C_{12}H_{17}NOS$  requires: C, 64.54; H, 7.67; N, 6.27%.

### *N*-Allyloxy-2(1*H*)-pyridinethione



Allyl mesylate was prepared on a 40 mmol scale in 98% yield by the reaction of allyl alcohol with mesyl chloride/ $Et_3N$  in  $CH_2Cl_2$ . It was stored at  $-70^\circ C$  due to its expected lability.

$^1H$  nmr: 3.03 (s, 3H,  $CH_3$ ), 4.72 (d, 2H, O- $CH_2$ ), 5.40 (d, 1H, *Htrans*), 5.48 (d, 1H, *Hcis*), 5.98 (m, 1H, *Hgem*).

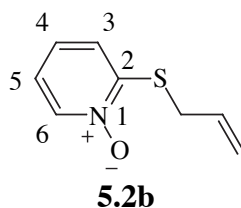
The reaction between **5.1i** (14.00 g, 54.6 mmol) and allyl mesylate (7.43 g, 54.6 mmol), in 175 mL of dry DMF at  $0^\circ C$  for 1.5 hr afforded a viscous, yellow oil, upon removal of solvent. This residue was taken up in 140 mL of 0.1 M NaOH and 210 mL of diethyl ether and the mixture was filtered to remove insoluble products. Repeated ethereal extraction of the aqueous phase was continued until no further yellow colour was present in the organic phase. Combined extracts were washed with 100 mL saturated aqueous  $NaHCO_3$ , 100 mL saturated NaCl, then dried over  $MgSO_4$ . The solvent was removed under vacuum to give a yellow oil. Purification was achieved by flash chromatography ( $R_f = 0.64$ ) using ether as the eluent. Compound **5.1b** was obtained as a viscous, yellow oil (1.83 g, 10.9 mmol, 20%).

$^1H$  nmr: 4.97 (dd, 2H,  $^3J = 6.7$  Hz,  $^4J$  not res., O- $CH_2$ ), 5.42 (m, 1H,  $^2J = 1.3$  Hz,  $^3J = 10.2$  Hz, *Htrans*), 5.45 (m, 1H,  $^2J$  not res.,  $^3J = 17.2$  Hz,  $^4J = 0.7$  Hz, *Hcis*), 6.11 (m, 1H,  $^3J = 6.7, 10.2, 17.2$  Hz, *Hgem*), 6.66 (ddd, 1H, H5), 7.21 (ddd, 1H, H4), 7.65 (dd, 1H, H3), 7.80 (dd, 1H, H6).

$^{13}C$  nmr: 76.2 (O- $CH_2$ ), 112.9 (5), 123.4 ( $H_2C=CH$ ), 129.8 ( $CH=CH_2$ ), 133.2 (4), 137.5 (3\*), 138.9 (6\*), 175 3 (2).

EIMS: 167 (9)  $M^+$ , 150 (33), 136 (27), 127 (4), 120 (13), 111 (79), 110 (11), 109 (11), 83 (15), 79 (24), 78 (44), 67 (100), 58 (28), 56 (10), 51 (16), 44 (12), 42 (15), 41 (51).

Found: C, 57.22; H, 5.12; N, 8.38%.  $C_8H_9NOS$  requires: C, 57.46; H, 5.42; N, 8.38%.

2-(Allylsulfanyl)pyridine *N*-oxide

The reaction of sodium 2(1*H*)-pyridinethione *N*-oxide (1.00 g, 6.71 mmol) and allyl bromide (0.58 mL, 6.7 mmol) in 10 mL of dry DMF at 80°C for 2 hr yielded a yellow, viscous suspension upon removal of solvent. This was treated twice with 25 mL portions of CHCl<sub>3</sub>, filtering each time to remove NaBr. After removal of solvent from the filtrate, the resulting oil was treated twice with 30 mL portions of pentane and the solvent decanted to remove the yellow, *O*-alkylated product **5.1b**. After decolourising with charcoal in hot benzene, the crude product was recrystallized from benzene/hexane to yield a crop of off-white plates (0.90 g, 80%), mp 69-70.5°C, following drying under high vacuum overnight.

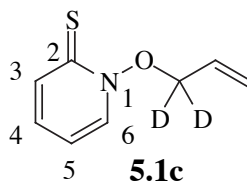
<sup>1</sup>H nmr: 3.62 (dd, 2H <sup>4</sup>*J* = 1.2 Hz, <sup>3</sup>*J* = 6.3 Hz, S-CH<sub>2</sub>), 5.27 (m, 1H, <sup>2</sup>*J* (<sup>4</sup>*J*) = 1.2 Hz, <sup>3</sup>*J* = 10.0 Hz, *H*<sub>trans</sub>), 5.41 (m, 1H, <sup>2</sup>*J* = 1.2 Hz, <sup>3</sup>*J* = 17.0 Hz, *H*<sub>cis</sub>), 5.93 (m, 1H, <sup>3</sup>*J* = 10.0, 17.0, 6.3 Hz, *H*<sub>gem</sub>), 7.08 (ddd, 1H, H<sub>5</sub>), 7.18 (dd, 1H, H<sub>3</sub>), 7.27 (ddd, 1H, H<sub>4</sub>), 8.28 (dd, 1H, H<sub>6</sub>).

<sup>13</sup>C nmr: 32.9 (S-CH<sub>2</sub>), 119.3 (CH=CH<sub>2</sub>), 120.4 (5), 121.8 (3), 125.6 (4), 131.4 (CH<sub>2</sub>=CH), 139.6 (6) 151.7 (2).

ir (mull): 3105 w, 3065 m, 3057 m, 3035 m, 1640 s, 1583 w, 1549 m, 1414 s, 1402 s, 1270 s, 1252 s, 1239 s, 1225 s, 1205 m, 1145 s, asym, 1089 s, 990 s, 940 w, 923 s, 915 m, 838 s, 763 s, 757 s, 748 w.

EIMS: 167 (2) M<sup>+</sup>, 150 (90), 136 (15), 120 (15), 117 (45), 111 (100), 78 (71), 67 (30), 51 (15), 41 (12), 39 (20).

Found: C, 57.33; H, 5.67; N, 8.30%. C<sub>8</sub>H<sub>9</sub>NOS requires: C, 57.46; H, 5.42; N, 8.38%.

*N*-(Allyloxy-1,1-*d*<sub>2</sub>)-2(1*H*)-pyridinethione

Allyl alcohol-1,1-*d*<sub>2</sub> was synthesized according to Faller et al.,<sup>113</sup> by the reduction at -10°C of acryloyl chloride (1.80 mL, 22.1 mmol) with lithium aluminium deuteride (1.00 g, 23.8 mmol, Aldrich, 98 atom% *d*), in diethyl ether (45 mL). After 5



hours, the mixture was quenched carefully with 5 mL of 3% NaOH and stirred overnight. Extraction of the aqueous phase was achieved with 3 × 30 mL of diethyl ether and the combined extracts were dried over Na<sub>2</sub>SO<sub>4</sub> and evaporated under vacuum at 0°C to yield a colourless oil (1.27 g). Nmr analysis showed the crude product to be impure. Purification by kugelrohr distillation (50°C/115 mmHg) gave the desired product (0.64 g, 10.6 mmol, 48%, lit.<sup>113</sup> 80% undistilled). Isotopic composition determined from <sup>1</sup>H nmr peak integrals is 98 atom% *d*.

<sup>1</sup>H nmr: 1.67 (br, 1H, OH), 4.15 (m, ≈ 0.02 H residual O–CH<sub>2</sub> and O–CDH), 5.17 (dd, 1H, *Htrans*), 5.30 (dd, 1H, *Hcis*), 5.97–6.17 (m, 1H, *Hgem*).

Allyl-*1,1-d*<sub>2</sub> mesylate (0.67 g, 4.8 mmol, 68%) was then prepared by the reaction at 0°C of the labelled alcohol (0.43 g, 7.2 mmol), mesyl chloride (0.610 mL, 7.88 mmol) and Et<sub>3</sub>N (1.50 mL, 10.7 mmol) in 35 mL of CH<sub>2</sub>Cl<sub>2</sub>. An estimated isotopic composition from <sup>1</sup>H nmr peak integrals is 98 atom% *d*.

<sup>1</sup>H nmr: 3.03 (s, 3H, CH<sub>3</sub>), 4.71 (m, ≈ 0.02 H, residual O–CH<sub>2</sub> and O–CDH), 5.40 (d, 1H, <sup>3</sup>*J* = 10.5 Hz, *Htrans*), 5.48 (d, 1H, <sup>3</sup>*J* = 16.9 Hz, *Hcis*), 5.97 (dd, 1H, <sup>3</sup>*J* = 10.5, 16.9 Hz, *Hgem*).

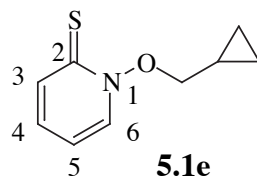
The reaction between **5.1i** (2.86 g, 11.2 mmol), and the labelled allyl mesylate (0.67 g, 4.85 mmol) in 17.5 mL of dry DMF at 0°C for 2.5 hr afforded a yellow, cloudy oil upon removal of the solvent. The residue was treated with 12 mL of aqueous 0.1 M NaOH and extracted with 5 × 10 mL of diethyl ether until the extracts were no longer yellow in colour. Combined extracts were washed with 10 mL of water, dried over MgSO<sub>4</sub> and evaporated to afford a yellow oil (0.21 g). Purification of this crude product by vacuum-liquid chromatography (VLC, hexane→ether) gave **5.1c** (0.15 g, 0.89 mmol, 8%) as a viscous, yellow oil.

<sup>1</sup>H nmr: 4.97 (m, ≈0.017H, <sup>3</sup>*J* = 6.7 Hz, <sup>4</sup>*J* not res., O–CH<sub>2</sub>), 5.43 (dd, 1H, <sup>3</sup>*J* = 10.2 Hz, <sup>2</sup>*J* = 1.4 Hz, *Htrans*), 5.45 (dd, 1H, <sup>3</sup>*J* = 17.2 Hz, <sup>2</sup>*J* = 1.4 Hz, *Hcis*), 6.10 (dd, 1H, <sup>3</sup>*J* = 17.2, 10.2 Hz, *Hgem*), 6.62 (ddd, 1H, H5), 7.18 (ddd, 1H, H4), 7.66 (dd, 1H, H3), 7.75 (dd, 1H, H6).

<sup>13</sup>C nmr: 77.2 (O–CD<sub>2</sub>), 113.5 (5), 124.4 (CH<sub>2</sub>=CH), 130.5 (CH<sub>2</sub>=CH), 133.8 (4), 138.5 (3\*), 139.6 (6\*), 176.3 (C=S).

EIMS: 169 (4) M<sup>+</sup>, 152 (8), 136 (6), 127 (4), 121 (17), 112 (48), 83 (15), 78 (45), 68 (100), 58 (13), 51 (22), 43 (23).

<sup>2</sup>H nmr (30.7 MHz, CHCl<sub>3</sub>): 4.97 (s, br, O–CD<sub>2</sub>).

***N*-Cyclopropylmethoxy-2(1*H*)-pyridinethione**

Cyclopropylmethyl mesylate was prepared by the reaction at 0°C between cyclopropanemethanol (3.00 g, 41.6 mmol), methanesulfonyl chloride (3.6 mL, 47 mmol) and Et<sub>3</sub>N (8.7 mL, 62 mmol) in 200 mL of CH<sub>2</sub>Cl<sub>2</sub>. After the usual work-up,<sup>99</sup> the desired mesylate was obtained as a colourless oil (5.64 g, 90%).

<sup>1</sup>H nmr: 0.40 (m, 2H, *H*<sub>cis</sub> × 2), 0.69 (m, 2H, *H*<sub>trans</sub> × 2), 1.25 (m, 1H, S-CH<sub>2</sub>), 3.04 (s, 3H, CH<sub>3</sub>), 4.09 (d, 2H, <sup>3</sup>*J* = 7.6 Hz, O-CH<sub>2</sub>).

<sup>13</sup>C nmr: 3.7 (cyclopropyl CH<sub>2</sub> × 2), 10.0 (cyclopropyl CH), 37.7 (CH<sub>3</sub>), 75.4 (CH<sub>2</sub>O).

The reaction between **5.1i** (9.70 g, 37.8 mmol) and cyclopropylmethyl mesylate (5.64 g, 37.6 mmol) in 100 mL of dry DMF at 0°C for 3 hr afforded a cloudy yellow residue upon removal of solvent. This was treated with 0.1 M aqueous NaOH and extracted thrice with 50 mL aliquots of CCl<sub>4</sub> to remove **5.1e** preferentially. The same aqueous solution was then extracted similarly with CHCl<sub>3</sub> to obtain the isomeric *N*-oxide **5.2e**.

Evaporation of the solvent from the CCl<sub>4</sub> solution yielded crude **5.1e** as yellow oil (3.23 g, 17.8 mmol, 47%) which was purified by flash chromatography, using diethyl ether as the eluent. Pure **5.1e** was obtained as a clear, yellow oil (1.91 g, 10.5 mmol, 28%).

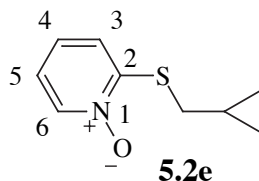
<sup>1</sup>H nmr: 0.36 (m, 2H, *H*<sub>cis</sub> × 2), 0.65 (m, 2H, *H*<sub>trans</sub> × 2), 1.59 (m, 1H, OCH<sub>2</sub>-CH), 4.32 (d, 2H, <sup>3</sup>*J* = 7.4 Hz, OCH<sub>2</sub>), 6.65 (ddd, 1H, H<sub>5</sub>), 7.18 (ddd, 1H, H<sub>4</sub>), 7.64 (dd, 1H, H<sub>3</sub>), 7.86 (dd, 1H, H<sub>6</sub>).

<sup>13</sup>C nmr: 3.3 (cyclopropyl CH<sub>2</sub> × 2), 8.5 (cyclopropyl CH), 80.4 (CH<sub>2</sub>O), 112.8 (5), 132.9 (4) 137.5 (3\*), 138.7 (6\*), 175.4 (2).

ir (neat): 3085 w, 3010 w, asym, 1710 m, asym, 1608 s, 1527 s, 1448 s, 1418 s, 1277 m, 1227 m, 1176 m, 1132 s, 1089 m, 1026 m, 958 m, 757 m.

EIMS: 220 (6), 181 (17) M<sup>+</sup>, 164 (21), 150 (5), 136 (32), 127 (55), 111 (65), 79 (45), 67 (35), 55 (100).

Found: C, 59.49; H, 6.39; N, 7.72; S, 17.67%. C<sub>9</sub>H<sub>11</sub>NOS requires: C, 59.64; H, 6.12; N, 7.73; S, 17.69%.

**2-(Cyclopropylmethylsulfanyl)pyridine *N*-oxide**

Evaporation of solvent from the  $\text{CHCl}_3$  extract (from preparation of **5.1e**) gave crude **5.2e** as a brownish-white solid (3.33 g, 18.4 mmol, 49%). This was purified by flash chromatography (eluent 5% methanol in  $\text{CH}_2\text{Cl}_2$ ), followed by recrystallisation from ethyl acetate/hexane to yield 2-(cyclopropylmethylsulfanyl)pyridine *N*-oxide (**5.2e**, 1.68 g, 9.27 mmol, 25%) as white prisms, mp 57-58°C.

$^1\text{H}$  nmr: 0.37 (m, 2H,  $H_{\text{cis}} \times 2$ ), 0.68 (m, 2H,  $H_{\text{trans}} \times 2$ ), 1.13 (m, 1H,  $\text{SCH}_2\text{-CH}$ ), 2.87 (d, 2H,  $^3J = 7.0$  Hz, S- $\text{CH}_2$ ), 7.06 (ddd, 1H, H5), 7.18 (dd, 1H, H3), 7.27 (ddd, 1H, H4), 8.25 (dd, 1H, H6).

$^{13}\text{C}$  nmr: 5.7 (cyclopropyl  $\text{CH}_2 \times 2$ ), 8.8 (cyclopropyl CH), 36.0 (S- $\text{CH}_2$ ), 120.0 (5), 121.3 (3), 125.4 (4), 138.4 (6), 152.3 (2).

ftir (KBr): 3084 w, 2994 w, 2922 w, 2851 w, 1466 s, 1443 m, 1405 s, 1268 m, 1249 s, 1216 s, 1196 s, 1132 s, 838 s, 754 s, 705 s, 531 s.

EIMS: 181 (2)  $\text{M}^+$ , 164 (100), 149 (6), 136 (10), 127 (28), 118 (6), 111 (15), 96 (7), 85 (7), 78 (48), 67 (20), 55 (33).

Found: C, 59.64; H, 6.01; N, 7.46; S, 17.72%.  $\text{C}_9\text{H}_{11}\text{NOS}$  requires: C, 59.64; H, 6.12; N, 7.73; S, 17.69%.

**Procedure to test the catalytic activity of a reagent**

Due to the photolability of *N*-alkoxy-2(1*H*)-pyridinethiones, the following manipulations were carried out under minimal lighting. In an ampoule of 2-3 mL capacity was placed, nominally, 25 mg (0.115 mmol) of *N*-benzyloxy-2(1*H*)-pyridinethione **5.1a**. This was dissolved in 500  $\mu\text{L}$  of the solvent of choice, usually  $\text{CDCl}_3$ . The resulting solution was treated with the test reagent (commonly 0.50 mol%), added as a measured volume of a solution of the reagent in the reaction solvent.

Solutions were degassed with two freeze/pump/thaw cycles, then frozen, pumped and flame sealed under vacuum. A deviation from this procedure was taken when air and oxygen were used as reagents. In these cases, the solution was either degassed and the chosen atmosphere was admitted before freezing and flame sealing (air and oxygen), or the degassing procedure was omitted (air). Sealed ampoules were wrapped in aluminium foil and placed into thermostatted oil baths at  $80 \pm 1^\circ\text{C}$  for a measured time, usually 4.00 hours.

When withdrawn from the baths, the ampoules were washed to remove the oil,

opened and the contents were transferred to an nmr tube. When the solvents  $C_6D_6$  and  $CD_3CN$  were used, 500  $\mu L$  of  $CDCl_3$  was added to ensure complete solubility of all components. Analysis was performed by  $^1H$  nmr. The results are listed in table 5.1. "Extent of reaction" was calculated by dividing the sum of the relative concentrations of identifiable products by the total. "Yield of *N*-oxide" represents the concentration of **5.2a** divided by the sum of the concentrations of all identifiable compounds.

### Procedure for conducting kinetics experiments

These experiments were performed in three different groups. In the first, kinetic data was measured as a function of the proportion of the catalyst iodine. The second set of experiments was concerned with obtaining kinetic data for four different types of catalyst. In the third, kinetic data was measured as a function of changing both pyridinethione and iodine concentrations whilst keeping their ratio the same.

#### 1. Kinetic data as a function of the proportion of iodine present

Into a 3 mL Reactivial, was placed of *N*-benzyloxy-2(1*H*)-pyridinethione (**5.1a**, nominally 50.0 mg, 0.230 mmol), which was dissolved in 2.00 mL of purified, dry  $CHCl_3$ . The vial was capped with a Mininert valve and the solution was degassed using three freeze/pump/thaw cycles *via* a needle through the valve and placed under a dry nitrogen atmosphere. Iodine was then injected by microsyringe from a  $5.755 \times 10^{-4}$  M solution of iodine in  $CHCl_3$ . Proportions of 0.500 (20.0  $\mu L$ ), 1.01 (40.0  $\mu L$ ) and 2.00 mol% (80.0  $\mu L$ ) were added, for the three reactions.

The vials were placed in an  $80 \pm 1^\circ C$  thermostatted oil bath and aliquots of 25.0 mL were withdrawn over time and diluted to 10.00 mL with spectroscopic grade ethanol. Analysis was performed by UV-vis spectrophotometry, by monitoring with time the absorbance of the absorption peak with  $\lambda_{max} = 361$  nm, belonging to the compound *N*-benzyloxy-2(1*H*)-pyridinethione (**5.1a**).

**Table 5.10.** Kinetic data for experiments involving different proportions of iodine:  $[\mathbf{5.1a}]_0 = 0.114 \text{ M}$ ,  $[\text{I}_2]_0 = 0.575 \text{ mM}$ ,  $1.15 \text{ mM}$ ,  $2.30 \text{ mM}$ 

0.50 mol% iodine		1.01 mol% iodine		2.00 mol% iodine	
time (s)	absorbance	time (s)	absorbance	time (s)	absorbance
0	1.687	0	1.654	0	1.631
150	1.709	370	1.591	481	1.498
480	1.648	1745	1.378	1326	1.254
963	1.566	2387	1.273	2266	1.022
1490	1.547	3783	1.081	3136	0.8331
2368	1.479	5770	0.8584	4074	0.6840
3638	1.412	7280	0.7574	5279	0.5266
5290	1.257	10540	0.5653	6456	0.4080
7430	1.104	12752	0.4393	7739	0.3101
9421	1.023	16313	0.3196	9454	0.2167
11366	0.9424	21450	0.1822	10904	0.1649
13867	0.8445	27287	0.1005	13118	0.1102
16550	0.7255				
19240	0.6217				

## 2. Kinetic data as a function of the type of catalyst

The four catalysts iodine, ferrocenium hexafluorophosphate, tris(4-bromophenyl)aminium hexachloroantimonate (**5.33**) and nickel (III) sarcophagine perchlorate were used in this set of experiments. Reactions were performed identically to the previous set, with the following exceptions: all catalysts were added in a proportion of 1.00 mol% and reactions were performed in a 1:1 (v/v) mixture of  $\text{CHCl}_3$  and  $\text{CH}_3\text{CN}$ , to avoid catalyst solubility problems.

**Table 5.11.** UV-Vis spectrophotometric data from 4 rearrangement reactions, each with a different catalyst, where  $[\mathbf{5.1a}]_0 = 0.115 \text{ M}$ ,  $[\text{catalyst}]_0 = 1.15 \text{ mM}$ 

1.00 mol% iodine		1.00 mol% $\text{Fc}^+\text{PF}_6^-$	
time (s)	absorbance	time (s)	absorbance
0	1.80	0	1.808
835	1.180	1025	1.166
2108	0.5574	2291	0.5797
3654	0.2126	3852	0.2503
5801	0.0597	5396	0.0887
9196	0.0110	9392	0.0237
13697	0.0026	13772	0.0084

1.00 mol% (BrC <sub>6</sub> H <sub>4</sub> )NSbCl <sub>6</sub> ( <b>5.33</b> )		1.00 mol% Ni (III) SAR (ClO <sub>4</sub> ) <sub>3</sub>	
time (s)	absorbance	time (s)	absorbance
0	1.711	0	1.826
1235	1.610	1415	0.9902
2480	1.562	2809	0.5706
4081	1.504	4301	0.2820
6196	1.443	6398	0.0986
9607	1.348	9796	0.0216
13966	1.243	14172	0.0058
18846	1.135	19064	0.0042

3. Kinetic data as a function of changes in the concentrations of both iodine and the pyridinethione, whilst keeping their ratio the same

These reactions were conducted similarly to the last two types, although the solutions of **5.1a** were heated at temperature for 15 minutes prior to introducing the catalyst. The chloroform was washed with water, dried over MgSO<sub>4</sub> and distilled from P<sub>2</sub>O<sub>5</sub>.

**Table 5.12.** Kinetic data for reactions in CHCl<sub>3</sub> at 81.5±1°C in which the ratio of [5.1a]<sub>0</sub> to [I<sub>2</sub>]<sub>0</sub> remains the same, but absolute concentrations are varied

[5.1a] <sub>0</sub> = 57.4 mM, [I <sub>2</sub> ] <sub>0</sub> = 0.294 mM		[5.1a] <sub>0</sub> = 225 mM, [I <sub>2</sub> ] <sub>0</sub> = 1.16 mM	
time (s)	absorbance	time (s)	absorbance
0	0.8936	0	1.780
200	0.8788	60	1.668
540	0.8709	365	1.603
1410	0.8472	775	1.506
3240	0.8044	1692	1.325
5520	0.7559	3000	1.115
7650	0.6952	4700	0.8830
10350	0.6500	6600	0.6671
14595	0.5799	12925	0.2865
22575	0.4603	19930	0.1148
70940	0.1326		

### Iodine catalysed rearrangement of *N*-(allyloxy-1,1-*d*<sub>2</sub>)-2(1*H*)-pyridinethione (5.1c)

Pyridinethione **5.1c** (25.3 mg, 0.149 mmol) was placed in an ampoule. To it was added 500  $\mu\text{L}$  of  $\text{CDCl}_3$  and 10.0  $\mu\text{L}$  of a 0.149 M solution of iodine in  $\text{CDCl}_3$  ( $1.49 \times 10^{-6}$  mol, 1.00 mol%). The solution was degassed in the usual manner, then flame-sealed under vacuum. The solution was heated at 80°C in the dark for 4 hr, then cooled and examined by  $^1\text{H}$  nmr. Approximately half of the original amount of **5.1c** remained. The solution was then treated with another 1.00 mol% iodine and a little more  $\text{CDCl}_3$ , degassed and flame-sealed in an identical manner to the first time and heated under identical conditions for another 4.5 hr, then cooled. This time,  $^1\text{H}$  nmr indicated that about 80% of **5.1c** had been consumed. From the  $^1\text{H}$  nmr spectrum, the ratio of products indicated was **5.2c**: 94% and **5.2c'**: 6%. When normalised to compensate for the isotopic composition of **5.1c**, these values indicate that formally 96% of the rearrangement occurs *via* 1,4 rearrangement and 4% in a 3,4 sense.

$^1\text{H}$  nmr: 3.62 (d, 0.065H S- $\text{CH}_2$ ), 5.27 (dd, 1H,  $^2J = 1.1$  Hz,  $^3J = 10.3$  Hz, *Htrans*), 5.41 (dd, 1H,  $^2J = 1.1$  Hz,  $^3J = 17.0$  Hz, *Hcis*), 5.93 (dd, 1H,  $^3J = 10.3$ , 17.0 Hz, *Hgem*), 7.08 (ddd, 1H, H5), 7.18 (dd, 1H, H3), 7.27 (ddd, 1H, H4), 8.26 (dd, 1H, H6).

$^2\text{H}$  nmr (30.7 MHz,  $\text{CHCl}_3$ ): 3.62 (s, br, 2D, S- $\text{CD}_2$ ), 5.27 (d, 0.07D, *Dtrans*), 5.41 (d, 0.07D, *Dcis*).

### Triflic-acid-catalysed rearrangement of *N*-(allyloxy-1,1-*d*<sub>2</sub>)-2(1*H*)-pyridinethione (5.1c)

Pyridinethione **5.1c** (6.70 mg,  $4.01 \times 10^{-5}$  mol) was dissolved in 500  $\mu\text{L}$  of  $\text{CDCl}_3$  in an ampoule and was treated with 5.0  $\mu\text{L}$  of a 0.277 M solution of trifluoromethanesulfonic acid in  $\text{CDCl}_3$  ( $1.39 \times 10^{-6}$  mol, 3.46 mol%). After degassing and sealing in a manner identical to the previous reaction, the solution was heated at  $80 \pm 1^\circ\text{C}$  for 19 hours and 42 minutes. Analysis was performed by  $^1\text{H}$  nmr, which revealed that about 60% of the starting material had been consumed. The relative yield of products was **5.2c**: 96%, **5.2c'**: 4%. After normalisation to compensate for the isotopic composition of **5.1c**, these values indicate that formally 98% of the rearrangement occurs *via* 1,4 rearrangement and 2% in a 3,4 sense.

**Procedure used to investigate the stereochemistry of the catalysed rearrangement of enantiomerically enriched *N*-(1-phenylethoxy)-2(1*H*)-pyridinethiones 5.1d(+) and 5.1d(-)**

*Reactions with 5.1d(-)*

All the reactions, except those performed under an oxygen atmosphere, were performed in the following manner. In an ampoule of capacity 2-3 mL was prepared a 0.22 M solution of **5.1d(-)** in the solvent of choice. This was treated with a measured volume of a solution of a catalyst. After degassing by freeze/pump/thaw degassing in the usual manner, the resulting mixture was flame-sealed under vacuum and placed into an 80±1°C oil bath, in the absence of light for a measured time.

Reactions involving oxygen as a catalyst were done in two ways. In acetonitrile, the pyridinethione solution was contained in a Reactival capped with a Mininert valve and oxygen gas was bubbled through solution for five min, *via* a needle. The valve was then closed and the reaction heated in the usual manner. In chloroform, the pyridinethione solution was contained in an Ace reaction tube (9 mL capacity) which was degassed by freeze/pump/thawing and sealed after admitting an oxygen atmosphere.

After reactions were complete, separation of the *N*-oxide product was performed by flash chromatography over silica, eluting with 5% MeOH in CH<sub>2</sub>Cl<sub>2</sub>. The *N*-oxide was purified further by complete sublimation at 0.08 Torr and 100°C to produce a crop of white crystals. The specific optical rotation was then determined at 589 nm in CDCl<sub>3</sub> solution at a concentration of about 10 mg/mL and at approximately 21°C. Purity was then checked by <sup>1</sup>H nmr and all samples were pure. Enantiomeric composition was determined relative to *R* (+) -2-(1-phenylethylsulfanyl)pyridine *N*-oxide (**5.2d(+)**), which has a specific optical rotation (at 589 nm) of + 130±1° in chloroform.

**Table 5.13.** Specific optical rotation data for the *N*-oxide product, isolated from the catalysed rearrangement reactions of **5.1d(-)**

Catalyst	Quantity (mol%)	Solvent	Time (hr)	Product specific optical rotation
I <sub>2</sub>	5.0	CDCl <sub>3</sub>	4.0	- 65.2±0.9°
I <sub>2</sub>	2.00	CDCl <sub>3</sub>	4.0	- 76.6±0.9°
I <sub>2</sub>	1.92	CD <sub>3</sub> CN	4.0	+ 5.4±0.2°
I <sub>2</sub>	2.03	CH <sub>3</sub> CN	4.0	+ 5.0±0.2°
O <sub>2</sub>	145	CDCl <sub>3</sub>	24	- 13.8±0.2°
O <sub>2</sub>	unknown	CH <sub>3</sub> CN	24	+ 48.4±0.7°
Fc <sup>+</sup> PF <sub>6</sub> <sup>-</sup>	1.00	CH <sub>3</sub> CN	4.0	+ 22.6±0.4°
Ni (III) SAR	1.00	CH <sub>3</sub> CN	4.0	+ 32.8±0.4°



*Rearrangement reactions of 5.1d(+)*

1. Pyridinethione **5.1d(+)** (48.33 mg, 0.2090 mmol) was dissolved in 1.00 mL of CDCl<sub>3</sub> and treated with 9.30 μL of a 0.116 M solution of iodine in CDCl<sub>3</sub> ( $1.08 \times 10^{-6}$  mol, 0.518 mol%). This solution was degassed and flame sealed under vacuum in the usual manner, then heated in the dark at 80±1° for 4.00 hours. Analysis by <sup>1</sup>H nmr revealed that only 30% of the starting material had been consumed. After treatment with a further 20.0 μL of the iodine solution (total moles =  $3.40 \times 10^{-6}$  mol, 1.63 mol%) and degassing and resealing, the mixture was heated for a further 11 hours. Treatment with a little hexane produced a yellow precipitate to form, then the solvents were removed under vacuum. The resulting solid was washed three times with hexane to remove iodine and any remaining pyridinethione. Reprecipitation from benzene/hexane gave a white solid of specific optical rotation (589 nm) of + 53.1±0.8°.

2. A reaction was performed in the same way as for **5.1d(-)**, using 2.04 mol% iodine, and heating at 80°C for 5.0 hours. The *N*-oxide product was isolated by flash chromatography, followed by sublimation, to give a white solid of specific optical rotation of + 58.2±0.8°.

**The iodine catalysed rearrangement of *N*-cyclopropylmethoxy-2(1*H*)-pyridinethione (5.1e)**

In an Ace brand pressure reaction tube (9 mL capacity) was placed pyridinethione **5.1e** (0.40 g, 2.2 mmol) and 8.0 mL of purified CHCl<sub>3</sub>. To the resulting solution was added iodine (33.0 mg, 0.130 mmol, 5.9 mol%) and the mixture was swirled until the iodine dissolved. Deoxygenation was accomplished by three freeze/pump/thaw cycles, then the solution was placed under a dry nitrogen atmosphere. The vessel was heated at 80±1°C in a thermostatted oil bath for 5.5 hours under minimal light. After cooling, the solvent was removed by rotary evaporation then high vacuum to yield a yellow, viscous oil (0.44 g). Analysis by <sup>1</sup>H nmr indicated the following compounds were present in the molar ratios shown: 2-(cyclopropylmethylsulfanyl)pyridine *N*-oxide (**5.2e**, 100); *N*-cyclopropylmethoxy-2(1*H*)-pyridinethione (**5.1e**, 20); and cyclopropylmethanol (2.7). There was no detectable resonance in the range 5.0-6.5 ppm, indicating an absence of alkene functionality. In addition, no peak was detected in the ranges 1.5-2.5 ppm and 3.5-4.1 ppm, which is where hydrogens of sulfur-substituted cyclobutyl rings normally resonate. It can be concluded that the cyclopropylmethyl group does not undergo ring opening to an alkene to any measurable extent, nor ring expansion to a cyclobutane compound.

### Investigation of the effect of alkoxy substituent structure upon migration rate (product yield)

The following procedure was used for each pyridinethione undergoing testing. A  $\text{CDCl}_3$  solution of the pyridinethione was prepared in an ampoule, such that the concentration of the solute was approximately 50 mg/mL. This corresponded with molarities in the range 0.2-0.3 M. After treating the solution with a measured amount of a solution of iodine in  $\text{CDCl}_3$  (usually 0.50 mol%), the mixture was degassed with two freeze/pump/thaw cycles, then frozen, pumped and flame-sealed under vacuum. The ampoule was placed in an  $80 \pm 1^\circ\text{C}$  thermostatted oil bath for a measured period (commonly 4.0 hours) under minimal light. After cooling, the yield of the *N*-oxide product was determined by  $^1\text{H}$  nmr spectroscopy. Results of these experiments are listed in table 5.6.

### Attempted detection/interception of intermediates in the rearrangement of *N*-benzyloxy-2(1*H*)-pyridinethione (5.1a)

#### *Effect of a radical scavenger*

A 0.230 M solution of *N*-benzyloxy-2(1*H*)-pyridinethione in  $\text{CDCl}_3$ , a 0.342 M solution of the radical scavenger 1,4-benzoquinone in  $\text{CDCl}_3$  and a 0.140 M solution of iodine in  $\text{CDCl}_3$  were prepared. Three different reactions were conducted, in ampoules, to determine the effect the scavenger had upon the rate of the iodine-catalysed rearrangement of the pyridinethione. The contents of each ampoule were:

- 500  $\mu\text{L}$  (0.115 mmol) of the pyridinethione solution, 10.0  $\mu\text{L}$  ( $3.42 \times 10^{-6}$  mol, 2.97 mol%) of the benzoquinone solution and 4.10  $\mu\text{L}$  ( $5.74 \times 10^{-7}$  mol, 0.50 mol%) of the iodine solution;
- 500  $\mu\text{L}$  (0.115 mmol) of the pyridinethione solution and 4.10  $\mu\text{L}$  ( $5.74 \times 10^{-7}$  mol, 0.50 mol%) of the iodine solution; and
- 500  $\mu\text{L}$  (0.115 mmol) of the pyridinethione solution and 10.0  $\mu\text{L}$  ( $3.42 \times 10^{-6}$  mol, 2.97 mol%) of the benzoquinone solution.

Each solution was degassed and flame-sealed under vacuum in the usual manner, then heated under minimal light in an  $80 \pm 1^\circ\text{C}$  thermostatted oil bath for a total of 2.00 hours. Yields of the product 2-(benzylsulfanyl)pyridine *N*-oxide (**5.2a**) were established using  $^1\text{H}$  nmr spectroscopy. The yields were: a) 72.2%; b) 74.7%; and c) 3.2%.

*Isolation and attempted identification of products resulting from the reaction of N-benzyloxy-2(1H)-pyridinethione (5.1a) and tris(p-bromophenyl)aminium hexachloroantimonate (5.33)*

The aminium salt **5.33** (0.2991 g, 0.3663 mmol) was added under a nitrogen blanket to 25 mL of dichloromethane, forming a deep blue solution. To this was added, in small portions, *N*-benzyloxy-2(1H)-pyridinethione **5.1a**, which caused a gradual colour change. Additions were continued until there was a permanent loss of the blue colour and a yellow/brown precipitate in a brown solution resulted. At this stage 0.1025 g (0.4717 mmol, 1.29 eq.) of **5.1a** had been added. Centrifugation settled the solids and the liquid phase was drawn off. The remaining precipitate (0.1864 g) was dried under high vacuum. If the molecular formula of  $C_{12}H_{11}NOSSbCl_6$  is correct, 0.3378 mmol (92%) was obtained.

$^1H$  nmr ( $CD_3OD$ ): 4.63 (s, 2H), 5.82 (s, 2H), 7.30-7.45 (m, 4H), 7.50-7.60 (m, 7H), 7.66 (d, 2H), 8.02 (dt, 1H), 8.28 (d, 1H), 8.43 (t, 1H), 8.48 (d, 1H), 9.49 (d, 1H).

MS (+FAB, 1:1 glycerol:thioglycerol matrix 160-730 amu): 497 (80), 429 (7), 391 (19), 308 (33), 280 (54), 218 (100).

MS (+Electrospray,  $CH_3CN$ ): 343 (100), 308 (3), 253 (43), 233 (70), 218 (6), 186 (7), 142 (8), 132 (9).

Found: C, 27.34; H, 1.70; N, 2.97; Sb, 22.79%.  $C_{12}H_{11}NOSSbCl_6$  requires: C, 26.12; H, 2.01; N, 2.54; Sb, 22.07%.

The liquid phase from centrifugation was evaporated and the components were separated by flash chromatography. Eluent polarity was gradually increased in the order light alkanes, diethyl ether, 50/50 methanol/dichloromethane, then methanol. By far the largest component was tris(*p*-bromophenyl) amine (0.1528 g, 0.3170 mmol, 87%), identified by comparison of nmr spectra with those of an authentic sample. A second fraction (14.9 mg) was a yellow/brown solid which had a  $^1H$  nmr spectrum consisting of aromatic resonances ranging from 6.6 to 7.9 ppm, but its structure remains unknown. A third fraction (32.0 mg) was a yellow solid but no reasonable  $^1H$  nmr spectrum could be obtained in  $CDCl_3$  solution. The mass recovery for the reaction was 0.3861 g (96%).

## 5.7 References

1. Wagner, G. and Pischel, H. *Arch. Pharm.* **1963**, 296, 576.
2. Pluijgers, C. W.; Berg, J. and Thorn, G. D. *Recl. Trav. Chim. Pays-Bas* **1969**, 88, 241.
3. Jeffcoat, A. R.; Gibson, W. B.; Rodriguez, P. A.; Turan, T. S.; Hughes, P. F. and Twine, M. E. *Toxicol. Appl. Pharmacol.* **1980**, 56, 141.
4. Tachikawa, R.; Wachi, K.; Sato, S. and Terada, A. *Chem. Pharm. Bull.* **1981**, 29, 3529.
5. Beckwith, A. L. J. and Hay, B. P. *J. Am. Chem. Soc.* **1988**, 110, 4415.
6. Beckwith, A. L. J. and Hay, B. P. *J. Am. Chem. Soc.* **1989**, 111, 230.
7. Hay, B. P. and Beckwith, A. L. J. *J. Org. Chem.* **1989**, 54, 4330.
8. Lampard, C.; Murphy, J. A. and Lewis, N. *Tetrahedron*, **1993**, 49, 3841.
9. Hartung, J. and Gallou, F. *J. Org. Chem.* **1995**, 60, 6706.
10. Girard, P.; Guillot, N.; Motherwell, W. B. and Potier, P. *J. Chem. Soc. Chem. Commun.* **1995**, 2385.
11. Hartung, J.; Hiller, M. and Schmidt, P. *Chem. Eur. J.* **1996**, 2, 1014.
12. Hartung, J.; Hiller, M. and Schmidt, P. *Liebigs Ann.* **1996**, 1425.
13. Hartung, J.; Hiller, M.; Schwarz, M.; Svoboda, I. and Fuess, H. *Liebigs Ann.* **1996**, 2091.
14. Hartung, J. *Synlett* **1996**, 1206.
15. Hartung, J.; Svoboda, I.; Fuess, H. and Duarte, M. T. *Acta Cryst. C.* **1997**, 53, 1629.
16. Adam, W.; Grimm, G. N. and Saha-Moller, C. R. *Free Radic. Biol. Med.* **1998**, 24, 234.
17. Adam, W.; Grimm, G. N.; Marquardt, S. and Saha-Moller, C. R. *J. Am. Chem. Soc.* **1999**, 121, 1179.
18. Hartung, J.; Kneuer, R.; Schwarz, M.; Svoboda, I. and Fuess, H. *Eur. J. Org. Chem.* **1999**, 97.
19. Hartung, J. and Kneuer, R. *Eur. J. Org. Chem.* **2000**, 1677.

20. Wiselogle, F. Y.; Losee, K. A. and Bernstein, J. *Chemical Abstracts* **1957**, *51*, P2881d.
21. Crich, D. *Aldichimica Acta* **1987**, *20*, 35.
22. Zamojski, A. *Chemtracts - Org. Chem.* **1995**, *8*, 181.
23. Barton, D. H. R. and Ferreira, J. A. *Phosphorus Sulfur Silicon Relat. Elem.* **1997**, *120*, 1.
24. Barton, D. H. R.; Crich, D. and Motherwell, W. B. *J. Chem. Soc. Chem. Commun.* **1983**, 939.
25. Barton, D. H. R.; Jaszberenyi, J. Cs. and Morrell, A. I. *Tetrahedron Lett.* **1991**, *32*, 311.
26. Adam, W.; Ballmaier, D.; Epe, B.; Grimm, G. N. and Saha-Moller, C. R. *Angew. Chem. Int. Ed. Engl.* **1995**, *34*, 2156.
27. Epe, B.; Ballmaier, D.; Adam, W.; Grimm, G. N. and Saha-Moller, C. R. *Nucleic Acids Res.* **1996**, *24*, 1625.
28. Aveline, B. M.; Kochevar, I. E. and Redmond, R. W. *J. Am. Chem. Soc.* **1996**, *118*, 10113.
29. Adam, W.; Marquardt, S. and Saha-Moller, C. R. *Photochem. Photobiol.* **1999**, *70*, 287.
30. Newcomb, M. and Kumar, M. U. *Tetrahedron Lett.* **1991**, *32*, 45.
31. Beckwith, A. L. J. and Davison, I. G. E. *Tetrahedron Lett.* **1991**, *32*, 49.
32. Newcomb, M.; Park, S. -U.; Kaplan, J. and Marquardt, D. J. *Tetrahedron Lett.* **1985**, *26*, 5651.
33. Newcomb, M. and Deeb, T. M. *J. Am. Chem. Soc.* **1987**, *109*, 3163.
34. Esker, J. L. and Newcomb, M. *Tetrahedron Lett.* **1992**, *33*, 5913.
35. Horner, J. H.; Musa, O.; Bouvier, A. and Newcomb, M. *J. Am. Chem. Soc.* **1998**, *120*, 7738.
36. Avila, L. Z. and Frost, J. W. *J. Am. Chem. Soc.* **1988**, *110*, 7904.
37. Koenig, T. in *Free Radicals*; Kochi, J. K., Ed.; John Wiley and Sons: New York, 1973, vol. 1, p. 113.

38. Walling, C. and Padwa, A. *J. Am. Chem. Soc.* **1963**, 85, 1593.
39. Walling, C. and Clark, R. T. *J. Am. Chem. Soc.* **1974**, 96, 4530.
40. Brun, P. and Waegell, B. *Tetrahedron* **1976**, 32, 517.
41. Barton, D. H. R. *Pure Appl. Chem.* **1968**, 16, 1.
42. Hesse, R. H. *Adv. Free-Radical Chem.* **1969**, 3, 83.
43. Mihailovic, M. Lj. and Cekovic, Z. *Synthesis* **1970**, 209.
44. Beckwith, A. L. J.; Hay, B. P. and Williams, G. W. *J. Chem. Soc., Chem. Commun.* **1989**, 1202.
45. Pasto, D. J. and Cottard, F. *Tetrahedron Lett.* **1994**, 35, 4303.
46. Aveline, B. M.; Kochevar, I. E. and Redmond, R. W. *J. Am. Chem. Soc.* **1995**, 117, 9699.
47. Yadav, V. K.; Yadav, A.; Pande, P. and Kapoor, K. K. *Indian J. Chem. Sect. B.* **1994**, 33, 1129.
48. Wagner, G. and Pischel, H. *Arch. Pharm.* **1962**, 295, 897.
49. Shaw, E. *J. Am. Chem. Soc.* **1949**, 71, 67.
50. Dinan, F. J. and Tieckelmann, H. *J. Org. Chem.* **1964**, 29, 1650.
51. Litster, J. E. and Tieckelmann, H. *J. Am. Chem. Soc.* **1968**, 90, 4361.
52. Schollkopf, U. and Hoppe, I. *Tetrahedron Lett.* **1970**, 4527.
53. Schollkopf, U. and Hoppe, I. *Liebigs Ann. Chem.* **1972**, 765, 153.
54. Gerhart, F. and Wilde, L. *Tetrahedron Lett.* **1974**, 475.
55. le Noble, W. J. and Daka, M. R. *J. Am. Chem. Soc.* **1978**, 100, 5961.
56. Alker, D.; Mageswaran, S.; Ollis, W. D. and Shahriari-Zavareh, H. *J. Chem. Soc., Perkin Trans. 1* **1990**, 1631.
57. Alker, D.; Ollis, W. D. and Shahriari-Zavareh, H. *J. Chem. Soc., Perkin Trans. 1* **1990**, 1637.
58. Jones, R. A. and Katritzky, A. R. *J. Chem. Soc.* **1960**, 2937.
59. Kohrman, R. E.; West, D. X. and Little, M. A. *J. Heterocycl. Chem.* **1974**, 11, 101.
60. Wallace, T. J.; Schriesheim, A. and Bartok, W. *J. Org. Chem.* **1963**, 28, 1311.

61. Gilbert, B. C. and Whitwood, A. C. *J. Chem. Soc. Perkin Trans. 2* **1989**, 1921.
62. Janes, R. and Symons, M. C. R. *J. Chem. Soc. Faraday Trans.* **1990**, 86, 2173.
63. Hart, H.; Rodgers, T. R. and Griffiths, J. *J. Am. Chem. Soc.* **1969**, 91, 752.
64. Childs, R. F. and Winstein, S. *J. Am. Chem. Soc.* **1974**, 96, 6409.
65. Miller, B. and Saidi, M. R. *Tetrahedron Lett.* **1975**, 1365.
66. Miller, B. *Acc. Chem. Res.* **1975**, 8, 245.
67. Vittorelli, P.; Peter-Katalinic, J.; Mukherjee-Muller, G.; Hansen, H. J. and Schmid, H. *Helv. Chim. Acta* **1975**, 58, 1379.
68. Miller, B. and Saidi, M. R. *J. Am. Chem. Soc.* **1976**, 98, 2227.
69. Miller, B. and Lin, W.-O. *J. Org. Chem.* **1979**, 44, 887.
70. Felkin, H. and Tambute, A. *Tetrahedron Lett.* **1969**, 821.
71. Biellman, J. F. and Ducep, J. B. *Tetrahedron Lett.* **1970**, 2899.
72. Magid, R. M. and Wilson, S. E. *Tetrahedron Lett.* **1971**, 19.
73. Felkin, H. and Frajerman, C. *Tetrahedron Lett.* **1977**, 3485.
74. Rautenstrauch, V. *Helv. Chim. Acta* **1972**, 55, 594.
75. Garst, J. F. and Smith, C. D. *J. Am. Chem. Soc.* **1976**, 98, 1526.
76. Crombie, L.; Darnbrough, G. and Pattenden, G. *J. Chem. Soc., Chem. Commun.* **1976**, 684.
77. Briere, R.; Cherest, M.; Felkin, H. and Frajerman, C. *Tetrahedron Lett.* **1977**, 3489.
78. See references 56 and 57.
79. Bellville, D. J.; Wirth, D. D. and Bauld, N. L. *J. Am. Chem. Soc.* **1981**, 103, 718.
80. Bauld, N. L.; Bellville, D. J.; Pabon, R.; Chelsky, R. and Green, G. *J. Am. Chem. Soc.* **1983**, 105, 2378.
81. Bellville, D. J. and Bauld, N. L. *Tetrahedron* **1986**, 42, 6167.
82. Bauld, N. L.; Bellville, D. J.; Harirchian, B.; Lorenz, K. T.; Pabon, R. A.; Reynolds, D. W.; Wirth, D. D.; Chiou, H. -S. and Marsh, B. K. *Acc. Chem. Res.* **1987**, 20, 371.
83. Reynolds, D. W.; Lorenz, K. T.; Chiou, H. -S.; Bellville, D. J.; Pabon, R. A. and

- Bauld, N. L. *J. Am. Chem. Soc.* **1987**, *109*, 4960.
84. Bauld, N. L. *Tetrahedron* **1989**, *45*, 5307.
85. Yueh, W. and Bauld, N. L. *J. Am. Chem. Soc.* **1995**, *117*, 5671.
86. Valentine, D.; Turro, N. J., Jr and Hammond, G. S. *J. Am. Chem. Soc.* **1964**, *86*, 5202.
87. Konig, W. A.; Francke, W. and Benecke, I. *J. Chromatogr.* **1982**, *239*, 227.
88. Huck, H. and Schmidt, H.-L. *Angew. Chem. Int. Ed. Engl.* **1981**, *20*, 402.
89. Cavalieri, E. and Roth, R. *J. Org. Chem.* **1976**, *41*, 2679.
90. Smejtek, P.; Honzl, J. and Metalova, V. *Coll. Czech. Chem. Commun.* **1965**, *30*, 3875.
91. Wheeler, L. O.; Santhanam, K. S. V. and Bard, A. J. *J. Phys. Chem.* **1966**, *70*, 404.
92. Forbes, W. F. and Sullivan, P. D. *J. Am Chem. Soc.* **1966**, *88*, 2862.
93. Lucken, E. A. C. *Theor. Chim. Acta.* **1963**, *1*, 397.
94. Gassman, P. G. and Singleton, D. A. *J. Am Chem. Soc.* **1984**, *106*, 7993.
95. Katritzky, A. R. *J. Chem. Soc. (London)* **1957**, 191.
96. Duggan, D. M. and Hendrickson, D. N. *Inorg. Chem.* **1975**, *14*, 955.
97. Coates, R. M. and Chen, J. P. *Tetrahedron Lett.* **1969**, 2705.
98. Benecke, I. and Konig, W. A. *Angew. Chem., Int. Ed. Engl.* **1982**, *21*, 709.
99. Crossland, R. K. and Servis, K. L. *J. Org. Chem.* **1970**, *35*, 3195.
100. Hutchins, R. O.; Masilamani, D. and Maryanoff, C. A. *J. Org. Chem.* **1976**, *41*, 1071.
101. Isola, M.; Ciuffarin, E. and Sagramora, L. *Synthesis* **1976**, 326.
102. Rinaldi, P. L. *Prog. NMR Spectrosc.* **1982**, *15*, 291.
103. Jacques, J.; Collet, A. and Wilen, S. H. *Enantiomers, Racemates and Resolutions*; Wiley-Interscience, 1981, pp 162-165.
104. Suckling, C. J. *Angew. Chem. Int. Ed. Engl.* **1988**, *27*, 537.
105. Beckwith, A. L. J.; Bowry, V. W. and Moad, G. *J. Org. Chem.* **1988**, *53*, 1632.
106. Cacace, F.; Chiavarino, B. and Crestoni, M. E. *Chem. Eur. J.* **2000**, *6*, 2024.



107. Szeimies, G.; Schlosser, A.; Philipp, F.; Dietz, P. and Mickler, W. *Chem. Ber.* **1978**, *111*, 1922.
108. Kimmelma, R. *Acta Chem. Scand. Ser. B* **1987**, *41*, 344.
109. March, J. *Advanced Organic Chemistry, 3rd Ed.*; Wiley-Interscience, New York, 1985, p 145.
110. Smie, A. and Heinze, J. *Angew. Chem. Int. Ed. Engl.* **1997**, *36*, 363.
111. Claridge, R. F. C. and Dohrmann, J. *Landolt-Bornstein Group 2; Vol. 18, Subvolume E1*; Springer-Verlag, Berlin-Heidelberg; 1997; pp 40-133.
112. Ito, O.; Tamura, S.; Murakami, K. and Matsuda, M. *J. Org. Chem.* **1988**, *53*, 4758.
113. Faller, J. W.; Blankenship, C.; Whitmore, B. and Sena, S. *Inorg. Chem.* **1985**, *24*, 4483.
114. Nakata, R.; Okazaki, S. and Fujinaga, T. *J. Electroanal. Chem.* **1981**, *125*, 413.
115. Compound and  $E^0$  value supplied by Professor A. M. Sargeson, Research School of Chemistry, Australian National University.
116. Mehta, S. and Pinto, B. M. *Carbohydr. Res.* **1998**, *310*, 43.
117. Ballesteros, P.; Senent, S. and Elguero, J. *Bull. Soc. Chim. Belg.* **1990**, *99*, 595.
118. Wolfe, S.; Yang, K.; Weinberg, N.; Shi, Z.; Hsieh, Y.-H.; Sharma, R. D.; Ro, S. and Kim, C.-K. *Chem. Eur. J.* **1998**, *4*, 886.
119. Wolfe, S.; Hsieh, Y.-H.; Batchelor, R. J.; Einstein, F. W. B. and Gay, I. D. *Can. J. Chem.* **2001**, *79*, 1272.
120. Barton, D. H. R.; Bridon, D.; Fernandez-Picot, I. and Zard, S. Z. *Tetrahedron* **1987**, *43*, 2733.
121. Kurzer, F. *Org. Synth.* **1963**, *Coll. Vol. 4*, 937.
122. Wilt, J. W.; Stein, R. G. and Wagner, W. G. *J. Org. Chem.* **1967**, *32*, 2097.
123. Hoffmann, H. M. R. and Hughes, E. D. *J. Chem. Soc.* **1964**, 1244.
124. Gilman, H. and Catlin, W. E. *Org. Synth.* **1941**, *Coll. Vol. 1*, 188.
125. Hartung, J. *Eur. J. Org. Chem.* **2001**, 619.
126. Hartung, J.; Kneuer, R.; Schwarz, M. and Heubes, M. *Eur. J. Org. Chem.* **2001**,

4733.

127. Hartung, J.; Kneuer, R.; Kopf, T. M. and Schmidt, P. *C. R. Acad. Sci. Paris, Chimie* **2001**, *4*, 649.

128. See Harman, D. G. *This thesis*, Chapters 1, 2 and 3 and references within.

129. Hartung, J., Gottwald, T. and Špehar, K. *Synthesis* **2002**, 1469.

130. Tschugaeff, L. *Ber. Dtsch. Chem. Ges.* **1899**, *32*, 3332.

## Chapter 6

### General discussion and conclusions

6.1	Introduction	285
6.2	The $\beta$ -trifluoroacetoxyalkyl radical rearrangement	285
6.3	Related radical-mediated rearrangements and $\beta$ -eliminations	297
6.4	The mechanism of the rearrangement of <i>N</i> -alkoxy-2(1 <i>H</i> )-pyridinethiones	301
6.5	Final remarks	301
6.6	References	303

## 6.1 Introduction

This chapter begins with a summary of what the current research has revealed about the mechanism of the rearrangement of the 2-methyl-2-trifluoroacetoxy-1-heptyl radical. The relative magnitude of migrating group effects of the  $\beta$ -trifluoroacetoxyalkyl radical rearrangement and an analogous ionic process are then discussed. The relationship between rearrangement regiochemistry and kinetics is then examined. Low-level theoretical calculations are performed in order to discover whether the *E/Z* conformational distribution in the ester group is controlled by solvent polarity and can therefore account for the observed rearrangement regiochemistry. The dynamics for a radical ion pair are investigated to determine whether such an intermediate is plausible and conclusions about the mechanism of the  $\beta$ -trifluoroacetoxyalkyl radical rearrangement are provided. Conclusions are drawn about the mechanism of the  $\beta$ -trifluoroacetoxyalkyl radical rearrangement.

Rearrangements and  $\beta$ -elimination reactions related to the  $\beta$ -acyloxyalkyl radical rearrangement are briefly discussed. The mechanism of the rearrangement of *N*-alkoxy-2(1*H*)-pyridinethiones and its relationship to that of the  $\beta$ -acyloxyalkyl radical rearrangement are discussed. The chapter concludes with a summary of the mechanism of the  $\beta$ -trifluoroacetoxyalkyl radical rearrangement and the differences between pericyclic processes and radical ion pairs. The chapter concludes with reflections on the differences between polarized pericyclic processes and radical ion pairs and with hypotheses as to the chemical physics of reactions which occur over an extremely short time period.

## 6.2 The $\beta$ -trifluoroacetoxyalkyl radical rearrangement

### 6.2.1 What is known about the rearrangement of the 2-methyl-2-trifluoroacetoxy-1-heptyl radical?

The rearrangement is definitely radical in nature. Trifluoroacetoxy group migration occurs under conditions known to produce carbon-centred radicals and stalled reactions are restarted by the addition of the radical initiators AIBN or di-*tert*-butyl

hyponitrite. The esr spectra of several  $\beta$ -trifluoroacetoxyalkyl radicals have been recorded during this research and by other groups.

There is no rearrangement observed until the  $\beta$ -trifluoroacetoxyalkyl radical is generated. Experiments in which an oxygen-labelled  $\beta$ -bromotrifluoroacetate is heated in the presence of a radical initiator but in the absence of the hydrogen atom source demonstrate that there is no fission of the alkoxy C–O bond until after the bromine atom is removed.

The rearrangement is intramolecular. A crossover experiment has demonstrated that there is no significant amount of exchange of trifluoroacetoxy groups between radicals or molecules.

Furthermore, free trifluoroacetate ions are not significantly involved in the rearrangement step. An experiment designed to trap a possible intermediate—the radical cation of 2-methyl-1-heptene—with unlabelled trifluoroacetate ion yielded results which indicated that the extent of trapping does not exceed 3% in the rearranged product.

There is no strong electronic effect which acts to lock the radical into a conformation favourable for rearrangement. Esr spectroscopy has established that the barrier to rotation about the  $C_{\alpha}$ – $C_{\beta}$  bond in  $\beta$ -acyloxyethyl radicals is approximately the same of that for the propyl radical.

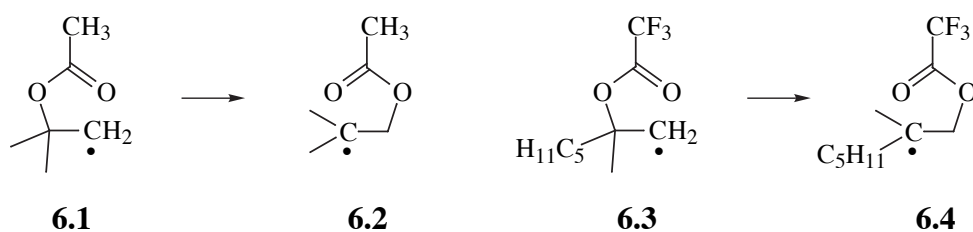
The  $\beta$ -trifluoroacetoxyalkyl radical rearrangement has polar character. The rearrangement is promoted by polar solvents, although the solvent effects are only a fraction of that of comparable ionic reactions. Trifluoroacetoxy groups have been shown to migrate more rapidly than acetoxy groups in otherwise identically-structured radicals.

A trifluoroacetoxy group does not appear to migrate cleanly by either 1,2 or 3,2 rearrangement. Studies with radicals bearing an  $^{17}\text{O}$ - and  $^{18}\text{O}$ -labelled trifluoroacetoxy group reveal that the rearrangement proceeds predominantly with label transposition (3,2 shift), but the degree of 1,2 shift increases with increasing solvent polarity, increasing temperature and decreasing reducing agent concentration. The rearrangement has also been shown to be reversible.

### 6.2.2 Migrating group electronic effects

In chapter 2, it was established that the solvent effects upon the rate of the rearrangement of the 2-methyl-2-trifluoroacetoxy-1-heptyl radical were only a fraction as large as those observed in the solvolysis of *tert*-butyl chloride. A comparison will now be made between the difference in reactivity of acetoxy and trifluoroacetoxy groups in the  $\beta$ -acyloxyalkyl radical rearrangement and in solvolysis reactions.

Arrhenius parameters and rate constants at 75°C for the migration of acetoxy and trifluoroacetoxy groups in similarly-constituted  $\beta$ -acyloxyalkyl radicals are displayed in table 6.1. A trifluoroacetoxy group migrates with a rate constant approximately 560 times as great as that for an acetoxy group.



**Table 6.1.** Rearrangement of  $\beta$ -acetoxyalkyl and  $\beta$ -trifluoroacetoxyalkyl radicals

Rearrangement	Solvent	$\log_{10}(A/s^{-1})$	$E_a$ (kJmol <sup>-1</sup> )	$k_r$ (s <sup>-1</sup> ) at 75°C
<b>6.1</b> → <b>6.2</b> <sup>a</sup>	<i>t</i> -butyl benzene	13.9±1.1	75±8	4.5 × 10 <sup>2</sup>
<b>6.3</b> → <b>6.4</b> <sup>b</sup>	benzene	12.0±0.2	43.7±0.8	2.5 × 10 <sup>5</sup>

a: From table 2.1, chapter 2; b: Current research

Table 6.2 contains Arrhenius parameters and calculated rate constants at 75°C for the first order hydrolysis of *t*-butyl acetate<sup>1</sup> and *t*-butyl trifluoroacetate<sup>2</sup> in water. Unfortunately, solvolysis rate data in aromatic hydrocarbon solution could not be found. By comparison, the ratio of rate constants at 75°C is about 24000, approximately 44 times that for the radical rearrangements.

**Table 6.2.** Hydrolysis of tertiary esters in water

Ester	$\log_{10}(A/s^{-1})$	$E_a$ (kJmol <sup>-1</sup> )	$k_{SN1}$ (s <sup>-1</sup> ) at 75°C
<i>t</i> -butyl acetate	12.3	112.1	$3.00 \times 10^{-5}$
<i>t</i> -butyl trifluoroacetate	16.2	109.0	$7.35 \times 10^{-1}$

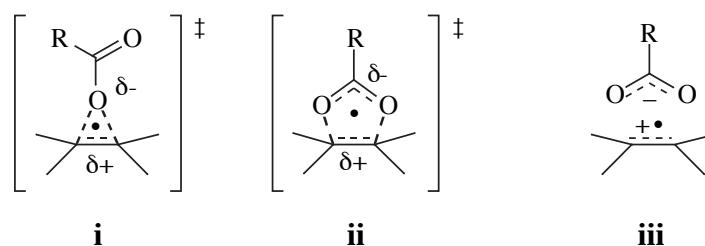
The magnitude of the electron-withdrawing effect of the ester group upon the rate constant is much smaller in the case of the radical rearrangement. This is consistent with the absence of free carboxylate ions during the rearrangement. The source of the rate effect is reflected primarily in the  $E_a$  (enthalpic) term for the radical rearrangements, but in the  $\log_{10}A$  (entropic) term for the hydrolysis reactions. The relative closeness of the  $\log_{10}A$  values for the radical rearrangements indicates a similar entropy in the respective transition states to the rate-limiting step.

### 6.2.3 Relationship between rearrangement regiochemistry and kinetics

Table 6.3 illustrates the relationship between the kinetics and regiochemistry for the rearrangement of the 2-methyl-2-trifluoroacetoxy-1-heptyl radical (**6.3**) as a function of solvent polarity. It is clear that an increase in solvent polarity is accompanied by an increase in the rearrangement rate constant ( $k_r$ ), and in the degree of 1,2 shift ( $R_E$ ). The differences observed in both  $k_r$  and  $R_E$  between the reactions in hexane and benzene are remarkable considering the relatively small increase in solvent polarity. A sizeable reduction in the activation energy term ( $E_a$ ) accompanies the increase in solvent polarity.

In chapter 3 an estimate of the difference in Arrhenius parameters between the hypothetical concerted, polarized 1,2 (i) and 3,2 (ii) shifts was made from experimental data. The 1,2 shift had  $\Delta E_a = +9.5$  kJmol<sup>-1</sup> and  $\Delta \log_{10}(A/s^{-1}) = +1.01$  compared with the respective parameters for the 3,2 shift in benzene solution. If  $R_E$  increases, the proportion of 1,2 shift must increase relative to that for the 3,2 shift. But no significant increase in either  $\log_{10}A$  or  $E_a$  accompanies the increase in  $R_E$  in polar solvents. However, recent MO calculations do predict that  $\Delta \Delta G$  between the 5-membered transition

structure **ii** and the 3-membered structure **i** decreases in polar solvents.<sup>15</sup>



**Table 6.3.** Solvent effects upon the rearrangement **6.3**→**6.4**.

Solvent	$\epsilon$ at 25°C	$E_T(30)$ (kcalmol <sup>-1</sup> )	$\log_{10}A$ (s <sup>-1</sup> )	$E_a$ (kJmol <sup>-1</sup> )	$k_T$ at 75°C (s <sup>-1</sup> )	$R_E$ (%) <sup>a</sup>
hexane	1.88	31.0	11.8	48.9	$2.91 \times 10^4$	18.5
benzene	2.27	34.3	12.0	43.7	$2.78 \times 10^5$	26.4
EtCN	28.86 <sup>b</sup>	43.6	11.9	42.0	$3.97 \times 10^5$	36.0

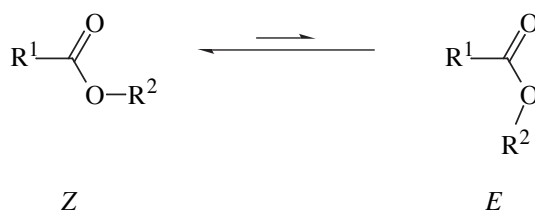
a: From table 3.5, Chapter 3. Average [Bu<sub>3</sub>SnH] = 6 mM; b: at 20°C

#### 6.2.4 Is the regiochemistry controlled by the conformation of the ester group?

From table 3.1 of chapter 3 it can be seen that the migration of acetoxy (entry 4), benzyloxy (entries 3 and 6) and butanoyloxy (entry 3) substituents in the rearrangement of simply-constituted  $\beta$ -acyloxyalkyl radicals proceeds with essentially complete transposition of ester oxygens ( $R_E = 0\%$ ). However, the present results and other work<sup>3</sup> have demonstrated that the rearrangement of  $\beta$ -trifluoroacetoxyalkyl radicals proceeds with predominant ester oxygen transposition together with a significant proportion of a formal 1,2 shift. The question then arose as to whether the increase in  $R_E$  observed with the migration of the electronegative trifluoroacetoxy group was caused by the presence of a significant amount of the *E* ester conformation and whether the proportion of this conformation is increased by polar solvents.

It is well accepted that the lowest energy conformation of esters is the *Z* form, being lower in energy than the *E* form by approximately 12 kJmol<sup>-1</sup>.<sup>4</sup>





The most favourable conformation of *t*-butyl trifluoroacetate in the gas phase was determined to be *Z* by low resolution microwave spectroscopy.<sup>5</sup> No signals attributable to the *E* form were detected and *ab initio* calculations (STO-3G basis set) revealed that the *E* form was 24 kJmol<sup>-1</sup> higher in energy.<sup>5</sup>

The dipole moment of the *E* conformation of an ester (~3.4 D) is generally significantly greater than that for the *Z* conformer (~1.5 D).<sup>6</sup> Oki and Nakanishi have reported that the proportion of the *E* conformer increases with increasing solvent polarity.<sup>6</sup> This solvent effect is particularly pronounced with *t*-butyl alkoxy substituents, where steric compression of the bulky alkyl group against the carbonyl oxygen becomes more significant. Even so, the effect is not large. At 30°C in DMF/DME (95/5 *v/v*) solution, the *E* isomer of *t*-butyl formate constitutes only 36% of the mixture of the two conformers.<sup>7</sup>

In an effort to determine whether  $\beta$ -trifluoroacetoxyalkyl radicals might favour the *E* ester group conformation in polar solution, theoretical dipole moments were calculated for the *E* and *Z* forms of both *t*-butyl acetate and *t*-butyl trifluoroacetate. Low-level semi-empirical calculations were performed with the AM1, PM3 and AM1-SM2 basis sets, using the program MacSpartan. Results are provided in table 6.4.

**Table 6.4.** Results of molecular orbital calculations

Compound	Conformer	$\mu$ (D) AM1	$\mu$ (D) PM3	$\mu$ (D) AM1-SM2	$\mu$ (D) (average)
<i>t</i> -butyl acetate	<i>E</i>	4.63	4.40	5.95	4.99±0.84
<i>t</i> -butyl acetate	<i>Z</i>	1.73	1.79	2.37	1.96±0.35
<i>t</i> -butyl trifluoroacetate	<i>E</i>	4.22	3.68	5.41	4.44±0.89
<i>t</i> -butyl trifluoroacetate	<i>Z</i>	3.35	3.19	4.20	3.58±0.54

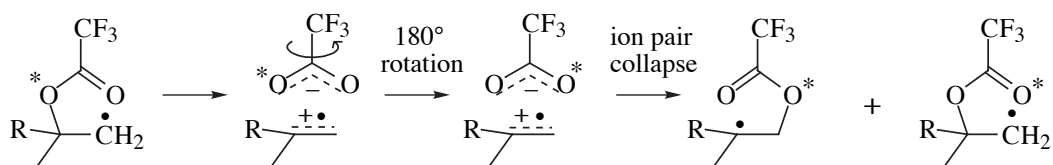
These simple calculations reveal that although the *Z* conformer of the ester always has a smaller predicted dipole moment than its *E* counterpart, the difference in magnitude of the dipole moment is much greater between the *E* and *Z* conformers of *t*-butyl acetate than for the corresponding trifluoroacetate. The effect of solvent stabilisation of the *E* trifluoroacetate should therefore be significantly smaller than for the acetate. There does not appear to be a large enough proportion of the *E* conformer in the incipient  $\beta$ -trifluoroacetoxyalkyl radical to rationalise the increasing proportion of 1,2 shift observed with increasing solvent polarity. Therefore, the stabilisation of the *E* conformation of the trifluoroacetoxy group does not appear to be the cause of the observed regiochemistry. This conclusion was also supported by the difference in the calculated heats of formation for the *E* and *Z* conformations of each of the esters.

### 6.2.5 The predicted dynamics for a radical ion pair intermediate

A preference for the *E* ester conformation has now been excluded as the cause of the observed rearrangement regiochemistry for the rearrangement of  $\beta$ -trifluoroacetoxyalkyl radicals. Although experimental kinetics and labelling results are consistent with a rearrangement mechanism which involves the cooperation of concerted 1,2 (i) and 3,2 (ii) shifts, the possibility of the intermediacy of an alkene-radical-cation/trifluoroacetate-anion pair (iii, R = CF<sub>3</sub>) cannot be excluded. The predicted dynamics of such an ion pair have been investigated in an effort to decide whether such an intermediate is feasible.

It is envisaged that a radical ion pair, formed by heterolysis of the alkoxy ester C–O bond, could experience relative rotation between the oppositely-charged fragments before collapsing to form the rearranged product radical, or to regenerate the initial radical in which the oxygen label has been scrambled. The collapse of this pair cannot be rate-limiting because the rearrangement rate constant increases with increasing solvent polarity and polar solvents would be expected to stabilise this complex. This process is depicted in scheme 6.1, the asterisk representing an oxygen label. For this process to be feasible, the half-life for the collapse of the ion pair and the period for a half-rotation of the

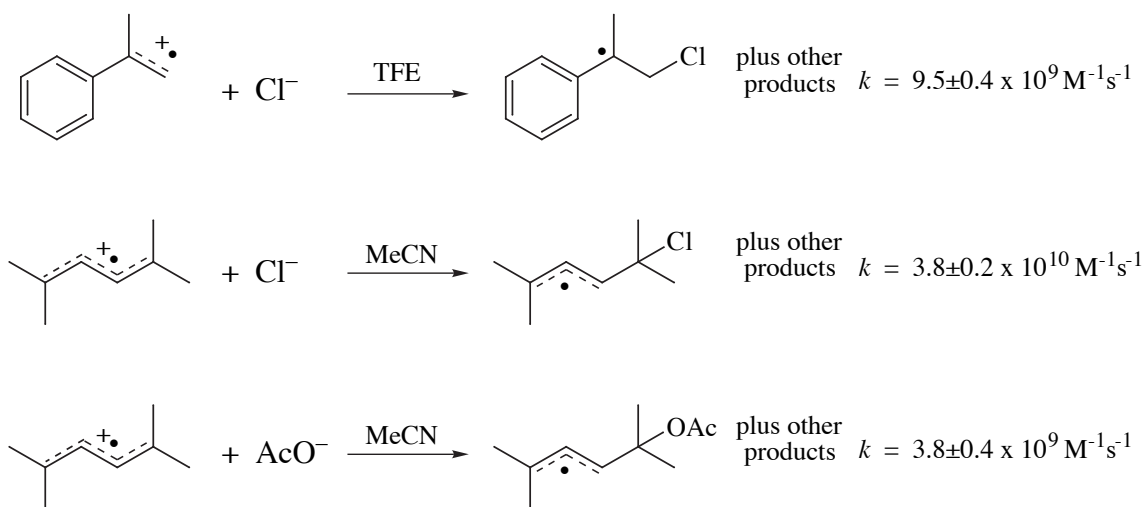
trifluoroacetate ion need to be approximately the same.



Scheme 6.1

No kinetic data could be found for the collapse of ion pair radicals in solution. Neither could data be found for the frequency of rotation of carboxylate ions in aprotic solvents. However, reasonable approximations could be made using literature data for model systems.

Laser flash photolysis has been used to determine the second order rate constants (at room temperature) for the reactions of a series of substituted styrene radical cations with nucleophiles in trifluoroethanol ( $\epsilon = 27.68$  at  $20^\circ\text{C}$ ) and acetonitrile/water mixtures<sup>8</sup> and for the reaction of 1,3 diene radical cations with nucleophiles in acetonitrile solution.<sup>9</sup> Both of these reactions are very fast, occurring at almost diffusion-controlled rates. Some model systems are illustrated below with accompanying rate constants at room temperature.



To approximate the first order rate constant for the collapse of an intimate radical ion pair, an effective concentration of trifluoroacetate ion is taken to be the concentration of neat trifluoroacetic acid (approximately 13 M at room temperature). So the first order rate constant for collapse of the radical ion pair is estimated to be in the range  $5 \times 10^{10}$  to  $5 \times 10^{11} \text{ s}^{-1}$  at room temperature, corresponding to a radical-ion pair half-life of about 1.4 ps to 14 ps. It is likely that 2-methyl-1-heptene radical cation is more reactive than the model systems due to decreased spin and charge delocalisation, yet trifluoroacetate is a weaker nucleophile than chloride or acetate. The rate constants will increase at elevated temperatures, but not by much because such reactions must have a low activation energy and hence a low temperature dependence.

Rate constants for the conversion of a contact ion pair (CIP) to a solvent-separated ion pair (SSIP) are of the order of  $10^8$ – $10^9 \text{ s}^{-1}$  for the 1,2,4,5-tetracyanobenzene (e-acceptor)/*p*-xylene (e-donor) system.<sup>10</sup> These results are expected to be typical for a larger range of ion pairs. The rate constant for the collapse of the radical ion pair in question is much larger than  $10^9 \text{ s}^{-1}$ , so there is little probability that a CIP has time to form a SSIP during the  $\beta$ -trifluoroacetoxyalkyl radical rearrangement.

The rotational constants have been determined for trifluoroacetic acid (an asymmetric top) in the gas phase by microwave spectroscopy.<sup>11</sup> From these were calculated the moments of inertia,  $I_a$ ,  $I_b$ ,  $I_c$ , about the mutually perpendicular axes  $A$ ,  $B$  and  $C$ , using equation 6.1,<sup>12a</sup>.  $B$  is the rotational constant (in Hz) for a particular axis and  $h$  is the Planck constant.

$$I = \frac{h}{8\pi^2 B} \quad (6.1)$$

The most populated rotational quantum state,  $J$ , may be calculated at any temperature,  $T$ , using equation 6.2:<sup>12b</sup>

$$\text{Maximum population: } J = \sqrt{\frac{kT}{2hB}} - \frac{1}{2} \quad (6.2)$$

and the angular velocity  $\omega$ , in  $\text{rad s}^{-1}$ , is given by:<sup>12c</sup>

$$\omega = \frac{h\sqrt{J(J+1)}}{2\pi I} \quad (6.3)$$

Hence, the frequency,  $\nu$ , in rotations per second is obtained by division by  $2\pi$ :

$$\nu = \frac{h\sqrt{J(J+1)}}{4\pi^2 I} \quad (6.4)$$

Rotational frequencies were calculated for trifluoroacetic acid in the gas phase, for the three mutually perpendicular axes,  $A$ ,  $B$  and  $C$  and appear in table 6.5.

**Table 6.5.** Frequencies of rotation of trifluoroacetic acid about its rotational axes

$B$ (MHz) about rotational axes $A, B$ and $C$	$I$ ( $\text{kgm}^2$ )	Most populous $J$ at $20^\circ\text{C}$	Most populous $J$ at $75^\circ\text{C}$	$\nu$ at $20^\circ\text{C}$ (GHz)	$\nu$ at $75^\circ\text{C}$ (GHz)
$A = 3865.098$	$2.171 \times 10^{-45}$	28	30	220	236
$B = 2498.738$	$3.359 \times 10^{-45}$	34	38	172	192
$C = 2075.188$	$4.044 \times 10^{-45}$	39	41	164	172

Due to solvent friction, molecular rotation frequencies are lower in solution than in the gas phase. It is possible to approximate the magnitude of this effect from work done using other, similar-sized molecules, such as aniline. Effective orientational relaxation times for aniline in solution have been derived from ultraviolet fluorescence upconversion measurements.<sup>13</sup> By comparison with gas phase data, aniline rotates about 65% as fast in isopentane and about 15% as fast in acetonitrile, as in the gas phase.

For the current analysis, the solvent effect is assumed to be the same for trifluoroacetic acid and aniline. Therefore, the frequency of rotation of trifluoroacetic acid—and presumably the trifluoroacetate anion—is of the order of  $1 \times 10^{11} \text{ s}^{-1}$  in aliphatic hydrocarbon solvent at rearrangement temperatures. The corresponding period

of rotation is about 10 ps, or 5 ps per half rotation.

From these approximations, the rotation period of the trifluoroacetate ion and the half-life for the collapse of the radical ion pair are predicted to be of approximately the same duration. Therefore, it is possible that these processes may effectively compete with each other, enabling the rearrangement regiochemistry to be affected by subtle changes in the dynamics of the tight ion pair, in turn governed by temperature and solvent polarity. Furthermore, low concentrations of the reducing agent allow radicals more time on average for intramolecular reactions and therefore a greater proportion of rearrangement reversibility. From the similarity of the rotational frequencies about the *A*, *B* and *C* axes of trifluoroacetic acid, it is assumed that the trifluoroacetate group can also rotate about these three axes with approximately equal ease in solution in the absence of directional electrodynamic influences. Some modes of rotation may favour a 1,2 shift of oxygen by positioning the initial ether oxygen of the trifluoroacetate group closest to C1 of the alkene radical cation when the radical ion pair collapses.

### 6.2.6 The mechanism of the rearrangement of $\beta$ -trifluoroacetoxyalkyl radicals

The bulk of the evidence tends to support the theory that the mechanism of the  $\beta$ -trifluoroacetoxyalkyl radical rearrangement involves a cooperation of reversible, polarized and concerted 1,2 (i) and 3,2 (ii) shifts ( $R = CF_3$ ). Experiments with radicals bearing an oxygen-labelled trifluoroacetoxy group have shown that the migration occurs with 55.5-82.3% transposition of label, demonstrating that a formal 3,2 shift predominates under all the conditions investigated in this study. These labelling experiments also revealed some scrambling of the oxygen label in the unrearranged product, necessitating that any concerted rearrangement processes be reversible.

Solvent exerted only a modest effect upon the rearrangement rate constant, compared with the solvent effects observed in comparable ionic chemistry. Likewise, migrating group electronic effects were small in comparison with those observed in solvolysis reactions.

Attempts to trap the 2-methyl-1-heptene radical cation—a fragment of a

hypothetical ion pair intermediate—with unlabelled trifluoroacetate ion were largely unsuccessful, indicating that a dissociated ion pair or a solvent-separated ion pair cannot be involved.

Plots of  $\ln k_{\text{T}}$  against  $1/T$  showed slight, but consistent, curvature which suggests that two competing mechanistic paths are in operation.

Others' high-level theoretical *ab initio* calculations<sup>15</sup> indicated that the difference in energy between transition states for the 1,2 (i) and 3,2 (ii) concerted shifts of a trifluoroacetoxy group was  $12 \text{ kJmol}^{-1}$ , which compared favourably with an experimental value for the difference in activation energies for the two reaction paths of  $9.5 \text{ kJmol}^{-1}$  in benzene.

Evidence in support of the intermediacy of an alkene-radical-cation/trifluoroacetate-anion pair is weaker than for the concerted shifts theory. Experimental evidence indicates that  $\log_{10}A$  for the 1,2 shift is about one unit larger than that for the 3,2 shift. However, there is no significant increase in the overall experimental  $\log_{10}A$  value as the amount of 1,2 shift increases.

There have been claims that a 1,2 concerted shift is faster than the 3,2 shift because it is more polarized.<sup>3,14,39,41</sup> In contrast are the results of MO calculations which reveal that the TS for 3,2 shift is actually slightly more polarized than its 1,2 counterpart, for the rearrangement of 1,2 acyloxy-2-methyl-1-propyl radicals.<sup>15</sup>

Significant proportions of the isomeric alkenes 2-methyl-1-heptene and 2-methyl-2-heptene were sometimes detected by GC in the reactions between 1-bromo-2-methyl-2-trifluoroacetoxyheptane and tributyltin hydride or tris(trimethylsilyl)silane, particularly at low concentrations of the hydrogen atom source. It is possible that trifluoroacetate ion is being eliminated from the 2-methyl-2-trifluoroacetoxy-1-heptyl radical (**6.3**), although the mechanism for the formation of the alkenes has not been studied in detail.

Simple calculations predict that the half-life of the 2-methyl-1-heptene-radical-cation/trifluoroacetate-anion pair is of the same order of magnitude as the time taken for a half-rotation of the trifluoroacetate group, namely a few picoseconds. The short lifetime of such an intermediate may explain why an alkene radical cation cannot be trapped with a

nucleophile.

Esr spectroscopy experiments showed there to be no strong conformational locking of the  $\beta$ -acyloxyalkyl radicals. In  $\beta$ -substituted ethyl radicals, electronic effects were about as strong as steric effects. This indicates that if there is a significant electronic interaction between the unpaired spin and either of the ester oxygen atoms, it does not occur until there is considerable breakage of the alkoxy C–O bond.

### **6.3 Related radical-mediated rearrangements and $\beta$ -eliminations**

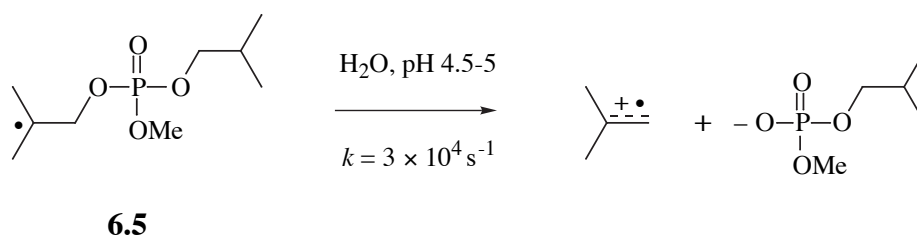
The rearrangements of  $\beta$ -acyloxyalkyl,  $\beta$ -phosphatoxyalkyl,  $\beta$ -nitroxyalkyl and  $\beta$ -sulfonatoxyalkyl radicals have recently been reviewed.<sup>14</sup> Also covered in the same review were the fragmentation reactions of  $\beta$ -acyloxyalkyl radicals, their thiocarbonyl analogues,  $\beta$ -phosphatoxyalkyl and  $\beta$ -sulfatoxyalkyl radicals. Most of the elimination reactions are considered to take place by what the authors termed a "radical-ionic" mechanism, where an alkene radical cation is created by the departure of an anionic  $\beta$ -substituent. The authors considered that  $\beta$ -substituted alkyl radicals prone to rearrangement are intermediate in reactivity between those showing no reactivity and those undergoing fragmentation. This leaves the question: at what point does the reaction path change from apparently polarized and concerted to eliminative? It is only reasonable to expect that there is a transitional reaction path consisting of inner-sphere elimination and subsequent recombination.

Zipse and Bootz could not locate a stationary point on the energy surface corresponding to a contact radical-cation/anion pair for the rearrangement of either the 2-methyl-2-acetoxy-1-propyl or 2-methyl-2-trifluoroacetoxy-1-propyl radicals using *ab initio* MO calculations.<sup>15</sup> There is little evidence for carboxylate elimination from radicals of this type.

Zipse and coworkers have identified stationary points corresponding to contact radical ion pairs in an *ab initio* study of the  $\beta$ -phosphatoxyalkyl radical rearrangement, provided the system contains strongly stabilising substituents.<sup>16</sup> Unfortunately, the

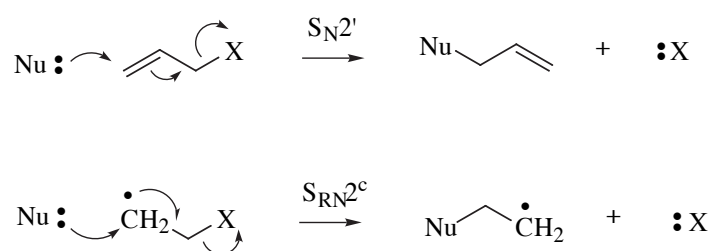


energetics as well as the characteristics of these intermediates depend on the level of theory. Eliminations from  $\beta$ -phosphatoxyalkyl radicals, however, are well documented and play a crucial role in the fragmentations of nucleotide C4' radicals.<sup>14</sup> For example, radical **6.5** eliminates a disubstituted phosphate anion under slightly acidic aqueous conditions at room temperature, forming isobutylene radical cation with a rate constant of  $3 \times 10^4 \text{ s}^{-1}$ .<sup>17</sup> Rate constants have also been measured by a pulsed-radiolysis/conductivity method for the elimination of chloride, bromide, methyl sulfonate and propyl sulfate anions from alkyl radicals with leaving groups in the  $\beta$  position under the same conditions.<sup>17</sup> The 1,2 rearrangements of  $\beta$ -chloroalkyl and  $\beta$ -bromoalkyl radicals are also well documented.<sup>18-21</sup>



Recently, the UV-vis spectra have been recorded for stabilised alkene radical cations produced by elimination of diphenyl<sup>22</sup> or diethyl<sup>23</sup> phosphate from  $\beta$ -phosphatoxyalkyl radicals during laser flash photolysis experiments. A general method for the detection of alkene radical cations under these conditions using a triarylamine reporter has been published.<sup>24</sup> There are reports that alkene radical cations, formed by elimination of substituted phosphate from  $\beta$ -phosphatoxyalkyl radicals, have been trapped intermolecularly<sup>25,26</sup> and intramolecularly<sup>27,28</sup> with nucleophiles. One system exhibits stereochemical memory effects.<sup>28</sup> Of course, like the old  $S_N1$  vs.  $S_N2$  mechanistic debates, it can be notoriously difficult to establish whether the leaving group has actually departed prior to nucleophilic attack. Zipse's calculations<sup>29-33</sup> provide substantial theoretical support for the  $S_{RN}2^c$  reaction (a radical analogy of  $S_N2'$ ), thus allowing scope for a bimolecular displacement step in the trapping experiments. General

$S_N2'$  and  $S_{RN}2^c$  reaction types are illustrated below (scheme 6.2).



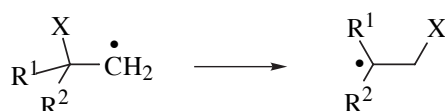
Scheme 6.2

The bulk of evidence indicates that the factors which accelerate  $\beta$ -oxyalkyl radical rearrangements (and  $\beta$ -eliminations) include hydrocarbon framework substituents capable of stabilising a radical cation, polar solvents, elevated temperature and a high propensity for the migrating group to act as a leaving group. Giese and coworkers have published a Brønsted plot correlating  $pK_a$  of the dialkylphosphate leaving group with rate constant for the fragmentation of 4'-nucleotide radicals.<sup>34</sup>

A similar comparison is provided for a larger variety of rearrangements (table 6.6). Where data was available, values for the rearrangement rate constant ( $k_r$ ) and  $R_E$  are provided. Most rearrangements were conducted in organic solvents, but the rearrangement of the protonated hydroxyl radical is in aqueous acid. The  $pK_a$  values for the parent acid HX are for aqueous solution, and may differ from values in hydrocarbon solvents. Values of  $R_E$  were recalculated from original data when mistakes were found in the original papers.

It is difficult to establish structure-activity relationships when the nature of the carbon framework, temperature and solvent varies. However, it is clear that migrating substituents which are also good leaving groups tend to migrate more quickly and with a higher proportion of 1,2 shift, than poor leaving groups. Chlorine undergoes a 1,2 shift very rapidly and bromine ( $pK_a \text{ HBr} = -8$ ) even more so.<sup>20</sup> The size and shape of the migrating group must play a role in the regiochemical outcome of the rearrangement. There is little doubt that a systematic investigation into the effect of migrating group structure upon  $k_r$  and  $R_E$  would provide valuable mechanistic information.

Elimination reactions tend to occur when the carbon framework has substituents which stabilise positive charge (particularly  $\alpha$ -alkoxy groups) and where the  $\beta$ -substituent may easily depart with an electron pair. It appears that it is the hardness (concentration or lack of delocalisation) of the charge on the carbon skeleton and on the migrating group which determines whether there is enough electrostatic attraction to keep the radical ion pair fragments together. Hardness of charge in both fragments will only result in rearrangement. Softness in both fragments will result in elimination. Mixed hardness will produce results somewhere between these two extremes. Studies of radicals which undergo both  $\beta$ -acyloxyalkyl rearrangement and  $\beta$ -elimination should prove fruitful.



**Table 6.6.** Rate constants and  $R_E$  as a function of  $\text{p}K_a$

X	R <sup>1</sup>	R <sup>1</sup>	T (°C)	$k_T$ (s <sup>-1</sup> )	$R_E$ (%)	$\text{p}K_a$ of HX	Ref.
-Cl	Me	Me		$\sim 10^{10}$		-7	20
-OH <sub>2</sub> <sup>+</sup>	Me	Me				-1.74	35
-ONO <sub>2</sub>	Ph	H	80		84	-1.37	36
-OCOCF <sub>3</sub>	Ph	H	80	$\approx 10^5 ?$	19	0.52	36
-OCOCF <sub>3</sub>	<i>n</i> -C <sub>5</sub> H <sub>11</sub>	Me	80	$3.4 \times 10^5$	18-45	0.52	37
-OSO <sub>2</sub> tol	Ph	H	80		81	0.70	38
-OPO(OPh) <sub>2</sub>	Ph	H	80	$8.0 \times 10^5$	81	1.1	39
-OCOPh	Me	Me	75	$3.5 \times 10^2$	$\sim 0$	4.20	40
-OCOPr	Ph	Me	75	$1.6 \times 10^5$	$\sim 0$	4.82	41

## 6.4 The mechanism of the rearrangement of *N*-alkoxy-2(1*H*)-pyridinethiones

The mechanism of the catalysed rearrangement of *N*-alkoxy-2(1*H*)-pyridinethiones is not fully understood. Kinetic evidence indicates that the rate limiting step may be the intermolecular transfer of the migrating group. Results from a mass spectrometric analysis of an isolated intermediate also support the participation of intermolecular processes. An intermolecular process has previously been shown to be in operation in the analogous rearrangement of 2-alkoxypyridine *N*-oxides. A crossover experiment is necessary to establish whether the rearrangement of *N*-alkoxy-2(1*H*)-pyridinethiones occurs with intermolecular alkyl transfer.

Stereochemical experiments have demonstrated that the rearrangement cannot occur *via* one, concerted mechanism. It remains possible that this isomerization does belong to a class of rearrangements which proceed *via* a transition structure in which 5 electrons are delocalised over 5 atoms, although other processes must also be in operation alongside this 1,4 concerted shift.

## 6.5 Final remarks

It is difficult to devise experiments which would enable one to distinguish between the cooperation of two concerted, pericyclic processes and the intermediacy of a radical ion pair. This endeavour is sure to provide continuing challenges to workers in the field. In the case of the rearrangement of the 2-methyl-2-trifluoroacetoxy-1-heptyl radical (**6.3**) to the 2-methyl-1-trifluoroacetoxy-2-heptyl radical (**6.4**), it has not been possible to unequivocally establish the mechanism.

It became evident that solvent plays an important role in the rate of rearrangement and in the regiochemistry. Therefore, future theoretical calculations must take into account solvent effects since the mechanism in the gaseous state may differ markedly from that observed in not only a polar solvent, but non-polar solvents also.

One might expect the rate of processes which involve contact ion pairs to show considerably smaller solvent effects than reactions with more completely solvated

intermediates. For CIPs, the overall charge within the solvent sphere sums to zero. The solvation enthalpy will be less for CIPs since each of the oppositely-charged fragments are less stabilised due to an incomplete solvent sphere. The solvation entropy will also be lower for CIPs because the solvent molecules are less ordered than in a completely-solvated solvent-separated (SSIP) or solvent-shared ion pair.

For intermediates with very short lifetimes, it is possible that the distinction between polarized, concerted transition states and tight ion pairs may become an artificial one. The parameters which determine this segregation are bond length, bond strength and charge distribution. The location of the valence electrons in two adjacent atoms formally governs whether they are covalently bonded. Solvents exert a significant influence on the positions of valence electrons in solutes at any point in time. For  $\beta$ -acyloxyalkyl radical rearrangements in which the migrating group is a stronger conjugate base (weaker leaving group) and in which the alkyl framework does not readily delocalise a developing positive charge, any such radical ion intermediate must have a half life of considerably less than 10 picoseconds (cf. section 6.2.5). For species with little stabilisation, it is envisaged that the actual time interval may not be much larger than the period of a molecular vibration (10-50 fs).

The rate constants for valence bond tautomerism have been measured for the trimethylcyclopropenyl radical ( $> 10^8 \text{ s}^{-1}$ )<sup>42</sup> and for a number of conjugated and highly hindered aryloxy radicals ( $\approx 2 \times 10^7 \text{ s}^{-1}$  at RT).<sup>43-45</sup> One is led to wonder whether it is possible that the resonance structures of a carboxylate ion become time-resolved on the timescale of the lifetime of a radical ion intermediate in such a way that regiochemistry is directly affected.

From a quantum-mechanical perspective, a tight radical ion pair should exist in a number of discrete, quantised geometries. Are there two of these allowed states which are isomorphic with the polarized transition structures? At what point does a strong electrostatic interaction become a partial bond?

## 6.6 References

1. Adam, K. R., Lauder, I. and Stimson, V. R. *Aust. J. Chem.* **1962**, *15*, 467.
2. Barnes, D. J., Cole, M., Lobo, S., Winter, J. G. and Scott, J. M. W. *Can. J. Chem.* **1972**, *50*, 2175.
3. Crich, D. and Filzen, G. F. *J. Org. Chem.* **1995**, *60*, 4834.
4. Deslongchamps, P. *Stereoelectronic effects in organic chemistry* 1983, Pergamon, Oxford, p 54.
5. True, N. S. and Bohn, R. K. *J. Phys. Chem.* **1978**, *82* (4), 478.
6. Oki, M. and Nakanishi, H. *Bull. Chem. Soc. Jpn* **1970**, *43*, 2558.
7. Drakenberg, T. and Forsen, S. *J. Phys. Chem.* **1972**, *76* (24), 3582.
8. Johnston, L. J. and Schepp, N. P. *J. Am. Chem. Soc.* **1993**, *115*, 6564.
9. Lew, C. S. Q., Brisson, J. R. and Johnston, L. J. *J. Org. Chem.* **1997**, *62*, 4047.
10. Arnold, B. R.; Farid, S.; Goodman, J. L. and Gould, I. R. *J. Am. Chem. Soc.* **1996**, *118*, 5482.
11. Stolwijk, V. M. and van Eijck, B. P. *J. Mol. Spectrosc.* **1985**, *113*, 196.
12. Banwell, C. N. *Fundamentals of molecular spectroscopy*, 2nd Ed. 1972, McGraw-Hill, London. a: p 33, b: p 41, c: p 38.
13. Pereira, M. A., Share, P. E., Sarisky, M. J. and Hochstrasser, R. M. *J. Chem. Phys.* **1991**, *94* (4), 2513.
14. Beckwith, A. L. J.; Crich, D.; Duggan, P. J. and Yao, Q. *Chem. Rev.* **1997**, *97*, 3273.
15. Zipse, H. and Bootz, M. *J. Chem. Soc., Perkin Trans. 2* **2001**, 1566.
16. Wang, Y. and H. Zipse, H. unpublished results (as of April 2003)
17. Koltzenburg, G. Behrens, G. and Schulte-Frohlinde, D. *J. Am. Chem. Soc.* **1982**, *104*, 7311.
18. Wilt, J. W. in *Free Radicals*; Kochi, J. K., Ed.; John Wiley and Sons: New York, 1973, vol. 1, p. 333.
19. Skell, P. S. and Shea, K. J. in *Free Radicals*; Kochi, J. K., Ed.; John Wiley and Sons: New York, 1973, vol. 2, p. 809.

20. Beckwith, A. L. J. and Ingold, K. U. in *Rearrangements in Ground and Excited States*; de Mayo, P., Ed.; Academic Press: New York, 1980, vol. 1, p. 161.
21. Freidlina, R. Kh. and Terent'ev, A. B. *Adv. Free-Radical Chem.* **1980**, 6, 1.
22. Bales, B. C.; Horner, J. H.; Huang, X.; Newcomb, M.; Crich, D. and Greenberg, M. M. *J. Am. Chem. Soc.* **2001**, 123, 3623.
23. Whitted, P. O.; Horner, J. H.; Newcomb, M.; Huang, X. and Crich, D. *Org. Lett.* **1999**, 1, 153.
24. Newcomb, M.; Miranda, N.; Huang, X. and Crich, D. *J. Am. Chem. Soc.* **2000**, 122, 6128.
25. Crich, D.; Huang, X. and Newcomb, M. *Org. Lett.* **1999**, 1, 225.
26. Crich, D.; Huang, X. and Newcomb, M. *J. Org. Chem.* **2000**, 65, 523.
27. Crich, D. and Neelamkavil, S. *Org. Lett.* **2002**, 4, 2573.
28. Crich, D. and Ranganathan, K. *J. Am. Chem. Soc.* **2002**, 124, 12422.
29. Zipse, H. *Angew. Chem. Int. Ed. Engl.* **1994**, 33, 1985.
30. Zipse, H. *J. Am. Chem. Soc.* **1994**, 116, 10773.
31. Zipse, H. *J. Chem. Soc. Perkin Trans. 2* **1996**, 1797.
32. Zipse, H. *J. Chem. Soc. Perkin Trans. 2* **1997**, 2691.
33. Zipse, H. *Acc. Chem. Res.* **1999**, 32, 571.
34. Giese, B.; Beyrich-Graf, X.; Burger, J.; Kesselheim, C.; Senn, M. and Schafer, T. *Angew. Chem. Int. Ed. Engl.* **1993**, 32, 1742.
35. Gilbert, B. C.; Norman, R. O. C. and Williams, P. S. *J. Chem. Soc. Perkin Trans. 2* **1981**, 1401.
36. Crich, D. and Filzen, G. F. *J. Org. Chem.* **1995**, 60, 4834.
37. Harman, D. G. *This thesis*, Chapters 2 and 3.
38. Filzen, G. F. *Ph.D. Thesis*, University of Illinois at Chicago, 1996.
39. Crich, D.; Yao, Q. and Filzen, G. F. *J. Am. Chem. Soc.* **1995**, 117, 11455.
40. Beckwith, A. L. J. and Thomas, C. B. *J. Chem. Soc., Perkin Trans. 2* **1973**, 861.
41. Beckwith, A. L. J. and Duggan, P. J. *J. Am. Chem. Soc.* **1996**, 118, 12838.
42. Closs, G. L.; Evanochko, W. T. and Norris, J. R. *J. Am. Chem. Soc.* **1982**, 104,

350.

43. Kirste, B.; Harrer, W.; Kurreck, H.; Schubert, K.; Bauer, H. and Gierke, W. *J. Am. Chem. Soc.* **1981**, *103*, 6280.

44. Kirste, B. *J. Magn. Reson.* **1987**, *73*, 213.

45. Gersdorff, J.; Kirste, B.; Niethammer, D.; Harrer, W. and Kurreck, H. *Magn. Res. Chem.* **1988**, *26*, 416.



## Chapter 7

### General Experimental

7.1	Melting points	307
7.2	Elemental analyses	307
7.3	Infrared spectroscopy	307
7.4	Optical rotations	307
7.5	Molecular ultraviolet and visible spectra	307
7.6	Bulb to bulb distillations	307
7.7	Liquid chromatography	307
7.8	Gas chromatography	308
7.9	Mass spectrometry	309
7.10	Electron spin resonance spectroscopy	310
7.11	Nuclear magnetic resonance spectroscopy	310
7.12	Cyclic voltammetry	312
7.13	Purification of solvents for radical reactions	312
7.14	Purification of solvents for other purposes	314
7.15	Reagents for synthesis	314
7.16	Evaporation of solvents	314
7.17	Drying of extract solutions	315
7.18	Nomenclature	315
7.19	References	316

**7.1** Melting points are uncorrected and were determined using a Reichert microscope Kofler hot-stage apparatus.

**7.2** Elemental analyses were performed by the ANU Microanalytical Services Unit, Canberra.

### **7.3 Infrared spectroscopy**

Routine infrared spectra were recorded with a Perkin-Elmer 686 infrared spectrophotometer. Liquid samples were generally prepared as a thin film, smeared between NaCl plates. Solid samples were run as either a Nujol mull smeared between NaCl plates, or as a solution contained in a NaCl cell of cavity thickness 0.5 mm run with a reference cell to balance solvent absorptions. Polystyrene film was used as a wavenumber reference.

FTIR spectra were generally recorded by the ANU Infrared Spectrometry Service on a Perkin-Elmer 1800 fourier transform infrared spectrophotometer, coupled to a Perkin-Elmer 7500 computer. Samples were prepared as KBr pellets. Some FTIR spectra were recorded on a Perkin-Elmer 1600 series instrument, using 4 scans for both background and sample spectra.

Infrared data are listed as the wavenumber ( $\nu_{\max}$ ) in units of  $\text{cm}^{-1}$ , followed by a description of the peak's size and/or shape. Abbreviations used to indicate peak characteristics are: vs (very strong); s (strong); m (medium); w (weak); asym (asymmetric); and br (broad).

**7.4** Optical rotations were measured on a Perkin-Elmer 241 polarimeter, at a wavelength of 589 nm and at ambient temperature, in spectroscopic grade solvents.

**7.5** Molecular ultraviolet and visible spectra were recorded using a Hewlett-Packard 8450A spectrophotometer. Spectroscopic grade solvents were used in preparing solutions.

**7.6** Bulb-to-bulb distillations were performed with a Buchi GKR-50 Kugelrohr apparatus. The boiling temperature quoted is that which just causes the liquid to distil.

### **7.7 Liquid Chromatography**

**7.7.1** Flash chromatography was performed according to an established method,<sup>1</sup> using Merck Kieselgel 60 (230-400 mesh ASTM).

**7.7.2** Vacuum liquid chromatography (VLC) was performed according to an established

method,<sup>2</sup> with the same type of silica.

**7.7.3** Analytical thin layer chromatography (TLC) was performed using either Whatman type MK6F, precoated silica microscope slide plates (75 mm × 25 mm × 10-12 μm), or Merck Kieselgel 60 plates (100 × 200 × 0.25 mm), both containing a 254 nm fluorescence indicator. Once developed, chromatograms were first inspected under ultraviolet light, then sprayed with either 3% vanillin in conc. H<sub>2</sub>SO<sub>4</sub> or alkaline KMnO<sub>4</sub> solutions, and heated at *ca.* 200°C until spots became visible.

**7.7.4** Preparative scale thin layer chromatography was undertaken using Merck 20 × 20 cm glass plates coated with Kieselgel 60 (with F<sub>254</sub> indicator), generally of thickness 2 mm.

**7.7.5** Radial chromatography was performed on a Chromatotron, model 7924, using plates coated 2 mm thick with Merck Kieselgel 60 PF<sub>254</sub> (with gypsum). A hand-held short-wave ultraviolet lamp was used to detect UV-absorbing compounds on the plate during chromatography.

## 7.8 Gas Chromatography

### 7.8.1 Analytical

Three capillary GC instruments were used for analytical gas chromatography. High-purity helium was used as the carrier and make-up gas for each. Each instrument employed flame ionisation detection. Capillary columns with prefix "BP" were purchased from SGE. The details for each instrument follow.

i) A Varian 6000 Vista Series instrument, fitted with an SGE Unijector control module (replacing the original injector), was used for the majority of the work. A dimethylpolysiloxane (BP1) capillary of dimensions 25 m × 0.32 mm I.D. × 0.5 μm film thickness was employed, with a carrier gas average linear velocity of 30 cm s<sup>-1</sup>. A Hewlett-Packard 3390A integrator controlled signal plotting and integration.

ii) A Varian 3400 instrument with an on-board integrator was fitted with both a 25 m × 0.32 mm I.D. × 0.5 μm film thickness Carbowax (BP20), and a 25 m × 0.32 mm I.D. × 0.5 μm film thickness 95% dimethyl, 5% diphenyl polysiloxane (BP5) capillary. Both capillaries employed a carrier gas average linear velocity of 40 cm s<sup>-1</sup>.

ii) A Varian 3400 instrument, coupled to an HP 3390A integrator, contained a 14% cyanopropylphenyl, 86% dimethyl polysiloxane (BP10) capillary, of dimensions 25 m ×

0.5  $\mu\text{m}$   $\times$  0.32 mm I.D. The average linear carrier gas velocity was 40  $\text{cm s}^{-1}$ .

### 7.8.2 Chiral analytical GC<sup>3</sup>

The ratios of enantiomers in selected optically active mixtures were determined by using a Chirasil-Val WCOT capillary column (Applied Science), of length 25 m and I.D. of 0.30 mm. The film thickness was not stated. This column was installed in either instrument i) or ii).

### 7.8.3 Preparative scale gas chromatography

This work was performed using a Varian 6000 Vista Series GC equipped with a thermal conductivity detector (TCD), containing a 2 m  $\times$  4 mm I.D. glass column, packed with 10% SE30 (dimethyl polysiloxane) on 80/100 Gas-Chrom Q support (Applied Science). The carrier gas flow was set to 20  $\text{mL min}^{-1}$  (average linear velocity = 2.65  $\text{cm s}^{-1}$ ); the injector temperature to 200°C; detector oven temperature to 200°C; and detector filament an indicated 230°C, giving a detector current of 150 mA. The column oven temperature was usually 60°C. A Hewlett-Packard 3396A integrator controlled signal plotting and integration.

## 7.9 Mass Spectrometry

Mass spectral data are listed as values of  $m/z$ , followed by the intensity of the ion as a percentage of the base peak intensity (in parentheses). The symbol  $\text{M}^{+\bullet}$  accompanies the  $m/z$  value assigned to the molecular ion. The symbols  $\text{MH}^+$  and  $\text{MNH}_4^+$  correspond respectively to the protonated molecule and the species corresponding to the molecular addition of the ammonium ion, commonly seen using CIMS with ammonia as the reagent gas.

### 7.9.1 EIMS

Direct-probe, low resolution, electron impact mass spectra (EIMS) were recorded at 70 eV on either a VG 7070F or a VG ZAB-2SEQ mass spectrometer. Where necessary, the compounds were frozen in the sample cup using liquid nitrogen, before insertion into the vacuum lock.

### 7.9.2 HRMS

High resolution mass spectrometry (HRMS) provided accurate mass measurements using EIMS at a resolution (10% valley) of *ca.* 6,000. Peaks were nominally matched using perfluorokerosene (PFK) to provide reference ions.

### 7.9.3 CIMS

Chemical ionisation mass spectra (CIMS) were measured on the VG 7070F instrument using  $\text{NH}_3$  as the reagent gas. The ion source temperature was generally maintained at *ca.* 200°C, although lower temperatures were used for samples which were temperature-sensitive.

### 7.9.4 GCMS

Gas-chromatography/mass-spectrometry was performed using a Hewlett-Packard system, comprised of an HP 5890 gas chromatograph (splitless injection) connected to an HP 5970 mass-selective detector (70 eV electron beam energy), fitted with an HP 59822A gauge controller. An HP 59970 MS Chemstation computer was used to control the system. A dimethylpolysiloxane (HP1) capillary of 12.5 m length, 0.33  $\mu\text{m}$  film thickness and 0.2 mm I.D. was fitted to the chromatograph. High purity helium was used as the carrier gas, employing an average linear velocity of 40  $\text{cm s}^{-1}$ .

### 7.9.5 FAB MS

Fast atom bombardment mass spectra were recorded on the ZAB-2SEQ instrument, using a 1:1 glycerol:thioglycerol matrix and a beam of  $\text{Cs}^+$  ions.

### 7.9.6 Electrospray MS

Positive electrospray mass spectra were obtained on a ZAB-AutoSpec instrument, using acetonitrile as the solvent.

## 7.10 Electron Spin Resonance Spectroscopy

A Bruker 200D-SRC EPR spectrometer was used to measure esr spectra. Values of  $g$  were determined relative to a marker at  $g = 2.00333$ , in turn calibrated using a Bruker ER 035 NMR gaussmeter. The spectrometer was equipped with a Bruker ER 4111 calibrated variable temperature unit and an irradiation system containing a Hanovia L5175 Hg (Xe) lamp. A more comprehensive description of the system used has been supplied by Beckwith and Brumby,<sup>4</sup> the only differences being that a frequency counter was omitted and the IBM XT computer was replaced with an IBM 386 clone. A simulation program, designed by Brumby<sup>5</sup> was used to aid in the analysis of the spectra.

## 7.11 Nuclear Magnetic Resonance Spectroscopy

### 7.11.1 $^1\text{H}$ nmr

The  $^1\text{H}$  nmr spectra of all compounds, unless stated otherwise, were obtained in  $\text{CDCl}_3$  solution, internally referenced with tetramethylsilane (TMS). Spectra were recorded on these machines at their respective frequencies : a Varian Gemini (300.1

MHz); a Varian VXR 300S, equipped with an Oxford magnet and broad-band probe (299.9 MHz); and a Varian XL 200, with a broad-band probe (200.0 MHz). Spectral information is listed for each resonance as : chemical shift in parts per million (ppm) downfield of TMS (0.00 ppm); multiplicity; peak integration (number of nuclei); coupling constant,  $J$ , in hertz, if appropriate; and peak assignment. Abbreviations used are s (singlet), d (doublet), t (triplet), q (quartet), m (multiplet), br (broad), Ar, (aryl), Ph (phenyl), *o* (*ortho*), *m* (*meta*), *p* (*para*), *a* (*axial*), *e* (*equatorial*), exch. (exchangeable proton). Combinations of multiplicities are listed as their consecutive respective abbreviations, the multiplicities of clearly larger coupling constants cited first.

### 7.11.2 $^2\text{H}$ nmr

The spectra of deuterium-labelled compounds were recorded at 30.7 MHz on a Varian XL 200 spectrometer, equipped with a broad-band probe. Samples were run as  $\text{CHCl}_3$  or  $\text{CHCl}_3/\text{CDCl}_3$  solutions, using  $\text{C}_6\text{D}_6$  (benzene- $d_6$ ) as an internal reference (7.27 ppm). Spectral information is quoted as the chemical shift followed by peak integration and assignment.

### 7.11.3 $^{13}\text{C}$ nmr

Unless stated otherwise, the  $^{13}\text{C}$  nmr spectra of compounds were recorded at 75 MHz, in  $\text{CDCl}_3$  solution. The middle line of the 1:1:1  $\text{CDCl}_3$  resonance (77.00 ppm) was used to reference spectra indirectly to TMS (0 ppm). Spectral information is listed for each resonance as a chemical shift, a coupling constant with a heteronucleus (if appropriate), followed by an assignment. To establish the degree of hydrogen substitution on carbons, the Attached Proton Test (APT)<sup>6</sup> was used, in the first instance. Where necessary, discrimination of APT carbon resonances of the same phase, but differing in degree of hydrogen substitution was enabled by obtaining a fully- $^1\text{H}$ -coupled carbon spectrum. A group of resonances that could not be assigned unambiguously were given tentative assignments and marked with asterisks (\*), or a similar symbol if there was more than one group.

Spectra were recorded on the following machines at their respective frequencies: a Varian Gemini (75.5 MHz); a Varian VXR 300S, equipped with an Oxford magnet and broad-band probe (75.4 MHz); and a Jeol PNM FX200 (50 MHz). Abbreviations used for assignments include Ar (aryl), Ph (phenyl), *o* (*ortho*), *m* (*meta*), *p* (*para*), and *i* (*ipso*).

### 7.11.4 $^{17}\text{O}$ nmr

Oxygen-17 nmr spectra were recorded at 298 K in a field of 7.04 T, using a Varian VXR 300S (broad-band probe) spectrometer, operating at 40.7 MHz. Chemical shifts are listed in ppm, downfield of  $\text{H}_2^{17}\text{O}$  (0 ppm). For a more detailed description of

how these experiments were performed, see Appendix B.

#### 7.11.5 $^{19}\text{F}$ nmr

The  $^{19}\text{F}$  spectra of compounds were obtained with their  $\text{CDCl}_3$  solutions, using a Varian Gemini spectrometer (with a broad-band probe) operating at 282.2 MHz, with a transmitter offset of 9770 Hz. The compound  $\text{CFCl}_3$  was used as an internal reference (0.00 ppm). Spectral information is quoted as: chemical shift, downfield of  $\text{CFCl}_3$ ; multiplicity; peak integration (number of nuclei); coupling constant,  $J$ , in Hz; and assignment.

#### 7.11.6 2-D nmr spectra: COSY, HETCOR and LR HETCOR

Two-dimensional nmr experiments were performed on a Varian VXR 300S, equipped with an Oxford magnet and broad-band probe, using  $\text{CDCl}_3$  solutions of compounds.

### 7.12 Cyclic Voltammetry

Electrochemical measurements were taken using a PAR Model 170 Electrochemical System. The cell was of a standard electrode configuration, consisting of a polished platinum disc working electrode (0.5-1.0 mm diameter), platinum bar counter electrode and a double-fritted  $\text{Ag}/\text{AgCl}$  reference electrode (Metrohm). The internal compartment of the reference electrode was filled with 0.45 M  $n\text{-Bu}_4\text{NBF}_4$ /0.05 M  $n\text{-Bu}_4\text{NCl}$  in  $\text{CH}_3\text{CN}$  (or  $\text{CH}_2\text{Cl}_2$ ). The external compartment was filled with standard electrolyte solutions, *i.e.* 0.50 M  $n\text{-Bu}_4\text{NBF}_4$  in  $\text{CH}_3\text{CN}$  (or  $\text{CH}_2\text{Cl}_2$ ). The ferrocenium/ferrocene couple was recorded at +0.41 V in  $\text{CH}_3\text{CN}$  at room temperature.

The electrolyte solutions were deoxygenated with nitrogen and the cell was maintained under an inert atmosphere. Low temperature measurements were recorded in a jacketed cell, connected to a Lauda RL6 circulating cooling bath. The temperature was monitored by a Comark 2001 digital thermometer, with the probe located directly in the electrochemical solution.

### 7.13 Purification of solvents for radical reactions

Purification procedures for solvents in which reactions with tributyltin hydride would be performed were chosen so that contaminants which might interfere with processes mediated by carbon and tin-centred radicals, would be removed. These contaminants included alkenes, halogenated compounds, acids, bivalent sulfur-containing compounds and carbonyl-containing compounds. Solvents for reactions involving trifluoroacetate esters were also dried to limit the extent of hydrolysis of the esters. Procedures for the purification of solvents for other physico-chemical studies are also

described. Many of these procedures were performed as reported in the literature,<sup>7-12</sup> or are adaptations of these procedures. All distillations were performed under dry nitrogen. The air pressure in Canberra averages 720 mmHg and boiling points are uncorrected. All solvents were stored in well sealed, dark glass bottles, under an atmosphere of dry nitrogen, unless specified otherwise.

#### 7.13.1 Hexane

A sample of AR grade 95% hexanes was washed repeatedly with *ca.* 5% of its volume of concentrated H<sub>2</sub>SO<sub>4</sub>, until the acid layer no longer became coloured. The organic phase was then washed consecutively with 10% of its volume of distilled water, 25% aqueous Na<sub>2</sub>CO<sub>3</sub>, distilled water, and then filtered through silica. The hexanes were distilled from sodium wire under nitrogen, collecting the fraction of bp 65-66°C.

#### 7.13.2 Benzene

AR grade benzene was treated with one quarter its volume of AR grade ethanol and crystallized whilst stirring vigorously at -10°C. The resulting slurry was filtered under vacuum and the precipitate was melted and washed thrice with distilled water, filtered through a column of silica, then distilled from sodium wire (no benzophenone), under nitrogen.

#### 7.13.3 Toluene

AR grade toluene was distilled twice from sodium wire.

#### 7.13.4 *tert*-Butylbenzene

Aldrich (99%) *tert*-butylbenzene was washed repeatedly with *ca.* 10% of its volume of concentrated H<sub>2</sub>SO<sub>4</sub>, until a fresh portion of acid was no longer discoloured, then consecutively with 10% aqueous NaOH, twice with distilled water, and dried over MgSO<sub>4</sub>. The drying agent was removed by filtration and the solvent was distilled, collecting the fraction of bp 166-167°C.

#### 7.13.5 Acetonitrile

HPLC grade acetonitrile was distilled under nitrogen, from CaH<sub>2</sub> (2g/L) and stored over dried 4Å molecular sieves.

#### 7.13.6 Propionitrile

A slightly yellow sample of Aldrich propionitrile (reported purity 98% by GC) was washed successively with 30% of its volume of 2 M aqueous HCl, distilled water, 1 M aqueous K<sub>2</sub>CO<sub>3</sub>, distilled water, then saturated aqueous NaCl solution. After filtering



through silica, the nitrile was stirred with 15g/L CaH<sub>2</sub>, then filtered through celite and distilled from 10g/L P<sub>2</sub>O<sub>5</sub>. The distillate was treated with 10g/L CaH<sub>2</sub> and redistilled, collecting the fraction of bp 93.8-94.2°C (99.3% by GC).

#### 7.13.7 *N*-Methylacetamide

Aldrich (99%) *N*-methylacetamide was preliminarily dried over powdered CaO, filtered, then distilled by kugelrohr under reduced pressure. It was then dried more rigorously in the presence of P<sub>2</sub>O<sub>5</sub>, in a dessicator at 0.5 mmHg. It was stored under nitrogen, in a flask, sealed with two septa (one inverted on top of the other).

#### 7.13.8 Perfluoromethylcyclohexane

Perfluoromethylcyclohexane was filtered through silica, then fractionally distilled, collecting the fraction of bp 72.5-74.5°C.

### 7.14 Purification of solvents for other purposes

#### 7.14.1 Chloroform for pyridinethione rearrangements

UV-spectroscopic grade chloroform was washed twice with distilled water to remove ethanol, filtered through a short plug of anhydrous K<sub>2</sub>CO<sub>3</sub>, then distilled from P<sub>2</sub>O<sub>5</sub>.

#### 7.14.2 Acetonitrile for electrochemistry

A literature procedure (Method B)<sup>13</sup> was followed to obtain solvent of sufficient purity for electrochemistry.

### 7.15 Reagents for synthesis

For synthetic purposes, most commercial fine chemicals and AR grade solvents were used without further purification. Purification and/or drying (when necessary) was usually performed by established methods.<sup>7</sup> Mention is usually made in the text or respective experimental sections where purification of reagents has been necessary.

### 7.16 Evaporation of solvents

Unless stated to the contrary, the terms "evaporation", "evaporated", "removal" and "removed" when concerning solvents, mean that solvent(s) were vaporised from solutes, under reduced pressure, using a Buchi Rotavapor. If the residues were sufficiently involatile, high vacuum ( $\geq 0.001$  mmHg) was used to remove traces of solvent. When compounds have been purified by wet chromatographic methods, it is inferred that the solvent(s) have been evaporated afterward. Relative proportions of solvents in mixtures are expressed as *v/v* %.

**7.17** Organic extracts were dried with powdered, anhydrous  $\text{MgSO}_4$ , unless otherwise stated. It is implied that the drying agent is removed by filtration, before evaporation of the solvent.

### **17.18 Nomenclature**

Compounds have been named according to IUPAC rules<sup>14</sup> in the experimental sections of each chapter. Isotopically-labelled compounds have been indexed by the Boughton System (see the ACS Chemical Abstracts indexing system) applied to the IUPAC rules. Numbers in square brackets adjacent to the names of compounds in experimental sections are CAS registry numbers.

### 17.19 References

1. Still, W. C.; Kahn, M. and Mitra, A. *J. Org. Chem.* **1978**, *43*, 2923.
2. Coll, J. C. and Bowden, B. F. *J. Nat. Prod.* **1986**, *49*, 934.
3. Konig, W. A.; Francke, W. and Benecke, I. *J. Chromatogr.* **1982**, *239*, 227.
4. Beckwith, A. L. J. and Brumby, S. *J. Magn. Reson.* **1987**, *73*, 252.
5. Brumby, S. *Appl. Spectrosc.* **1992**, *46*, 176.
6. Williams, K. R. and King, R. W. *J. Chem. Educ.* **1990**, *67*, A93.
7. Perrin, D. D. and Armarego, W. L. F. *Purification of Laboratory Chemicals*; Pergamon Press: Oxford, 1988, 3rd ed.
8. Burfield, D. R.; Lee, K.-H. and Smithers, R. H. *J. Org. Chem.* **1977**, *42*, 3060.
9. Burfield, D. R. and Smithers, R. H. *J. Org. Chem.* **1978**, *43*, 3966.
10. Burfield, D. R.; Smithers, R. H. and Tan, A. S. C. *J. Org. Chem.* **1981**, *46*, 629.
11. Burfield, D. R. and Smithers, R. H. *J. Org. Chem.* **1983**, *48*, 2420.
12. Burfield, D. R. *J. Org. Chem.* **1984**, *49*, 3852.
13. Walter, M. and Ramaley, L. *Anal. Chem.* **1973**, *45*, 165.
14. IUPAC *Nomenclature of Organic Chemistry*; Rigaudy, J. and Klesney, S. P., Eds.; Pergamon Press: Oxford, 1979 (Blue Book) Website: [www.chem.qmw.ac.uk/iupac/](http://www.chem.qmw.ac.uk/iupac/) or [www.iupac.org](http://www.iupac.org)

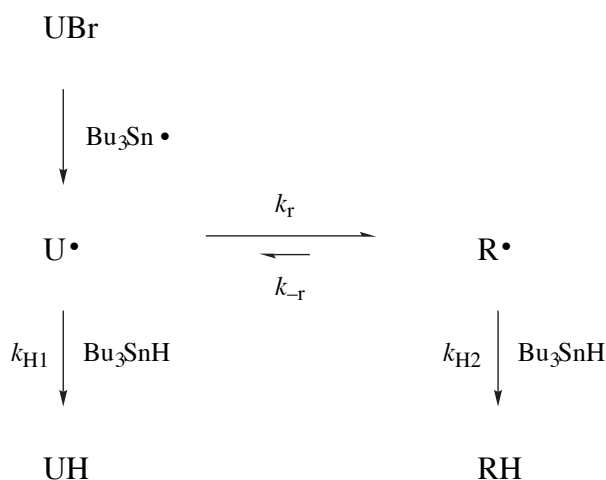
## Appendix A

### A description of the analytical method used to obtain rearrangement rate constants and a derivation of the integrated rate expression

#### A1. Analytical method

Rate constants for radical rearrangement processes have been determined directly by methods such as kinetic esr spectroscopy<sup>1</sup> and laser flash photolysis<sup>2</sup>. However, these techniques involve the use of complicated and expensive instruments and sometimes limited by the range of temperatures over which measurements may be taken. A reliable clock method was therefore developed<sup>3</sup> for the indirect determination of radical rearrangement rate constants, making it possible to obtain these desired kinetic data cheaply and conveniently.

Such a method relies upon the fact that the initial radical, once formed, may react by one of two competing paths, one of which has a known rate constant. If the reagent and product concentrations can be determined, a computer program may be used to calculate the ratio of the rate constants for these two processes, at each reaction temperature. The unknown rate constant is easily determined with knowledge of one rate constant and the ratio of the two.



Scheme A.1

Scheme A.1 represents this concept diagrammatically. Here U represents *unrearranged* and R represents *rearranged*. This scheme illustrates the overall reaction of an organobromide, UBr, with the radical-mediated reducing agent tributyltin hydride. However, the analytical method is also applicable to any other system in which chain reactions take place and reactive intermediates of low concentration are present, which can either rearrange or react directly with a chain propagating reagent of steadily decreasing concentration.

Radical U• is formed by the reaction of UBr with tributyltin radicals, the kinetics of which are unimportant to the analysis. U• may then either rearrange to radical R• in a first order process, with rate constant  $k_r$ , or react with a molecule of tributyltin hydride in a second order manner, forming the non-rearranged product, UH, with rate constant  $k_{H1}$ .

## A2. Derivation of the integrated rate expression

The rate law for the latter reaction may be written:

$$\frac{d[\text{UH}]}{dt} = k_{H1}[\text{U}\cdot][\text{Bu}_3\text{SnH}] \quad (\text{A.1})$$

Radical R• also reacts with tributyltin hydride, forming the rearranged product, RH, with rate constant  $k_{H2}$ . For an irreversible process ( $k_r \gg k_{-r}$ ), the rate of formation of RH is approximately equal to that for R•. We can then write:

$$\frac{d[\text{RH}]}{dt} \approx k_r[\text{U}\cdot]. \quad (\text{A.2})$$

By division of equation A.1 by A.2, we get:

$$\frac{d[\text{UH}]}{d[\text{RH}]} = \frac{k_{H1}[\text{Bu}_3\text{SnH}]}{k_r}. \quad (\text{A.3})$$

The equality:

$$[\text{UH}]_t + [\text{RH}]_t + [\text{Bu}_3\text{SnH}]_t = [\text{Bu}_3\text{SnH}]_0 \quad (\text{A.4})$$

holds for all times  $t$ . By differentiating A.4 with respect to  $[\text{RH}]$ , we obtain:

$$\begin{aligned} \frac{d[\text{UH}]}{d[\text{RH}]} + \frac{d[\text{RH}]}{d[\text{RH}]} + \frac{d[\text{Bu}_3\text{SnH}]}{d[\text{RH}]} &= \frac{d[\text{Bu}_3\text{SnH}]_i}{d[\text{RH}]} = 0 \\ \therefore \frac{d[\text{UH}]}{d[\text{RH}]} + 1 + \frac{d[\text{Bu}_3\text{SnH}]}{d[\text{RH}]} &= 0 \\ \therefore \frac{d[\text{UH}]}{d[\text{RH}]} &= - \left( 1 + \frac{d[\text{Bu}_3\text{SnH}]}{d[\text{RH}]} \right). \end{aligned} \quad (\text{A.5})$$

By combining equations A.3 and A.5, we get:

$$\begin{aligned} \frac{k_{\text{H1}}[\text{Bu}_3\text{SnH}]}{k_{\text{r}}} &= - \left( 1 + \frac{d[\text{Bu}_3\text{SnH}]}{d[\text{RH}]} \right) \\ \therefore \frac{k_{\text{H1}}[\text{Bu}_3\text{SnH}]}{k_{\text{r}}} + 1 &= - \frac{d[\text{Bu}_3\text{SnH}]}{d[\text{RH}]} \\ \therefore \frac{k_{\text{H1}}[\text{Bu}_3\text{SnH}] + k_{\text{r}}}{k_{\text{r}}} &= - \frac{d[\text{Bu}_3\text{SnH}]}{d[\text{RH}]} \\ \therefore d[\text{RH}] &= - \frac{k_{\text{r}} d[\text{Bu}_3\text{SnH}]}{k_{\text{H1}}[\text{Bu}_3\text{SnH}] + k_{\text{r}}} \\ \therefore d[\text{RH}] &= - \frac{k_{\text{r}}}{k_{\text{H1}}} \left( \frac{d[\text{Bu}_3\text{SnH}]}{[\text{Bu}_3\text{SnH}] + k_{\text{r}} / k_{\text{H1}}} \right) \end{aligned} \quad (\text{A.6})$$

Equation A.6 is in a form suitable for integration, so it can be written:

$$\int_i^f d[\text{RH}] = - \frac{k_{\text{r}}}{k_{\text{H1}}} \int_i^f \frac{d[\text{Bu}_3\text{SnH}]}{[\text{Bu}_3\text{SnH}] + k_{\text{r}} / k_{\text{H1}}}. \quad (\text{A.7})$$

Since it is known<sup>4</sup> that:

$$\int \frac{dx}{a+bx} = \frac{1}{b} \ln(a+bx)$$

we can integrate A.7 to obtain:

$$\begin{aligned} [\text{RH}]_f &= -\frac{k_r}{k_{\text{H1}}} \left[ \ln \left( \frac{k_r}{k_{\text{H1}}} + [\text{Bu}_3\text{SnH}] \right) \right]_i^f \\ &= -\frac{k_r}{k_{\text{H1}}} \left[ \ln \left( \frac{k_r}{k_{\text{H1}}} + [\text{Bu}_3\text{SnH}]_f \right) - \ln \left( \frac{k_r}{k_{\text{H1}}} + [\text{Bu}_3\text{SnH}]_i \right) \right] \\ \therefore [\text{RH}]_f &= \frac{k_r}{k_{\text{H1}}} \left[ \ln \left( \frac{k_r}{k_{\text{H1}}} + [\text{Bu}_3\text{SnH}]_i \right) - \ln \left( \frac{k_r}{k_{\text{H1}}} + [\text{Bu}_3\text{SnH}]_f \right) \right]. \quad (\text{A.8}) \end{aligned}$$

Since the equation A.8 could not be solved analytically, a computer program was used to iteratively solve for  $k_r/k_{\text{H1}}$ , the ratio of rate constants, when supplied with values for the variables  $[\text{RH}]_f$ ,  $[\text{Bu}_3\text{SnH}]_i$  and  $[\text{Bu}_3\text{SnH}]_f$ . The quantity  $[\text{Bu}_3\text{SnH}]_f$  was equal to zero in this work by simply making it the limiting reagent. The concentration of the rearranged product, RH, was determined by gas chromatography. The value of  $k_r/k_{\text{H1}}$  and that of  $k_{\text{H1}}$  obtained from the literature<sup>5,6</sup> for that temperature, are multiplied to yield the desired rate constant,  $k_r$ .

### A3. References

1. Luszytk, J.; Maillard, B.; Deycard, S.; Lindsey, D. A. and Ingold, K. U. *J. Org. Chem.* **1987**, *52*, 3509.
2. Sciano, J. C. *J. Am. Chem. Soc.* **1980**, *102*, 7747.
3. Beckwith, A. L. J. and Moad, G. *J. Chem. Soc. Chem. Commun.* **1974**, 472.
4. *CRC Handbook of Chemistry and Physics*, 75th ed. Lide, D. R., Ed., CRC Press: Boca Raton, 1995, p A 21.

5. Chatgililoglu, C.; Ingold, K. U. and Sciano, J. C. *J. Am. Chem. Soc.* **1981**, *103*, 7739.
6. Johnston, L. J.; Luszyk, J.; Wayner, D. D. M.; Abeywickreyma, A. N.; Beckwith, A. L. J.; Sciano, J. C. and Ingold, K. U. *J. Am. Chem. Soc.* **1985**, *107*, 4594.



## Appendix B

### **$^{17}\text{O}$ nmr spectroscopy: Optimisation of acquisition parameters for accurate quantification of the ratio of $^{17}\text{O}$ label in carbonyl and alkoxy oxygens of esters**

#### ***B.1 Introduction***

Oxygen is an important element, forming compounds with all of the elements except some of the noble gases. It is a constituent of many functional groups and is fundamental in living systems. Oxygen has three stable, naturally occurring isotopes:  $^{16}\text{O}$  (99.762%),  $^{17}\text{O}$  (0.038%) and  $^{18}\text{O}$  (0.200%).<sup>1</sup> Chemical and biological studies based on the properties of oxygen have usually focussed on the mass spectrometry of  $^{18}\text{O}$  enriched molecules. This technique is limited because the exact location of the label can be difficult to assign with confidence and a high enrichment is usually required for accurate quantitative work. In recent years advantage has been taken of the difference in chemical shift of an nmr-active nucleus (eg.  $^{13}\text{C}$ ,  $^{31}\text{P}$ ) attached to an  $^{16}\text{O}$  and to an  $^{18}\text{O}$  atom.<sup>2</sup> The position of an  $^{18}\text{O}$  label in a molecule can often be established this way, but the technique suffers from a difficulty encountered in accurate quantitation and, being an indirect method of observation,  $^{18}\text{O}$  nuclei attached solely to nmr-inactive nuclei escape detection.

In  $^{17}\text{O}$  nmr, the site of substitution (type of functional group or position within a functional group with inequivalent oxygens) is determined directly from the chemical shift. If two or more oxygens are labelled, the relative amount present in each can be obtained from the ratio of the respective peak integrals.

The field of  $^{17}\text{O}$  nmr spectroscopy has been the subject of chapters in monographs,<sup>3-6</sup> whole monographs,<sup>7</sup> as well as reviews.<sup>8</sup> Of particular interest are topics such as  $^{17}\text{O}$  enrichment methods<sup>9</sup> and the use of  $^{17}\text{O}$  nmr as a mechanistic probe in chemistry.<sup>10</sup> Directly relevant to the work in this thesis is the use of  $^{17}\text{O}$  nmr in establishing the proportions of label in ether and carbonyl positions of esters,<sup>11-15</sup> to enable the determination of rearrangement regiochemistry.

Two problems, perceived as significant barriers to using  $^{17}\text{O}$  as an analytic tool, are the labelling cost and the limit on molecular size. Perhaps the most useful source of a heavy-oxygen label is labelled water. The price of  $^{17}\text{O}$  labelled water (A\$ 700  $\text{g}^{-1}$  for 36.8 atom%  $^{17}\text{O}$ ,<sup>15</sup>) is significantly greater than that for  $\text{H}_2^{18}\text{O}$  (A\$ 175 for 98 atom%  $^{18}\text{O}$ ,<sup>14</sup>), yet  $^{17}\text{O}$  is still a relatively cheap isotope and the cost is by no means prohibitive if efficient labelling methods are used. As a marked decrease in the rate of molecular orientation accompanies increasing size the line widths associated with  $^{17}\text{O}$  signals from large molecules ( $MW > 500$ ) can be quite substantial, sometimes too great for signal detection.<sup>8</sup> However, high-field magnets greatly decrease the effects of this problem. A line width of 500 Hz will correspond to only 12.2 ppm at 41 MHz, which is relatively small when one considers that most oxygen resonances in organic molecules appear over a range of 600 ppm.

It requires only a relatively low enrichment of  $^{17}\text{O}$  to obtain good, quantitative spectra for small to medium-sized molecules. Natural abundance spectra can be obtained in reasonable time, but to double the spectral signal-to-noise ratio one must double the  $^{17}\text{O}$  concentration (isotopic content) of the sample or square the number of transients acquired. Therefore, isotopic enrichment of samples makes a great deal of sense.

**Table B.1.** Nmr parameters for the  $^{17}\text{O}$  nucleus

Spin number	$\frac{5}{2}$
Nuclear magnetic moment	$-1.894 \mu_{\text{N}}$
Gyromagnetic ratio	$-3.628 \text{ rad s}^{-1} \text{ T}^{-1}$
Electric quadrupole moment	$-0.0263 \times 10^{-24} \text{ e cm}^2$
Resonant frequency at 1T	5.772 MHz
Natural abundance	0.038 %
Chemical shift range	$\geq 1500 \text{ ppm}$
Magnitude of one-bond coupling constants (examples)	16.1 Hz for $^{13}\text{CO}$ ; (-)106 Hz for $^1\text{H}_3\text{O}^+$ ; 692 Hz for $^{129}\text{XeOF}_4$
Relaxation times	$\leq 200 \text{ ms}$
Relative sensitivity ( $^1\text{H} = 1$ )	$2.91 \times 10^{-2}$

The  $^{17}\text{O}$  nucleus has spin number  $\frac{5}{2}$  and is the only stable nmr-active isotope of oxygen. Although  $^{17}\text{O}$  is a reasonably sensitive nucleus, its combination of low natural abundance and large spectral line widths have made  $^{17}\text{O}$  nmr a relatively unpopular method of chemical and biological research. However, by increasing the abundance of  $^{17}\text{O}$  in a sample to 10 atom percent, the relative receptivity becomes  $3.12 \times 10^{-3}$  times that for  $^1\text{H}$ , atom for atom. This now compares favourably with a value of  $1.76 \times 10^{-4}$  for  $^{13}\text{C}$  at natural abundance. Relaxation times are relatively short because the principal mode of relaxation is through the electric quadrupole. The equality  $T_1 = T_2$  generally holds and  $T_2$  values may be obtained easily from spectral line widths by the relationship:

$$w_{\frac{1}{2}} = \frac{1}{\pi T_2}$$

where  $w_{\frac{1}{2}}$  is the line width at half-height and  $T_2$  is the transverse relaxation time constant.  $T_1$  represents the longitudinal relaxation time constant. For a typical line width of 200 Hz,  $T_2$  is 1.6 ms. Line widths may be reduced ( $T_2$  values increased) by increasing the rate of molecular reorientation. This is achieved in practice by using non-viscous, non-hydrogen-bonding solvents and acquiring data at elevated temperature. Reasonable line widths may be achieved for molecules with molecular weight  $\leq 500 \text{ g mol}^{-1}$ .

## ***B.2 Overcoming transmitter breakthrough***

An additional hindrance to obtaining good  $^{17}\text{O}$  nmr spectra has been the combination of relatively low Larmor resonance frequencies and fast relaxation times. At lower frequencies high resolution FT nmr probes are prone to acoustic ringing, where the residual RF signal resonates for a short time within the probe after the pulse has been switched off. This effect becomes significant for nuclei with short relaxation times because the decaying RF pulse signal significantly distorts a large proportion of the FID, causing "transmitter breakthrough", which manifests as an undulating baseline in spectra. Elimination of this effect is possible by leaving a delay of up to several hundred  $\mu\text{s}$  between the  $90^\circ$  excitation pulse and acquisition. This is done at the expense of losing a

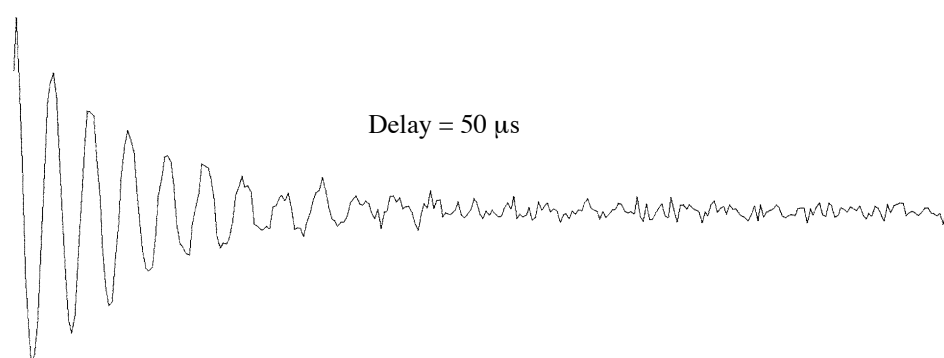
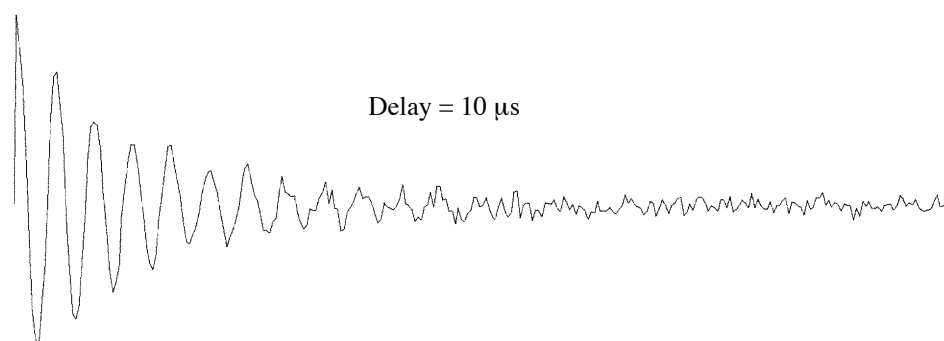
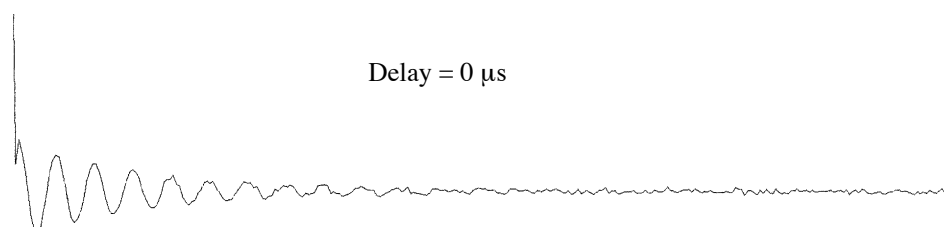
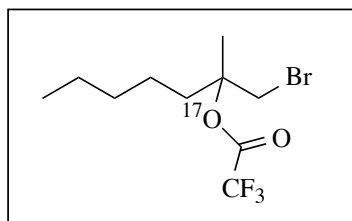
sometimes significant proportion of the signal and introducing phase errors, which in turn causes considerable errors when accurate peak integrals are required. Acoustic ringing decreases markedly at higher pulse frequencies however, so that shorter pre-acquisition delay times are required with high-field spectrometers. Baseline roll is also less of a problem when  $^{17}\text{O}$  enriched samples are used owing to higher signal-to-noise ratios.

Figure B.1 illustrates how the transmitter spike at the beginning of the FID can be eliminated by the correct choice of a pre-acquisition delay time. Here the FID (total time = 10,000  $\mu\text{s}$ ) for the relaxation of the  $^{17}\text{O}$  nucleus in the *oxy*-labelled  $\beta$ -bromoester is shown for delays of 0, 10 and 50  $\mu\text{s}$ . No delay results in a marked spike at the beginning of the FID, whereas a 10  $\mu\text{s}$  delay eliminates this spike. A 50  $\mu\text{s}$  delay eliminates this spike, but an unnecessarily large amount of the start of the FID is also lost. A 10  $\mu\text{s}$  delay was therefore used in data acquisition.

### ***B.3 Spectrometer parameters and method of acquisition***

#### **B.3.1 Spectrometer parameters**

All of the  $^{17}\text{O}$  spectra were obtained in a field of 7.05 T on a Varian VXR 300 spectrometer operating at 40.681 MHz. A spectral width of 30,030 Hz and transmitter offset of 10,000 Hz were employed, corresponding with the transmitter RF pulse being centred at about 235 ppm. For each spectrum 16,384 complex data points were collected and zero filled to 32,768 complex points prior to Fourier transform, without exponential weighting. A  $90^\circ$  pulse of 21.0  $\mu\text{s}$  duration was followed by a 10  $\mu\text{s}$  delay before acquisition, to arrest transmitter breakthrough. The total acquisition time for each cycle was 273 ms and the number of transients collected varied from 8192 (30 min acquisition time) to *ca.*  $2 \times 10^5$  (16 hours), depending upon sample concentration. The S/N ratio for the smallest peak of interest in each of the spectra was always greater than 6. Quantitatively reliable spectra have been obtained with samples containing as little as  $7 \times 10^{-6}$  moles of  $^{17}\text{O}$  in 16 hours. The longitudinal relaxation time constant ( $T_1$ ) for the *oxy*-labelled ester, 1-bromomethyl-1-methylhexyl trifluoroacetate, was determined to be  $847 \pm 90$   $\mu\text{s}$  and  $T_2$  values for all compounds were calculated from spectral line widths and were in the range 500 - 2300  $\mu\text{s}$ .



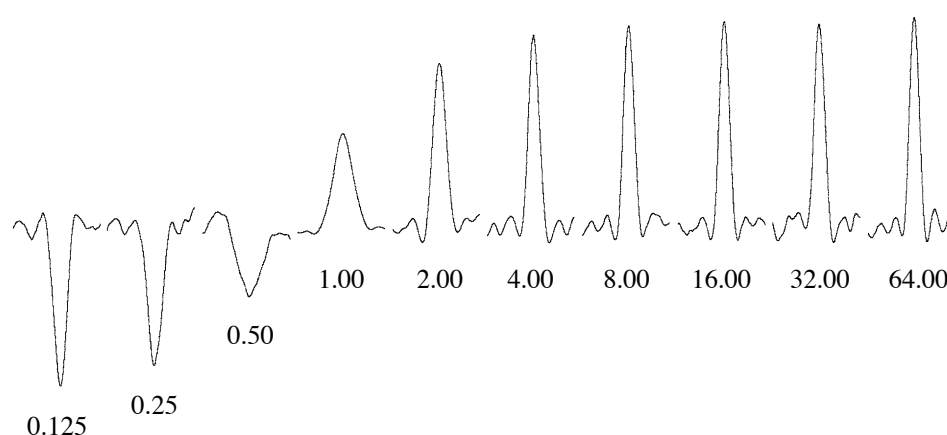
**Figure B.1.** A delay between the end of the excitation pulse and acquisition eliminates "transmitter breakthrough".

### B.3.2 Method for obtaining spectra

Once purified by preparative GC, samples of the labelled esters (3-20 mg of compound of  $MW \sim 227 \text{ gmol}^{-1}$ ) were dissolved in  $\geq 400 \mu\text{L}$  of distilled pentane (viscosity = 0.240 cp at 20°C) in 5 mm nmr tubes. Spectra of reaction mixtures were

obtained in their respective solvents, occasionally with a little pentane added. To optimise field homogeneity throughout the sample solution, the spectrometer was locked and shimmed (in  $^1\text{H}$  mode) with a solution of equal volumes of pentane and  $\text{CDCl}_3$ . The acquisition parameters for the spectrometer were then set to those for the  $^{17}\text{O}$  nucleus, the probe was tuned to the transmitter frequency and the field was referenced externally to  $\text{H}_2^{17}\text{O}$  (0 ppm), by placing a Wilmad capillary insert containing  $\text{H}_2^{17}\text{O}$  (48.6 atom%  $^{17}\text{O}$ ) into the sample tube and acquiring four transients. Acquisitions of sample spectra were run unlocked at 298 K while spinning at 24 Hz. The chemical shift data is reproducible to within  $\pm 2$  ppm and the ratios of the integrals of ether and carbonyl oxygens are estimated to have a precision of  $\pm 0.3\%$  between spectra of identical samples.

Figure B.2 shows the spectra for a  $T_1$  determination of the *oxy*-labelled  $\beta$ -bromoester (46.5%  $^{17}\text{O}$  enriched). A zero amplitude for the resonance occurs at time  $T_1$ , which was determined to be  $847 \pm 90$   $\mu\text{s}$ . A total acquisition time of 273 ms for each transient is therefore more than 300 times that of  $T_1$  value for the  $^{17}\text{O}$  nucleus in this ester, so it can be assumed that complete relaxation of  $^{17}\text{O}$  nuclei in each of the labelled compounds is occurring before the next excitation pulse occurs.

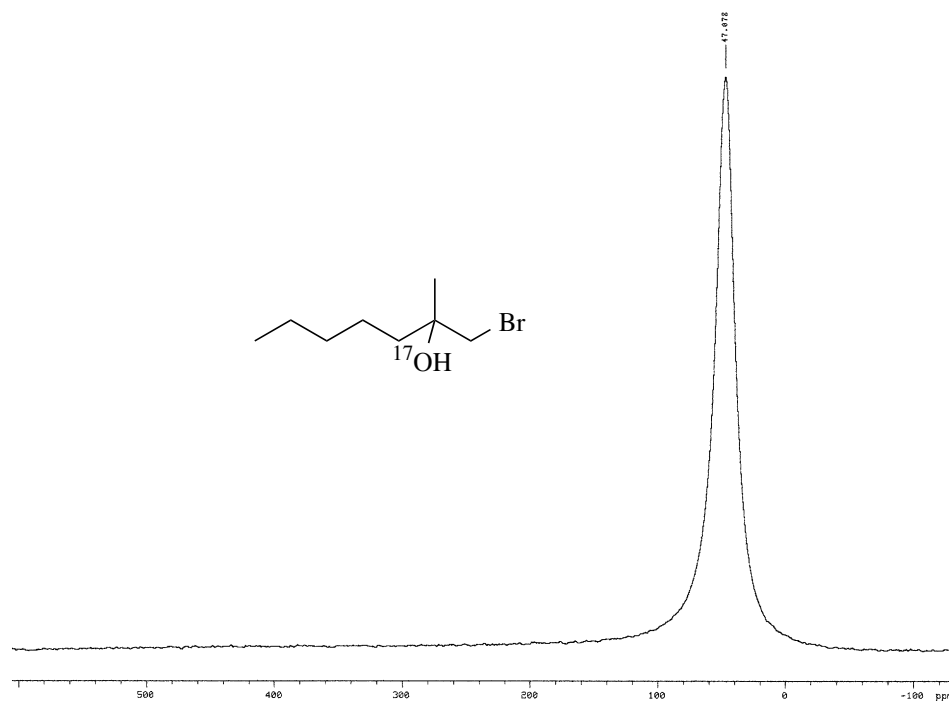


**Figure B.2.** An inversion-recovery experiment to determine the spin-lattice (longitudinal) relaxation time constant,  $T_1$ , for the  $^{17}\text{O}$  nucleus of the *oxy*-labelled ester 1-bromomethyl-1-methylhexyl trifluoroacetate. The time values indicated are given in milliseconds.

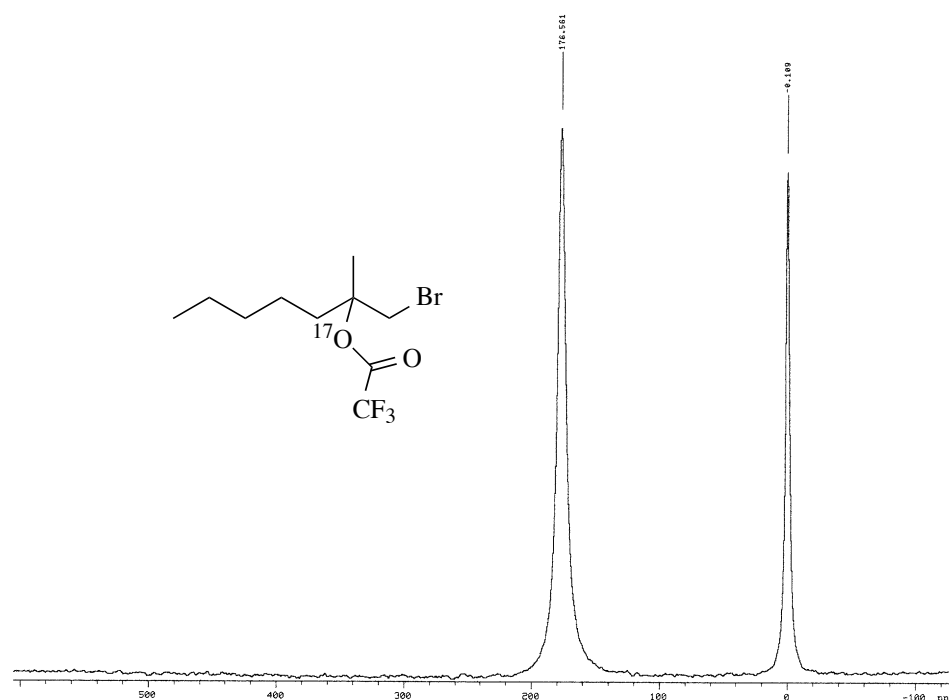
### B.4 $^{17}\text{O}$ nmr spectra

The  $^{17}\text{O}$  nmr spectrum of 1-bromo-2-methylheptan-2-ol (46.5%  $^{17}\text{O}$  enriched) is shown in figure B.3. The peak is centred at 47.1 ppm and is broadened due to the effects of hydrogen bonding which decrease the rate of molecular reorientation in solution. A computer line-broadening function was used to improve the apparent S/N ratio. The coupling of  $^{17}\text{O}$  to  $^1\text{H}$  cannot be resolved but would be expected to be approximately 80 Hz, like most alcohols.<sup>3</sup>

Figure B.4 shows the  $^{17}\text{O}$  nmr spectrum of *oxy*-labelled  $\beta$ -bromoester (46.5%  $^{17}\text{O}$  enriched) in pentane solution, externally referenced to  $\text{H}_2^{17}\text{O}$  (0 ppm). The ether oxygen resonates at 176.7 ppm. A line-broadening function was again used to improve apparent S/N. In this spectrum, coupling of  $^{17}\text{O}$  to  $^1\text{H}$  is not observed in the water peak. It is interesting to note that the line width of the ether-type oxygen resonance is greater than that for water owing to the larger molecular size of the ester.



**Figure B.3.** The  $^{17}\text{O}$  nmr spectrum of labelled 1-bromo-2-methylheptan-2-ol in pentane solution

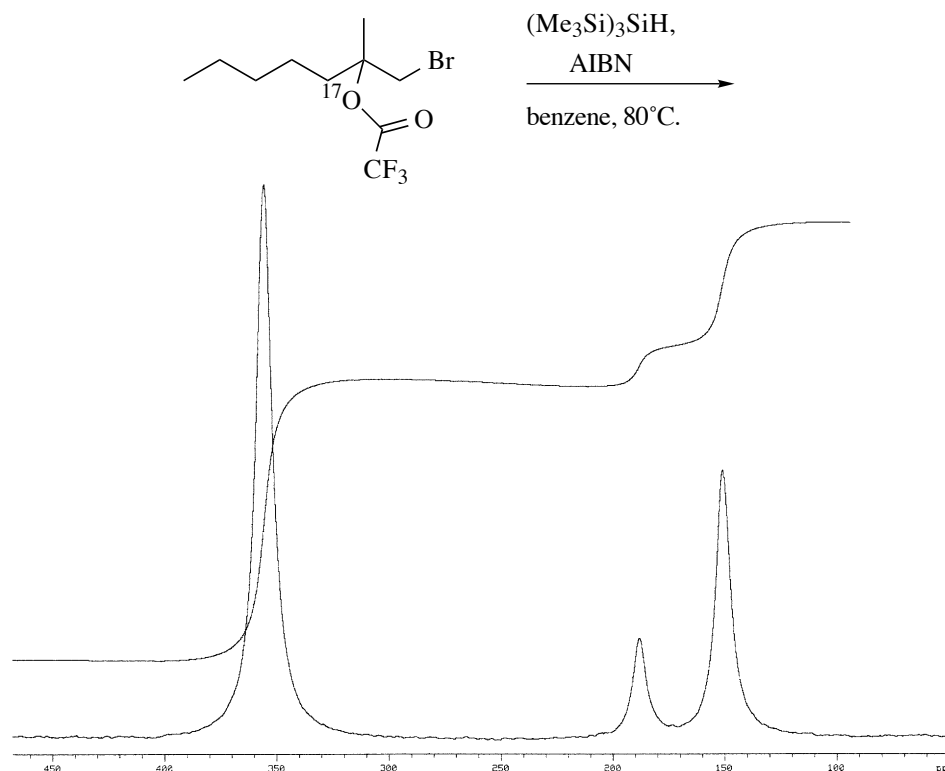


**Figure B.4.** The  $^{17}\text{O}$  nmr spectrum of *oxy*-labelled 1-bromomethyl-1-methylhexyl trifluoroacetate in pentane solution, externally referenced to  $^{17}\text{O}$ -labelled water (0 ppm)

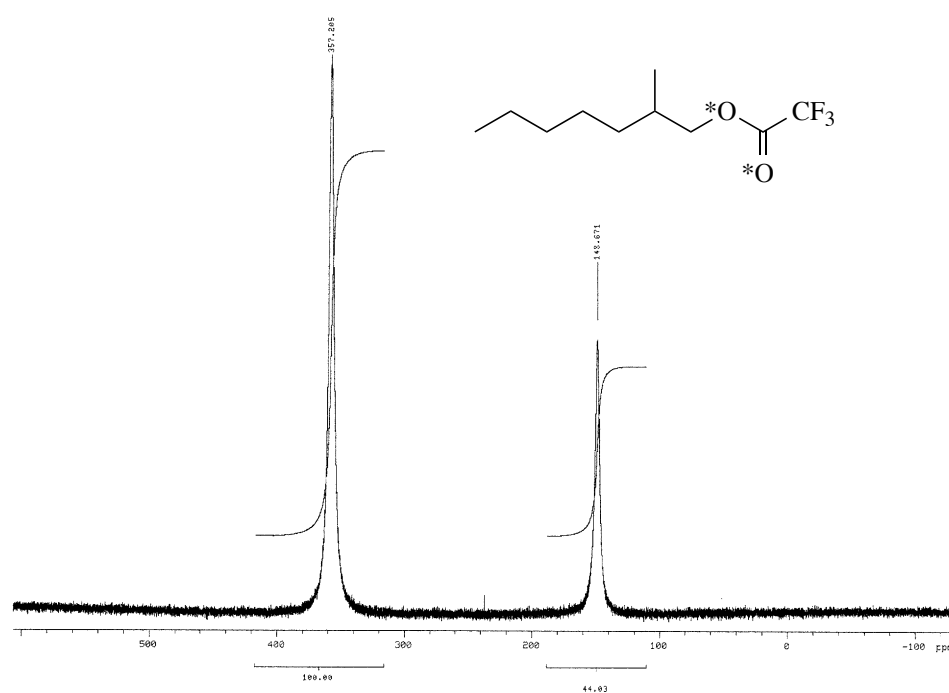
A spectrum of the mixture from the reaction of the  $\beta$ -bromoester with tris(trimethylsilyl)silane (av. conc. = 0.030 M) and AIBN in benzene solution at  $80^\circ\text{C}$  is shown in figure B.5. To prepare the sample for nmr the bulk of the benzene was carefully distilled from the reaction solution and a small volume of pentane was added to lower the viscosity. The viscosity of benzene (0.65 cp at  $20^\circ\text{C}$ ) is significantly greater than that of pentane (0.24 cp) and the effect of this and the viscosity of the by-products upon spectral line widths is apparent.

A line-broadening function was used to improve apparent signal-to-noise. The peaks represent the alkoxy and carbonyl resonances of the rearranged product, 2-methyl-1-heptyl trifluoroacetate and the directly-reduced product, 1,1-dimethylhexyl trifluoroacetate. The ratio of these products was determined by analytical GC to be 9.15:1 respectively. Following this spectrum are the spectra of each of the constituents, which were separated from each other and from by-products by preparative GC.

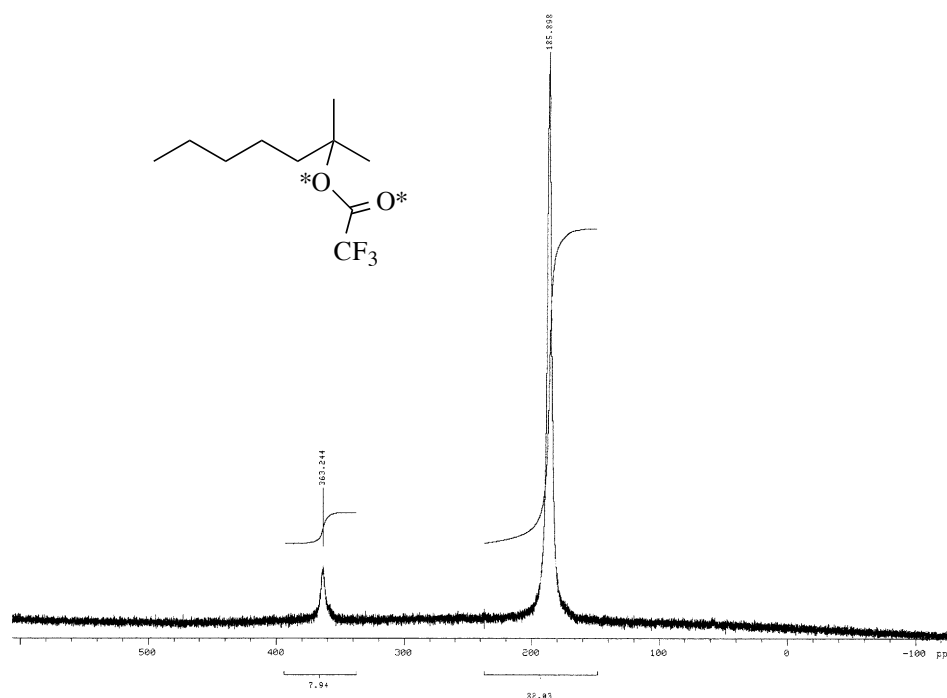




**Figure B.5.** The  $^{17}\text{O}$  nmr spectrum of the mixture from the completed reaction of the labelled bromoester with tris(trimethylsilyl)silane in benzene



**Figure B.6.** The  $^{17}\text{O}$  nmr spectrum of the labelled, rearranged product in pentane solution, after being isolated from the rearrangement reaction mixture by preparative GC



**Figure B.7.** The  $^{17}\text{O}$  nmr spectrum of the labelled, directly-reduced product in pentane solution, after being isolated from the rearrangement reaction mixture by preparative GC

The  $^{17}\text{O}$  spectrum of the rearranged product ester is shown in figure B.6. The smaller peak at 148.7 ppm is due to the alkoxy oxygen and the large peak at 357.2 ppm to the carbonyl oxygen. Figure B.7 shows the  $^{17}\text{O}$  nmr spectrum of the non-rearranged product. The peak at 185.9 ppm is due to the alkoxy oxygen and that at 363.2 ppm to the carbonyl oxygen. Note that there is a measurable proportion of label in the carbonyl oxygen. The line-broadening function was not used with either of these spectra.

## B.5 References

1. *CRC Handbook of Chemistry and Physics*; Lide, D. R., Ed.; CRC Press: Boca Raton, 75th Ed., 1994-1995, p. 8-64.
2. Risley, J. M. and Van Etten, R. L. *J. Am. Chem. Soc.* **1980**, *102*, 4609.
3. Kintzinger, J.-P. in *Oxygen-17 and Silicon-29*; Diehl, P., Fluck, E and Kosfeld, R., Eds.; Springer Verlag: Berlin, 1981, p. 1.
4. Kintzinger, J.-P. in *NMR of Newly Accessible Nuclei*; Laslo, P., Ed.; Academic Press: New York, 1983, vol. 2, p. 79.

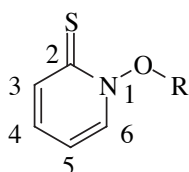
5. Klemperer, W. G. in *The Multinuclear Approach to NMR Spectroscopy*; Lambert, J. B. and Riddell, F. G., Eds.; D. Reidel Publishing: Dordrecht, 1983, p. 245.
6. McFarlane, W. and McFarlane, H. C. E. in *Multinuclear NMR*; Mason, J., Ed.; Plenum Press: New York, 1987, p. 403.
7. *<sup>17</sup>O NMR Spectroscopy in Organic Chemistry*; Boykin, D. W., Ed.; CRC Press: Boston, 1991.
8. Klemperer, W. G. *Angew. Chem., Int. Ed. Engl.* **1978**, *17*, 246.
9. Kabalka, G. W. and Goudgaon, N. M. in *<sup>17</sup>O NMR Spectroscopy in Organic Chemistry*; Boykin, D. W., Ed.; CRC Press: Boston, 1991, p. 21.
10. Woodard, R. W. in *<sup>17</sup>O NMR Spectroscopy in Organic Chemistry*; Boykin, D. W., Ed.; CRC Press: Boston, 1991, p. 115.
11. Nakanishi, W.; Jo, T.; Miura, K.; Ikeda, Y.; Sugawara, T.; Kawada, Y. and Iwamura, H. *Chem. Lett.* **1981**, 387.
12. Creary, X. and Inocenio, P. A. *J. Am. Chem. Soc.* **1986**, *108*, 5979.
13. Beckwith, A. L. J. and Duggan, P. J. *J. Chem. Soc., Perkin Trans. 2* **1993**, 1673.
14. Beckwith, A. L. J. and Duggan, P. J. *J. Am. Chem. Soc.* **1996**, *118*, 12838.
15. Crich, D.; Huang, X. and Beckwith, A. L. J. *J. Org. Chem.* **1999**, *64*, 1762.
16. Cambridge Isotope Laboratories, Inc., Andover, MA, USA.
17. Isotec Inc., Miamisburg, OH, USA.

## Appendix C

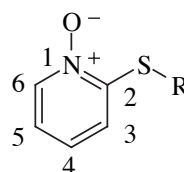
### The assignment of the $^{13}\text{C}$ and $^1\text{H}$ nmr chemical shifts of the heterocyclic ring systems of *N*-alkoxy-2(1*H*)-pyridinethiones and 2-(alkylsulfanyl)pyridine *N*-oxides

#### C.1 Introduction

A search through the chemical literature failed to find reliable assignments of the  $^1\text{H}$  and especially  $^{13}\text{C}$  chemical shifts of the atoms in the heterocyclic rings of *N*-alkoxy-2(1*H*)-pyridinethiones (**C.1**) and their isomers 2-(alkylsulfanyl)pyridine *N*-oxides (**C.2**). Hartung and coworkers have investigated the structures of **C.1a** and **C.2a** ( $\text{R} = \text{CH}_3$ ) in various solvents by  $^1\text{H}$  and  $^{13}\text{C}$  nmr but made only partial assignments.<sup>1</sup> Two-dimensional shift-correlated nmr spectroscopy was hence used to correctly assign the resonances.



**C.1**



**C.2**

*N*-Cyclohexylmethoxy-2(1*H*)-pyridinethione (**C.1b**,  $\text{R} = \text{CH}_2c\text{-C}_6\text{H}_{11}$ ) and 2-(cyclohexylmethylsulfanyl)pyridine *N*-oxide (**C.2b**,  $\text{R} = \text{CH}_2c\text{-C}_6\text{H}_{11}$ ) were chosen as the representatives of the two classes of compound. Both these compounds are crystalline (solid pyridinethiones decompose less quickly than those in a liquid state) at room temperature, can be readily purified and the aliphatic substituents ensure that no unnecessary complexity arises due to overlap of signals from the conjugated or aromatic  $\pi$ -electron ring systems.

The  $^1\text{H}$  and  $^{13}\text{C}$  nmr spectra, obtained at 300 and 75 MHz respectively in deuteriochloroform solution, are provided for each compound. Arrows are included where an APT<sup>2</sup> spectrum was run. "Up" arrows represent  $\text{CH}_2$  and quaternary carbons

and "down" arrows CH and CH<sub>3</sub> groups. It was possible to correctly assign some closely separated resonances from their relative peak heights, as the magnitude of the signal resonance is often approximately proportional to the numbers of degenerate atoms contributing to the signal.

## C.2 Assignment of the chemical shifts of *N*-cyclohexylmethoxy-2(1*H*)-pyridinethione

The one-dimensional nmr spectra for *N*-cyclohexylmethoxy-2(1*H*)-pyridinethione are provided below:

<sup>1</sup>H: 1.13 (m, 2H), 1.20-1.40 (m, 3H), 1.65-1.82 (m, 4H), 1.81-2.00 (m, 3H), 4.24 (d, 2H, *J* = 6.1 Hz), 6.66 (ddd, 1H), 7.17 (ddd, 1H), 7.68 (dd, 1H), 7.77 (dd, 1H); and

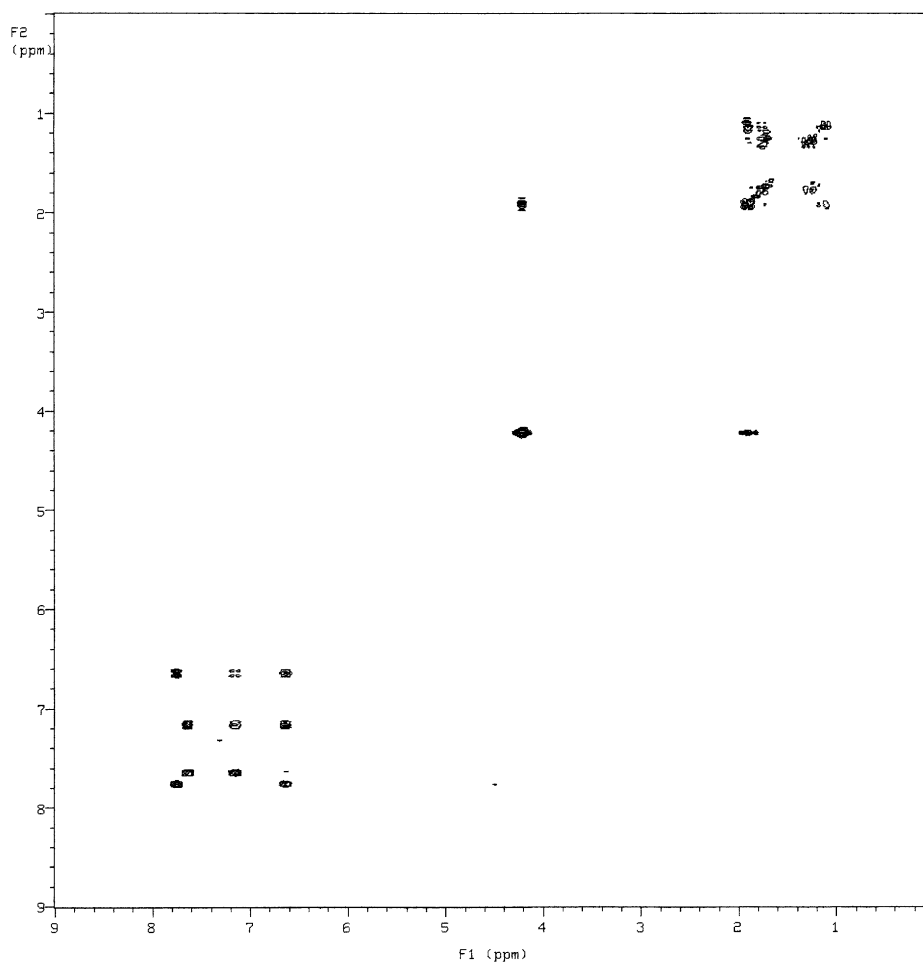
<sup>13</sup>C: 25.2↑, 25.9↑, 29.2↑, 36.0↓, 81.6↑, 113.6↓, 133.1↓, 137.8↓, 138.0↓, 175.6↑.

In the <sup>1</sup>H spectrum, it is clear from the multiplicities of the double doublet resonances at 7.68 and 7.77 ppm that the hydrogens corresponding to these signals lie at the extremities (positions 3 and 6) of the four sequential ring protons. The two remaining downfield signals at 6.66 and 7.17 hence represent the hydrogens at positions 4 and 5, but absolute assignment of any one of these resonances cannot be made with certainty on the basis of this spectrum alone.

A homonuclear shift-correlated spectrum (COSY) was obtained (figure C.1) and the correlations for the pyridinethione ring function are listed in table C.1.

**Table C.1.** <sup>1</sup>H–<sup>1</sup>H shift correlations for the heterocyclic ring of *N*-cyclohexylmethoxy-2(1*H*)-pyridinethione

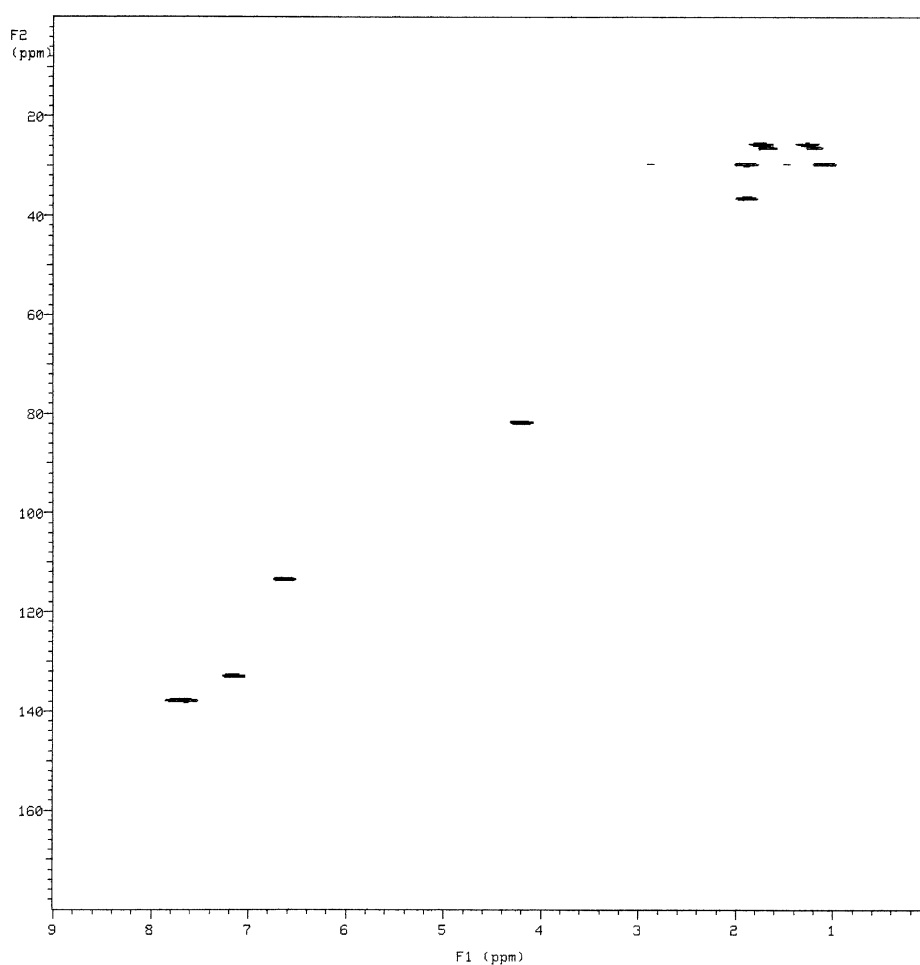
<sup>1</sup> H chemical shift (ppm)	<sup>1</sup> H chemical shift (ppm)
6.66	7.17 and 7.77
7.17	6.66 and 7.68
7.68	7.17
7.77	6.66



**Figure C.1.** COSY spectrum of *N*-cyclohexylmethoxy-2(1*H*)-pyridinethione

From the correlations the chemical shifts of the consecutive hydrogens around the pyridinethione ring were established to be  $7.77 \rightarrow 6.66 \rightarrow 7.17 \rightarrow 7.68$ . In addition, the  $\text{OCH}_2$  doublet at 4.24 ppm correlates strongly with a multiplet centred around 1.9 ppm. The latter multiplet therefore corresponds to the methine of the cyclohexyl ring. The sequential order of the hydrogens around the ring, despite being valuable information, still does not allow absolute assignment of any of the heterocyclic ring hydrogens or carbons.

A one-bond,  $^{13}\text{C}$ - $^1\text{H}$  heteronuclear shift-correlated (HETCOR) spectrum (figure C.2) was recorded in order to establish carbon-hydrogen connectivity. Table C.2 lists the C–H correlations extracted from the HETCOR spectrum.



**Figure C.2.** HETCOR spectrum of *N*-cyclohexylmethoxy-2(1*H*)-pyridinethione. The horizontal axis represents  $^1\text{H}$  and the vertical axis  $^{13}\text{C}$  chemical shifts.

**Table C.2.**  $^{13}\text{C}$ - $^1\text{H}$  (1 bond) shift correlations for *N*-cyclohexylmethoxy-2(1*H*)-pyridinethione

$^{13}\text{C}$ chemical shift (ppm)	$^1\text{H}$ chemical shift (ppm)
25.2	1.32 and 1.80
25.9	1.25 and 1.74
29.2	1.13 and 1.94
36.0	1.94
81.6	4.24
113.6	6.66
133.1	7.17
137.8	7.68 or 7.77 (not resolved)
138.0	7.77 or 7.68 (not resolved)
175.6	no correlations

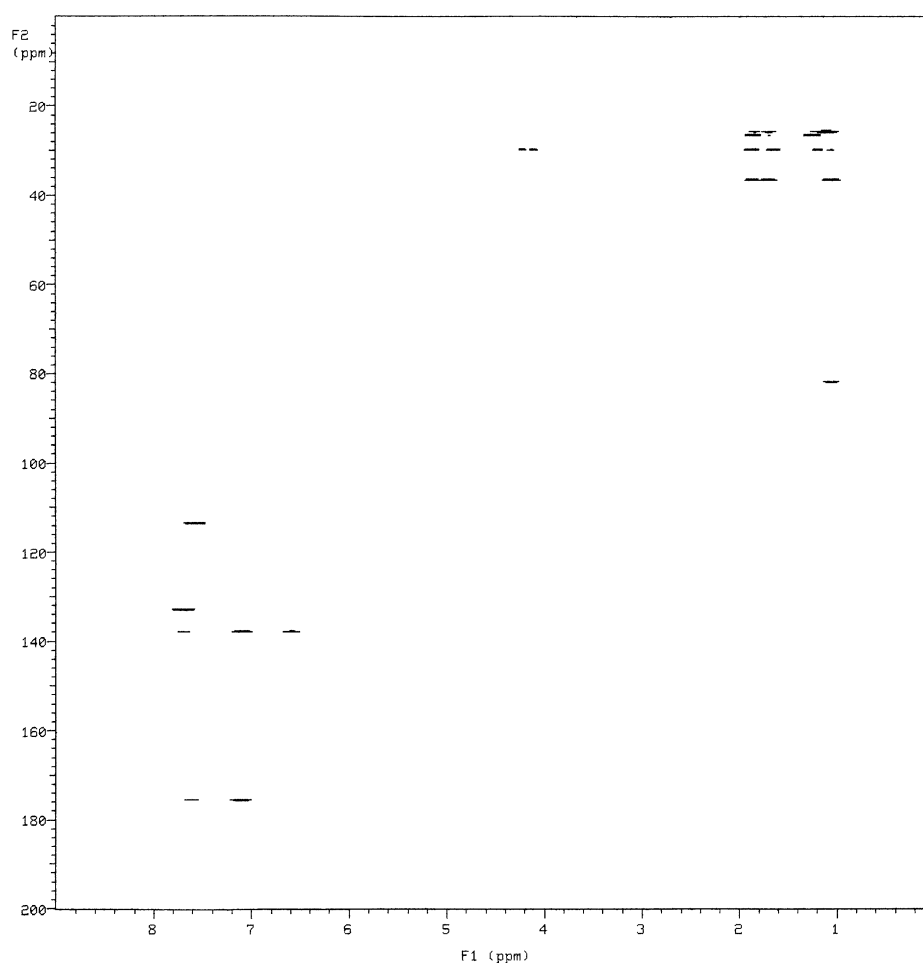
The HETCOR spectrum permitted most C–H connectivity to be established. There was also resolution of the signals contributing to the several-proton multiplets of the cyclohexyl ring system, allowing accurate chemical shifts to be assigned. However, the unambiguous assignment of the heterocyclic ring protons was still not possible.

A long-range (2 and 3 bond)  $^{13}\text{C}$ – $^1\text{H}$  shift-correlated heteronuclear nmr (LR HETCOR) spectrum was hence obtained (figure C.3), which made unambiguous assignment of the heterocyclic ring chemical shifts possible. One-bond correlations are absent in LR HETCOR spectra. In addition, in aromatic and other extended  $\pi$ -systems, 3-bond interactions are usually more intense than 2-bond interactions. The LR HETCOR acquisition parameters were configured so that coupling constants of 9.0 Hz would produced maximum correlation intensity. Coupling constants significantly greater, or less than, this value may cause correlations to appear absent from the spectrum. The 2 and 3-bond C–H correlations are listed in table C.3.

**Table C.3.**  $^{13}\text{C}$ – $^1\text{H}$  (2 and 3-bond) correlations for the heterocyclic ring of *N*-cyclohexylmethoxy-2(1*H*)-pyridinethione

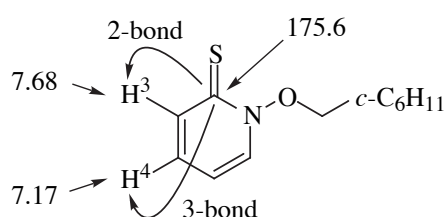
$^{13}\text{C}$ chemical shift (ppm)	$^1\text{H}$ chemical shift (ppm)
113.6	7.68
133.1	7.77
137.8 and 138.0 (not res.)	7.77 (weak), 7.17 and 6.66
175.6	7.17 and 7.68 (weak)





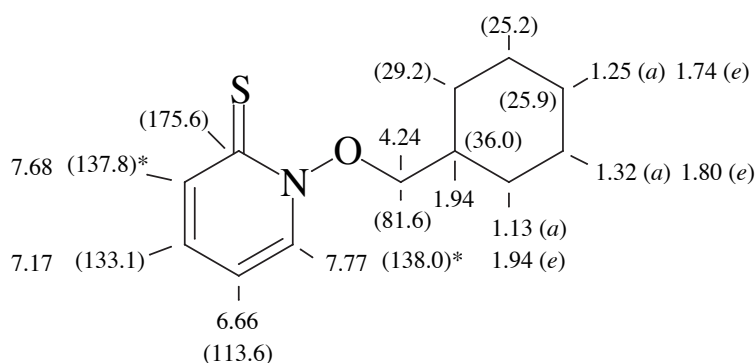
**Figure C.3.** LR HETCOR spectrum of *N*-cyclohexylmethoxy-2(1*H*)-pyridinethione. The vertical axis represents  $^{13}\text{C}$  and the horizontal axis  $^1\text{H}$  chemical shifts.

The correlations most easily enabling the correct assignment of the heterocyclic ring protons were that of the quaternary carbon at 175.6 ppm with the hydrogen resonances at 7.17 (ddd) and at 7.68 ppm (dd). These resonances thus belong to hydrogens at positions 4 and 3 respectively. The latter, 2-bond interaction is considerably less intense than the former, 3-bond interaction. Hydrogens at positions 5 and 6 hence resonate at 6.66 and 7.77 ppm respectively.



It was not possible, due to the limits of resolution, to unambiguously assign the carbon resonances at 137.8 and 138.0 ppm. It is expected that the greater downfield shift of H6 will be reflected in the carbon shift as well, making 138.0 ppm the more likely resonance attributable to the carbon at position 6.

All the aliphatic resonances have also been confidently assigned. Complete assignments are provided in figure C.4 ( $^{13}\text{C}$  shifts in brackets). Geminal axial and equatorial hydrogens were differentiated by chemical shift, the equatorial protons resonating further downfield. For cyclohexane, the axial and equatorial protons resonate at 1.19 and 1.67 ppm respectively.<sup>3</sup> Asterisks represent signals which could not be unambiguously assigned, due to the resolution limits of the nmr experiments.



**Figure C.4.** The complete assignment of the  $^{13}\text{C}$  and  $^1\text{H}$  nmr resonances for *N*-cyclohexylmethoxy-2(1*H*)-pyridinethione, **C.1b**

These assignments agree with the partial assignments given by Hartung and coworkers to *N*-methoxy-2(1*H*)-pyridinethione, but they have incorrectly assigned the hydrogens at ring positions 4 and 5 of *N*-pentoxy-2(1*H*)-pyridinethione.<sup>1</sup>

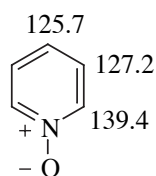
### C.3 Assignment of the chemical shifts of 2-(cyclohexylmethylsulfanyl)pyridine *N*-oxide

The one-dimensional nmr spectra for 2-(cyclohexylmethylsulfanyl)pyridine *N*-oxide are provided below:

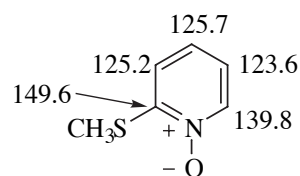
$^1\text{H}$ : 1.10 (m, 2H), 1.18-1.35 (m, 3H), 1.60-1.82 (m, 4H), 1.97 (dm, 2H), 2.78 (d, 2H,  $J = 6.8$  Hz), 7.05 (ddd, 1H), 7.13 (dd, 1H), 7.27 (ddd, 1H), 8.28 (dd, 1H); and

$^{13}\text{C}$ : 25.6, 25.8, 32.8, 36.5, 37.5, 120.0, 121.3, 125.9, 138.9, 153.3.

The  $^{13}\text{C}$  chemical shifts for a model compound, 2-(methylsulfanyl)pyridine *N*-oxide, were estimated by applying the shift values for the substituent  $-\text{SCH}_3$  from nmr tables for substituted benzenes,<sup>4</sup> to the known shifts of pyridine *N*-oxide.<sup>5</sup>

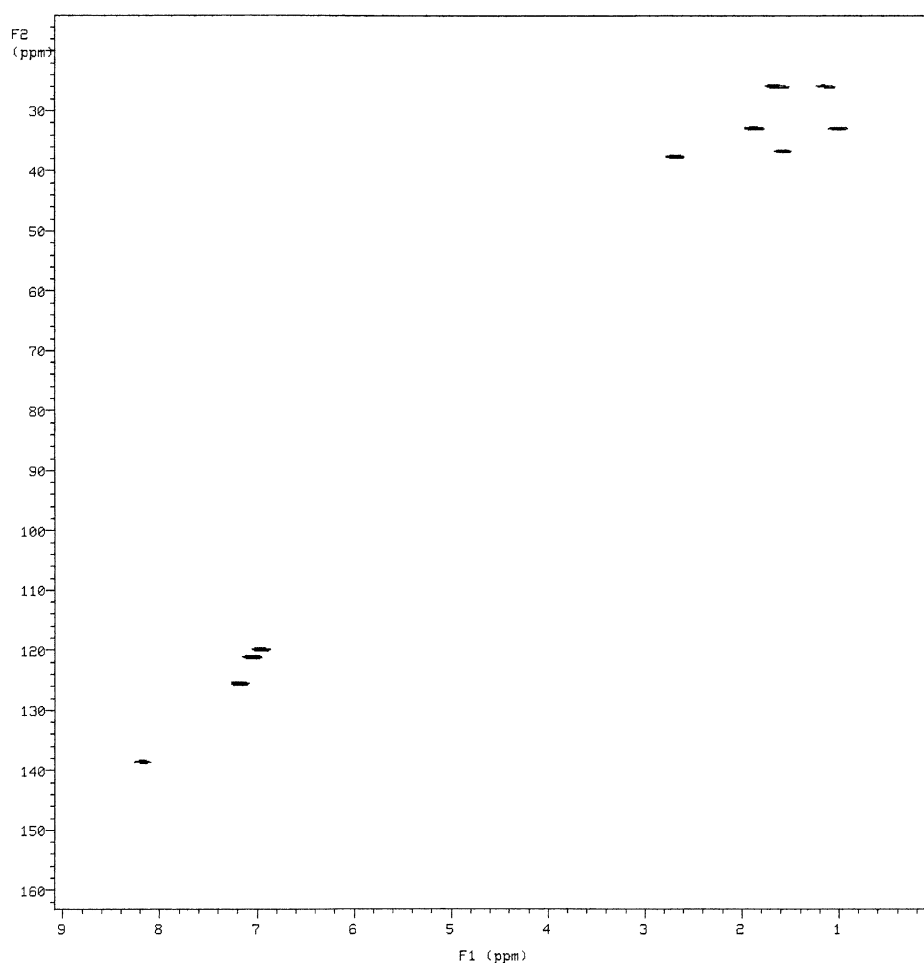


Known  $^{13}\text{C}$  chemical shifts for pyridine *N*-oxide



Estimated  $^{13}\text{C}$  chemical shifts for 2-(methylthio)pyridine *N*-oxide

It was therefore probable that the quaternary carbon of 2-(cyclohexylmethylsulfanyl)pyridine *N*-oxide would have the highest chemical shift and the methine with the highest shift would be at position 6. The resonance at 139.8 ppm in the  $^{13}\text{C}$  nmr spectrum of 2-(cyclohexylmethylsulfanyl)pyridine *N*-oxide was tentatively assigned to position 6 of the heterocyclic ring. A HETCOR spectrum was obtained to establish carbon-hydrogen connectivity (figure C.5) and table C.4 lists the pertinent correlations.



**Figure C.5.** HETCOR spectrum for 2-(cyclohexylmethylsulfanyl)pyridine *N*-oxide. The vertical axis represents  $^{13}\text{C}$  and the horizontal axis  $^1\text{H}$  chemical shifts.

**Table C.4.**  $^{13}\text{C}$ - $^1\text{H}$  (1 bond) shift correlations for 2-(cyclohexylmethylsulfanyl)pyridine *N*-oxide

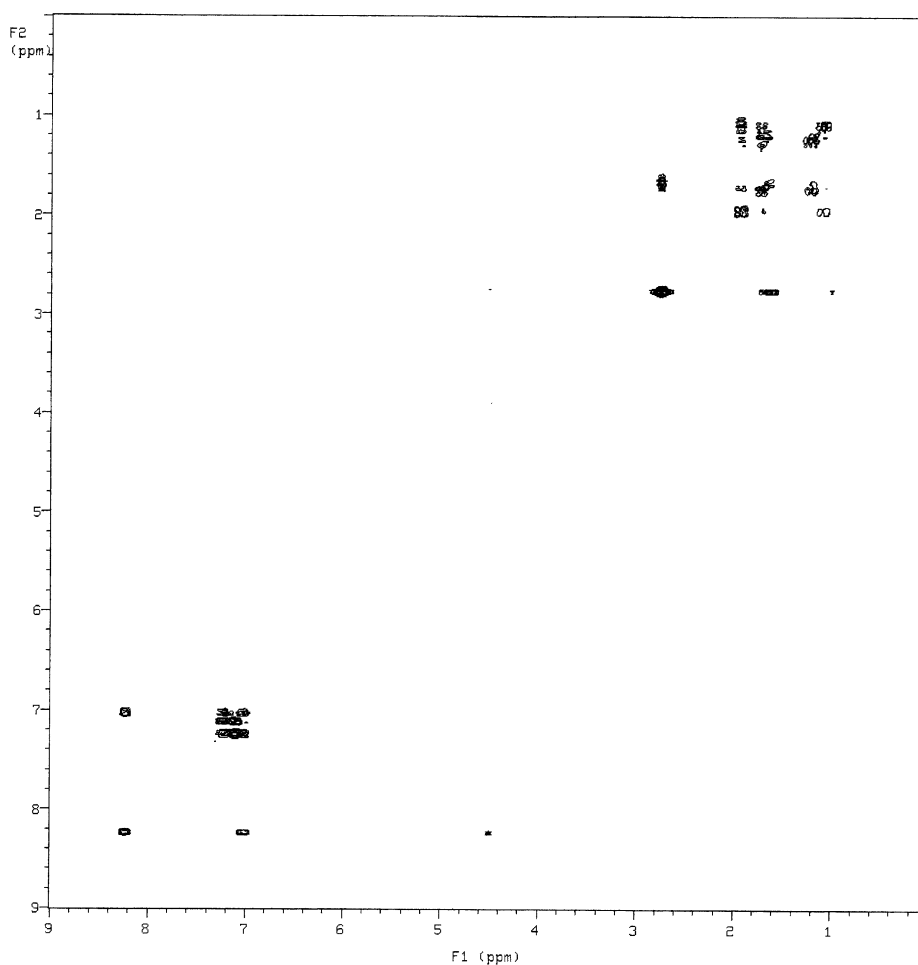
$^{13}\text{C}$ chemical shift (ppm)	$^1\text{H}$ chemical shift (ppm)
25.6	1.23 and 1.76
25.8	1.19 and 1.69
32.8	1.10 and 1.97
36.5	1.66
37.5	2.78
120.0	7.05
121.3	7.13
125.9	7.27
138.9	8.28
153.3	no correlation

Indeed, the quaternary carbon does have the highest shift at 155.3 ppm. It can also be immediately established that the proton connected to the carbon at position 6 (138.9 ppm) resonates at 8.28 ppm.

A COSY spectrum (figure C.6) was obtained to establish the sequential order of heterocyclic ring hydrogens. The correlations are listed in table C.5.

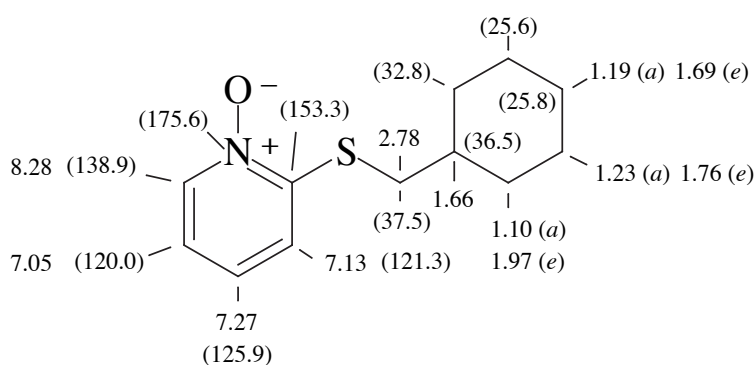
**Table C.5.**  $^1\text{H}$ - $^1\text{H}$  shift correlations for the aromatic ring portion of 2-(cyclohexylmethylsulfanyl)pyridine *N*-oxide

$^1\text{H}$ chemical shift (ppm)	$^1\text{H}$ chemical shift (ppm)
7.05	7.27 and 8.28
7.13	7.27
7.27	7.05 and 7.13
8.28	7.05



**Figure C.6.** COSY spectrum of 2-(cyclohexylmethylsulfanyl)pyridine *N*-oxide

The order of hydrogens around the ring is therefore 8.28 (6)→7.05 (5)→7.27 (4)→7.13 ppm (3). These hydrogens are connected respectively to the carbons which resonate at 138.9 (6), 120.0 (5), 125.9 (4) and 121.3 ppm (3). The correct assignments for the cyclohexymethyl resonances were established similarly to those for the pyridinethione. The complete assignments are illustrated in figure C.7 ( $^{13}\text{C}$  chemical shifts in brackets) and agree with partial assignments published.<sup>1</sup>



**Figure C.7.** The complete assignment of the  $^{13}\text{C}$  and  $^1\text{H}$  nmr resonances for 2-(cyclohexylmethylsulfanyl)pyridine *N*-oxide, **C.2b**

## C.4 References

- Hartung, J.; Kneuer, R.; Schwarz, M.; Svoboda, I. and Fuess, H. *Eur. J. Org. Chem.* **1999**, 97.
- Patt, S. L. and Shoolery, J. N. *J. Magn. Reson.* **1982**, 46, 535.
- Abraham, R. J. and Loftus, P. *Proton and Carbon-13 NMR Spectroscopy*; Heyden and Son: London, 1978, p. 179.
- Silverstein, R. M.; Bassler, G. C. and Morrill, T. C. *Spectrometric Identification of Organic Compounds*; John Wiley and Sons: New York, 1981, 4th Ed., p. 265.
- Katritzky, A. R. *The Handbook of Heterocyclic Chemistry*; Pergamon Press: Oxford, 1985, p. 35.

## Appendix D

### The preparation, purification, purity determination and storage of tributyltin hydride

#### *D.1 Introduction*

Tributyltin hydride is a mild, selective reagent used frequently to replace a variety of functional groups with a hydrogen atom, or to mediate in the generation of carbon-centred radicals which then undergo a variety of useful reactions including cyclisation, addition and substitution.<sup>1-3</sup> Considering the importance and widespread use of this compound, a short description of its inexpensive preparation, purification, purity determination and recommended storage will be presented.

Several problems with the use of tributyltin hydride have been encountered in the ANU laboratories, the first of which is the substantial cost of the reagent at A\$ 1.45 per gram.<sup>4</sup>

The second problem was the difficulty associated with the purification of tributyltin hydride. Distillation can be a difficult procedure, especially if finely divided solids are present in the sample.

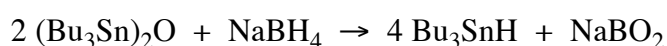
The third problem is the determination of purity. Rigorous kinetic work, for instance, requires that the concentration of tributyltin hydride in reaction solutions is accurately known, in turn demanding that the purity of the neat hydride is known accurately.

The fourth problem is preservation of sample purity upon storage. Pure tributyltin hydride (a colourless liquid) often decomposes slowly to a white solid upon storage, especially when leakage of air into the container is suspected. Neumann claims that the hydride is oxidised first to the colourless liquid bis(tributyltin) oxide, then further to the white solid dibutyltin oxide.<sup>3</sup> Support for this claim is found in the observation that formation of the white solid appears to cease once partially-oxidised tributyltin hydride samples are stored in the absence of air. Interestingly, no experimental support could be found for the claim that tributyltin hydride is moisture-sensitive,<sup>4</sup> as a pure sample could

be left in contact with air-free water overnight with negligible decomposition.

## **D.2 Preparation**

Tributyltin hydride is commonly prepared by the reduction of either tributyltin chloride or bis(tributyltin) oxide with lithium aluminium hydride in diethyl ether.<sup>2</sup> Other methods include the reduction of bis(tributyltin) oxide with borane,<sup>5</sup> reaction of tributyltin chloride and sodium borohydride,<sup>6</sup> or from the reaction of bis(tributyltin) oxide and polymeric methyl siloxane.<sup>7</sup> However, a simpler, cheaper, safer and higher-yielding method has been described by Szammer and Otvos.<sup>8</sup> This procedure consists of the treatment of a 0.33 M ethanolic solution of bis(tributyltin) oxide with 0.7 molar equivalents of sodium borohydride at room temperature. The sodium borohydride dissolves and the reaction proceeds according to the following equation, producing tributyltin hydride and precipitating sodium metaborate. Reaction progress can be monitored by thin layer chromatography, using iodine as an indicator.<sup>8</sup>



The original workers reported that the solvent was removed after 30 minutes by rotary evaporation and the residue was extracted with hexane. No further purification was attempted. Dry ethanol need not be used since the authors of the original procedure claim that small proportions of water (< 10%) in the reaction solvent does not affect the yield.<sup>8</sup> It is important that there is no acetic acid present since acids react with  $\text{Bu}_3\text{SnH}$  and  $\text{NaBH}_4$ . We suggest that several changes be made to the original procedure.

Stirring the reaction overnight (30 min recommended by authors), provided the reaction is kept under an oxygen-free atmosphere, is convenient and does not affect the yield adversely. The crude tributyltin hydride is purified by distillation after first removing the ethanol by rotary evaporation and filtering off the precipitate. Light petroleum is added to the residue and the resulting suspension is filtered through a short column of silica, eluting with several portions of the same solvent. Fine particles should



be removed since they cause frothing and bumping upon distillation. The solvent is removed under rotary evaporation, leaving crude tributyltin hydride as a colourless oil.

High yields ( $\geq 95\%$ ) of the tin hydride were usually obtained prior to distillation. This procedure enabled the cost of the reagent to decrease to approximately A30c per gram, 20% the price of that purchased commercially.<sup>4</sup> This method has been used to prepare tributyltin deuteride successfully and it is reported<sup>8</sup> that tributyltin tritide has been similarly prepared on a 0.1 mol scale.

### **D.3 Purification**

Contaminants in the crude tributyltin hydride would be expected to be small amounts of: unreacted bis(tributyltin) oxide, which is a colourless liquid with a boiling point of  $180^{\circ}\text{C}/2\text{ mmHg}^4$  (equivalent to  $135^{\circ}\text{C}/0.15\text{ mm}$ ); light petroleum from the work-up procedure; non-polar impurities in the reagents and their possible reaction products; and any of the decomposition products resulting from the atmospheric oxidation of tributyltin hydride (very high boiling points expected).

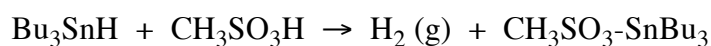
It is possible to purify the crude tributyltin hydride by reduced-pressure kugelrohr distillation, but since several distillations have bumped using this technique we recommended conventional reduced-pressure distillation through a short-path apparatus. Packed distillation columns flood easily during these distillations so their use is best avoided. Other workers have reported significant decomposition upon distillation,<sup>9</sup> so care must be taken during this step to avoid both excessive temperature and distillation time. We found the best method was to place the distillation flask—containing a rapidly magnetically-stirred, homogeneous sample of the crude  $\text{Bu}_3\text{SnH}$ —under a nitrogen atmosphere and lower it into an oil bath maintained at  $95\text{-}100^{\circ}\text{C}$ , then decrease the pressure gradually using a bleed valve and high vacuum until distillation commences ( $75^{\circ}\text{C}/0.15\text{ mmHg}$ ). This technique has reliably produced samples in good recovery, of purities in excess of 98% (w/w).

### D.4 Purity Determination

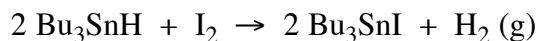
Neumann<sup>3</sup> lists several ways by which the purity of tributyltin hydride has previously been measured: halide titration; treatment with 3 mols of ethylmagnesium bromide which forms ethyl tributyltin, in turn analysed by GC against an internal standard; infrared spectroscopy; and gas volumetrically by reaction with dichloroacetic acid. Recently, Crich and coworkers used <sup>119</sup>Sn nmr spectroscopy with trimethylphenyl tin as an internal standard.<sup>10</sup> Three other methods of purity assay will be discussed: gas chromatography; volumetric measurement of hydrogen evolved by reaction with methanesulfonic acid; and titration with iodine.

Analytical gas chromatography, using a dimethylpolysiloxane-coated capillary column, provides a method of detecting and quantifying all stable, volatile compounds present in the tributyltin hydride sample. Bis(tributyltin) oxide, hexabutylditin, dibutyltin dihydride and possibly atmospheric degradation products may be detected in this way. Purity determination precision of  $\pm 0.1\%$  has been obtained.

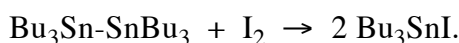
The measurement by gas burette of the volume of hydrogen evolved by reaction of a known mass of Bu<sub>3</sub>SnH with a large excess of stirred methanesulfonic acid is a reliable method provided the equipment is well maintained and skilfully used and that the sample does not contain a significant proportion of Bu<sub>2</sub>SnH<sub>2</sub> (detectable by GC) or other compounds which also liberate hydrogen upon reaction with acid. Methanesulfonic acid ( $pK_a -2.0$ ) is stronger than dichloroacetic acid ( $pK_a 1.1$ ), providing a faster and more complete reaction. The apparatus used for this measurement can be left permanently assembled so purity determinations are quick and convenient. Precision to  $\pm 1\%$  is usually possible.



Titration of a known mass of Bu<sub>3</sub>SnH with a 0.1 M solution of iodine in benzene to a permanent, pale pink endpoint (iodine excess)<sup>11</sup> has been recommended by Szammer and Otvos.<sup>8</sup> We performed these titrations under nitrogen in a small two-necked flask.



The reaction proceeds rapidly and this method can achieve a precision of better than  $\pm 0.3\%$ . However, hexabutylditin also reacts with iodine (see below), interfering with the analysis if it is present.<sup>11</sup> We have observed that bis(tributyltin) oxide also reacts with iodine in an as yet undetermined manner, producing a pale yellow solution. Dibutyltin dihydride is reported to form hydrogen iodide when the same procedure is used, although accurate quantitation is reportedly still possible by back-titration with alkali to determine the amount of acid present.<sup>11</sup>



In summary, all three methods are quick and convenient. Gas chromatography is a good method of assay if a very accurate determination of purity is required—for kinetic work for instance—although it does not easily provide a measure of "available H• equivalent" as the other methods do. Both of the other methods are reliable, although they don't inform the analyst of the identity and proportion of contaminants. Only the iodometric analysis is practical for neat samples with a large proportion of solids present.

### **D.5 Storage**

The choice and correct use of a storage container will determine the amount of time the tributyltin hydride retains its purity. For synthetic work samples are best stored below 4°C under dry nitrogen, in a container which is completely gastight and robust enough to tolerate high vacuum. A suitable container is a two-necked, round-bottomed flask fitted with a greased stopper in one neck and a teflon "rotaflo" tap with a greased Quickfit male joint in the other. Before opening, the container is evacuated and the contents are blanketed with oxygen-free nitrogen or argon *via* the rotaflo tap. The stopper is removed, ensuring that a stream of the inert gas is flowing continually over the liquid and from the flask. Slightly more of the reagent than needed is withdrawn.

Contamination is avoided by ensuring not to pump the syringe in the reagent nor return any excess. Before re-storage the container is evacuated again and sealed under an inert atmosphere. Samples of tin hydride have been kept like this for months with no measurable decrease in purity.

For kinetic work, where small volumes of tributyltin hydride of identical purity are required, it is handy to store the reagent in 1-5 mL portions in sealed ampoules which can be opened immediately before use. The reagent is placed in the ampoule, freeze/pump/thaw degassed several times and the ampoule is flame-sealed under vacuum. Samples stored in this way may be kept indefinitely at 4°C.

## **D.6 References**

1. Menapace, L. W. and Kuivila, H. G. *J. Am. Chem. Soc.* **1964**, 86, 3047.
2. Kuivila, H. G. *Synthesis* **1970**, 499.
3. Neumann, W. P. *Synthesis* **1987**, 665.
4. *Aldrich Catalogue of Fine Chemicals*, 1994-1995.
5. Chopa, A. B.; Koll, L. C.; Podesta, J. C. and Thorpe, F. G. *Synthesis* **1983**, 722.
6. Corey, E. J. and Suggs, J. W. *J. Org. Chem.* **1975**, 40, 2554.
7. Keinan, E. and Peretz, M. *J. Org. Chem.* **1983**, 48, 5302.
8. Szammer, J. and Otvos, L. *Chem. Ind (London)* **1988**, 23, 764.
9. Kuivila, H. G. *Adv. Organomet. Chem.* **1964**, 1, 47.
10. Crich, D.; Suk, D.-H. and Hao, X. *Tetrahedron* **2002**, 58, 5789.
11. Hayashi, K.; Iyoda, J. and Shiihara, I. *J. Organometal. Chem.* **1967**, 10, 81.